AD NUMBER

AD276249

NEW LIMITATION CHANGE

TO

Approved for public release, distribution unlimited

FROM

Distribution authorized to U.S. Gov't. agencies and their contractors; Mar 1962. Other requests shall be referred to Air Force Systems Command, ASD, Wright-Patterson AFB, OH 43433.

AUTHORITY

AFWAL ltr, 21 Nov 1984

AD 276249

AUTHORITY: AFWAL ltr, 21 Nov 84

UNCLASSIFIED

AD 276249

DEFENSE DOCUMENTATION CENTER

FOR

SCIENTIFIC AND TECHNICAL INFORMATION

CAMERON STATION ALEXANDRIA, VIRGINIA

UNCLASSIFIED

DISCLAIMER NOTICE

THIS DOCUMENT IS BEST QUALITY PRACTICABLE. THE COPY FURNISHED TO DTIC CONTAINED A SIGNIFICANT NUMBER OF PAGES WHICH DO NOT REPRODUCE LEGIBLY.

276249

AN ENGINEERING EVALUATION OF METHODS FOR THE PREDICTION OF FATIGUE LIFE IN AIRFRAME STRUCTURES

TECHNICAL REPORT No. ASD-TR-61-434

MARCH 1962

FLIGHT DYNAMICS LABORATORY
AERONAUTICAL SYSTEMS DIVISION
AIR FORCE SYSTEMS COMMAND
WRIGHT-PATTERSON AIR FORCE BASE, OHIO

Project No. 1367, Task No. 136710

(Prepared under Contract No. AF 33(616)-6574 by Lockheed-[illegible] Lockheed Aircraft Corporation, [illegible] Young, and M. A. Melcon.)

NOTICES

When Government drawings, specifications, or other data are used for any purpose other than in connection with a definitely related Government procurement operation, the United States Government thereby incurs no responsibility nor any obligation whatsoever; and the fact that the Government may have formulated, furnished, or in any way supplied the said drawings, specifications, or other data, is not to be regarded by implication or otherwise as in any manner licensing the holder or any other person or corporation, or conveying any rights or permission to manufacture, use, or sell any patented invention that may in any way be related thereto.

Qualified requesters may obtain copies of this report from the Armed Services Technical Information Agency, (ASTIA), Arlington Hall Station, Arlington 12, Virginia.

ASTIA release to OTS NOT authorized

Copies of ASD Technical Reports and Technical Notes should not be returned to the Aeronautical Systems Division unless return is required by security considerations, contractual obligations, or notice on a specific document.

300 - May 1962 - 33-1463 & 1464

FOREWORD

This report was prepared by the Lockheed-California Company, a Division of Lockheed Aircraft Corporation, Burbank, California, under USAF Contract No. AF 33(616)-6574. This contract was performed under Project No. 1367, "Structural Design Criteria," Task No. 136710, "Structural Analysis Methods." This Project and Task are part of Air Force Systems Command's Applied Research Program 750A, "The Mechanics of Flight." The contract was administered initially under the technical direction of the Aircraft Laboratory by the Project Engineer, Mr. Bernard Nagal. It was completed in the Flight Dynamics Laboratory under the direction of Mr. Vincent Kearney.

The program was conducted at the Lockheed-California Company under the technical administration of Mr. M. A. Melcon, Department Manager, Structural Methods. Technical supervision was under the direction of Mr. W. J. Crichlow, Group Engineer, Structural Static, and Mr. A. J. McCulloch. The details of the methods review and computations were developed by Mr. Louis Young with the assistance of other technical personnel in the Structural Methods Department and from the Mathematical Analysis Department in programming for digital computers. The statistical analysis of the S-N data was performed by Dr. F. M. Mueller.

The laboratory experimental program was under the technical administration of Mr. H. W. Foster, Division Manager, Lockheed Structures Research Laboratory. The design and assembly of the experimental equipment and the development of operational techniques were under the technical supervision of Mr. J. Redman, Group Engineer, Structural Development Research. He was also assisted in the assembly of electronic equipment for magnetic tape signal analysis, the recording of special loading spectra, and for fatigue test machine control equipment by Mr. W. B. Brewer, Group Engineer, Electrical Instrumentation, aided by Mr. R. A. Meyer, electrical design; Mr. J. B. Harlan, tape equipment; Mr. P. A. [illegible]tham, electrical calibration, monitoring, and maintenance.

The testing performed under this contract was under the direct supervision of Mr. H. W. Greene, Mr. R. H. Wells, and Mr. J. B. Ryan, assisted by Mr. J. Cox, Mr. R. L. Lowe, and Mr. L. Silvas.

Typing of the report was done by Mrs. Emily A. Baldwin, assisted by Mrs. Joyce Ponder and Miss Pat Daly.

\- - -

The assembly of the electronic equipment for magnetic tape reading, counting, tape recording of special loading spectra, and for the magnetic tape controlled fatigue test equipment, along with the development of the calibration and monitoring techniques, and the testing of the spectrum loaded coupons reported herein, was shared between this contract and the companion contract, No. AF 33(616)-6575, "Research Study to Establish Fatigue Test Loading Spectra from Flight Records."

ABSTRACT

The results of a research study are presented for the comparison and verification of methods of fatigue life prediction suitable for handling the complex problems encountered in the design and operation of modern aircraft. A general introduction to the problems of airframe fatigue analysis is given from the overall viewpoint of a system of design, development testing, and interpretation of fleet service history to maintain a necessary comparative basis for relating a practical fatigue life prediction method to operational results. From a study of twenty proposed fatigue life prediction methods ten of the procedures were chosen for evaluation numerically with a group of seventy-eight complex spectral test results representing approximately 206 individual specimens.

An experimental program generated constant amplitude and S-N type data on simple notched coupons of 7075-T6 aluminum alloy sheet for use in the analysis procedures. Ordered spectral fatigue test data from these same type coupons were utilized from another concurrent ASD fatigue research program. New magnetic tape controlled fatigue test machines were utilized to apply simple spectra of gust, maneuver, ground, composite spectra of flight gust, ground taxi, and ground-air-ground transitions and composite spectra of flight maneuver, ground taxi, and ground-air-ground transitions. A series of specimens of a complex joint were also [illegible] the same simple ordered gust and maneuver spectra, and to the [illegible] gust, ground taxi, and ground-air-ground transition composite spectra of flight maneuver, ground taxi, and ground-air-ground cycles, and to composite fli[illegible] were analyzed by the selected procedures to confirm transition cycles. These [illegible] of improving the selected fatigue life prediction or provide a possible means methods.

PUBLICATION REVIEW

This report has been reviewed and is approved.

FOR THE COMMANDER:

William C. Nielsen

WILLIAM C. NIELSEN
Colonel, USAF
Chief, Flight Dynamics Laboratory

TABLE OF CONTENTS

LIST OF ILLUSTRATIONS

LIST OF ILLUSTRATIONS (Continued)

LIST OF ILLUSTRATIONS (Continued)

LIST OF ILLUSTRATIONS (Continued)

LIST OF ILLUSTRATIONS (Continued)

LIST OF ILLUSTRATIONS (Continued)

LIST OF ILLUSTRATIONS (Continued)

LIST OF ILLUSTRATIONS (Continued)

LIST OF ILLUSTRATIONS (Continued)

LIST OF ILLUSTRATIONS (Continued)

LIST OF ILLUSTRATIONS (Continued)

LIST OF TABLES

LIST OF TABLES (Continued)

LIST OF TABLES (Continued)

LIST OF TABLES (Continued)

LIST OF TABLES (Continued)

LIST OF TABLES (Continued)

LIST OF TABLES (Continued)

LIST OF SYMBOLS

a, b, c, d	exponents
e	exponential = 2.718282
f_v	varying stress in KSI
f_E	varying stress at the endurance limit in KSI
f_{max}	maximum stress in KSI
f_{min}	minimum stress in KSI
f_{mean}, f_m	mean stress in KSI
$f_{v_{peak}}$	peak or largest varying stress
f_{red}	reduced or equivalent constant stress which gives the same damage ratio as a spectrum of varying stresses above the endurance limit
g	load factor
h	parameter
k	proportionality factor
m	number of cracks
n	number of load cycles applied at a varying load of specific amplitude
p	α^u
r	coefficient of crack propagation
u	$\frac{1}{\beta}$
u_i	number of load cycles applied before crack initiation
w	internal work absorbed by a material at a varying load of specific amplitude
x	log N
x_i	number of load cycles applied between initiation of fatigue crack and the final failure of a specimen at a varying load of specific amplitude
y	log $(S_v - S_E)$
y_o	log p

ψ	per cent of the number of cycles to failure that is used up in initiating cracks at a varying load of specific amplitude
A	area
D	damage ratio
$F_{varying}$	allowable varying stress in KSI
F_{mean}	allowable mean stress in KSI
F_{tu}	tensile ultimate strength in KSI
G-A-G	ground-air-ground
H, H_T, $\sum n$	total number of load cycles applied at or above a varying stress of specific amplitude
H_o	value of H at S_v equal zero
H_s	total number of load cycles in one application of a unit loading spectrum
K	damage boundary or K_T of standardized S-N curves
K_T	theoretical elastic stress concentration factor
$\frac{M}{h}$	force due to bending moment in lbs.
$\frac{Mc}{I}$	stress due to bending moment in KSI
N	number of cycles to failure when a varying load of constant amplitude is applied to a specimen
N_L	fatigue life in terms of the total number of load cycles that are applied at varying loads of two or more amplitudes prior to failure
N'	number of cycles to failure when only the highest load in a unit loading spectrum is applied to a specimen
N"	number of cycles to failure at a varying load of constant amplitude for a "fictitious" S-N curve
P	force or load in lbs.
R	ratio of the coefficient of the rate of crack propagation at a lower varying load to that at the highest varying load in a unit loading spectrum

S_v	relative or nondimensional varying stress $= \frac{f_{max} - f_{mean}}{F_{tu}} = \frac{f_v}{F_{tu}}$
S_E	relative or nondimensional varying stress at the endurance limit $= \frac{f_E}{F_{tu}}$
S_E'	relative varying stress at the endurance limit after fatigue damage is produced by the application of varying loads above the endurance limit
S_R	relative or nondimensional reduced varying stress $= \frac{f_{red}}{F_{tu}}$
S_{max}	relative or nondimensional maximum stress $= \frac{f_{max}}{F_{tu}}$
S_{mean}	relative or nondimensional mean stress $= \frac{f_{mean}}{F_{tu}}$
W	maximum amount of internal work that is absorbed by a material before failure
W.S.	wing station
α, and γ	S-N parameters
β, δ, and ψ	exponents
Γ	gamma function
σ	standard deviation and multiplicative standard deviation
ω	stress interaction factor having a value that always exceeds unity
$\sqrt[i]{N_{L_1} \cdot N_{L_2} \cdot \cdot \cdot N_{L_i}}$	geometric mean of N_L

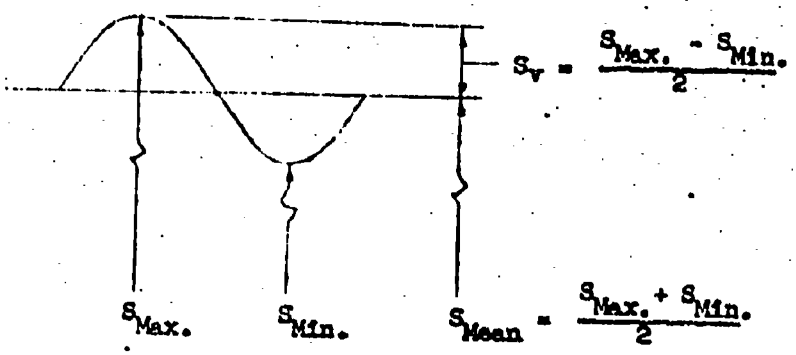

Definition of Maximum, Minimum, Mean and Varying Relative Stresses.

SECTION I

INTRODUCTION AND BACKGROUND

The problem of the fatigue of airframe structures is of vital importance not only to the operators of both military and commercial aircraft but also to the designers. The importance of fatigue of the airframe has been well recognized by the military and industry for many years. However, the complexities involved have successfully defied satisfactory solution in spite of the massive effort, time, and expense which have been invested in fatigue research in past years. In addition to the operational problems on current aircraft, future trends to high performance VTOL/STOL and spacecraft, with their acutely more critical weight problems, foretells even greater urgency of reaching a practical solution of the "fatigue problem."

A satisfactory analytical solution for the problem of fatigue life prediction has eluded the intense efforts of some of the best scientists, engineers and research specialists for the past 130 years. This is so because of the immense number of variables involved, the statistical qualities of nature, and the inherent limitations of the analytical achievements in detail stress analysis, impressive as these are. Progress is being made in the area of the statistical definition of the external loading environment, and in the area of the definition of the material resistance to fatigue cracking under complex loading environments.

There is, however, a most important middle area between these two which is the crux of the whole problem of fatigue life prediction. This area is that concerned with the definition of a "fatigue quality" as a property of complex, composite structure. The analytical assessment of this key property of a complex structure is fraught with the most formidable of difficulties. The purely analytical approach offers no immediate fruitfulness. This is not to imply neglect of this area, rather, that the solution must be pursued with vigor; but the primary approach must be experimental. Some of the reasons for this statement are as follows:

a. Joint friction and its attendant nonlinear slippage characteristics is highly unpredictable and nonrepeatable.

b. Local plastic yielding at points of high stress concentrations with resulting residual stresses, and, for some materials, the changing work hardening properties, is too complex a process to expect analytical solutions to follow clearly the path through intricate service histories.

c. Fretting and fretting corrosion can create unpredictable stress concentrations which often compound with normal design concentrations.

d. Repairs, reconstruction, and accidental damage place unforeseen and unpredictable fatigue-critical areas in the structure.

e. The micro-detailed geometrical stress analysis required at the multitudinous points in a complex structure is as yet beyond the capabilities of the modern analyst.

Manuscript released by the authors 21 August, 1961 for publication as an ASD Technical Report

Time and complexity preclude reliance on purely analytical solutions which would realistically encompass these variables.

An important distinction must be made between various stages of the external loads and stress analysis of a complex structure and a theory of fatigue damage. It is a process of definitive stress analysis that is required to define the complex stress history at a critical point in the structure. It is a process of fatigue damage that defines the formation of a crack in a critical point in the structure as a function of the definitive stress history.

Even if a perfect fatigue damage theory were available the fatigue life prediction problem would not be solved until the stress analysis problem is also solved.

However, the problem of fatigue life prediction is amenable to solution in spite of all the difficulties cited. This solution makes use of analytical formulations where feasible, and supported by the proper kind of laboratory fatigue testing and field service comparisons, a reasonably good job may be accomplished, consistent with the uncertainties which will always be inherent in the definition of the external basic loads.

It must be recognised from the outset that the development of fatigue cracks in metal is a statistically random process. The loads and stresses in the airframes of individual aircraft are subject to extremely wide variations. Many of the operating variables are beyond direct control. The integrated influence of all these variables yields a large scatter of results. Thus it cannot be expected to precisely predict the fatigue life of a single article. Life insurance companies with the best facilities and statisticians do not yet attempt to predict the life span of a single individual however well their prediction holds for a large-enough population.

A considerable background of successful service history on other aircraft models can provide a basis for significant comparisons. When coupled with this foundation of service history, and with judicious testing of critical areas of the structure, it is possible to develop a system which has good potential of achieving fatigue quality control as well as reasonable predictability of fatigue life.

OBJECTIVES

The objectives of this research study are as follows:

1. To review, compare and evaluate proposed methods of fatigue life prediction suitable for application to the special problems of airframe structure.

2. To provide experimental fatigue life data of constant load amplitude S-N type for use in evaluating selected prediction methods.

3. To provide experimental fatigue life data under complex loading spectra representative of realistic airframe loading history on both coupon-type specimens and on specimens of a complex joint representative of contemporary airframe construction.

4. From an analysis of the new experimental data to verify the adequacy or provide a possible improvement in the selected fatigue life prediction method.

PLAN OF THE STUDY

This research program was organized into three basic phases to meet the stated objectives:

Phase I.

A study of proposed methods for the prediction of fatigue life was made and those suitable for application to the problems of airframe fatigue were selected for evaluation using available published data. This portion is discussed in Sections I through III and Appendices A, B, and C.

Phase II.

Experimental fatigue data were generated to provide additional verification or a basis for the improvement of selected methods of fatigue life prediction under loadings more realistic of airframe environment than was previously available. These data are described in Appendix D.

Phase III.

Analyses were made of the experimental results of Phase II using the selected methods from Sections II and III. A summary of the results and conclusions drawn is presented in Section VI.

SECTION II

METHODS OF ANALYSIS

Fatigue analysis follows the same general pattern as developed in static strength analysis. These subjects may be classified into three broad fields.

1. External loads
2. Internal loads
3. Allowable loads

The differences in fatigue analysis compared with conventional static strength analysis are associated primarily with the specification of the multitudes of external loadings, with the detail requirements, or precision demanded of internal load (or stress) distributions, and with the form or specification of the allowable loads. Another major difference is the convention of expressing the results of static strength analysis as a comparison of internal loads (stresses) with allowable loads (stresses) to show a "Margin of Safety." Inherent in this "Margin of Safety" is the concept of a "Factor of Safety." Fatigue analyses for this discussion will not contain this concept of "Margins of Safety" nor "Factors of Safety," but will be limited to the direct prediction of a "fatigue life." That the predicted lifetime in whatever units measured (hours, cycles, missions, or any other) is "safe" or not is, of course, dependent not only upon the precision of all input data, precision of operations performed, but also on many other factors, some not even a part of the fatigue process.

1. Such factors as "fail safe" may change completely the complexion of a "Margin of Safety" in fatigue.
2. Periodic and special inspections, maintenance, and repair can have the quality of extending the "life" of an airframe to an indefinite period, probably determined by economic or performance obsolescence rather than fatigue.

The subject of factors or margins of safety will be discussed in a later section of the report (see Section III).

A method of analysis is a formal procedure to attain the solution of a problem. The method chosen will depend heavily on two facets:

1. The problem to be solved, and
2. The data available on which to base the solution.

To illustrate, one of the oldest and simplest fatigue problems to be solved is that of the plain rotating shaft in bending. Assuming the external loading to be known, measured, or limited, the internal stresses may be simply computed by the engineering beam theory. The remaining question is the determination of

the allowable stresses for the lifetime desired or to predict the life of a given design. An impressive amount of experimental S-N data is available for most materials under this type of loading. This is highly important in the solution of this problem, which may be considered solved, provided:

A. External loads are

   1. Constant, known, or
   2. Measured, or
   3. Limited.

B. Internal loads (stresses) are

   1. Predictable or
   2. Measurable.

C. Allowable loads (stresses) are

   1. Known or
   2. Determinable for

      a. Material chosen,
      b. Processing variables,
      c. Environment,
      d. Rate of loading,
      e. Laboratory simulation compatible with service conditions, etc.

The effects of more than one load level on fatigue life were minimized in most industrial problems of this type by restricting the loads produced in service to levels below an endurance limit, or the maximum repeated load for an indefinite life on the S-N curve. This is still the practice for certain propeller and other rotating machinery for aircraft use.

The internal loads or stresses in the simple example were assumed predictable or measurable. The simple shaft, without notches, is both an easily predictable and an easily tested article. Years of laboratory experience have envolved specimen designs which achieve consistent fatigue failure in almost straight shafts unaffected by grips and loading fixtures. The experimentally determined allowable stresses are thus compatible with the actual part under its expected loading. This point is of primary importance to the precision and success of the solution to the assigned problem.

Suppose the shaft had a notch. The solution of the problem may now take one of two divergent paths.

<u>Path 1</u>. The influence of the notch may be computed in the second stage of the solution dealing with the prediction of internal loads or stresses. Geometrical analyses of stress concentration factors, supported by experimental measurements, photoelastic optical methods, and others, constitute a large body of data to accomplish this step. (References 1, 2 & 3)

Successfully accomplished, the predicted maximum repeated stress to be applied may be compared with the allowable S-N data of virgin unnotched material to predict a fatigue life or to design to a specific life.

However, attempts to follow Path 1 have run into difficulties. The theoretical elastic or photoelastically determined stress concentration factor is, in the actual part, profoundly affected by yielding, residual stresses, work hardening, and other effects so that the net fatigue effect is not directly predictable. This is well illustrated in Figure 1 taken from reference 4, which indicates the fatigue effective concentration factor compared with the geometrical stress concentration factor at several different fatigue lives. Some recent work at the NACA has provided empirical plasticity corrections which work well in certain steels (non-work hardenable), but these corrections are as yet unsuccessful in aluminum alloy (work hardenable). (Reference 3)

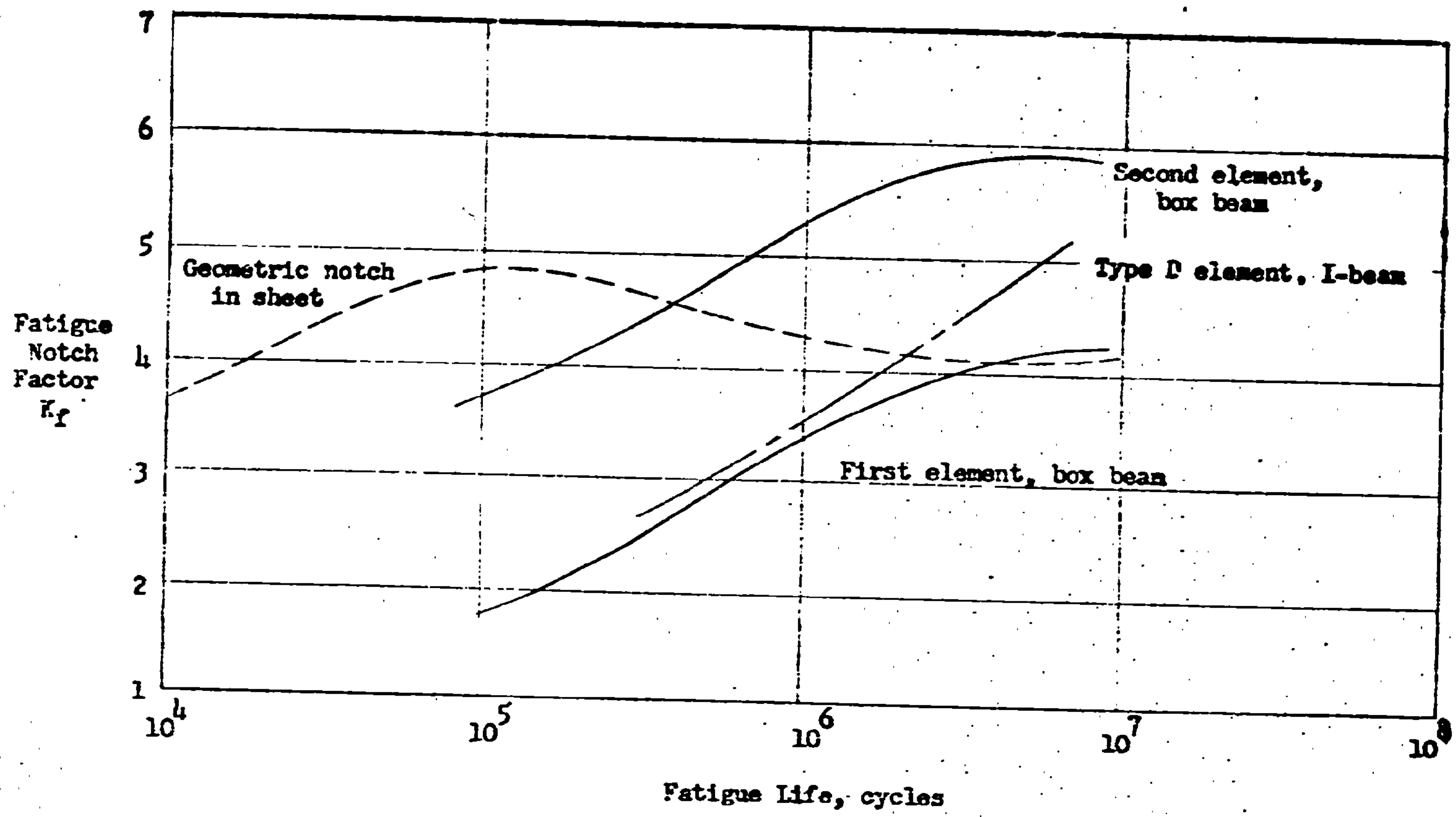

Figure 1 Fatigue notch factors for simulation elements. (Ref. No. 4)

Path 2. The internal loads or stresses may be computed as if the notch were not there (gross area basis) or at the root of the notch (net area basis) without any influence of stress concentration.

The stress concentration influence of the notch is assigned to the third stage of the solution dealing with the allowable stress determination. The actual notch or a graded series of notches is fatigue tested and S-N or allowable data are plotted for the specific part. (Stresses must, of course, be consistent with the internal stresses of step 2.) The fatigue effectiveness of the notch is in this manner determined experimentally.

Following Path 2 is seen to be fundamentally an improvement over the method or procedure of Path 1 in that some of the previous difficulties unaccountable by analysis are now experimentally determined and the precision of prediction of the fatigue life of the notched part is improved. However, experimental data for the actual configuration must be made available for the achievement of this improvement. Lack of these data may force an estimate by the best means available (Path 1), but imprecision is then inevitable.

The type of experimental data required to assess the fatigue problem varies at different stages of a design. Broadly categorized, these may be scaled in complexity by the following list:

1. Material and Processing Data are needed in the earlier preliminary design stages. These are usually S-N type or simple spectrum-type fatigue tests to provide comparative data for decisions among possible design choices.

2. Development Tests are designed to assure achievement of a satisfactory fatigue quality at critical joints or discontinuities.

3. Full-Scale Component or Airframe Fatigue Test may be planned if the fleet size warrants the time and cost.

4. Fleet Service History is a factor of importance. The structure designed by the best means available must be observed in service. The integrated influence of many factors may reduce fatigue life below the best engineering and laboratory estimates. Some of these factors are:

    a. Service loading variations, changing operational demands,
    b. Installation stresses, misalignments,
    c. Workmanship, nicks, scratches not duplicated in laboratory test specimens,
    d. Material alloy, heat treat, batch variations,
    e. Environmental conditions, corrosive atmosphere,
    f. And many others.

The factors that bring about fatigue life reductions must be ferreted out and field service experience obtained to provide a feed-back loop to improve the life predictions. Engineering estimates of fatigue life conditioned by fleet-wide field service experience are another stage of improvement beyond that provided by calculations and laboratory experiments. Laboratory testing and analysis of parts which have a known service failure history provide a required overall check of the laboratory-analysis life-prediction system.

Within this context of an overall system approach for the deliberate scheduling of improvements in airframe fatigue life predictions, depending on the data available at various stages of a design, specific facets of the airframe life prediction problem will be examined in more detail.

EXTERNAL LOADING DATA

The aircraft exists and operates in a complex physical environment. The list of service loading is extensive. It includes:

1. Gust loadings

    1.1 In clear air
    1.2 In storms

2. Maneuver loadings

    2.1 Transport

        2.1.1 Routine route maneuvers
        2.1.2 Training maneuvers

    2.2 Military aircraft

        2.2.1 Operational maneuvers
        2.2.2 Training maneuvers

3. Landing impacts

4. Taxiing and ground handling

5. Ground-air cycle

6. Buffeting

    6.1 Stall
    6.2 Supersonic shock wave instability

7. Acoustical noise

    7.1 Propeller tip or jet noise
    7.2 Aerodynamic noise (boundary layer)

The contribution of some of these types of loading to fatigue damage has been debated for many years. Other concurrent research programs are investigating experimentally some important facets of these loadings. (See reference 5) Preliminary results indicate that the fatigue influence of some of these items may be unimportant while others are of considerable importance. It is too early to determine a clear cut simplification.

A detailed investigation of the generation of external applied loading data and its influence on the fatigue life prediction process is considered beyond the scope of this study. It will be assumed that complete external applied loading spectra for all the critical loading conditions can be developed for a mission phase synthesis utilizing basic environmental statistics currently available for each type of loading. However, a brief review of the general characteristics of several pertinent types of loading is given to describe the complex form of these external applied loads and to demonstrate the versatility required of a practical fatigue life prediction method necessary to handle this complexity.

1. Gust Loading

a. The gust loading record is characterized by a varying load factor or stress component oscillating about a substantially constant mean load level. At different positions in the structure and in different types of aircraft the mean load level can cover a wide range of values. This is significant for fatigue life predictions.

b. The natural sequence of varying gust loading magnitudes is substantially random. However, examination of sufficient length of record shows an eventual symmetry of positive loads and negative loads. Past practice has been to regroup positive half cycles with equal negative half cycles and re-order the sequence of occurrence into a graduated spectra of frequency of occurrence or probability of exceedance. This process is illustrated in Figure 2. It can be seen that a number of basic assumptions are involved in tampering with the original load record to convert it into the ordered spectrum. The fatigue significance of the order of load application has been well demonstrated. (Reference 16) Physical considerations of the process of crack propagation confirm the importance of order of loading. This information is not reported in the current service load data reduction methods. Some experimental evidence of the fatigue life significance of this property of ordered vs. random loading is being generated in a concurrent research project reported in reference 5.

2. Maneuver Loading

a. Bomber, Transport, and Cargo-Type Aircraft

Maneuver loadings of large bomber, transport, and cargo-type aircraft are characterized by near symmetry of incremental or varying load component about the constant flight mean load level. For records of sufficient duration the loads are substantially random in sequence, and, in general, the above comments regarding gust loadings are applicable to maneuver loadings for this class of aircraft.

b. Military Fighter-Trainer Aircraft

The maneuver load record for high load factor military fighter-trainer type aircraft has a considerable bias in the positive direction, reflecting the pilot's inherent avoidance of uncomfortable negative accelerations of any appreciable magnitude. The resulting load record has a substantially constant minimum load at the steady static 1g level. The positive acceleration increments rise from this level to a maximum load increment and return to the steady static 1g level with only minor excursions in the negative range. This is characterized by a varying mean load for each load cycle as contrasted with gust loads which occur with a substantially constant mean load level. The character

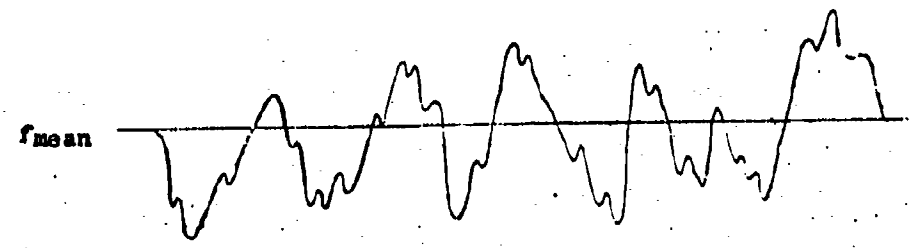

Random Sequence of Flight Loads

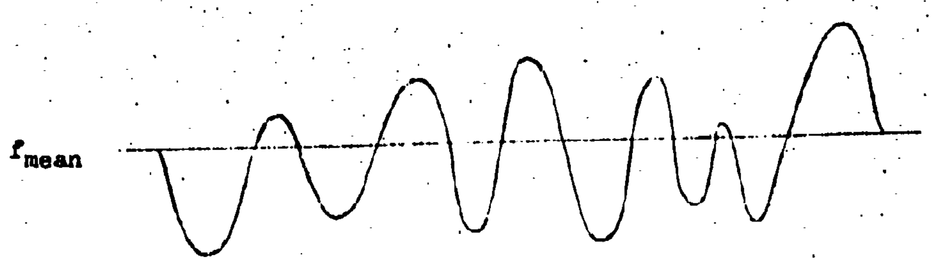

Random Grouping of Faired Flight Loads

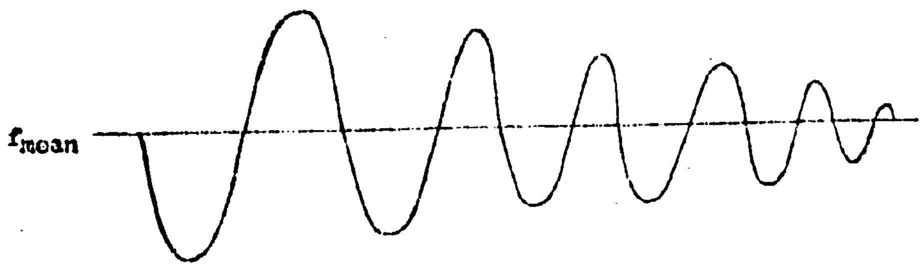

Ordered Grouping of Faired Flight Loads

Figure 2 Development of Gust Loading Spectra

of this type of loading is illustrated in Figure 3 . Incremental load levels may approach random sequence over a long-enough time period. As discussed above, the sequence information is lost in current data reduction techniques. This fact produces a significant difference in handling the fatigue life predictions, which will be discussed in more detail in later sections.

3. Landing Impacts

Landing loads are applied to the airframe while it is in the flight steady mean load condition. The varying loads are a complex function of the dynamic response of the structure and are affected by the usually nonlinear characteristics of the tire-shock strut combination. The sequence of load application is not accounted for in the usual analysis.

4. Taxi and Ground Handling

These conditions create varying loads of a generally random sequence oscillating about a ground-supported mean load level. Depending on the aircraft configuration, the mean load level for these conditions can become compressive for fatigue critical structures which are normally loaded in tension in the flight conditions. This condition can be aggravated by configurations which carry large external stores and/or tip tanks. Thus the range of the mean load can be quite large for each flight.

5. Ground-Air-Ground Cycle

The change in load distribution from ground borne to air borne during the take-off run and the transition from air borne to ground borne during the landing run is a loading cycle that takes place once each flight. There is general agreement that this cycle is an important contributor to fatigue damage. However, there is no general agreement on the specific definition of the effective amplitude of this loading. One definition could be the cycle of loading from the maximum negative (ground load) to the maximum positive (flight load) occurring in each flight. This overall load cycle per flight is not yet precisely defined; it may become a spectrum of load amplitudes over the life duration of a fleet. Another definition, popular in many quarters though not universally accepted, is the transition cycle from the ground-borne static mean load level to the air-borne static mean load, and return on each flight. Various other definitions have been proposed such as the RMS value of negative ground level loads to the RMS value of positive flight level loads and return for each flight.

Whatever the load level definition, the ground-air-ground cycle is generally broken down into its own substantially constant varying load component acting once per flight about its own mean load level.

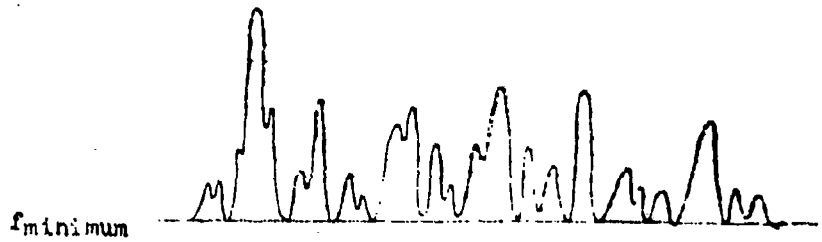

Random Sequence of Flight Loads

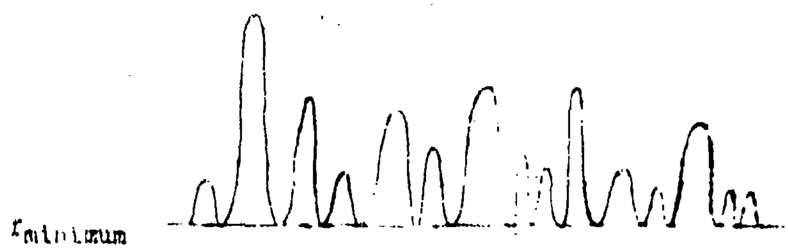

Random Grouping of Faired Flight Loads

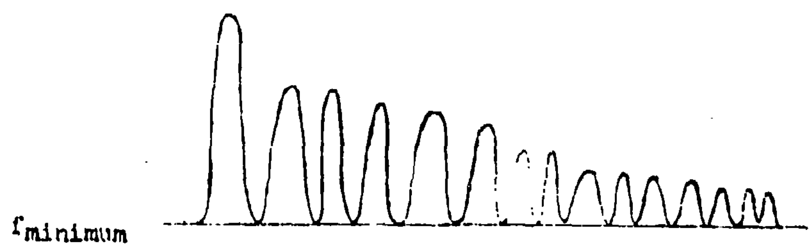

Ordered Grouping of Faired Flight Loads

Figure 3 Development of Maneuver Loading Spectra

6. Buffeting

Buffeting from stall or supersonic shock wave instability is a phenomenon to be avoided wherever possible. When fatigue accounting is necessary, these loads are generally considered random in sequence and act symmetrically about a specific mean or steady load condition. The comments on gust loads are therefore also applicable for buffet loadings.

7. Acoustic Noise

Although an important source of fatigue damage for some areas of structure in certain configurations, this specialized problem is not within the scope of this study.

8. Composite of Mission Loads

The total load history at a point on the airframe structure during one flight mission may be made up of each of the major types discussed above. These may be schematically illustrated as in Figure 4.

Pre-take-off ground handling and take-off run.	-	Taxi load spectrum at a negative mean load (compression).
Ground-air	-	Transition from ground- to air-borne state.
Turbulence	-	Random loads varying about a positive mean load (tension).
Fighter Maneuver	-	Varying increments to a maximum above the static level flight mean load.
Landing impact	-	Nonrandom varying loads about a level flight mean load.
Air-ground	-	Transition from flight- to ground-borne state.
Landing run, taxi, and ground handling	-	Same as take-off and pre-take-off ground handling.

Each of the several types of loadings may appear in each flight.

9. Summary

This discussion of the loads to which airframe structures are subjected during their lifetime is primarily to demonstrate the type of input data which the method of analysis for fatigue life prediction must be capable of handling in order to solve the problem posed. Some methods proposed for fatigue life prediction, while elegant and useful in certain

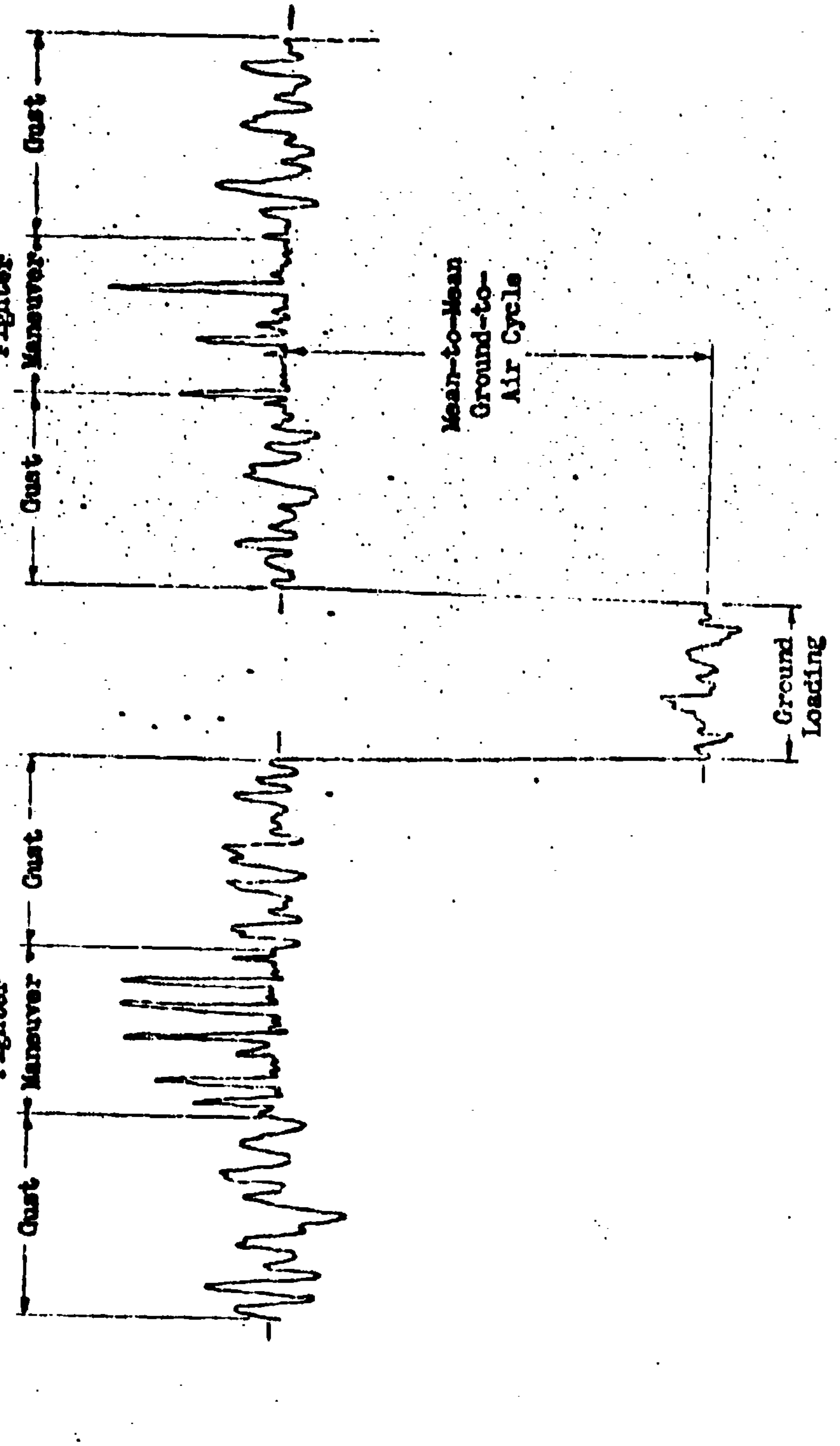

Figure 4 Schematic of Composite Loading Spectrum

fields, are limited in capability to handling only simple definitions of loads. These limited methods cannot be successful in the solution of the problem at hand.

INTERNAL LOAD DISTRIBUTION

Structural designs which achieve the highest efficiency place the greatest amount of material into pure tension or compression, reducing bending stresses from local discontinuities to the least possible. Great pains are taken to achieve this desirable goal. The process of design and analysis goes through several circuits of ever increasing precision, each stage successively miniaturizing the structural element under consideration.

Design Stage	Method of Analysis	Structural Size
1. Preliminary design	$P = \frac{M}{h}$, $f = \frac{P}{A}$	Yards
2. Project design	$f = \pm \frac{Mc}{I} + \frac{P}{A}$	Feet
3. Final design	Redundant analysis	Inches
4. Proof of design	Experimental	Millimeters to microns
5. Research	Experimental	Millimeters to microns.

The precision of internal loads and stress distributions computed at various stages of the design is essentially consistent with the precision of the data available at that stage of design. However, it is well known that both the number of cycles to crack initiation and the additional cycles for growth to a critical crack size are extremely sensitive to small variations in the stress level existing at the critical points.

The desired precision of life prediction resolves into a required precision of stress prediction that is simply not attainable with the currently available analytical tools. This critical statement is not an indictment of the present state of the art of stress analysis for this is indeed impressive. Rather, it must be considered a recognition of critical factors which the current analysis techniques cannot handle and were never intended to handle. As discussed in the introduction, some of these factors are:

1. Joint friction with unpredictable, nonrepeatable, nonlinear slippage characteristics.

2. Local plastic yielding at points of high stress concentration with the resulting ever-changing residual stresses, and work hardening properties.

3. Fretting and fretting corrosion resulting from joint slippage under repeated loads.

4. The complexity of practical structures most generally results in shapes not readily amenable to the analytical approach.

Consideration of the formidable difficulties involved in this brief list indicates that the purely analytical approach cannot in the immediate future offer any hope of adequate solution. Therefore the only practical approach is to refer this problem to the experimental laboratory for solution. This is Path 2 of the analysis methods discussed in the introduction. However, for timely success in this approach a number of conditions must be considered.

1. There must be a specimen design to test. The designer is called upon to make decisions without benefit of final test knowledge. The best tools available and the data on hand at decision time are used to make the best possible estimates. These estimates can only be considered crude at best. The stress concentration factor procedure finds its greatest usefulness at this stage. As explained in the sample problem in the introduction, by judicious use of a large body of stress concentration literature (for example, reference 1) and with the full realization of the limitations on fatigue effectiveness of these predictions, design comparisons and choices can be made, subject to later confirmation and refinement.

2. The fatigue test specimen must be complete. The test specimen must be a large-enough sample of the structure to encompass local redistributions of load due to yielding, joint slippage; it must contain an exact representation of all critical local eccentricities and a reasonable representation of local supporting structure. It must have all secondary attachments which would in any way affect the fatigue life of the primary element; for example, attachment holes for hose clamps, tubing, electrical wiring bundles, drain holes, and holes for secondary support brackets may be fatigue critical but are too easily overlooked. All processing operations, cleaning, coating, etching, sealing, etc., which the airframe parts undergo during manufacture should also be included in the build-up of the fatigue test specimen.

3. Nominal structure adjacent to joint. The loads introduced into a complex joint or material discontinuity are generally controlled by the stress state of the average material in the structure surrounding the joint. It is also often considered good practice that joints and fatigue-critical discontinuities, and especially blind areas, should be as good as or better than adjacent structure with a nominal hole. To most directly demonstrate achievement of this quality level and to aid in the definition and monitoring of the test load spectra, the test specimen should include such sections.

4. The full range of loads are necessary. There is considerable evidence accumulated from full-scale airframe fatigue tests (references 20 and 21 and others) and from laboratory attempts to duplicate service failures, that the location of fatigue failures in complex structure is dependent on the applied load levels. Constant load amplitude S-N type tests on multiple specimens must therefore cover the full range of the anticipated operational service loads. Spectrum-type tests offer the advantage of requiring fewer specimens to cover the full range of operational loads. However, the test variables of unit spectrum block size, stress interval, order of load application, etc., exert some influence on the test results. The influence of these test variables must be minimized by judicious choices. (Reference 5)

The internal loads from the normal static stress analysis are generally considered adequate to define the test spectra for development tests of the joint or discontinuity. Strain gage surveys taken during component or full-scale static tests are an aid in either setting the fatigue test load level, or, if scheduled later, provide data for corroboration or corrective analyses to improve the precision of prediction when necessary.

The successful fatigue test of a fully detailed specimen of a critical area of the airframe structure under the full range of expected loads provides experimentally the micro-detailed analysis which includes most of the factors which current purely analytical approaches find insurmountable.

It is necessary, however, that allowable fatigue data for complex structure be provided by laboratory development tests of fully detailed specimen(s) of the critical areas of the structure, tested under the full range of loads representative of those expected in service. To define an S-N curve for a specific element of structure requires a minimum of six to nine specimens with sixteen or twenty desirable depending upon the statistical confidence level required. In the interests of economy, schedule, and the availability of large scale fatigue equipment, in addition to the technical reasons discussed above, it is advantageous to perform the development tests on fewer specimens with each to experience the full spectrum of loadings anticipated for operational service. This aspect is especially important in the consideration of a full scale airframe fatigue test in which the economic justification of a single test specimen is of paramount importance.

The interpretation of the results of these more complex specimen tests is not quite so simple as the interpretation of the allowable fatigue life (vs. Stress) of constant amplitude type loadings. However, a number of methods have been used such as the comparison of the test results with the results of tests of a (good quality) standard joint, or the Tangent Intercept Method, or the Fatigue Quality Index procedure. The latter two are described in detail in Appendix A.

One of the objectives of this study is to explore the possibilities and limitations in the use of spectrum type fatigue test results as a means for fatigue life prediction.

SUMMARY

A discussion of the complexities involved in the prediction of the fatigue life of airframe structure and the requirements of a practical method has emphasized these points.

1. External loadings are complex in range and sequence. A fatigue life prediction method must be versatile in scope to handle the many types of loadings likely to be critical.

2. The prediction of the fatigue life of complex structure requires a precision and reliability of local stress history under complex external loading which is not currently available by purely analytical means, nor likely to be available in the near future.

3. A satisfactory fatigue damage theory is not available for the analytical prediction of the allowable stress history of complicated structure under complex loadings.

4. The crux of the problem of fatigue life prediction is, therefore, a fatigue quality of complex structure which embodies the effects of the complex internal stress history and the allowable stress history for the formation of a critical crack, both of which are dependent on the range and sequence of applied loading.

5. Laboratory development tests of fully detailed specimens of fatigue critical structure are required to assess this fatigue quality of complex structure. Either spectrum type tests which cover the full range of loads anticipated for operational service, or constant amplitude S-N type tests may be used for this purpose.

6. For spectrum type tests, test variables such as loading block size, stress interval size, and loading sequence affect the laboratory results. These effects must be eliminated, reduced to insignificance, or accounted for by some empirical means.

7. Interpretation of operational service history by consistent laboratory testing and analysis means is required to provide a comparative base for any method of fatigue life prediction.

SECTION III

EVALUATION AND SELECTION OF FATIGUE LIFE PREDICTION METHODS

From a search of the literature a number of methods for the prediction of fatigue life proposed by various authors was selected for comparative study and evaluation. During this study, simplifications, modifications, and generalizations were developed to better adapt some of these methods to the problem of fatigue life prediction of aluminum airframe structure. For brevity and continuity of this section, these methods and their extensions are described in detail in Appendix A.

While all these methods (except one, the Tangent Intercept Method) were fundamentally the concept of the gradual accumulation of fatigue damage during the progress of loading, each author emphasized some particular aspect or formula for the representation of either or both the applied loading spectra or the allowable S-N data. These variations could be considered in three general categories. The methods studied in this phase of the project are classified in the three categories as listed below, with the Tangent Intercept method unclassified. In addition, those methods chosen for comparison by numerical evaluation with the selected test data are indicated by the asterisk.

Class I. Linear Cumulative Damage (based on specific S-N data for each specimen type).

* 1. Miner's Method (reference 6)

This is the well-known linear summation of the fractions of fatigue damage expressed as the cycle ratio $\left(\frac{n_i}{N_i}\right)$ where failure is hypothesized when the sum of all cycle ratios is one.

* 2. Lundberg's FFA Method (reference 7)

Lundberg and his associates at the Aeronautical Research Institute of Sweden (FFA) utilized mathematical formulas for representing the applied loading spectrum and the allowable S-N data and, based on Miner's linear cumulative damage hypothesis, obtained a closed form solution for the total damage, and, thus, for the corresponding predicted fatigue life. This method was evaluated in two parts, one utilizing equations for the applied load spectra and for the S-N curves with parameters determined by an average best fit for the full stress range, while the second application, in an attempt to improve the precision of prediction, restricted the best fit to the mid-range of stress levels in the region of highest cycle ratios.

* 3. Shanley's "1X" Method (references 8, 9 and 10)

Based on a concept of rate of formation of slip bands, Shanley's "1X" method derives an equation for the fatigue damage which results in the linear cumulative damage expression of Miner, utilizing a mathematical formula for the S-N curve.

4. Langer's Method (reference 11)

Langer separated the fatigue process into two parts - first, the initiation of cracks, and second the growth of the cracks, and, based on linear accumulation of cycle ratios, derived a prediction of fatigue life.

5. Grover's Method (reference 12)

Grover's method is essentially the same as Langer's method. Both of these methods require experimental S-N data which separate the crack initiation stage from the crack growth stage. These data were not available for this evaluation.

6. Smith's Residual Stress Method (reference 13)

Using Miner's linear cumulative damage, Smith proposes inclusion of the residual stresses from plastic yielding at higher load levels with the stresses from external loads. This very elegant method of stress analysis is not practical for the complexity of loading history met in service, and could not be evaluated in this study.

Class II. Nonlinear Cumulative Damage (based on specific S-N data for each specimen type.)

7. Henry's Method (reference 14)

Henry developed a procedure for reducing the allowable S-N curve in a step-by-step procedure to account for damage of prior loadings. By ingenious means of cycle ratio corrections, the reductions are achieved by reference to only the original S-N curve. The result is a nonlinear accumulation of damage. Knowledge of the order of load application is necessary for the use of this method. In its original form the mathematical representation of the S-N data could be applied only to a limited class of materials.

* 8. Generalization of Henry's Method

Henry's original development is extended in this report to accept a more general representation of the S-N data. This development is discussed in detail in Appendix "A".

9. <u>Corten and Dolan's Method</u> (reference 15)

Corten and Dolan based their method on a concept of relating fatigue damage to the number of cracks formed as a function of the largest varying load in the sequence, with the growth of such cracks to occur at all load levels of the sequence. The result is a form of nonlinear cumulative damage in terms of stress ratios of the various loads in the spectrum, and, as such, contributes damage from the low stresses below the endurance limit. This point is discussed in detail in Appendix A.

* 10. <u>Modified Corten and Dolan Method</u>

The Corten and Dolan method is modified to convert the basic formula to a cycle ratio basis, which assumes no contribution from loadings below the endurance limit. The nonlinearity coefficient, evaluated by the available test data in Appendix B, indicates the results to be so closely equivalent to the Linear Cumulative Damage Method that further evaluation was discontinued.

* 11. <u>A Simplified Nonlinear Cumulative Damage Method</u>

A simplified form of a nonlinear cumulative damage method is developed from the results of this survey by introducing an empirical exponent into the equation representing the damage ratio summation. This nonlinearity coefficient, evaluated from the available test data in Appendix B, indicates the results to be so closely equivalent to the Linear Cumulative Damage Method that further evaluation was discontinued.

* 12. <u>Shanley's "2X" Method</u> (reference 8)

Based on essentially the same reasoning as was used to develop his linear "1X" method, Shanley assumed one of the coefficients in the rate equation to be stress dependent. This increased strongly the rate of crack growth and resulted in a nonlinear form of the cumulative damage summation.

<u>Class III.</u> <u>Cumulative Damage (Linear or Nonlinear) from Damage Boundaries or Modified S-N Curves</u>

13. <u>Kommers' Nonlinear Damage Hypothesis</u> (reference 22)

Kommers pointed out the essential nonlinearity of the damage boundaries determined experimentally from two-step load tests of steel coupons. The damage boundaries were found to be functions of both the load levels and the cycle ratios in each load level.

14. <u>Richart and Newmark's Method</u> (reference 24)

Richart and Newmark devised a formal procedure with additional experimental verification for utilizing Kommers' nonlinear

damage hypothesis to create damage boundaries which vary with both stress level and the cycle ratio.

15. Marco and Starkey's Method (reference 25)

A method of defining damage boundaries by use of a power relation of the cycle ratio was developed by Marco and Starkey. The exponent was made stress or load dependent, which resulted in essentially a mathematical formulation of the damage boundaries for use in the procedure described previously by Richart and Newmark, and suggested by Kommers' earlier work.

16. Freudenthal and Heller's Method (reference 26)

Freudenthal and Heller have developed a procedure to construct a "fictitious" S-N curve by the use of a stress interaction factor, which is derived from a statistical analysis of a large number of samples tested under a number of spectra of loading. Lack of both the type and quantity of the necessary data precludes its practical application.

17. Levy's Method (reference 27)

Levy suggested a fatigue life prediction procedure based on deriving, from test data, empirical constants as exponents for each cycle ratio of a step spectrum, with one additional constant coefficient required for the life prediction equation. This method requires (q + 1) sets of test data and the solution of as many simultaneous equations where q is the number of steps of the loading spectrum. Data were not available in a form required to evaluate this method.

* 18. Stress Concentration Method

The stress concentration method in practice is a procedure of refined stress analysis to define the ratio of peak stress in a discontinuity of structure to the nominal stress in a region remote from the disturbance. It must be coupled with a damage theory to complete a life prediction method. The linear cumulative damage hypothesis is taken for that purpose in this study. The stress concentration factor derived analytically may be used in either of two ways:

A. When used to specifically define the peak stress, the allowable stress (or cycles) may be determined from an appropriate S-N curve for the virgin unnotched material.

B. The stress concentration factor may be used to select an appropriate S-N curve from a graded set of notched specimens of the material. This S-N curve may be arbitrarily considered as the damage boundary for the design for which no specific test data exist.

Once the peak stress history is defined (as in A.) or the equivalent notch concentration factor specified (as in B.) any of the fatigue life prediction methods could, in principle, be used.

* 19. Fatigue Quality Index Method

A fatigue test of a completely detailed specimen is conducted under the full spectrum of loads expected on the structure in service. The results of the spectrum test are analyzed with a set of standardized S-N data fixed for the purpose of providing a scale of measurement of fatigue quality. That stress concentration factor is determined which, by interpolation, makes the linear cumulative damage equation exactly unity under the application of the full test history. This concentration factor, defined as the Fatigue Quality Index for the tested specimen, is compared with an acceptance standard.

As a fatigue life prediction method, the establishment of the Fatigue Quality Index provides an arbitrary damage boundary based on a fatigue test of the specimen under its own anticipated load spectrum. By the linear cumulative damage procedure, fatigue life predictions are made from this damage boundary for the structure under other similar loading spectra.

Unclassified

* 20. Tangent Intercept Method (reference 28)

Originally developed as a method of interpretation of simple spectrum test results to derive a fatigue quality acceptance standard, the Tangent Intercept procedure has been proposed as a fatigue life prediction method. (reference 31)

Essentially a graphical procedure, the spectrum test result in cumulative cycles is plotted in an appropriate field of S-N curves. The interpolated K_T value of the S-N curve which is tangent to the total test spectrum becomes the Tangent Intercept Quality Index of the specimen.

As a fatigue life prediction method, an S-N curve of the specimen is provided by constant amplitude tests. The fatigue life under a spectrum of loads is defined by the multiple of the unit spectrum which becomes just tangent to the S-N curve.

EVALUATION OF METHODS OF PREDICTION

For use in evaluating numerically the various methods of fatigue life prediction which were chosen, an extensive search of the available published data turned up seventy-eight sets of tests conducted on approximately 266 specimens suitable for application to most of the proposed methods. These are all spectrum-type experiments in which spectrum shapes, unit spectrum block size, stress intervals, sequence of loadings, etc., cover a wide range of variations. Included also are pertinent spectrum test results from the Australian P-51 and the NACA C-46 wing full scale fatigue tests. Detailed descriptions of these test data are given in Appendix "C".

The evaluation was conducted in two forms, depending on the scale on which the comparisons are measured.

1. Comparisons of Life Cycles

   Each of the methods chosen for evaluation was required to predict the fatigue life of the test specimen from the unit applied loading spectrum, using whichever form of the allowable data that was specifically applicable to the method.

   The details of this numerical work pertinent to each method are given in Appendix "B".

   The results of the life predictions of each group of specimens are plotted in Figure 5 for sixty-five groups of gust-type spectrum results, and in Figure 6 for thirteen groups of maneuver-type spectrum results. The code identification of the various methods is given in Table 1. The experimental results are also plotted for direct comparison, indicating the geometrical mean of the group, and a vertical bar showing the band spread between the minimum and maximum experimental values of the group.

   Another comparison of the prediction with the actual test result is made by the ratio:

$$\text{Degree of conservatism} = \frac{N_{L(\text{Test})}}{N_{L(\text{Predicted})}}$$

If $\dfrac{N_{L(\text{Test})}}{N_{L(\text{Predicted})}} < 1.00$, the prediction is unconservative.

If $\dfrac{N_{L(\text{Test})}}{N_{L(\text{Predicted})}} \geq 1.00$, the prediction is conservative.

TABLE 1

LIST OF CODING USED IN FIGURES

Symbol	Meaning	
◆	Geometric Mean of Test Data	
I	Scatter Band for Test Data	
○	Miner's	
♡	FFA	Loading Spectrum and S-N Equations Best Fit in the Midstress Range.
◇	FFA	Loading Spectrum and S-N Equations Best Fit in the Full Stress Range.
△	Shanley "1X"	
▽	Shanley "2X"	
⌂	Modified Henry	S-N Equation Best Fit in the Midstress Range.
♡	Modified Henry	S-N Equation Best Fit in the Full Stress Range.
◠	Tangent Intercept	
⬡	Quality Index-Based on Standardized S-N Data of Figs. 58 to 62.	
⬯	Stress Concentration Factor-Based on Standardized S-N Data of Figs. 58 to 62.	

Loading Sequence in the Unit Spectrum Block

L-H	Low to High Loading Sequence
H-L	High to Low Loading Sequence
L-H-L	Low to High to Low Loading Sequence
H-L-H	High to Low to High Loading Sequence
QR	Quasi-Random Loading Sequence
TR	True Random Loading Sequence

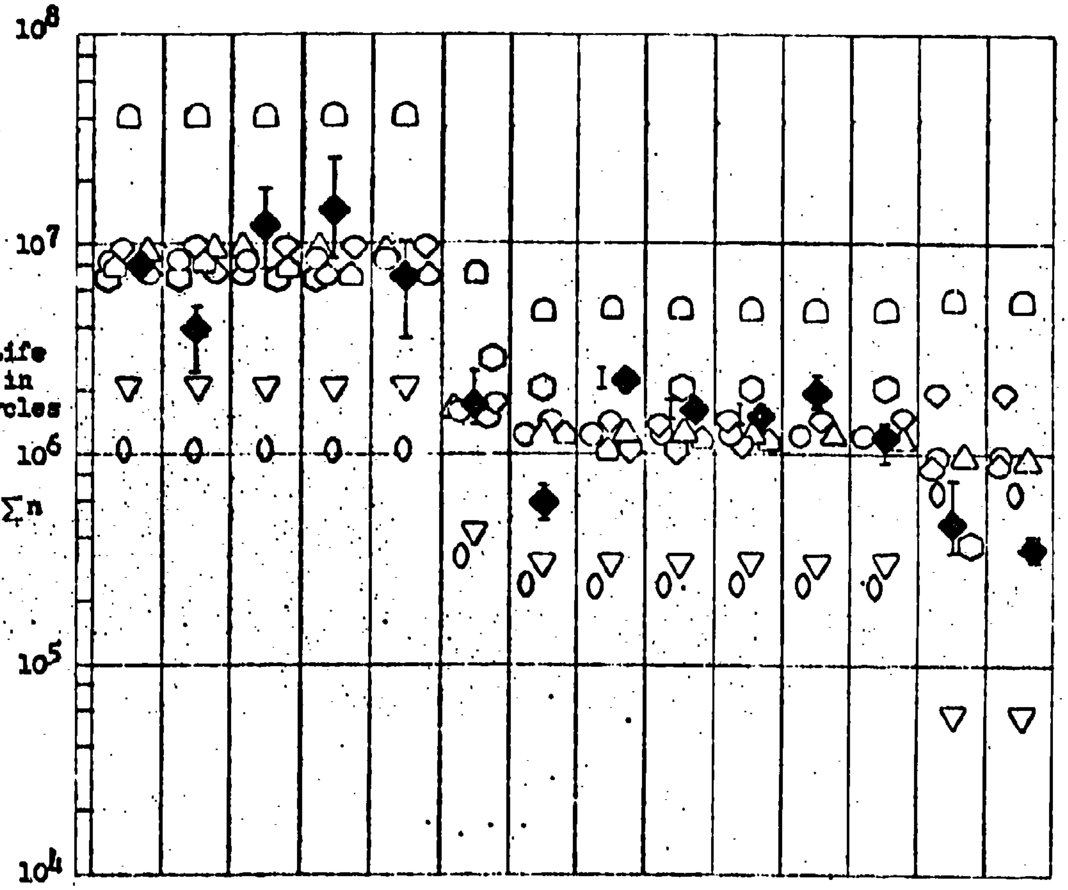

Test Group No.	G1	G2	G3	G4	G5	G6	G7	G8	G9	G10	G11	G12	G13	G14
Sequence	L-H		H-L		QR		L-H	H-L	L-H-L	H-L-H	QR			
Block Size (cycles)	100000	500000	100000	500000		100000	100200				50100	100200	50000	100000
Loading Steps	18						8							
Mean Stress	17.4 KSI												0 KSI	
Spectrum	Gust B					Gust A								
Specimen	Notched Sheet													
Material	2024-T3													
Reference for Test Data	16													

Coding for Points is Given in Table 1

Figure 5. Comparison of Predicted and Experimental Fatigue Life

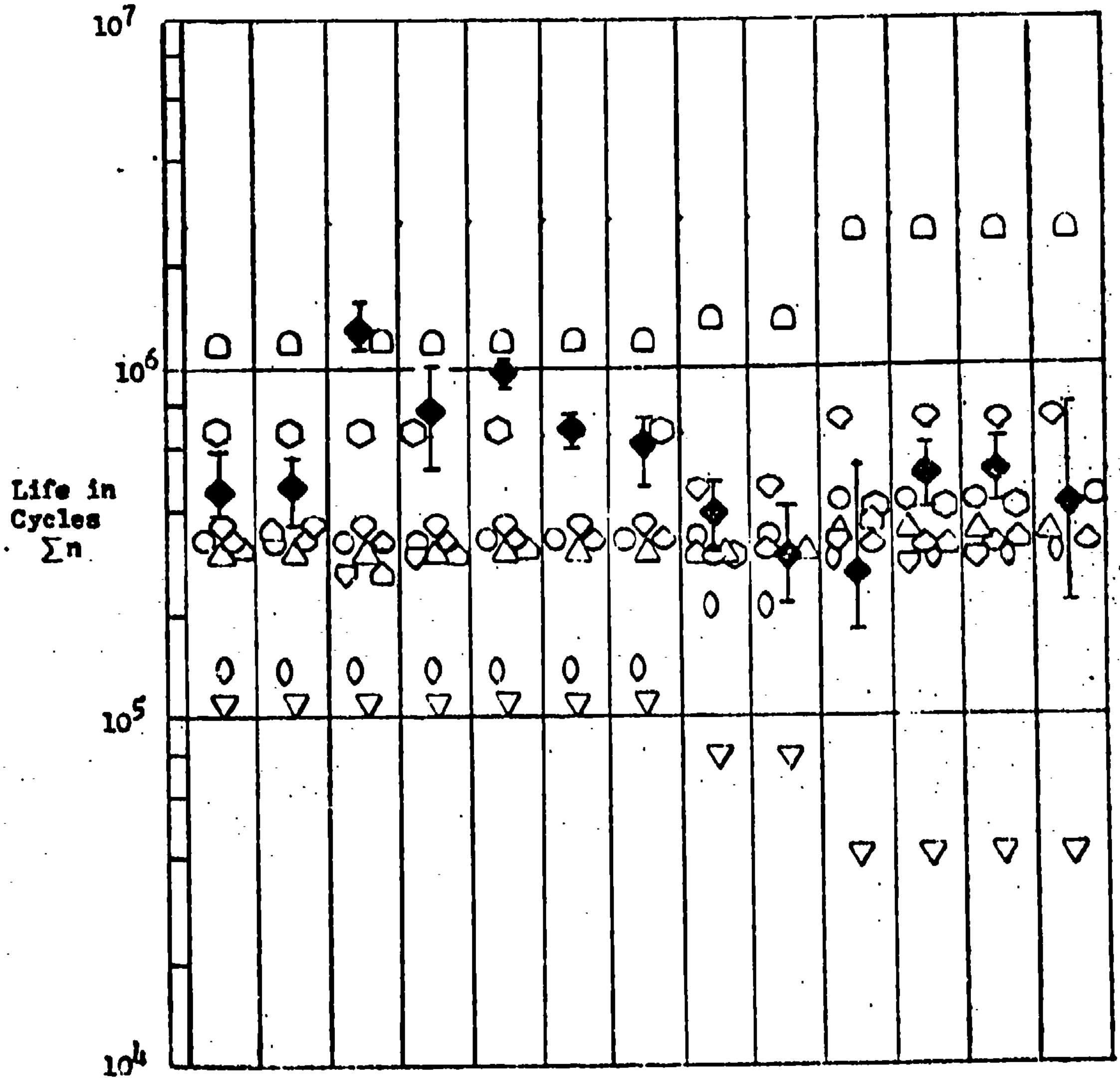

Test Group No.	015	016	017	018	019	020	021	022	023	024	025	026	027
Sequence	L-H		H-L	L-H-L	H-L-H	QR		L-H-L	QR	L-H	H-L	L-H-L	QR
Block Size (cycles)	10200	50900		10200	50900	10200	50900	30200		30000			
Loading Steps	8												
Mean Stress	20 KSI							10 KSI		0 KSI			
Spectrum	Gust A												
Specimen	Notched Sheet												
Material	7075-T6												
Reference for Test Data	16												

Coding for Points is Given in Table 1.

Figure 5 (continued) Comparison of Predicted and Experimental Fatigue Li

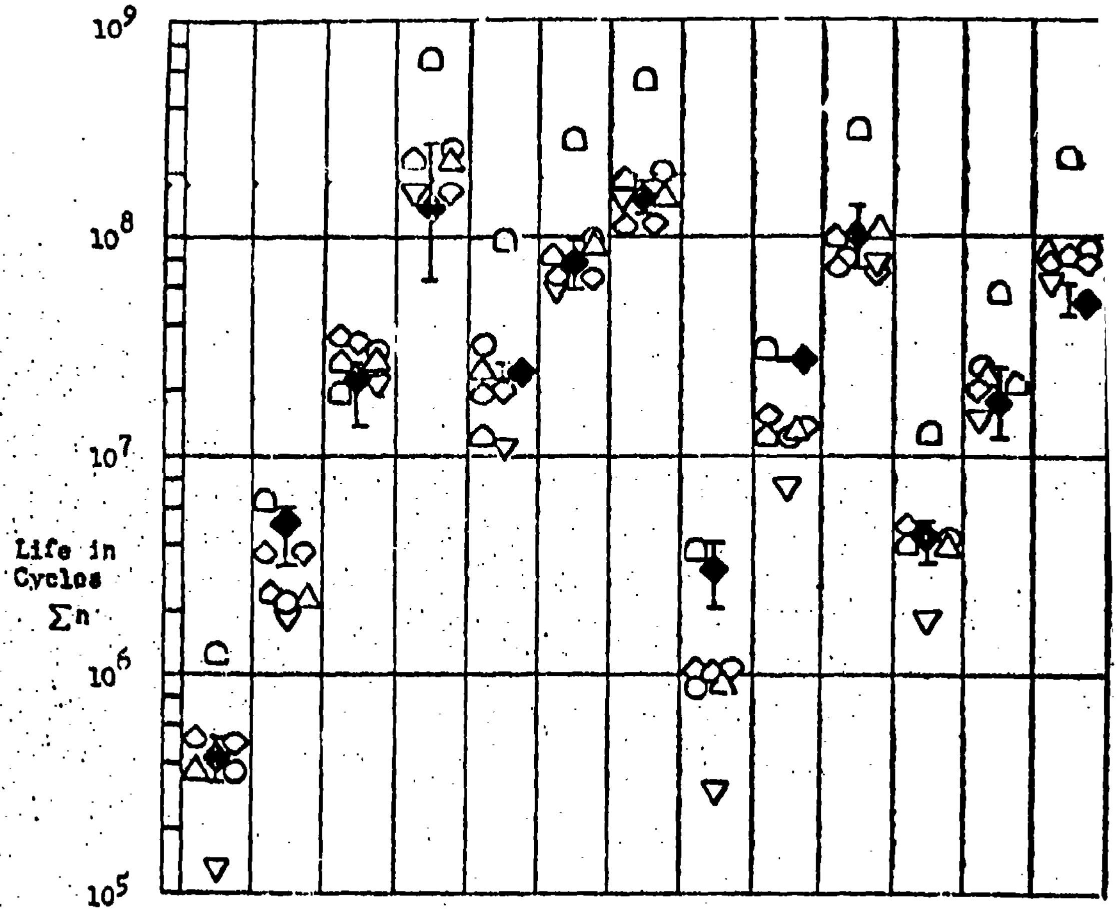

Test Group No.	G28	G29	G30	G31	G32	G33	G34	G35	G36	G37	G38	G39	G40
Sequence	L-H-L												
Block Size (cycles)	360280												
Loading Steps	9												
Mean Stress KSI	15.5	9.3	6.2	4.9	15.4	12.4	11.1	13.2	8.9	6.6	43.1	33.5	27.5
Spectrum	Gust												
Specimen	Double Shear Riveted Joint				Unnotched Sheet			Butt Joint			Strips with Hole		
Material	2024-T3 Alclad				7075-T6-Alclad						Cr-Mo Steel		
Reference for Test Data	17												

Coding for Points is Given in Table 1.

Figure 5. (continued) Comparison of Predicted and Experimental Fatigue Life

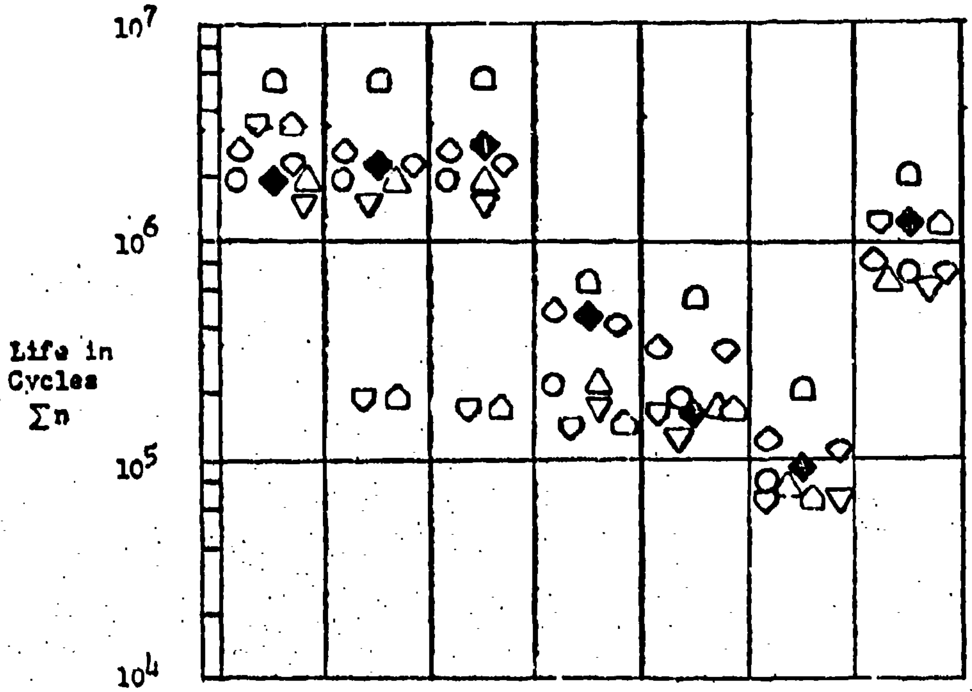

Test Group No.	G41	G42	G43	G44	G45	G46	G47
Sequence[a]	L-H	H-L					L-H
Block Size (cycles)	Same as Experimental Life						
Loading Steps	6			5			6
Mean Load LBS	975				1240	1055	
Spectrum	Gust						
Specimen	Lap Joint with One Row of Flush Rivets				b	c	
Material	2024-T3 Alclad					7075-T6 Alclad	
Reference for Test Data	18						

a sequence applied only once
b Lap Joint with two rows of flush rivets
c Lap Joint with one row of flush rivets

Coding for Points is Given in Table 1.

Figure 5. (continued) Comparison of Predicted and Experimental Fatigue Life

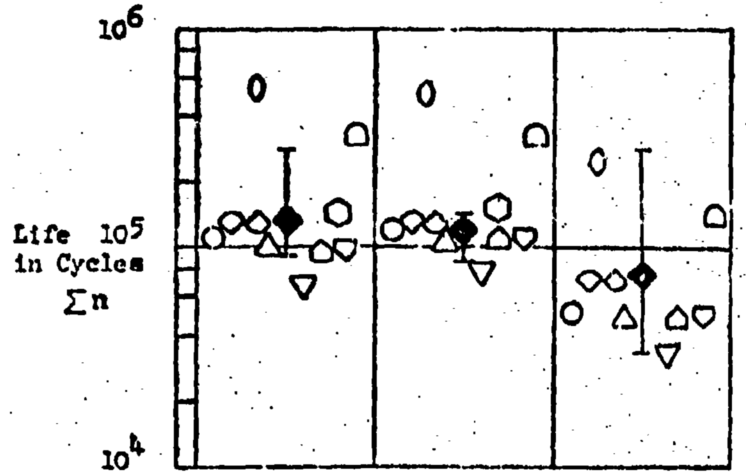

Test Group No.	G48	G49	G50
Sequence	L-H-L		
Block Size (cycles)	13290	6290	5410
Loading Steps	9		10
Mean Stress	14KSI		
Spectrum	Gust		
Specimen	Notched Plate		
Material	D.T.D. 363A Aluminum Alloy		
Reference for Test Data	19		

Coding for Points is Given in Table 1

Figure 5. (continued) Comparison of Predicted and Experimental Fatigue Life

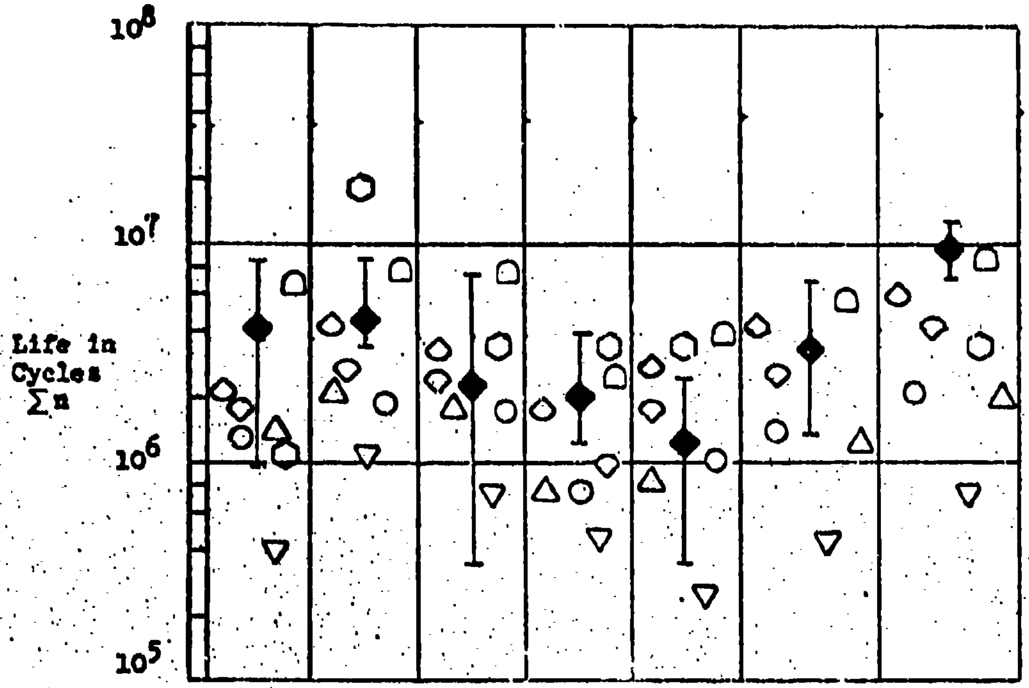

Test Group No.	G51	G52	G53	G54	G55	G56	G57
Type of Failure	Crack Initiation				First Crack	Critical Crack	Final Failure
Sequence	Quasi-Random						
Block Size (cycles)	59670						
Loading Steps	16						
Mean Load Factor	Unit Gravitational Acceleration						
Spectrum	Gust						
Location on C-46 Wing	Wing Station				Complete Wing		
	180	214	228	239			
Material	2024-T						
Reference for Test Data	20						

Coding for Points is Given in Table 1.

Figure 5. (continued) Comparison of Predicted and Experimental Fatigue Life

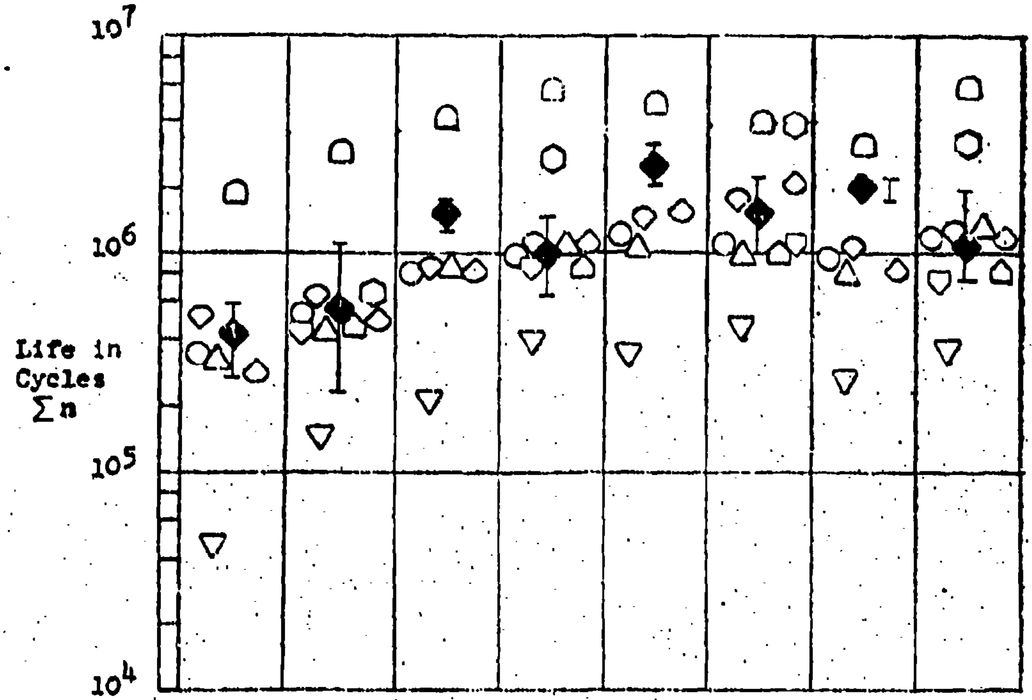

Test Group No.	G58	G59	G60	G61	G62	G63	G64	G65
Type of Failure	Initial				Final			
Sequence	T R	L-H-L	T R	L-H-L	T R	L-H-L	T R	L-H-L
Block Size (cycles)	500000	32860	500000	32860	500000	32860	500000	32860
Loading Steps	11	3	11	3	11	3	11	3
Mean Load LBS	17900							
Spectrum	Gust							
Location on P-51 Wing	Gun bay		Tank bay		Gun bay		Tank bay	
Material	2024-T							
Reference for Test Data	21							

Coding for Points is Given in Table 1

Figure 5. (continued) Comparison of Predicted and Experimental Fatigue Life

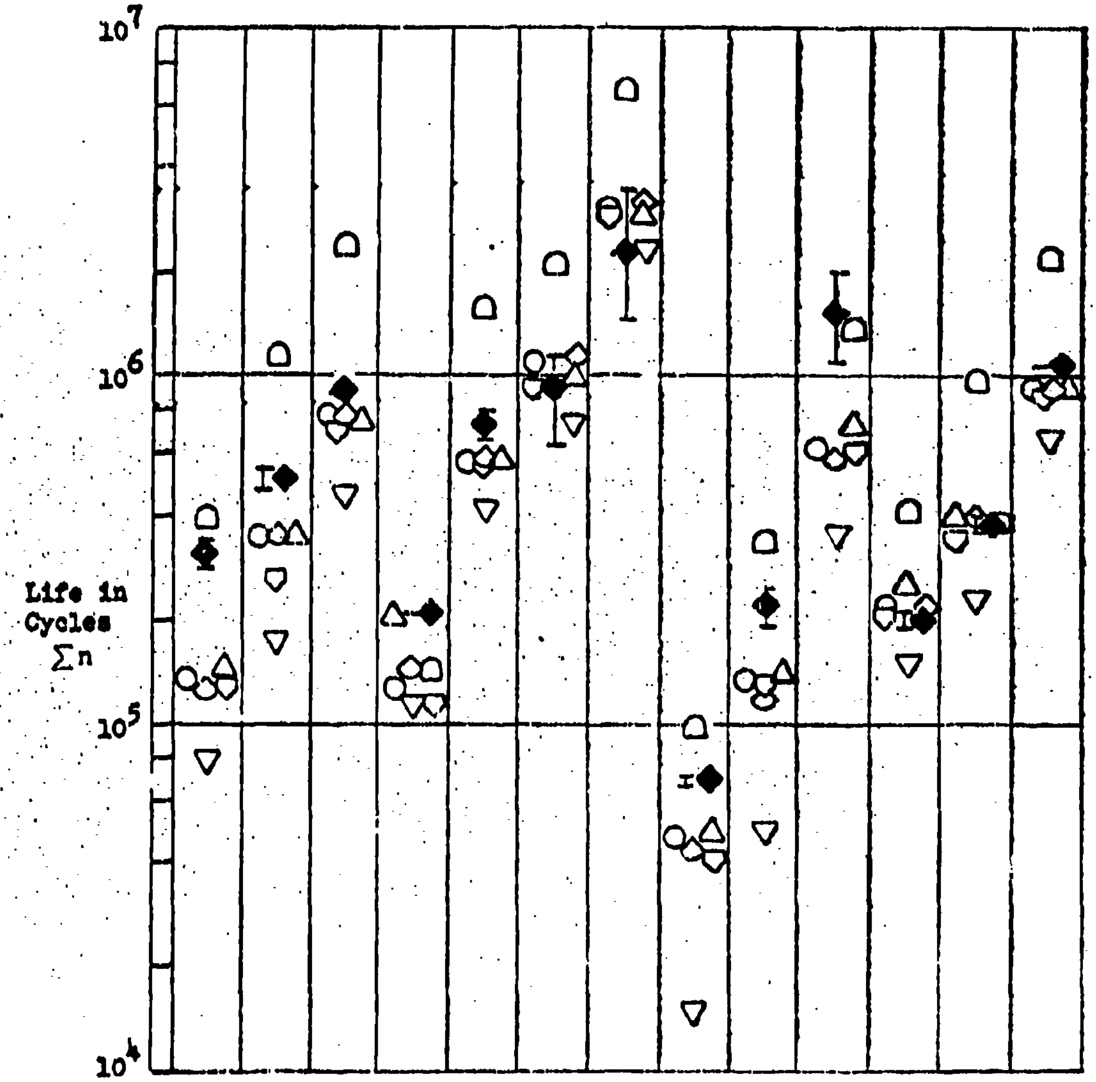

Test Group No.	M1	M2	M3	M4	M5	M6	M7	M8	M9	M10	M11	M12	M13
Sequence	L-H-L												
Block Size	7477												
Loading Steps	9												
Minimum Stress KSI	5.1	3.8	3.1	9.6	7.7	6.4	4.8	5.3	4.4	3.3	16.8	15.1	12.6
Spectrum	Maneuver												
Specimen	Double Shear Riveted Joint			Unnotched Sheet				Butt Joint			Strips with Hole		
Material	2024-T3 Alclad			7075-T6 Alclad							Cr-Mo Steel		
Reference for Test Data	17												

Coding for Points is given in Table I.

Figure 6. Comparison of Predicted and Experimental Fatigue Life.

This scale of comparison is most informative in assessing the life prediction effectiveness of the various methods and in providing information on the scatter factors which need consideration for assessing reliability on the life cycle scale.

2. Comparisons of the Change in Stress Level Required to Predict Exactly the Test Life

The stress scale may be used to evaluate the various prediction methods by the determination of a proportionality factor, k, by which all stress levels of the test spectrum are raised or lowered to arrive at the exact prediction of the specific test life.

The comparison of the prediction with the actual test result is made by the ratio:

$$\text{Degree of conservatism} = \frac{S_{v(Test)}}{S_{v(Adjusted)}} = \frac{S_{v(Test)}}{k\,S_{v(Test)}} = \frac{1}{k}$$

If $\dfrac{S_{v(Test)}}{S_{v(Adjusted)}} = \dfrac{1}{k} < 1.00$, the prediction is unconservative.

If $\dfrac{S_{v(Test)}}{S_{v(Adjusted)}} = \dfrac{1}{k} \geq 1.00$, the prediction is conservative.

This scale of comparison is informative to the designer with respect to the amount of material (and its corresponding weight) which is necessary to achieve a given fatigue life, and in the assessment of any factor of safety on loads which may need consideration in achieving any required degree of reliability of fatigue life.

The ratios of $\dfrac{N_{L(Test)}}{N_{L(Predicted)}}$, and $\dfrac{S_{v(Test)}}{S_{v(Adjusted)}}$ were ranked in ascending order and the percentage of the total number of samples equal to or less than a given degree of conservatism was determined and plotted as a function of that degree of conservatism. These correlation graphs are shown in Figures 7 and 9 for the life cycle prediction and in Figure 8 for the stress adjustment ratio.

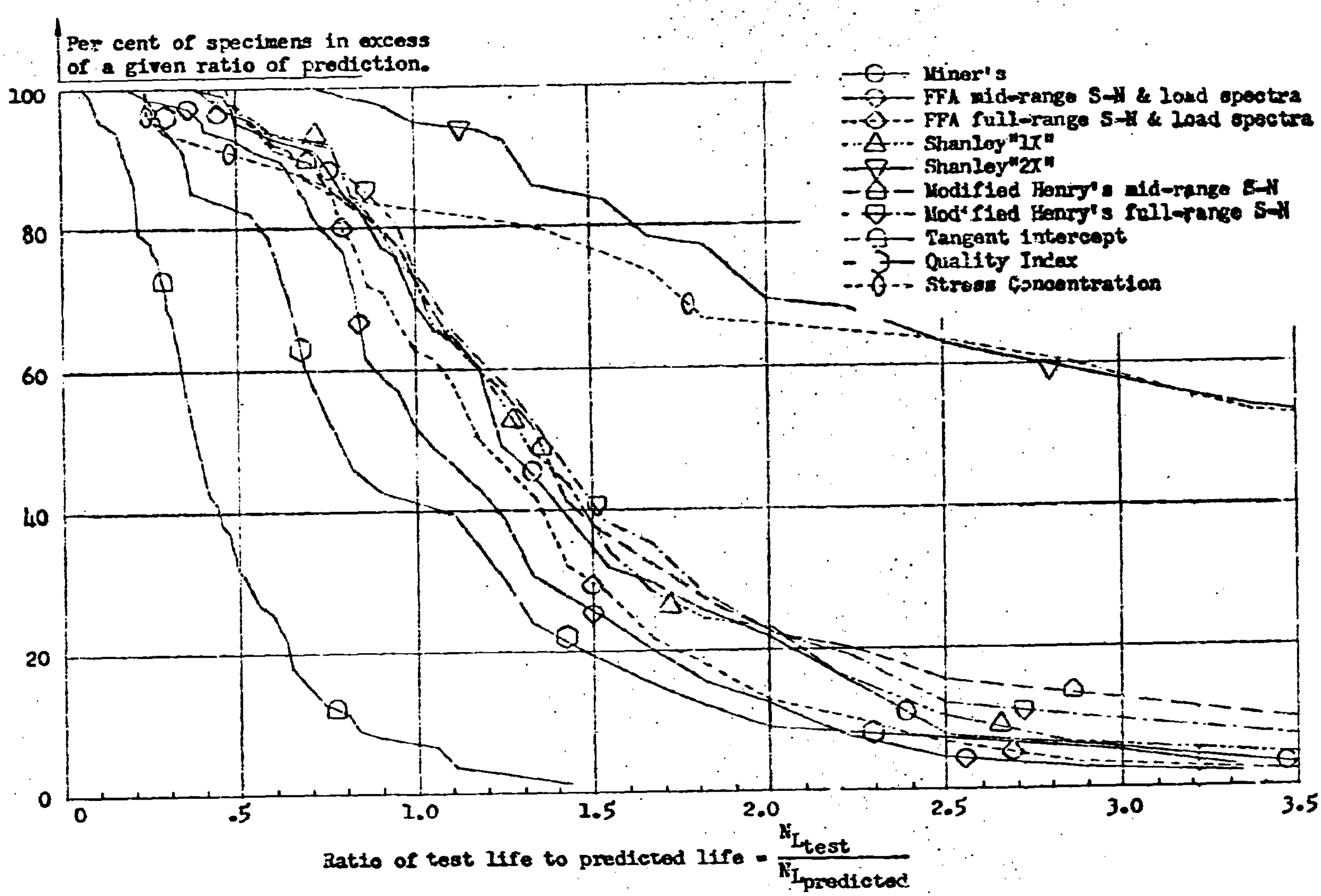

Figure 7. Cumulative Distributions for the Ratio of Test Life to Predicted Life

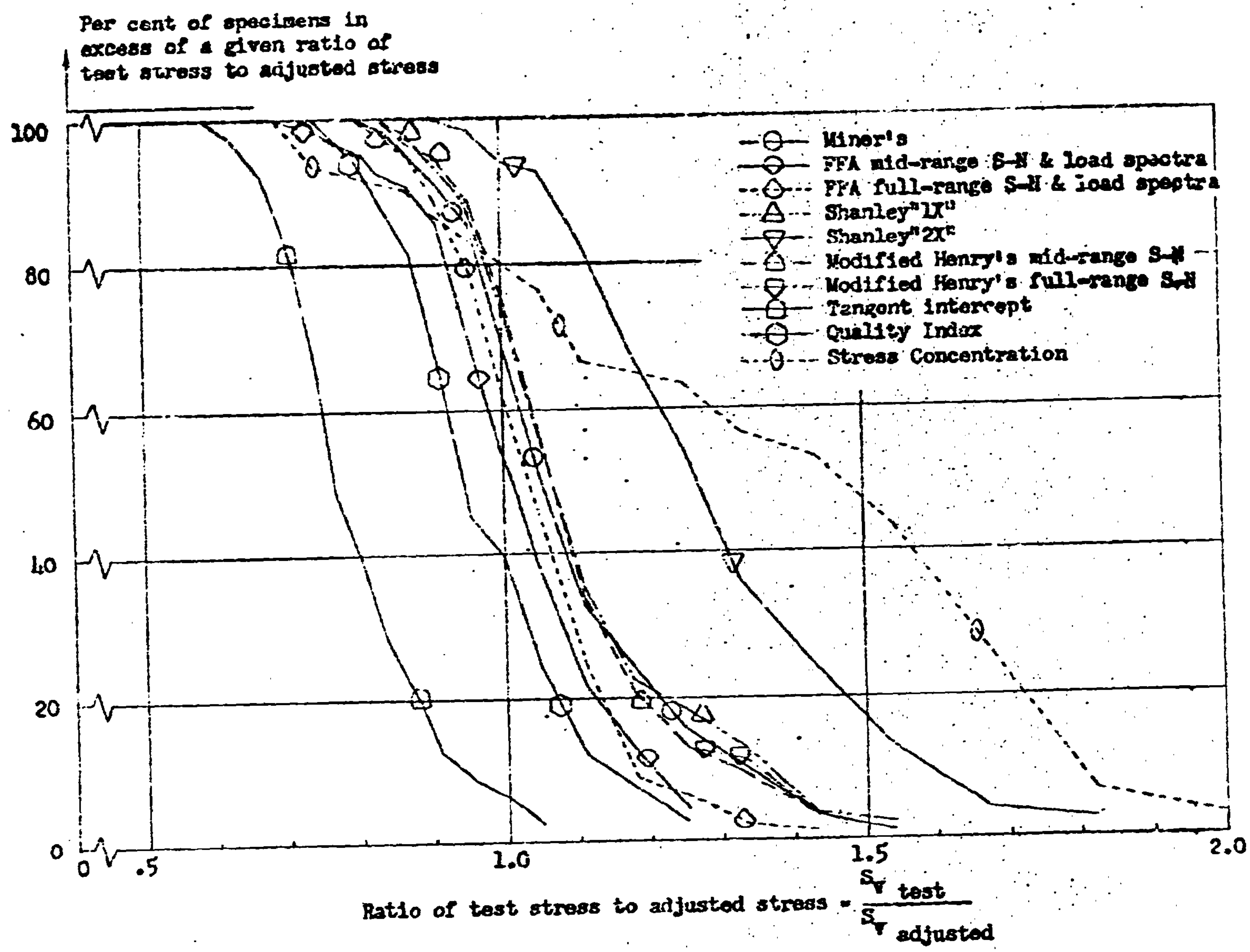

Figure 8. Cumulative Distributions for the Ratio of Test Stress to Adjusted Stress

The inherent spread of fatigue life predictions is evident in the rectilinear scale of Figure 7. To encompass a wider range of data, Figure 9 is presented with the degree of conservatism on a log scale. This latter figure also has the advantage that equal distances on each side of the ordinate of perfect correlation (degree of conservatism = 1.00) represent equal degrees of conservatism, whereas in the rectilinear plots of Figures 7 and 8, these distances are distorted between the unconservative and the conservative sides of the diagrams.

The appearance of these diagrams is roughly similar to the Gaussian normal distribution curve. Table 2 was therefore prepared from these data to indicate a quasi-statistical analysis of the error spread in terms of standard deviations (one sigma). From the properties of the logarithmic increments, the resulting multiplicative standard deviation is a factor to be multiplied or divided, not added or subtracted as is the case for the standard deviation.

Examination of these curves shows the Tangent Intercept method to be very unconservative for predicting the fatigue life of this group of tests. Also evident is the large degree of conservatism in the fatigue life predictions of Shanley's "2X" method and the lack of agreement, both conservative and unconservative, for the stress concentration procedure when using the concept of linear cumulative damage with standardized S-N curves. All other methods evaluated by these data group closely to the same band generally consistent with the linear cumulative damage prediction. This agreement is to be expected since all of these methods except the Tangent Intercept are variations of the basic cumulative damage procedure, some of which vary only in details of mathematical curve fitting.

Some of the methods which introduce nonlinearities do not demonstrate for these tests any strong divergence from the linear accumulation process, with the single exception of Shanley's "2X" method.

The evaluation of the two variants of the least squares best fit of the S-N data in the two methods showed no detectable difference in the generalized Henry method. A relatively minor overall improvement can be observed in Lundberg's FFA method when the best fit of S-N and loading spectra data is restricted to the midstress region of most damaging stresses.

In Figure 8 the correlation of the various methods as measured on the stress scale reveals the same general pattern among the various methods as was discussed above for the life cycle scale of comparison. The significant difference, from the viewpoint of design and control for the prevention of fatigue failures, is the relatively small change in the stress adjustment factor required to achieve a given degree of improvement on the life cycle scale.

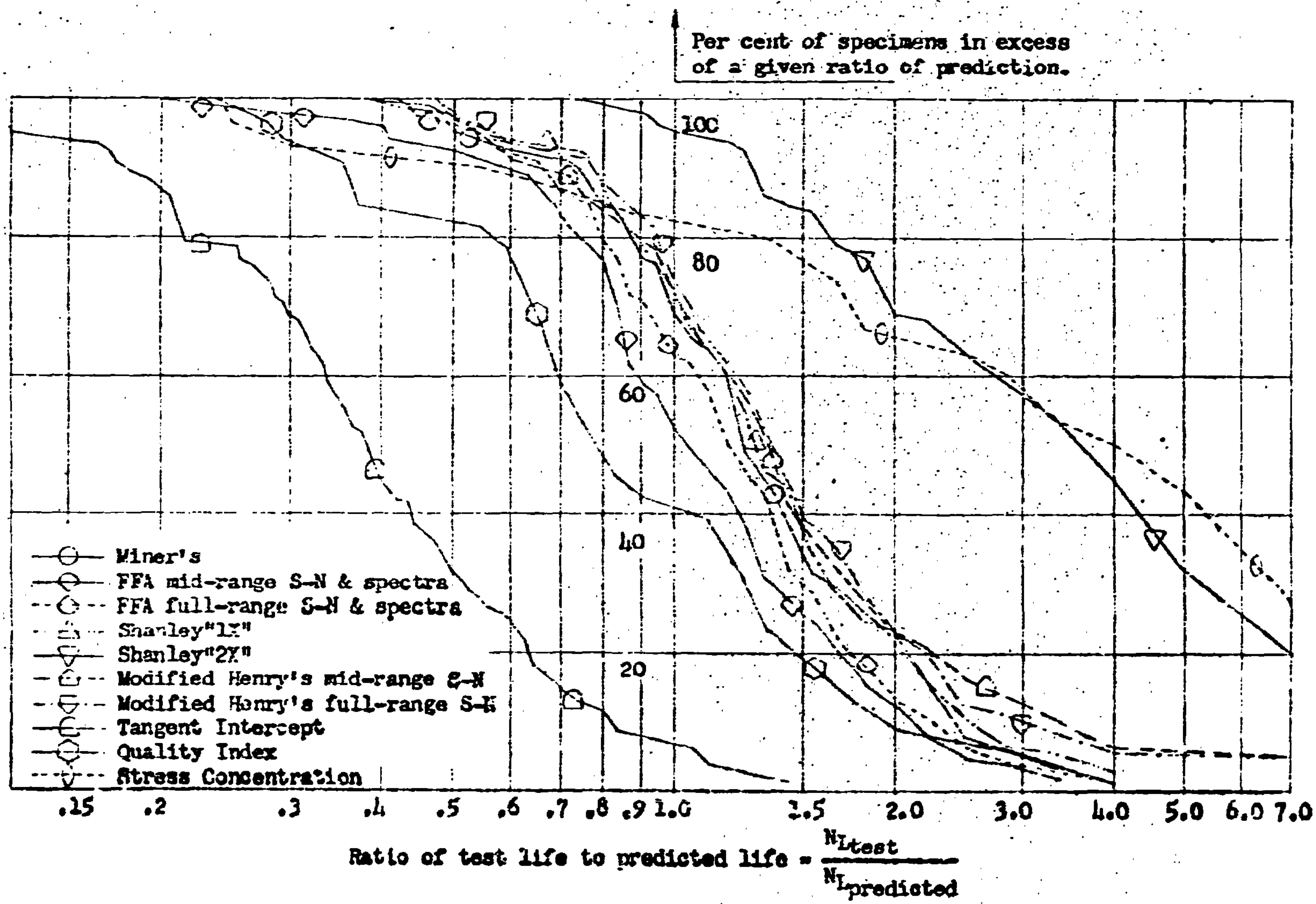

Figure 9. Log Cumulative Distributions for the Ratio of Test Life to Predicted Life

TABLE 2

STATISTICAL PARAMETERS ESTIMATED FROM THE CUMULATIVE DISTRIBUTION CURVES

Method Codes in Table 1	Ratio, $\frac{NL_{test}}{NL_{predicted}}$ Multiplicative Mean	Ratio, $\frac{NL_{test}}{NL_{predicted}}$ Multiplicative Standard Deviation One σ	Ratio, $\frac{S_{v\,test}}{S_{v\,adjusted}}$ Mean	Ratio, $\frac{S_{v\,test}}{S_{v\,adjusted}}$ Standard Deviation One σ
Tangent Intercept	.38	1.84	.79	±.10
FFA Code ⬡	1.07	1.74	1.02	±.12
FFA Code ◇	1.20	1.52	1.05	±.12
Miner's	1.29	1.64	1.09	±.16
Henry's Code ⌂	1.42	1.85	1.09	±.14
Henry's Code ▽	1.43	1.78	1.09	±.14
Shanley's 1X	1.34	1.65	1.10	±.15
Shanley's 2X	3.74	2.13	1.30	±.20
Quality Index	.87	1.93	.97	±.12
Stress Concentration	2.40	2.81	1.38	±.36

Derived from Figures 8 and 9.

THE FATIGUE QUALITY INDEX METHOD

The potential advantages of basing a fatigue life prediction method on one or a few spectrum test results of specimens of critical structure is worthy of special study. The simplest test of the effectiveness of the procedure is to compare the values of the test-derived quality index determined from all available tests in which two or more different loading spectra were applied to one specimen. If these quality indices are invariant (within a reasonable scatter factor) for all load spectra test results on the same type of specimen, the predictability of fatigue life is assured.

The fatigue quality index was derived for all the pertinent data available from the test groups chosen for this evaluation. These values are listed in Table 3 . The test data of these groups are of a similarly shaped spectrum of varying loads in which the general slope was changed as well as the mean stresses. Comparisons of the fatigue quality index values in Table 3 for a given specimen, however, indicate a considerable variance. The variance due to scatter of the test results is also indicated.

Groups 28 through 31 inclusive show the influence of progressively reduced slope of a gust-type spectrum on the derived fatigue quality index for a double shear riveted joint of 2024-T3 Aluminum Alloy. The maximum K-value (minimum life of each test group) is progressively higher for each reduction in slope of the loading spectrum. The geometric mean and the minimum K-value (maximum life of each test group) show a slight reversal in the general trend for the lowest sloped loading spectrum. However, the change in slope between these last two groups (G30 and G31 in Figure 10) is relatively much smaller than the changes among the others of the set. The trend of increasing K-value with decreasing slope of the loading spectrum is, in general, stronger than the scatter (except for the last two groups).

Groups G35, G36, and G37 provide a similar comparison for a butt-joint specimen of 7075-T6 Aluminum Alloy. The trend is clearer for this group, there being no overlapping of the minimum and maximum K-values of any of the groups.

Groups G32, G33, and G34 indicate, for 7075-T6 aluminum alloy unnotched sheet specimens, the same general trend of increasing K-value with reduction of loading spectrum slope. However, the variance is much weaker, and there is more overlap of minimum and maximum values of the groups from scatter. Contributing to this conclusion, however, is the relatively small difference in slope as indicated by Figure 10.

It is therefore concluded from this brief study that the relative maximum load content of a service record as exemplified by the mean load changes and the slope of the statistical load frequency spectrum has an important influence on the fatigue life of airframe structure.

TABLE 3

VARIATION OF THE FATIGUE QUALITY INDEX
WITH DIFFERENT LOADING SPECTRA SLOPE

Test Group	Slope Sequence	No. of Spec.		Max. K Min. Life	Geometric Mean	Min. K Max. Life
2024-T3 Double Shear Rivited Joint - 2(3/16) Round Head Rivets						
G28	High Lo-Hi-Lo	2	K	4.13	3.97	3.82
			Life	$.324 \times 10^6$	$.411 \times 10^6$	$.522 \times 10^6$
G29	High Intermediate Lo-Hi-Lo	3	K	5.06	4.70	4.52
			Life	3.20×10^6	5.98×10^6	4.788×10^6
G30	Low Intermediate	3	K	7.73	6.71	6.29
			Life	13.69×10^6	$21,73 \times 10^6$	27.4×10^6
G31	Low Lo-Hi-Lo	2	K	7.83	6.59	5.52
			Life	62.4×10^6	129.7×10^6	270.0×10^6
7075-T6 Butt Joint Specimens 5/32 CSK Rivets						
G35	High Lo-Hi-Lo	4	K	3.69	3.52	3.30
			Life	2.05×10^6	2.99×10^6	4.03×10^6
G36	Intermediate Lo-Hi-Lo	2	K	3.98	3.97	3.96
			Life	27.00×10^6	27.56×10^6	28.10×10^6
G37	Low Lo-Hi-Lo	2	K	4.59	4.41	4.25
			Life	72.75×10^6	101.00×10^6	140.00×10^6
7075-T6 Unnotched Sheet						
G32	High	2	K	1.91	1.90	1.89
			Life	24.1×10^6	25.71×10^6	27.4×10^6
G33	Intermediate	2	K	2.22	2.10	1.98
			Life	58.7×10^6	75.875×10^6	98.0×10^6
G34	Low	2	K	2.26	2.17	2.07
			Life	127.00×10^6	152.00×10^6	181.00×10^6

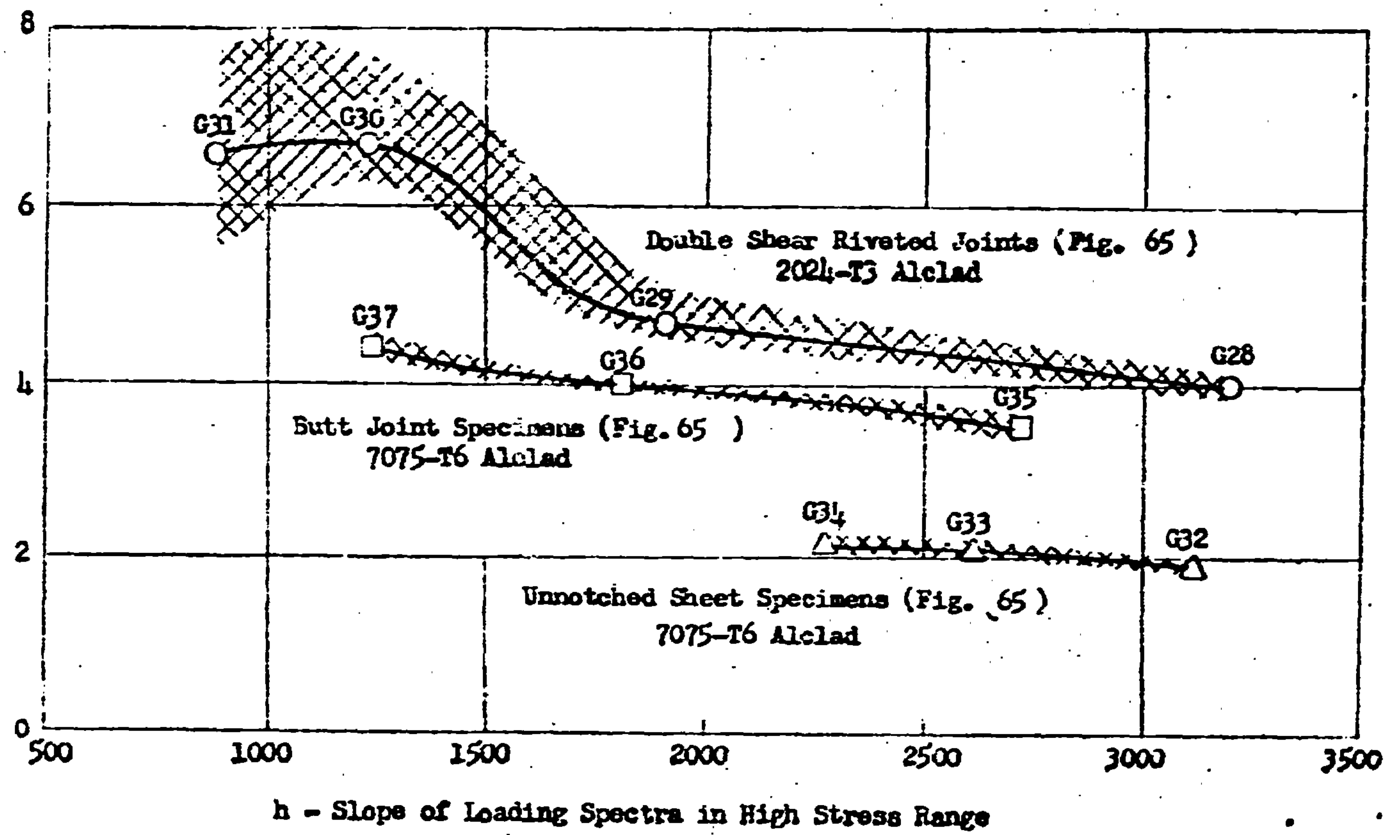

Figure 10 Variation of the Test Derived Fatigue Quality Index K versus Slope of the Loading Spectra

FACTORS OR MARGINS OF SAFETY FOR FATIGUE

Diagrams of the type of Figure 7 are often used for discussion on the necessity of factors of safety or margins of safety on fatigue life. Diagrams of the type of Figure 8 are correspondingly used for discussions of factors or margins on loads or stresses to achieve the same end; namely, a "safe-life" philosophy of design. However, there are many other facets of the problem which must be considered in the establishment of safety factors. A brief discussion of some of these facets is given, although it is not the purpose nor within the scope of this study to establish factors or margins of safety for fatigue.

Mission Objectives

The trend of design toward achievement of higher performance goals has led to an ever higher degree of specialization. For each major project, therefore, the subject of reassessment of factors of safety in relation to the specific mission objectives is a necessity.

Fail-Safe Philosophy

One of the most important aspects to be considered is the "fail-safe" philosophy of design. The "safe-life" and the "fail-safe" philosophy have been the subject of considerable controversy in the past by proponents of one or the other approaches to built-in safety in the flight structure. From practical considerations, both have a place, they are not mutually exclusive philosophies, and even though reliance may be placed on a "fail-safe" approach, the fatigue qualities of the structure cannot have any less degree of attention. However, in the case of successful "fail-safe" design, the need for reliance on fatigue life for flight safety is considerably reduced. The consideration of factors of safety on fatigue life thus may have an entirely different complexion in the presence of a "fail-safe" structure than it assuredly must have in a "safe-life" structure which is not "fail-safe."

Loads

The evaluation diagrams referred to above cover only a portion of the life prediction process; uncertainties in the external load predictions are not contained. The external loads as well as the interrelation of the static strength level loads and their factors of safety should be considered simultaneously in assessing factors of safety for designing against fatigue.

Inspection, Maintenance, and Repair

Inspection, maintenance, and repair as a means of prolonging indefinitely the "fatigue useful life" of a structure is another important subject, often overlooked in the assessment of factors of safety for fatigue. Catastrophic fatigue cracking of major structure early in the operational life of a fleet is not to be condoned. On the other hand, an airframe used long enough can be expected to develop fatigue cracks. The fatigue characteristics of some materials show no specific endurance limit, and the severe performance

requirements of flight force the use of the highest possible design allowable tensile stresses. However, means are available for designing to any specific fatigue life required, performance permitting. Scheduled inspection, maintenance, and repair or replacement of components may become a deliberate policy in the attainment of higher performance with safety from fatigue problems. Helicopter parts are an example.

Test Procedures

Factors in the laboratory testing procedures also affect the scatter of results, which should be considered in assessing factors for design. Constant amplitude loading appears to give wider scatter in results when compared with spectral load testing techniques. Notched coupon-type specimens appear also to give wider scatter in results than complex specimens in which load redistributions may take place. These factors should be taken into account, particularly in assessing a broad range of specimen types and loadings as represented in the Figures 5 and 6 of the methods evaluation phase of this study.

It may be concluded, therefore, that the results of this study demonstrates a need for factors or margins of safety in certain classes of structures (non-fail-safe). However, additional considerations are necessary, some of which are specific for each type of project. An evaluation of the need and the particular values for factors of safety should, therefore, be a process in the establishment of design criteria for each project.

CONCLUSIONS OF THE EVALUATION STUDY

From considerations of the problems involved in the prediction of fatigue life of airframe structure when this process is used as a tool for the prevention of fatigue failures in an operational fleet, and based on the test data utilized in this evaluation, the following conclusions may be drawn.

1. The Linear Cumulative Damage Method is currently the most practical, simple, and yet versatile method available and has sufficient accuracy commensurate with the other uncertainties, such as service load history, not included in this evaluation.

2. The Stress Concentration Factor Method of refined stress analysis, coupled with a fatigue damage theory such as the linear cumulative damage hypothesis used in this evaluation, is shown to be less than adequate as a fatigue life prediction method. However, since these procedures usually are the only means available for preliminary design assessments, their use must be followed up by development tests of fatigue critical areas.

   Development tests of fatigue critical joints and structural discontinuities are required to assess a fatigue quality of the structure which is as yet not attainable by theoretical means. To achieve satisfactory reliability from the laboratory results, the critical areas of the specimen must be as exact a simulation of the critical area as possible, including local eccentricities, supports, manufacturing processes and finishes, local attachments for secondary elements, etc., and should also include a nominal area of surrounding structure for load and stress monitoring and for comparing the joint results with the fatigue life of the nominal structure, if this is required. These development tests must encompass the full range of load magnitudes expected in service to properly assess location of cracks, crack growth, and final fracture. While the objectives of these tests might be achieved by constant load amplitude S-N type tests or the full spectral-type tests, there is considerable evidence (reference 20) for recommending the latter.

3. The Fatigue Quality Index Procedure, which was originally a means of interpreting spectrum-type fatigue tests, is investigated as a test-based method of fatigue life prediction. A spectrum test result is analyzed by the linear cumulative damage equation coupled with a fixed standard set of S-N data to define which K-value of the set will make the cumulative damage summation exactly unity. For success as a fatigue life prediction method, the test-defined K-value should be invariant for similar types of test spectra applied to identical specimens. Study of the applicable test data shows this not to be the case. Further exploration is therefore necessary to determine whether a consistent trend exists which might be used as an adjustment factor to improve the life prediction process.

4. The Tangent Intercept Method demonstrated the largest degree of unconservatism when applied to these test data. Graphical limitations make this method impractical to handle the more complex composite loading histories, often at several different mean load levels in each flight.

5. Shanley's "2X" Method of nonlinear cumulative damage, based on a more accelerated rate of crack growth than his "1X" method, demonstrated a larger degree of conservatism than all other methods investigated.

6. The remaining prediction methods which were evaluated (Lundberg's FFA method, Shanley's "1X", and the generalized Henry method) all show relatively small differences in reliability of life prediction, considering the large uncertainties remaining, for instance, in the service loads and operational history. The limitations of mathematical curve fitting in some of these methods and the complexity and lack of statistical information for other methods preclude their widespread application for aircraft fatigue life prediction.

7. The assessment of reliability on the scale of the stress adjustments necessary to achieve exact prediction of the fatigue test results show generally the same relationship among the various methods as for the scale of life cycles. However, as would be expected, far less absolute deviation occurred on the stress adjustment scale than on the life cycle scale.

8. The results of this study demonstrate a need for factors or margins of safety in certain classes of structures (non-fail safe). However, additional considerations are necessary, some of which are specific for each type of project. An evaluation of the need and the particular values for factors of safety should, therefore, be a process in the establishment of design criteria for each project.

SECTION IV

INVESTIGATION OF THE INFLUENCE OF SPECTRUM SHAPE ON FATIGUE LIFE PREDICTIONS

Based on the test data available, the evaluation study of fatigue life prediction methods discussed in Section III arrived at two basic conclusions. First, when adequate S-N data is available on the specific structure, fatigue life prediction under complex loading spectra by the simple linear cumulative damage procedure is of sufficient accuracy commensurate with other intangibles remaining in the problem. Secondly, the direct use of the fatigue quality index procedure was shown to be less capable of analysing different spectra of loads applied to identical specimens. While some of the discrepancy is attributable to artificial test variables, sufficient variation remains to indicate a considerable influence from the statistical load frequency content as exemplified by the spectrum shape (slope).

It is the purpose of this section of the study to explore the circumstances of this difference in fatigue life predictions for similar structure tested under different shaped loading spectra. The objective is to determine whether any regularity in the trend of fatigue life with shape of loading spectra exists which might be used an an empirical adjustment factor to improve the predictability under different types of loading spectra. An experimental program was conducted to generate data for this purpose.

EXPERIMENTAL PROGRAM

The experimental program was conducted in two parts to provide evidence for this study. The first part, using simple notched sheet coupons of 7075-T6 aluminum alloy, explored a variety of test spectra shapes including the use of the original random load record from which the ordered loading spectra was derived. The results of these tests, reported in detail in Appendix D, are analyzed in this section of the report. The second part of the experimental program was conducted on specimens of a complex joint design to determine whether the results of the coupon test program could be reproduced in complex structure more representative of contemporary aircraft. These results, reported in detail also in Appendix D, are analyzed in the following section of this report.

FATIGUE TEST EQUIPMENT

A magnetic tape controlled fatigue loading machine was assembled from available equipment. The system consisted essentially of a magnetic tape playback unit, associated electronic amplifiers, calibration equipment, load monitoring tape recording system, and an oscillograph. The amplified magnetic tape load demand signal was fed through a summing junction to a highly sensitive electrohydraulic servo-valve which controls the pressure on each side of a 17,000 lb. capacity, double-acting hydraulic loading jack. The fatigue test specimen was coupled to the hydraulic jack, in series through a calibrated electrical strain-gage load-measuring cell. The instantaneous load signal from the monitoring cell was amplified and fed through a specially tailored lead network to the tape demand signal summing junction. The error between the measured load signal and the

demand signal, suitable amplified, was applied to the servo valve in a direction to reduce the error to zero. This negative feed-back loop stabilizes the system up to relatively high frequence of load application, in this case approximately 60 cps for simple loading forms, determined primarily by the dynamics of the mechanical system and the hydraulic flow characteristics of the valve and associated power supply.

While most of the equipment is of commercially available units and the test arrangement is simple and straightforward, the precision and repeatability, demanded for quality results, require considerable efforts to develop control, maintenance, calibration, and monitoring techniques to a satisfactory degree of reliability. These techniques consist essentially of careful calibration of each set-up, and recording sampling load monitoring tapes which are counted on the electronic analogue computer set up for this purpose. The test data records reported herein are based on the load cell monitor count. The details of the equipment and a description of the complete test technique are more fully outlined in Appendix D, Part 2. Figures 11, 12, and 13 illustrate the test equipment, electronic control system, and a test specimen in place. Figure 14 illustrates the precision finally achieved by comparing the calibrated load cell output with the demand signal applied to the servo valve input terminals.

COUPON TEST SPECIMENS

The test specimens for the first phase of this program were made of a three-inch-wide strip of 0.040-inch thick 7075-T6 aluminum alloy sheet, Material Spec. QQ-A-277. Static tensile properties, taken in the longitudinal grain direction, are reported in Appendix D, Part 2, for samples from each sheet purchased for this program. The tensile test specimen conformed to ASTM standard E8-57T. These results indicate adequate uniformity and conformity of this material to the specification standards.

The specimens were notched by a series of central holes designed for two values of K_T = 4 and 7. The dimensions were as indicated in Figure 15. Floating edge-grooved stiffener blocks were installed to prevent buckling under the maximum compressive loads.

TEST SPECTRA ON MAGNETIC TAPE

A sample reproduced from a short length of an actual load trace from a B-47 aircraft flying in turbulence is shown in Figure 16. The general characteristics of varying magnitude cyclic loads are apparent, along with other irregularities of a nonrepetitive nature. There have been a number of methods proposed to reduce this type of load record to ordered cyclic load frequency spectra, three of which were explored in some detail in the research program reported in reference 5. A line through the average of the amplitudes of a short length of trace defines the local mean static load measured from a calibrated reference line. Perhaps the simplest of the counting methods is the mean crossing peak count which records each excursion from the local mean line to a maximum peak and return to the next crossing of the mean line as one half cycle of load, ignoring any secondary excursions within the time interval of mean line crossings. For records of sufficient duration, varying

magnitudes of positive peaks and negative peaks are substantially equal in number. Positive and negative half cycles are regrouped to form full cycles. These cycles are rearranged in order of magnitude and plotted in cumulative load frequency form as illustrated in Figure 17. The majority of service loading data is customarily reported in this form.

The other counting methods that were investigated, the range count and the interval crossing count, are defined in detail in reference 5. For the available loading traces, these were shown to be equivalent to the mean crossing peak count method described above. For this reason all the spectral fatigue results of this report are recorded in the form of mean crossing peak counts.

Analogue computing components were assembled to perform the counting procedure as described in Appendix D, Part 2. The computing techniques were calibrated against an average of several manual counts of approximately five minutes' length of the B-47 wing root bending moment record, which had been recorded on oscillograph paper for this purpose.

The relatively short length of B-47 data record (ninety-six minutes) produced a continuous frequency distribution spectra, with no gaps and discontinuities in the load intervals. However, the record was modified to provide a variety of spectra more suitable for testing. The modifications are discussed below.

1. The varying component of load was recorded separately from the local mean load so that independent amplification ratios could be applied to each load channel. An inequality of the maximum negative and the maximum positive load was equalized by nonlinear re-recording.

2. The varying spectra of loads were extended in length by linear amplifications and splicing, and was modified by special nonlinear amplifications to introduce the seldom encountered higher loads found on longer records. The technique used in producing this master gust spectrum tape is described in detail in Appendix D, Part 2.

3. During testing, suitable linear amplification ratios were used to produce high-slope high peak spectra, as illustrated in Figure 18.

4. Nonlinear amplification of the varying load record changed the spectrum shape to be predominately concave downward as illustrated in Figure 18.

5. The use of a diode rectifier suppressed all negative load peaks and resulted in a master record substantially representative of the random positive maneuver excursions from a constant minimum load level. The spectrum shape was modified by non-linear amplification to produce the characteristics of the maneuver spectrum of Specification MIL-A-8866. See Figure 19. A sample of the resulting random military maneuver loading trace is given in Figure 20. This type of trace represents the true random maneuver loading sequence denoted in Figure 25.

6. Unit step spectra were constructed and recorded on tape, from the average fatigue life on the various random mean crossing peak count curves of each type of spectrum, by the breakdown illustrated in Figure 21. The unit spectrum sizes were 1/10 and 1/20 of the total random test life,

and the stress interval was 1000 psi in each block size. One additional combination was produced with 4000 psi stress interval and 1/20 block size, as illustrated in Figure 22. A typical trace of an ordered step or Lo-Hi loading spectrum of a gust history is shown in Figure 23. The unit maneuver spectrum size was 1/20 of the total random test life with stress intervals of either 1000 or 4000 psi. A sample of an ordered military maneuver loading trace is shown in Figure 24, and the ordered or Lo-Hi maneuver loading sequence is illustrated in Figure 25.

7. Ordered composite gust and ground loading was simulated as sketched schematically in Figure 26, based on the 1/20 unit spectrum block size and 1000 psi stress interval. The load activity was the same as for the random composite tests in Reference 5 with approximately 11 to 12 gust loads per flight and approximately 6 to 7 taxi loads per flight. Test group CG4 had approximately 100 gust loads and 10 ground taxi loads per flight.

8. Random composite maneuver loading and ground taxi loading were simulated by running the master random maneuver tape during the flight portion and switching to the master gust random tape at the mean load level and amplification commensurate with ground taxi loads. The load activity was approximately 30 maneuver loads and approximately 35 taxi loadings per flight. A trace of this record is shown in Figure 27. Only those tests are used that were deemed of sufficient duration to provide adequate statistical sampling of both the maneuver and ground (gust) records.

The results of the fatigue tests conducted are tabulated and plotted in Appendix D, Part 2.

ANALYSIS OF THE COUPON TEST DATA

Miner's method was applied to the unit spectra using the specific S-N data for these coupons from Appendix D. The resulting predictions are compared with test results in Tables 4 and 5 and in Figures 37, 38, and 39. The fatigue life predictions by Miner's method for these coupons are in general less conservative than the results of the application of this method to the test data from the literature. This is illustrated in Figure 40 by the comparison of curve number 2 with curve number 1 taken from Figure 7 of Section III. The largest degree of unconservatism is shown for coupons of $K_T = 7.00$ loaded with the ground taxi spectra at compressive mean stress levels of $f_m = -3000$ psi. (Test group numbers T1 and T2.)

The effects of the shape of the loading spectra on fatigue life predictions by the Fatigue Quality Index method was investigated in two ways:

1. Adjustment of the Fatigue Quality Index by a function of the slope of the air loading spectrum in the high stress range.

2. Adjustment of the Fatigue Quality Index by a function of the slope of the air loading spectrum in the stress range of maximum fatigue damage as denoted by the largest cycle ratio $\left(\frac{n}{N}\right)_{max}$ in the unit loading spectrum.

The slope of the airloading portion of each test spectra is plotted as a function of the varying stress level for gust and maneuver type loading spectra in Figures 30 and 31, respectively, and for composite gust and composite maneuver load spectra in Figures 32 and 33, respectively.

The test results of Groups G74, G79, and G81 were selected to provide the empirical adjustment function for the variation of the Fatigue Quality Index with the slope of the test spectra. The test results of each of the three shapes of loading spectra in Figure 18 were used to derive the Fatigue Quality Index for the coupon specimen of $K_T = 4$. The geometric mean of the Quality Index for the test groups G74, G79, and G81 are plotted in Figure 28 as a function of the slope of the varying load spectra at 90% of the maximum peak load applied. Figure 29 is a graph of the same test derived Fatigue Quality Index values plotted as a function of the slope of the loading diagrams in the region of the stress level for maximum calculated fatigue damage, $(\frac{n}{N})_{max}$.

To predict the fatigue life of similar specimens tested under other types of loading spectra, the slope of the new unit loading spectrum is determined at the appropriate stress level, for example, at the level of 90% of the maximum applied load in the sequence. At this value of slope, the corresponding Fatigue Quality Index read from Figure 28 establishes the standard S-N curve set that is to be used in the prediction of fatigue life by the linear cumulative damage procedure. This is accomplished for twelve sets of data in Table 6, including low slope gust spectra, composite gust and ground load spectra, and composite maneuver and ground load spectra. These predictions are graphically compared with the corresponding test results in Figures 37 to 39. The degree of conservatism is indicated in Table 6 by the ratio of test fatigue life to predicted fatigue life. These degrees of conservatism are ranked in ascending order, and the percentage of the total number of samples equal to or less than a given degree of conservatism is determined and plotted as a function of that degree of conservatism as curve No. 4 in Figure 40.

The second procedure of adjustment is not quite so direct. As indicated in Table 7 and Figure 35, the stress level of the maximum cycle ratio $(\frac{n}{N})_{max}$ is a function of the Quality Index which, from Figure 29, is a function of the slope of the loading spectra at the stress level for maximum cycle ratio. The graphical procedure illustrated in Figure 36 was used to determine the compatible stress level, slope of the loading spectra, and Fatigue Quality Index. As an example, Figure 36 illustrates the procedure for Test Group No. G66. Arbitrarily chosen Fatigue Quality Index values were utilized to obtain the stress level at which the maximum cycle ratio exists for the unit loading spectra. These values of stress level are plotted as a function of the chosen Quality Index, K, in the center graph of Figure 36. The slope of the loading spectra is given as a function of the varying stress level in the graph to the left of Figure 36 (see Figures 30, 31, 32, and 33 for slope data from other loading spectra). Values of slope "h" and Quality Index "K" are determined at several trial varying stress levels a, b, and c, from the left and center graph as indicated, and these values are cross plotted on the right hand graph at points a, b, and c. The intersection of the interpolating curve abc with the curve of Figure 29 provides the value of the Fatigue Quality Index compatible with the other parameters as desired.

The adjusted value of the Fatigue Quality Index is used to predict fatigue lives of these specimens with the standard set of S-N data as in the normal procedure. Results of life predictions for thirteen of the sixteen groups of coupons of this series are given in Table 6. Two cases (G75 and G80) provided no compatible values. A third case (CM1) was of a slope beyond the range of the control test data of Figure 29 and was therefore omitted.

The comparison of these predicted results with their test results is given in Figures 37, 38, and 39. The ratio of the test life to the predicted life is determined, ranked, and the percentage of the total number of samples exceeding a given degree of conservatism is plotted as a function of that degree of conservatism as described previously. This is Curve No. 5 in Figure 40.

The basic version of the Fatigue Quality Index procedure was also applied to these coupon data. The Fatigue Quality Index values, derived from the 26 groups of coupon test results by the use of the standardized S-N curves, are listed in Tables 8 for simple gust type spectra of various shapes and in Table 9 for the simple fighter maneuver and the ground-taxi type of loading spectra, and for the composite gust and the composite maneuver flight type of loading spectra. The minimum, the maximum, and the geometrical mean of the test derived Fatigue Quality Index are given. In addition, the FQI value from the first specimen of each group is given. Its purpose is to assess the effectiveness of a reduced number of test results in the evaluation of other loading spectra on similar specimens. This is of importance in consideration of large size specimens, components, and full-scale airframe tests in which only one specimen may be economically feasible.

Comparison may be made of the results of Test Groups G66 through 69 which are low peak load, low slope gust spectra (at a low mean stress level) with those of Test Groups G72 through G75 which are high peak load, high slope gust spectra (with a high mean stress level) on the same type specimen ($K_T = 4.$). This comparison indicates a considerable variation in the derived Fatigue Quality Index. A life prediction derived from a test of the low slope variety of gust spectrum would under-predict the result of the high slope gust spectrum whereas the reverse situation would provide an unconservative prediction. It was not possible to evaluate the results of the specimen of $K_T = 7.0$ because the derived Fatigue Quality Index, in most cases, exceeded the maximum scale value of $K = 8.0$.

The comparison of the test derived FQI values for the first specimen of each of these two simple gust groups shows a similar trend. For the low slope spectra the geometric mean of the first specimen FQI values is 5.46 which compares well with the geometric mean of the means of all specimens of this group which is $K = 5.45$, even though by chance the first specimen of the first group was the maximum value of all in this group. The similar comparison for the high slope group has a geometric mean of the first specimen of $K = 4.43$ to compare with the geometric mean of the means for all the specimens of this group of $K = 4.53$. The first specimen basis for life predictions in this case would be only slightly unconservative.

The two groups G78 and G79 (concave upward loading spectra) and G80 and G81 (concave downward loading spectra) show a somewhat reversed trend from that discussed above in that the concave upward group has a relatively higher Fatigue Quality Index value although this spectra has higher peak stresses and slope than the concave downward loading spectra.

The simple fighter maneuver spectra test results from groups M14, M15, and M16 show derived Fatigue Quality Index values more closely approximating the concave upward gust spectra (group G78 and G79) than any of the others. However, the results of these simple maneuver spectra encompass the widest scatter of all the groups. The values of the Fatigue Quality Index range from the minimum of K = 3.60 to the maximum of K = 7.10.

The derived FQI values for the composite test results bear no close correspondence to their counterparts in the simple spectrum groups. From Tables 8 and 9, compare, for instance, groups G66 through G69 with composite gust Group C01 (low slope spectra) and groups G72 through G75 with composite gust groups C03 and C04 (high peak, high slope spectra), and the fighter maneuver groups M14, M15 and M16 with the composite maneuver group CM1. Fatigue life predictions are made in Table 10 for the composite loading spectra by the use of the derived Fatigue Quality Index value from the first coupon specimen result of the corresponding simple spectra of flight loads. As indicated these results were unconservative in the composite tests by approximately 12% of the predicted value for the low slope gust spectra, 43 to 60% of the prediction for the high slope gust spectra and 33% of the prediction for the maneuver spectra. Comparisons in Tables 4 and 5, of the fatigue life predictions for these same groups by Miner's method utilizing the specific S-N curves for these coupons show only moderately improved predictions. This is a fundamental result inherent in the test data which none of the life prediction methods studied in this report can cope with in their current form.

To determine the effectiveness of a Fatigue Quality Index derived from a gust test spectra as a means of predicting the fatigue life of coupons under maneuver type spectra, Table 11 was prepared. This comparison indicates results ranging from relatively conservative predictions to values of test results of half the predictions. While this range of the ratios of test life to predicted life is within the normal scatter band of other prediction methods, this data group is much too small for reliance.

An unexpected result of this series of tests is indicated in the comparisons shown in Table 12. The flight portion of the composite spectrum tests is compared with the simple spectrum test results for corresponding types of loading. The ratio of the number of cycles of flight loadings in the composite spectrum test to the number of cycles of loading in the simple spectrum test may be considered to be the damage fraction for this portion of the loading. Assigning the remaining fraction $(1-\Sigma D_{(flight)})$ to the rest of the loadings and noting that the damage due to ground taxi loadings is relatively small, the ground-air-transition cycle is seen to be a predominant producer of fatigue damage. This portion of the loading is seen to provide approximately 50% to 73% of the total damage ratio for this series of tests. The importance of this transition cycle is thus established on an experimental basis. Reviewing the results in Table 5 of the simple linear cumulative damage procedure (Miner's method) utilizing the specific S-N data for these specimens indicates that the effect of the ground-air transition cycle is not predictable by this method either. The test results vary unconservatively from approximately 24% to 86% of the predicted value.

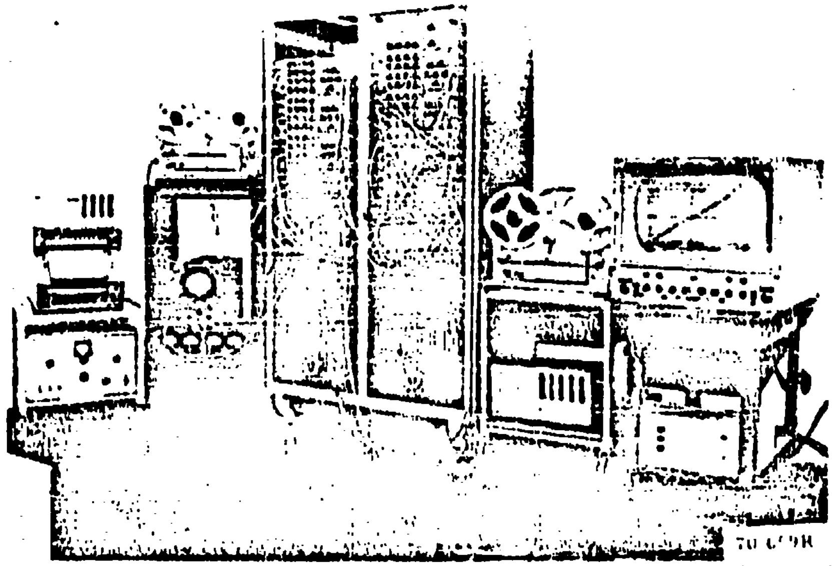

Figure 11 General View of Tape Handling Equipment

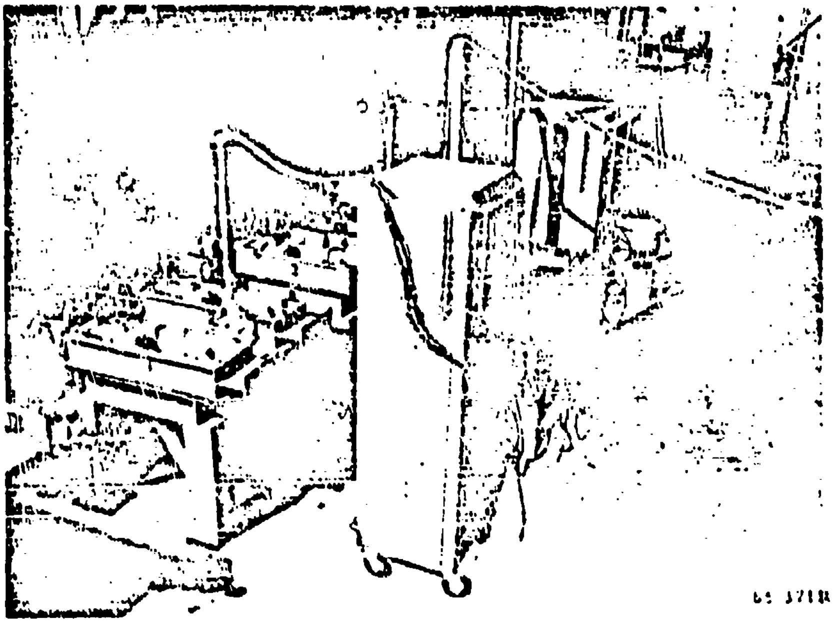

Figure 12 General View of Specimen Loading Apparatus

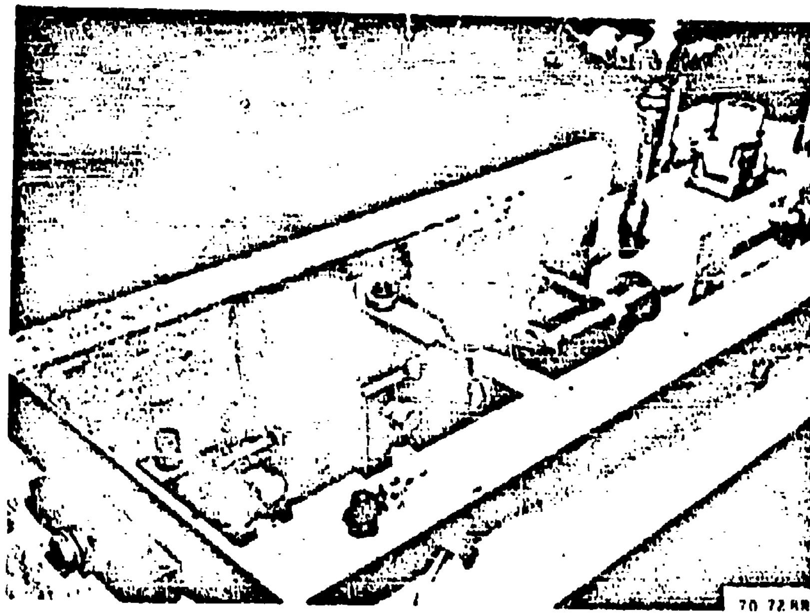

Figure 13 Close-up of Test Specimen Installation

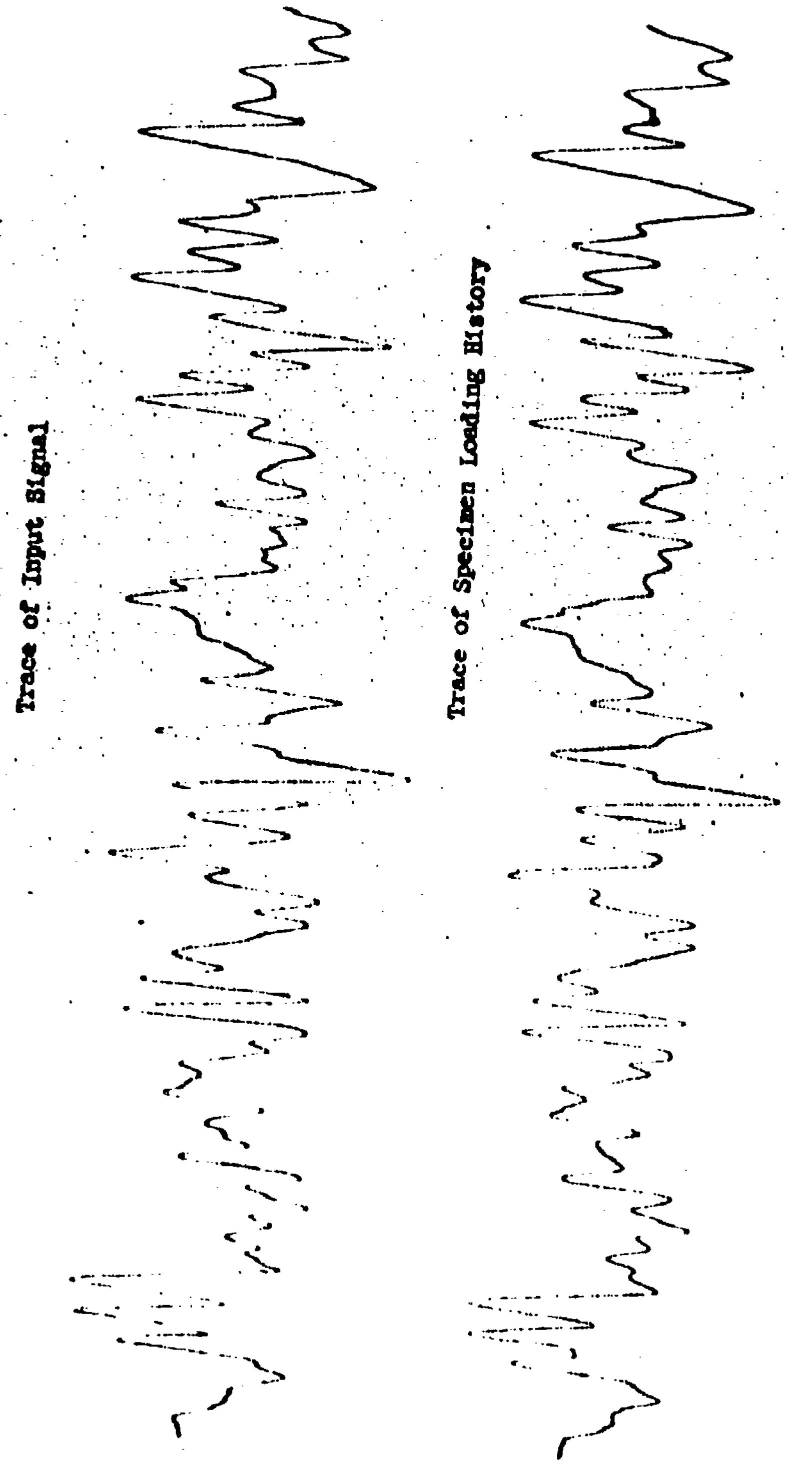

Figure 14 Comparison of Servo Valve Input Signal with Specimen Loading History

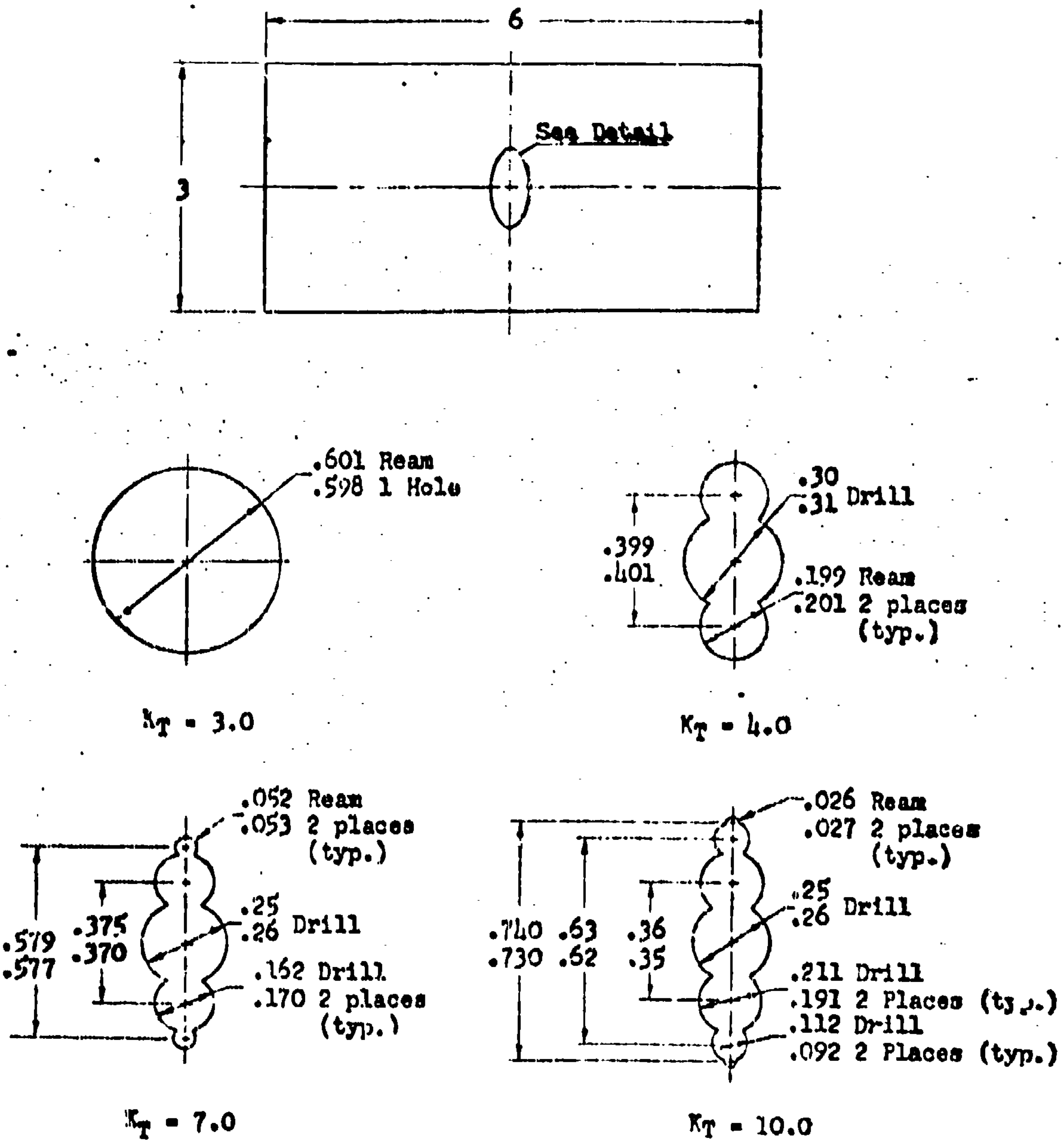

Note: All Dimensions Given In Inches

MATERIAL: 7075-T6 Bare Aluminum Alloy Sheet (.04 inches thick)
FABRICATION: Specimen Blanks Sheared to Size
Holes Drilled and Reamed
Burrs Removed by Light Stoning

Figure 15. Notched Sheet Test Coupons

Figure 16 Sample Flight Loading Trace

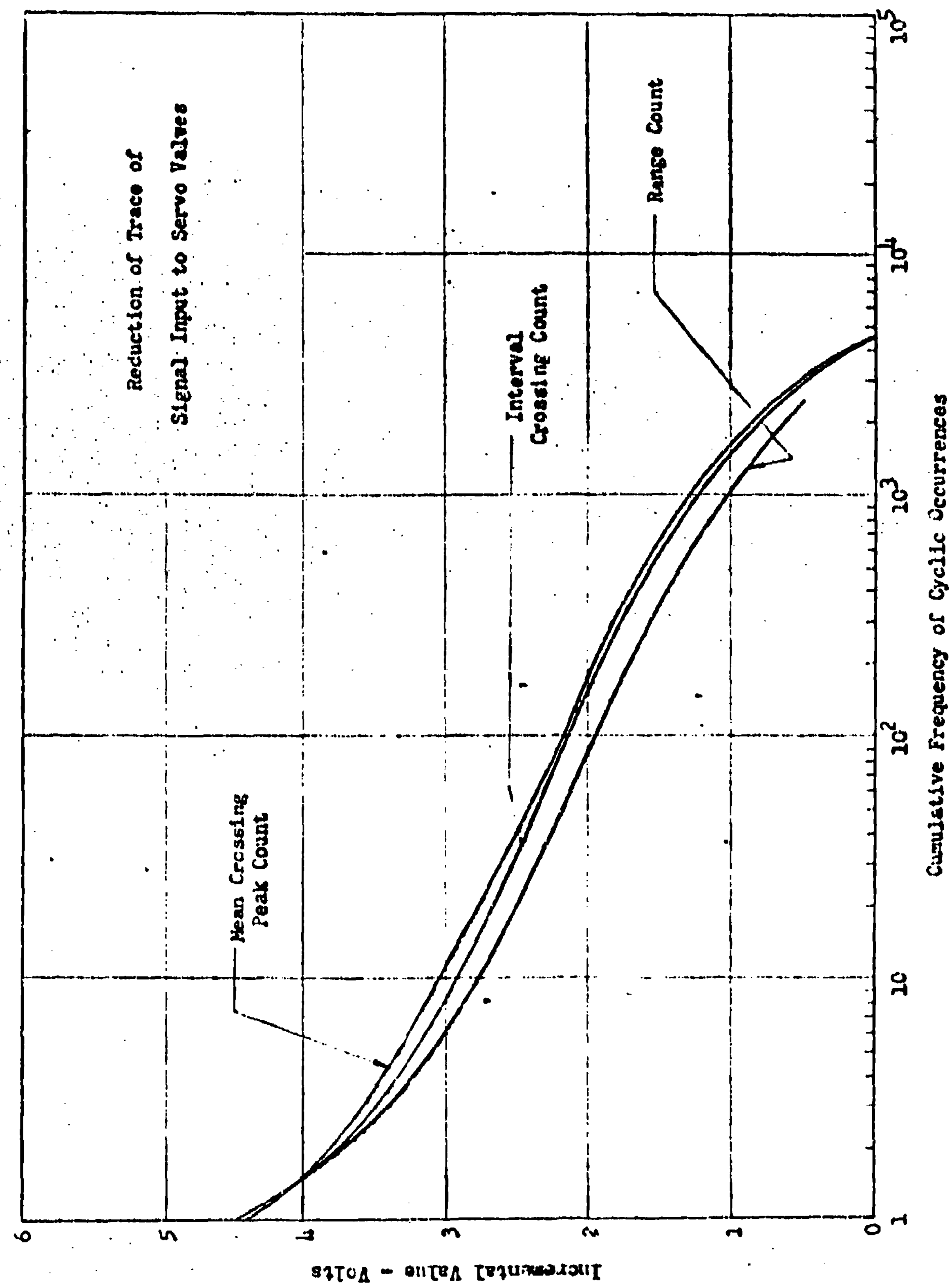

Figure 17 Comparison of Trace Reductions - Wing Root Random Loading Trace

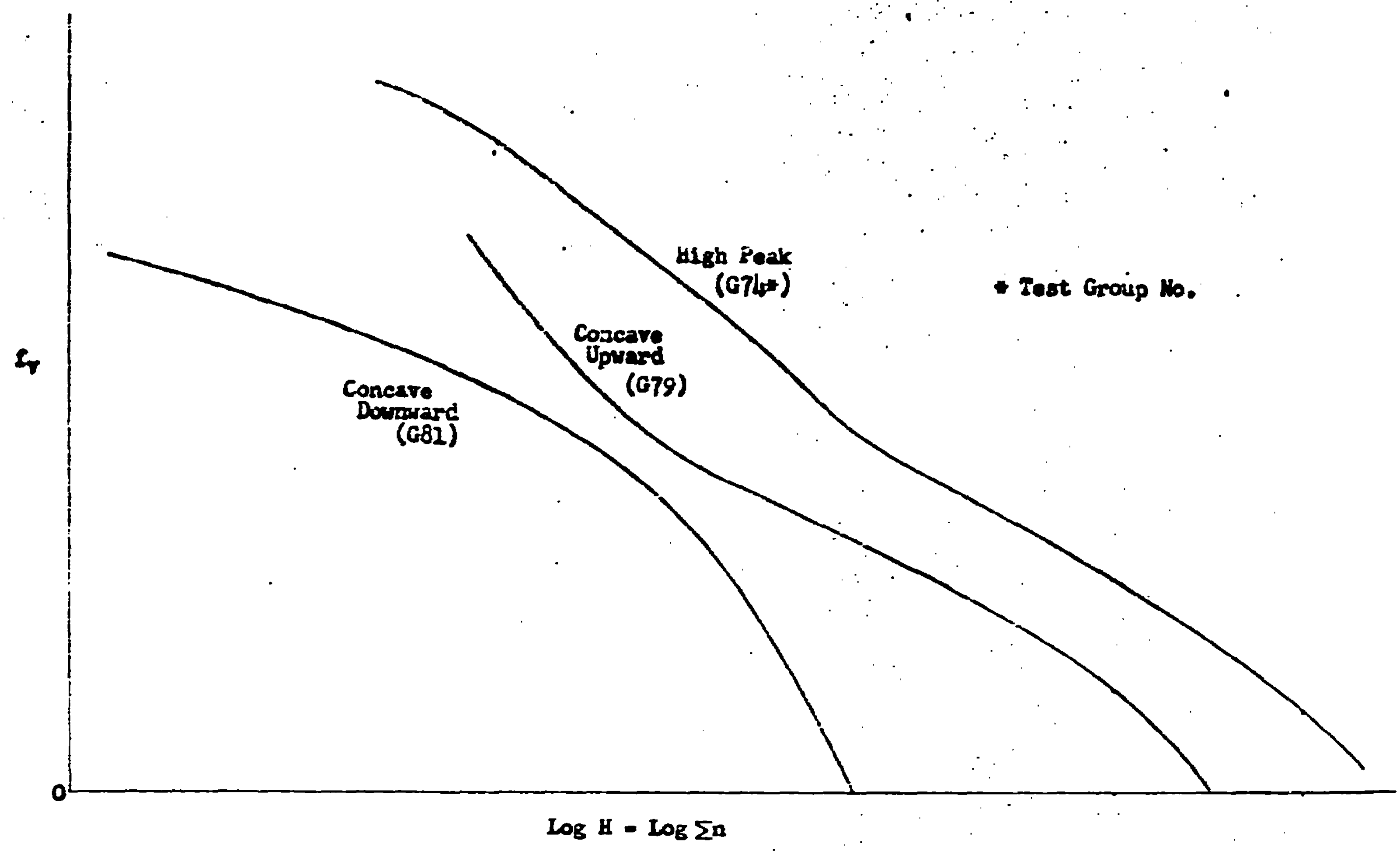

Figure 13. Schematic of High Peak, Concave Upward and Concave Downward Gust Loading Spectra.

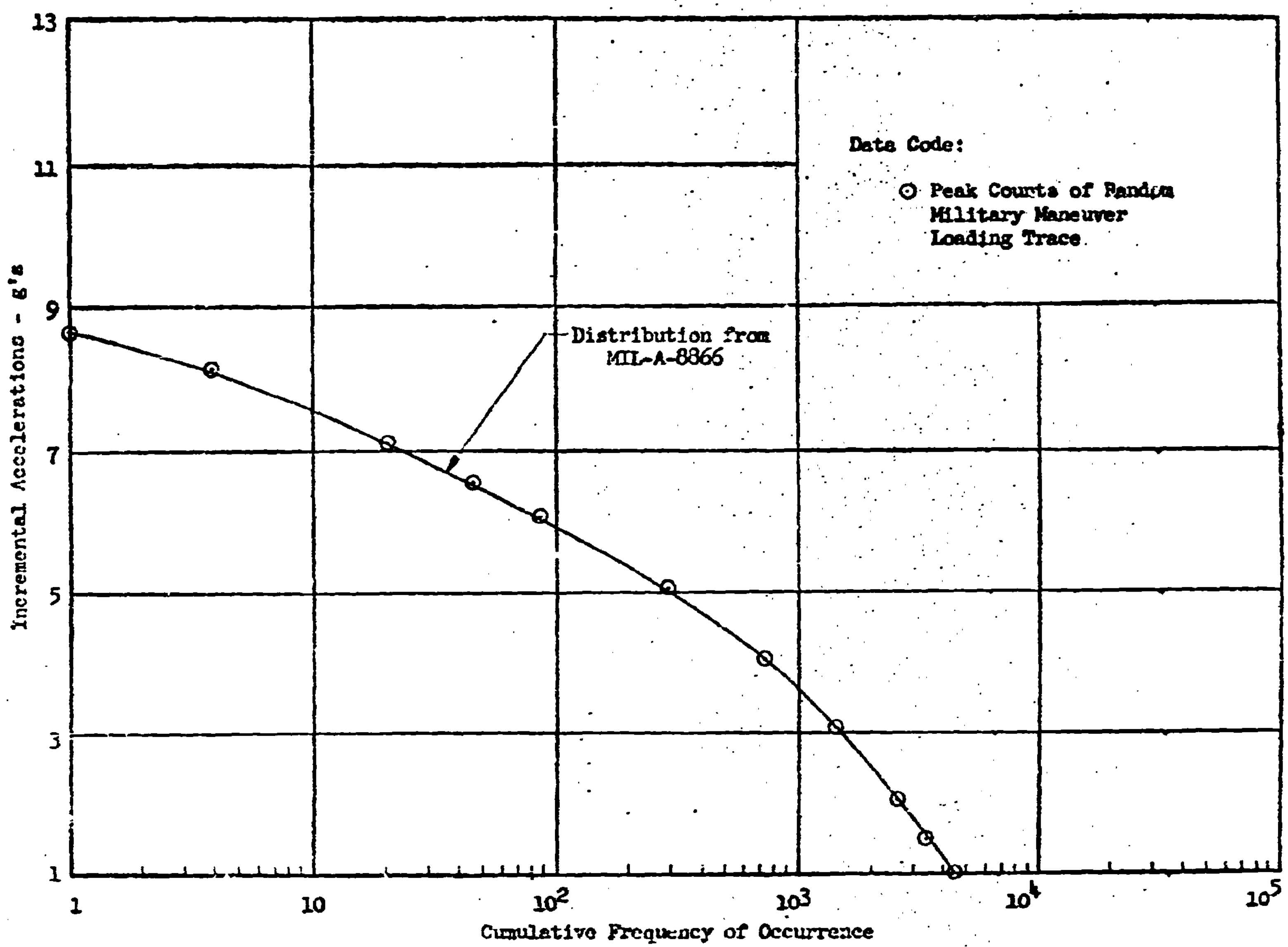

Figure 19 Comparison of Military Maneuver Loading Spectrum with Distribution Specified in MIL-A-8866 for Class "A" Aircraft

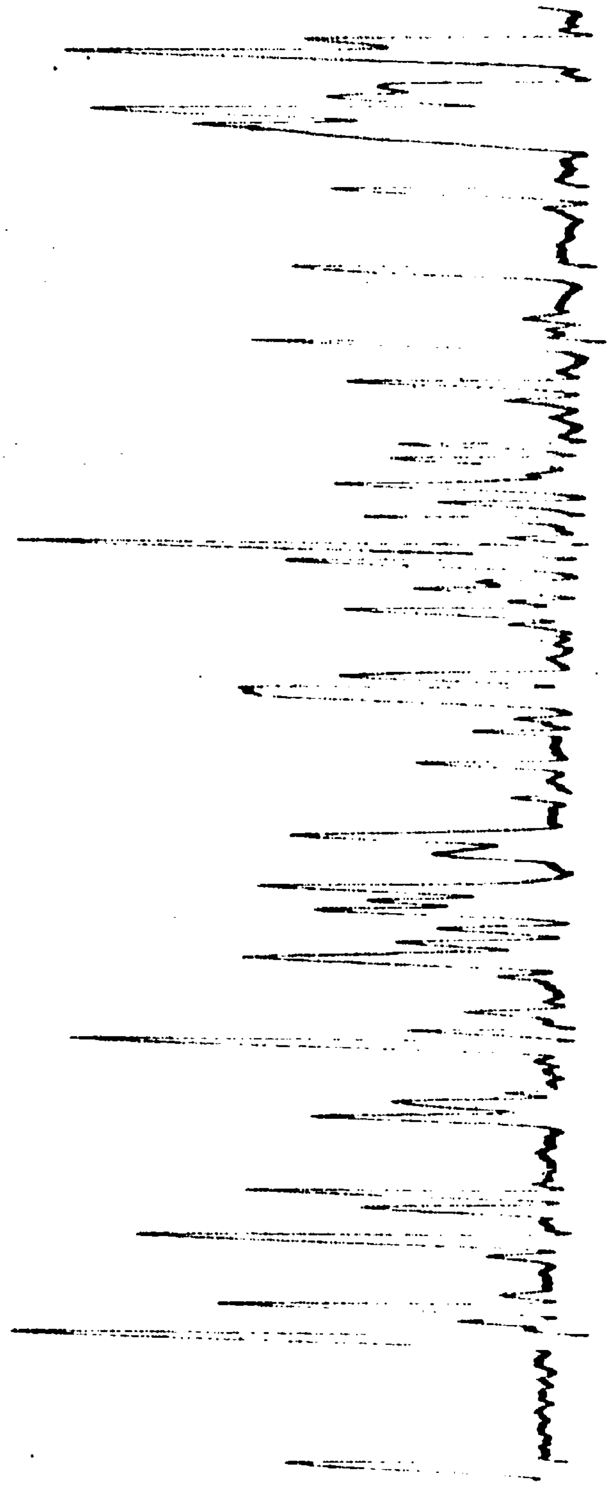

Figure 20 Sample of Random Military Maneuver Loading Trace

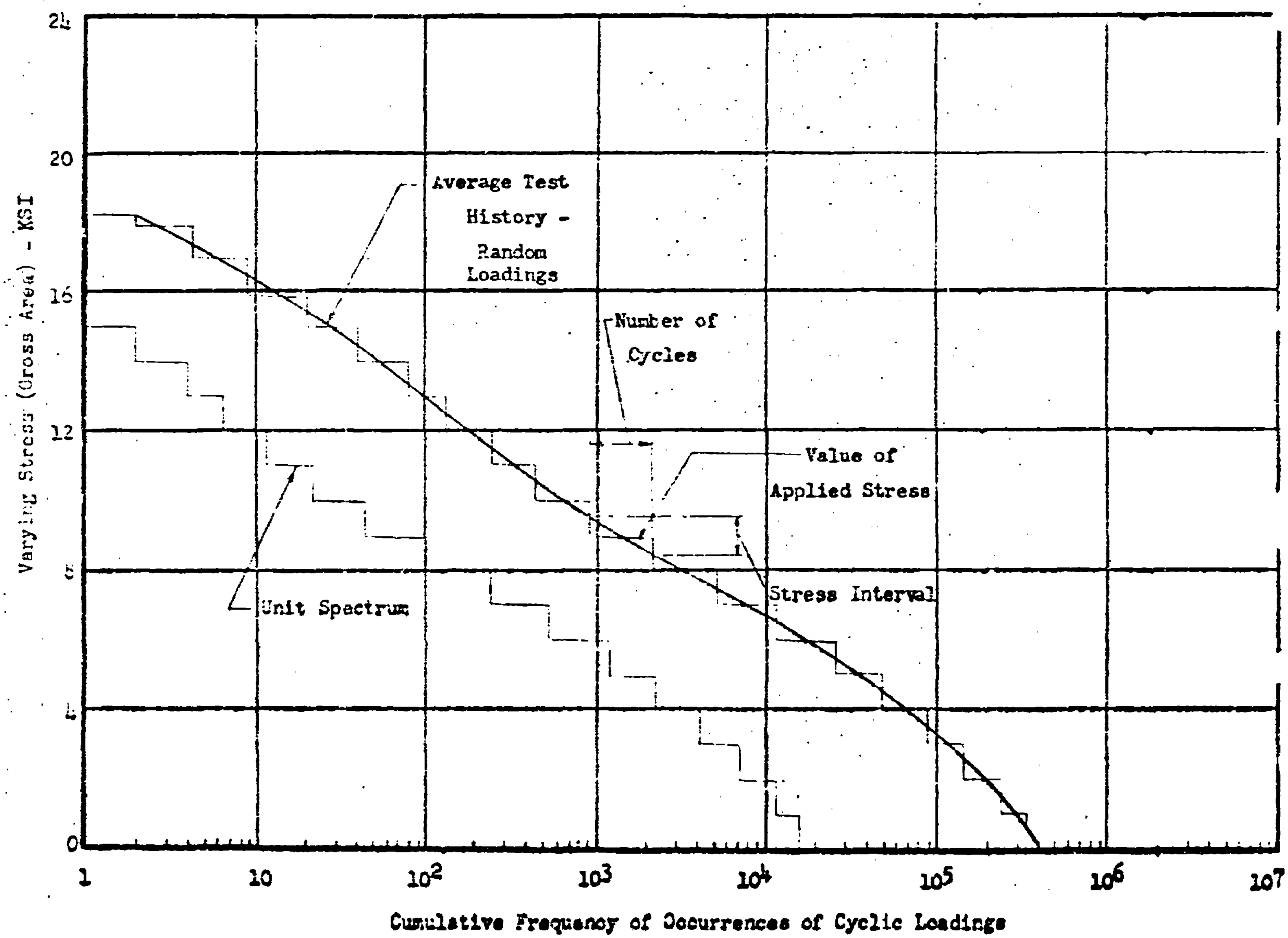

Figure 21 Development of Ordered Loading Spectrum

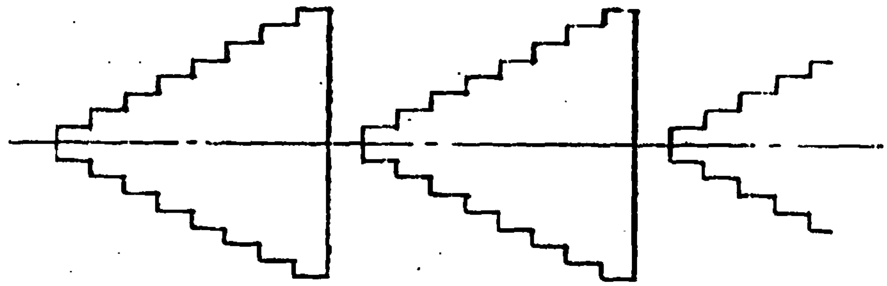

Low-High Sequence, Small Stress Interval, Small Unit Spectrum

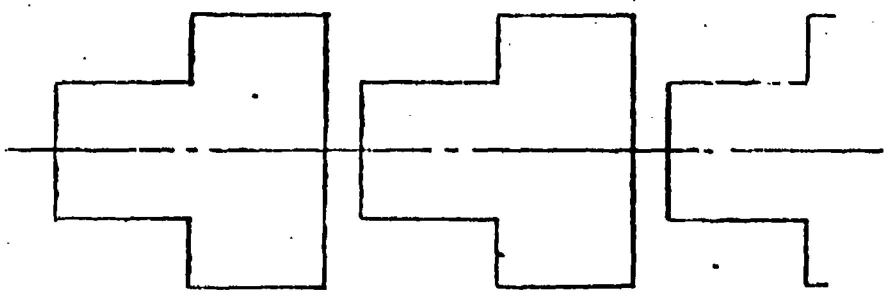

Low-High Sequence, Large Stress Interval, Small Unit Spectrum

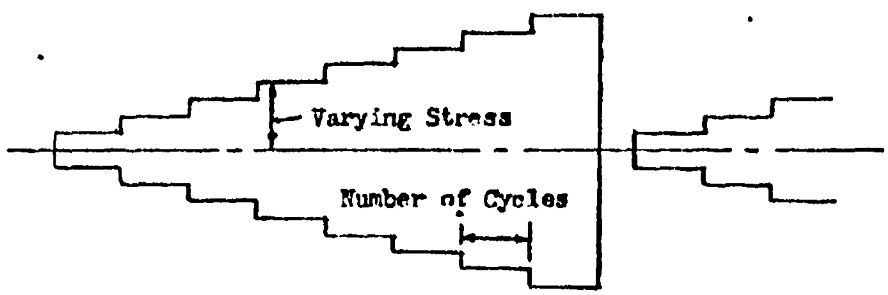

Low-High Sequence, Small Stress Interval, Large Unit Spectrum

Figure 22. Schematic Representation of Sequence Stress Interval, and Unit Spectrum Size

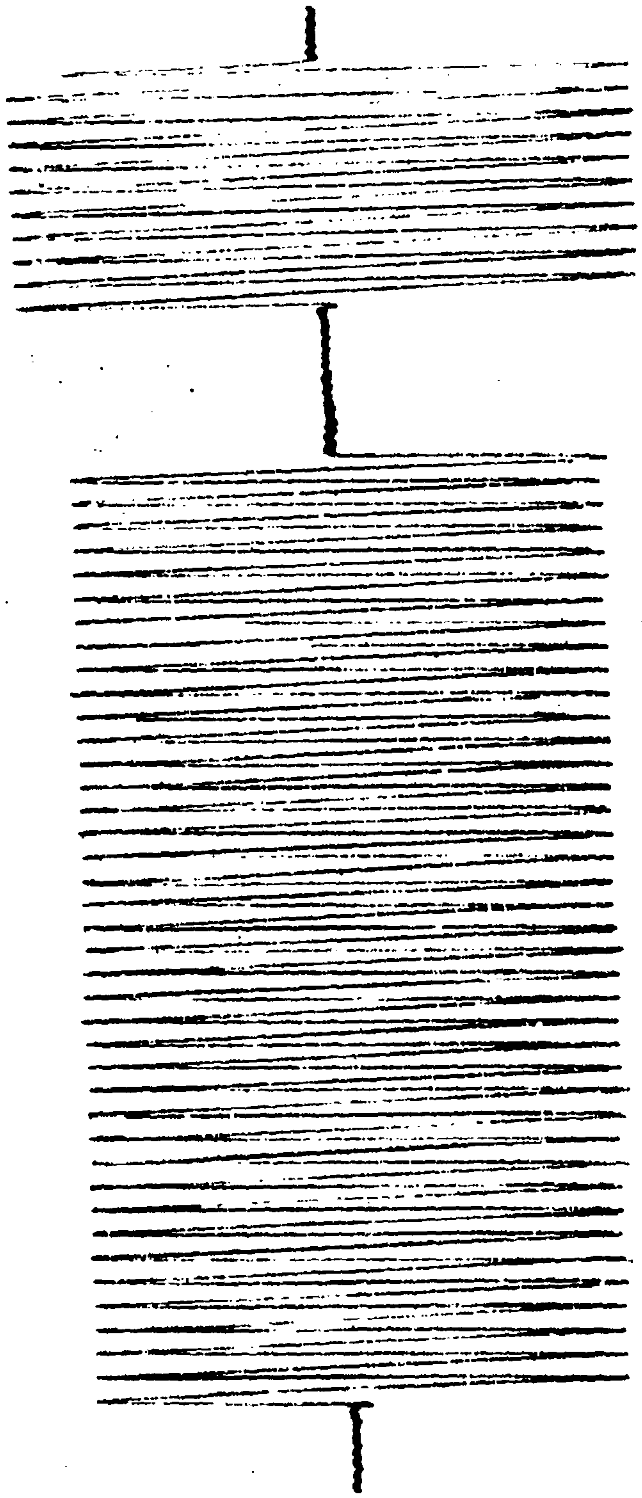

Figure 23 Partial Trace of an Ordered Gust Loading History

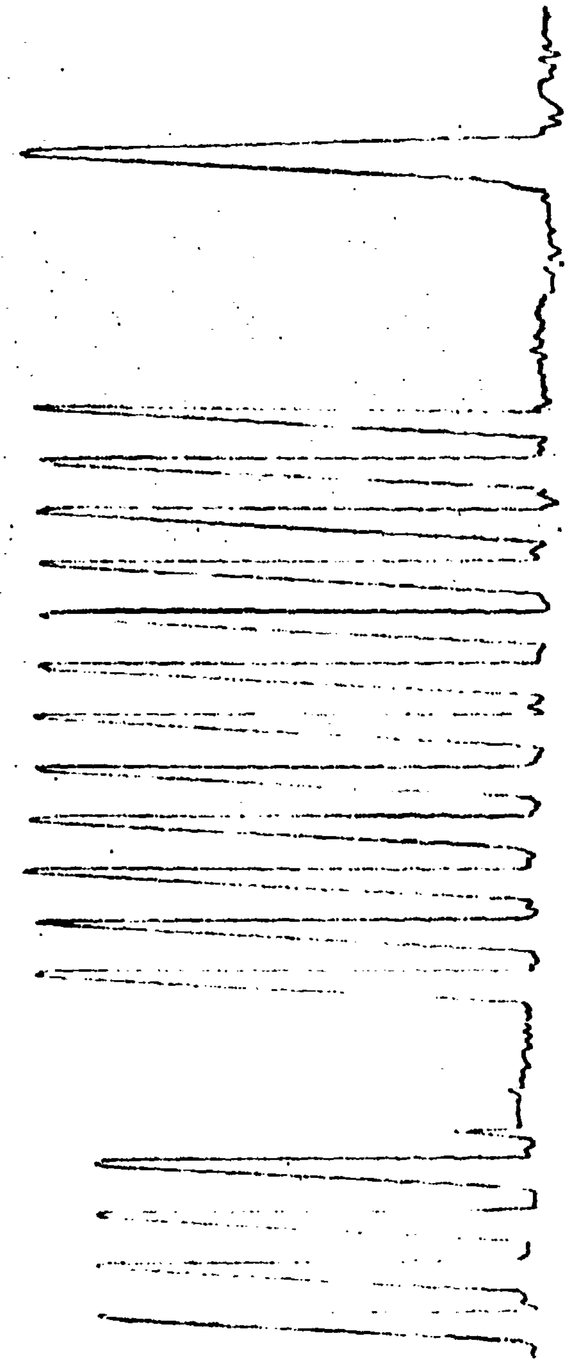

Figure 24 Sample of Ordered Military Maneuver Loading Trace

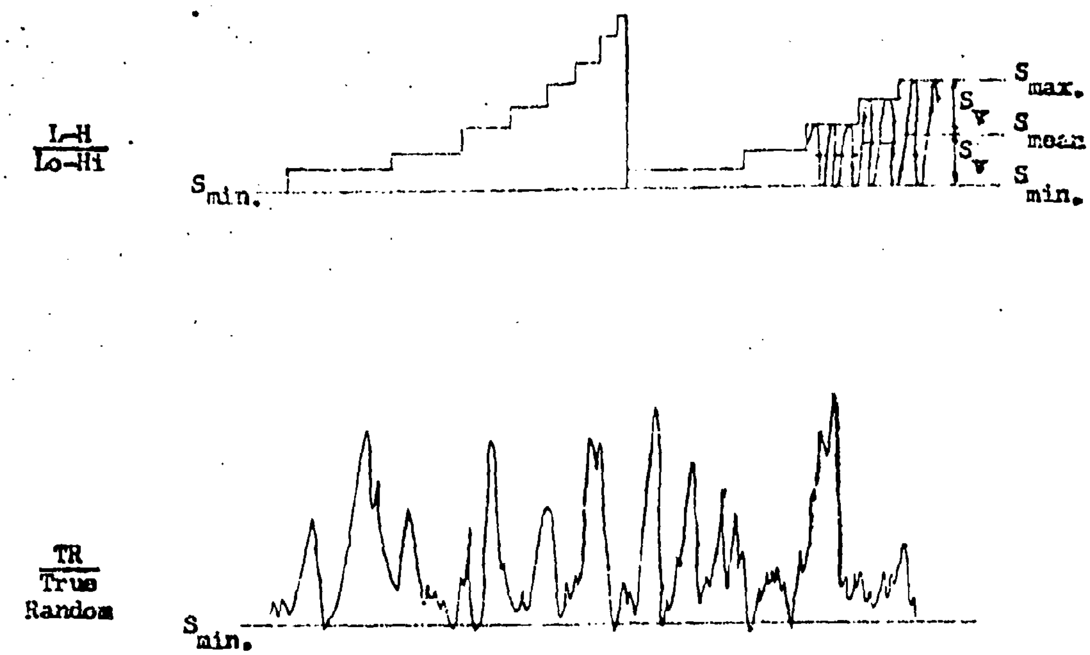

Figure 25. Schematic Diagrams of Maneuver Loading Sequences for Coupons

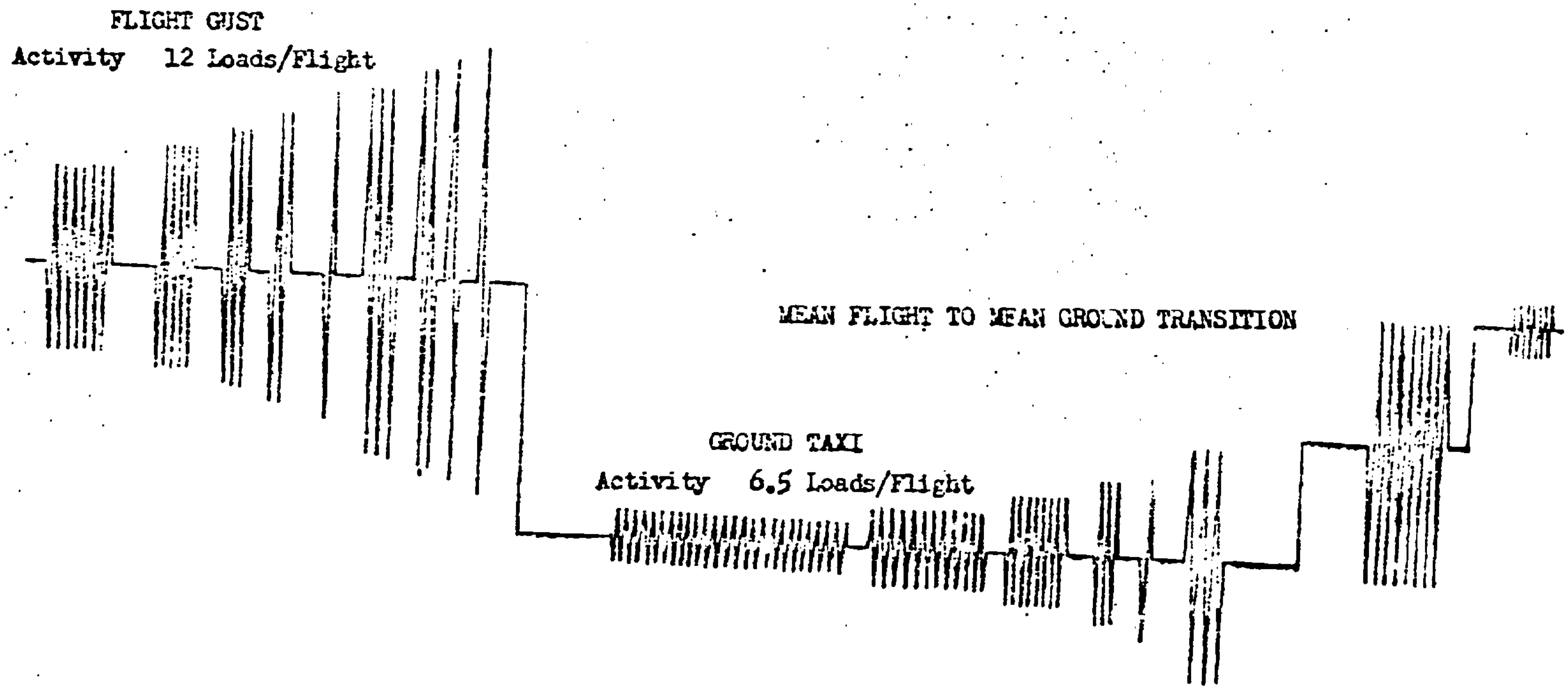

Figure 26 Schematic Representation of Ordered Loading Trace — Gust and Ground Loadings plus Ground-to-Air Cycles.

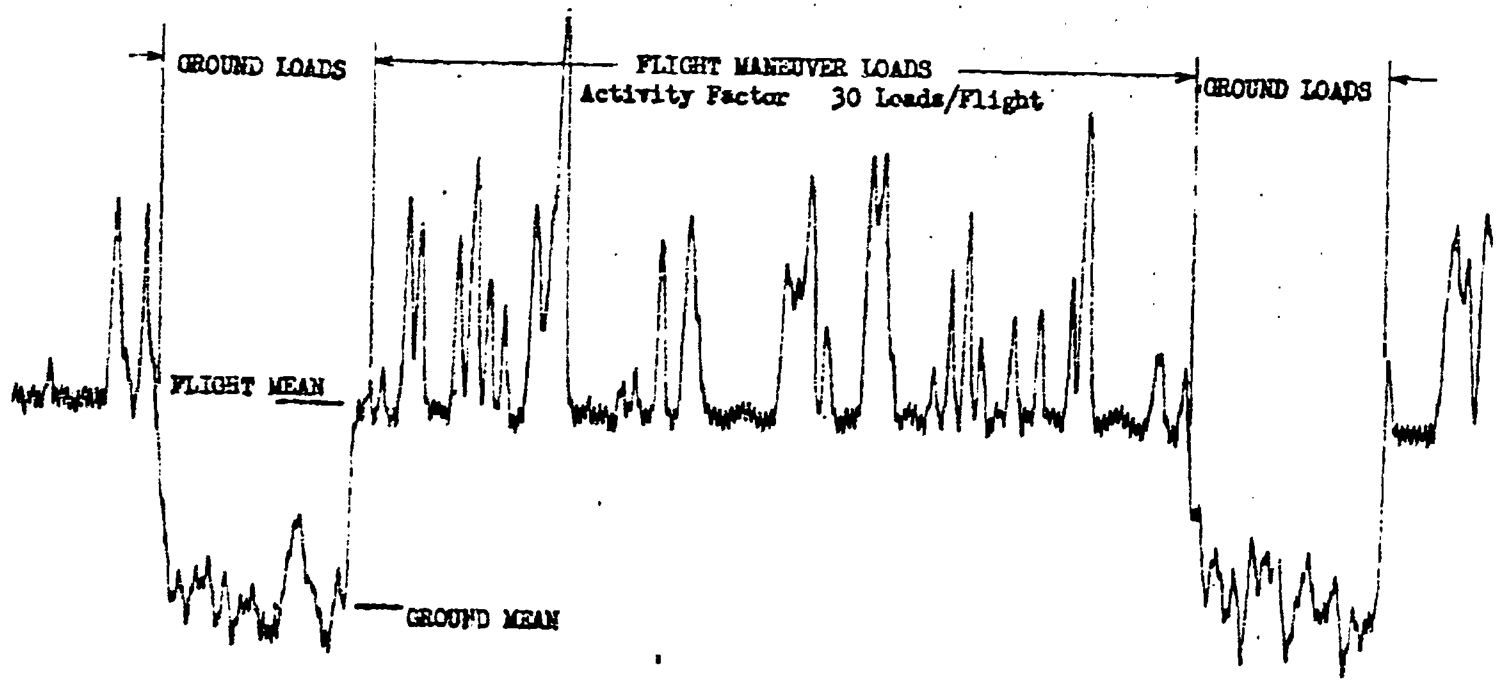

Figure 27 Sample Random Loading Trace - Composite of Military Maneuver and Ground Loadings

TABLE 4

FATIGUE LIVES PREDICTED BY MINER'S METHOD FOR GUST SPECTRA ON COUPONS

Test Group No.	Sequence	Geometric Mean of Test Life (10^6 cycles)	Predicted Life (10^6 cycles) Miner's Method	N_L Test / N_L Pred.
066	True Random	1.650	4.296	.384
067	Lo-Hi	1.230	.668	1.841
068	Lo-Hi	4.165	3.074	1.355
069	Lo-Hi	6.005	3.178	1.890
070	True Random	.229	.484	.473
071	Lo-Hi	.255	.518	.492
072	True Random	.359	.290	1.238
073	Lo-Hi	.248	.099	2.505
074	Lo-Hi	.579	.353	1.640
075	Lo-Hi	.274	.196	1.398
076	True Random	.057	.057	1.000
077	Lo-Hi	.058	.055	1.055
078	True Random	.270	.317	.852
079	Lo-Hi	.804	.453	1.775
080	True Random	.193	.082	2.354
081	Lo-Hi	.144	.052	2.769

UND,

N_L Test / N_L Pred.
1.780
1.133
.769
.078
.112
.271
.238
.597
.862
.611

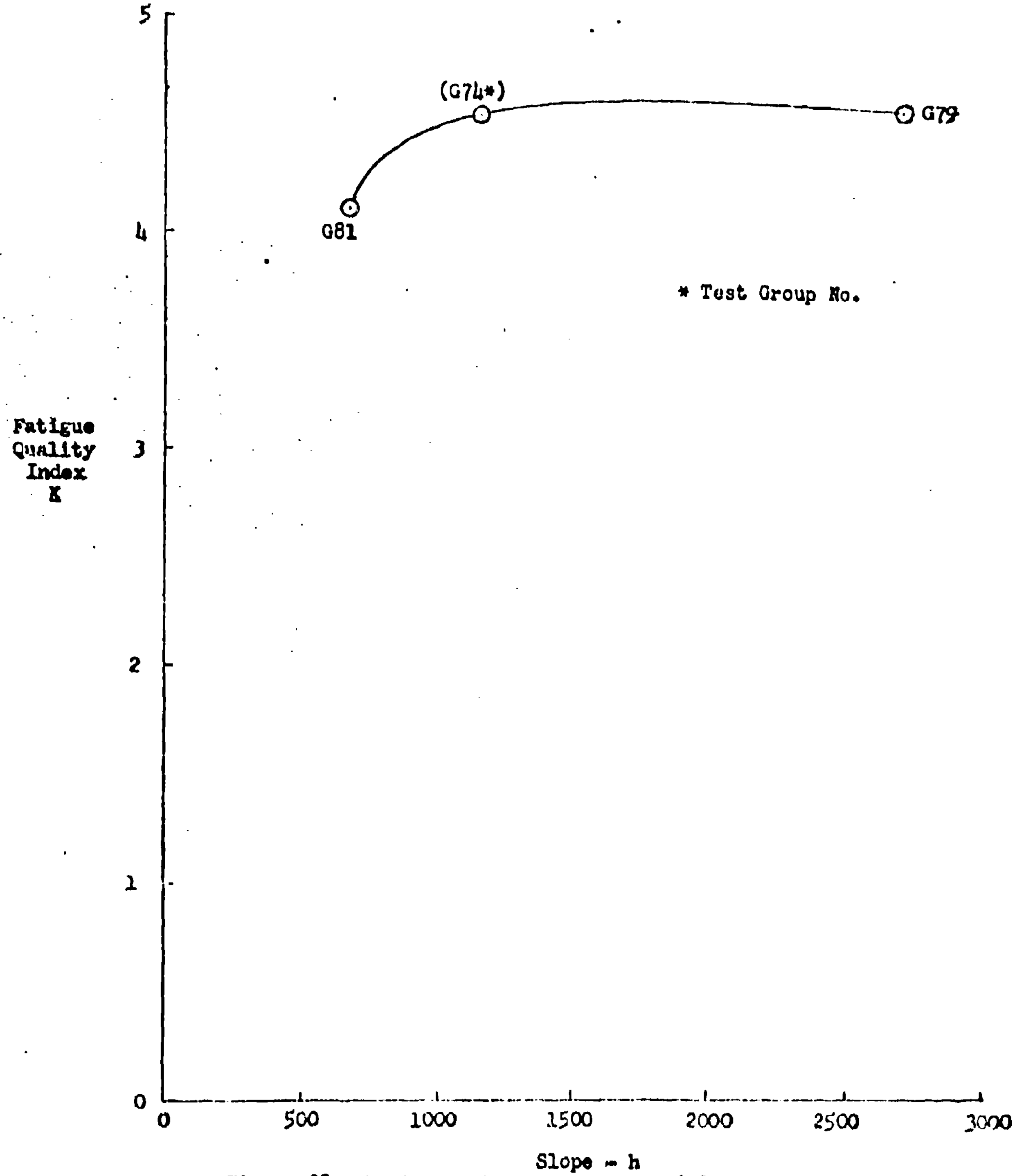

Figure 28. Variation in Quality Index (K) with slope of gust loading spectra in the high stress range.

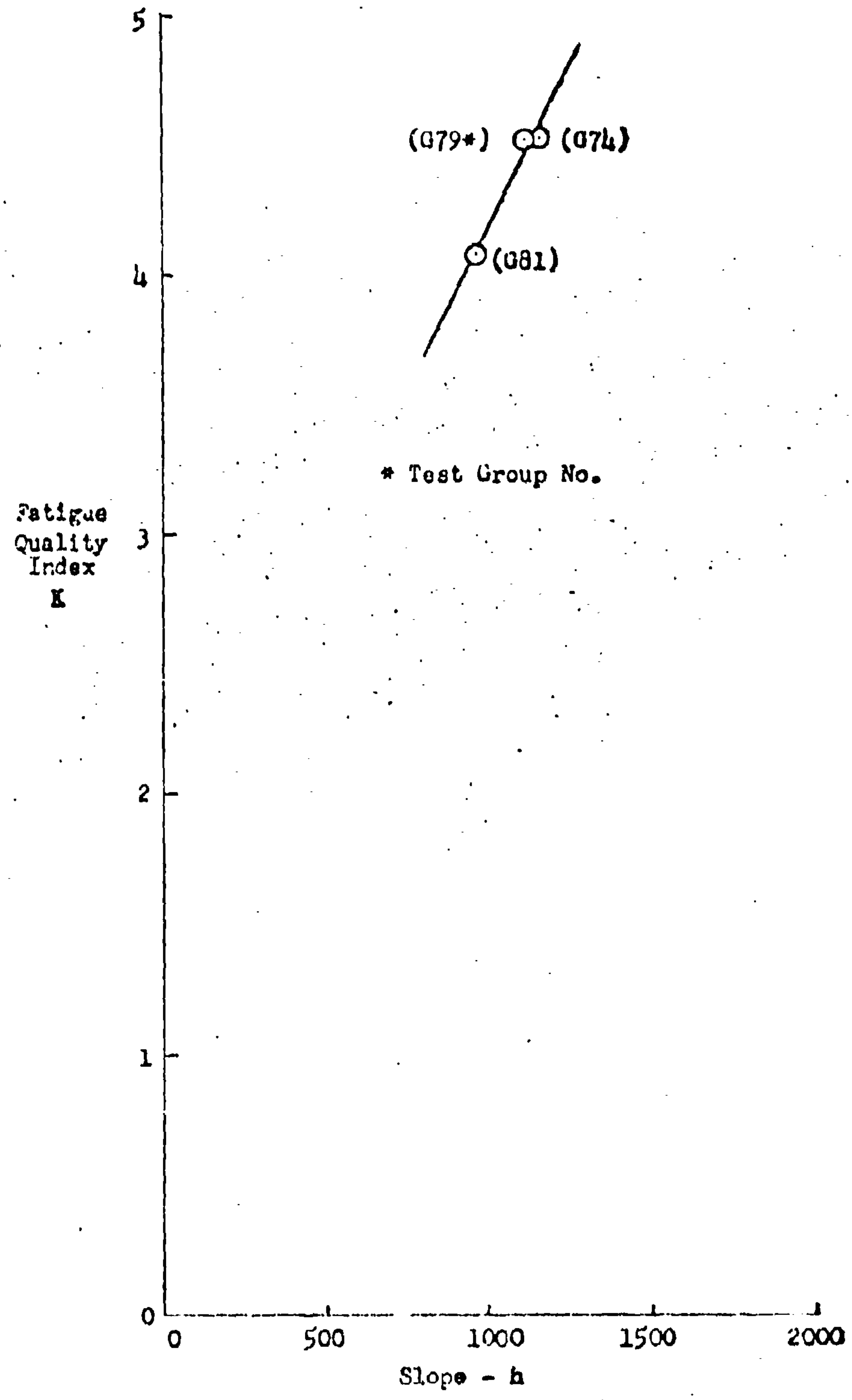

Figure 29 Variation in Quality Index (K) with Slope of Gust Loading Spectra in Midstress Range of Maximum Calculated Fatigue Damage.

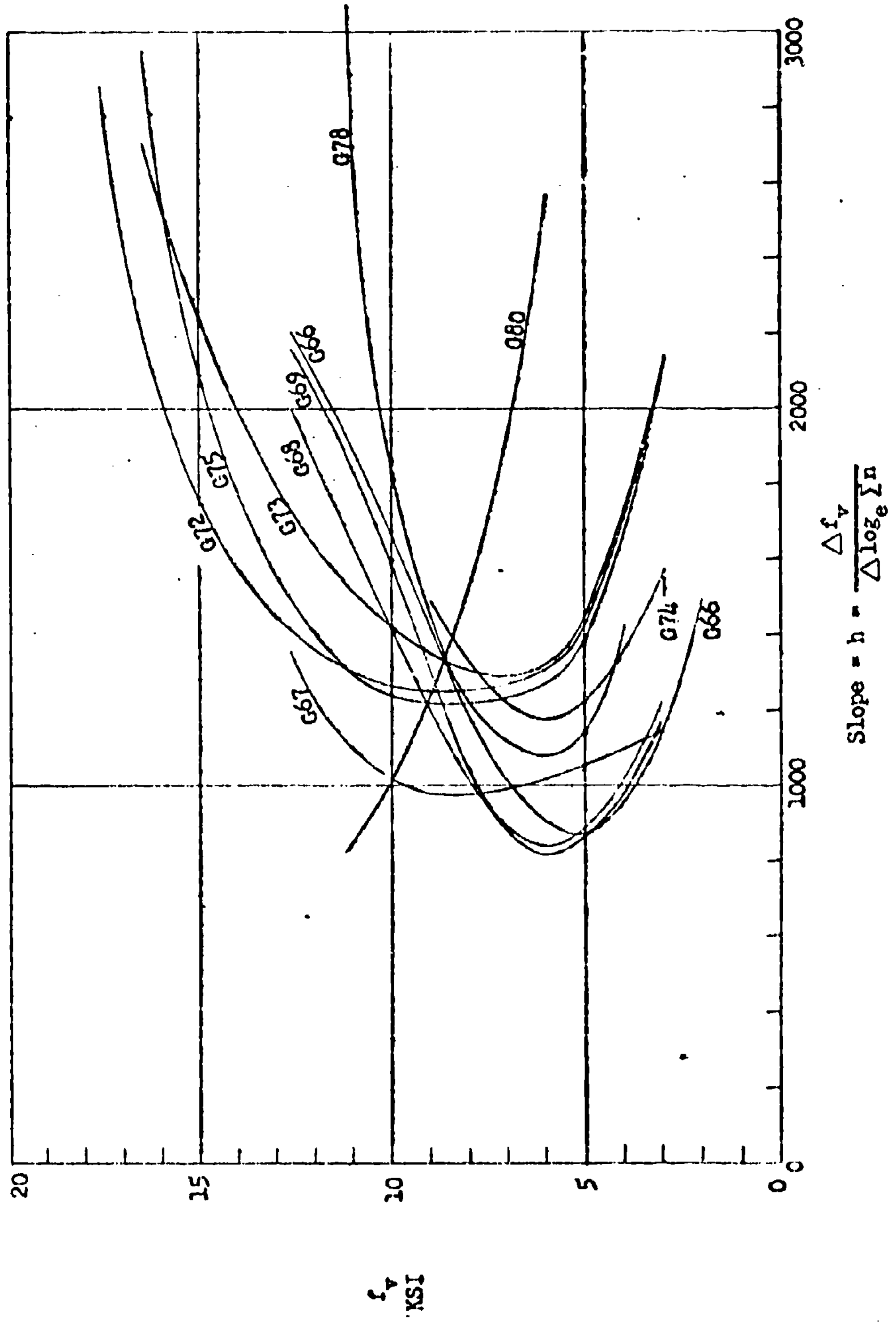

Figure 30. Varying Stress versus Slope of Gust Loading Spectra

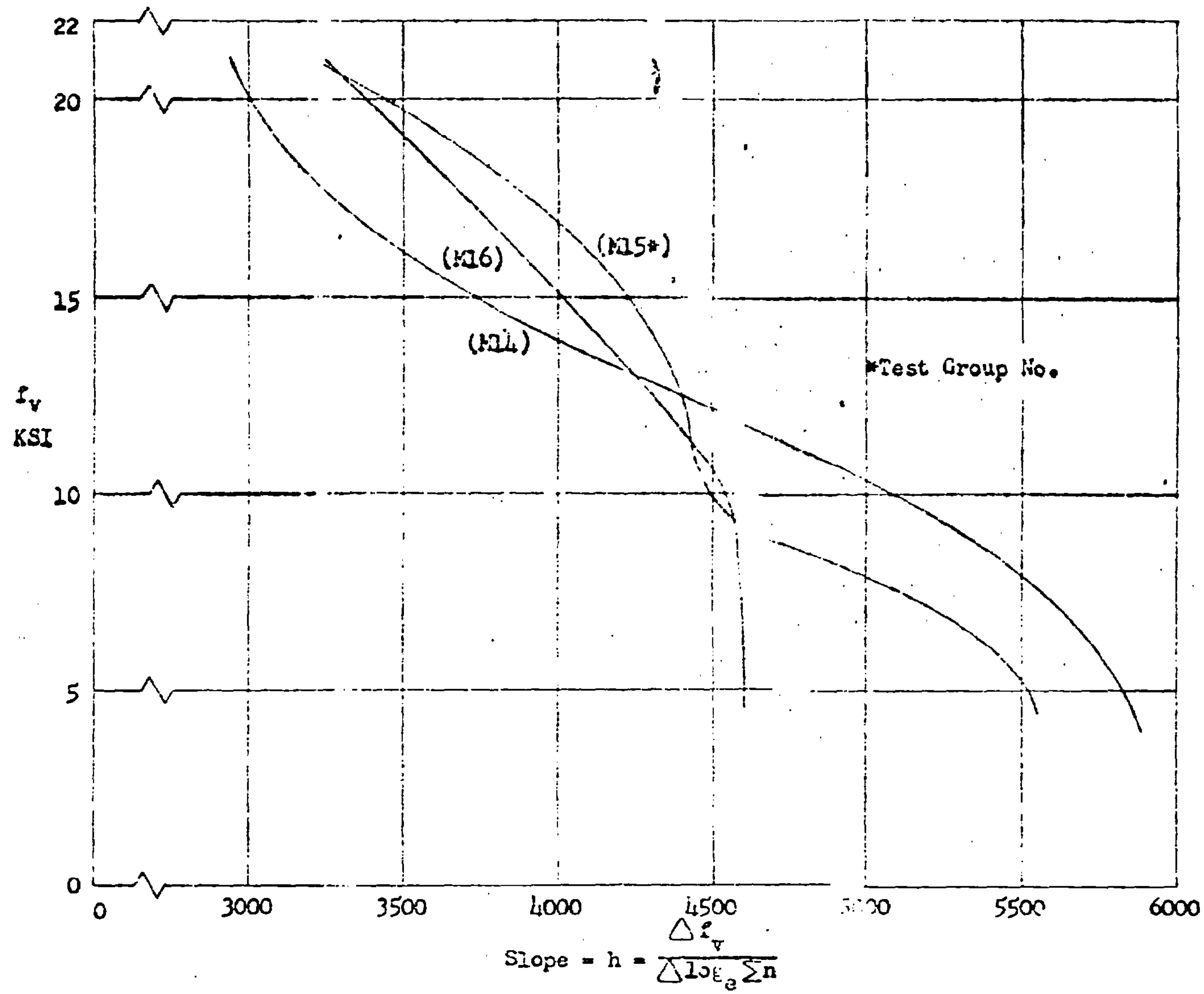

Figure 31 Varying Stress versus Slope of Maneuver Loading Spectra

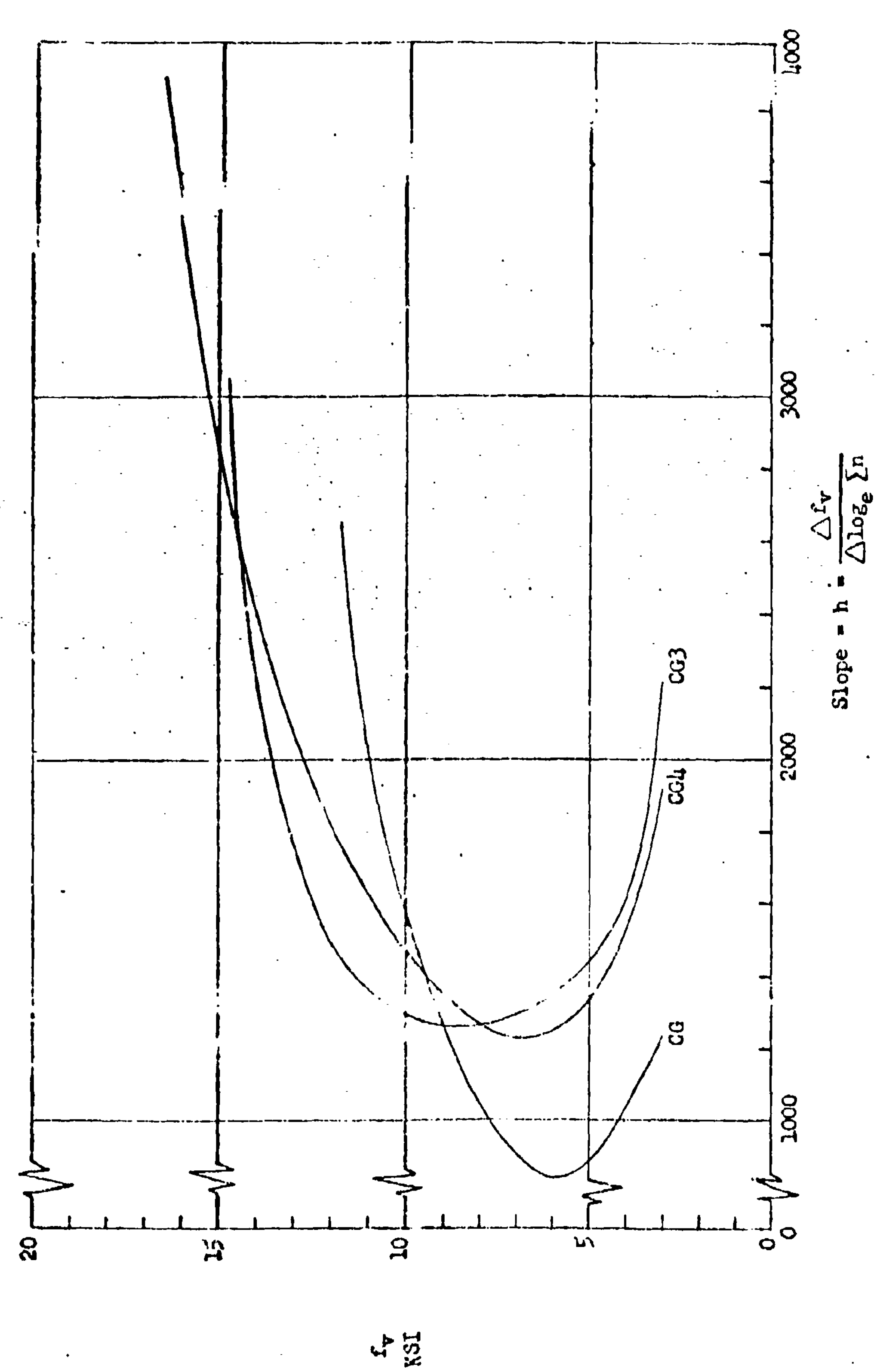

Figure 32 Varying Stress versus Slope of Composite Gust Loading Spectra

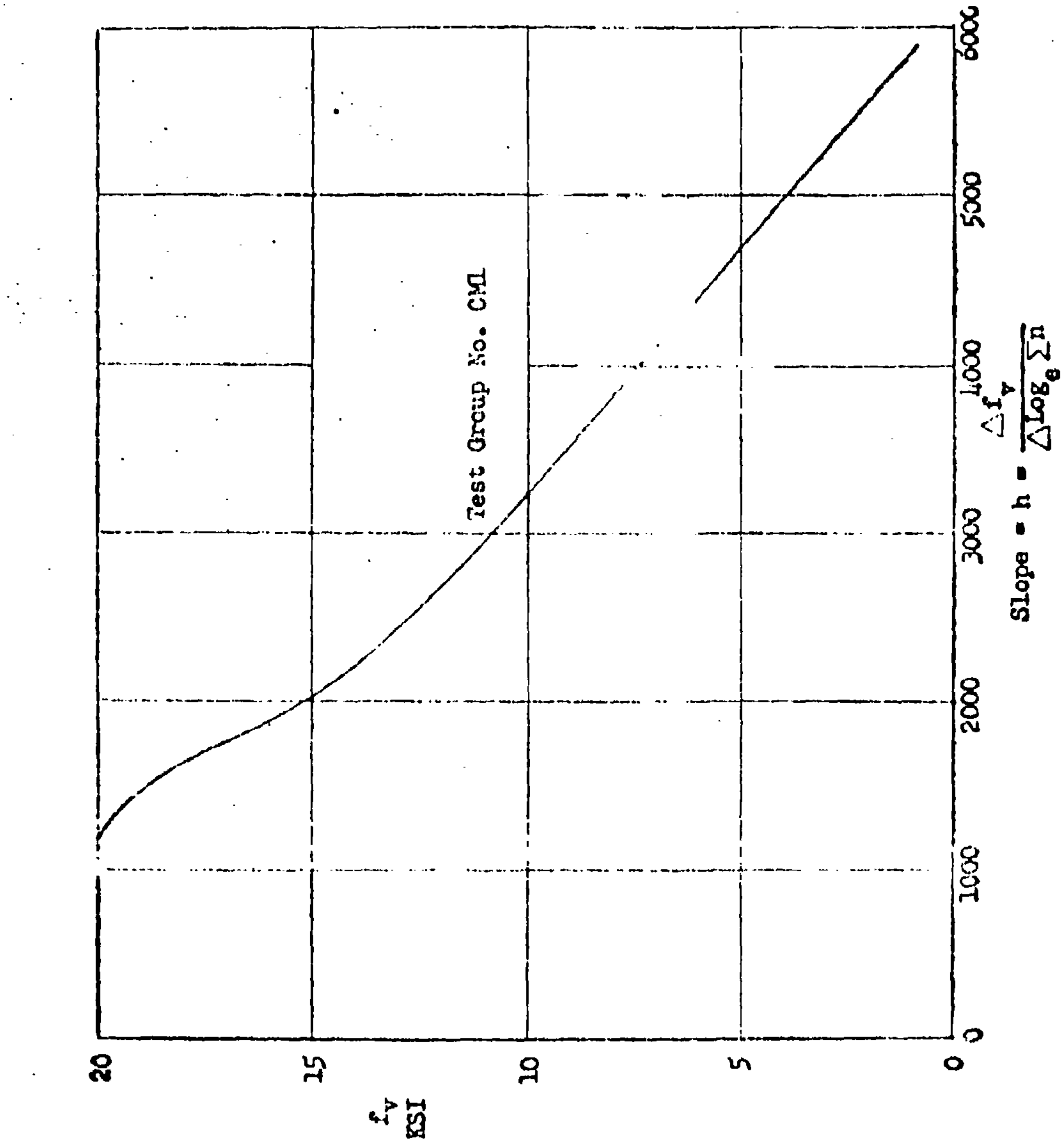

Figure 33. Varying Stress versus Slope of Composite Maneuver Spectrum

TABLE 6

FATIGUE LIVES PREDICTED FOR COUPONS WITH ADJUSTMENTS IN K FOR SLOPE OF LOADING SPECTRA

Test Group No.	f_{mean} KSI (Air Load Only)	Geom. Mean of Test Life (10^6 Cycles)	Midstress Slope Adjustment (a) f_v KSI Max. Cal. Dam.	h_{af_v} $\frac{\Delta psi}{\Delta Log \Sigma n}$	K Fig. 29	$N_{L_{pred}}$ (10^6 Cycles)	$\frac{N_{L_{Test}}}{N_{L_{Pred}}}$	High Stress Slope Adjustment (b) $f_{v_{peak}}$ KSI (Air Load Only) (c)	$0.9f_{v_{peak}}$ KSI	$h_{\ni .9f_{v_{peak}}}$ $\frac{\Delta psi}{\Delta Log \Sigma n}$	K Fig. 28	$N_{L_{pred}}$ (10^6 Cycles)	$\frac{N_{L_{Test}}}{N_{L_{Pred}}}$
G66	6	1.650	6.50	940	4.02	50.000	.033	14.00	12.60	2200	4.56	19.000	.087
G67		1.230	8.15	980	4.18	4.300	.286	14.00	12.60	1350	4.55	2.100	.585
G68		4.165	6.20	840	3.76	100.000	.0416	14.00	12.60	2000	4.57	8.400	.496
G69		6.005	6.30	820	3.70	90.000	.0667	14.00	12.60	2150	4.56	8.400	.715
G72	6	.359	5.35	1370	5.00	.280	1.282	19.52	17.57	2850	4.50	.480	.748
G73	12	.248	6.60	1290	4.91	.110	2.253	18.30	16.47	2700	4.52	.170	1.460
C75		.274			(f)			18.30	16.47	2950	4.49	.350	.783
C78		.312	5.65	1080	4.41	.620	.504	13.50	11.15	3080	4.47	.600	.520
G80	12	.226			(f)			13.50	11.15	830	4.38	.110	2.053
M14	(d)	.027	12.42	890	3.89	.032	.844	20.81	17.73	3680	(e)		
M15	(d)	.014	13.50	870	3.83	.026	.539	21.00	18.90	4750	(e)		
M16	(d)	.012	14.70	810	3.62	.044	.273	21.00	18.90	3620	(e)		
CG1	6	.998	7.77	1000	4.18	33.900	.0294	13.00	11.70	2650	4.52	1.800	.554
CG3	12	.142	6.10	1340	5.00	.266	.534	16.30	14.67	3050	4.48	.462	.307
CG4	12	.250	5.70	1270	4.90	.374	.669	18.30	16.47	3900	(e)		
CM1	(d)	.011	12.50	2570	(g)			21.20	19.00	2480	4.56	.025	.44

(a) Prediction Based on Quality Index Adjustment for Slope of Loading Spectra in Midstress Range of Maximum Calculated Fatigue Damage.
(b) Prediction Based on Quality Index Adjustment for Slope of Loading Spectra at 90% of the Peak Varying Stress.
(c) Peak or Largest Varying Stress in Spectra.
(d) f_{min} of 5.4 KSI
(e) Slope of Loading Spectra is Outside Range of Figure 28.
(f) Compatible Combinations of K and h do not Satisfy Curve in Figure 29.
(g) Slope of Loading Spectra is Outside Range of Figure 29.

TABLE 7

EVALUATION OF FATIGUE DAMAGE FOR QUALITY INDICES OF 2, 4, AND 6

Unit Spectra for Test Group No. 366

Varying Stress f_v KSI	Applied Cycles n	Cycles to Failure N $f_m = 6$ KSI	Cycle Ratio $10^{-5}(\frac{n}{N})$	Fatigue Damage % $\frac{n}{N}$	Cycles to Failure N $f_m = 6$ KSI	Cycle Ratio $10^{-3}(\frac{n}{N})$	Fatigue Damage % $\frac{n}{N}$	Cycles to Failure N $f_m = 6$ KSI	Cycle Ratio $10^{-1}(\frac{n}{N})$	Fatigue Damage % $\frac{n}{N}$
		K = 2			K = 4			K = 6		
.55	612800	-	0		-	0	0	-	0	0
1.55	460000	-	0		-	0	0	-	0	0
2.55	310000	-	0		-	0	0	-	0	0
3.55	180000	-	0		-	0	0	4200000	.43	6.3
4.55	64000	-	0		-	0	0	430000	1.49	21.9
5.55	25500	-	0		5200000	4.90	13.2	120000	2.13	31.4
6.55	7000	-	0		580000	7.95	21.4	58000	1.21	17.8
7.55	2300	-	0		300000	7.67	20.6	34000	.68	10.0
8.55	650	-	0		135000	4.81	12.9	21000	.31	4.6
9.55	280	-	0		73000	3.84	10.3	14000	.20	2.9
10.55	150	7000000	2.14	12.8	46000	3.26	8.8	10000	.15	2.3
11.55	70	1500000	4.67	27.9	30000	2.33	6.3	7100	.10	1.5
12.55	32	590000	5.42	32.4	20500	1.56	4.2	5400	.06	.9
13.55	13	290000	4.48	26.9	15000	.87	2.3	3900	.03	.4
			Σ 16.71	Σ 100.0		Σ 37.19	Σ 100.0		Σ 6.79	Σ 100.0

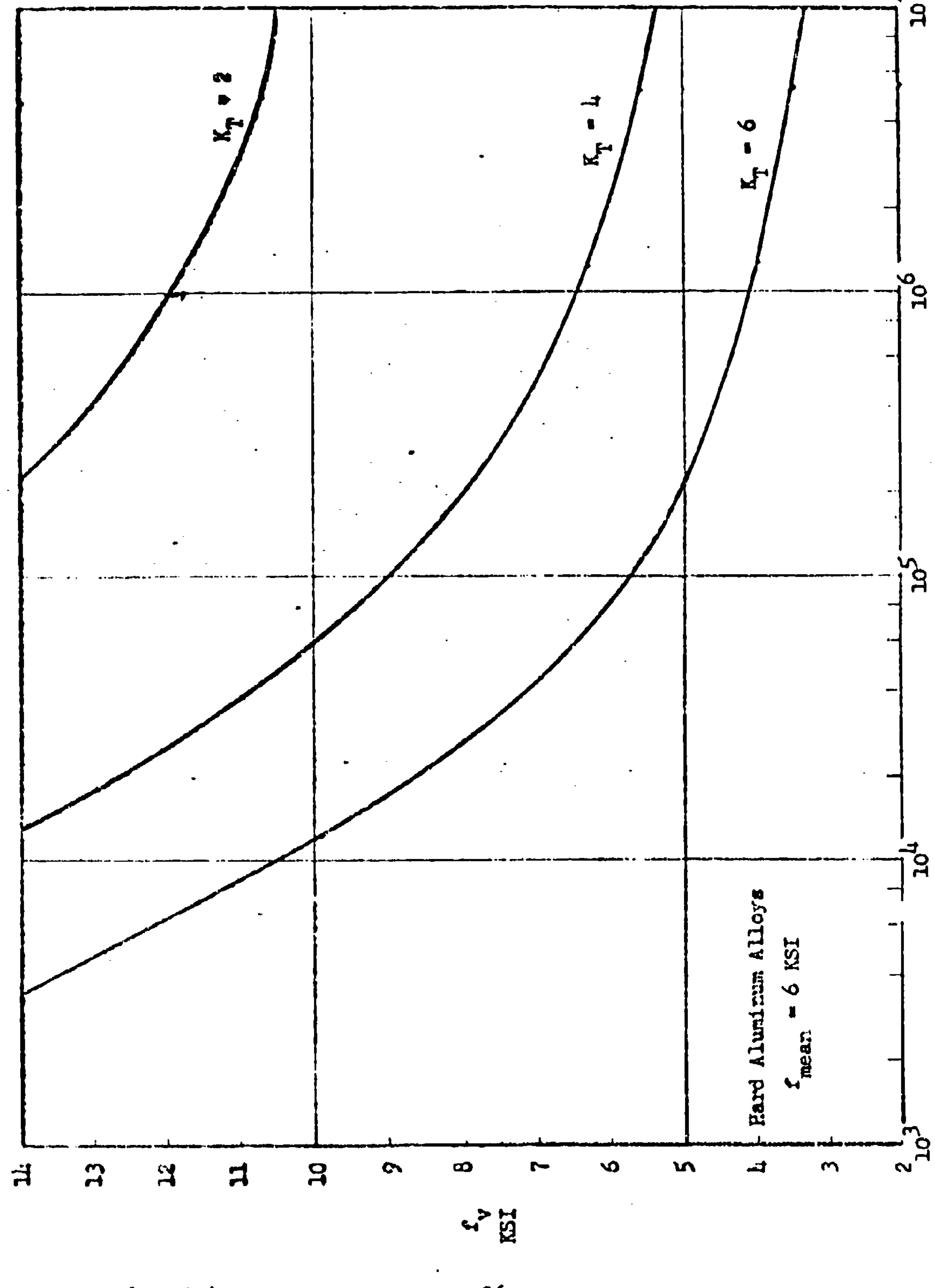

$K_T = 2$
$K_T = 4$
$K_T = 6$
Hard Aluminum Alloys
$f_{mean} = 6$ KSI
f_v KSI
N
14
13
12
11
10
9
8
7
6
5
4
3
2
10^3
10^4
10^5
10^6
10^7

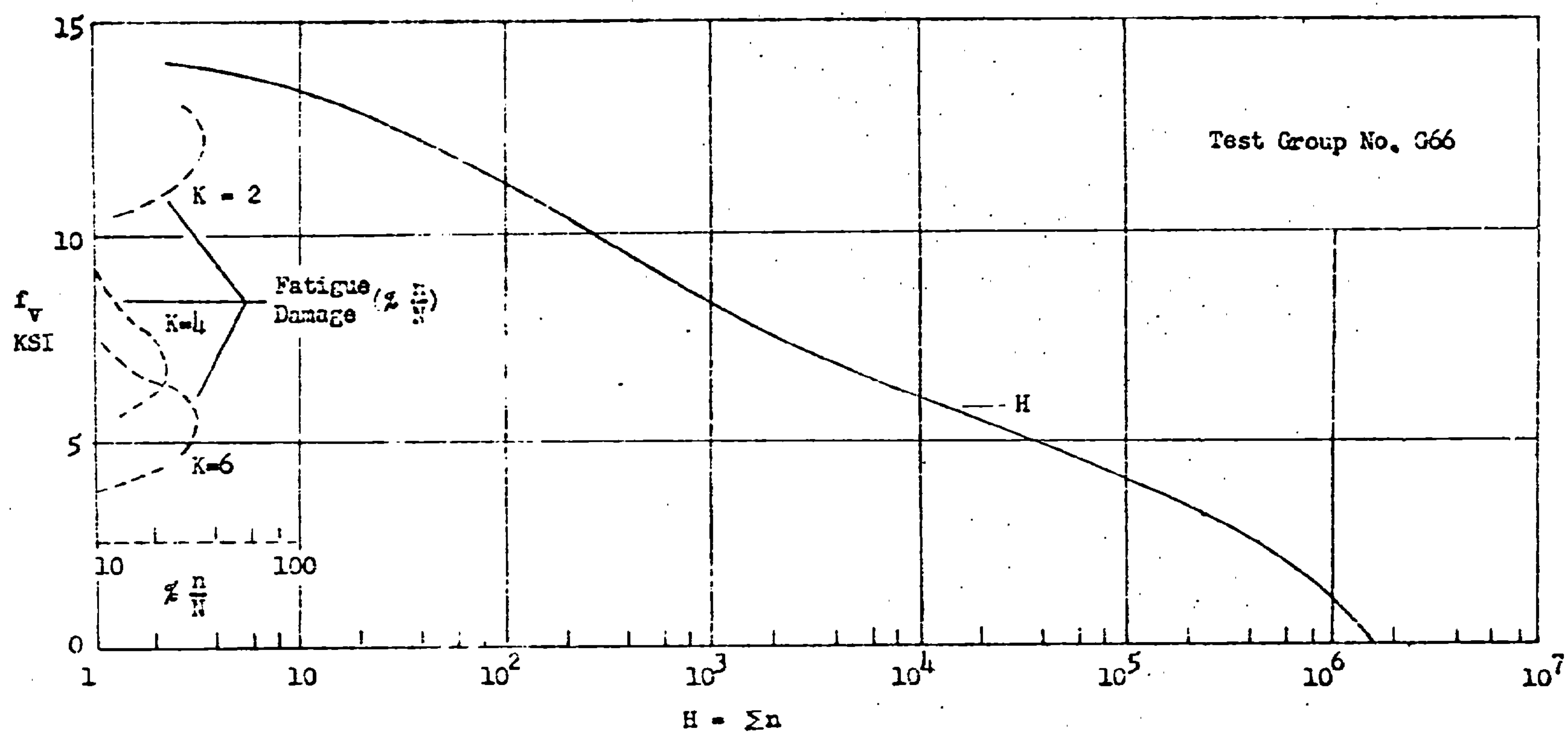

Figure 35. Illustration of a Gust Loading Spectra and the Corresponding Curves for Fatigue Damage at Quality Indices of 2, 4, and 6.

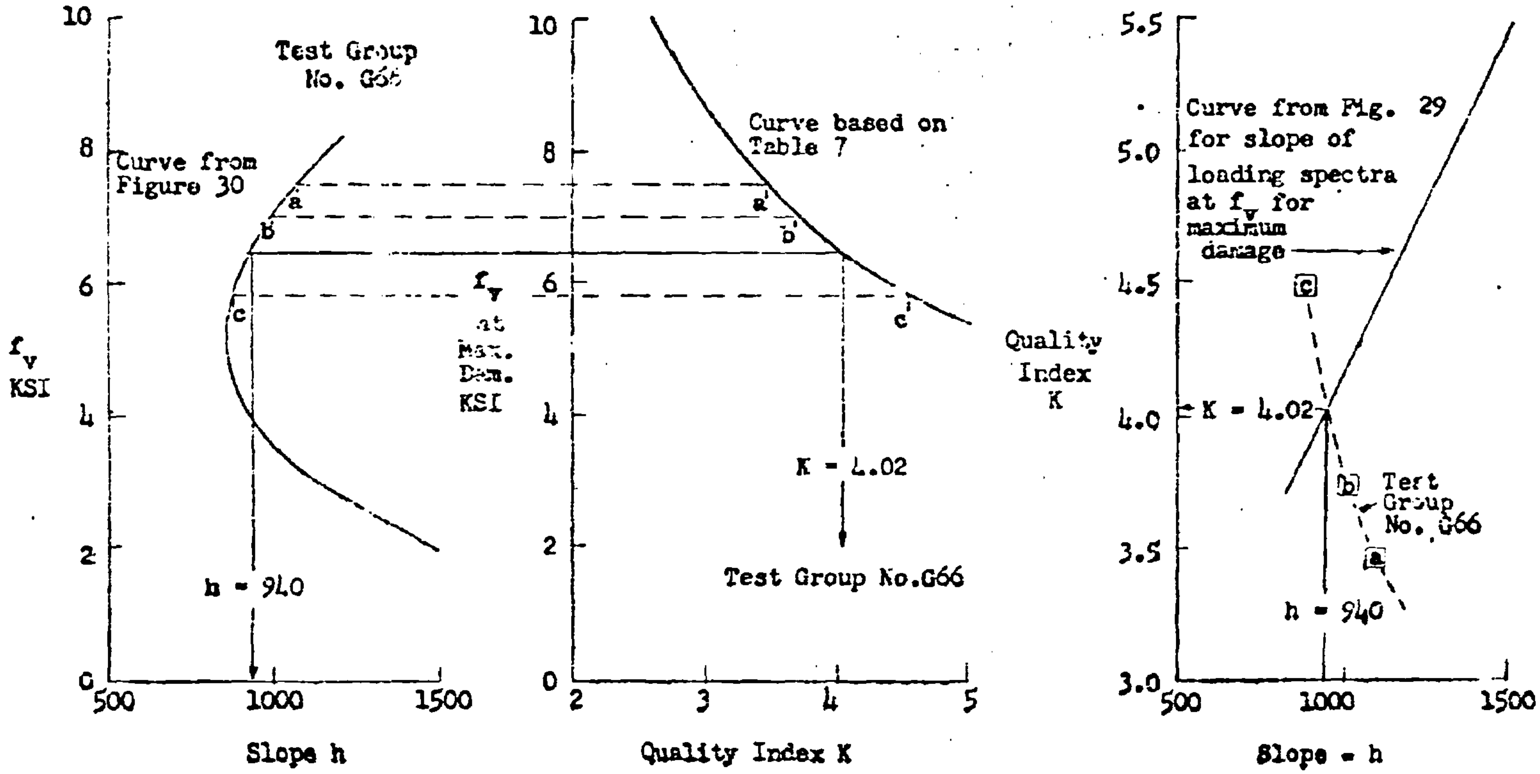

Figure 36. Illustration of procedure used to correlate quality index and slope of loading spectra in stress range of maximum fatigue damage.

TABLE 8

FATIGUE QUALITY INDEX FOR GUST SPECTRA ON COUPONS

Specimen, Figure 15

Test Group No.	Type of Spectrum	Sequence	Number of Specimens	Geometric K_T	K First Specimen in Test Group	K Quality Index Method Minimum	Maximum	Geometric Mean
G66		True Random	4	4	7.18	6.62	7.18	6.92
G67		Lo-Hi	5	4	4.63	4.57	6.23	5.05
G68	Low	Lo-Hi	5	4	5.01	4.97	5.50	5.19
G69	Peak	Lo-Hi	5	4	5.11	4.53	5.11	4.85
G70		True Random	6	7	>8	7.38	>8	>8
G71		Lo-Hi	5	7	>8	>8	>8	>8
G72		True Random	7	4	4.32	4.32	5.27	4.78
G73		Lo-Hi	8	4	4.12	3.81	4.63	4.24
G74	High	Lo-Hi	5	4	4.78	4.22	4.78	4.52
G75	Peak	Lo-Hi	5	4	4.52	4.52	4.76	4.61
G76		True Random	6	7	>8	7.58	>8	>8
G77		Lo-Hi	6	7	>8	>8	>8	>8
G78	Concave	True Random	10	4	5.25	4.87	5.60	5.33
G79	upward	Lo-Hi	5	4	4.20	4.36	4.74	4.52
G80	Concave	True Random	4	4	4.30	3.98	4.30	4.17
G81	downward	Lo-Hi	5	4	4.40	3.81	4.22	4.08

TABLE 9

FATIGUE QUALITY INDEX FOR MANEUVER GROUND AND COMPOSITE SPECTRA ON COUPONS

Specimen, Figure 15

Test Group No.	Type of Spectrum	Sequence	Number of Specimens	Geometric K_T	K First Specimen in Test Group	K Quality Index Method: Minimum	K Quality Index Method: Maximum	K Quality Index Method: Geometric Mean
M14	Fighter Maneuver	True Random	7	4	4.15	3.60	4.75	4.18
M15	Fighter Maneuver	Lo-Hi	5	4	4.85	4.20	5.40	4.76
M16	Fighter Maneuver	Lo-Hi	5	4	7.10	4.80	7.10	5.61
T1	Ground	True Random	6	7	>8	>8	>8	>8
T2	Ground	Lo-Hi	6	7	>8	>8	>8	>8
CG1	Low Peak	Lo-Hi	5	4	8.00	6.80	>8	>8
CG2	Composite	Lo-Hi	5	7	>8	>8	>8	>8
CG3	High Peak	Lo-Hi	5	4	5.70	5.40	6.20	5.85
CG4	Composite	Lo-Hi	8	4	5.60	5.00	5.80	5.35
CM1	Composite Maneuver	True Random	5	4	7.45	5.87	7.45	6.69

TABLE 10

FATIGUE LIVES PREDICTED FOR COMPOSITE GUST AND COMPOSITE MANEUVER SPECTRA ON COUPONS FROM QUALITY INDEX FOR FIRST SPECIMEN IN A SIMILAR TYPE OF SIMPLE FLIGHT SPECTRA

Test Group No.	Geometric Mean of Test Life (10^6 Cycles)	Low Peak Gust		High Peak Gust		Fighter Maneuver	
		$N_{L_{Pred}}$ (10^6 Cycles)	$\frac{N_{L_{Test}}}{N_{L_{Pred}}}$	$N_{L_{Pred}}$ (10^6 Cycles)	$\frac{N_{L_{Test}}}{N_{L_{Pred}}}$	$N_{L_{Pred}}$ (10^6 Cycles)	$\frac{N_{L_{Test}}}{N_{L_{Pred}}}$
		K = 5.01*		K = 4.78**		K = 4.15***	
CG1	.998	8.475	.118				
CG3	.142			.332	.428		
CG4	.250			.414	.604		
CM1	.011					.033	.333

* K for first specimen in Test Group No. G68 (Specimen No. 372)
** K for first specimen in Test Group No. G74 (Specimen No. 313)
*** K for first specimen in Test Group No. M14 (Specimen No. 342)

TABLE 11

FATIGUE LIVES PREDICTED FOR MANEUVER AND COMPOSITE MANEUVER SPECTRA ON COUPONS FROM QUALITY INDEX FOR FIRST SPECIMEN IN A GUST SPECTRUM

Test Group No.	Geometric Mean of Test Life (10^6 Cycles)	Based on Low Peak Gust Spectrum		Based on High Peak Gust Spectrum	
		$N_{L_{Pred}}$ (10^6 Cycles)	$\frac{N_{L_{Test}}}{N_{L_{Pred}}}$	$N_{L_{Pred}}$ (10^6 Cycles)	$\frac{N_{L_{Test}}}{N_{L_{Pred}}}$
		K = 5.01*		K = 4.78**	
M14	.027	.015	1.800	.017	1.588
M15	.014	.012	1.167	.013	1.077
M16	.012	.016	.750	.018	.667
CM1	.011	.019	.579	.022	.500

* K for first specimen in Test Group No. G68 (Specimen No. 372)
** K for first specimen in Test Group No. G74 (Specimen No. 313)

TABLE 12

COMPARISON OF TEST FATIGUE LIFE OF SIMPLE LOADING SPECTRA WITH THE FLIGHT PORTION OF COMPOSITE TESTS

Composite Spectra		Simple Spectra			
Test Group No.	$N_{L_{Test}}$ (10^6 Cycles)	Test Group No.	$N_{L_{Test}}$ (10^6 Cycles)	$\frac{N_{L_{Test\ Composite}}}{N_{L_{Test\ Simple}}}$	Damage Attributed to All Other Loadings*
CG1	.615	G67	1.23	.500	.500
CG2	.068	G71	.255	.267	.733
CG3	.090	G73	.248	.363	.637
CG4	.223	G74	.579	.385	.615
CM1	.0086	M14	.0267	.322	.678

* Damage Attributable to All Other Loadings is $\Delta D = 1 - \frac{N_{L_{composite}}}{N_{L_{simple}}}$

TABLE 13

CODING IN FIGURES FOR COUPONS AND PANELS

(All Predictions are Based on Linear Cumulative Damage.)

Symbol	Meaning
◆	Geometric mean of test data.
I	Scatter band for test data.
○	Prediction based on actual S-N curve for specimen configuration (Coupons). (Miner's Method)
□	Prediction based on standardized S-N curves with adjustment in K for slope of loading spectra in the mid-stress range. (Coupons)
×	Prediction based on standardized S-N curves with adjustment in K for slope of loading spectra in the high stress range. (Coupons)
	Prediction based on standardized S-N curve corresponding to the Quality Index for the first specimen in a simple gust spectrum.
	a) S-N data based on stresses for minimum gross area.
	1) Quality Index for first panel in gust spectrum.
	2) Quality Index for first coupon in a low peak gust spectrum.
	3) Quality Index for first coupon in a high peak gust spectrum.
	b) S-N data based on stresses for local gross area in fractured structural element. (Panels)
	Prediction based on standardized S-N curve corresponding to the Quality Index for the first specimen in a simple maneuver spectrum.
	a) S-N data based on stresses for minimum gross area. (Coupons and panels)
	b) S-N data based on stresses for local gross area in fractured structural element. (Panels)

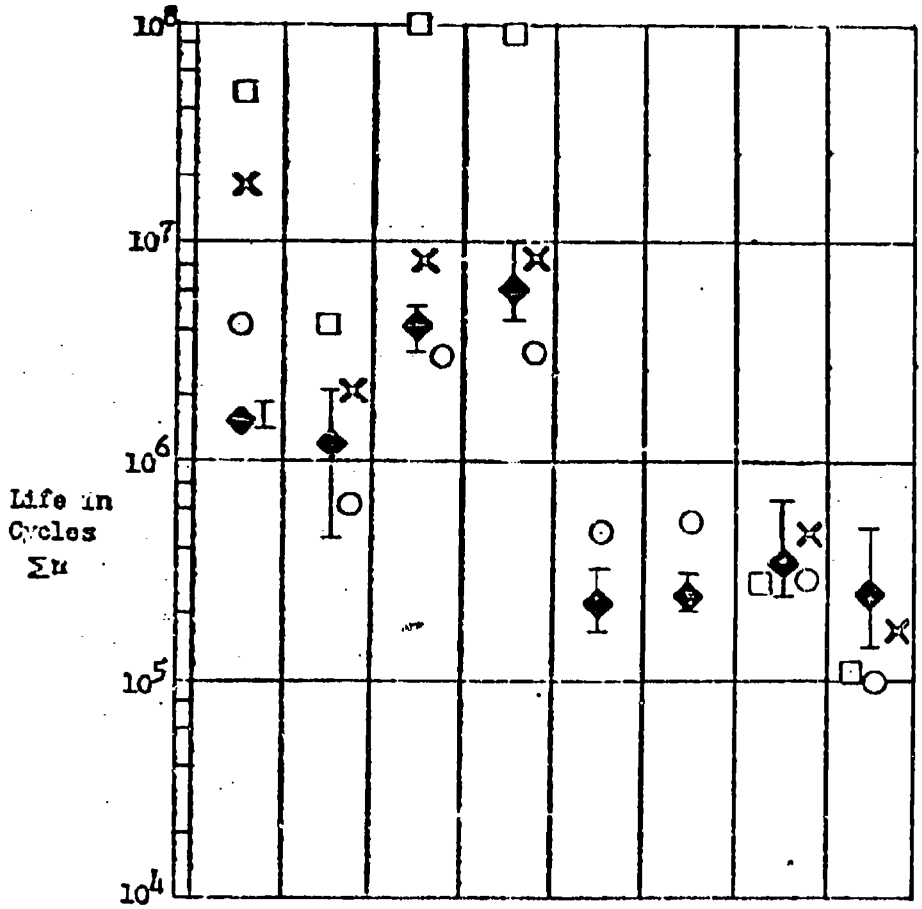

Test Group No.	G66	G67	G68	G69	G70	G71	G72	G73
Sequence	TR	L-H			TR	L-H	TR	L-H
Block Size (10^3 Cycles)	1663	26	60	120	233	9	379	9.25
Number of Loading Steps	18	4	14		17	13	23	5
Mean Stress KSI	6					12		
Type of Spectrum	Gust							
Specimen	Notched Sheet Coupons							
K_T	4				7		4	
Material	7075-T6							

For Coding See Table 13

Figure 37. Comparison between Predicted and Experimental Fatigue Lives for Gust Spectra on Coupons

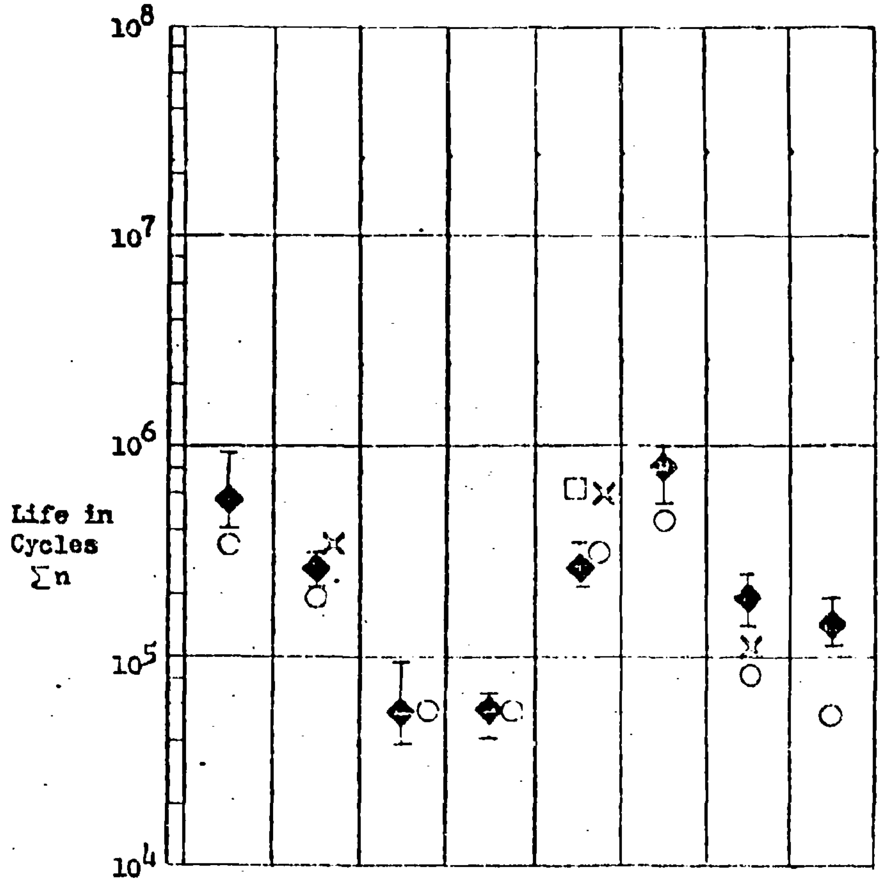

Test Group No.	G74	G75	G76	G77	G78	G79	G80	G81
Sequence	L-H		TR	L-H	TR	L-H	TR	L-H
Block Size (10^3 Cycles)	16	32	58.7	2.5	273	826	197	145
Number of Loading Steps	19		14	17	7			
Mean Stress KSI	12							
Type of Spectrum	Gust							
Specimen	Notched Sheet Coupons							
K_T	4		7		4			
Material	7075-T6							

For Coding See Table 13

Figure 38. Comparison between Predicted and Experimental Fatigue Lives for Gust Spectra on Coupons

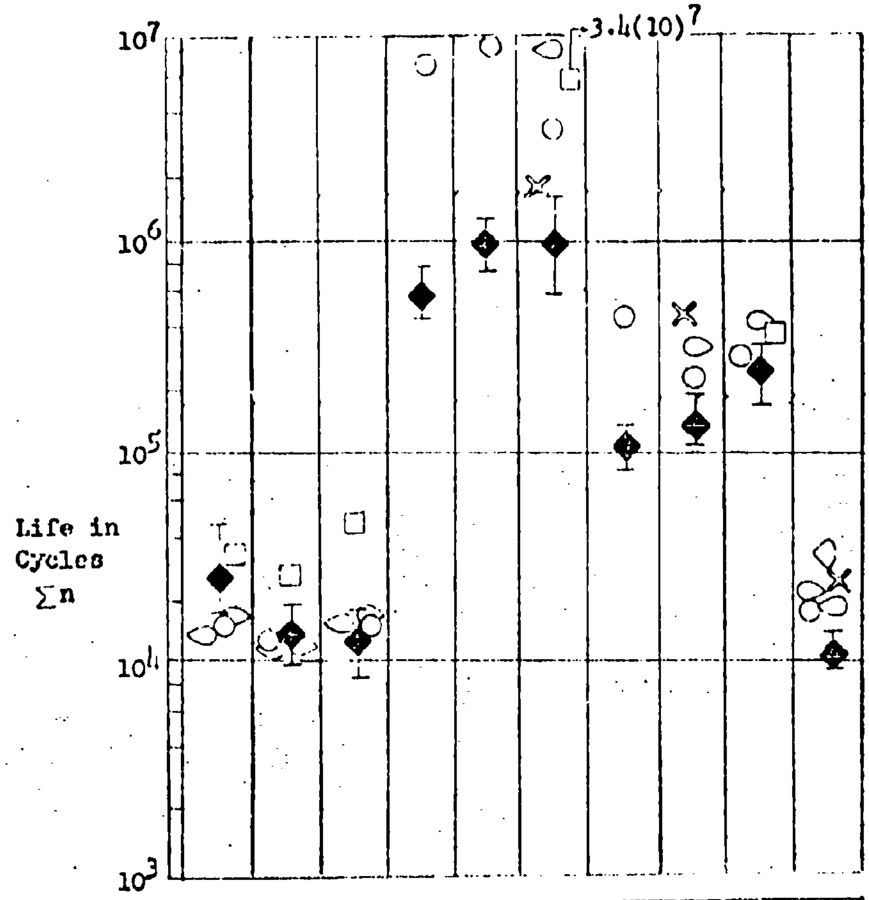

Test Group No.			M14	M15	M16	T1	T2	CG1	CG2	CG3	CG4	CM1
Sequence			TR	L-H		TR	L-H					TR
Block Size (10^3 Cycles)			27.7	1.1	1	560	21.5	21.2	1.9	3.3	10.1	11
Number of Loading Steps			11		40	18	11	26	21	29		
Minimum Stress	K S I	Air	5.4									5.45
Mean Stress		Air						6		12		
		Ground				-3						
		G-A-G						1.5		4.5		1.22
Type of Spectrum			Maneuver			Ground		Composite Gust				*
Specimen			Notched Sheet Coupons									
K_T			4			7		4	7	4		
Material			7075-T6									

* Composite Maneuver
For Coding See Table 13

Figure 39 Comparison between Predicted and Experimental Fatigue Lives for Maneuver, Ground, and Composite Spectra on Coupons

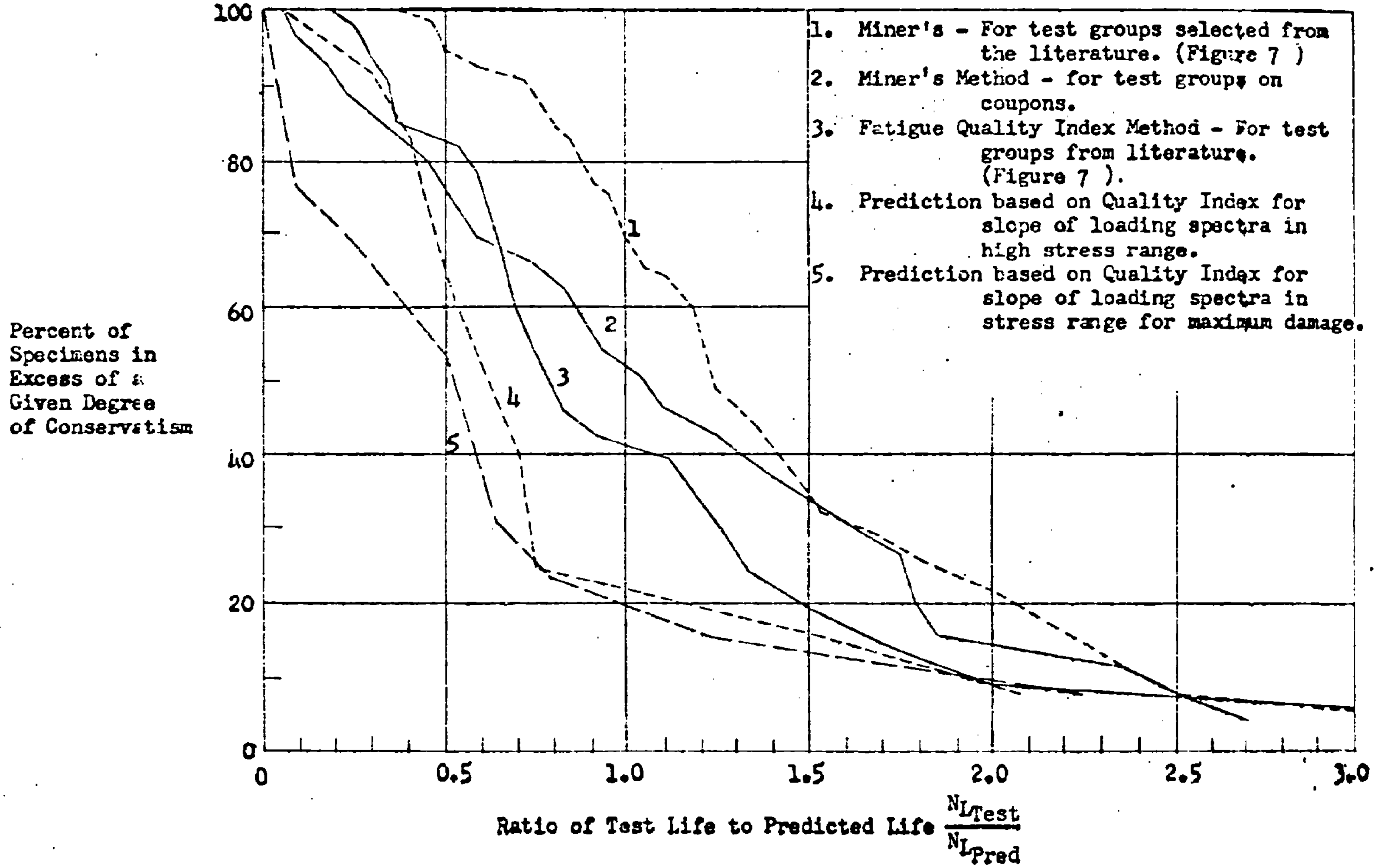

Figure 40. Cumulative Distributions for the Ratio of Test Life to Predicted Life

SECTION V

ANALYSIS OF COMPLEX JOINT SPECIMENS

Many of the problems of full scale complex structure are not present in the simple notched strip coupon-type specimen used in the majority of research projects for reasons of economy. To determine the effectiveness of the selected life prediction method on specimens more representative of aircraft structure, a series of spectrum-type fatigue tests was conducted on a splice design adapted from an integrally stiffened tension surface of a current wing structure. A splice joint is made of two panels consisting of machined plates of 7075-T6 extrusion material approximately six inches wide, each containing three vertical stiffeners which run out or taper off into a tongue flange across the width of the plates. A double butt splice is formed by a flush recessed outer surface splice plate and an inner tee splice plate with an integral flange for a rib connection. Attachments are by twelve one-quarter inch diameter Hi-Lok fasteners, six on each side of the splice. The neutral axis location throughout the length was carefully tailored in the aircraft design to reduce as much as possible eccentrically induced bending stresses. The recessed outer splice plate, in addition to providing flush aerodynamic surfaces, also aids materially in achieving a uniform load axis. The details of the panel are sketched in Figure 41 .

The panels were to be tested in an adaptation of the magnetic tape controlled fatigue test machine described in the preceding section. Two electro-servo controlled loading jacks were coupled in tandem to operate on one magnetic tape demand signal, providing 34,000 lb. load capacity. This proved insufficient, however, when the first panel had not failed after approximately 350 applications (over 5.25×10^6 cycles) of the unit low peak-low slope gust spectra illustrated in Figure 42. After careful inspection of this panel had revealed no visible damage, it was reassembled in the large 500,000 lb. fatigue machine illustrated in Figure 43. The principle of operation of this machine is illustrated schematically in Figure 44. Static loading was applied to determine the ultimate strength of the panel as a guide to stress levels to apply in the remaining fatigue tests.

Pertinent data are as follows:

Static failure load	= 66,000 lbs.
Minimum gross area	= 0.815 in.^{2} (Section BB in Figure 41)
Minimum gross area ultimate tensile strength	= 81,000 psi

The remaining panels were fatigue tested in the large 500,000 lb. fatigue machine (Figure 43) as described in detail in Appendix D Part 3. Two additional panels, No. 11 and 12, were accidentally destroyed by compression collapse through malfunction of a loading valve in the hydraulic loading system.

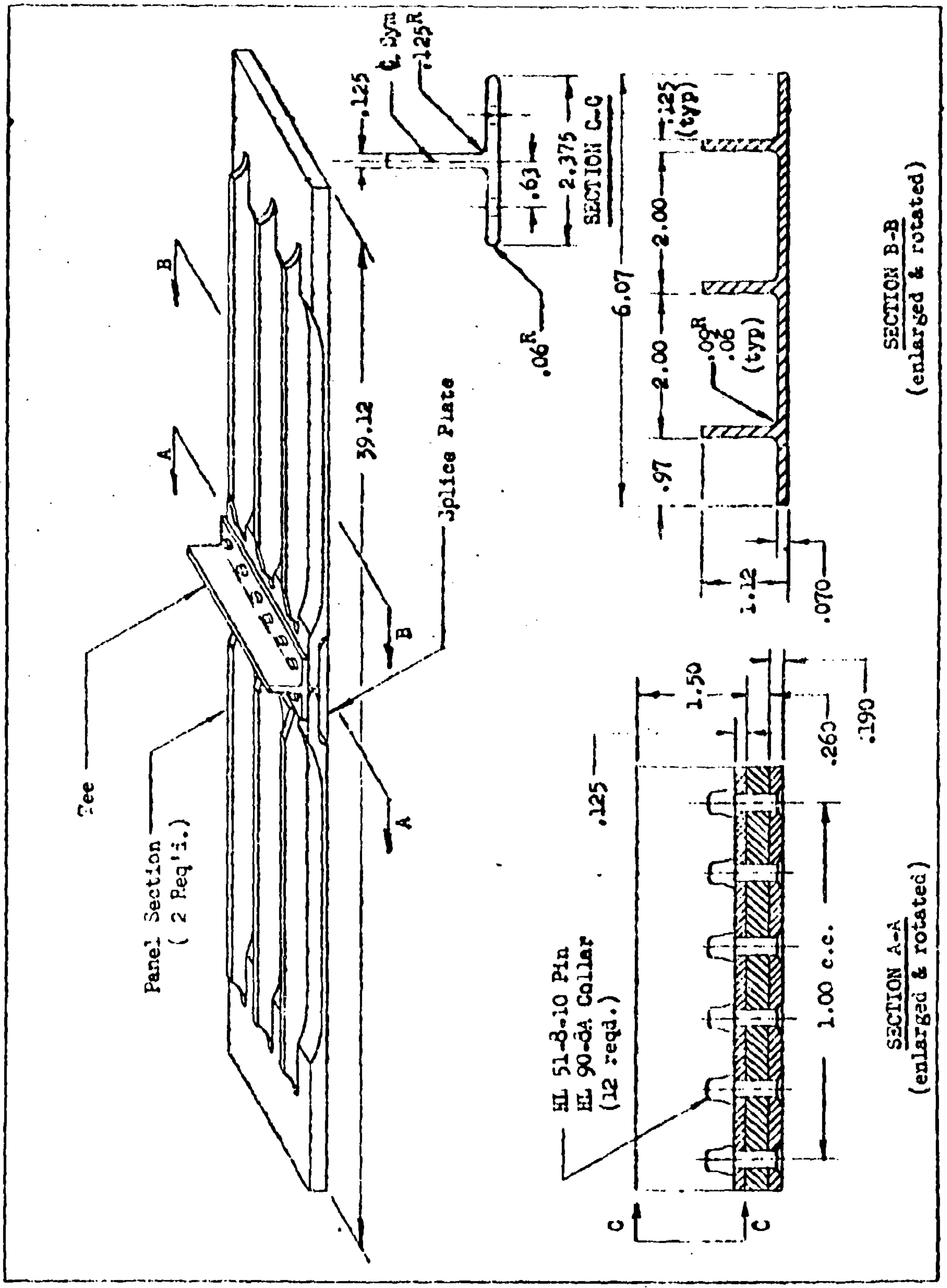
Tee
Panel Section
(2 Req'd.)
Splice Plate
39.12
A
B
.125
℄ Sym
.125R
.63
2.375
SECTION C-C
.06R
6.07
2.00
.97
.125
(typ)
.06
(typ)
1.12
.070
SECTION B-B
(enlarged & rotated)
1.50
.260
.190
.125
HL 51-8-10 Pin
HL 90-6A Collar
(12 reqd.)
1.00 c.c.
C
SECTION A-A
(enlarged & rotated)

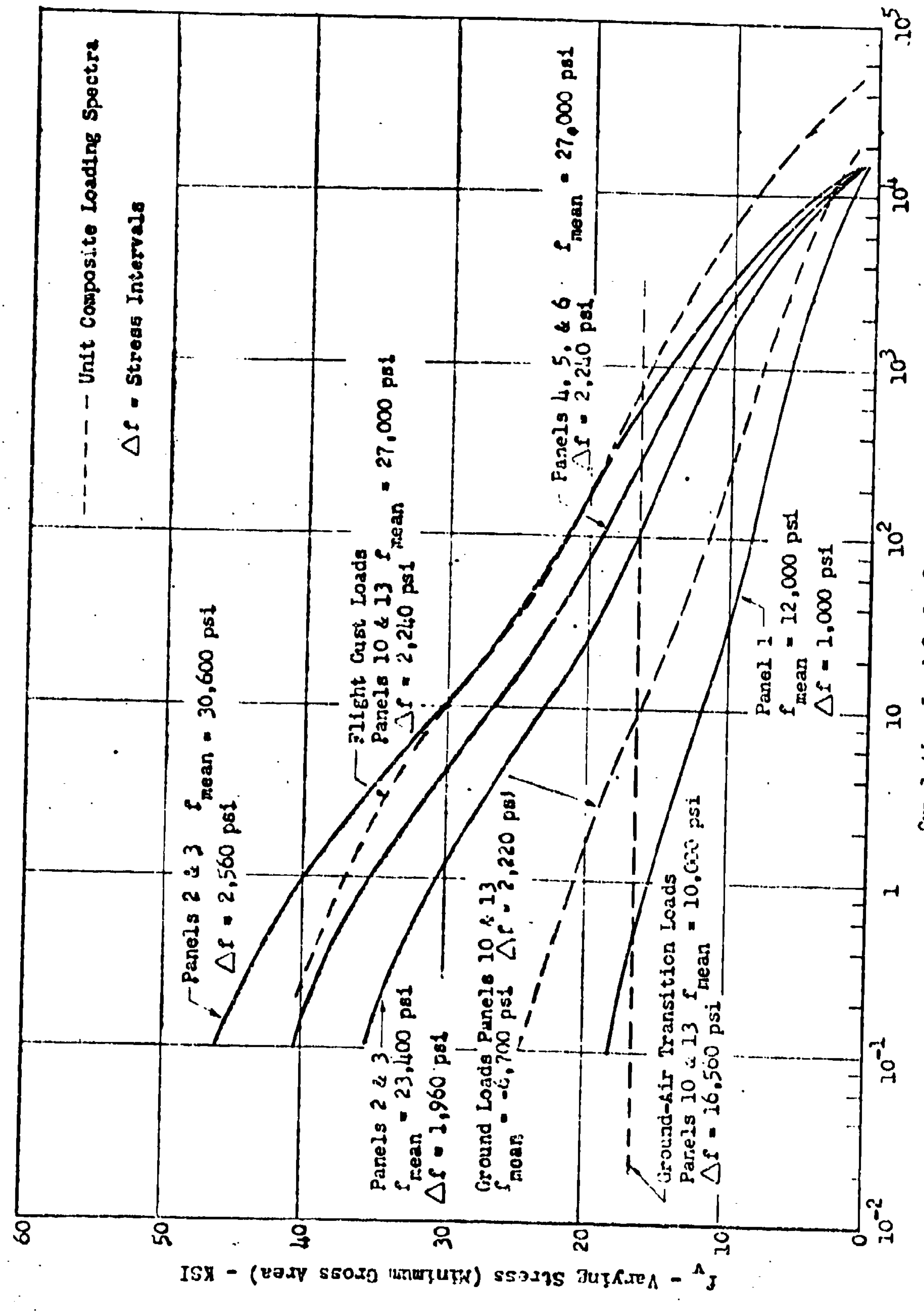

Figure 42. Basic Ordered Unit Gust and Unit Composite Gust Loading Spectra

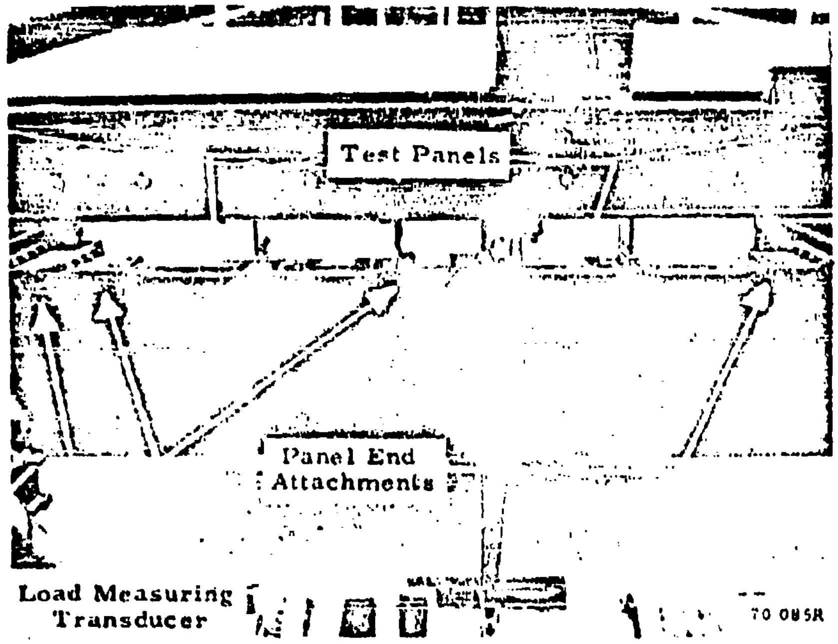

Figure 43 Two-Joint Test Panel Assemblies Installed in Tandem in a Lockheed 500,000-pound Fatigue Test Machine

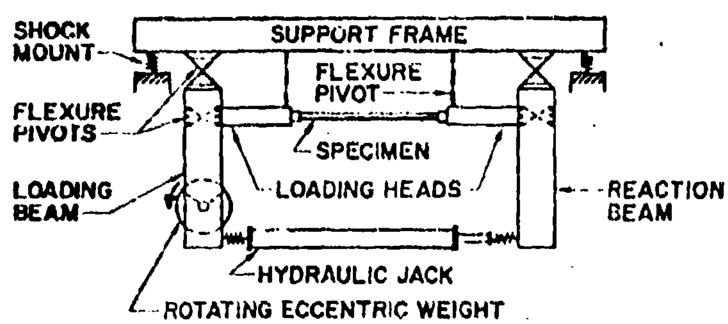

Figure 44 Schematic Diagram of the 500,000-pound Fatigue Machine Shown in the Above Photograph

Eight of the twelve panels successfully fatigue tested were apportioned five to the unit gust spectra that is illustrated in Figure 42, and three to the unit maneuver spectra in Figure 45. The remaining four were tested two to the composite gust, ground taxi, and mean load level ground-air transition cycle shown in Figure 42 and two to the composite maneuver, ground taxi, and mean load level ground-air transition cycle shown in Figure 45. The spectral test results are presented in terms of minimum gross area stress in Tables 99 to 104 and Figures 179 to 184 of Appendix D, Part 3. These same test results are also presented in terms of gross area stress at the point of fracture in Tables 106 to 110 of Appendix D. Photographs of the various types of failures that occurred are also presented there.

In the composite tests, the gust loading activity was approximately 12 loads per flight along with approximately 6.5 ground taxi loads per flight. The maneuver load activity was 30 loads per flight along with 35 ground loads per flight. In both cases, the ground-air cycle applied was the mean ground load transition to the mean flight load. These loads were grouped into ordered step spectra broken down to approximately 2000 to 2500 psi stress intervals in the gust and ground taxi loadings, and approximately 5500 psi intervals for the maneuver loadings. Block sizes varied from 1/48th to 1/600th of the final test life for the simple ordered spectral loading tests. However, due to the unexpectedly shorter test life under the composite loadings, these block sizes were from 1/5th to 1/10th of the final test life. The low-to-high load sequence was applied within the block interval. Further test details are given in Appendix D Part 3.

GROUND-AIR TRANSITION CYCLE

The importance of the ground-to-air-to-ground transition cycle discussed in connection with the analysis of the coupon data in Section IV was confirmed by these tests of the complex joint. The following comparison is developed relating the geometric mean of the number of flight cycles in the composite tests to the geometric mean of the number of flight cycles of a simple spectrum test:

TABLE 14 INFLUENCE OF GROUND-AIR TRANSITION

Simple Spectra		Composite Spectra			
Panel or (Group) Numbers	N_L (test) (10^6 Cycles)	Panel or (Group) Numbers	N_L (test) (10^6 Cycles)	$\frac{N_L \text{ (composite)}}{N_L \text{ (simple)}}$	$1 - \frac{N_L \text{ (composite)}}{N_L \text{ (simple)}}$
4	.912				
5	.783	10	.397		
6	.928	13	.516		
(G83)	.872*	(CG5)	.452*	.518	.482
7	.298				
8	.421	14	.099		
9	.474	15	.179		
(M17)	.391*	(CM2)	.133*	.340	.660

* Geometric mean of the group.

Assuming the ratio of the number of flight loading cycles in the composite test to the number of cycles in the simple spectrum test to be representative of fatigue damage done by the flight loads, the residual damage due to other than flight loadings of the composite spectra is seen to be 0.48 for the gust loading case and 0.66 for the fighter maneuver case. Since it is known that the damage contributed by the ground taxi portion of the spectra is relatively small, it can be concluded that the ground-air-ground transition cycle per flight is the predominant contributor of this residual damage. It should be noted also that the mean ground load to mean flight load level as used in these tests is a minimum (conservative) definition of this transition cycle per flight. The predominance of the ground-air transition would be expected to vary with the flight duration, reducing in importance with increased duration to the flight phase per landing. The gust loading spectra of these tests represents relatively short range flights; the fighter maneuver activity, however, is moderately high for long time average usage.

MINER'S METHOD

There were no specific S-N data available for this joint design, consequently Miner's method of simple linear cumulative damage could not be directly applied.

FATIGUE QUALITY INDEX PROCEDURE

Since a consistent influence of the shape or slope of the cumulative load frequency spectrum on the Fatigue Quality Index was not apparent in the analysis of the coupon data discussed in the previous section, this type of analysis was not applied to the data from the complex joint tests. However, several combinations of the Fatigue Quality Index procedure were applied.

The Fatigue Quality Index was derived for each of the test groups utilizing the standardized S-N data in the usual manner. Each of two base stress levels was used:

Stress Basis I. Minimum gross area stress in the uniform panel adjacent to the joint,

Stress Basis II. Actual gross area stress through the section of fracture.

The derived FQI values for Stress Basis I are given in Table 15, while those for Stress Basis II are given in Table 16. Examination of these values shows the general separation of the groups by the type of load spectra. In both bases of stress definition, the simple and composite gust loading values of K are similar within moderate scatter, and the simple and composite maneuver loading values are similar to each other but considerable different than the values from the gust-type spectra tests.

The Fatigue Quality Index is seen to be not invariant as would be required for satisfactory predictability of fatigue life. However, for similar spectra the predictability of variations on the basic load frequency spectrum is of interest. The large leverage factor between the Fatigue Quality Index value "K" and the corresponding fatigue life in number of cycles makes difficult the assessment of predictability. Therefore, several combinations of Fatigue Quality Index calculations were made to compare with the test results.

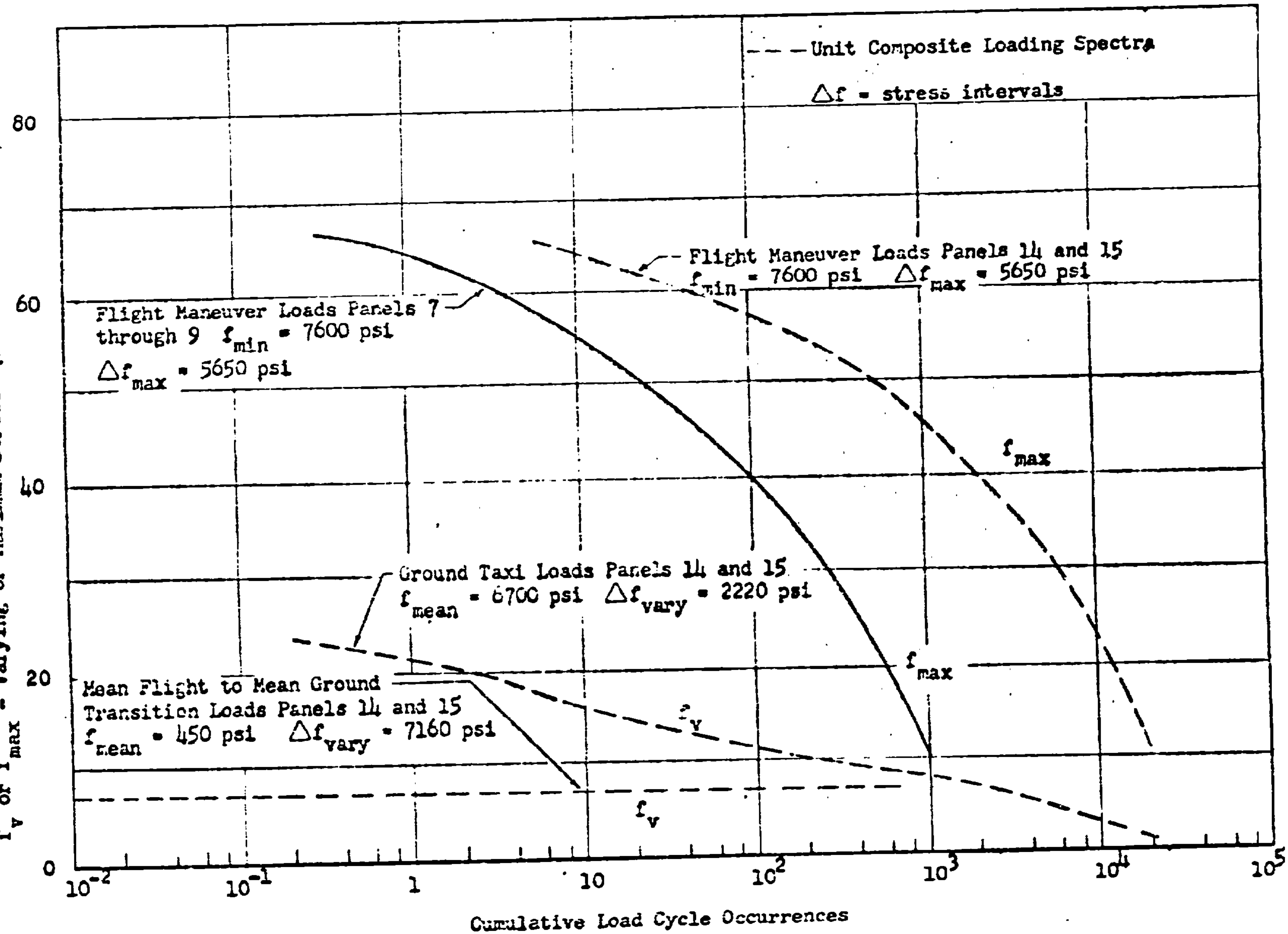

Figure 45. Basic Ordered Unit Maneuver and Unit Composite Maneuver Loading Spectra

FATIGUE QUALITY INDEX FROM FIRST PANEL TEST RESULT

A. SIMPLE GUST SPECTRUM

Fatigue life predictions based on a single specimen test result are an important consideration for large component and airframe fatigue tests in which more than one specimen is economically unfeasible. This investigation therefore utilizes the results of the gust spectrum test on Panel No. 4 to derive the Fatigue Quality Index with the standardized S-N curves. This value of Quality Index is used to predict the fatigue life of each specimen under the composite gust, simple maneuver, and composite maneuver load frequency spectra. Comparison of these predictions with the test results is given in Table 17 for both bases of stress definition.

The composite gust fatigue life by test is approximately 63.9 per cent and 75.8 per cent of the prediction when based on the Fatigue Quality Index for the simple gust load spectra and the minimum gross area stress outside the joint (Stress Basis I). When the stress is defined by the gross area at the point of fracture, the test result is 17.6 per cent to 30.4 per cent of the prediction.

The simple maneuver loading results are conservatively predicted by the Fatigue Quality Index from the simple gust spectrum test result, by factors of 10.5 to 74.5 times the predicted lifetime by the minimum gross area Stress Basis I. The corresponding composite maneuver test result is 6.36 to 8.07 times the predicted value on the same stress basis. However, on the basis of the stress through the point of fracture (Stress Basis II), the simple manouver load spectrum test results were from 23.4 per cent of prediction (unconservative) to 206 per cent of prediction (conservative), whereas the composite manouver load spectra test result was only 5.2 per cent and 58.8 per cent of the predicted lifetime (unconservative) on this stress basis. These variations in predictability are much greater than the test scatter within each group.

B. SIMPLE MANEUVER SPECTRUM

The first test result from a simple maneuver loading spectrum (Panel No. 7) was also used to derive a Fatigue Quality Index with the standard S-N curves for use in predictions of the panel fatigue life under the composite maneuver loading spectra. These results are shown in Table 18. Predictions for both bases of stress definition were unconservative, comparing test lives with approximately 5.2 per cent and 6.6 per cent of the predicted values for a panel interpreted for each stress basis and 48.4 per cent and 61.6 per cent for the alternate panel in each case. This wide divergence is greater than the test scatter.

The results of these predictions are graphically compared with the test results from each of the panels in Figure 46. Too few test results were available to justify the statistical rank ordering of the ratio of test life to predicted life as was done for the more numerous coupon test data.

TABLE 15

CLASS I FATIGUE

QUALITY INDEX FOR MINIMUM GROSS AREA STRESSES IN GUST, MANEUVER, AND COMPOSITE SPECTRA

Specimen, Figure 41

Test Group No.	Type of Spectrum	Sequence	Number of Specimens	K First Specimen in Test Group	K Quality Index Method Minimum	K Quality Index Method Maximum	K Quality Index Method Geometric Mean
GS2	Gust	Lo-Hi	2	1.52	1.20	1.52	1.35
GS3	Gust		3	1.24	1.24	1.33	1.29
M17	Maneuver		3	.60	.60	.98	.83
CG5	Composite Gust		2	1.40	1.38	1.40	1.39
CM2	Composite Maneuver	Lo-Hi	2	.70	.70	.99	.83

TABLE 16

CLASS II FRACTURE

QUALITY INDEX FOR GROSS AREA STRESSES IN VICINITY OF FRACTURE IN GUST, MANEUVER, AND COMPOSITE SPECTRA

Test Group No.	Type of Spectrum	Sequence	Number of Specimens	K First Specimen in Test Group	K Quality Index Method Minimum	K Quality Index Method Maximum	K Quality Index Method Geometric Mean
G82	Gust	Lo-Hi	2	5.01	4.01	5.01	4.48
G83	Gust		3	3.26	3.26	4.57	3.74
M17	Maneuver		3	3.28	2.81	4.04	3.34
CG5	Composite Gust		2	3.88	3.88	4.12	4.00
CM2	Composite Maneuver	Lo-Hi	2	5.41	3.61	5.41	4.41

TABLE 17

FATIGUE LIVES PREDICTED FOR MANEUVER, COMPOSITE GUST, AND COMPOSITE MANEUVER SPECTRA ON PANELS FROM QUALITY INDEX FOR FIRST SPECIMEN IN A SIMPLE GUST SPECTRUM

Test Group No.	Panel No.	N_L Test (10^6 Cycles)	N_L Pred. (10^6 Cycles)	$\frac{N_L \text{ Test}}{N_L \text{ Pred.}}$	N_L Pred. (10^6 Cycles)	$\frac{N_L \text{ Test}}{N_L \text{ Pred.}}$
			K based on stresses for minimum gross area		K based on stresses for local gross area at fracture	
			K = 1.24 *		K = 3.26 *	
M17	7	.298	.004	74.500	.310	.961
	8	.421	.040	10.525	1.800	.234
	9	.474	.040	11.850	.230	2.061
CG5	10	.639	1.000	.639	2.100	.304
	13	.758	1.000	.758	4.300	.176
CM2	14	.218	.027	8.074	4.200	.052
	15	.394	.062	6.355	.670	.588

* K for Panel No. 4 in Test Group No. G83

TABLE 18

FATIGUE LIVES PREDICTED FOR COMPOSITE MANEUVER SPECTRA ON PANELS FROM QUALITY INDEX FOR FIRST SPECIMEN IN A SIMPLE MANEUVER SPECTRUM

Test Group No.	Panel No.	N_L Test (10^6 Cycles)	N_L Pred. (10^6 Cycles)	$\frac{N_L \text{ Test}}{N_L \text{ Pred.}}$	N_L Pred. (10^6 Cycles)	$\frac{N_L \text{ Test}}{N_L \text{ Pred.}}$
			K based on stresses for minimum gross area		K based on stresses for local gross area at fracture	
			K = .6 *		K = 3.28 *	
CM2	14	.218	.450	.484	4.200	.052
	15	.394	6.000	.066	.640	.616

* K for Panel No. 7 in Test Group No. M17

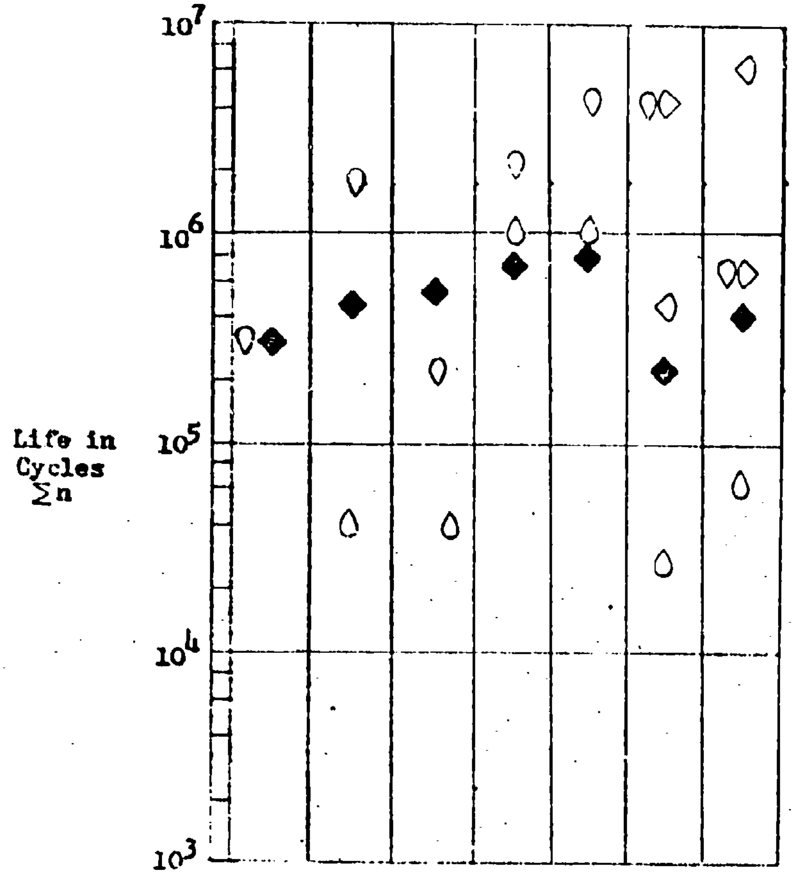

Panel No.		7	8	9	10	13	14	15
Test Group No.		M17			CC5		CM2	
Sequence		Lo - Hi						
Block Size (10^3 Cycles)		1			76		44	
Number of Loading Steps		11			32		24	
Mean Stress KSI	Air	7.7*			26.6		7.7*	
	Ground				-6.6		-6.7	
	G-A-G				9.9		.45	
Type of Spectrum		Maneuver			Composite Gust		Composite Maneuver	
Specimen		Panel						
Material		7075-T6						

* f_{min} for maneuver loading

For coding see Table 13

Figure 46. Comparison between Predicted and Experimental Fatigue Lives

CONCLUSIONS FROM THE PANEL TESTS

The analysis of the spectral fatigue tests conducted on the complex panels result in the following conclusions.

1. The influence of the ground-air-ground transition cycle which occurs once per flight was found to be important in reducing the fatigue life of these joints when compared with the results of similar panels tested by the flight load spectra alone. This confirms the conclusions reached in the analysis of the coupon test results.

2. A Fatigue Quality Index derived from the first test result of a simple gust spectrum by use of standard S-N curves was used as a test-based fatigue life prediction procedure for other types of loading spectra. The predictions were somewhat unconservative for composite gust loading spectra which included the ground-air-ground cycle based on the mean ground to mean flight load transition. When based on the minimum gross area stress adjacent to the joint, this Fatigue Quality Index produced unduly conservative predictions for both the simple and the composite fighter maneuver test results. When based on the gross area through the point of fracture, they were both conservative and unconservative for the simple maneuver results and unconservative for the composite maneuver results.

3. The use of a Fatigue Quality Index derived from a simple fighter maneuver test spectrum was unconservative in predicting the composite fighter maneuver which contained the ground-air cycle based on the transition of mean ground to mean flight load.

SECTION VI

SUMMARY AND CONCLUSIONS

The main difficulty in the task of the prediction of fatigue life lies in the definition of a fatigue quality of complex structure. This quality embodies an intergration of the dual effects of a complicated localized internal stress history and the physics of the creation and propagation of a fatigue crack. The problem is complicated by a very complex loading history, plastic yielding at peak stress points, progressive work hardening of some materials, changing residual stress patterns, nonlinear, nonrepeatable slippage of friction joints, redistribution of local internal loads, and many other factors not amenable to analytical treatment. Means of analytical prediction of this fatigue quality of a complex structure will not likely be available in the near future. The statistical nature of many facets of the fatigue problem precludes hope of any specific fatigue life prediction of a single article. The best that can be achieved is broad comparisons of the expectations of new structure compared with current and past fleet performance. However, the problem of fatigue control is amenable to solution.

An engineering evaluation of the available practical methods of fatigue life prediction was conducted by the application of selected procedures to a large body of experimental fatigue test results. From this study, the use of the Linear Cumulative Damage Hypothesis is recommended as best qualified from the standpoint of simplicity, versatility, and of sufficient accuracy (in view of other intangibles in the problem) for use in three areas of design:

1. Preliminary Design

   The Stress Concentration Method (essentially a refined method of stress analysis) must be coupled with a damage theory to constitute a life prediction method. The direct use of theoretical (or photoelastic or experimental) elastic stress concentration factors coupled with the linear cumulative damage procedure is inadequate and may provide misleading comparisons. Therefore, development tests of fatigue-critical areas are required.

2. Development Tests

   The development tests are an important link in any system for the control of fatigue cracks in fleet operations. The specimens must be complete in all fatigue-critical details. Where feasible, constant amplitude S-N type tests may be conducted to provide specific S-N data for fatigue life predictions by the simple cumulative damage procedure. This requires a considerable number of identical specimens for any resonable degree of confidence. Where constant amplitude S-N type testing is not economically feasible (for large size specimen, component, or airframe testing) it is recommended that spectral type tests impose the full range of loading anticipated for operational

service. Spectral tests results are known to depend on many variables and assumptions made in the reduction of service loading records to practical test loading history. Some of these include unit spectrum size and stress interval size, both of which should be made relatively small (block size 1/20 or less of anticipated life; stress interval 1000-2000 psi). Flight by flight load sequence is one means of avoiding arbitrary definitions of the ground-air-ground transition cycle.

The sequence of the higher loads in the schedule has a large influence on the results; if applied early in the loading history, the test life may be unconservatively prolonged. Only the Henry Method, extended for more general application, had the potential of accounting for block size and loading sequence. However, for the test data used in this evaluation, the Generalized Henry Method offered no overall improvement over the more simple Linear Cumulative Damage Hypothesis. This problem cannot be satisfactorily resolved until sufficient statistical information on the sequence of occurrence of the highest loadings is made available from service records.

An interpretation of the full spectrum type fatigue test is outlined by a special application of the Linear Cumulative Damage Procedure in connection with a standardized set of S-N curves. The procedure is to find, by interpolation, which set of K_T curves from the standardized group is required to make the cumulative damage equation exactly unity for the total applied test history. This K-value defines the Fatigue Quality Index demonstrated by the specimen under these test conditions.

3. Analysis of Service History

Many intangibles remain in the laboratory test based analysis system, including the wide range of operational loads in service, among others. It is necessary, therefore, to maintain a comparative base in service history by the consistent application of any analysis system to laboratory tests of structure which has a known operational history - both successful and unsuccessful. This is most important in the establishment of the fatigue quality acceptance standards for new structure.

The application of the Linear Cumulative Damage procedure in the prediction of the fatigue life of airframe structure as described has many unexplored areas. One of the most pertinent questions raised is the validity of the extrapolation of one or a few test results to other loading conditions. The experimental program conducted for this study explored briefly the influence of the statistical load content, as exemplified by the shape of the cumulative load frequency spectra, on the Fatigue Quality Index derived from the tests and their use in a test-based fatigue life prediction method for loading spectra of other shapes. A number of different loading spectra were applied to notched 7075-T6 aluminum alloy coupon specimens, including both the random loading sequences based on actual flight load measurements, and various ordered cyclic loading spectra derived from this flight record, and from various modifications of it.

A new magnetic tape controlled fatigue test machine and auxiliary equipment was assembled and testing, calibration, monitoring and maintenance techniques perfected to precisely reproduce almost any desired loading record which could be imposed on magnetic tape.

The experimental data derived from these tests were analyzed to determine what correlation, if any, existed between the derived quality index values and the slopes of the various loading spectra, and whether there was any trend that could be used as a corrective step for the improvement of the fatigue life prediction method. The slopes of the loading spectra were measured both at the high stress region and in the mid-stress level in the region of the maximum computed damage ratios. Fatigue life predictions using the experimentally derived relationship between spectrum slopes and the quality index were compared with the normal predictions based on the fatigue quality index derived from the first test result of a group.

The second group of experiments was conducted on a complex joint specimen representative of contemporary aircraft construction. Except for one specimen, these tests were conducted in a 500,000 lb. resonant pendulum type fatigue test machine. The same step-ordered cyclic load spectra were used as for some of the coupon experiments. These included gust type spectra of various slopes and maneuver type loadings, and two composite spectra of ground taxi loads, ground-to-air cycles based on the transition from ground mean load to flight mean load, and containing, in one case spectra of high peak-high slope flight gust loads, and in the other case spectra of military maneuver flight loads.

From an analysis of the experimental results of coupon tests, no consistent trend in the derived fatigue quality index could be developed as a function of the slope of the various loading spectra curves in either the high stress region or the mid-stress range of maximum computed fatigue damage. Fatigue life predictions of coupon type specimens loaded by composite spectra, including a ground-to-air transition based on the mean load level, from a test derived fatigue quality index based on a simple spectrum test of similar specimens loaded only by the flight portion of the spectrum of loads were less conservative than predictions by the simple linear cumulative damage hypothesis. This conclusion is equally applicable for gust-type loads or for military maneuver-type flight loads.

The use of a fatigue quality index based on a gust-type test to predict the fatigue life of specimens loaded by military maneuver-type spectra was not satisfactory.

These conclusions, with respect to the Fatigue Quality Index procedure initially based on coupon tests, were confirmed by a brief series of tests on a complex joint specimen.

A general observation is made that the scatter of coupon data obtained by spectrum-type tests is somewhat smaller than the scatter obtained in the constant amplitude-type tests, and that the scatter in results of the limited number of complex joints under spectral loading is even less than that on coupons tested by either constant amplitude or spectral-type loading. This may be significant in any study which might be conducted to establish factors of safety or margins of safety on fatigue loads or life. It is suggested that

these factors or margins of safety for fatigue cannot be established from a study of fatigue results alone, but must be considered in perspective with many other considerations such as static design criteria, fail-safe philosophy, and inspection, maintenance, and repair policy, as well as performance penalties which might accrue. These considerations are beyond the scope of this study.

CONCLUSIONS

Based on the test data applied in the engineering evaluations conducted in this study and the analysis of the experimental results generated for the investigation of extrapolations of a test-based fatigue life prediction method for airframe structure, the following conclusions may be drawn.

1. When satisfactory constant amplitude S-N type data can be provided for the specific structure, the Linear Cumulative Damage procedure is recommended for its simplicity, versatility, and sufficient accuracy commensurate with the data currently available for this type of analysis.

2. Development tests are required for all fatigue-suspect areas of the structure. Either constant amplitude S-N type tests or full load range spectrum-type tests can be used for this purpose.

3. An important link in a fatigue quality control system is the establishment of realistic fatigue quality acceptance standards. These should be based on the consistent analysis of laboratory test results of structure with known service history, both successful and unsuccessful.

4. For spectral type tests, the technique for load simulation such as unit spectrum block size, stress intervals, and the order in which the higher peak loads appear in the sequence of loading has an important bearing on the fatigue life predictions based on test results. The unit block size and the stress interval should be relatively small. The question of where in the sequence of loading to place the highest loads cannot be satisfactorily resolved until this type of statistical information is made available from service records. A compromise is to place the highest loads approximately into the mid-range of the anticipated life sequence.

5. A special use of the Linear Cumulative Damage procedure in the interpretation of test results under complex composite spectral-type loading histories is a useful tool to accomplish two functions:

   a. To provide a simple index number on a scale of fatigue quality by which various structures may be compared and evaluated against fatigue quality acceptance standards established by similar consistent analysis of service history.

   b. To provide a test basis for the extrapolation of fatigue life predictions of complex structure under other similar loading spectra than the specific test condition, when specific constant amplitude S-N type data cannot be made available.

6. Test results indicate that the ground-air-ground transition cycle which occurs once per flight has a strong influence in reducing the fatigue life of coupons and complex panel specimens when compared with spectral tests with flight loads alone.

7. The use of simple gust-type spectral test results to derive a Fatigue Quality Index is less adequate for the life prediction of gust-type composite spectrum tests which include ground taxi, and ground-air transition cycles as well as flight gust loads. The same conclusion is made for the military maneuver-type loading conditions. The use of a Quality Index derived from a simple gust loading condition was completely inadequate to predict the fatigue life of specimens under military manouver-type of loads, and vice versa. More experimental data are needed to explore the problems of composite loading. In the meantime, it is concluded that development tests should contain the best possible representation of all loads expected in service. Flight by flight spectral loading technique is recommended to avoid arbitrary definition of the ground-air-ground transition cycle.

8. A versatile magnetic tape controlled fatigue test machine is now available with adequate calibration and monitoring techniques for precisely reproducing onto test specimens actual flight records and almost any simulation of ordered loading spectra which may be required.

REFERENCES

1. Peterson, R.E., Stress Concentration Design Factor, John Wiley and Sons., 1953

2. Neuber, H., Theory of Notch Stresses: Principles of Exact Stress Calculations, J.W. Edwards, Ann Arbor, Michigan, 1946

3. Hardrath, H.F. and Ohman, L., A Study of Elastic and Plastic Stress Concentration Factors Due to Notches and Fillets in Flat Plates NACA Tech. Report No. 1117, 1953

4. Hyler, W.S., Popp, H.G., et al., Fatigue Behavior of Aircraft Structural Beams, NACA Tech. Note No. 4137, January 1958

5. McCulloch, A.J., Melcon, M.A., Crichlow, W.J., Foster, H.W., and Rebman, J., Investigation of the Representation of Aircraft Service Loading in Fatigue Tests, WADD Contract No. AF 33(616)-6575, Project No. 1367, Task 14025, ASD TR 61 - 435, September, 1961

6. Miner, M.A., Cumulative Damage in Fatigue. J. Appl. Mech., Vol. 12, No. 3, pp. A-159 - A-164, Sept. 1945

7. Lundberg, B., Fatigue Life of Airplane Structures, J. Aero. Sci. Vol. 22, No. 6, pp. 349 - 402, June 1955

8. Shanley, F.R., A Theory of Fatigue Based on Unbonding during Reversed Slip. RAND Corp. Report P-350-1, 11 Nov. 1952

9. Shanley, F.R., A Theory of Fatigue Based on Unbonding during Reversed Slip: Supplement. RAND Corp. Report P-350-Supplement, 1 May 1953

10. Shanley, F.R., Fatigue Analysis of Aircraft Structures, RAND Corp. Paper No. RM1127, 31 July 1953; AD 210794

11. Langer, B.F., Fatigue Failure from Stress Cycles of Varying Amplitude, J. Appl. Mech., Vol. 4, pp. A-160 - A-162, December, 1937

12. Grover, H.J., Cumulative Damage Theories. (In Proceedings of the Symposium on Fatigue of Aircraft Structures) WADC Tech. Rept. 59-507, pp. 207-225, August 1959

13. Smith, C.R., Prediction of Fatigue Failures in Aluminum Alloy Structures, SESA Proceedings, Vol. 12, No. 2, pp. 21-28, 1955

14. Henry, D.L., A Theory of Fatigue-Damage Accumulation in Steel. ASME Trans., Vol. 77, No. 6, pp. 913-918, August 1955

15. Corten, H.T. and Dolan, T.J., Cumulative Fatigue Damage. Session 3-Paper 2 (Advance copy of paper presented at the International Conference on Fatigue of Metals at the IME, London, 10-14 Sept. 1956, and at the ASME, N.Y., 28-30 November 1956)

16. Naumann, E.C., Hardrath, H.F., and Guthrie, D.E., Axial-Load Fatigue Tests of 2024-T3 and 7075-T6 Aluminum-Alloy Sheet Specimens under Constant-and Variable-Amplitude Loads, NASA Tech. Note No. D-212, December 1959

17. Wallgren, G., Fatigue Tests with Stress Cycles of Varying Amplitude, FFA Report No. 28, 1949

18. Russell, H.W., Jackson, L.R., et al., Fatigue Strength and Related Characteristics of Aircraft Joints - Part II - Fatigue Characteristics of Sheet and Riveted Joints of 0.040-inch 24S-T, and R 303-T275 Aluminum Alloys, NACA Tech. Note No. 1485, February 1948

19. Fisher, W.A.P., Programme Fatigue Tests on Notched Bars to a Gust Load Spectrum, R. A. E. Tech. Note No. Structures 236, March 1958

20. Whaley, R.E., Fatigue Investigation of Full-Scale Transport-Airplane Wings: Variable-Amplitude Tests with a Gust-Loads Spectrum, NACA Tech. Note No. 4132, November 1957

21. Payne, A.O., Random and Programmed Load Sequence Fatigue Tests on 24ST Aluminum Alloy Wings, Dept. of Supply, Melbourne, A.R.L. Report No. SM 244, Sept. 1956

22. Kommers, J.B., The Effect of Overstress in Fatigue on the Endurance Life of Steel, ASTM Proceedings, Vol. 45, pp. 532-541, 1945

23. McGuigan, Jr., M.J., Bryan, D.F., and Whaley, R.E., Fatigue Investigation of Full-Scale Transport-Airplane Wings: Summary of Constant-Amplitude Tests through 1953, NACA Tech. Note No. 3190, March 1954

24. Richart, Jr., F.E., and Newmark, N.M., A Hypothesis for the Determination of Cumulative Damage in Fatigue, ASTM Proceedings, Vol. 48, pp. 767-798, 1948

25. Marco, S.M. and Starkey, W.L., A Concept of Fatigue Damage. ASME Trans., Vol. 76, No. 4, pp. 627-632, May 1954

26. Freudenthal, A.M. and Heller, R.A., On Stress Interaction in Fatigue and a Cumulative Damage Rule - Part 1 - 2024 Aluminum and SAE 4340 Steel Alloys, WADC Tech. Rept. 58-69-Pt. 1, June 1958, AD 155687

27. Levy, J.C., Cumulative Damage in Fatigue - A Design Method Based on the S-N Curves, J. Royal Aero. Soc. Vol. 61, No. 559, pp. 485-491, July 1957

28. Foster, H.W., and Wells, R.H. "Fatigue Test of Lower Wing Surface Splice at Station 317" Lockheed Aircraft Corp., Lockheed Report No. 4612, 11 Feb 1944

29. Roylance, T.F., "A Review of Cumulative Damage in Fatigue", British Ministry of Supply S and T Memo No. 8/57 Dated May 1957

30. Kuhn, P. and Hardrath, H.F. "An Engineering Method for Estimating Notch Size Effect in Fatigue Tests on Steel NACA TN 2805 - Oct 1952

31. Aircraft Fatigue Handbook - Vol. II - Design and Analysis - Aircraft Industries Association - ARTC/W-76 Aircraft Structural Fatigue Panel, January 1957

32. Rhode, R.V., and Donely, P., Frequency of Occurrence of Atmospheric Gusts and of Related Loads on Airplane Structures, NACA War Report No. L-121, 1944

33. Weibull, W., Statistical Handling of Fatigue Data and Planning of Small Test Series. The Aeronautical Research Institute of Sweden (FFA), Report No. 69, October 1956

34. Cramer, H., Mathematical Methods of Statistics. Princeton Univ. Press, Princeton, N.J. (1954)

35. Pearson, K., Tables of the Incomplete Γ - Function, Cambridge, 1951

APPENDIX A

DESCRIPTION OF FATIGUE LIFE PREDICTION METHODS

A survey of the literature revealed some seventeen procedures by different authors dealing with some aspect of fatigue life predictions. This section of the report presents a detailed description of most of these methods. In a number of cases, study of the methods revealed essentially a common basis with variations in handling certain aspects of the problem. For instance, the form of the mathematical equations for representing the loading spectra, or the S-N data were subject to differences by different authors who, nevertheless, were each performing, in a slightly different way, the basic linearly cumulative damage analysis.

In addition, study of some of these methods showed that modifications, extensions, and generalizations could be derived which would improve the application of certain specific methods. These extensions are derived and explained in detail. They provide three additional procedures for consideration, making twenty in all.

Study of these methods revealed some which could not be evaluated because of the lack of proper data. The methods which were studied include the following: (Those underlined were chosen for comparative evaluation.)

1. <u>Linear Cumulative Damage - Miner's Method</u>
2. <u>Shanley's "1X" Method</u>
3. <u>Shanley's "2X" Method</u>
4. <u>Lundberg's FFA Method</u>
5. Henry's Method
6. <u>Generalization of Henry's Method</u>
7. Corten and Dolan's Method
8. <u>Modified Corten and Dolan Method</u>
9. <u>A Simplified Nonlinear Cumulative Damage</u>
10. Kommers' Method
11. Richart and Newmark's Method
12. Marco and Starkey's Method
13. Freudenthal-Heller's Method

14. Langer's Method

15. Grover's Method

16. Levy's Method

17. Smith's Residual Stress Method

18. Tangent Intercept Method

19. Stress Concentration Method

20. A Fatigue Quality Index Method

LINEAR CUMULATIVE DAMAGE - MINER'S METHOD

In 1945 Miner derived, in reference 6, the first logical basis for the method of linear cumulative damage, which had been previously proposed by Palmgren in 1924. In deriving this method, the following assumptions were applied to a simple distribution of discrete loads:

1. The amount of internal work absorbed by the material during each load cycle was constant at a given load level.

2. The maximum amount of internal work that could be absorbed from cyclic loads prior to failure was always the same.

3. The amount of internal work absorbed at each discrete load level in a simple loading spectrum was linearly cumulative and independent of the sequence of loading.

The first two assumptions lead to the following relationship between the amount of internal work absorbed and the number of load cycles applied at a specific load level.

$$\frac{w_i}{W} = \frac{n_i}{N_i} \qquad \text{(A1)}$$

where

w_i = work absorbed at the i^{th} varying load,

W = maximum amount of internal work that is absorbed by a material before failure (note that $W = W_i$ = constant),

n_i = number of cycles applied at the i^{th} varying load, and

N_i = number of cycles required for failure at the i^{th} varying load.

Assumptions two and three were used to derive the equation which is given below for relating the increments of internal work absorbed at two or more load levels to the maximum amount of internal work absorbed before failure.

$$\sum w_i = W$$

or (A2)

$$\sum \frac{w_i}{W} = 1$$

Elimination of $\frac{w_i}{W}$ in Equations (A1) and (A2) results in the following expression.

$$\sum \frac{n_i}{N_i} = 1 \tag{A3}$$

Failure is specified by the above equation in terms of a damage level of unity when the left hand side of the equation is considered to represent fatigue damage in the form

$$D = \sum \frac{n_i}{N_i} \tag{A4}$$

where

D = damage ratio or the fraction of fatigue life used up by the total number of load cycles that are applied at all load levels.

In using this expression, a unit distribution of discrete loads is usually selected that represents some specific service time or flight distance. When the damage ratio D has been calculated for this unit distribution, the predicted life is obtained as follows:

$$\text{Predicted Life (in hours or miles)} = \frac{1}{D} \times \text{(Life in hours or miles associated with a unit spectrum of discrete loads)}$$

or, in terms of the predicted fatigue life in cycles

$$N_L = \frac{\sum n_i}{D} = \frac{(\sum n_i)_{flight} + (\sum n_i)_{G-A-G} + (\sum n_i)_{ground}}{\left(\sum \frac{n_i}{N_i}\right)_{flight} + \left(\sum \frac{n_i}{N_i}\right)_{G-A-G} + \left(\sum \frac{n_i}{N_i}\right)_{ground}} \tag{A5}$$

where

N_L = predicted total number of cycles applied at loads of all magnitudes,

$\sum n_i$ = total number of load cycles in the unit distribution, and

D = damage ratio for the unit distribution.

SHANLEY'S "1X" METHOD

Shanley's "1X" method (references 8, 9, and 10) is similar to Miner's method in using the concept of linear cumulative damage that is expressed in Equation (A4). In this method S-N data are represented by an equation of the form:

$$N = \frac{\gamma}{S_v^{\delta}} \tag{A6}$$

where

γ = a parameter which is equal to the vertical intercept at N = 1 of the straight line fit to a plot of log S_v versus log N, and

δ = exponent defining the slope of the straight line fit.

This equation provides a linear approximation for the log-log form of S-N data that is illustrated in Figure 47.

A relative reduced stress or equivalent stress is also used in this method. This equivalent reduced stress is associated with a load of constant magnitude that may be applied the same number of times as all the loads above the endurance limit in a unit loading spectrum and may be defined in terms of Equation (A6) as

$$S_R = \left(\frac{\gamma}{N_R}\right)^{\frac{1}{\delta}} \tag{A7}$$

where

S_R = relative equivalent or reduced stress of constant amplitude, and

N_R = the total number of cycles that may be applied at all load levels above the endurance limit prior to failure.

Equation (A5) may be modified so that it becomes applicable to only the loads applied above the endurance limit in a unit loading spectrum. This is accomplished by multiplying this equation by the ratio of load cycles above the endurance limit $(\sum n_i)_{S_{v_i} > S_E}$ to the block size of the spectrum or $(\sum n_i)_{\text{all } S_{v_i}}$. Use of this ratio in Equation (A5) will lead to

$$N_R = \frac{(\sum n_i)_{S_{v_i} > S_E}}{\sum \frac{n_i}{N_i}} \tag{A8}$$

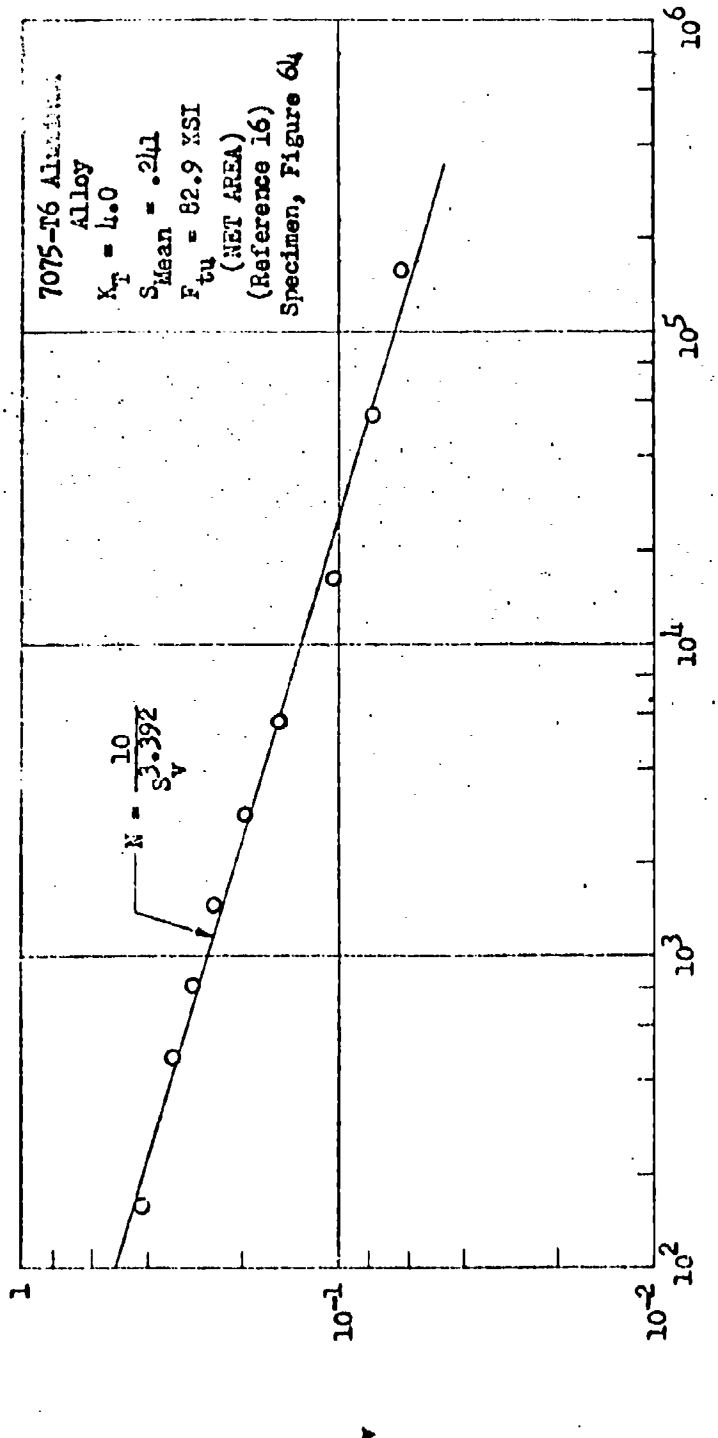

Figure 47. S-N Data for Notched Sheet Specimens

The following equation will result when Equations (A6) and (A7) are used to eliminate N_i and N_R in Equation (A8).

$$S_R = \left[\frac{\sum n_i\, S_{v_i}^{\delta}}{\sum n_i}\right]^{\frac{1}{\delta}} \quad S_{v_i} > S_R \tag{A9}$$

This equation was derived in reference 8 from a concept of crack growth that leads to the following relationship for depth of crack:

$$h = Ae^{an} \tag{A10}$$

where

- h = depth of crack,
- A = constant,
- e = exponential,
- a = factor that depends on the magnitude of the varying load, and
- n = number of loading cycles.

To complete the derivation of the "1X" method in terms of the quantities specified in Equation (A10) the reduced stress in Equation (A9) was assumed to cause the same crack growth as the unit loading spectrum for which the reduced stress was calculated.

SHANLEY'S "2X" METHOD

By using an assumption that the constant, A, in Equation (A10) was dependent on stress level, Shanley derived his "2X" method in the preceding reference. This assumption leads to a rate of crack growth which is higher than that used in the "1X" method, with the reduced stress expressed in the form:

$$S_R = \left[\frac{\sum n_i \, S_{v_i}^{\,2\delta}}{\sum n_i} \right]^{\frac{1}{2\delta}}_{S_{v_i} > S_E} \tag{A11}$$

By using Equations (A6) and (A7) to eliminate the relative stress terms in Equation (A11), the "2X" method may be expressed in terms of cycles as:

$$N_R = \sqrt{\frac{\left(\sum n_i\right)_{S_{v_i} > S_E}}{\sum \frac{n_i}{N_i^{\,2}}}} \tag{A12}$$

The relative reduced stress in Equations (A9) or (A11) may be used to predict fatigue life with the "1X" or "2X" method. To evaluate the reduced stress, S-N data must be analytically defined by Equation (A6) to evaluate the exponent δ that is used in Equations (A9) and (A11). The value of the relative reduced stress from either of these equations is used to read from an S-N curve the appropriate number of cycles N_R that may be applied at load levels above the endurance limit. Fatigue life is predicted by "1X" and "2X" methods when N_R is multiplied by the ratio of the total number of cycles of the associated unit loading spectrum to the total number of cycles above the endurance limit.

$$N_L = N_R \frac{\left[\sum n_i\right]_{\text{unit block size}}}{\left[\sum n_i\right]_{S_{v_i} > S_E}} \tag{A13}$$

The value of N_R could be evaluated by substituting the relative reduced stress in Equation (A7) or (A14). When these equations provide a good fit to the S-N curve in the vicinity of S_R, their analytical definition will be the same as

the value of N_R obtained by reading an S-N curve. Equations (A8) and (A12) may also be used to determine the value of N_R without requiring an analytical definition of S-N data or of reduced stress. However, these equations were not used in making predictions from the "1X" and "2X" methods.

THE FFA METHOD

Bo Lundberg and his colleagues at the Aeronautical Research Institute of Sweden (FFA) developed mathematical equations in reference 7 for simplified forms of the gust loading spectra and S-N data. By use of these equations in the linear cumulative damage concept, a closed form solution was obtained for fatigue life predictions.

In this method, S-N curves are represented by equations of the form:

$$N = \frac{\alpha}{(S_v - S_E)^{\beta}} \tag{A14}$$

where

- N = number of cycles to failure at a varying load of constant magnitude corresponding to the relative varying stress, S_v,
- S_v = relative varying stress,
- S_E = relative varying stress at the endurance limit (may be arbitrarily defined by the relative varying stress at $N = 10^7$),
- α = S-N curve parameter, given by the vertical intercept at $N = 1$ of the straight line fit to S-N data, when log $(S_v - S_E)$ is plotted vs. log N, and
- β = exponent defined by the slope of the straight line fit.

A graphical picture of S-N data is given in Figure 48 to illustrate the basis for this equation. This figure also indicates that Equation (A14) may not closely represent the behavior of S-N data in both the high and low stress ranges.

The cumulative loading spectrum is represented [illegible] in the FFA method by functions of the form:

$$H = H_0 e^{-h S_v} \tag{A15}$$

where

- H = total number of load cycles applied at or above the relative varying stress corresponding to S_v,
- H_0 = intercept of the straight line fit to the cumulative unit loading spectrum at $S_v = 0$ when S_v is plotted versus log H,
- h = slope of the straight line fit to the cumulative unit loading spectrum, and
- e = exponential.

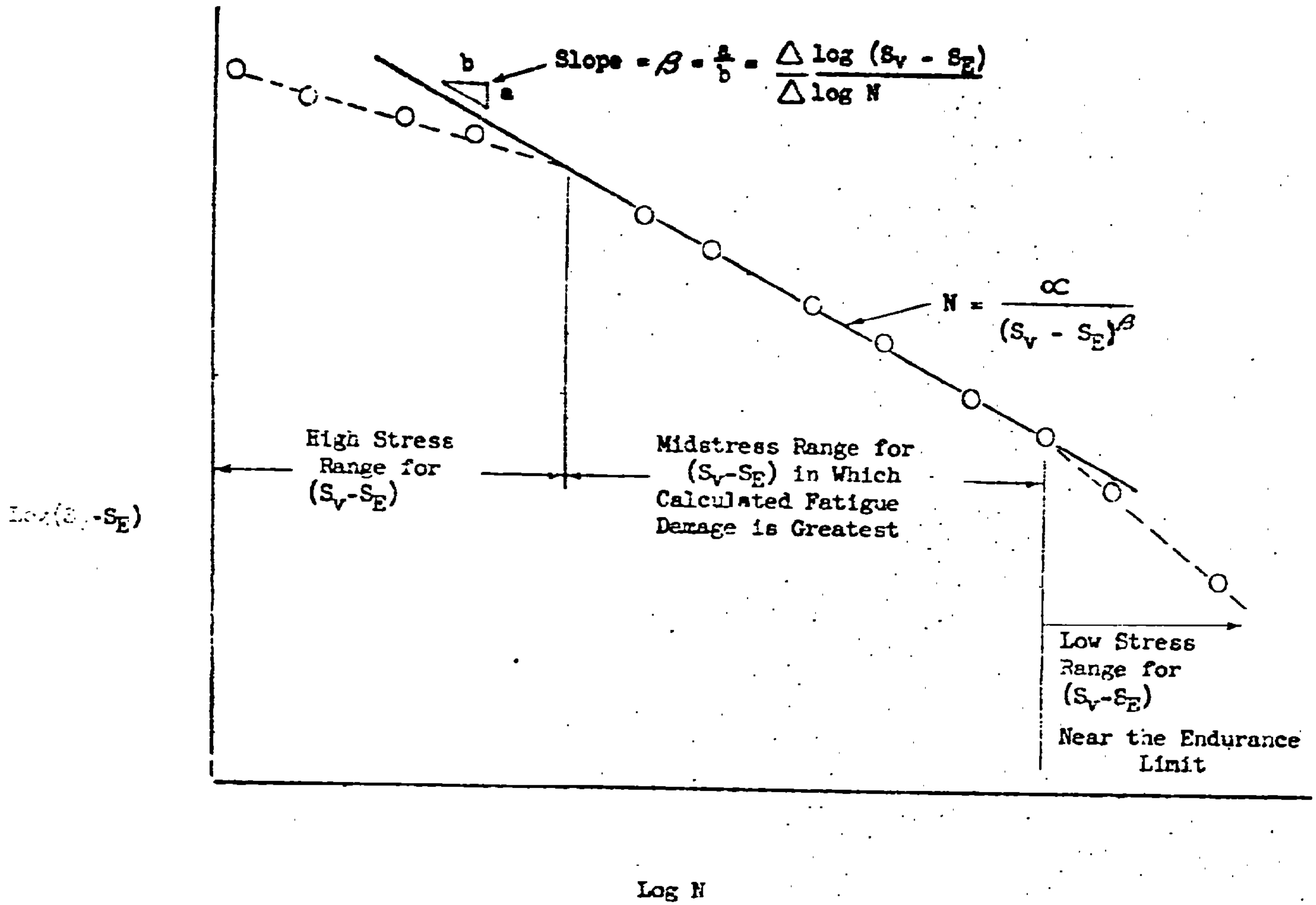

Figure 48. Analytical Representation of S-N Data

The type of curve fitting that is required for an adequate representation of cumulative loading spectra by this equation is illustrated in Figure 49. When more complex analytical functions are used, the solution of the resulting damage equation in the method can become very difficult. Complications are also involved when the shape of the unit loading spectrum cannot be adequately defined by a straight line fit in the stress range for maximum calculated fatigue damage.

To show how Equations (A14) and (A15) are used, Equation (A4) must be written in the form:

$$D = \sum \frac{-\Delta H}{N} \tag{A16}$$

where

ΔH = the number of cycles applied within the varying load interval represented by ΔS_v.

The minus sign is required in the above definition for consistency with the negative exponent in Equation (A15).

For an infinitesimal increment in relative varying stress, ΔS_v, Equation (A16) may be transformed into the following equation for defining fatigue damage over a wide range of varying stress.

$$D = - \int_{S_E}^{\infty} \frac{dH}{d\,S_v} \, \frac{1}{N} \, d\,S_v \tag{A17}$$

S. Eggwertz used Equations (A14) and (A15) in Appendix A of Reference 7 to eliminate $\frac{d\,H}{d\,S_v}$ and N in Equation (A17). He then integrated Equation (A17) between limits of S_E to ∞ arrive at the following approximate solution.

$$D = \frac{H_o}{\alpha} h^{-\beta} e^{-h\,S_E} \, \Gamma(\beta + 1) \tag{A18}$$

where

$\Gamma(\beta + 1)$ = Gamma function of $(\beta + 1)$ which

may be obtained from mathematical tables such as Reference 35.

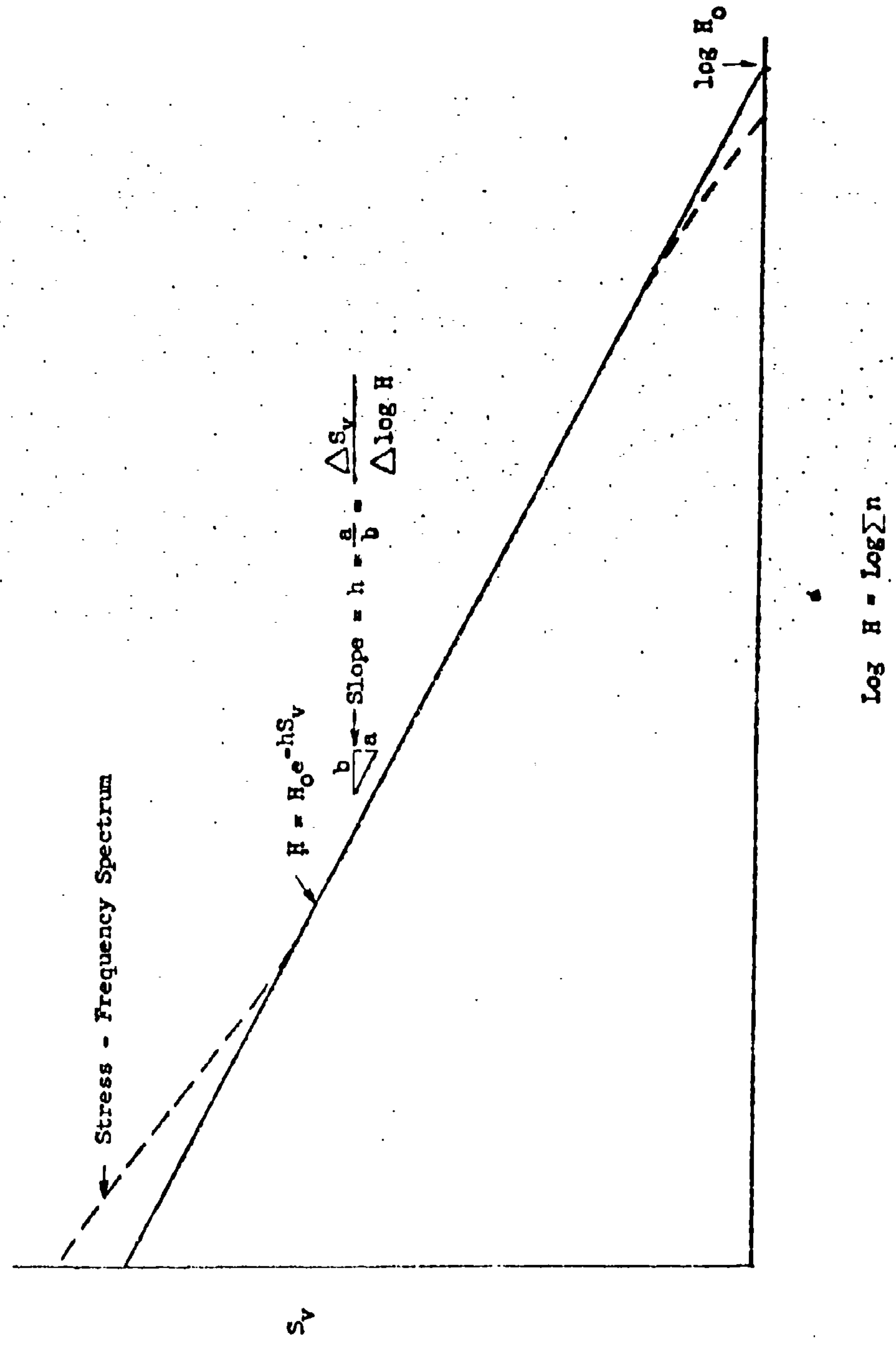

Figure 49. Analytical Interpretation of Unit Loading Spectrum

Within the usual accuracy of S-N and loading spectrum data, the approximate solution in Equation (A18) was considered to be more than adequate in Reference 7 for all practical applications of the FFA method.

When unit cumulative loading spectra are considered, fatigue damage may be calculated by using Equation (A18); and the predicted total number of cycles to failure may be obtained by using Equation (A5). In this last step, the actual total number of loading cycles in the unit spectrum must be used rather than the value of H_o that was determined in the analytical definition of the spectrum.

HENRY'S METHOD

Henry (reference 14) derived a method of nonlinear cumulative damage by defining fatigue damage in terms of a reduction in the S-N curve. This decrease in fatigue strength reflected the effects of increased local stress concentration when loading cycles were applied at any load level above the endurance limit. As originally proposed, Henry's method could be used only with materials which had S-N curves which fit the following equation:

$$N = \frac{\alpha}{S_v - S_E} \tag{A19}$$

Fatigue damage at any varying stress greater than S_E but less than $1.5\,S_E$ was evaluated in this method from the following equation:

$$D = \frac{S_E - S_E'}{S_E} = \frac{n/N}{1 + \frac{S_E}{S_v - S_E}(1 - n/N)} \tag{A20}$$

where

S_E = relative varying stress at the endurance limit from S-N data prior to the initiation of any fatigue damage, and

S_E' = relative varying stress at the endurance limit after fatigue damage is produced by applying varying loads associated with relative stresses larger than S_E.

The above equation becomes indeterminate when $S_v = S_E$ and cannot be used when $S_v \leq S_E$. Equation (A20) is also used to compute fatigue damage when two or more varying loads are applied above the endurance limit. The damage after applying one or more varying loads is first defined in terms of an equivalent cycle ratio $\left(\frac{n}{N}\right)_i$ at the next varying load above the endurance limit.

This equivalent cycle ratio is then used as the starting point from which additional damage will be computed by Equation (A20) at the new varying load. This is shown in Figure 50. The equation for the equivalent cycle ratio is

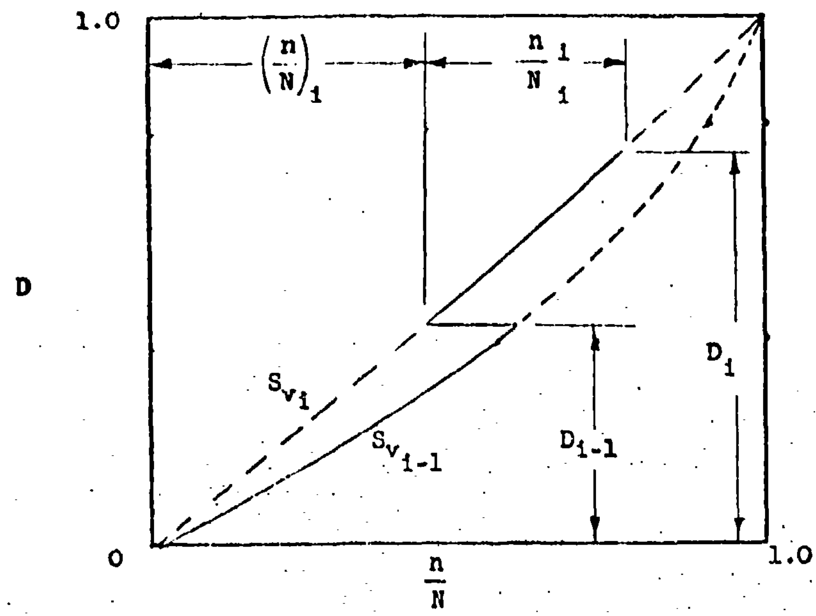

a) Lo-Hi - Sequence of Loading

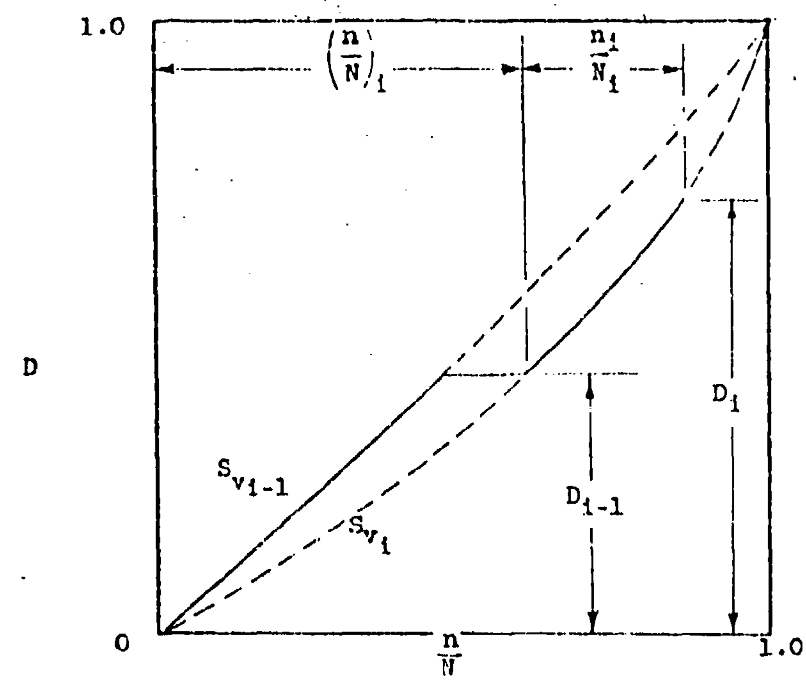

b) Hi-Lo - Sequence of Loading

Figure 50 Equivalent Cycle Ratio $\left(\frac{n}{N}\right)_i$ For Lo-Hi and Hi-Lo Sequence of Loading

$$\left(\frac{n}{N}\right)_i = \frac{D_{i-1}\left(1 + \frac{S_{v_i} - S_E}{S_E}\right)}{D_{i-1} + \frac{S_{v_i} - S_E}{S_E}} \qquad \text{(A21)}$$

where

$\left(\frac{n}{N}\right)_i$ = equivalent cycle ratio at a new relative varying stress greater than S_E that computes the level of damage reached by applying loading cycles at other relative varying stresses,

D_{i-1} = damage ratio after applying loading cycles at the last previous relative varying stress greater than S_E, and

S_{v_i} = the new relative varying stress greater than S_E at which damage is to be calculated.

The use of an equivalent cycle ratio may be further clarified in terms of stress levels and equivalent S-N curves by referring to the Hi-Lo loading sequence in Figure 51. In this figure, n_1 load cycles are applied at the larger relative varying stress of S_{v_1}. The constant amplitude fatigue life of N_1 on the original S-N curve is reduced by n_1 cycles to $(N_1 - n_1)$. An equivalent S-N curve that accounts for this reduction is defined in terms of a new relative endurance limit S_E'. The cycles to failure on the equivalent S-N curve at S_{v_1} can be read from the original S-N curve at the increased stress level of $C_1 \cdot S_{v_1}$ where C_1 is a function of the new relative endurance limit. The cycles to failure on the equivalent S-N curve at a new relative varying stress of S_{v_2} are also read from the original S-N curve, but not at S_{v_2}. They are read at the adjusted stress level defined by multiplying the new varying stress by C_1 which was previously evaluated at S_{v_1}. This results in the definition of a fatigue life under constant amplitude loading of S_{v_2} that is shorter than the original S-N curve by ΔN_2 cycles or the equivalent cycle ratio $(\frac{n}{N})_2$ in Equation (A21). Applying n_2 load cycles at the relative varying stress of S_{v_2} will result in another new equivalent S-N curve with a still lower endurance limit of S_{E_1}'. Points on this second equivalent S-N curve in Figure 51 at other relative varying stresses S_{v_i} are defined by reading the original S-N curve

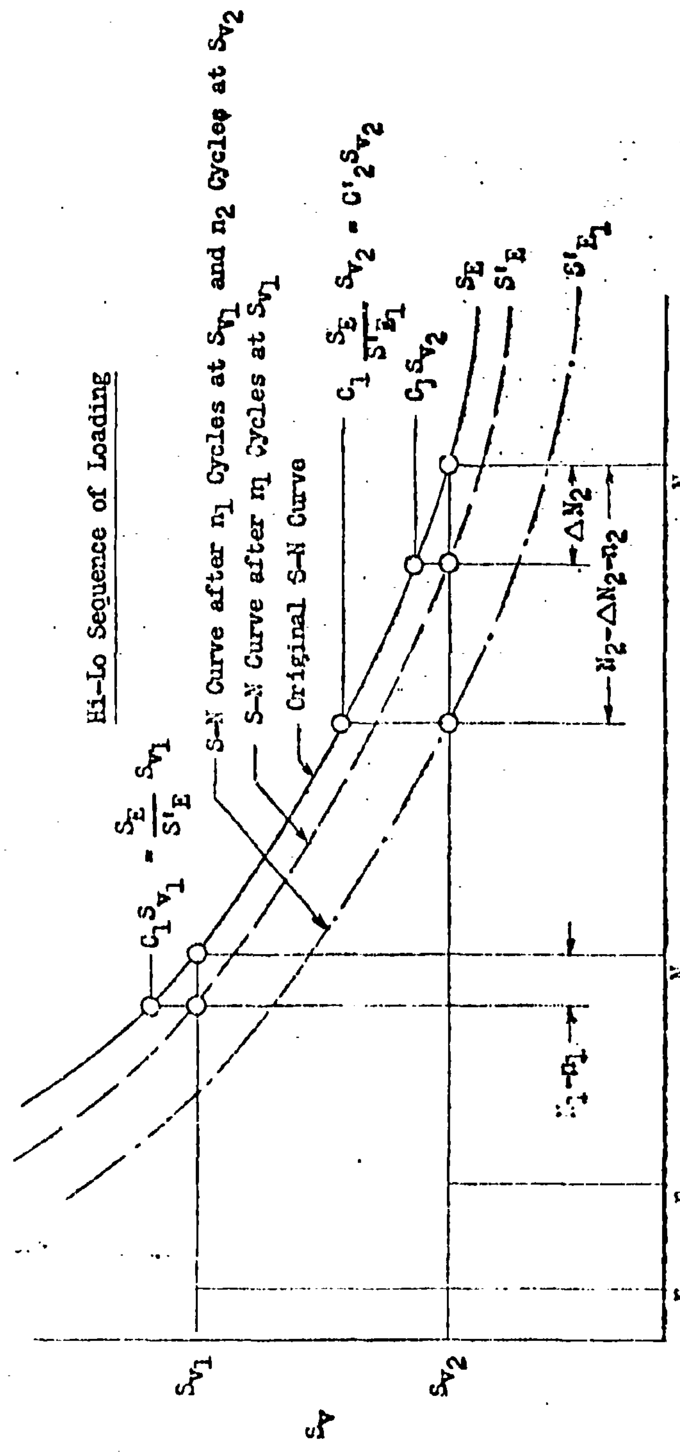

Figure 51. The Influence of Prior Fatigue Loading on the Selection of an Equivalent S-N Curve

stress levels of $C_2' S_{v_i}$. In this manner, the equivalent S-N data after any number of loading steps may be defined in terms of the original S-N curve. Since the exponent on $(S_v - S_E)$ in Equation (A19) has a fixed value of unity, the equivalent S-N curves have the same slope and are parallel to the original S-N curve when log $(S_v - S_E)$ is plotted versus log N.

If subscripts are added to Equation (A20), the equivalent cycle ratio in Equation (A21) could be used in the following manner to evaluate damage at the end of applying cycles of the next relative varying stress:

$$D_i = \frac{\left(\frac{n}{N}\right)_i + \frac{n_i}{N_i}}{1 + \frac{S_E}{S_{v_i} - S_E}\left[1 - \left\{\left(\frac{n}{N}\right)_i + \frac{n_i}{N_i}\right\}\right]} \qquad \text{(A22)}$$

where

D_i = damage ratio after applying cycles at the next relative varying stress greater than S_E,

n_i = number of cycles applied at the next relative varying stress, and

N_i = the number of cycles to failure from S-N data for the next relative varying stress.

Fatigue damage can be determined through repeated use of Equation (A22) as a function of the magnitude and sequence of application of varying loads above the endurance limit. The block size of a simple spectrum of discrete load levels affects the cycle ratio n_i/N_i used in this equation. Hence, the effects of block size are also a parameter in Henry's method.

After two loading steps, Equation (A22) would take the form given below, with n_1 load cycles applied in the first loading step and n_2 cycles in the second loading step.

$$D_2 = \frac{\frac{n_1}{N_1} + \frac{n_2}{N_2} - \frac{n_1}{N_1}\frac{S_E}{S_{v1}}\left(I + \frac{n_2}{N_2}\right) - \frac{n_2}{N_2}\cdot\frac{S_E}{S_{v2}}\left(1 - \frac{n_1}{N_1}\right)}{1 - \frac{n_1}{N_1}\frac{S_E}{S_{v_1}} - \frac{n_2}{N_2}\frac{S_E}{S_{v_2}} - \frac{n_1}{N_1}\frac{n_2}{N_2}\frac{S_E^{\,2}}{S_{v_1}\cdot S_{v_2}}\left(\frac{S_{v_1} - S_{v_2}}{S_{v_2} - S_E}\right)} \qquad \text{(A23)}$$

All terms except the first and second in the numerator and the first in the denominator are zero when S_E is zero, or tend to become zero when S_{v_1} and S_{v_2} are much greater than the relative endurance limit S_E. In such a case, Equation (A23) reduces to Equation (A4) in Miner's method. The added complexity in considering more than two load levels in Equation (A22) obscures this simple picture. When S_{v_1} and S_{v_2} are of the same order of magnitude as S_E, the difference in the fatigue damage predicted by Equations (A4) and (A23) will depend largely on the values of the cycle ratios $\frac{n_1}{N_1}$ and $\frac{n_2}{N_2}$. While this difference in fatigue damage would be slight for small cycle ratios, the difference will increase essentially as a linear function of these cycle ratios for fixed values of S_{v_1} and S_{v_2}.

Another important feature indicated by Equation (A23) is the effects of the order in which the larger varying load is applied to the specimen. When the larger relative varying load is applied first as S_{v_1}, the last term in the denominator is negative. This makes the resulting damage larger and the fatigue life shorter than it would be when the larger varying load is applied in the second loading step as S_{v_2}. Test results, however, tend to indicate that the fatigue damage is smaller and the resulting fatigue life longer when the largest of two or more varying loads is applied first. This may be seen by comparing the test lives for Hi-Lo and Lo-Hi loading sequences such as Test Groups No. G1 and G3 in Table 48. In certain loading ranges this effect may be due to beneficial residual stresses resulting from plastic yielding. (Reference 30)

GENERALIZATION OF HENRY'S METHOD

A more general version of Henry's method is derived to cover the cases where S-N data can be expressed in terms of Equation (A14). Unlike the S-N function expressed in Equation (A19) and used in the original derivation of Henry's method, Equation (A14) permits the slope of S-N data to have values other than unity. Removal of this slope restriction on S-N data permits Henry's method to have much wider application and to be used with many more materials than previously possible.

The general equation for damage is given by

$$D = \frac{1 - \left(1 - \frac{n}{N}\right)^{1/\beta}}{1 + \frac{S_E}{S_v - S_E}\left(1 - \frac{n}{N}\right)^{1/\beta}} \qquad \text{(A24)}$$

where

β = exponent from Equation (A14).

The equation replacing Equation (A21) for the equivalent cycle ratio at a subsequent relative varying stress is given below.

$$\left(\frac{n}{N}\right)_i = 1 - \left[\frac{\frac{S_{v_i} - S_E}{S_E}\left(1 - D_{i-1}\right)}{D_{i-1} + \frac{S_{v_i} - S_E}{S_E}}\right]^{\beta} \qquad \text{(A25)}$$

Equations (A24) and (A25) reduce to Equations (A20) and (A21) when the exponent β is unity.

This modified set of equations for Henry's method was used to calculate fatigue damage for most of the test spectra used in this report, with the exception of spectra employing random sequences. The random sequences were generally inadequately defined for the required step-by-step application of the equations.

CORTEN AND DOLAN'S METHOD

Corten and Dolan (reference 15) base the evaluation of fatigue damage on the number of fatigue cracks that are formed and the rate of crack propagation. While cracks are propagated at all load levels, the number of cracks is considered to be a function only of the largest varying load used in a fatigue test. With these basic concepts, fatigue damage is assumed on the first cycle of loading and is related to the number of cycles applied at each varying load through the following equation:

$$D = m r n^{a} \tag{A26}$$

where

m = number of cracks,

r = coefficient of the rate of crack propagation, and

a = exponent that could change with the amplitude of the varying load.

The total calculated damage for a periodically repeated sequence of two different varying loads was generalized from this equation in terms of applied load cycles. This generalization considered the actual number of cycles applied at the larger varying load , and the equivalent number of cycles required at the larger varying load to obtain damage increments equal to those accrued at the smaller varying load. In subsequent development of the equations, however, the authors used the actual number of cycles applied in each step at the smaller load rather than the equivalent number of cycles at the larger load, as mentioned in reference 29. Because of this, their resulting equation for fatigue life falls within the original concept of their theory only when the exponent "a" does not depend on the magnitude of the varying load, and fails to do so when the exponent is affected by changes in the magnitude of the varying load. Hence, the method must be used with a load invariant exponent, where the total number of cycles applied in a periodically repeated sequence of two different varying loads is given by

$$N_L = \frac{N_2}{\frac{n_2}{n_1 + n_2} + R^{1/a} \left(1 - \frac{n_2}{n_1 + n_2}\right)} \tag{A27}$$

where

N_2 = number of cycles to failure at the larger varying load when it is the only varying load applied to the specimen,

n_2 = the number of cycles applied at the larger varying load,

n_1 = the number of cycles applied at the smaller varying load, and

R = ratio of the coefficient of the rate of crack propagation at the smaller varying load to that at the larger varying load = $\frac{r_1}{r_2}$

The ratio R in the above equation was empirically related in reference 15 to the ratio of the smaller to the larger varying stress as shown below.

$$R^{1/a} = \left[\frac{S_{v_1}}{S_{v_2}} \right]^d \qquad \text{(A28)}$$

where

S_{v_1} = relative varying stress, at the smaller load;

S_{v_2} = relative varying stress, at the higher load; and

d = stress invariant exponent.

Equation (A28) was eventually used to extend equation (A27) into a more general equation for fatigue spectra involving any number of varying loads. The resulting equation is:

$$N_L = \frac{N'}{\frac{1}{\sum n_i} \sum n_i \left[\frac{S_{v_i}}{S'_v} \right]^d} \qquad \text{(A29)}$$

where

N' = number of cycles to failure from S-N data for the largest varying load, and

S'_v = relative varying stress for the largest load.

Use of the above equation will be discussed in the following section of this report.

MODIFIED CORTEN AND DOLAN METHOD

The method of Corten and Dolan is modified by replacing the stress ratios in Equation (A29) by a ratio involving the number of cycles to failure. This is readily accomplished when S-N data for a material can be analytically represented by Equation (A6).

In such cases, the following relationship between cycles to failure and relative varying stresses can be derived for the two-step spectrum under the restrictive condition where the relative varying stresses S_{v_1} and S_{v_2} are both greater than the relative endurance limit, S_E.

$$\frac{N_2}{N_1} = \left(\frac{S_{v_1}}{S_{v_2}}\right)^{\delta}$$

$$\text{or} \qquad \left(\frac{S_{v_1}}{S_{v_2}}\right)^{d} = \left(\frac{N_2}{N_1}\right)^{d/\delta} = \left(\frac{N_2}{N_1}\right)^{b} \tag{A30}$$

with

$$b = \frac{d}{\delta}$$

By generalizing Equation (A30) to cover any number of varying loads, this last equation can be used to eliminate the relative varying stress in Equation (A29). This results in

$$N_L = \frac{N'}{\frac{1}{\sum n_i} \sum n_i \left(\frac{N'}{N_i}\right)^{b}} \tag{A31}$$

Since Equation (A29) was derived in terms of stresses, it implies that all varying loads, including those below the endurance limit, are effective in propagating fatigue damage. On the other hand, Equation (A31) does not consider fatigue damage to be propagated below the endurance limit. This is because the number of cycles to failure, N_i, is infinite in this region of the S-N data.

Values of the exponents d in Equation (A29) or b in Equation (A31) can be determined by using test data to define all other terms in the applicable equations.

S-N curves define N' and N_i, the unit loading spectra define S_{v_i} or n_i, while N_L may best be defined by the geometric means of the test lives of a set of nominally identical specimens. Evaluation of the exponent b from the test data is discussed in Section III.

A SIMPLIFIED NONLINEAR CUMULATIVE DAMAGE METHOD

While several of the methods which have been described use nonlinear accumulations of damage, an investigation of the simplest type of nonlinear representation was considered to be desirable. For this purpose the available test data will be used to evaluate the exponent in the equation

$$N_L = \frac{\sum n_i}{\sum \left[\frac{n_i}{N_i} \right]^c} \tag{A32}$$

where

c = empirical exponent that is independent of the magnitude of the varying load.

When the exponent c is assumed independent of load amplitude, it is found to vary with material, specimen configuration, number of loading cycles in the unit spectrum, the number of loading steps, and the sequence in which the varying loads are applied to the specimen.

The exponent c is related to the exponent b in the modified version of Corten-Dolan's method. For a spectrum involving just two loading steps, the relationship between these exponents may be found by equating N_L in Equations (A31) and (A32). This will result in:

$$b = \frac{\log_e\left(\frac{N_2}{n_1}\right) + \log_e\left[\left(\frac{n_1}{N_1}\right)^c + \left(\frac{n_2}{N_2}\right)^c - \frac{n_2}{N_2}\right]}{\log_e\left(\frac{N_2}{N_1}\right)} \tag{A33}$$

where

n_1 = number of cycles applied in the spectrum at the smaller varying load,

n_2 = number of cycles applied at the larger varying load,

b = exponent in Equation (A31), and

c = exponent in Equation (A32).

The above relationship becomes rather complex and neither exponent can be expressed as a simple function of the other when a loading spectrum contains more than two different varying loads.

One pertinent difference between the exponent b in Equation (A31) and the exponent c in Equation (A32) lies in the fact that the value of c is more dependent upon block size than the exponent b. If the exponent c were evaluated for a unit loading spectrum which had the same fatigue life when applied at two different block sizes, the value of this exponent would be larger for the smaller block size as illustrated in Figure 52. The value of c is affected by block size through the number of applied load cycles that appear under different exponents in the numerator and denominator of Equation (A32). Figure 52 also indicates that the value of the exponent b is independent of block size at a specific fatigue life. The only effect that block size can have on the exponent b in Equation (A31) is from experimental variations in the fatigue lives used to evaluate this exponent.

Equations (A31) and (A32) both reduce to the simple linearly cumulative damage hypothesis, Equation (A5), when the exponents b and c are made equal to unity.

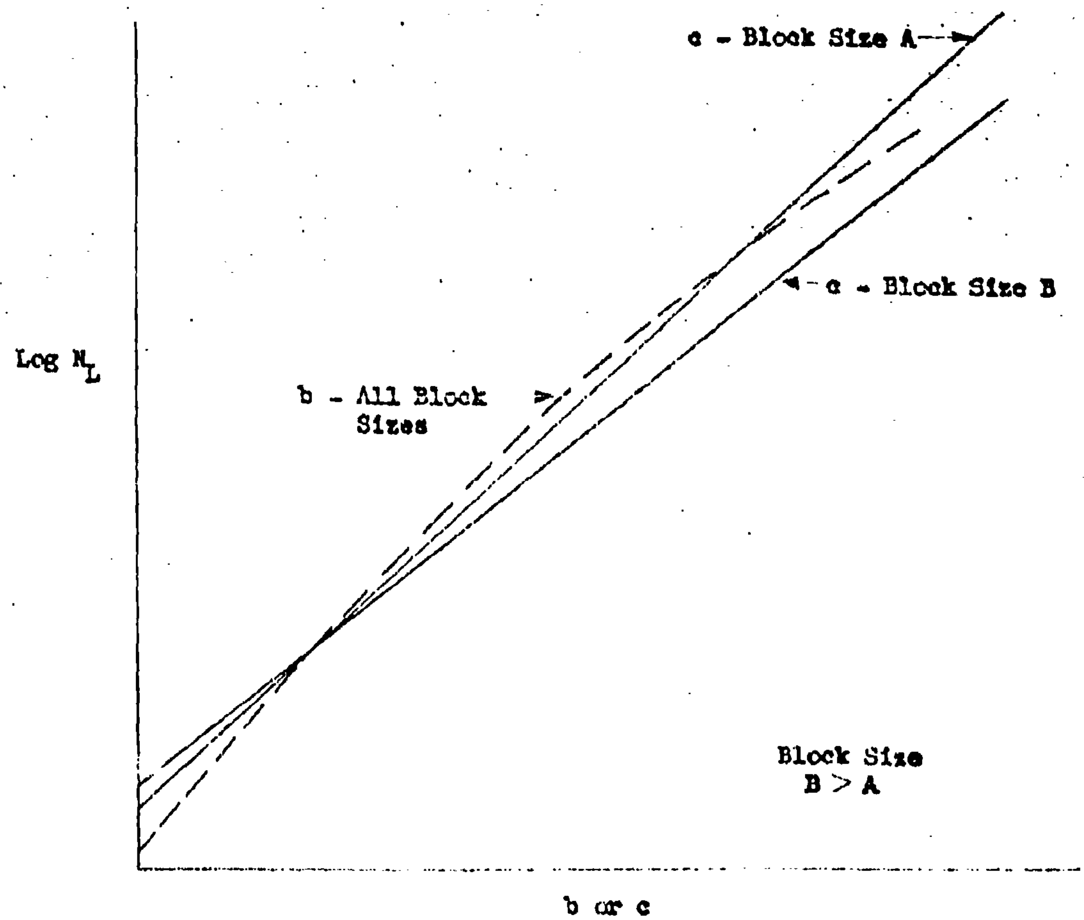

Figure 52 Typical Variation in Fatigue Life with the Exponents b and c for a Specific Unit Loading Spectrum.

KOMMERS' HYPOTHESIS AND RICHART-NEWMARK'S AND MARCO-STARKEY'S METHODS

The concept that damage curves are a function of both the varying load and the cycle ratio, n/N, was first presented as a hypothesis by Kommers in 1945 (Reference 22). In 1948 Richart and Newmark (Reference 24) and later (1954) Marco and Starkey (Reference 25) proposed graphical and analytical methods for the application of these damage curves to fatigue life predictions. This hypothesis placed only one restriction on the curves. They could have any shape, but each curve was required to indicate a damage level of one when the cycle ratio was unity. Damage curves of this general type are shown in Figure 50. The evaluation of the actual damage curves is difficult because of the problems involved in assessing any degree of damage less than failure. The most important factor, however, is the relationship between damage curves rather than their absolute values. From this concept, Richart and Newmark developed a method for experimentally securing damage curves at a specific varying load relative to an arbitrary damage curve at any reference varying load.

Marco and Starkey (Reference 25) developed an analytical form for damage curves that is similar to that of Richart and Newmark. These authors make the shape of the damage curve at each load amplitude a function of the cycle ratio raised to a load or stress-dependent exponent.

$$D = \left(\frac{n}{N} \right)^{\psi} \tag{A34}$$

where

D = damage at a specific varying load level,

n = number of cycles applied at the referenced varying load level,

N = number of cycles to failure, and

ψ = load-dependent exponent

In applying the above methods to test results, specially obtained two-step loading test data would be required in large quantities to experimentally determine the relationship between damage boundaries. Since this type of data was not available in sufficient quantity for any of the test conditions being considered, Kommers', Richart-Newmark's, or Marco-Starkey's methods could not be applied.

FREUDENTHAL-HELLER'S METHOD

Freudenthal and Heller (reference 26) proposed the use of a stress-interaction factor to construct a fictitious S-N curve. The fatigue life, associated with a randomly applied unit spectrum of loading, is predicted from the fictitious S-N curve by the concept of linear cumulative fatigue damage, with Equation (A4) being replaced by

$$\sum \frac{n_i \, \omega_i}{N_i} = 1$$

or (A35)

$$\sum \frac{n_i}{N_i''} = 1$$

where

ω_i = stress interaction factor that reduces the cycles to failure at the i^{th} varying load after the specimen has had prior exposure to larger varying loads, and

$N_i'' = \frac{N_i}{\omega_i}$ = cycles to failure at the i^{th} varying load from the fictitious S-N curve.

Determination of the stress interaction factor in the above equations depends on the statistical analysis of a large number of test results from a number of loading spectra applied to each type of specimen of interest. Experimental data may eventually be obtained that shows the nature of these interaction factors and some rules for their evaluation. Lack of both the type and quantity of data prevented application of this particular method to the test results used in this report.

LANGER'S METHOD AND GROVER'S METHOD

Langer (reference 11) and Grover (reference 12) have each divided the process of fatigue damage development into two stages. The first stage involves crack initiation, and the other crack propagation. In Grover's development of this type of analysis, it is assumed that

$$\sum \frac{u_i}{v_i N_i} = 1 \qquad \text{(A36)}$$

and

$$\sum \frac{x_i}{N_i (1 - v_i)} = 1 \qquad \text{(A37)}$$

where

$$(u_i + x_i) = n_i$$

u_i = number of load cycles applied before crack initiation,

x_i = number of load cycles applied between crack initiation and final failure, and

v_i = per cent of the number of cycles to failure that is used up in initiating cracks at the i^{th} varying load level.

Use of Equations (A36) and (A37) requires information on the number of cycles at each load level for crack initiation and the additional number of cycles to critical fracture. However, if the S-N curves for crack initiation and for failure are parallel, this method reduces to the simple linear cumulative damage equation.

No evaluation of this method was possible because the information required was not reported in the available data selected for this study.

LEVY'S METHOD

Another approach to analyzing fatigue has been developed by Levy (reference 27). In this approach the following equation was derived for two-step loading by assuming that less than one application of the higher load level in 10,000 total load cycles would have no effect on the S-N curve at the lower varying load.

$$N_L = \sqrt[4]{\left(N_2^{\log_{10}\frac{10000\,n_2}{n_1 + n_2}}\right)\left(N_1^{\log_{10}\frac{n_1 + n_2}{n_2}}\right)} \qquad (A38)$$

where

N_L = predicted fatigue life,

N_1 = number of cycles to failure at the lower varying load,

N_2 = number of cycles to failure at the higher varying load,

n_1 = number of cycles applied at the lower varying load, and

n_2 = number of cycles applied at the higher varying loads.

This method was extended to three loading steps, with the following equation being suggested for fatigue life predictions with more than three loading steps:

$$\log N_L = a \log \frac{n_1}{\sum n_i} + b \log \frac{n_2}{\sum n_i} + \cdots\cdots + M \qquad (A39)$$

where a, b, ... and M are functions of N_1, N_2, etc.

This equation is tedious to apply, as it becomes necessary to evaluate (q + 1) constants in Equation (A39), where q is the total number of loading steps in a unit spectrum. An eight-loading-step spectrum, for example, would require nine different sets of relative load frequencies as well as nine corresponding test results in order to solve the resulting system of simultaneous equations for the applicable constants. Once the constants have been determined from this system of equations, only one equation involving these constants would be necessary to predict fatigue life for any one of the specified unit spectra. The type of test data used in this report could not generally be adapted to applications of Levy's method.

SMITH'S METHOD

Smith, by considering two stress levels, has developed a method in Reference 13 that places primary emphasis on the effects of residual stresses in regions of stress concentration. These residual stresses are induced by plastic deformations during the first high load cycle. Their presence modifies the internal stresses associated with each additional loading, and, as such, is a stress analysis procedure rather than a damage theory or a life prediction method.

The modified stress, including the residual stress component, is used with the unnotched S-N curves and the linear cumulative damage equation to predict the fatigue life.

Since this method considers the influence of local stress variations on the fatigue strength of the material, an accurate stress history at the critical point is required. While this procedure has been demonstrated for simple two-step loading on a simple coupon, its application to multi-spectra in complex structure is not practical as yet. It was not possible to evaluate this method with the data chosen for this study.

TANGENT-INTERCEPT METHOD

The Tangent-Intercept approach (reference 28) was originally conceived to aid in interpretation of spectrum-type fatigue tests. It is in essence a graphical procedure of plotting the total cumulative load frequency spectrum of varying stresses achieved in the fatigue test at failure upon a graded set of S-N curves of the same mean stress level. The K_T value of the S-N curve which is tangent to the test total cumulative load frequency curve becomes the effective fatigue quality associated with the joint tested. Since both the test spectrum and the S-N curves were standardized for all fatigue tests of this era, simply comparing the effective K_T values gives a relative scale of joint quality. The method is schematically demonstrated in Figure 53. Joint A demonstrated a $K_T = 4.00$; Joint B did not last as long under the standardized test spectrum of loading and indicates a tangency to the S-N curve for $K_T = 8.00$. Fatigue tests of many joints which had proven satisfactory in service life showed better than, for example, $K_T = 4.5$. Some joints which developed cracks in service tested worse than K_T of 4.5. By this means $K_T \leq 4.5$ became established as the fatigue quality acceptance standard. New joints were required to be redesigned and retested until they demonstrated acceptably low K_T (≤ 4.5).

The standard test spectrum was derived from a peak count reduction of flight test records from an instrumented (VGH) Lockheed Model 18 Transport flown approximately 1000 miles through Rocky Mountain weather. Later more extensive records reduced by NACA show that for small service times this spectrum is good. However, with longer service times, relatively greater number of high load levels are developed producing a concave upward shape to the load frequency curve. Other loadings such as landing, taxiing, ground-air cycle, etc., became known as prominent producers of fatigue damage, each at considerably different mean stress levels. When these loadings were included in the test program, the Tangent Intercept approach proved inadequate to handle the added complexities. Its use for the purpose of interpretation of spectrum fatigue tests has since been entirely superseded by the application of the linearly cumulative damage concept.

Proposals have been made to convert this graphical process into a procedure to predict fatigue life (reference 31). As a life prediction procedure, the tangent-intercept method is illustrated on Figure 54. In this method, the prediction of fatigue life is based on the number of times the complete unit loading spectrum can be applied to a specimen before the spectrum becomes tangent to (or intercepts) the S-N curve defined for the test specimen.

As indicated on Figure 54.

$$N_L = \frac{N_T}{H_T} H_S \qquad (A40)$$

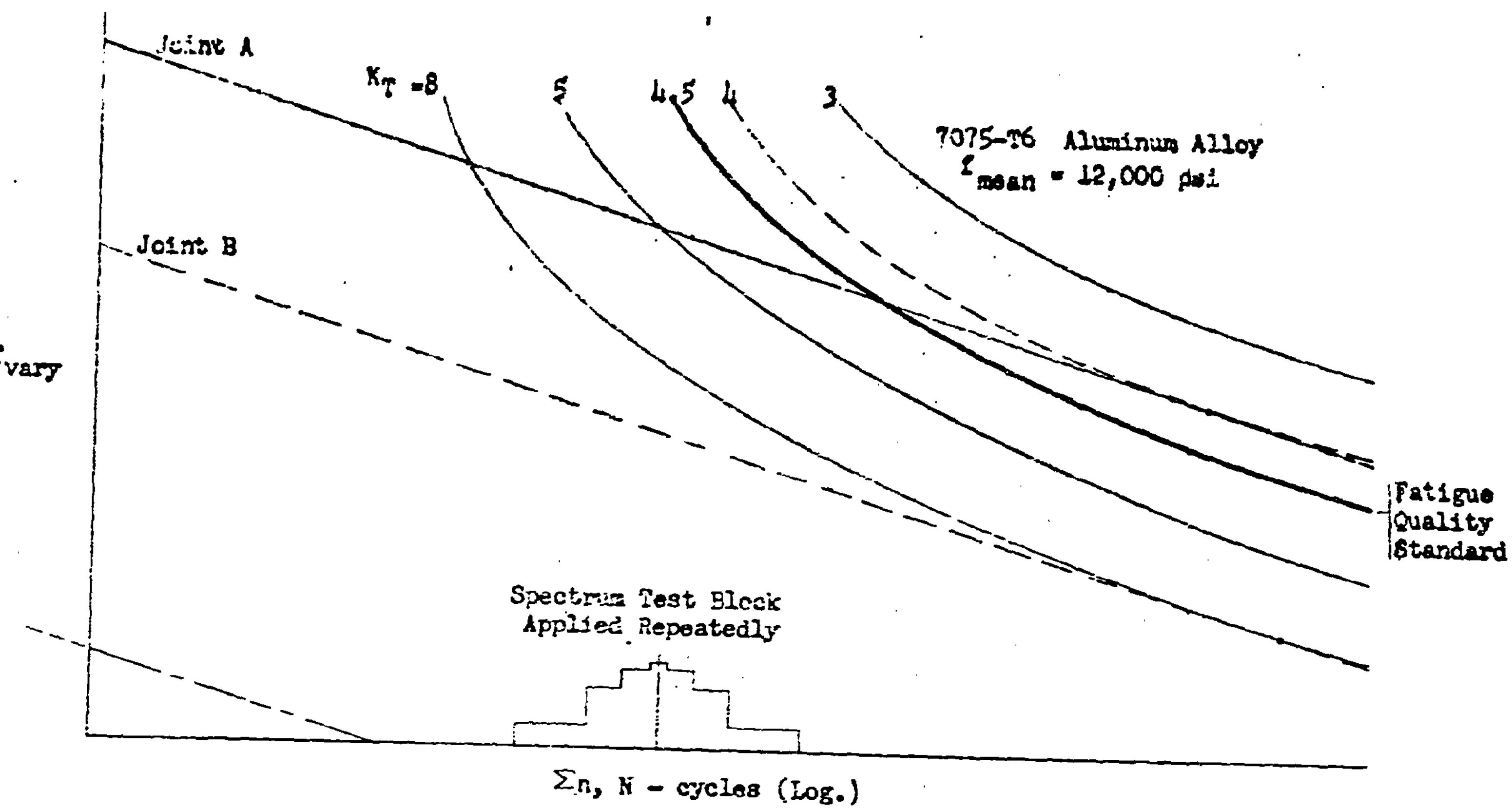

Figure 53 Tangent Intercept Method of Spectrum Fatigue Test Interpretation

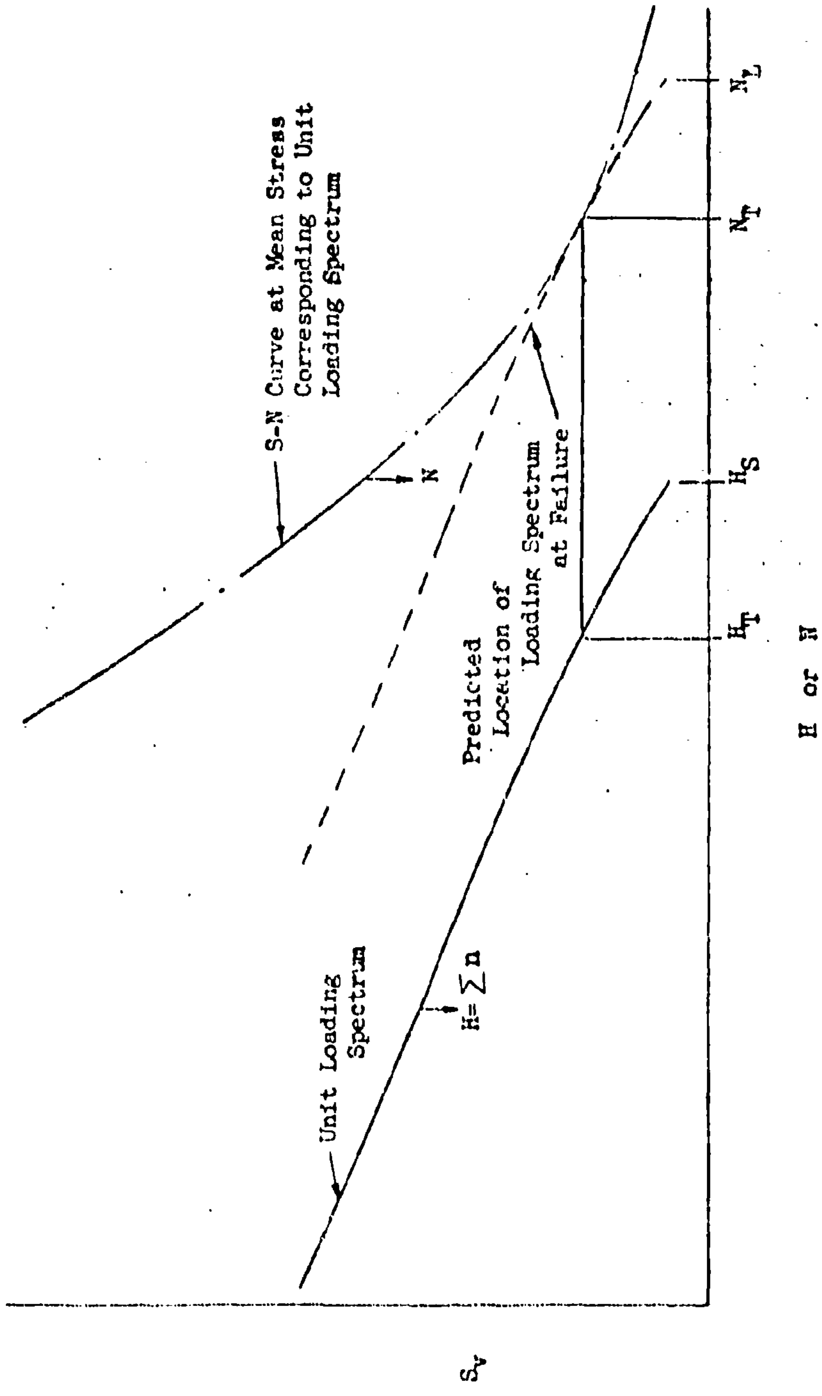

Figure 54 Schematic of Tangent Intercept Method

where

N_T = number of cycles to failure at the point of tangency of the cumulative loading spectrum and S-N curves,

H_T = the total number of cycles in the unit loading spectrum that are applied at or above the varying load at which the cumulative loading curve is tangent to the S-N curve, and

H_S = total number of cycles applied at all varying loads in one complete application of the unit loading spectrum.

Once the unit loading spectrum and the S-N data are specified, the tangent intercept method will give the same predicted life irrespective of the loading sequence or the block size of the unit spectrum.

In terms of the linear cumulative damage process, the basic procedure outlined for the tangent-intercept method implies that the one constant amplitude load in the test spectrum at the point of tangency with the S-N curve is the only load which creates damage, and all other loads, both above and below this level, contribute no fatigue damage. This is, of course, known to be unconservative.

In the graphical application of the procedure, one test spectrum of a gust or a maneuver type may be conveniently compared with an appropriate set of S-N curves at a time. If the required total loading spectrum contains other significant types of loadings, such as combined gust, maneuver, ground taxi, and ground-air-ground transitions, the graphical procedure becomes hopelessly inadequate and impractical.

For these reasons no attempt was made to develop an empirically corrective procedure to reduce the unconservatism of the tangent-intercept fatigue life predictions.

STRESS CONCENTRATION METHOD

The stress concentration procedure is a method of stress analysis to define as accurately as possible the stress distribution in local regions of discontinuities. (Typical references 1, 2 & 3) Before specific fatigue test data are available on a part, coupon, or joint specimen, the analytical assessment of the fatigue quality of a design is possible only through means of highly refined theoretical and/or photo-elastic or experimental stress analysis procedures. This type of analysis has in the past received a large amount of attention. This attention is currently no less, and work will continue to expand in the future. A large body of literature exists which provides solutions for many types of discontinuities and applied loading systems. However, for the reasons discussed in the introduction, applications of this analytical approach (including, as well, both experimental photoelasticity and static experimental stress analysis by means of strain gages and others) can only be considered a rough approximation until specific fatigue tests can be run.

To complete a life prediction method, the stress concentration procedure must be coupled with a fatigue damage theory. For evaluation in this study, the Miner's simple linear cumulative damage hypothesis was chosen. This method, used with a standardized set of S-N data for various geometrical K_T values, constitutes the basic information usually available in early stages of design. The choice of the standard S-N curves is, in essence, arbitrarily specifying a damage boundary shape before this boundary has been determined or confirmed by tests. For important complex joints or critical areas of the structure, the timely confirmation or correction of the fatigue quality and the life prediction by fatigue tests through the full range of the loading spectrum is of utmost importance.

FATIGUE QUALITY INDEX METHOD

The Fatigue Quality Index method was developed to overcome the difficulties inherent in the use of the Tangent Intercept method for the interpretation of a composite spectrum test on a complex joint. The composite test spectrum is generally made up of a taxi-load spectrum at the ground static mean load level, a gust and/or manouver and landing spectrum at the flight static mean load level, and ground-air-ground transition cycles for each flight. The spectrum fatigue results are interpreted by the use of the simple linearly cumulative damage equation to specifically define (by interpolation) which of the standardized S-N curves (identified by K_T value), when used in conjunction with the actually applied test spectrum, will exactly satisfy the equation:

$$\sum \frac{n_i}{N_i} = \text{[illegible]} \qquad \text{(A41)}$$

The stress concentration factor whi[illegible] identifies these curves becomes the Fatigue Quality Index demonstrated [illegible] the test specimen under its expected loading spectrum. The Quality Index [illegible] must be equal to or smaller than the established quality standard or [illegible] redesign and retest is necessary until satisfactory quality is achieved. [illegible] established quality standard is based on the results obtained in an ident[illegible], consistent analysis of many joints which have a known service history.

For comparative purposes the quali[illegible] scale must remain fixed and the analysis system consistent between the anal[illegible] of service history and the analysis of tests of new structure. Generally [illegible] complete S-N curve is not available for each complete joint or critica[illegible] area of the structure. For these reasons one set of S-N data for the hard [illegible] minum alloys has been fixed and all test interpretations and life predictio[illegible] are based on the consistent use of this standardized set. This standardi[illegible] set of S-N curves may be considered an arbitrarily defined damage bounda[illegible] and, in the usage outlined, have no longer any significant relationship to th[illegible] data from which they were derived.

For its use as a life prediction [illegible] hod a Fatigue Quality Index is determined from a fatigue test in which a com[illegible] site spectrum of all anticipated service loads is applied to suspect areas [illegible] the structure. The Fatigue Qualit[illegible] derived from this test result may [illegible] considered as a test-de[illegible] boundary on which life predictions [illegible] may be made for other similarly shaped loading spectra.

The Quality Index procedure as a [illegible] prediction method is evaluated along with the other selected methods by [illegible] ication to suitable data from the literature and to the special fatig[illegible] ata generated for this program. These evaluations are discussed in the ap[illegible] iate places elsewhere in this report. See Sections III through VI.

APPENDIX B

APPLICATION OF SELECTED FATIGUE LIFE PREDICTION METHODS TO PUBLISHED TEST DATA

The study of the twenty proposed fatigue life prediction methods, conducted in Appendix "A", reduced the list to ten which were to be evaluated numerically by application and comparison with the selected spectral fatigue test data described in Appendix "C". It was also decided to vary the procedure of mathematical curve fitting in two of these methods to determine the significance of alternate equation parameters for S-N curves, one set derived for a least square "best fit" for all data points, and the other set derived for a least square "best fit" in the local region of the midstress levels, where usually the maximum calculated damage is found. These twelve applications are those listed:

1. Miner's Linear Cumulative Damage Method.
2. Lundberg's FFA Method - Variant "A", with best fit to the midstress range of S-N and loading spectra data.
3. Lundberg's FFA Method - Variant "B", with best fit to the full-stress range of S-N and loading spectra data.
4. Shanley's "1X" Method.
5. Shanley's "2X" Method.
6. Henry's Method - Generalized Form - Variant "A", with best fit to the midstress range of S-N data.
7. Henry's Method - Generalized Form - Variant "B", with best fit to the full-stress range of S-N data.
8. Tangent Intercept Method.
9. Stress Concentration Procedure with Linear Cumulative Damage.
10. Fatigue Quality Index Method.
11. Modified Corton-Dolan.
12. Nonlinear Cumulative Damage.

The following sections explain the applications of each of these methods to the prediction of the fatigue lives of test specimens for which spectral and S-N data are listed in Appendix C.

The comparisons of the predicted fatigue life and experimental fatigue life are given in Section III of the main body of the report.

In addition to the direct comparison of fatigue lives on the cycle scale, a constant proportional adjustment in the varying stress levels was determined to make the predicted life exactly the experimental life for each test group by each method. The application of the proportionality factor to the mean

stress would, of course, make a more meaningful assessment of the effect of cross-section material changes in design. However, since the influence of the mean stress is not expected to change the order of ranking of the methods, the more simple comparison was chosen. The results of the analysis and comparisons of the various methods by the stress adjustment factor are given in Section III of the main body of the report.

1. Miner's Linear Cumulative Damage Method

The direct application of Miner's linear cumulative damage method is simple and straightforward. The unit cumulative frequency spectrum for the applied loads of each group is reduced to the simple number of cycles, n_i, in each stress interval in Tables 31 through 47 of Appendix C. The stress intervals are those used in each particular test, and the reduction from the accumulated spectrum to the simple spectrum is in accordance with the definitions given in Figure 55. Assuming all the cycles within one stress interval to act at the equivalent stress level approximately the mid point of the interval, the allowable number of cycles, N_i, at that stress level was interpolated from the appropriate form of the S-N curve; i.e., symmetrical varying stresses about a constant mean stress for gust-type spectra, while varying stresses that maintain a constant minimum stress were used for the maneuver-type spectra. The interpolating function is a straight line segment in S_v - Log N from tabulated input data taken at relatively close intervals. These values of N_i are also listed in the Tables 31 through 47. The individual damage ratios are formed and summed for all the stress intervals to form the damage for the unit spectrum. The life prediction for the group is then computed by Equation (B1):

$$N_L = \frac{\left(\sum n_i\right)_{\text{unit block}}}{\left(\sum \frac{n_i}{N_i}\right)_{\text{unit block}}} \qquad \text{(B1)}$$

These computations were performed on the IBM 7090 computer.

The stress adjustment ratio was determined by the change in slope of the accumulative spectra (i.e., constant proportional change to the stresses of all intervals) to require the process to exactly predict the test life. This was accomplished by an iteration procedur programmed for digital computation on the IBM 7090 computer.

Special handling was found necessary for some cases in which small changes of the stress adjustment factor would increase or decrease the mid-interval stress of the lower block in the vicinity of the endurance limit stress. Bringing in or dropping out of the large number of cycles in this last block could indicate a disproportionate

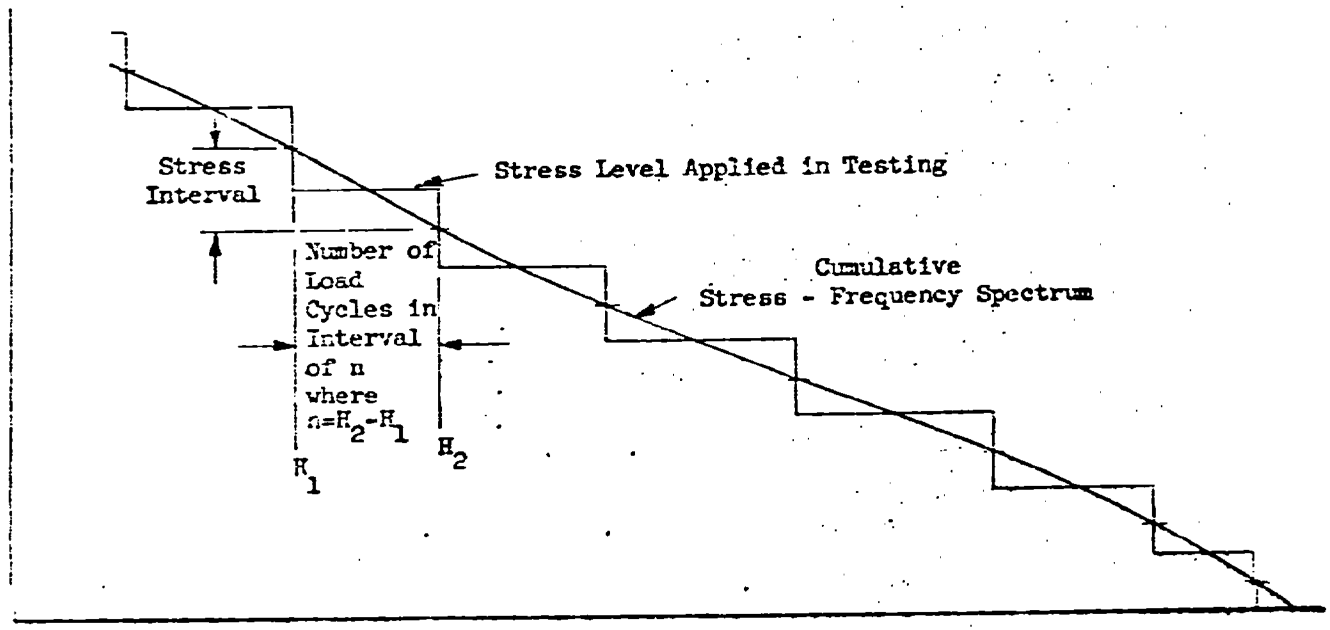

S_v

Cumulative Cycles = $H = \sum n$

Figure 55 Method used to Reduce Cumulative Stress - Frequency Spectrum into Simple Cyclic Loading Steps.

shift in the predicted fatigue life for those cases where the S-N data indicate an actual endurance limit, or those cases in which an arbitrary endurance limit had been defined at 10^7 cycles.

2. Lundberg's FFA Method

Since Lundberg's FFA method is basically an analytical form of the linear cumulative damage procedure, application consists of the determination of the mathematical curve parameters for the best fit to the unit applied loading spectrum, and those for best fit to the appropriate S-N curve. The suggested equation for gust-type spectra Equation (A15) has two adjustable parameters, H_o, the intercept, and h, the slope of the straight line, which is a best fit of the unit cumulative relative varying stress history when plotted in semi-log form of S_v vs. $\log \sum n$, as in Figure 56. The parameters for the S-N curve, α and β from Equation (A14), represent, respectively, the intercept and the slope of the straight line which best fits the S-N data in a $\log(S_v - S_E)$ vs. $\log N$ plot as in Figure 57. These four parameters were determined for each test case using the applied unit loading spectra and the appropriate type of S-N data for gust spectra, or for maneuver-type spectra. The S-N curves for each type of specimen were determined for the applicable mean stress or minimum stress through interpolation on the Christensen diagram as discussed in Section D. Where necessary, parameters for the unit loading spectra were biased to best fit the midstress range in the region of maximum calculated damage. The parameters for the S-N curves were determined for two cases:

Case (A) for a best fit to the midstress range of S-N data in the region of maximum calculated fatigue damage ratios, and

Case (B) for a best fit to the full stress range.

The parameters for the equations of Case (A) are given in Table 19; those for Case (B) are given in Table 22 for the gust spectra tests. The unit damage computed from the unit spectra is given in terms of these four parameters by Equation (A18) of Appendix A, and the predicted fatigue life is computed by Equation (A5) of Appendix A. These fatigue life predictions are listed in Table 21 for the gust spectra by Case (A) and in Table 22 for Case (B). The fatigue life predictions for the maneuvering spectra tests are given in Table 23. The geometric mean of the experimental fatigue life of each group of tests is given in each table for direct comparison. These data are plotted in Figures 5 and 6 in Section III, where comparisons of these results with those of other methods are discussed.

The stress adjustments required to predict exactly the experimental fatigue life were determined for each test group by trial manipulations of the unit test spectra slope parameter h, maintaining H_o the intercept constant. The resulting stress adjustment factors are listed in Table 24 for the gust loading spectra, and in Table 25 for the maneuvering-type spectra.

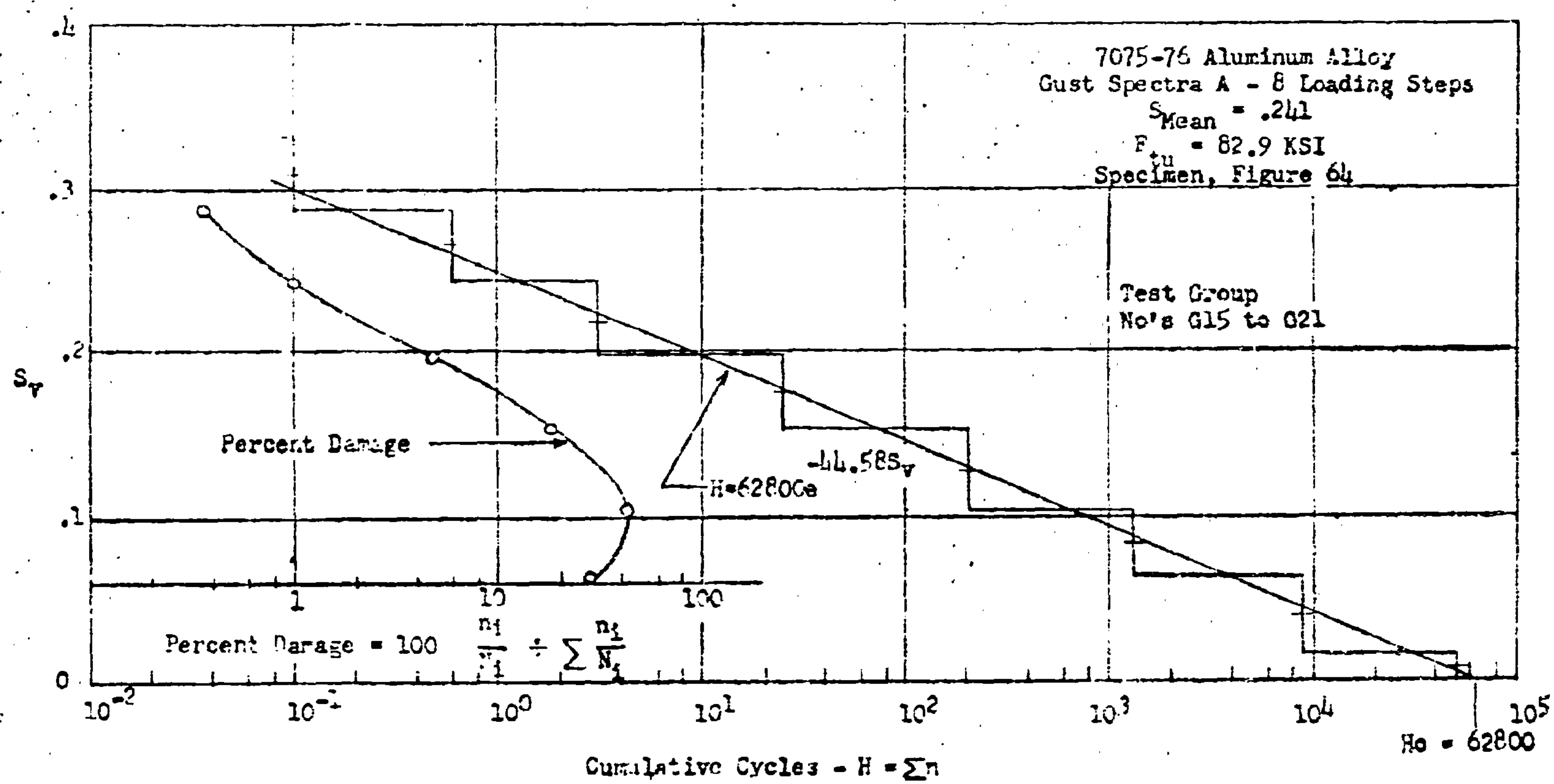

Figure 56 Comparison of Analytical and Experimental Unit Gust Loading Spectrum for Notched Sheet Specimens

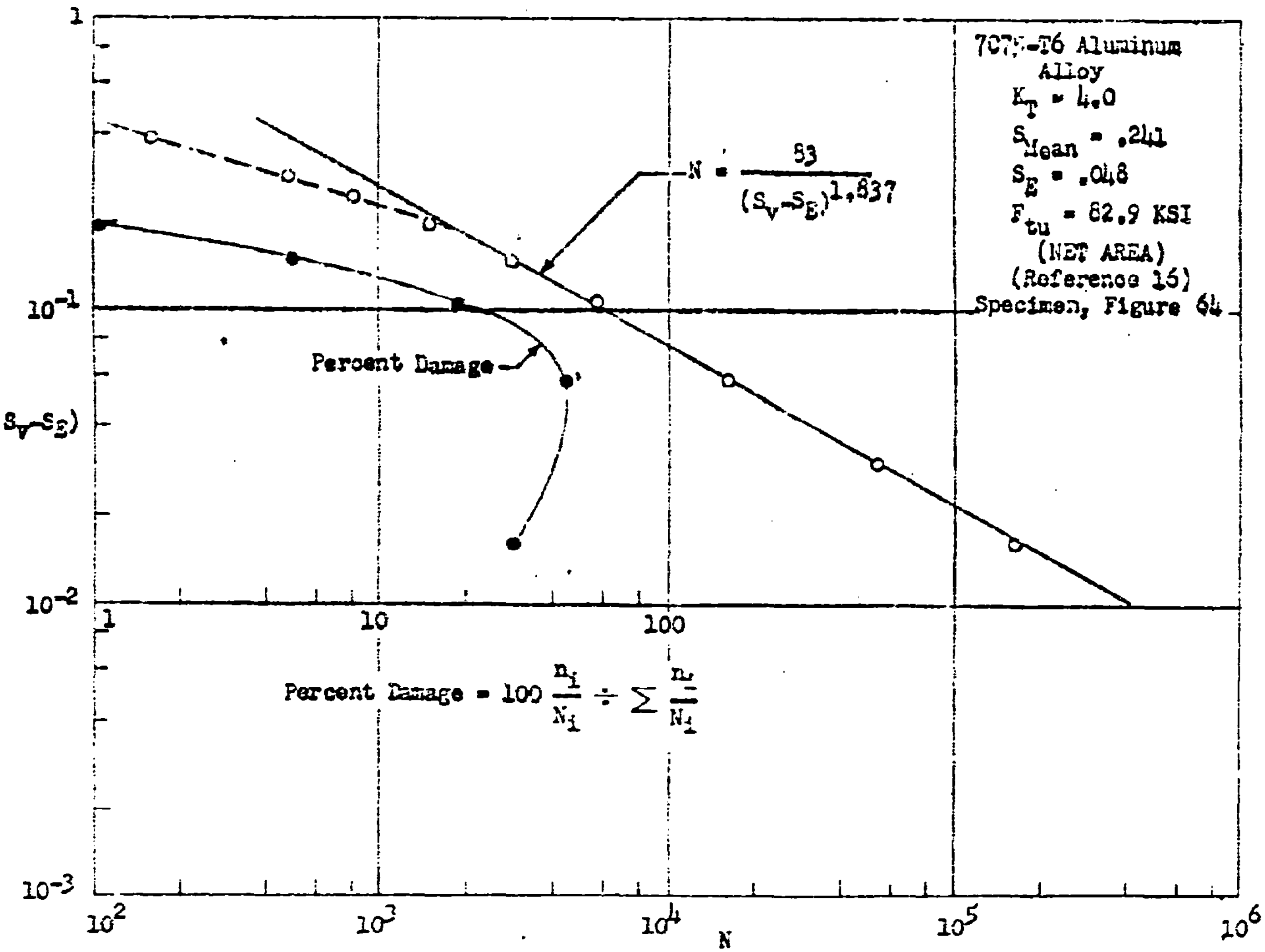

Figure 57 $(S_V - S_E)$ Versus N for S-N Data on Notched Sheet Specimens

3. Shanley's "1X" Method

In predicting fatigue life with Shanley's "1X" method, reduced varying stresses were computed for each of the loading spectra that were compared with test data. The number of applied cycles n_i and the corresponding relative varying stresses S_{v_i} above the endurance limit were provided from the test spectra in Tables 31 and 47 of Appendix C. The exponent δ in Equation (A6) was evaluated from the pertinent S-N data by a least square straight line fit to a plot of log S_v versus log N. In securing this fit, S-N data points for the low stresses near the endurance limit were omitted because these stresses did not generally lie on or near the straight line which fit best the rest of the S-N data. After the exponent δ has been obtained from S-N data, the solution of Equation (A9) for a relative reduced stress S_R corresponding to the stresses above the endurance limit in a loading spectrum is straightforward. The predicted number of cycles, N_R, to failure for load levels above the endurance limit are then read from the appropriate S-N curve at the computed value of S_R. Predictions of fatigue life in terms of cycles of applied loads at all levels, including those below the endurance limit, in a unit loading spectrum are then obtained from Equation (A13) by multiplying N_R by the ratio of total number of cycles in the unit block to the number of load cycles applied above the endurance limit. The resulting life predictions, N_L, are listed in Table 21 for gust loading spectra and Table 23 for maneuver loading spectra.

Stress adjustments were also computed by interpolations to make the "1X" method exactly predict the test results. These adjustments are given in Tables 24 and 25.

4. Shanley's "2X" Method

The fatigue lives for Shanley's "2X" Method in Tables 21 and 23 were determined from Equations (A11) and (A13) in a similar manner as for Shanley's "1X" Method. The proportional stress adjustment factors determined by this method to exactly predict fatigue test lives are given in Tables 24 and 25.

5. Generalized Henry's Method

Fatigue life predictions by the generalized Henry's Method were computed for each of the test groups by the alternate application of Equations (A24) and (A25) of Appendix A, and accounting for the sequence of loading in the test block of each unit spectrum until the damage reached a value of unity. The number of blocks repeatedly applied to reach the damage value of unity is then the measure of the predicted fatigue life.

The parameters β & S_E in Equations (A24) and (A25) were determined for each of two cases of curve fitting.

Case (A) is the best fit line in the limited mid-stress range in the region of maximum calculated damage, from the graphs of $\log (S_v - S_E)$ vs. $\log N$.

Case (B) is the best fit line for the full stress range on the graphs of $\log (S_v - S_E)$ vs. $\log N$.

These parameters are given for each test group in Table 19 for the gust loading spectra utilizing the Case (A) curve parameters for the S-N data, and in Table 22 for the Case (B) curve parameters. The S-N curve parameters for the maneuvering spectra tests are given in Table 20. The cycles to failure N at each of the stress levels used in testing were read from an S-N curve.

The fatigue life calculated for each group of tests is given in Tables 21 and 22 for the gust spectra loadings with the Case (A) and Case (B) forms of S-N data, respectively, and in Table 23 for the maneuver spectra test groups in which only Case (B), the best fit for the full range of S-N data, was used. The experimental test results are also given in these tables for direct comparison. These predictions are plotted along with the prediction results of the other methods and with the experimental results for comparative evaluation of each of the methods in Section III in the main body of the report.

In addition to the fatigue life evaluation, the Generalized Henry procedure is used to determine the proportional stress adjustment factor required to predict exactly the test life. These factors are listed in Table 24 for the gust spectra test groups and in Table 25 for the maneuver spectra groups. These results are also compared with the results of other methods in Section III of the report.

In several of the test groups (G42 and G43) it was noted that a damage ratio in excess of unity was achieved within one of the stress intervals. The computing procedure, of course, recognizes this as failure and predicts life as less than the unit block size although, experimentally, these groups lasted from approximately twelve to sixteen times longer than predicted. These were extreme cases of the High-to-Low sequence of loading within the test block in which very few blocks were applied. Residual stresses from early plastic yielding no doubt greatly benefited the net effective fatigue stress at the peak stress point. These examples point up the important influence test variables often have on fatigue life in the laboratory. The probability of these type events occurring in service cannot be deduced from current data reduction procedures.

6. The Tangent Intercept Method

The fatigue lives predicted by the Tangent Intercept method were secured by locating the point at which the cumulative loading spectrum was tangent to the appropriate S-N curve and applying Equation (A40) to arrive at the total cumulative number of cycles in the tangent spectrum.

The stress adjustment factor was also derived by trial changes in the slope of the loading spectrum until the total cycles predicted agreed with the experimental test results.

The fatigue life predictions are listed in Table 21 for each group of gust loading spectra tests, and in Table 23 for each group of maneuver loading spectra tests. The experimental values are also given for direct comparison. The stress adjustment factors are listed in Tables 24 and 25 for the gust and maneuver loadings, respectively.

7. Stress Concentration Factor Method

The stress concentration factor method as described in Appendix A is an analytical stress analysis procedure for defining the local critical stress state which, when coupled with a fatigue damage theory, may be used to predict fatigue life. Its area of usage is limited to preliminary design assessments in which only minimum information is available. The application of this procedure makes use of the simple linear cumulative damage hypothesis. The appropriate S-N curve is selected from the group of standardized S-N data in Figures 58 to 62 by means of the theoretical stress concentration factor reported for each particular test specimen. Thirty groups of data from those listed in Appendix C were analyzed by this procedure. The resulting fatigue life predictions are listed in Table 21 for the gust spectra tests. The experimental fatigue life for each test group is also listed for comparison.

The stress adjustment factors were determined, using the same sets of data, to make the predicted fatigue life equal to the experimental fatigue life. These factors are listed in Table 24 for the gust spectra tests. Comparisons of the results of these predictions with those of the other methods chosen for evaluation are given in Section III in the main body of the report.

8. Fatigue Quality Index Method

The Fatigue Quality Index method was used to predict fatigue life for thirty-three test groups. The application of this method requires the use of one spectral fatigue test result to determine by interpolation which K curve, of the standard set of S-N data (Figures 58 to 62), is

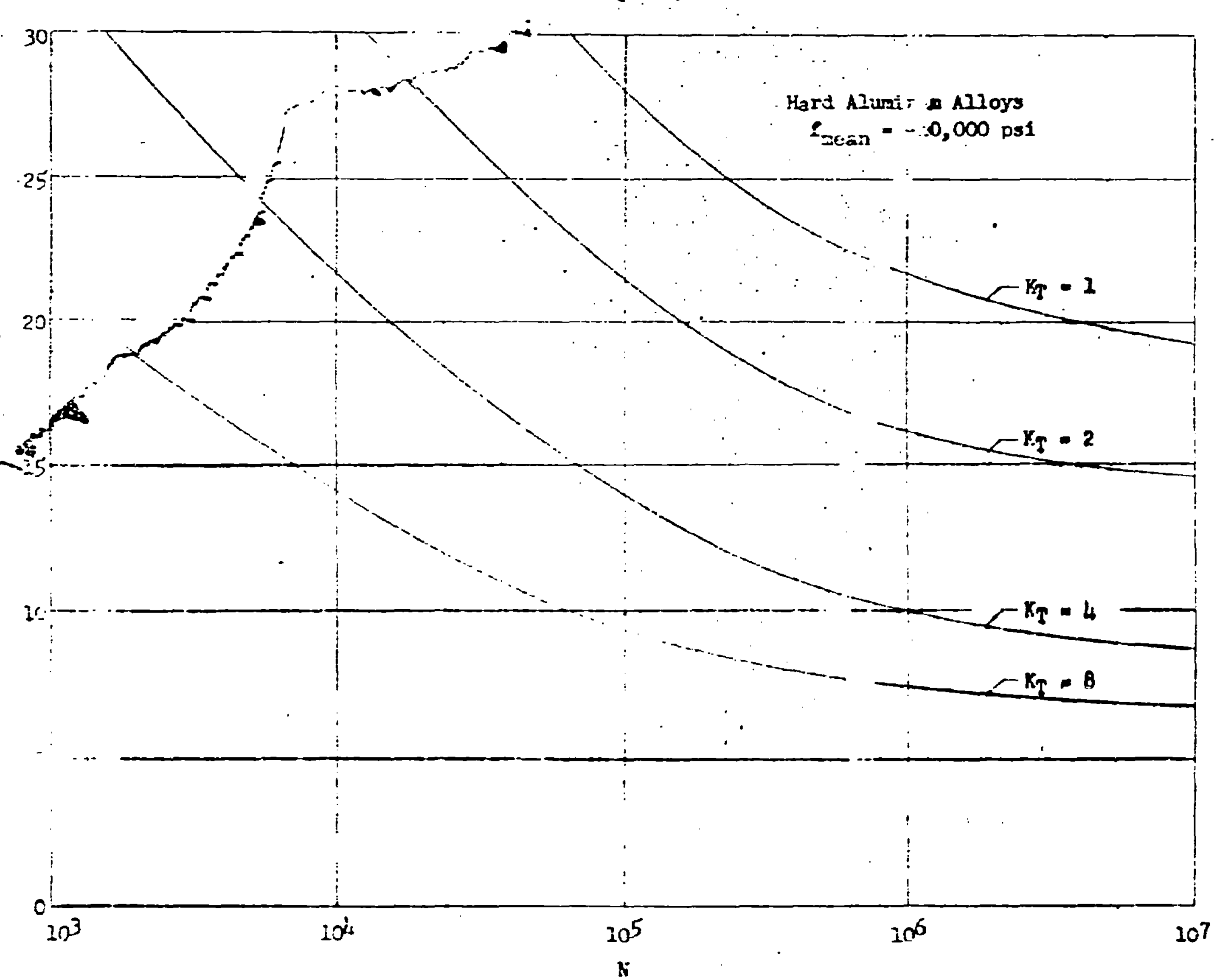

Figure 58 Standardized S-N Curves

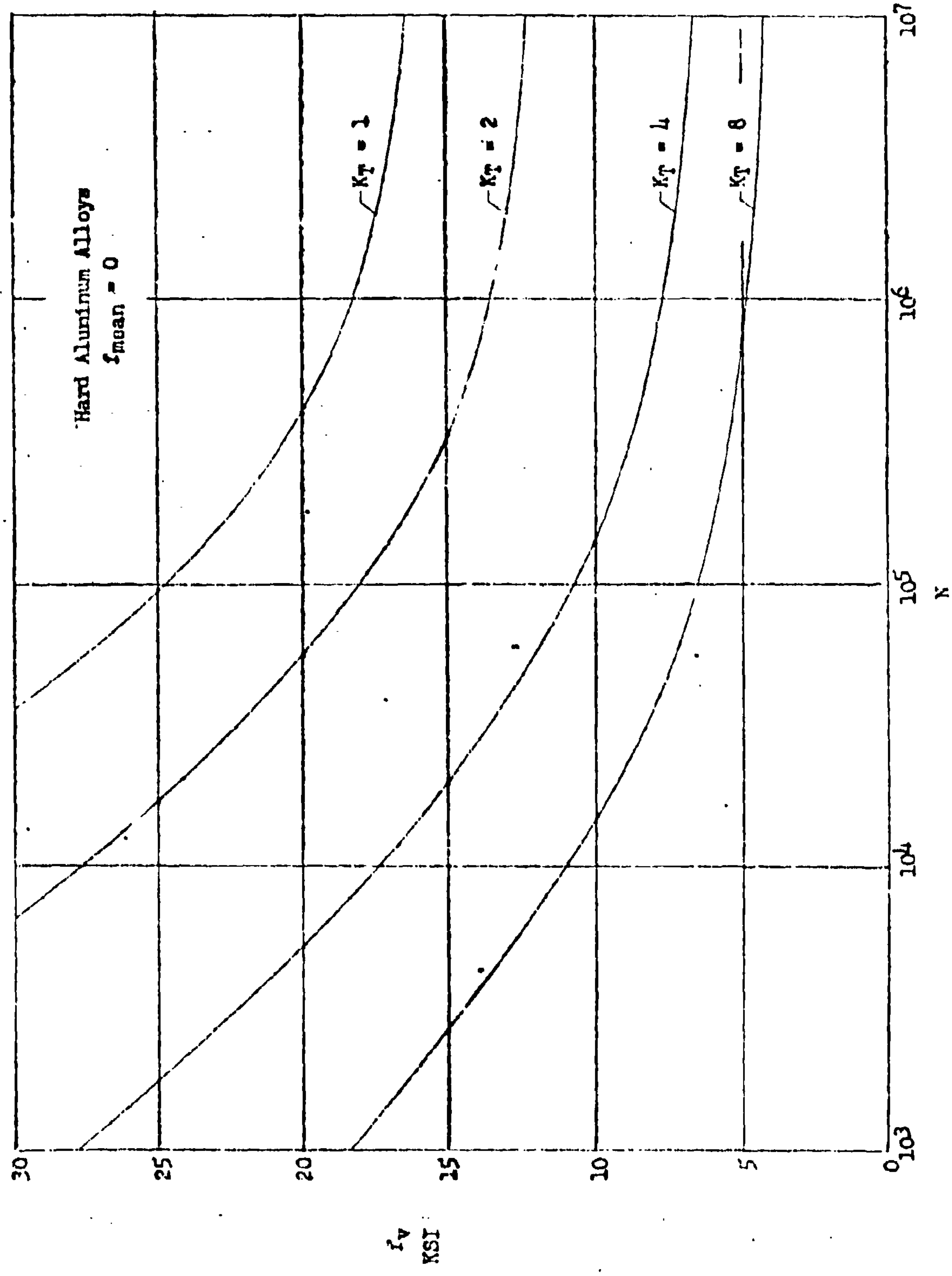

Figure 59 Standardized S-N Curves

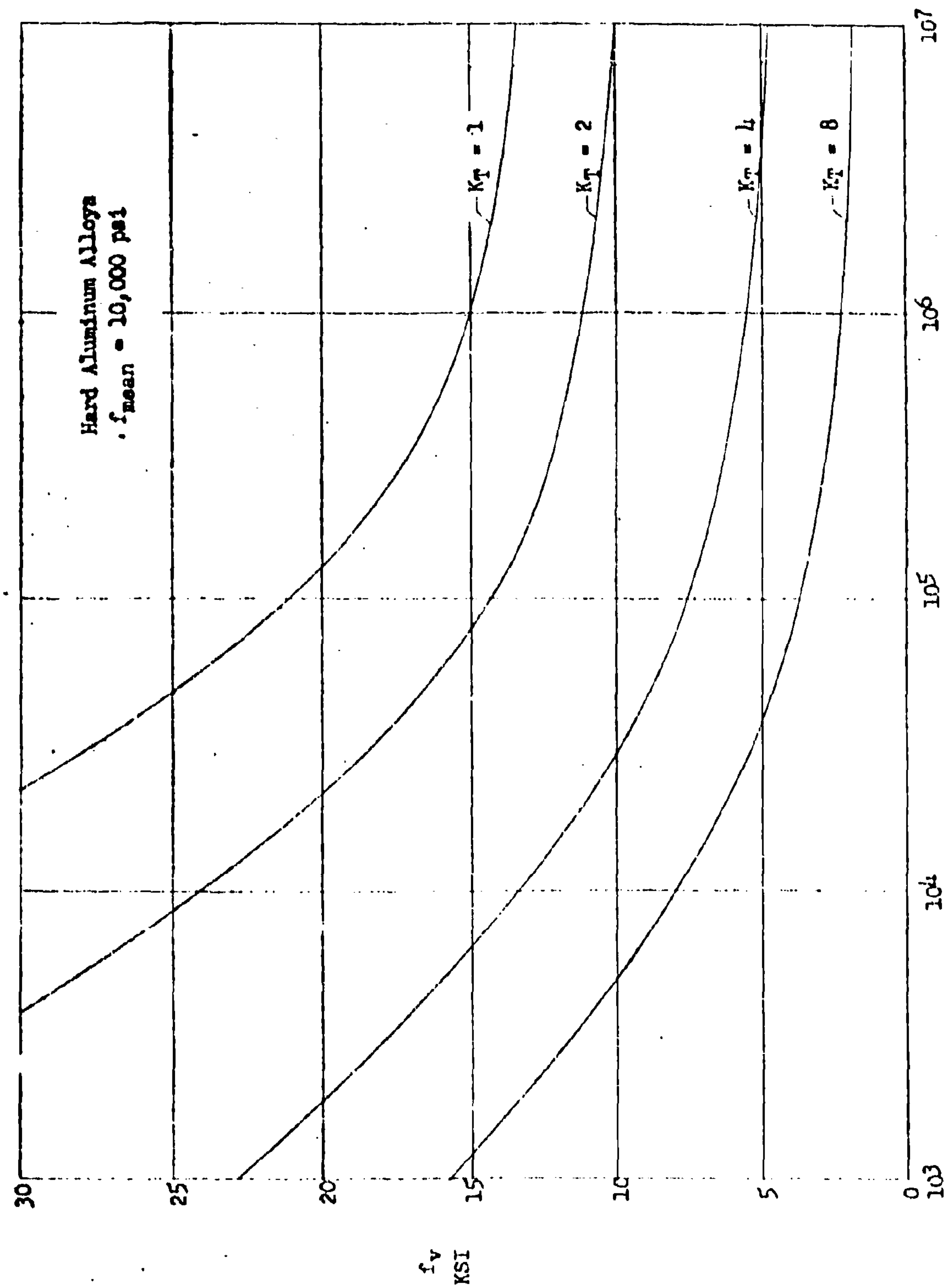

Figure 60 Standardized S-N Curves

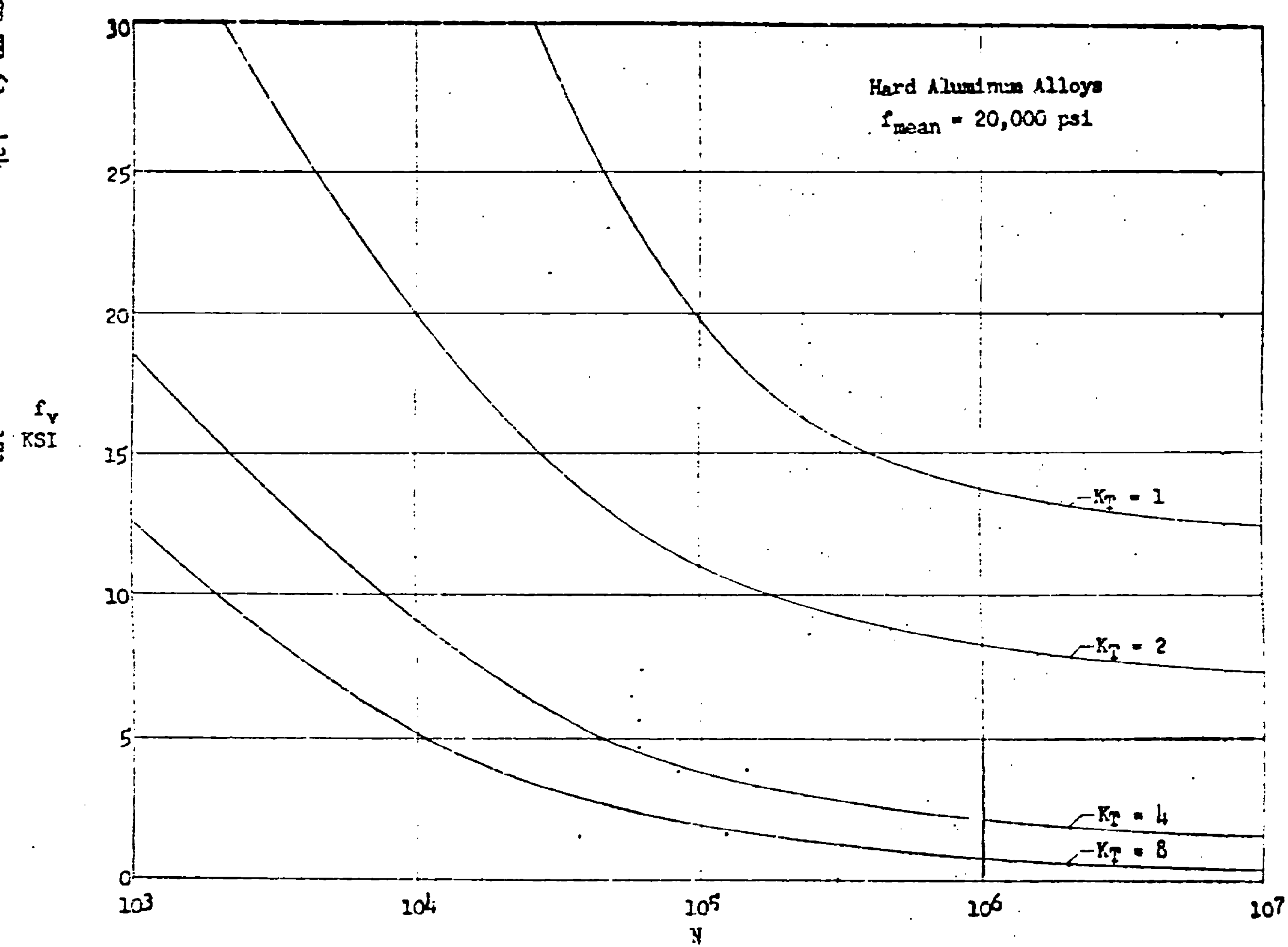

Figure 61 Standardized S-N Curves

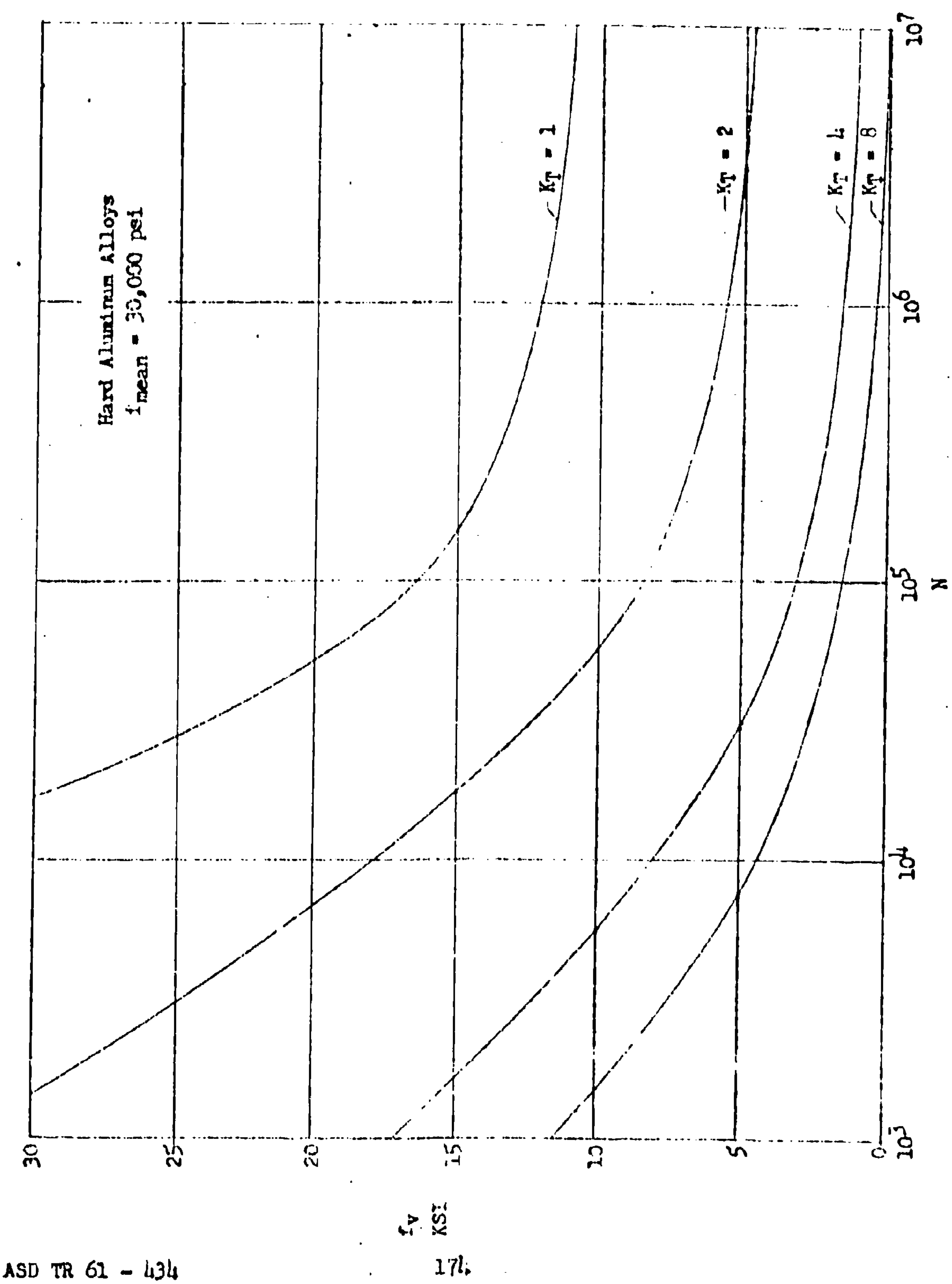

Hard Aluminum Alloys
f_{mean} = 30,000 psi
K_T = 1
K_T = 2
K_T = 4
K_T = 8
0
5
10
15
20
25
30
10^3
10^4
10^5
10^6
10^7
N
f_v KSI

required to make the linear cumulative damage equation equal unity for this test result. Interpolation of these standardized S-N curves to the mean stress of each test group is made from Christensen diagrams similar to those described in Appendix D. The test-derived Fatigue Quality Index or K is listed in Table 26 for all of the gust spectra that were applied to aluminum specimens and in Table 27 for maneuver spectra applied to aluminum specimens. One of these test-derived K is used as a base test to predict the fatigue life of identical specimens loaded under other similar types of spectra.

To reduce the bias in choice of the base test, only those test groups were selected which had a quasi-random or Lo-Hi-Lo loading sequence in conjunction with the same and other types of loading sequences in similar test groups. These selected spectrum test groups were first used to derive the K for which Equation (A41) was exactly satisfied. The resulting value of K was then used to obtain fatigue life predictions for the test groups that are noted in Table 21.

The stress adjustment factors in Table 24 were also determined for this same set of test groups to make the predicted fatigue life exactly match the test life when using the previously derived Quality Index in the linear cumulative damage procedure.

The Quality Index Procedure is effective only when fatigue life predictions are made for loading spectra that have approximately the same shape of slope, the same number of loading steps, relatively similar stress increments, fairly close mean loads, equivalent block sizes, identical loading sequences and essentially the same point of fatigue failure. All of these conditions were not satisfied between any two of the Test Groups that were analyzed. Just to consider, for example, the point of failure on the C-46 wing, in Test Group No. G56 where the occurrence of a critical crack on the complete wing was used to select a test-derived K for analyzing Test Groups G51 to G55 and G57. A total of six critical cracks occurred in Test Group G56, four at Wing Station 195, one at Wing Station 204, and one at the corner of the inspection cutout B at WS214 in Figure 68. Out of these Wing Stations at which critical cracks occurred, only Wing Station 214 was analyzed by the Quality Index Method. This analysis of Wing Station 214, however, was for crack initiation at the corner of the inspection cutout plate at H in Figure 68 rather than the corner of the inspection cutout at B.

9. <u>Modified Corten and Dolan and Nonlinear Cumulative Damage</u>

The exponent b in Equation (A31) of the Modified Corten-Dolan method and the exponent c in Equation (A32) of the nonlinear cumulative damage method were evaluated from the test data in the manner described in Appendix A. The resulting values are tabulated in Table 28 for gust loading spectra and in Table 29 for maneuver loading spectra.

Fatigue life predictions, however, were not made with either the Modified Corten-Dolan's or nonlinear cumulative damage methods, since the resulting average values of 1.097 for b and 1.077 for c were extremely close to the value of unity. When either of these exponents reach this value, the corresponding method reduces to the concept of linear cumulative fatigue damage.

TABLE 19

PARAMETERS FOR S-N DATA AND UNIT GUST LOADING SPECTRA[(a)]

(Table is completed on next page)

Material	Type of Specimen	S_{Mean}	Type of Spectrum	No. of Loading Steps	Block Size	α (b)	β (b)	S_E (b)	δ (c)	$\Gamma(\beta+1)$ (d)	H_o (d)	h (d)	Test Group No.
2024-T3	Notched Sheet	.241	Gust B	18	100000	67	2.473	.053	4.318	3.225	124900	59.59	G1-G5
			Gust A	18	100000	67	2.473	.053	4.318	3.225	165200	45.22	G6
		.241		8	100200	67	2.473	.053	4.318	3.225	176100	44.26	G7-G12
		0			50000	115	2.647	.100	6.604	3.922	63900	26.55	G13-G14
7075-T6		.241			50900	83	1.837	.048	3.391	1.731	62800	44.58	G15-G21
		.121			30200	159	1.828	.074	4.419	1.716	51100	34.32	G22-G23
	Notched Sheet	0	Gust A	8	30000	220	1.890	.105	5.788	1.811	50200	27.60	G24-G27
2024-T3 Alclad	Double Shear Riveted Joints	.253		9	360280	1368	1.620	.017	2.035	1.451	231800	26.99	G28
		.152				2650	1.684	.018	1.904	1.525	230400	44.89	G29
		.101				12340	1.145	.040	1.883	1.070	233700	67.66	G30
		.0806				26770	.900	.050	2.084	.961	231500	84.37	G31
7075-T6 Alclad	Unnotched Sheet	.201				9364	1.130	.097	2.875	1.062	231900	33.85	G32
		.161				10364	1.087	.100	2.641	1.040	232200	42.37	G33
		.145				14434	.976	.100	2.623	.990	230500	47.04	G34
	Butt Joints	.250				243	2.370	.042	3.376	2.388	232400	27.29	G35
		.167				988	2.080	.052	3.460	2.156	230800	40.94	G36
		.125				4414	1.551	.061	2.831	1.379	231300	54.55	G37
Cr-Mo Steel	Strips W/ Hole	.286				1400	1.741	.106	3.959	1.596	231800	23.85	G38
		.222				1237	1.721	.124	3.628	1.571	234300	30.79	G39
		.182		9	360280	1327	1.669	.130	3.700	1.508	227200	37.50	G40

(a) α, β, S_E, $\Gamma(\beta+1)$, H_o & h for FFA method
β and S_E for modified Henry's method
δ for Shanley's "1X" and "2X" methods.

(b) Parameter in Equation (A14) (Best fit in the midstress range.)

(c) Parameter in Equation (A6) (Best fit to the complete stress range.)

(d) Parameter in Equation (A18) (Best fit in the midstress range.)

TABLE 19

(Concluding Page of Table)

Material		Type of Specimen	S_{Mean}	No. of Loading Steps	Block Size	α (b)	β (b)	S_E (b)	δ (c)	$\Gamma(\beta+1)$ (d)	E_o (d)	h (d)	Test Group No.
2024-T3 Alclad		(e)	.212	6	1898800	3045	1.598	.049	2.601	1.428	2887000	34.96	G41-G43
				5	457700	3045	1.598	.049	2.601	1.428	3040700	32.54	G44
		(f)		5	164400	853	2.001	.053	2.823	2.002	1146200	31.58	G45
7075-T6 Alclad		(e)		5	92900	3514	1.125	.052	1.953	1.060	685600	31.25	G46
			.212	6	1228000	3514	1.125	.052	1.953	1.060	1874800	35.01	G47
D.T.D. 363A Aluminum Alloy		Notched Plate	.165	9	13290	222	1.422	.033	2.532	1.260	52900	62.94	G48
			.165	9	6290	222	1.422	.033	2.532	1.260	17100	56.18	G49
			.165	10	5410	222	1.422	.033	2.532	1.260	30300	58.43	G50
2024-T	C-46 Wing	WS 150	.2	16	59670	472	2.372	.039	3.624	2.893	202700	42.05	G51
		WS 214				2182	2.091	.032	2.687	2.178			G52
		WS 228				1318	2.155	.036	3.193	2.319			G53
		WS 239				1944	1.937	.020	2.472	1.889			G54
		(g)				309	2.676	.030	4.020	4.054			G55
		(h)				491	2.626	.032	3.709	3.828			G56
		(i)		16	59670	778	2.488	.040	3.548	3.279	202700	42.05	G57
	P51 Wing	(j) Gun Bay		11	500000	129	2.394	.039	4.881	2.964	998600	37.16	G58
				3	32860	129	2.394	.039	4.881	2.964	115200	45.04	G59
		(j) Tank Bay		11	500000	130	2.545	.041	3.682	3.495	998600	37.16	G60
				3	32860	130	2.545	.041	3.682	3.495	115200	45.04	G61
		(k) Gun Bay		11	500000	504	2.270	.039	3.782	2.602	998600	37.16	G62
				3	32860	504	2.270	.039	3.782	2.602	115200	45.04	G63
		(k) Tank Bay		11	500000	1624	1.549	.052	3.574	1.377	998600	37.16	G64
2024-T			.2	3	32860	1624	1.549	.052	3.574	1.377	115200	45.04	G65

(b), (c), and (d) See corresponding notes on previous page.
(e) Lap joint with one row of flush rivets
(f) Lap joint with two rows of flush rivets
(g) First crack initiated in complete wing
(h) Critical crack initiated in complete wing
(i) Final failure of complete wing
(j) Initial failure
(k) Final failure

TABLE 20

PARAMETERS FOR S-N DATA AND UNIT MANEUVER LOADING SPECTRA(*)

Material	Type of Specimen	$S_{Min.}$	No. of Loading Steps	Block Size	α (**)	β (**)	S_E (**)	δ (***)	$\Gamma(\beta+1)$ (****)	H_o (****)	h (****)	Test Group No.
2024-T3 Alclad	Double Shear Rivited Joints	.0833	9	7497	914	1.647	.033	2.544	1.481	9300	19.38	M1
		.0625			1001	1.708	.037	2.678	1.555	9400	25.83	M2
		.050			5109	1.095	.045	2.850	1.044	9300	32.30	M3
7075-T6 Alclad	Unnotched Sheet	.125			558	2.077	.095	4.028	2.150	9300	12.92	M4
		.100			3172	1.459	.099	2.955	1.292	9300	16.15	M5
		.0333			4840	1.302	.101	2.708	1.168	9300	19.38	M6
		.0625			5477	1.346	.092	3.015	1.200	9400	25.83	M7
	Butt Joints	.100			26	3.108	.055	4.669	6.382	9300	16.15	M8
		.0833			34	3.063	.059	4.674	6.497	9300	19.38	M9
		.0625			232	2.269	.063	4.654	2.599	9300	25.83	M10
Cr-Mo Steel	Strips W/hole	.111			554	1.857	.122	4.300	1.760	9300	14.53	M11
		.100			556	1.962	.122	4.122	1.931	9300	16.15	M12
		.0833	9	7497	2105	1.397	.122	3.869	1.240	9300	19.38	M13

(*) α, β, S_E, $\Gamma(\beta + 1)$, H_o & h are used in the FFA method
δ is used in the Shanley's "1X" and Shanley's "2X" methods
β & S_E are used in Henry's method.

(**) Parameter in Equation (A14) (Best fit to the full stress range.)
(***) Parameter in Equation (A6) (Best fit to the full stress range.)
(****) Parameter in Equation (A18) (Best fit to the full stress range.)

TABLE 21

PREDICTED FATIGUE LIVES FOR GUST LOADING SPECTRA
(Table is continued on next two pages)

Test Group No.	Sequence	Geometric Mean of Test Life (10^6 Cycles)	Predicted Life (10^6 Cycles) Miner	FFA Case A(a)	Shanley "1X"	Shanley "2X"	Modified Henry Case A (b)	Tangent Intercept	Quality Index	Stress Conc. Factor
G1	Lo-Hi	8.049	8.240	9.630	9.042	2.087	7.597	40.131	6.988	1.018
G2	Lo-Hi	3.872					7.986			
G3	Hi-Lo	11.888					7.403			
G4	Hi-Lo	11.555					7.013		6.988	
G5	QR	6.988	8.240	9.630	9.042	2.087	-	40.131	(c)	1.018
G6	QR	1.824	1.591	1.717	1.616	.426	-	7.065	2.848	.316
G7	Lo-Hi	.595	1.201	1.455	1.186	.305	1.194	4.754	2.020	.237
G8	Hi-Lo	2.294					1.014			
G9	Lo-Hi-Lo	1.612					1.145			
G10	Hi-Lo-Hi	1.519					1.103		2.020	
G11	QR	2.020					-		(d)	
G12		1.215	1.201	1.455	1.186	.305	-	4.754	2.020	.237
G13		.479	.944	1.913	.942	.058	-	5.361	.364	.656
G14	QR	.364	.944	1.913	.942	.058	-	5.361	(e)	.656
G15	Lo-Hi	.443	.320	.354	.288	.109	.304	1.171	.661	.138
G16	Lo-Hi	.452					.348			
G17	Hi-Lo	1.268					.257			
G18	Lo-Hi-Lo	.762					.291			
G19	Hi-Lo-Hi	.976					.304		.661	
G20	QR	.661					-		(f)	
G21	QR	.600	.320	.354		.109	-	1.171	.661	.138
G22	Lo-Hi-Lo	.385	.326	.445		.076	.287	1.360	.282	.209
G23	QR	.282	.326	.445	.288	.076	-	1.360	(g)	.209
G24	Lo-Hi	.255	.409	.697	.331	.040	.355	2.399	.394	.288
G25	Hi-Lo	.496					.301			
G26	Lo-Hi-Lo	.498					.316		.394	
G27	QR	.394	.409	.697	.331	.040	-	2.399	(h)	.288

(a) Analytical representation of unit loading spectrum and S-N data is based on best fit in the midstress range.

(b) Analytical intrepretation of S-N data is based on best fit in the midstress range.

(c), (d), (e), (f), (g), and (h) See corresponding notes on last pages of table.

TABLE 21

PREDICTED FATIGUE LIVES FOR GUST LOADING SPECTRA
(Table is completed on next page)

Test Group No.	Sequence	Geometric Mean of Test Life (10^6 Cycles)	Predicted Life (10^6 Cycles): Miner	FFA Case A (a)	Shanley "1X"	Shanley "2X"	Modified Henry Case A (b)	Tangent Intercept	Quality Index	Stress Conc. Factor
G28	Lo-Hi-Lo	.411	.368	.482	.370	.132	.364	1.171		
G29		4.788	2.222	3.692	2.284	1.790	2.452	6.341		
G30		21.732	29.959	33.146	27.496	22.860	28.473	18.566		
G31		129.700	260.200	159.280	233.510	177.440	225.890	633.470		
G32		25.710	31.627	19.522	24.928	10.758	13.344	92.350		
G33		75.875	95.532	62.881	68.848	56.984	81.783	278.160		
G34		151.966	195.450	108.070	148.540	147.160	186.980	501.790		
G35		2.994	.876	1.037	.871	.299	1.034	3.681		
G36		27.558	12.133	13.560	12.167	7.030	11.879	30.003		
G37		100.986	80.410	68.619	106.730	76.536	103.400(i)	300.010		
G38		4.060	4.130	4.266	3.734	1.739	3.956	12.215		
G39		17.902	24.139	20.083	23.912	15.096	21.976	55.208		
G40	Lo-Hi-Lo	50.367	89.807	77.480	89.042	61.611	82.504	235.890		
G41	Lo-Hi	1.899	1.888	2.280	1.554	1.445	3.584	5.551		
G42	Hi-Lo	2.279	1.888	2.280	1.854	1.445	.192	5.551		
G43		2.848	1.888	2.280	1.854	1.445	.173	5.551		
G44		.458	.228	.114	.223	.174	.114	.654		
G45		.164	.138	.326	.174	.125	.166	.568		
G46	Hi-Lo	.093	.079	.110	.075	.065	.066	.207		
G47	Lo-Hi	1.228	.705	.732	.680	.601	1.178	2.050		
G48	Lo-Hi-Lo	.133	.107	.127	.100	.068	.096	.330	.143	.529
G49		.122	.116	.127	.106	.077	.108	.336	.150	.504
G50	Lo-Hi-Lo	.074	.049	.070	.047	.033	.048	.138	(j)	.244

(a) See note on previous page.
(b) See note on previous page.
(i) Prediction ignored singularity at a varying stress equal to the endurance limit in the loading spectrum.
(j) Used as master spectrum to determine damage boundary with K of 5.27 for test groups No. G48 & G49. Reference Table 26.

TABLE 21

PREDICTED FATIGUE LIVES FOR GUST LOADING SPECTRA
(Concluding page of Table)

Test Group No.	Sequence	Geometric Mean of Test Life (10^6 Cycles)	Predicted Life (10^6 Cycles): Miner	FFA Case A (a)	Shanley "1X"	Shanley "2X"	Modified Henry Case A (b)	Tangent Intercept	Quality Index
G51	QR	4.179	1.305	1.759	1.408	.393	-	6.667	1.099
G52		4.453	1.893	2.811	2.128	1.104	-	7.645	18.585
G53		2.307	1.695	2.402	1.751	.719	-	7.435	3.305
G54		2.070	.745	.961	.760	.447	-	2.548	3.344
G55		1.252	1.010	1.750	.810	.261	-	3.947	3.344
G56		3.344	1.424	3.658	1.196	.444	-	5.634	(k)
G57	QR	9.666	2.126	4.116	1.957	.715	-	8.452	3.344
G58	TR	.417	.354	.532	.321	.048	-	1.909	(l)
G59	Lo-Hi-Lo	.557	.510	.654	.423	.147	.474	2.923	.649
G60	TR	1.521	.798	.851	.870	.214	-	4.128	(m)
G61	Lo-Hi-Lo	.953	.956	1.092	1.086	.400	.865	5.557	2.715
G62	TR	2.520	1.175	1.516	1.039	.350	-	4.768	(n)
G63	Lo-Hi-Lo	1.495	1.090	1.818	.993	.471	1.014	3.922	3.940
G64	TR	2.017	.939	1.103	.806	.275	-	3.142	(o)
G65	Lo-Hi-Lo	1.039	1.181	1.275	1.312	.372	.818	5.708	3.311

(a), (b) See Corresponding note on first page of table

(c)	Used as Master Spectrum to determine damage boundary with	K of 3.22 for Test Group No.	G 1 to G 4	Ref. Table 26
(d)		K of 2.95	G 6 to G12	
(e)		K of 4.71	G13	
(f)		K of 3.10	G15 to G19	
(g)		K of 3.78	G21	
(h)		K of 3.76	G23 to G26	
(k)		K of 8.26	G51 to G57	
(l)		K of 4.10	G57	
(m)		K of 3.33	G61	
(n)		K of 3.08	G63	
(o)	Used as Master Spectrum to determine damage boundary with	K of 3.19 for Test Group No.	G65	

TABLE 22

PREDICTED LIVES BY THE FFA AND MODIFIED HENRY'S METHODS WITH REQUIRED ANALYTICAL PARAMETERS BASED ON THE COMPLETE S-N CURVE AND ENTIRE GUST LOADING SPECTRUM

(Table is continued on the next two pages)

TEST GROUP NO.	SEQUENCE	GEOMETRIC MEAN OF TEST LIFE (10^6 CYCLES)	PARAMETERS					PREDICTED LIFE (10^6 CYCLES)	
			α (a)	β (a)	$\Gamma(\beta+1)$ (b)	H_o (b)	h (b)	FFA Case B	MODIFIED HENRY Case B
G1	Lo-Hi	8.049	24	2.852	4.995	52300	47.74	7.109	7.500
G2	Lo-Hi	3.872				261500			7.983
G3	Hi-Lo	11.888				52300			7.400
G4	Hi-Lo	14.555				261500			7.010
G5	QR	6.968				261500	47.74	7.109	-
G6	QR	1.824				121000	42.30	1.631	-
G7	Lo-Hi	.595				147800	42.26	1.332	1.192
G8	Hi-Lo	2.294							1.012
G9	Lo-Hi-Lo	1.612							1.061
G10	Hi-Lo-Hi	1.519				147300			1.102
G11	QR	2.020				73900			-
G12		1.215	24	2.852	4.995	147800	42.26	1.332	-
G13		.479	11	3.494	11.529	54800	25.44	.873	-
G14	QR	.364	11	3.494	11.529	109600	25.44	.873	-
G15	Lo-Hi	.443	41	2.053	2.102	11500	43.55	.322	.304
G16	Lo-Hi	.452				57700			.348
G17	Hi-Lo	1.268				57700			.257
G18	Lo-Hi-Lo	.762				11500			.290
G19	Hi-Lo-Hi	.976				57700			.304
G20	QR	.661				11500			-
G21	QR	.600	41	2.053	2.102	57700	43.55	.322	-
G22	Lo-Hi-Lo	.385	24	2.420	3.048	42200	32.67	.295	.287
G23	QR	.282	24	2.420	3.048	42200	32.67	.295	-

(a) Parameter in Equation (A14)
(b) Parameter in Equation (A18)

TABLE 22

(Table is completed on the next page)

TEST GROUP NO.	SEQUENCE	GEOMETRIC MEAN OF TEST LIFE (10^6 CYCLES)	PARAMETERS α (a)	β (a)	$\Gamma(\beta+1)$ (b)	H_o (b)	h (b)	PREDICTED LIFE (10^6 CYCLES) FPA Case B	MODIFIED HENRY Case B
G24	Lo-Hi	.255	23	2.552	3.522	40200	26.05	.310	.325
G25	Hi-Lo	.496							.271
G26	Lo-Hi-Lo	.498							.286
G27	CR	.394	23	2.552	3.522	40200	26.05	.310	-
G28	Lo-Hi-Lo	.411	850	1.836	1.728	231800	26.99	.514	.364
G29		4.788	2650	1.684	1.525	230400	44.89	3.692	2.452
G30		21.732	9390	1.243	1.129	233700	67.66	36.226	27.034
G31		129.700	22000	.953	.982	231500	34.37	164.140	224.450
G32		25.710	6320	1.252	1.135	231900	33.85	19.008	12.617
G33		75.875	7370	1.206	1.105	232200	42.37	65.630	80.344
G34		151.966	12200	1.032	1.014	230500	47.04	110.080	186.980
G35		2.994	120	2.696	4.150	232400	27.29	1.060	1.032
G36		27.558	470	2.383	2.926	230800	40.94	14.700	11.878
G37		100.986	3210	1.667	1.505	231300	54.55	72.703	103.400
G38		4.060	320	2.458	3.176	231800	23.85	4.743	3.953
G39		17.902	910	1.856	1.758	234300	30.79	20.890	21.975
G40	Lo-Hi-Lo	50.367	1330	1.659	1.508	227200	37.50	77.480	82.504
G41	Lo-Hi	1.899	1400	1.941	1.896	2887000	34.96	2.674	3.534
G42	Hi-Lo	2.279				3464000	34.96	2.674	.191
G43		2.848				4330000	34.96	2.674	.172
G44		.458	1400	1.941	1.896	3041000	32.55	.473	.143
G45		.164	850	2.001	2.002	1146000	31.58	.326	.166
G46	Hi-Lo	.093	1890	1.366	1.215	685500	31.25	.118	.065
G47	Lo-Hi	1.228	1890	1.366	1.215	1875000	35.01	.808	1.178
G48	Lo-Hi-Lo	.133	170	1.501	1.330	52900	62.94	.128	.096
G49	Lo-Hi-Lo	.122	170	1.501	1.330	17100	56.18	.126	.108
G50	Lo-Hi-Lo	.074	170	1.501	1.330	30300	58.43	.070	.048

(a), (b) See corresponding note on previous page

TABLE 22

(Concluding page of Table)

TEST GROUP NO.	SEQUENCE	GEOMETRIC MEAN OF TEST LIFE (10^6 CYCLES)	PARAMETERS α (a)	β (a)	$\Gamma(\beta+1)$ (b)	H_o (b)	h (b)	PREDICTED LIFE (10^6 CYCLES) FFA Case B	MODIFIED HENRY Case B
G51	QR	4.179	160	2.785	4.609	71800	34.60	2.196	-
G52		4.453	1710	2.192	2.404			4.229	-
G53		2.307	530	2.516	3.381			3.391	-
G54		2.070	1090	2.192	2.405			1.783	-
G55		1.252	65	3.444	10.773			2.836	-
G56		3.344	180	3.142	7.191			4.210	-
G57	QR	9.656	350	2.367	5.086	71800	34.60	5.961	-
G58	TR	.417	5	3.584	13.077	805000	35.10	.296	-
G59	Lo-Hi-Lo	.557	5	3.584	13.077	115200	45.04	.490	.463
G60	TR	1.522	90	2.670	4.025	805000	35.10	.814	-
G61	Lo-Hi-Lo	.953	90	2.670	4.025	115200	45.04	1.094	.862
G62	TR	2.520	100	2.932	5.509	805000	35.10	1.563	-
G63	Lo-Hi-Lo	1.495	100	2.932	5.509	115200	45.04	2.199	1.004
G64	TR	2.017	200	2.245	2.536	805000	35.10	.887	-
G65	Lo-Hi-Lo	1.039	200	2.245	2.536	115200	45.04	1.196	.739

(a), (b) See corresponding note on first page of table.

TABLE 23

PREDICTED FATIGUE LIVES FOR MANEUVER LOADING SPECTRA

Test Group No.	Sequence	Geometric Mean of Test Life (10^6 Cycles)	Predicted Life (10^6 Cycles)					
			Miner	FFA Case B	Shanley "1X"	Shanley "2X"	Modified Henry Case B	Tangent Intercept
M1	Lo-Hi-Lo	.308	.132	.125	.145	.078	.128	.484
M2		.499	.342	.346	.341	.171	.259	1.127
M3		.903	.760	.758	.727	.452	.661	2.329
M4		.206	.126	.145	.203	.113	.115	.139
M5		.716	.555	.575	.563	.405	.546	1.539
M6		.903	1.008	1.122	.963	.714	.921	2.076
M7		2.219	2.944	3.128	2.612	2.255	2.781	6.583
M8		.069	.047	.043	.048	.015	.040	.096
M9		.214	.132	.118	.138	.049	.127	.331
M10		1.477	.611	.582	.712	.348	.592	1.332
M11		.156	.216	.215	.248	.146	.202	.406
M12		.370	.382	.390	.381	.227	.338	.962
M13	Lo-Hi-Lo	1.042	.903	.915	.890	.637	.848	2.141

TABLE 24

STRESS ADJUSTMENT FACTORS FOR EXACTLY PREDICTING THE GEOMETRIC MEAN OF TEST LIFE FOR GUST LOADING SPECTRA

(Table is continued on the next two pages)

Test Group No.	Sequence	Stress Adjustment Factors									
		Miner	FFA (a) Case A	FFA (d) Case B	Shanley "1X"	Shanley "2X"	Modified Henry (b) Case A	Modified Henry (d) Case B	Tangent Intercept	Quality Index	Stress Conc. Factor
G1	Lo-Hi	1.005	1.033	.977	1.017	.779	.989	.988	1.342	.983	.639
G2	Lo-Hi	1.152	1.185	1.123	1.167	.885	1.082	1.082	1.566	1.133	.739
G3	Hi-Lo	.939	.964	.911	.960	.779	.908	.905	1.244	.920	.597
G4	Hi-Lo	.904	.931	.879	.930	.765	.779	.779	1.198	.888	.575
G5	CR	1.037	1.060	1.003	1.038	.793	-	-	1.381	-	.650
G6	CR	.975	.988	.978	.975	.779	-	-	1.350	1.094	.635
G7	Lo-Hi	1.159	1.214	1.178	1.146	.868	1.183	1.181	1.626	1.300	.771
G8	Hi-Lo	.976	.912	.901	.895	(c)	.828	.820	1.171	.983	.562
G9	Lo-Hi-Lo	.939	.970	.963	.941		.918	.916	1.263	.936	.609
G10	Hi-Lo-Hi	.951	.991	.975	.949		.925	.923	1.280	.923	.620
G11	CR	.899	.935	.923	.912	(c)	-	-	1.203	-	.579
G12		.998	1.039	1.018	.995	.754	-	-	1.350	1.125	.657
G13		1.109	1.322	1.167	1.086	.848	-	-	1.476	.943	1.058
G14	CR	1.155	1.403	1.161	1.136	.985	-	-	1.538	-	1.120
G15	Lo-Hi	.933	.952	.933	.931	(c)	.911	.909	1.315	1.134	.672
G16	Lo-Hi	.929	.947	.929	.928	(c)	.929	.928	1.307	1.129	.669
G17	Hi-Lo	.745	(c)	.742	.727	.650	.739	.739	.979	.883	.494
G18	Lo-Hi-Lo	.818	.838	.827	.834	.743	(c)	(c)	1.122	.998	.563
G19	Hi-Lo-Hi	.793	.793	.784	.798	.685	(c)	(c)	1.049	.938	.530
G20	CR	.844	.866	.853	.875	(c)	-	-	1.168	-	.590
G21	CR	.863	.885	.871	.888	(c)	-	-	1.201	1.057	.796
G22	Lo-Hi-Lo	.969	1.034	.947	.944	.937	.933	.903	1.343	.948	.876
G23	CR	1.033	1.114	1.009	1.004	.860	-	-	1.146	-	1.004
G24	Lo-Hi	1.087	1.251	1.038	1.042	.858	1.082	1.076	1.495	1.072	1.021
G25	Hi-Lo	.970	1.075	.917	.955	.760	.955	.955	1.326	.959	.906
G26	Lo-Hi-Lo	.969	1.074	.915	.955	.759	.955	.955	1.325	.958	.907
G27	CR	[illegible]	1.131	.956	.972	.792	-	-	1.381	-	.946

(a), (b), (c), and (d) See corresponding note on last page of table.

TABLE 24

STRESS ADJUSTMENT FACTORS FOR EXACTLY PREDICTING THE GEOMETRIC MEAN OF TEST LIFE FOR GUST LOADING SPECTRA

(Table is completed on the next page)

Test Group No.	Sequence	Stress Adjustment Factors: Miner	FFA (a) Case A	FFA (c) Case B	Shanley "1X"	Shanley "2X"	Modified Henry (b) Case A	Modified Henry (c) Case B	Tangent Intercept	Quality Index	Stress Conc. Factor
G28	Lo-Hi-Lo	.958	1.080	1.104	.954	.580	.831	.831	1.654		
G29		.748	.903	.903	.715	.521	.725	.725	1.132		
G30		1.120	1.121	1.145	1.107	1.026	1.109	1.103	.956		
G31		1.204	1.042	1.048	1.166	1.055	1.135	1.154	1.440		
G32		1.027	.941	.937	.996	.990	.990	.990	1.306		
G33		1.057	.966	.974	1.032	.946	1.027	1.024	1.361		
G34		1.033	.943	.945	.964	.914	1.010	1.010	1.305		
G35		.700	.751	.772	.655	.575	.661	.655	1.073		
G36		.782	.851	.874	.734	.542	.751	.748	1.021		
G37		(c)	.926	.938	(c)	.719	(c)	(c)	1.262		
G38		1.005	1.012	1.032	.973	.757	.968	.963	1.396		
G39		1.088	1.021	1.025	1.056	.949	1.065	1.064	1.315		
G40	Lo-Hi-Lo	1.119	1.070	1.070	1.079	1.046	1.048	1.048	1.392		
G41	Lo-Hi	.997	1.058	1.100	.990	.854	1.032	1.035	1.488		
G42	Hi-Lo	.929	1.000	1.045	.911	.815	.895	.894	1.390		
G43		.853	.936	.983	.834	.745	.813	.813	1.266		
G44		.772	.969	1.009	.750	.670	.737	.737	1.129		
G45		1.048	1.215	1.215	1.023	.890	1.010	1.010	1.561		
G46	Hi-Lo	.950	1.063	1.084	.898	.828	.915	.914	1.321		
G47	Lo-Hi	.843	.847	.881	.824	.773	.869	.871	1.181		
G48	Lo-Hi-Lo	.939	.987	.990	.921	.816	.918	.917	1.344	1.019	1.380
G49	Lo-Hi-Lo	.984	1.011	1.011	.959	.854	.961	.960	1.397	1.056	1.419
G50	Lo-Hi-Lo	.888	.984	.985	.873	.779	.868	.867	1.211	-	1.318

(a), (b), (c), and (d) See corresponding note on next page of table.

TABLE 24

STRESS ADJUSTMENT FACTORS FOR EXACTLY PREDICTING THE GEOMETRIC MEAN OF TEST LIFE FOR GUST LOADING SPECTRA
(Concluding page of Table)

Test Group No.	Sequence	Stress Adjustment Factors								
		Miner	FFA (a) Case A	FFA (d) Case B	Shanley "1X"	Shanley "2X"	Modified Henry (b) Case A	Modified Henry (d) Case B	Tangent Intercept	Quality Index
G51	QR	.762	.814	.859	.768	.616	-	-	1.134	.771
G52		.719	.878	.985	.722	.711	-	-	1.227	1.246
G53		.911	1.011	1.111	.922	.800	-	-	1.438	1.078
G54		.651	.773	.950	.649	.523	-	-	1.088	1.146
G55		.936	1.090	1.205	.854	.667	-	-	1.505	1.248
G56		.739	.944	1.056	.711	.624	-	-	1.204	-
G57	QR	.649	.822	.894	.646	.533	-	-	.940	.876
G58	TR	.969	1.066	.934	.942	.674	-	-	1.373	-
G59	Lo-Hi-Lo	.981	1.040	.976	.944	.734	.965	.961	1.450	1.028
G60	TR	.858	.870	.862	.874	.579	-	-	1.257	-
G61	Lo-Hi-Lo	1.001	1.032	1.031	1.027	.823	.974	.974	1.464	1.245
G62	TR	.807	.875	.897	.767	.615	-	-	1.219	-
G63	Lo-Hi-Lo	.924	1.050	1.087	.887	.709	.894	.891	1.265	1.235
G64	TR	.843	.847	.825	.794	.688	-	-	1.137	-
G65	Lo-Hi-Lo	1.031	1.055	1.032	1.031	.945	.945	.945	1.361	1.277

(a) Analytical representation of S-N data and unit loading spectra is based on best fit in the midstress range of maximum calculated fatigue damage.

(b) Analytical definition of S-N data is based on best fit in the midstress range of maximum calculated fatigue damage.

(c) No incremental deviation because of mathematical discontinuity (See text)

(d) Analytical definitions are based on best fit over the full stress range.

TABLE 25

STRESS ADJUSTMENT FACTORS FOR EXACTLY PREDICTING THE GEOMETRIC MEAN OF TEST LIFE UNDER MANEUVER LOADING SPECTRA

Test Group No.	Sequence	Stress Adjustment Factors					
		Miner	FFA Case B	Shanley "1X"	Shanley "2X"	Modified Henry Case B	Tangent Intercept
M1	Lo-Hi-Lo	.741	.689	.722	.642	.667	1.150
M2		.877	.875	.887	.746	.867	1.337
M3		.958	.935	.926	.865	.900	1.418
M4		.959	.901	.994	.815	.948	.923
M5		.934	.933	.914	.814	.918	1.300
M6		1.041	1.070	1.024	.819	1.009	1.493
M7		1.082	1.100	1.051	1.005	1.048	1.445
M8		.931	.888	.932	.752	.915	1.076
M9		.902	.870	.916	.749	.894	1.102
M10		.837	.797	.834	.723	.811	.978
M11		1.014	1.023	1.061	.922	1.008	1.179
M12		1.008	1.014	1.007	.877	.979	1.253
M13	Lo-Hi-Lo	.972	.966	.958	.881	.958	1.222

TABLE 26

FATIGUE QUALITY INDEX FOR GUST LOADING SPECTRA

(Table is completed on next page)

Test Group No.	Sequence	Number of Specimens	Geometric K_T	K Quality Index Method Minimum	K Quality Index Method Maximum	K Quality Index Method Geometric Mean
G1	Lo-Hi	3	4	3.17	3.17	3.17
G2	Lo-Hi	9		3.33	3.62	3.44
G3	Hi-Lo	3		2.92	3.19	3.04
G4	Hi-Lo	6		2.80	3.15	2.98
G5	QR	8		3.10	3.46	3.22
G6	QR	4		2.99	3.23	3.12
G7	Lo-Hi	3		3.43	3.61	3.52
G8	Hi-Lo	3		2.84	2.95	2.91
G9	Lo-Hi-Lo	3		2.98	3.09	3.05
G10	Hi-Lo-Hi	3		3.00	3.11	3.06
G11	QR	3		2.88	3.02	2.95
G12		4		3.10	3.30	3.16
G13		6		3.92	4.75	4.38
G14	QR	3		4.58	4.98	4.71
G15	Lo-Hi	3		3.19	3.41	3.32
G16	Lo-Hi	4		3.21	3.44	3.32
G17	Hi-Lo	4		2.77	2.91	2.85
G18	Lo-Hi-Lo	4		2.96	3.25	3.08
G19	Hi-Lo-Hi	4		2.93	3.03	2.97
G20	QR	3		3.04	3.15	3.10
G21	QR	4		3.11	3.30	3.18
G22	Lo-Hi-Lo	3		3.43	3.75	3.56
G23	QR	6		3.54	4.01	3.78
G24	Lo-Hi	6		3.53	4.58	4.19
G25	Hi-Lo	5		3.39	3.77	3.56
G26	Lo-Hi-Lo	3		3.37	3.73	3.55
G27	QR	6	4	3.19	4.40	3.76

TABLE 26

FATIGUE QUALITY INDEX FOR GUST LOADING SPECTRA

(concluding page of Table)

Test Group No.	Sequence	Number of Specimens	Geometric K_T	K Quality Index Method Minimum	Maximum	Geometric Mean
G28	Lo-Hi-Lo	2		3.82	4.13	3.97
G29		3		4.53	5.06	4.70
G30		3		6.29	7.73	6.71
G31		2		5.52	7.83	6.59
G32		2	1	1.89	1.91	1.90
G33		2	1	1.98	2.22	2.10
G34		2	1	2.07	2.26	2.17
G35		4		3.30	3.69	3.52
G36		2		3.96	3.98	3.97
G37		2		4.25	4.59	4.41
G38		2		-	-	-
G39		2		-	-	-
G40	Lo-Hi-Lo	3		-	-	-
G41	Lo-Hi	1		-	-	>8
G42	Hi-Lo	1		-	-	>8
G43		1		-	-	>8
G44		1		-	-	>8
G45		1		-	-	4.47
G46	Hi-Lo	1		-	-	>8
G47	Lo-Hi	1		-	-	>8
G48	Lo-Hi-Lo	6	3.95	4.41	5.75	5.23
G49		6	3.95	5.22	5.94	5.43
G50	Lo-Hi-Lo	5	3.95	3.93	6.91	5.27
G51	QR	4		5.20	>8	6.25
G52		6		>8	>8	>8
G53		5		6.64	>8	>8
G54		5		>8	>8	>8
G55		6		>8	>8	>8
G56		6		6.96	>8	8.26
G57	QR	6		6.06	6.91	6.48
G58	TR	3		3.87	4.41	4.10
G59	Lo-Hi-Lo	4		3.77	4.62	4.11
G60	TR	2		3.23	3.44	3.33
G61	Lo-Hi-Lo	7		3.65	4.02	3.85
G62	TR	4		2.96	3.18	3.08
G63	Lo-Hi-Lo	3		3.46	3.83	3.64
G64	TR	2		3.12	3.25	3.19
G65	Lo-Hi-Lo	5		3.52	3.94	3.80

TABLE 27

FATIGUE QUALITY INDEX FOR MANEUVER SPECTRA

Test Group No.	Sequence	Number of Specimens	Geometric K_T	K Quality Index Method: Minimum	Maximum	Geometric Mean
M1	Lo-Hi-Lo	2		2.50	2.60	2.55
M2		2		3.50	4.20	3.83
M3		2		4.00	4.20	4.10
M4		2	1	.60	.60	.60
M5		2	1	1.15	1.22	1.19
M6		3	1	1.15	1.58	1.33
M7		2	1	1.51	1.92	1.70
M8		2		3.50	3.60	3.55
M9		2		3.20	3.50	3.35
M10	Lo-Hi-Lo	2		3.20	3.60	3.39

TABLE 28

EXPONENTS FOR THE MODIFIED CORTEN-DOLAN AND THE NON-LINEAR CUMULATIVE DAMAGE METHODS FROM GUST LOADING SPECTRA

(Table is completed on the next page)

Test Group No.	Sequence	Geometric Mean of Test Life (cycles)	Exponents: b Modified Corten & Dolan	Exponents: c Non-linear Cumulative Damage
G1	Lo-Hi	804900	.996	.995
G2	Lo-Hi	3872000	.860	.844
G3	Hi-Lo	11888000	1.072	1.058
G4	Hi-Lo	14555000	1.113	1.120
G5	QR	6988000	.969	.966
G6	QR	1824000	1.032	1.027
G7	Lo-Hi	595000	.846	.822
G8	Hi-Lo	2294000	1.156	1.168
G9	Lo-Hi-Lo	1612000	1.069	1.065
G10	Hi-Lo-Hi	1519000	1.055	1.051
G11	QR	2020000	1.124	1.114
G12	|	1215000	1.003	1.003
G13	|	478600	.865	.855
G14	QR	363600	.816	.762
G15	Lo-Hi	442800	1.086	1.069
G16	Lo-Hi	452400	1.091	1.113
G17	Hi-Lo	1268000	1.389	1.457
G18	Lo-Hi-Lo	762000	1.237	1.162
G19	Hi-Lo-Hi	975700	1.309	1.299
G20	QR	661400	1.196	1.155
G21	QR	600300	1.169	1.206
G22	Lo-Hi-Lo	385000	1.038	1.045
G23	QR	282400	.968	.961
G24	Lo-Hi	254600	.898	.886
G25	Hi-Lo	496300	1.044	1.047
G26	Lo-Hi-Lo	497700	1.045	1.041
G27	QR	393900	.991	.991

TABLE 28

EXPONENTS FOR THE MODIFIED CORTEN-DOLAN AND THE NON-LINEAR CUMULATIVE DAMAGE METHODS FROM GUST LOADING SPECTRA

(Concluding page of table)

Test Group No.	Sequence	Geometric Mean of Test Life (Cycles)	Exponents b Modified Corten & Dolan	Exponents c Non-linear Cumulative Damage
G28	Lo-Hi-Lo	410700	1.032	1.087
G29		4788000	1.293	1.292
G30		21732000	.849	.943
G31		129700000	.589	.914
G32		25710000	.919	.966
G33		75875000	.871	.968
G34		151966000	.802	.967
G35		2994000	1.323	1.549
G36		27558000	1.276	1.174
G37		100936000	1.088	1.032
G38		4060000	.995	.996
G39		17902000	.865	.948
G40	Lo-Hi-Lo	50367000	.647	.918
G41	Lo-Hi	1899000	1.004	1.016
G42	Hi-Lo	2279000	1.065	1.442
G43		2848000	1.142	-
G44		457700	1.241	-
G45		164400	.965	.894
G46	Hi-Lo	92900	1.073	1.296
G47	Lo-Hi	1228000	1.232	-
G48	Lo-Hi-Lo	132900	1.128	1.056
G49		121500	1.032	1.010
G50	Lo-Hi-Lo	74100	1.214	1.101
G51	QR	4179000	1.210	1.241
G52		4453000	1.186	1.171
G53		2307000	1.059	1.063
G54		2070000	1.232	1.257
G55		1252000	1.024	1.035
G56		3344000	1.138	1.180
G57	QR	9666000	1.267	1.293
G58	TR	416800	1.030	1.093
G59	Lo-Hi-Lo	556600	1.063	1.025
G60	TR	1521000	1.151	1.272
G61	Lo-Hi-Lo	953300	1.145	1.046
G62	TR	2520000	1.148	1.277
G63	Lo-Hi-Lo	1495000	1.222	1.076
G64	TR	2017000	1.164	1.312
G65	Lo-Hi-Lo	1038700	.948	.983
Average of Gust & Maneuver Spectra			1.097	1.077

TABLE 29

EXPONENTS FOR THE MODIFIED CORTEN-DOLAN AND NON-LINEAR CUMULATIVE DAMAGE METHODS FROM MANEUVER LOADING SPECTRA

Test Group No.	Sequence	Geometric Mean of Test Life (Cycles)	Exponents b Modified Corten & Dolan	Exponents c Non-linear Cumulative Damage
M1	Lo-Hi-Lo	.308	1.685	1.173
M2		.499	1.283	1.065
M3		.903	1.131	1.026
M4		.206	1.496	1.114
M5		.716	1.203	1.042
M6		.903	.905	.983
M7		2.219	.715	.963
M8		.069	1.311	1.107
M9		.214	1.462	1.105
M10		1.477	2.238	1.145
M11		.198	.945	.983
M12		.370	.976	.994
M13	Lo-Hi-Lo	1.042	1.144	1.022
Average of Gust & Maneuver Spectra			1.097	1.077

APPENDIX C

SPECTRAL FATIGUE TEST DATA FOR THE EVALUATION OF FATIGUE LIFE PREDICTION METHODS

To evaluate and compare the fatigue life prediction methods studied in this program, a search was made for suitable experimental data. The suitability was judged on the basis of the following criteria:

1. Complexity - To cover the range and types of loading encountered in aircraft service, spectral fatigue test results were required.

2. Loading type was restricted to axial loading as more representative of the efficient stressing of the shell structure; bending data were considered unsatisfactory, except for the full scale airframe component test data.

3. Constant amplitude S-N data on each of the specific specimens were required in addition to the spectral results.

Within these criteria 78 sets of data suitable for most of the methods were collected covering approximately 266 individual specimens.

GUST SPECTRA TEST RESULTS

While gust spectra were used in most of the tests, maneuvering type data were located for some specimens. These maneuver tests will be described in the next section. The gust spectra were applied to the various specimens in loading sequences that are shown in Figure 63. In the quasi-random loading tests, the order of application of the different varying loads was irregular, with the total number of cycles applied at each varying load being equal to those specified in the unit loading spectrum. The number of loading steps and the number of load cycles employed in the unit spectra covered wide ranges. Loading steps ranged from 3 to 18, the load cycles in the unit spectra ranged from approximately 5,000 to 3,000,000 cycles. Other pertinent test variables are noted in Table 30 and in the summary that follows. These include types of loading sequences, specimens, materials, and mean load levels used in the various tests. S-N data were also obtained on all fatigue specimens in part of each test program for which data are reported under loading of variable magnitude.

In general, the gust tests were conducted under the following conditions:

a. Lo-Hi, Hi-Lo, Lo-Hi-Lo, Hi-Lo-Hi, and quasi-random loading sequences were applied to the notched sheet specimens of Figure 64 which were made of 2024-T3 aluminum alloy and tested at net area mean stresses of 0 and 17.4 ksi; and of 7075-T6 aluminum alloy tested at net area mean stresses of 0, 10, and 20 ksi (reference 16). The gust spectra A and B specified in reference 32 were used in this testing. The

applicable unit loading spectra and S-N data are presented in Tables 31 and 32 and Figures 70, 71, 82, and 83. The brackets behind or under F_{tu} in these tables and some of these figures (S-N curves only) denote that this value of F_{tu} was divided into the net area stresses to obtain the relative varying and mean stresses, S_v and S_{mean}. The magnitude of the relative varying stress in Figures 70 and 71 was increased as mean stress was reduced in this series of tests, maintaining essentially the same maximum stress spectrum.

b. Lo-Hi-Lo sequence was applied on the double shear riveted joints of Figure 65 which were made of 2024-T3 as presented from Reference 17. These were tested at net area mean stresses of 15.5, 9.3, 6.2, and 4.9 ksi. The same loading sequence was applied in tests to unnotched sheet of 7075-T6 (Figure 65) at net area mean stresses of 15.4, 12.4, and 11.1 ksi; to butt joints of 7075-T6 (Figure 65) at gross area mean stresses of 13.2, 8.9, and 6.6 ksi; and on strips of Cr-Mo steel (Figure 65) with a centrally located hole, at net area mean stresses of 43.1, 33.5, and 27.5 ksi. Unit loading spectra and S-N data for this series of tests are presented in Tables 33 to 36 and in Figures 72 to 75, and 84 to 87. In this series, the varying loads were decreased when reductions were made in mean stress levels. This may be seen in Figures 72 to 75.

c. Hi-Lo or Lo-Hi sequence was applied only once to lap joints of 2024-T3 with a single row of flush rivets (Figure 66) and tested at a gross area mean load of 975 lbs.; to lap joints of 7075-T6 with a single row of flush rivets (Figure 66) and tested at a gross area mean load of 1,055 lbs. (Reference 18) The unit loading spectra used in these tests and the related S-N data are given in Tables 37 to 39 and shown in Figures 76 to 78 and 88 to 90. In these tables and figures, the relative stresses, S_v and S_{mean} are based on the ratio of applied-to-ultimate static load while in Tables 40 and 41 to follow, they correspond to a similar ratio of load factors. The applicability of net or gross area in securing relative stress levels is denoted in the brackets near the ultimate load or load factor on each table or S-N curve.

d. Lo-Hi-Lo sequence is applied to notched plates of D.T.D 363A (a British zinc-aluminum alloy that is similar to 7075-T6) at a net area mean stress of 14 ksi (Reference 19). The unit loading spectra in Table 40 and in Figure 79 were used in testing. Applicable S-N data are presented in the same table and in Figure 91.

e. A quasi-random sequence of loads was applied to a complete C-46 wing for the purpose of determining the experimental load history at the initiation of the first crack; at the initiation of the critical crack that propagated to failure under continued loading, and at the

estimated time for final failure of the wing (reference 20). Test results were also screened for crack initiation at W.S. 180, W.S. 214, W.S. 228, and W.S. 239 which had measured local mean stresses of 7.1, 5.2, 6.3, and 6.0 ksi, respectively. All tests were conducted under the gross area loading spectrum described in Tables 41 and 42 or in Figure 80. S-N data are also presented in these tables or in Figures 92 and 93.

f. Lo-Hi-Lo and true random sequences of loading were applied to a complete P-51 wing at a mean load of 17,900 lbs. for determining initiation of failure. (Reference 21) Final failure resulted in the gun bay (approximately W.S. 28) and in the tank bay (W.S. 80). The two gross area loading spectra in Table 43 or Figure 81 were used in this series of tests with the related S-N data presented in the same Table and in Figures 94 and 95.

Experimental results for each of the preceding series of tests are tabulated in Table 48. This table sorts the data from 239 individual gust spectrum tests into 65 groups of test results according to material, specimen configurations, loading spectrum, and other pertinent experimental variables.

MANEUVER SPECTRA TEST RESULTS

Unit maneuver spectra were used in some of the tests that were selected from the literature to be correlated with fatigue life prediction methods. These unit maneuver spectra were applied in a series of tests that are reported in Reference 17. These tests were conducted under the Lo-Hi-Lo sequence of Figure 96 on double shear riveted joints of 2024-T3 (Figure 65) at net area minimum stresses of 5.1, 3.8, and 3.1 ksi, and on unnotched sheet of 7075-T6 at net area minimum stresses of 9.6, 7.7, 6.4, and 4.8 ksi. Butt joints of 7075-T6 (Figure 65) were tested at gross area minimum stresses of 5.3, 4.4, and 3.3 ksi; and strips of Cr-Mo steel with a centrally located hole (Figure 65) were tested at net area minimum stresses of 16.7, 15.1, and 12.6 ksi. The unit loading spectra and S-N data for this series of tests are presented in Tables 44 to 47 and in Figures 97 to 104. Similar to the series of tests conducted under unit gust loading spectra in Reference 17, the magnitude of the varying loads was decreased with reductions in mean load levels as shown in Figures 97, 98, 99, and 100. Twenty-seven experimental fatigue lives under these unit maneuver spectra were sorted into the 13 test groups listed in Table 49.

The application of these data to the numerical evaluation of ten of the fatigue life prediction methods selected for this phase of the study is described in detail in Appendix B. The results and conclusions drawn from the evaluation are given in Section III in the main body of the report.

TABLE 30

TEST VARIABLES TO BE CONSIDERED WITH MEAN AND VARYING STRESS IN

ANALYZING FATIGUE LIFE PREDICTION METHODS

SEQUENCE	NO. OF TEST GROUPS
Lo-Hi	8
Hi-Lo	10
Quasi-Random	17
Lo-Hi-Lo	37
Hi-Lo-Hi	2
True Random	4

BLOCK SIZE	NO. OF TEST GROUPS
5410	1
6290	1
7500	13
10200	3
13290	1
30000	4
30200	2
32860	4
50000	1
50100	1
50900	4
59670	7
92900	1
100000	4
100200	5
164400	1
360280	13
457700	1
500000	7
1228000	1
1899000	1
2279000	1
2848000	1

MATERIAL	NO. OF TEST GROUPS
2024-T	41
7075-T6	28
Cr-Mo Steel	6
D.T.D. 363A	6

NO. OF LOADING STEPS	NO. OF TEST GROUPS
3	4
5	3
6	4
8	21
9	28
10	1
11	4
16	7
18	6

TYPE OF SPECIMEN	NO. OF TEST GROUPS
Notched Sheet	27
Double Shear Riveted Joints	7
Unnotched Sheet	7
Butt Joints	6
Strips with Hole	6
One Row Lap Joints	6
Two Row Lap Joints	1
Notched Plate	3
C-46 Wing	7
P-51 Wing	8

TYPE OF SPECTRUM	NO. OF TEST GROUPS
Gust	65
Maneuver	13

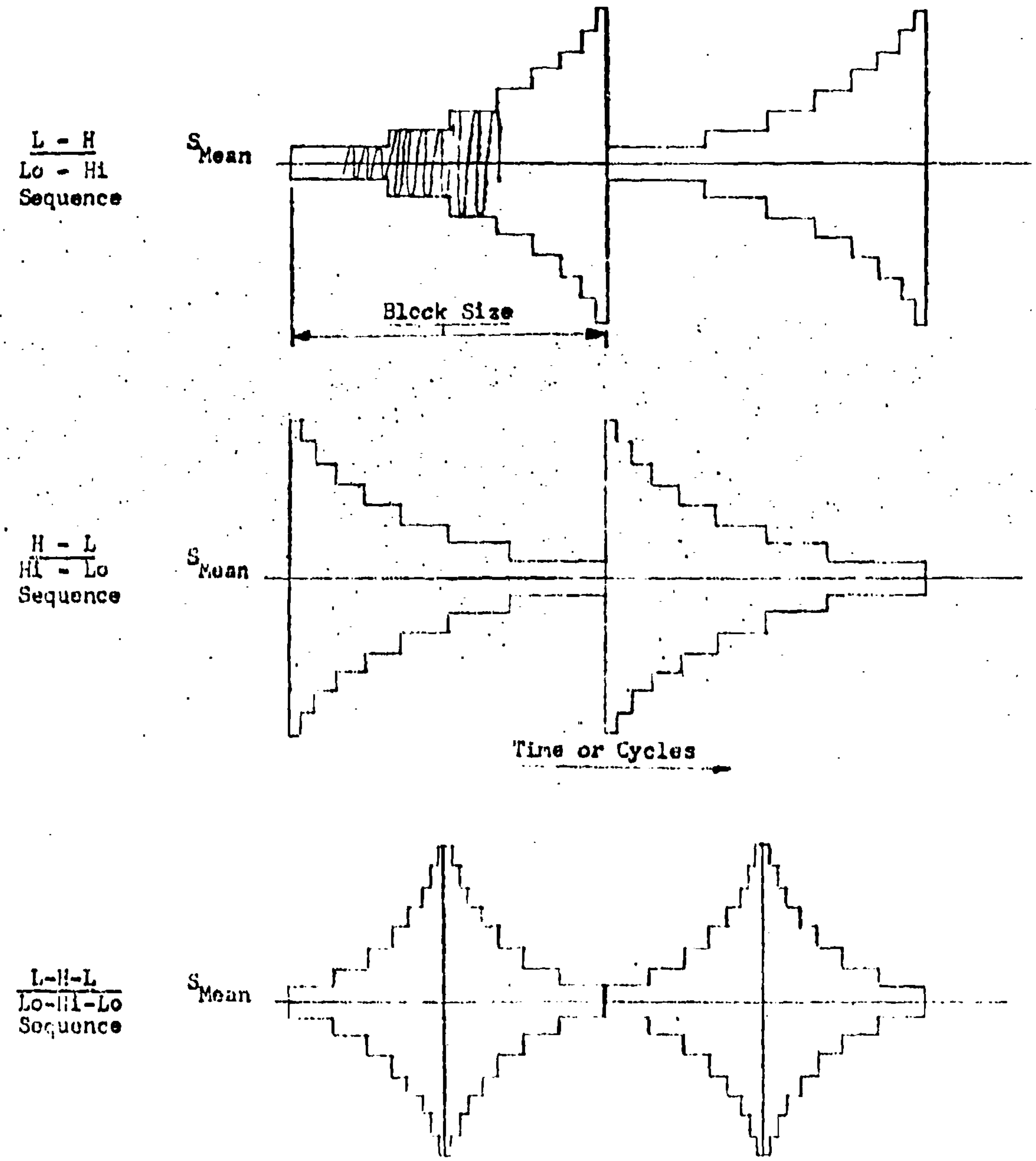

Figure 53. Schematic Diagrams of Gust Loading Sequences

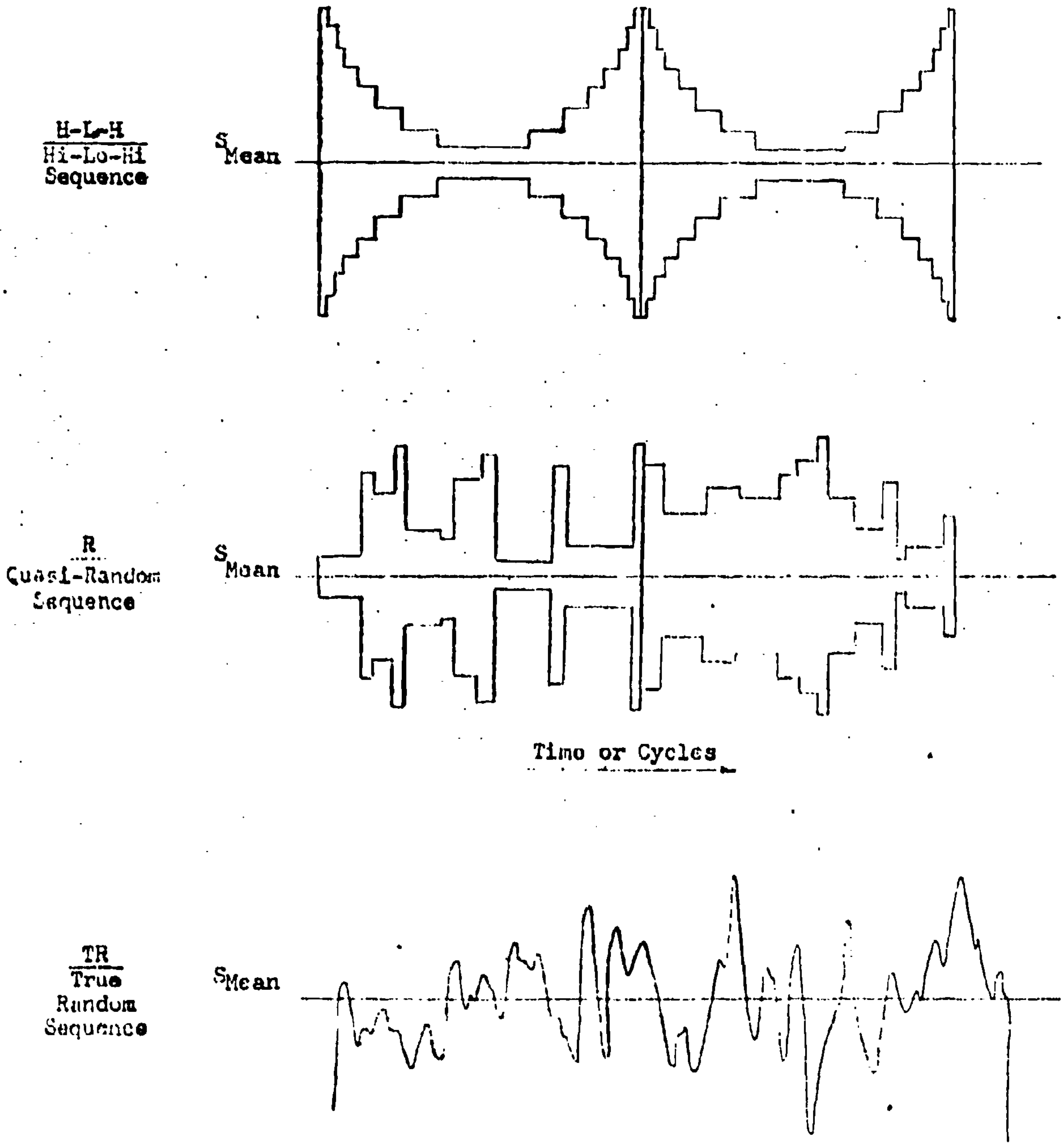

Figure 63 (continued) Schematic Diagrams of Gust Loading Sequences

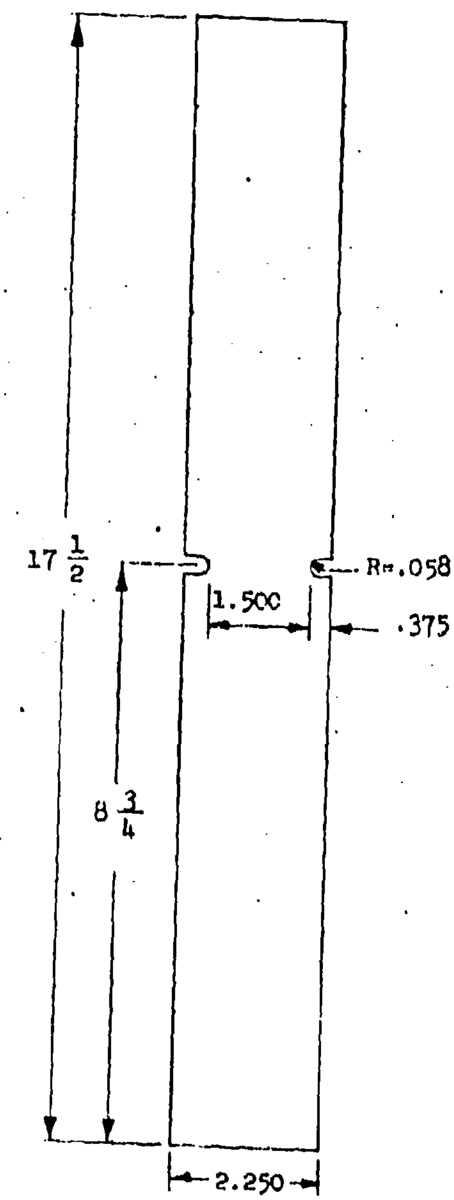

Theoretical Elastic Stress
Concentration Factor $K_T = 4.0$

Figure 64 Notched Sheet Specimen for which Fatigue Test Data are Presented in Reference 16

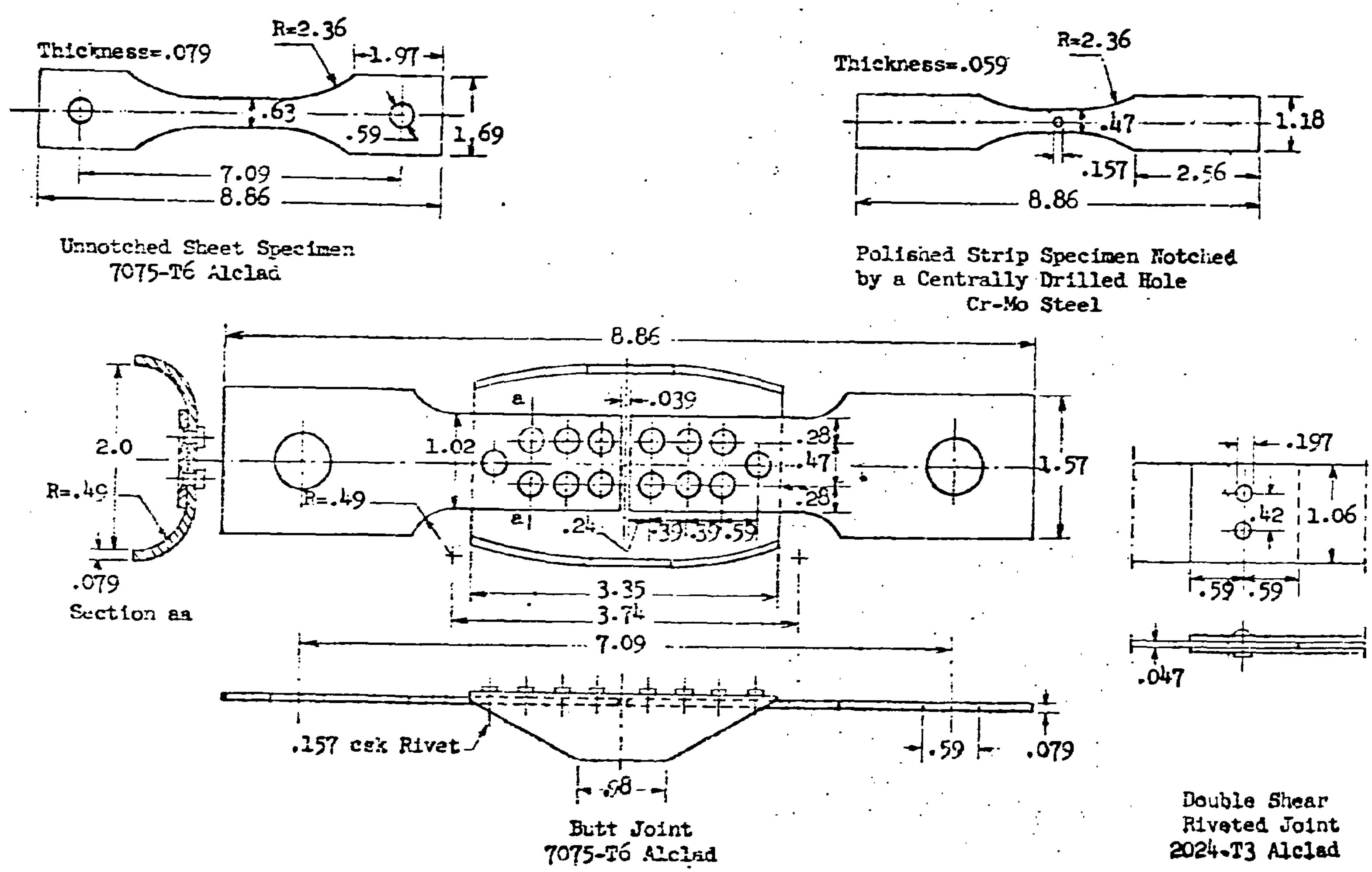

Figure 65 Specimens for which Fatigue Test Data are Presented in Reference 17

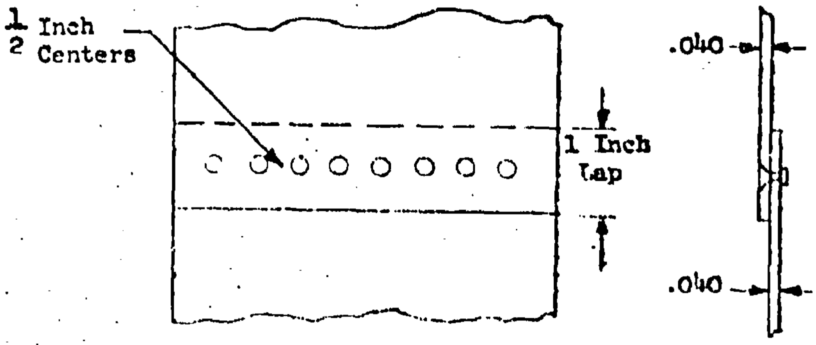

Single - Row Flush-Riveted Lap Joint

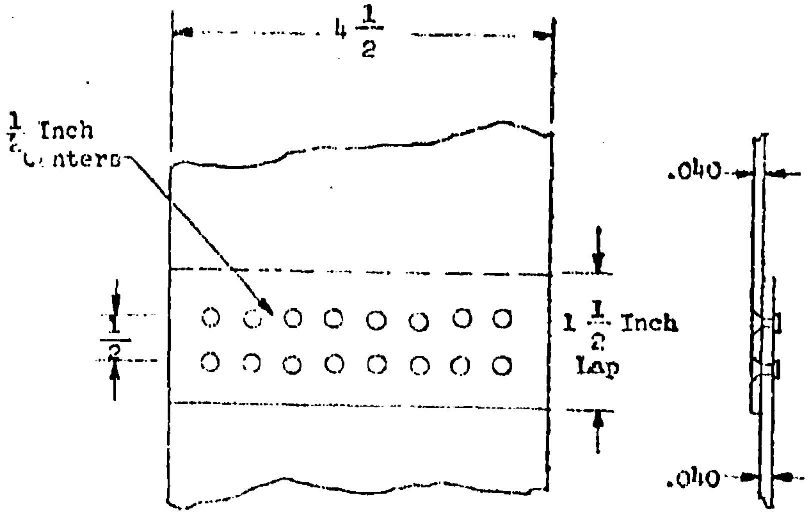

Double-Row Flush-Riveted Lap Joint

(Length between Grips is Approximately 12 Inches)

Figure 66 Riveted - Lap Joint Specimens for which Fatigue Test Data are Presented in Reference 18

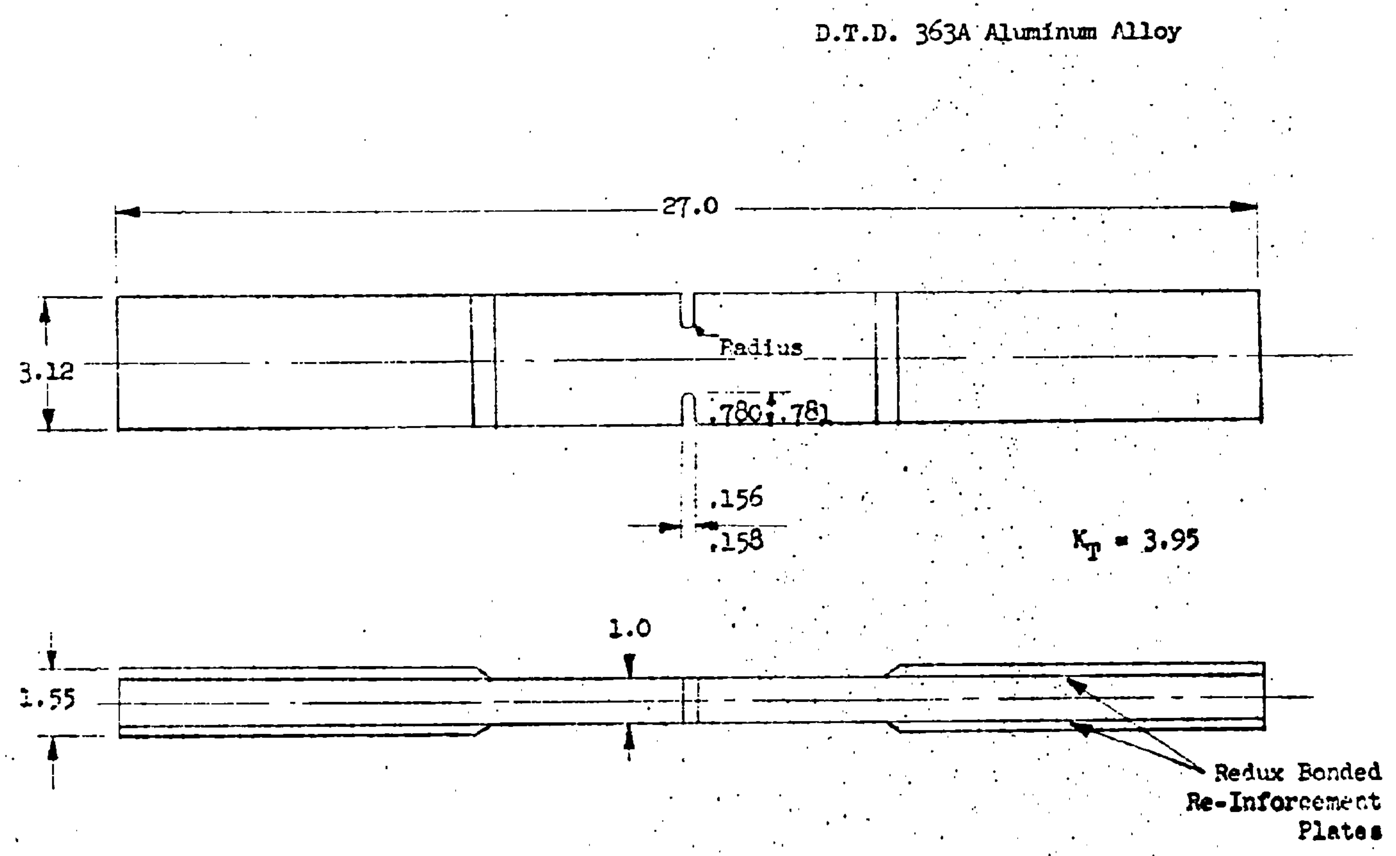

Figure 67 Notched Plate Specimen for which Fatigue Test Data are Presented in Reference 19

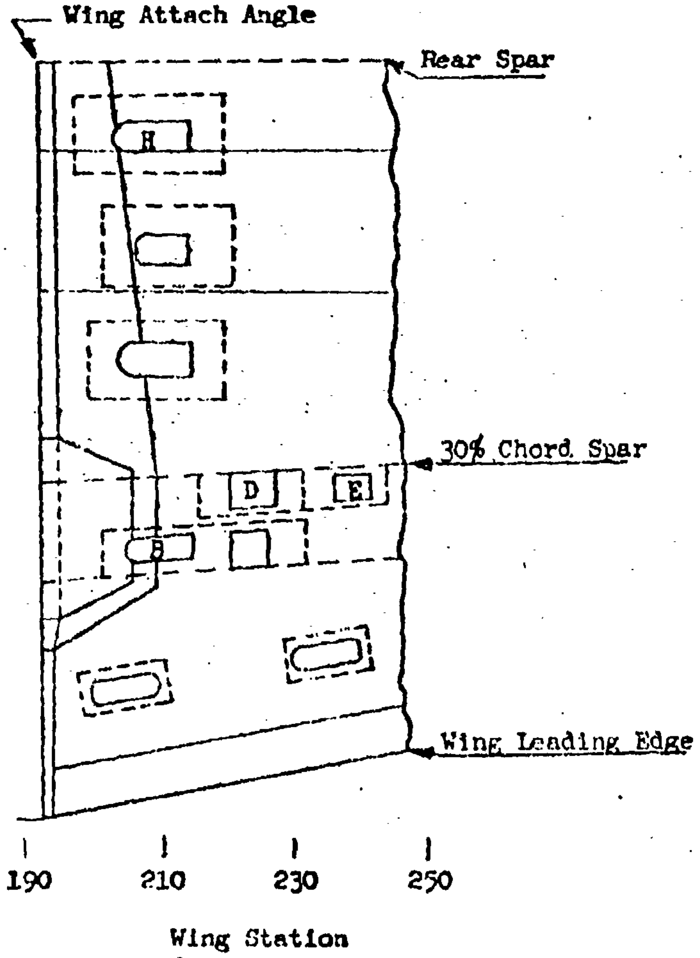

D Internal Doubler
E Internal Doubler
H Corner of Cutout

Figure 68 C-46 Wing Specimen for which Fatigue Test Data are Presented in References 20 and 23

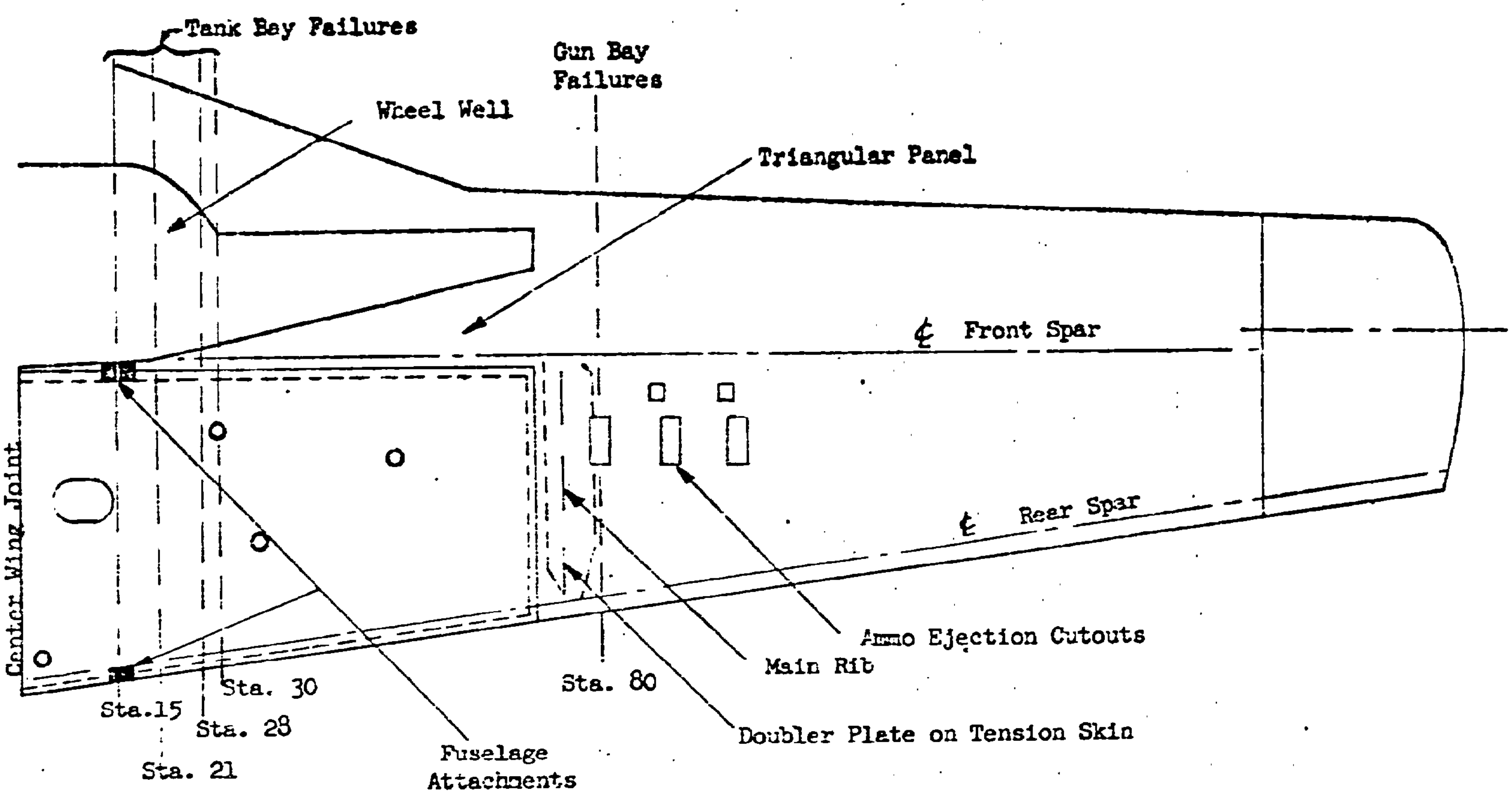

Figure 69 P51 Wing Specimen for Which Fatigue Test Data are Presented in Reference 21

TABLE 31

UNIT GUST LOADING SPECTRA AND S-N DATA FOR NOTCHED SHEET SPECIMENS
2024-T3 ALUMINUM ALLOY
(Reference 16)

F_{tu} = 72.1 KSI (Net Area)

Loading Step	f_{max} KSI	S_v	n	N	f_{max} KSI	S_v	n	N
	Gust Spectrum B f_{mean} = 17.4 KSI S_{mean} = .241				Gust Spectrum A f_{mean} = 17.4 KSI S_{mean} = .241			
1	18.1	.010	62000	-	18.1	.010	46800	-
2	19.5	.029	24000	-	19.5	.029	27200	-
3	20.9	.049	9400	-	20.9	.049	14500	-
4	22.3	.068	3400	1300000	22.3	.068	6800	1300000
5	23.7	.087	880	270000	23.7	.087	2750	270000
6	25.1	.107	220	96000	25.1	.107	1120	[illegible]
7	26.5	.126	60	44500	26.5	.126	450	44500
8	27.9	.146	26	26000	27.9	.146	200	26000
9	29.3	.165	7.8	15000	29.3	.165	80	15000
10	30.7	.185	3.2	9200	30.7	.185	39	9200
11	32.1	.204	1.8	6100	32.1	.204	18	6100
12	33.5	.223	.5	4200	33.5	.223	7.6	4200
13	34.9	.243	.34	2900	34.9	.243	3.0	2900
14	36.3	.262	.16	2050	36.3	.262	1.3	2050
15	37.7	.282	.08	1540	37.7	.282	.6	1540
16	39.1	.301	.054	1150	39.1	.301	.3	1150
17	40.5	.320	.024	860	40.5	.320	.25	860
18	41.9	.340	.012	700	41.9	.340	.09	700
	(G1 to G5****)		Σ100000 *			(G6)	Σ100000	

Loading Step	f_{max} KSI	S_v	n	N	f_{max} KSI	S_v	n	N
	Gust Spectrum A f_{mean} = 17.4 KSI S_{mean} = .241				Gust Spectrum A f_{mean} = 0 KSI S_{mean} = 0			
1	19.5	.029	82000	-	2.2	.031	41000	.
2	22.5	.071	15000	900000	8.0	.111	7850	[illegible]
3	25.6	.114	2800	73000	13.2	.183	980	80000
4	28.7	.157	350	18500	18.5	.257	143	10000
5	31.9	.201	46	6500	23.8	.330	23	1900
6	35.1	.246	7.4	2760	29.2	.405	3	480
7	38.4	.292	1.6	1320	34.8	.463	.73	170
8	41.5	.334	.35	750	40.4	.561	.11	58
	(G7 to G12)		Σ100205 **		(G13 & G14)		Σ50000 ***	

* tests also made at 5n (G2, G4, & G5)

** tests also made at $\frac{n}{2}$ (G11)

*** tests also made at 2n (G14)

**** Test Group No.

TABLE 32

UNIT GUST LOADING SPECTRA AND S-N DATA FOR NOTCHED SHEET SPECIMENS
7075-T6 ALUMINUM ALLOY
(Reference 16)

F_{tu} = 82.9 KSI (Net Area)

Loading Step	f_{max} KSI	S_v	n	N
Gust Spectrum A; f_{mean} = 20 KSI; S_{mean} = .241				
1	21.5	.018	42000	-
2	25.3	.064	7500	160000
3	28.7	.105	1190	16600
4	32.6	.152	175	5800
5	36.3	.197	23	2900
6	40.1	.242	2.5	1490
7	43.9	.288	0.5	820
8	47.[illegible]	.332	0.1	480
	(G15 to G21**)		≥ 30000 *	
Gust Spectrum A; f_{mean} = 10 KSI; S_{mean} = .121				
1	13.0	.036	24400	-
2	17.1	.086	4700	520000
3	21.9	.144	1000	20000
4	27.1	.206	92	4400
5	31.7	.262	14	1650
6	36.8	.323	1.8	670
7	42.5	.392	0.3	280
8	47.0	.446	0.07	160
	(G22 & G23)		≥ 30000	
Gust Spectrum A; f_{mean} = 0 KSI; S_{mean} = 0				
1	3.8	.046	24400	-
2	9.1	.110	4800	2300000
3	15.0	.181	690	27500
4	21.2	.256	98	4200
5	27.2	.328	14	1050
6	33.7	.406	1.8	320
7	39.9	.481	0.33	130
8	46.3	.559	0.074	58
	(G24 to G27)		≥ 30000	

* Tests also made at $\frac{n}{5}$ (G15, G18, & G20)

** Test Group No.

TABLE 33

UNIT GUST LOADING SPECTRA AND S-N DATA FOR DOUBLE SHEAR RIVETED JOINTS
2024-T3 ALCLAD
(Reference 17)

F_{tu} = 61.1 KSI (Net Area)

Loading Step	S_{max}	S_v	n	N	S_{max}	S_v	n	N
		S_{mean} = .253				S_{mean} = .152		
1	.278	.025	281000	2300000	.167	.015	281000	-
2	.327	.074	65700	120000	.196	.044	65700	650000
3	.376	.123	11500	54000	.226	.074	11500	260000
4	.426	.173	1440	29000	.256	.104	1440	160000
5	.475	.222	432	18000	.285	.133	432	100000
6	.524	.271	131	11700	.315	.163	131	72000
7	.574	.321	50	7600	.345	.193	50	53000
8	.623	.370	16	5400	.374	.222	16	38000
9	.672	.419	10	3700	.404	.252	10	29000
		(028*)	Σ 360280			(029)	Σ 360280	
		S_{mean} = .101				S_{mean} = .0806		
1	.111	.010	281000	-	.089	.008	281000	-
2	.131	.030	65700	-	.105	.024	65700	-
3	.150	.049	11500	1500000	.120	.039	11500	-
4	.170	.069	1440	610000	.136	.055	1440	3500000
5	.190	.089	432	390000	.152	.071	432	880000
6	.209	.108	131	270000	.168	.087	131	520000
7	.229	.128	50	200000	.184	.103	50	380000
8	.249	.148	16	145000	.199	.118	16	300000
9	.268	.167	10	120000	.215	.134	10	220000
		(030)	Σ 360280			(031)	Σ 360280	

*Test Group No.

TABLE 34

UNIT GUST LOADING SPECTRA AND S-N DATA FOR UNNOTCHED SHEET
7075-T6 ALCLAD
(Reference 17)

F_{tu} = 76.8 KSI

Loading Step	S_{max}	S_v	n	N
		S_{mean} = .201		
1	.221	.020	281000	-
2	.260	.059	65700	-
3	.299	.098	11500	5000000
4	.339	.138	1440	360000
5	.378	.177	432	180000
6	.417	.216	131	105000
7	.457	.256	50	66000
8	.496	.295	16	44000
9	.535	.334	10	31000
		(032*)	Σ 360280	
		S_{mean} = .161		
1	.177	.016	281000	-
2	.208	.047	65700	-
3	.240	.079	11500	-
4	.271	.110	1440	1500000
5	.302	.141	432	330000
6	.334	.173	131	181000
7	.365	.204	50	120000
8	.397	.236	16	82000
9	.428	.267	10	60000
		(033)	Σ 360280	
		S_{mean} = .145		
1	.159	.014	281000	-
2	.187	.042	65700	-
3	.216	.071	11500	-
4	.244	.099	1440	-
5	.272	.127	432	550000
6	.301	.156	131	260000
7	.329	.184	50	165000
8	.357	.212	16	120000
9	.385	.240	10	85000
		(034)	Σ 360280	

* Test Group No.

TABLE 35

UNIT GUST LOADING SPECTRA AND S-N DATA FOR BUTT JOINTS
7075-T6 ALCLAD
(Reference 17)

F_{tu} = 53.0 KSI (Gross Area)

Loading Step	S_{max}	S_V	n	N
		S_{mean} = .250		
1	.275	.025	281000	-
2	.323	.073	65700	380000
3	.372	.122	11500	95000
4	.421	.171	1440	31000
5	.470	.220	432	15000
6	.518	.268	131	8000
7	.567	.317	50	4200
8	.616	.366	16	2400
9	.665	.415	10	1400
		(035*)	Σ 360280	
		S_{mean} = .167		
1	.183	.016	281000	-
2	.216	.049	65700	-
3	.248	.081	11500	650000
4	.281	.114	1440	300000
5	.313	.146	432	150000
6	.346	.179	131	75000
7	.378	.211	50	42000
8	.411	.244	16	23000
9	.443	.276	10	14500
		(036)	Σ 360280	
		S_{mean} = .125		
1	.137	.012	281000	-
2	.162	.037	65700	-
3	.186	.061	11500	-
4	.210	.085	1440	1100000
5	.235	.110	432	460000
6	.259	.134	131	260000
7	.284	.159	50	170000
8	.308	.183	16	110000
9	.332	.207	10	72000
		(037)	Σ 360280	

*Test Group No.

TABLE 36

UNIT GUST LOADING SPECTRA AND S-N DATA FOR STRIPS
WITH CENTRALLY LOCATED HOLE
Cr-Mo STEEL
(Reference 17)

F_{tu} = 150.8 KSI (Net Area)

Loading Step	S_{max}	S_v	n	N
		S_{mean} = .286		
1	.314	.028	281000	-
2	.370	.084	65700	-
3	.426	.140	11500	260000
4	.481	.195	1440	92000
5	.537	.251	432	43000
6	.593	.307	131	22000
7	.649	.363	50	11000
8	.705	.419	16	5400
9	.760	.474	10	2600
		(038*)	Σ 360280	
		S_{mean} = .222		
1	.244	.022	281000	-
2	.288	.066	65700	-
3	.330	.108	11500	-
4	.374	.152	1440	270000
5	.417	.195	432	111000
6	.460	.238	131	56000
7	.503	.281	50	32000
8	.547	.325	16	18000
9	.590	.368	10	11000
		(039)	Σ 360280	
		S_{mean} = .182		
1	.199	.017	281000	-
2	.235	.053	65700	-
3	.270	.088	11500	-
4	.306	.124	1440	-
5	.341	.159	432	320000
6	.377	.195	131	125000
7	.412	.230	50	64000
8	.448	.266	16	37000
9	.483	.301	10	25000
		(040)	Σ 360280	

* Test Group No.

TABLE 37

UNIT GUST LOADING SPECTRA AND S-N DATA FOR SINGLE-ROW FLUSH-RIVETED LAP JOINTS
2024-T3 ALCLAD
(Reference 18)

Ultimate Load = 1600 lbs. (Gross Area)

Loading Step	Maximum Load-lbs.	S_{max}	S_v	n	N	Maximum Load-lbs.	S_{max}	S_v	n	N
	Mean Load = 759 lbs.					S_{mean} = .212				
	Six Loading Steps					Five Loading Steps				
1	1130	.246	.034	1670000	-					
2	1450	.315	.103	207500	280000	1450	.315	.103	415000	280000
3	1770	.384	.172	19200	91000	1770	.384	.172	38400	91000
4	2080	.452	.240	1920	40300	2080	.452	.240	3840	40300
5	2400	.520	.308	192	19200	2400	.520	.308	384	19200
6	2700	.588	.376	19	10000	2700	.588	.376	38	10000
		(G41, G42 & G43**)		Σ 1898830*				(G44)	Σ 457660	

* Tests also made at 1.2n and 1.5n. (G42 & G43, respectively)

** Test Group No.

TABLE 38

UNIT GUST LOADING SPECTRUM AND S-N DATA
FOR DOUBLE-ROW FLUSH-RIVETED LAP JOINTS
2024-T3 ALCLAD
(Reference 18)

Ultimate Load = 8690 lbs. (Gross Area)

Loading Step	Maximum Load-lbs.	S_{max}	S_v	n	N
Mean Load = 1840 lbs.				S_{mean} = .212	
Five Loading Steps					
1	2734	.315	.103	143800	250000
2	3333	.384	.172	18500	75000
3	3923	.452	.240	1850	31500
4	4514	.520	.308	185	13400
5	5104	.588	.376	19	6000
			(645*)	Σ 164350	

* Test Group No.

TABLE 39

UNIT GUST LOADING SPECTRA AND S-N DATA FOR SINGLE-ROW FLUSH-RIVETED LAP JOINTS
7075-T6 ALCLAD
(Reference 18)

Ultimate Load = 4975 lbs. (Gross Area)

Loading Step	Maximum Load-lbs.	S_{max}	S_v	n	N	Maximum Load-lbs.	S_{max}	S_v	n	N
	Mean Load = 1055 lbs.					S_{mean} = .212				
	Six Loading Steps					Five Loading Steps				
1	1222	.246	.034	1080000	-					
2	1567	.315	.103	134000	98000	1567	.315	.103	79100	98000
3	1910	.384	.172	12400	40500	1910	.384	.172	12400	40500
4	2248	.452	.240	1240	22100	2248	.452	.240	1240	22100
5	2587	.520	.308	124	12300	2587	.520	.308	124	12300
6	2920	.588	.376	12	7100	2920	.588	.376	12	7100
			(G47*)	Σ 1227780				(G46)	Σ 92880	

* Test Group No.

TABLE 40

UNIT GUST LOADING SPECTRA AND S-N DATA
FOR NOTCHED PLATE SPECIMENS
D.T.D. 363A ALUMINUM ALLOY
(British Zinc-Aluminum Alloy Similar to 7075-T6)
(Reference 19)

F_{tu} = 85 KSI (Net Area)
f_{mean} = 14 KSI
S_{mean} = .165

Loading Step	f_v KSI	S_v	n	N
		Nine Loading Steps		
1	2.62	.030	7400	-
2	3.68	.043	3100	150000
3	4.73	.056	1500	48000
4	5.78	.068	700	26000
5	6.84	.080	325	17000
6	7.88	.093	150	12500
7	8.93	.105	67	9200
8	9.98	.118	31	6800
9	11.02	.130	15	5200
		(048*)	Σ 13290	
		Nine Loading Steps Different Frequency		
1	2.62	.030	4400	-
2	3.68	.043	600	150000
3	4.73	.056	700	48000
4	5.78	.068	280	26000
5	6.84	.080	180	17000
6	7.88	.093	66	12500
7	8.93	.105	33	9200
8	9.98	.118	21	6800
9	11.02	.130	13	5200
		(049)	Σ 6290	
		Ten Loading Steps		
1	2.62	.030	810	-
2	3.68	.043	1800	150000
3	4.73	.056	1650	48000
4	5.78	.068	747	26000
5	6.84	.080	193	17000
6	7.88	.093	103	12500
7	8.93	.105	60	9200
8	9.98	.118	27	6800
9	11.02	.130	12	5200
10	11.60	.137	8	4000
		(050)	Σ 5410	

* Test Group No.

TABLE 41

UNIT GUST LOADING SPECTRUM AND S-N DATA
FOR WING STATIONS 180, 214, 228, AND 239 OF C-46 WING
2024-T ALUMINUM ALLOY
(Reference 20 and 23)

Ultimate Load Factor = 5.0 * (Gross Area)
S_{mean} = .2

Loading Step	Δg	$S_v = \frac{\Delta g}{5}$	n	N: WS 180	N: WS 214	N: WS 228	N: WS 239
				See Note on Figure 92			
1	.225	.045	39312	6500000	5000000	6000000	1750000
[illegible]	.375	.075	15444	1170000	1500000	1300000	520000
[illegible]	.525	.105	3510	320000	550000	470000	240000
4	.675	.135	1067	132000	260000	210000	130000
5	.825	.165	235	66000	150000	110000	81000
6	.975	.195	73	35000	92000	62000	56000
7	1.125	.225	20	20500	65000	39000	40000
8	1.275	.255	5.86	12500	48000	27000	29000
9	1.425	.285	1.48	8600	35000	18500	21500
10	1.575	.315	.69	6000	28000	14000	16000
11	1.725	.345	.19	4500	23000	10200	12500
12	1.875	.375	.12	3300	18000	8000	10000
13	2.025	.405	.06	2500	14500	6200	8500
14	2.175	.435	.02	1900	12000	4800	7000
15	2.325	.465	.02	1520	10000	4000	6000
16	2.475	.495	.01	1250	8800	3[illegible]00	5200
	(G51 to G54**)		Σ 59670				

* Arbitrary

** Test Group No.

TABLE 42

UNIT GUST LOADING SPECTRUM AND S-N DATA FOR COMPLETE C-46 WING
2024-T ALUMINUM ALLOY
(Reference 20)

Ultimate Load Factor = 5.0 * (Gross Area) S_{mean} = .2

Loading Step	Δg	$S_v = \frac{\Delta g}{5}$	n	N First Crack	N Critical Crack	N Final Failure
1	.225	.045	39312	3100000	4300000	6600000
2	.375	.075	15444	790000	1070000	1650000
3	.525	.105	3510	280000	400000	590000
4	.675	.135	1067	140000	200000	280000
5	.825	.165	235	72000	110000	152000
6	.975	.195	73	41000	65000	95000
7	1.125	.225	20	24000	40000	57000
8	1.275	.255	5.86	15000	26000	37000
9	1.425	.285	1.48	9500	17000	24000
10	1.575	.315	.69	6200	11500	16000
11	1.725	.345	.19	4000	7900	11000
12	1.875	.375	.12	2700	5400	8000
13	2.025	.405	.06	1800	3700	5900
14	2.175	.435	.02	1200	2600	4500
15	2.325	.465	.02	850	1820	3400
16	2.475	.495	.01	580	1270	2600
	(G55 to G57**)		Σ 59670			

* Arbitrary

** Test Group No.

TABLE 43

UNIT GUST LOADING SPECTRA AND S-N DATA FOR P51 WING
2024-T ALUMINUM ALLOY
(Reference 21 & 24)

Ultimate Load = 89600 lbs. (Gross Area)

S_{mean} = .200

Loading Step	S_v	n	N Initial Failure Gun Bay	N Initial Failure Tank Bay	N Final Failure Gun Bay	N Final Failure Tank Bay
			Eleven Loading Steps			
1	.0324	275300	–	–	–	–
2	.0540	118200	1585000	3020000	2089000	5888000
3	.0756	64310	346700	616600	660700	501200
4	.0972	26080	123000	211300	309000	218800
5	.1188	9452	53090	93330	162200	112200
6	.1512	5110	17780	38020	75860	53700
7	.1944	1139	5248	15140	33110	23500*
8	.2376	220.7	1950	7590	15850	10960
9	.2808	51.32	813	4360	7800*	5623
10	.3240	10.69	355	2660	4169	3020
11	.4100	4.343	83	1120	1120	1072
	(G58, G60, G62 & G64***)	Σ 499880 **				
			Three Loading Steps			
1	.055	26500	1513600	2691500	1905500	4365200
2	.075	5300	363080	630000*	676080	524810
3	.1325	1060	32359	61659	114820	81283
	(G59, G61, G63 & G65)	Σ 32860				

* These values have been corrected. The values listed in reference 21 are apparently in error.

** Specified in reference 21 as the number of positive load peaks in 10^6 load selections.

*** Test Group No.

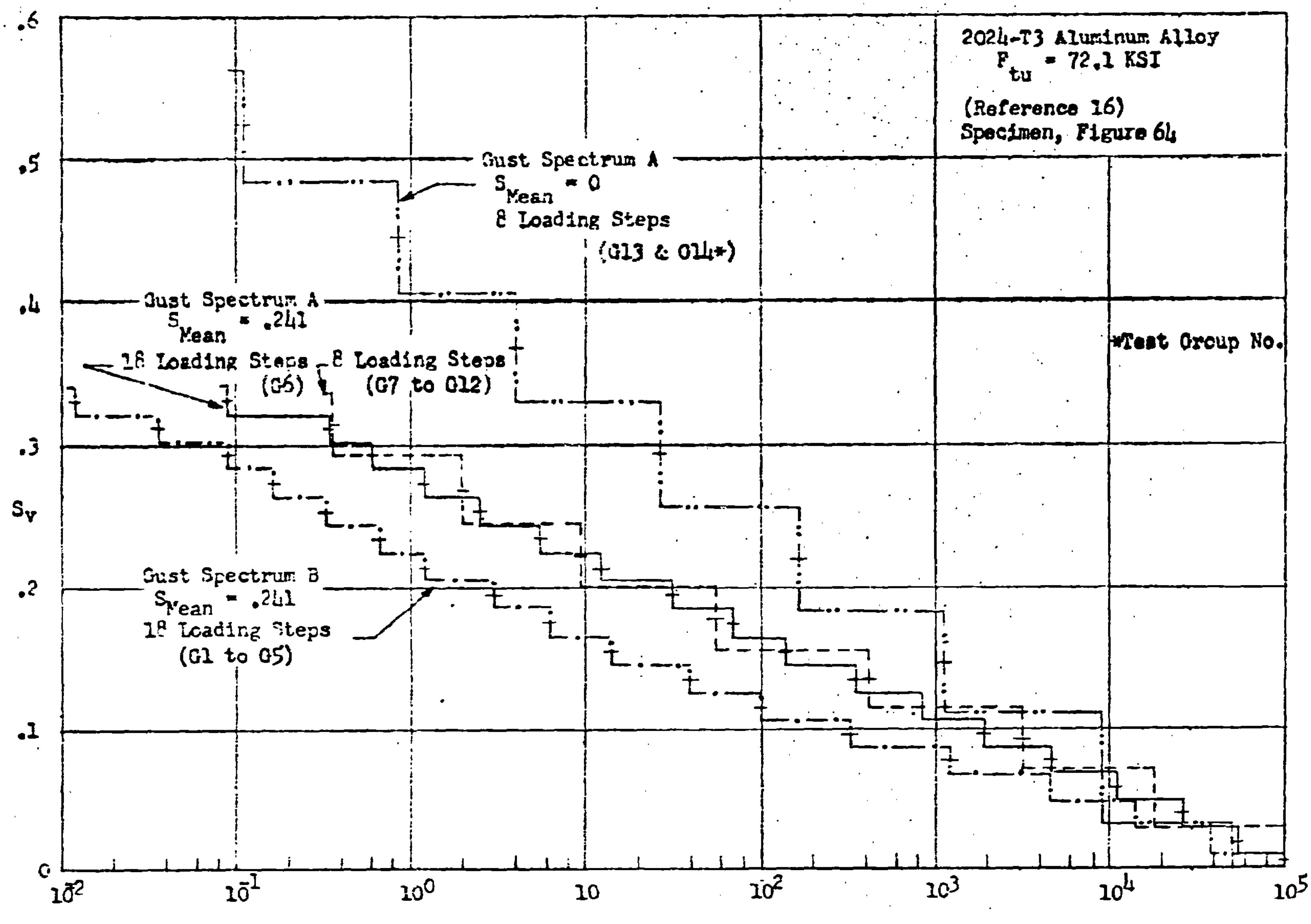

Figure 70 Unit Gust Loading Spectra For Notched Sheet Specimens

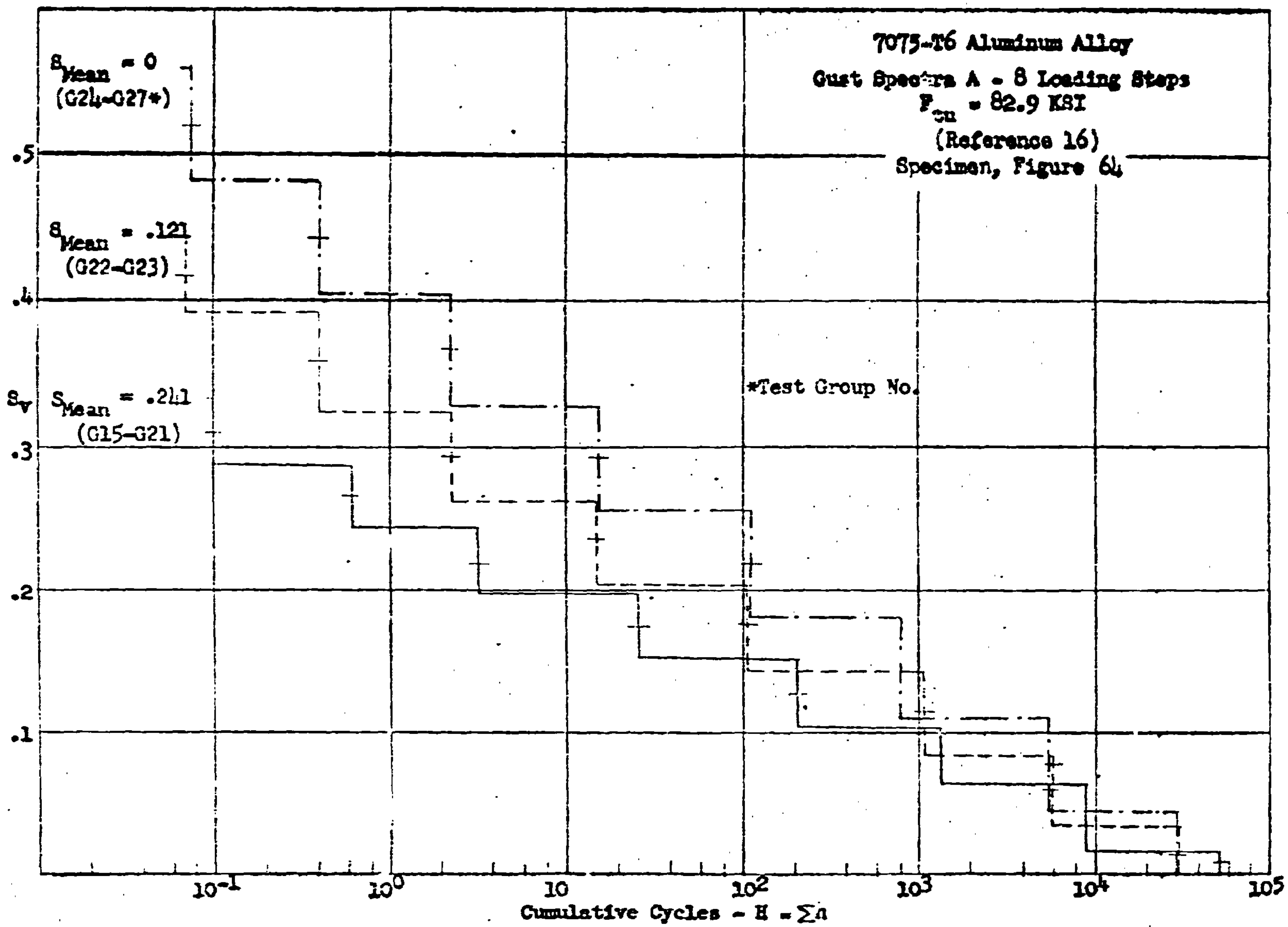

Figure 71 Unit Loading Spectra for Notched Sheet Specimens.

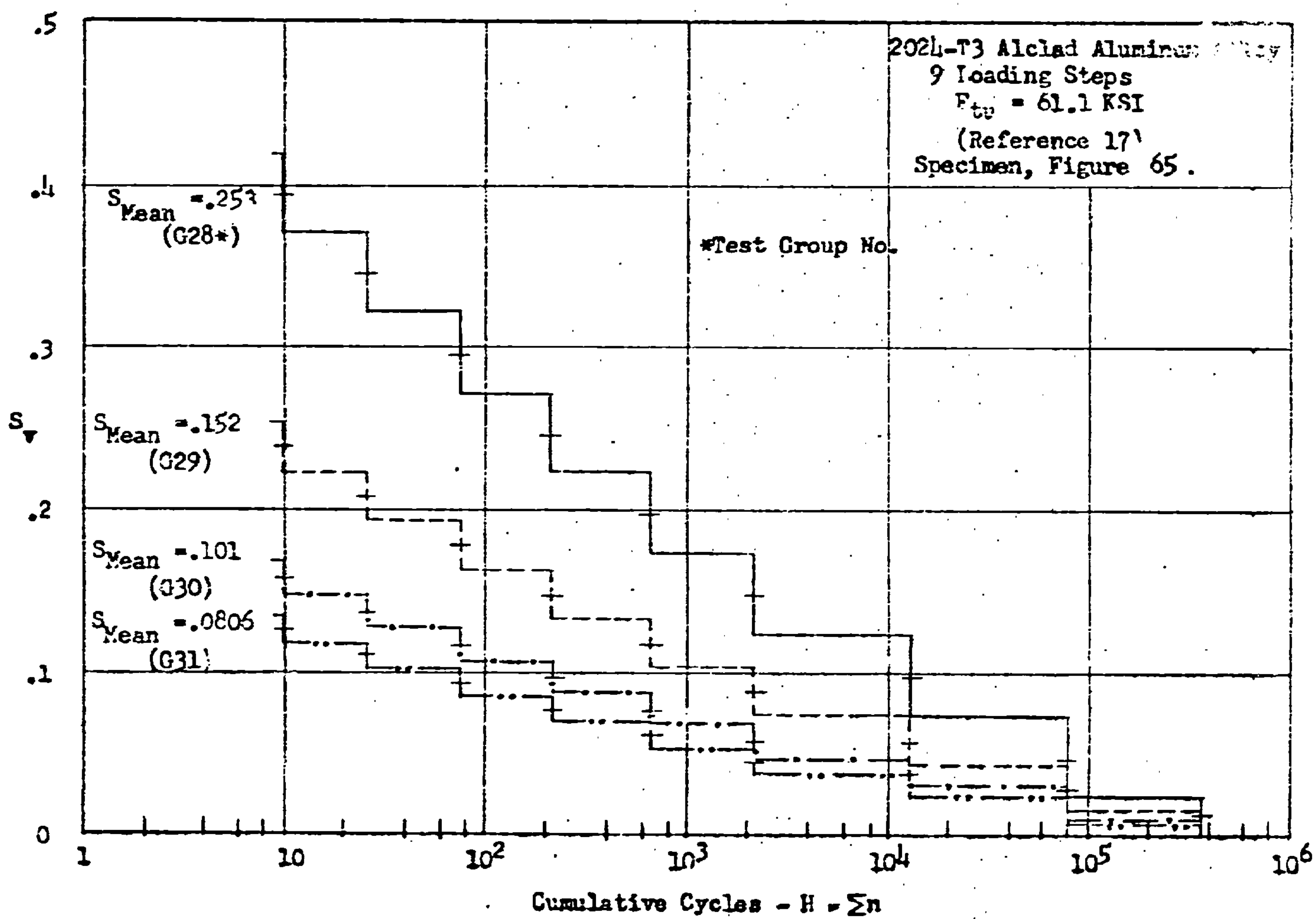

Figure 72 Unit Gust Loading Spectra for Double Shear Riveted Joint Specimens

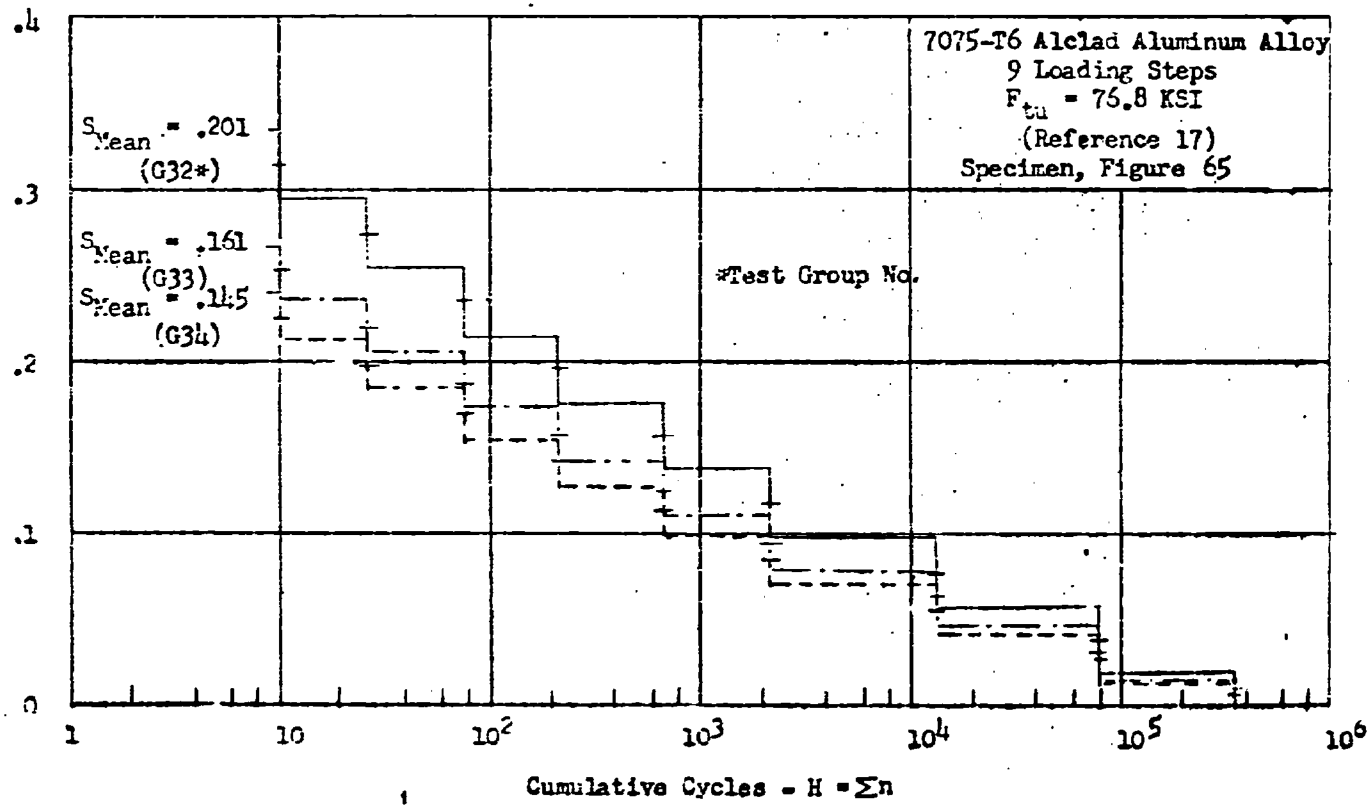

Figure 73 Unit Gust Loading Spectra for Unnotched Sheet Specimens

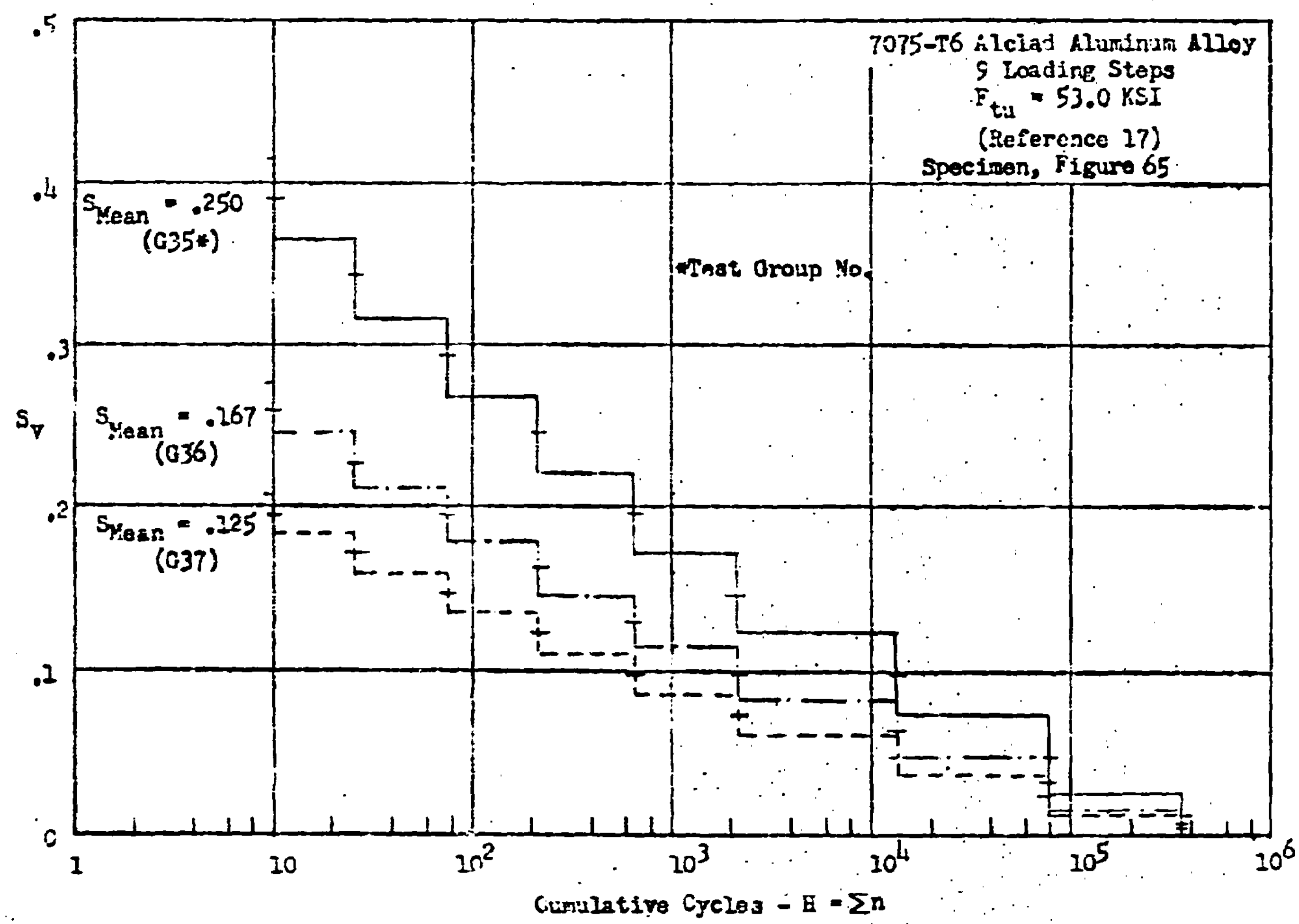

Figure 74 Unit Gust Loading Spectra for Butt Joint Specimens

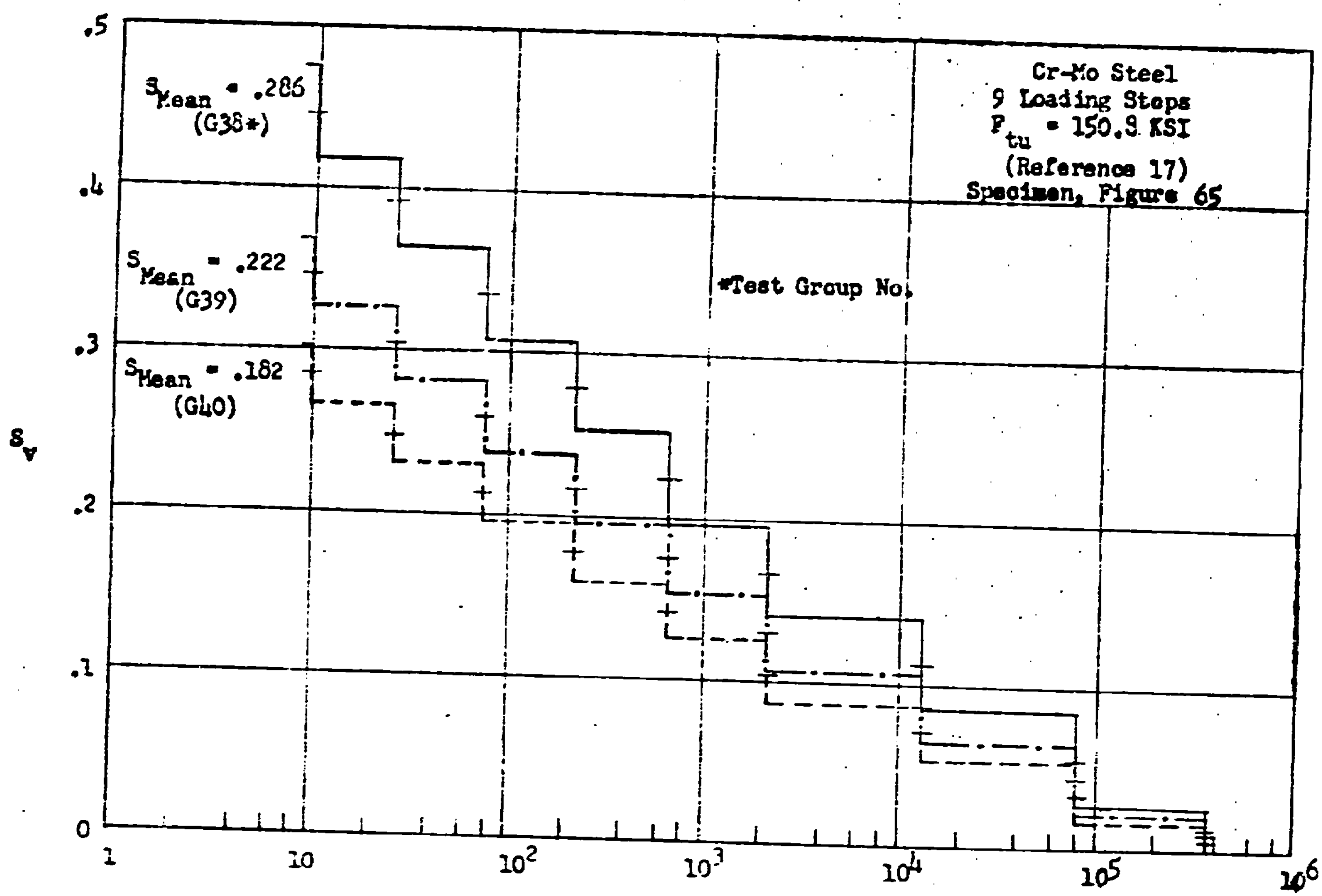

Figure 75 Unit Gust Loading Spectra for Strip Specimens with Centrally Located Hole

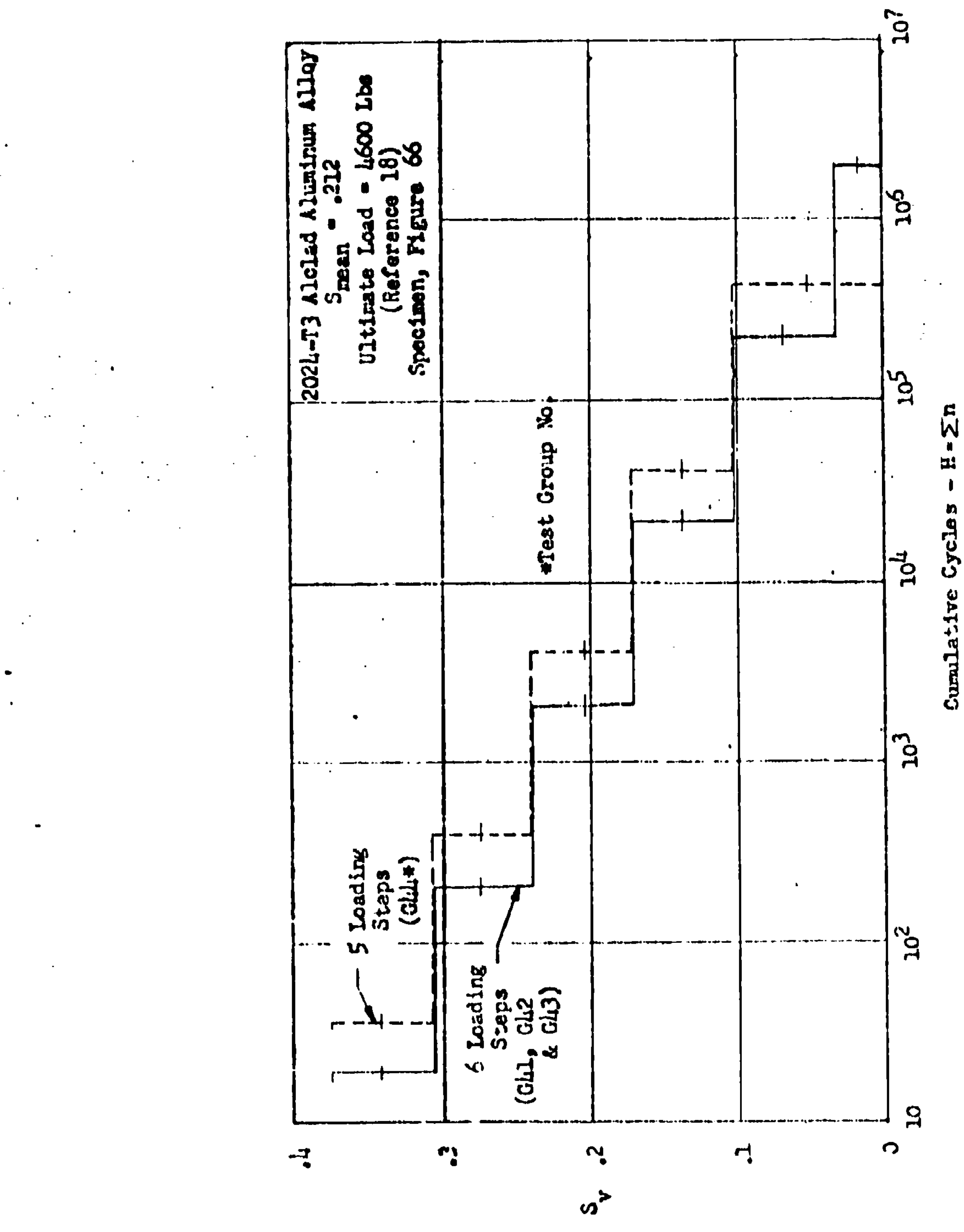

Figure 76 Unit Gust Loading Spectra for Lap Joint Specimens with a Single Row of Flush Rivets

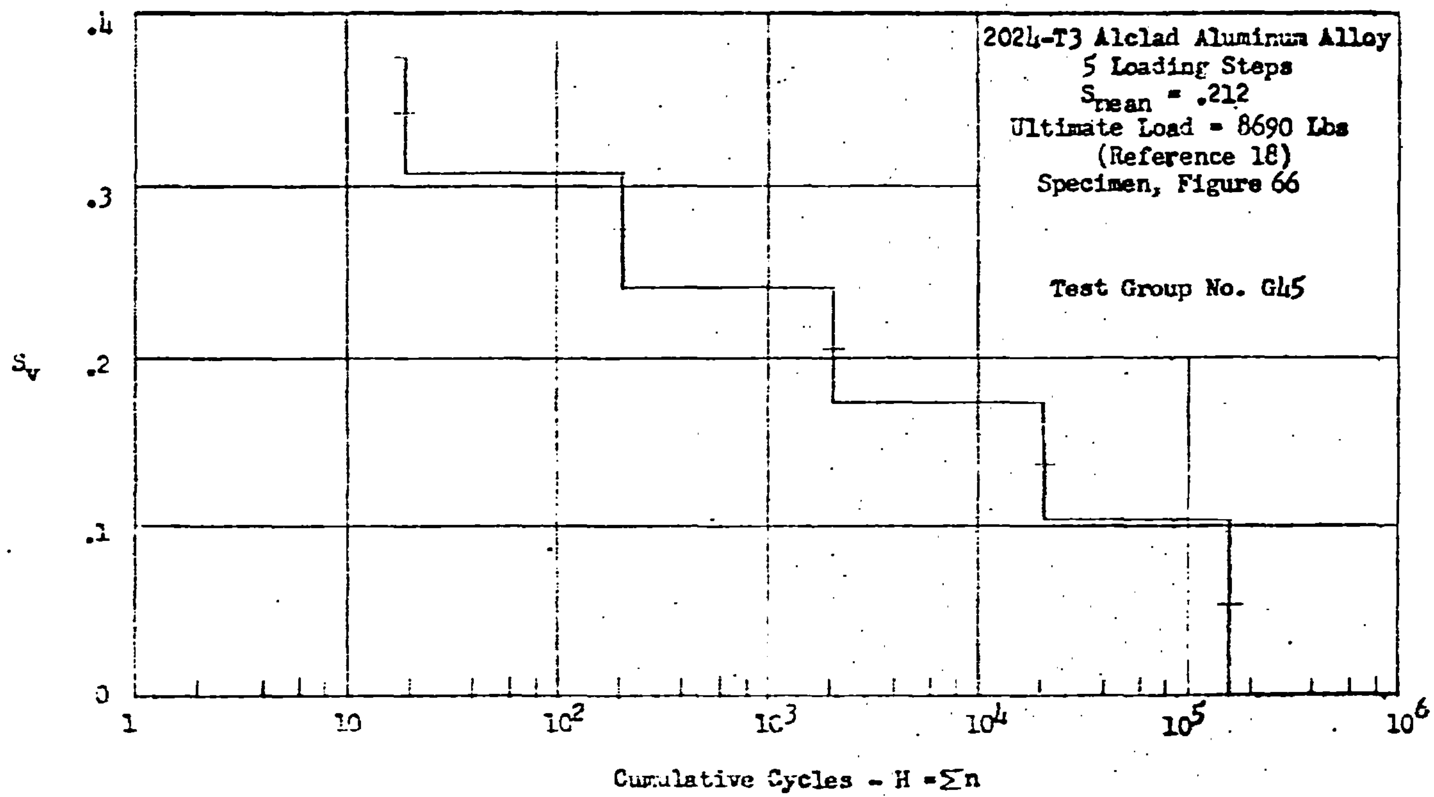

Figure 77 Unit Gust Loading Spectrum for Lap Joint Specimen with a Double Row of Flush Rivets

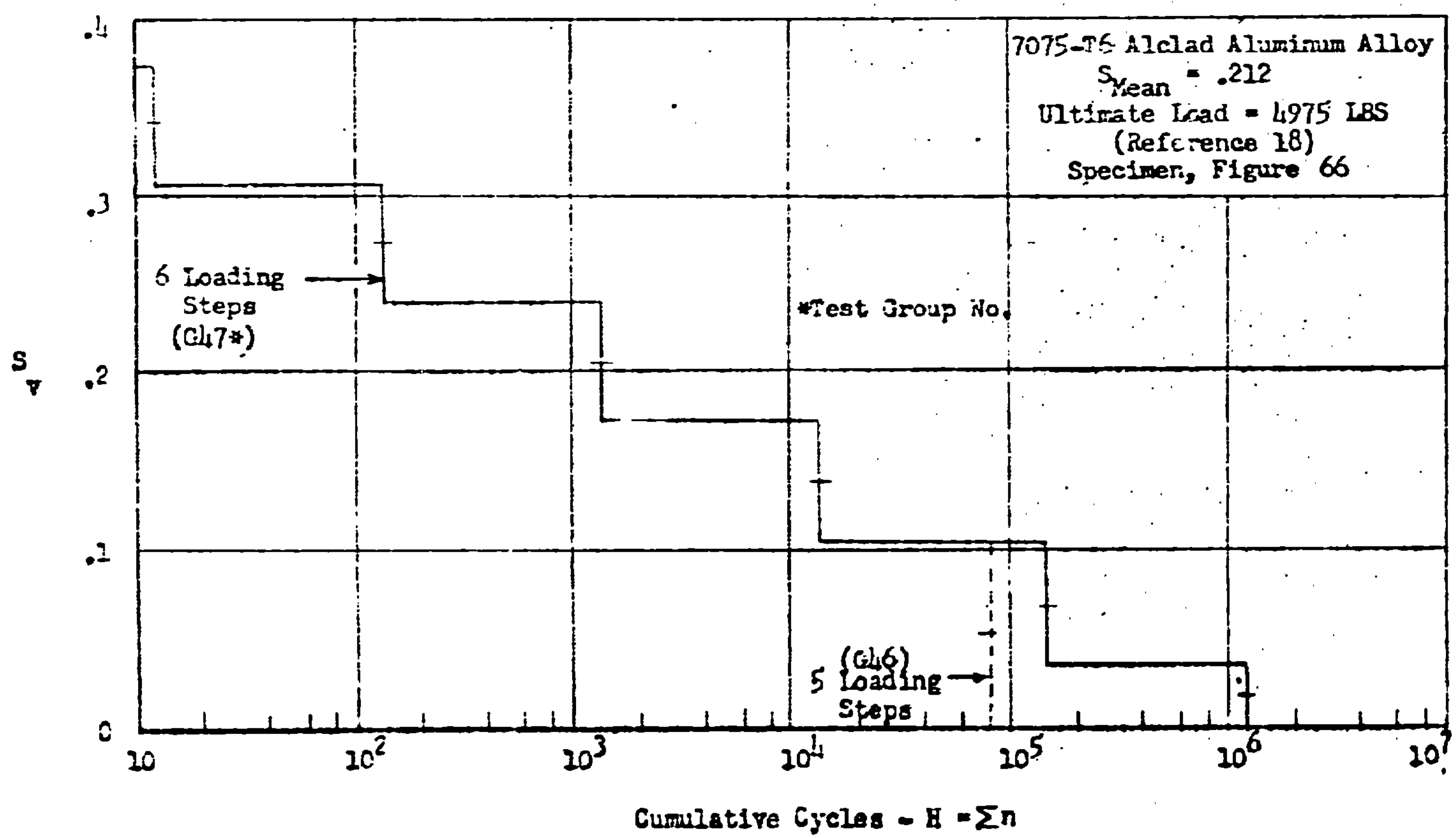

Figure 78 Unit Gust Loading Spectra for Lap Joint Specimens with a Single Row of Flush Rivets

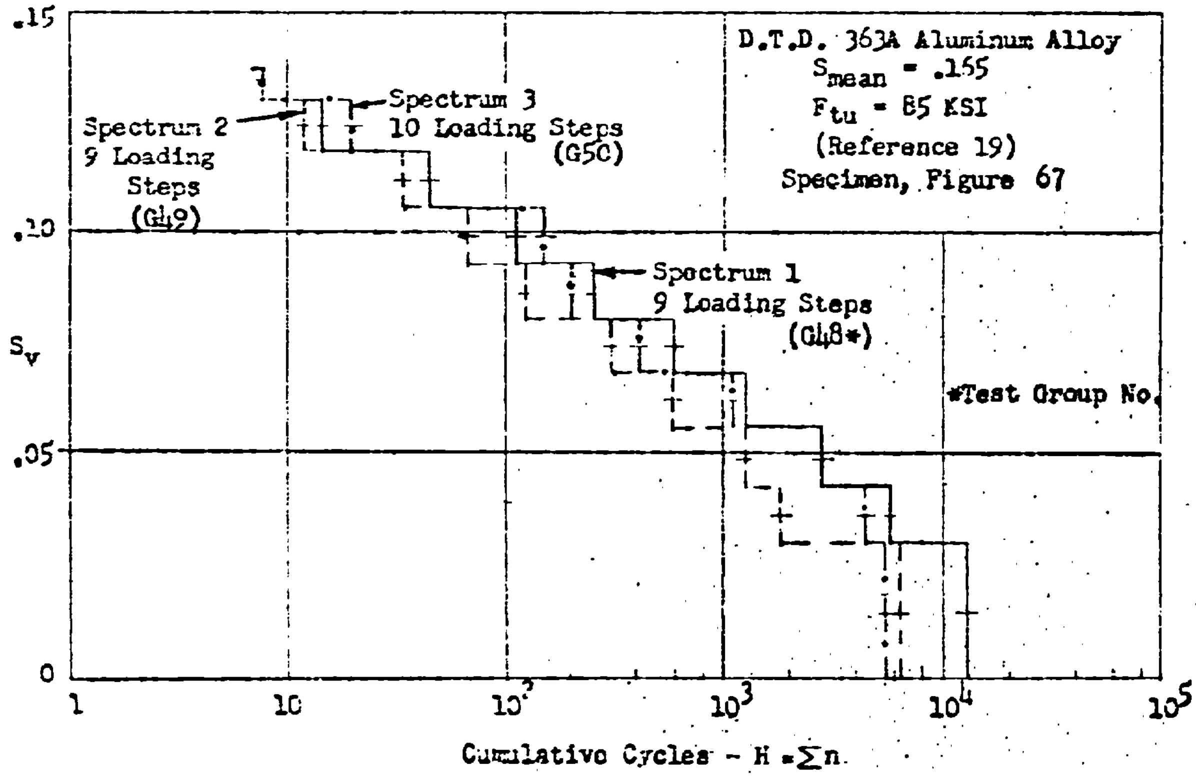

Figure 79 Unit Gust Loading Spectra for Notched Plate Specimens

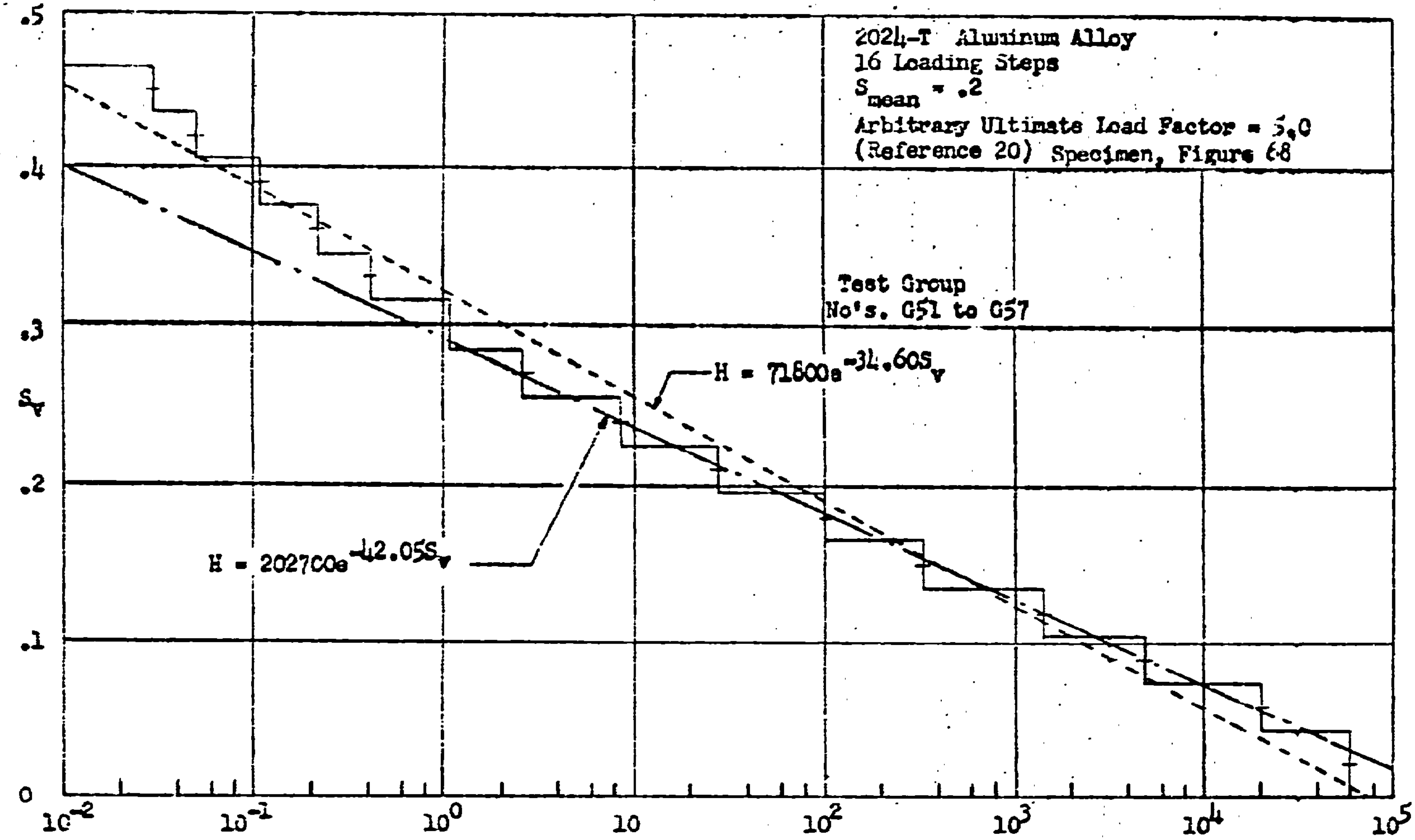

Figure 80. Unit Gust Loading Spectrum for C-46 Wing

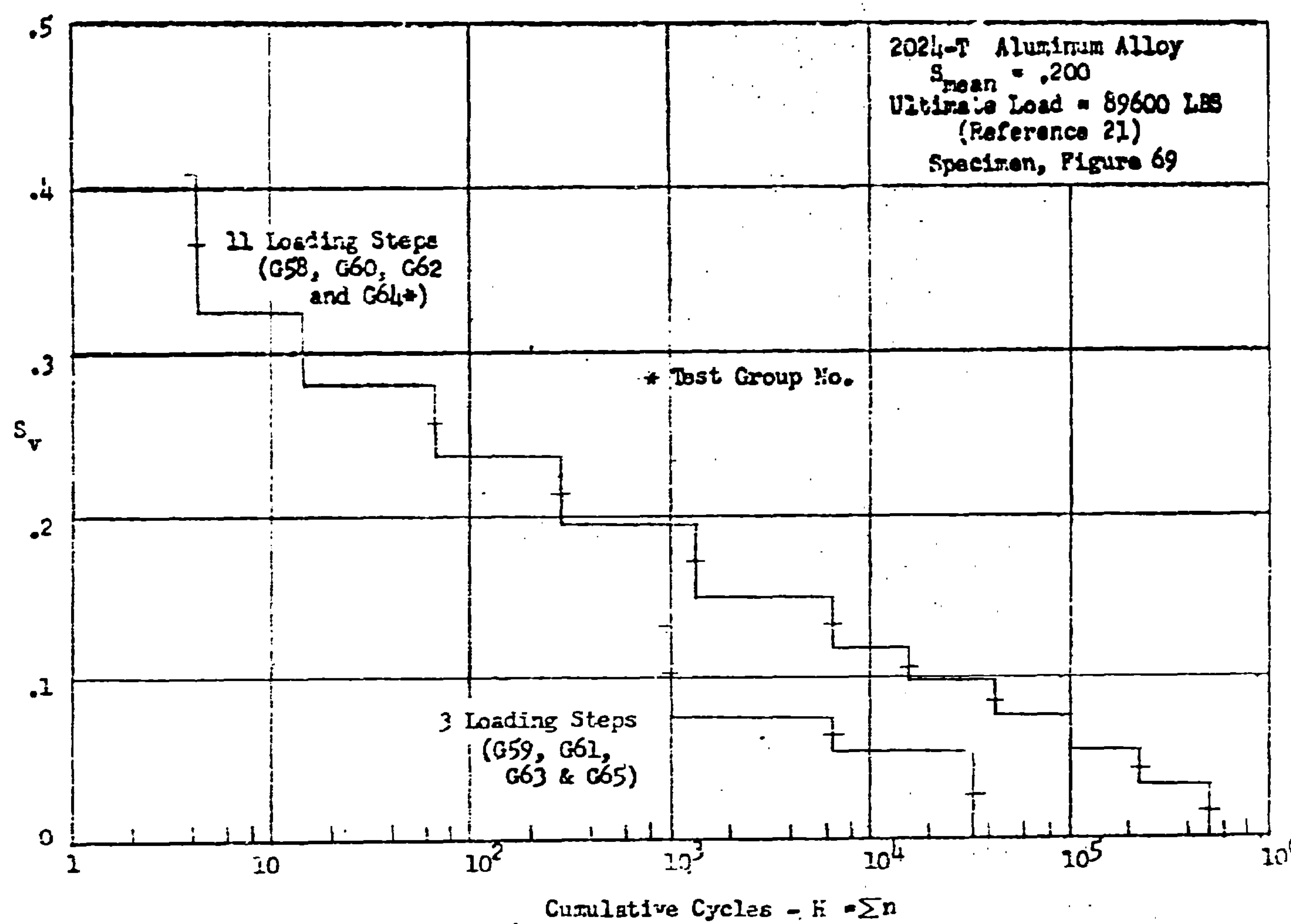

Figure 81 Unit Gust Loading Spectra for P51 Wing

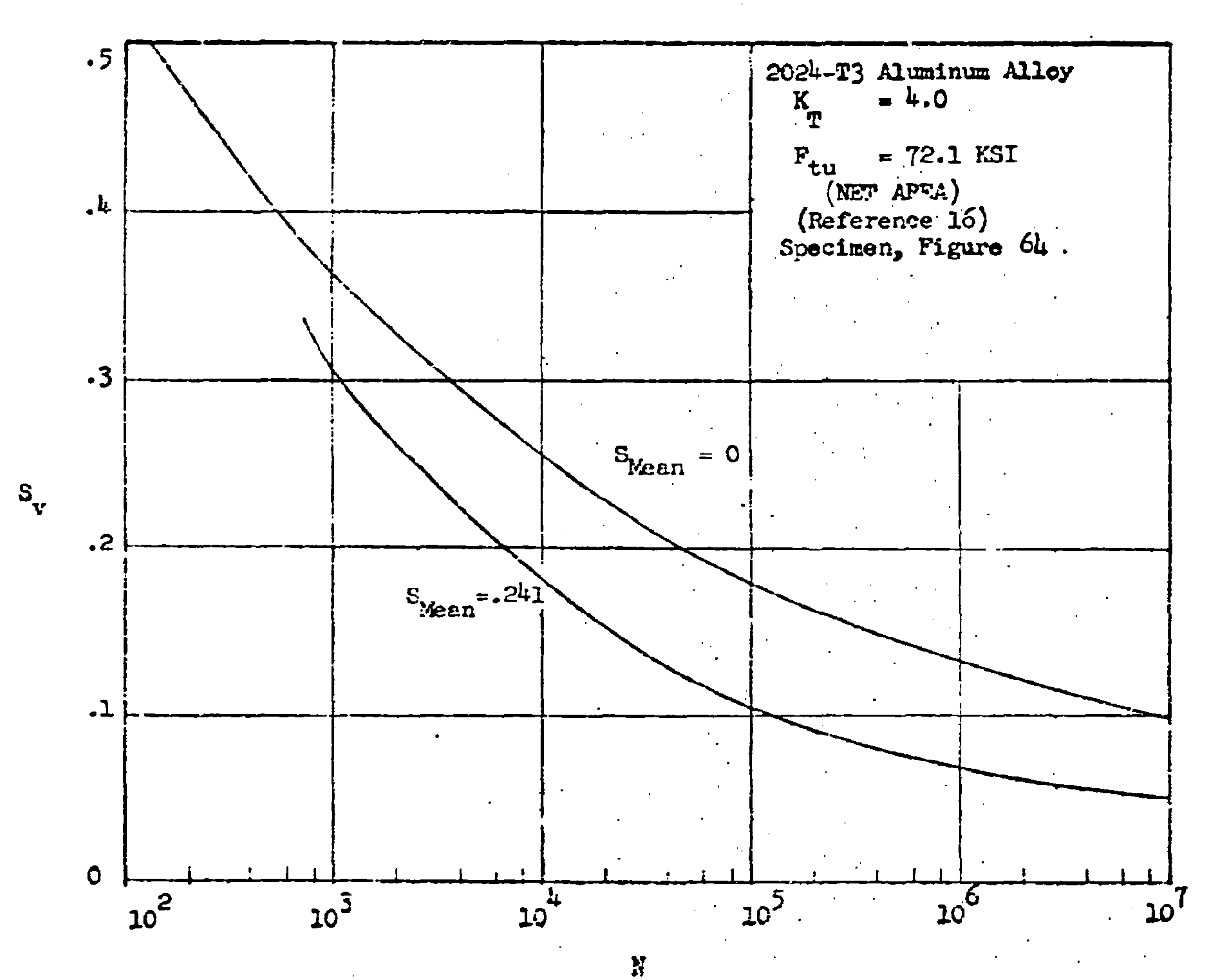

Figure 82 S-N Curves for Notched Sheet Specimens

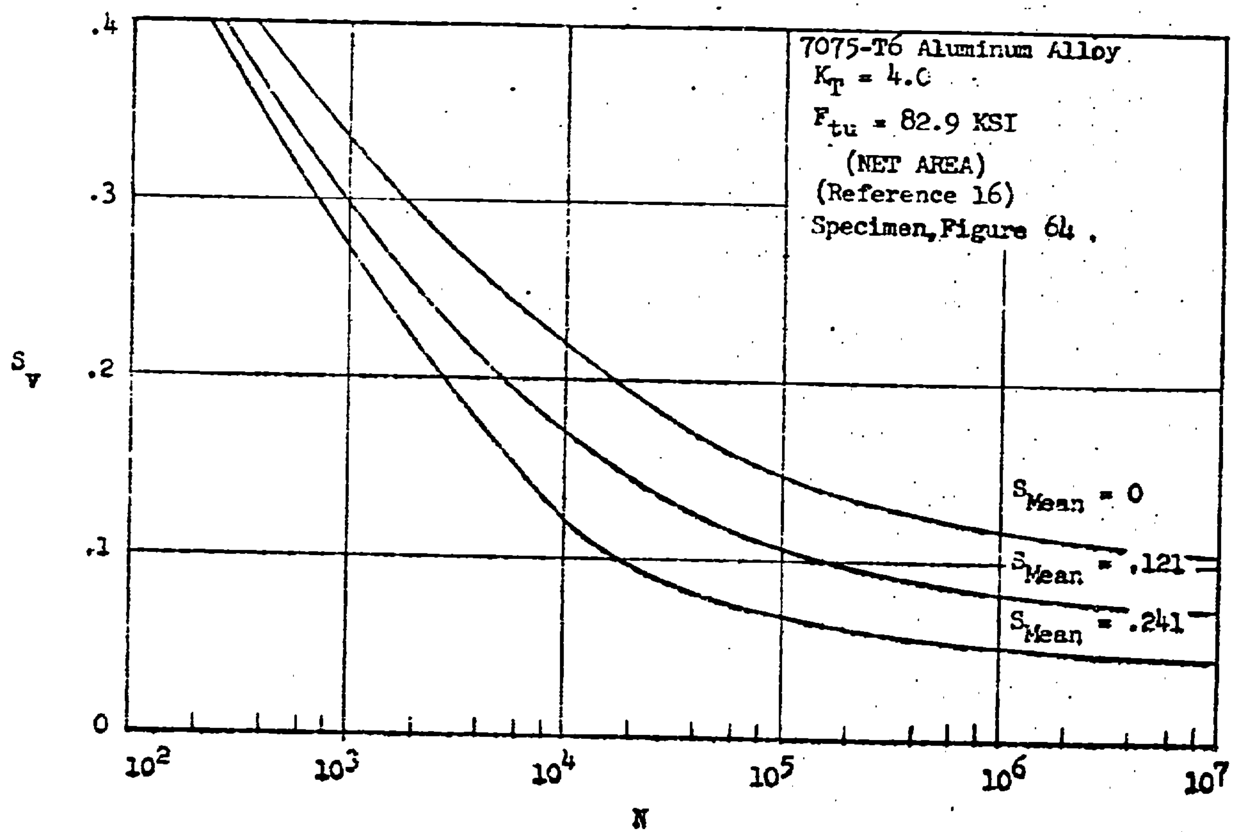

Figure 83 S-N Curves for Notched Sheet Specimens

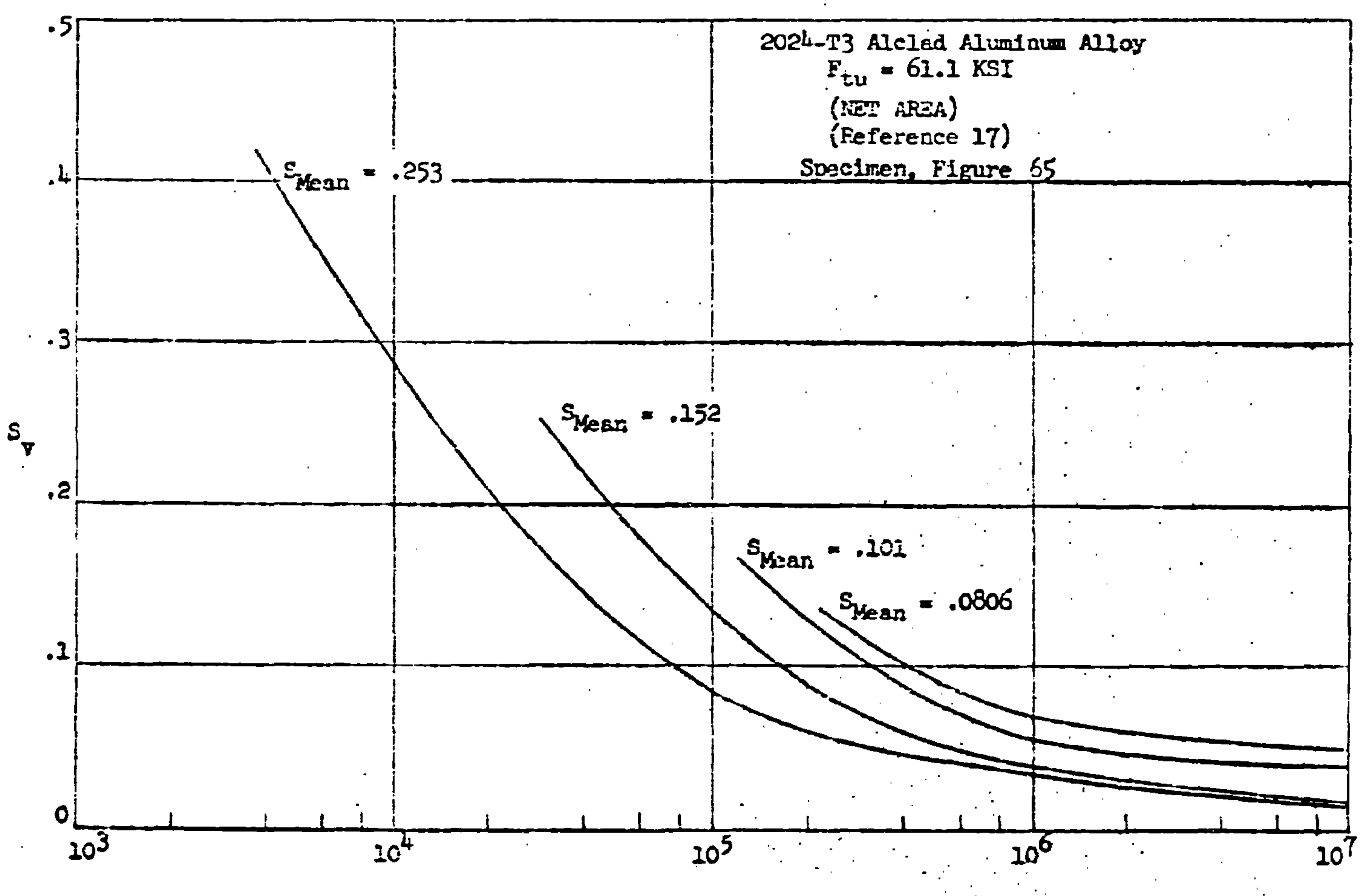

Figure 84 S-N Curves for Double Shear Riveted Joint Specimens

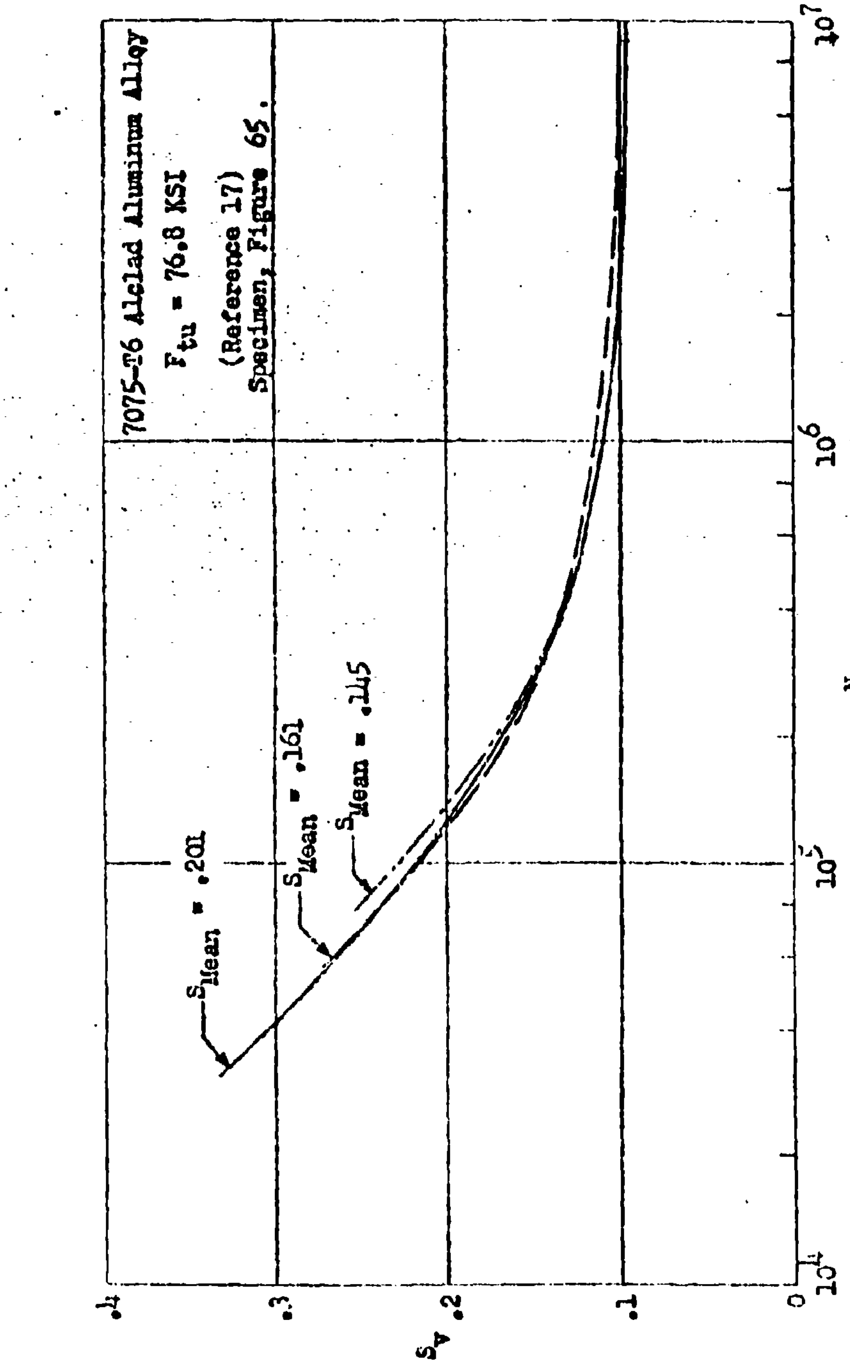

Figure 85 S-N Curves for Unnotched Sheet Specimens

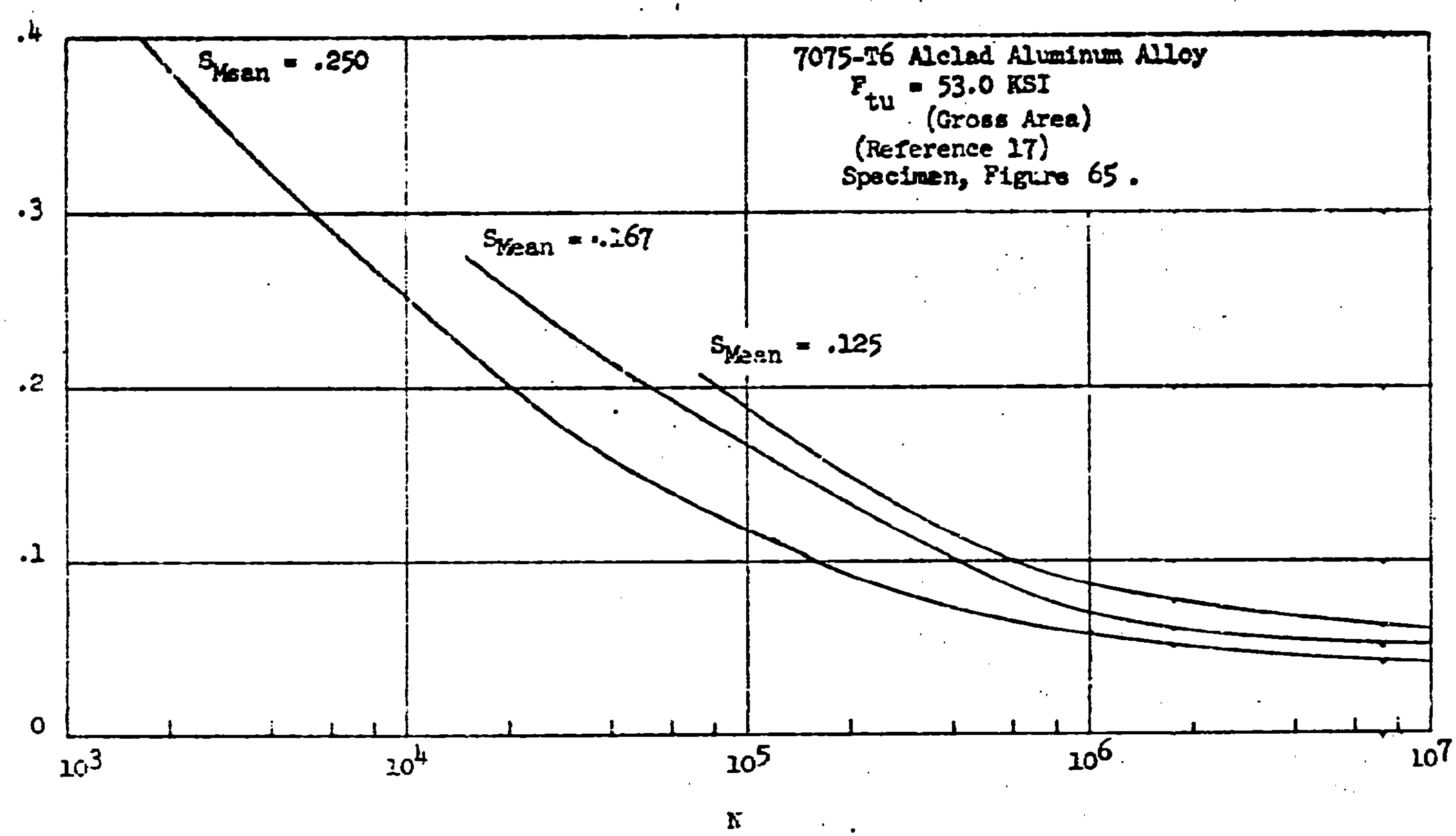

Figure 66 S-N Curves for Butt Joint Specimens

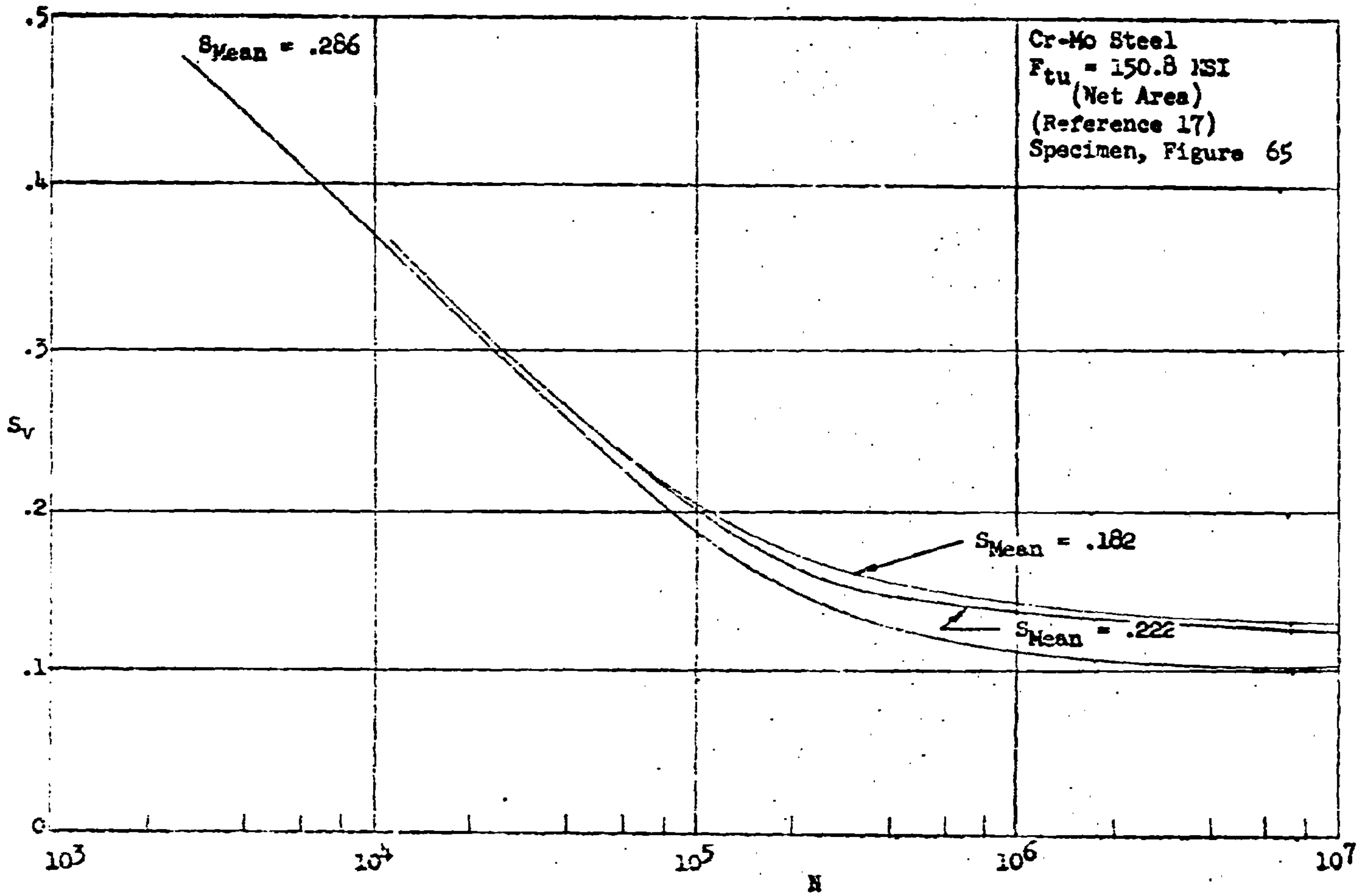

Figure 87 S-N Curves for Strip Specimens with Centrally Located Hole

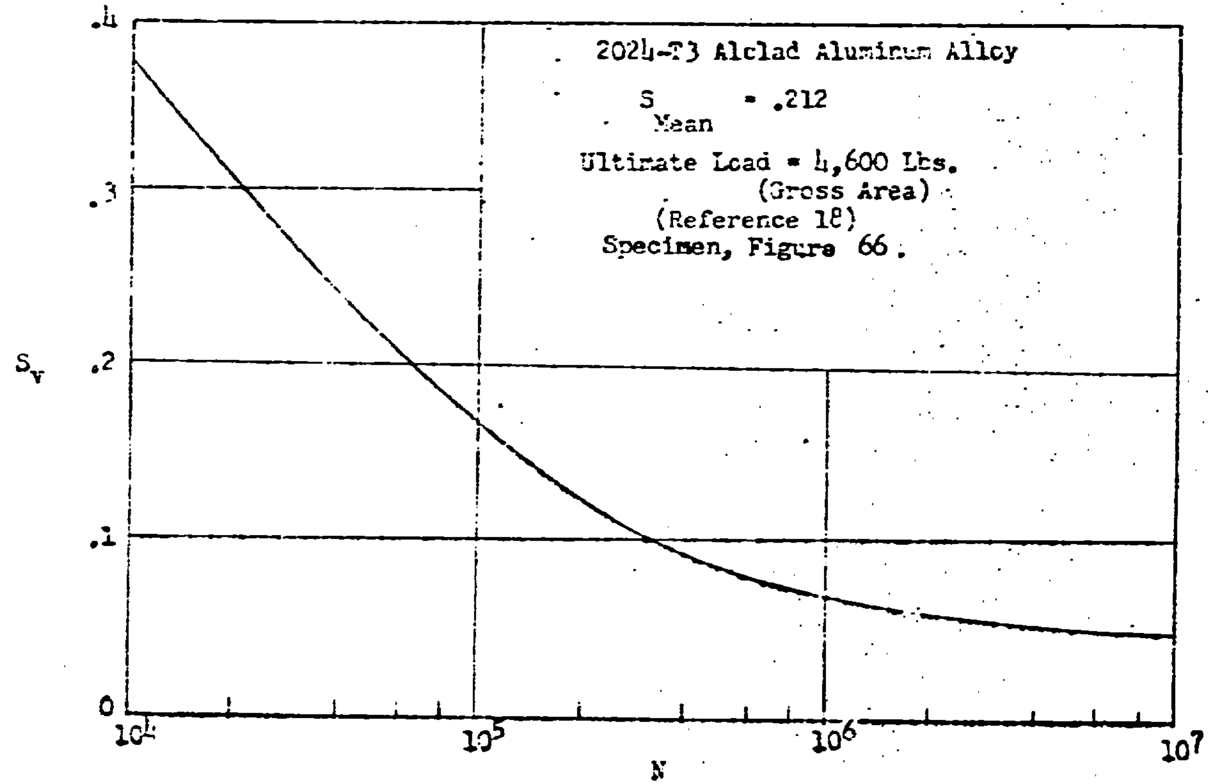

Figure 88 S-N Curve for Lap Joint Specimens with a Single Row of Flush Rivets

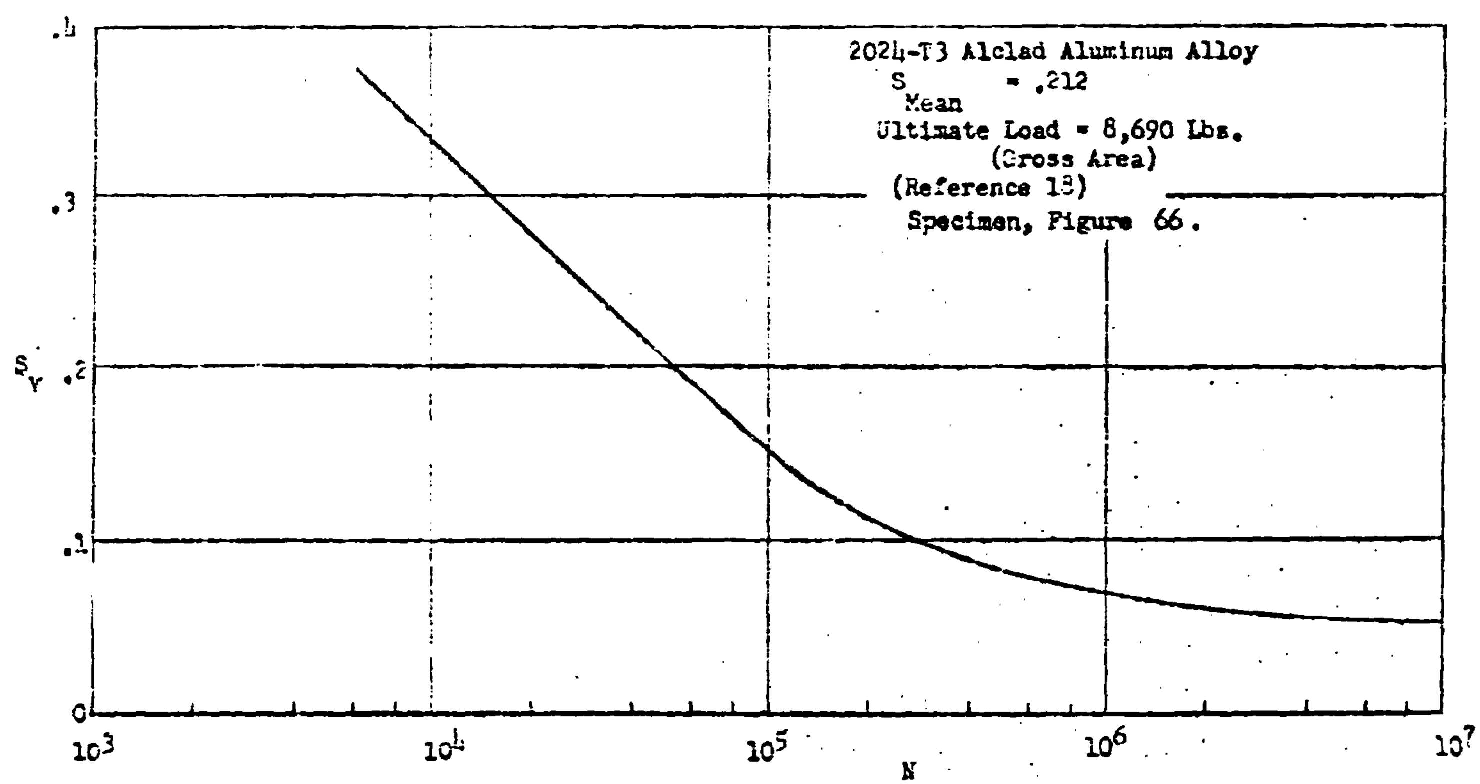

Figure 89 S-N Curve for Lap Joint Specimen with a Double Row of Flush Rivets

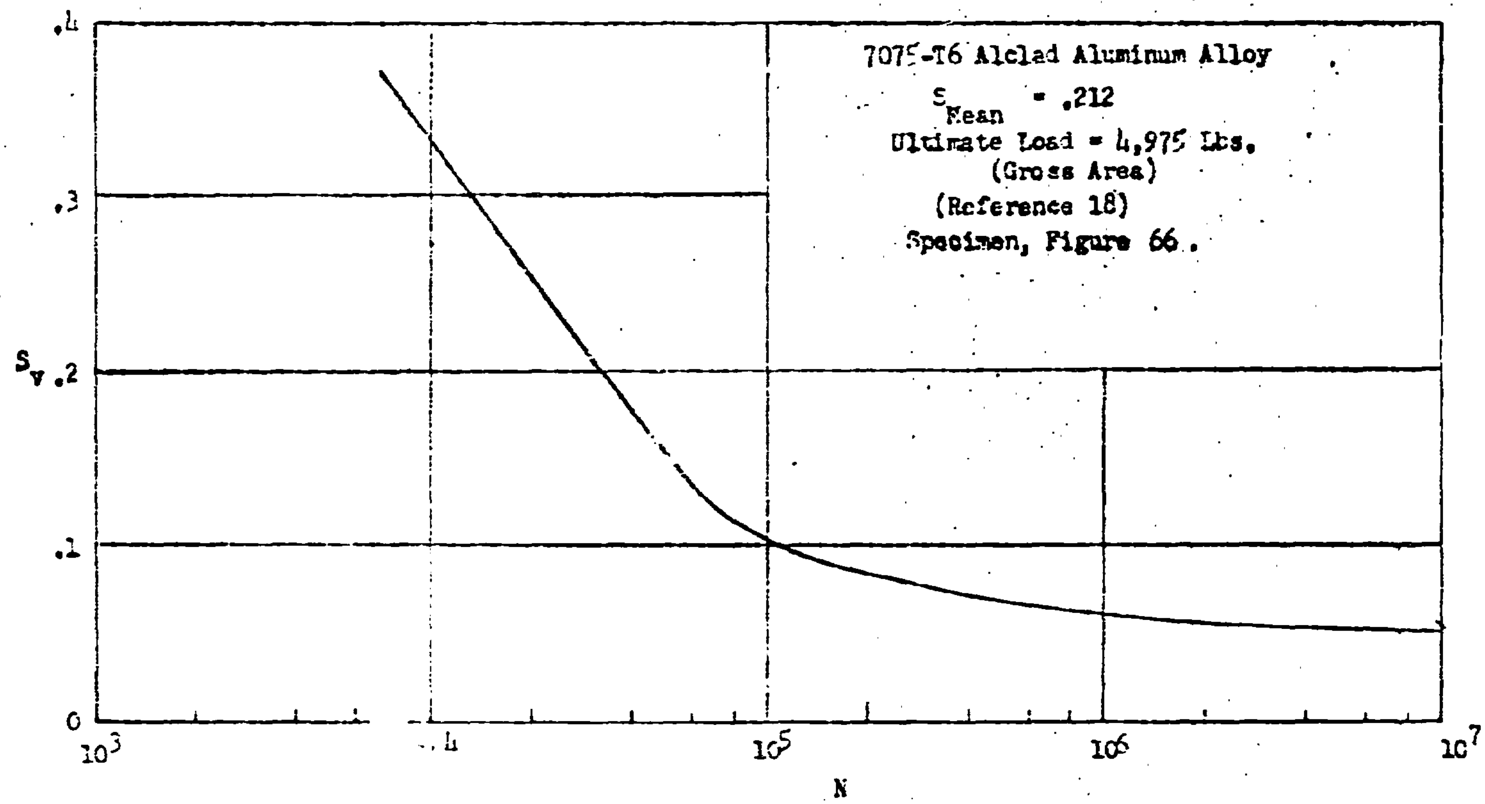

Figure 90 S-N Curve for Lap Joint Specimens with a Single Row of Flush Rivets

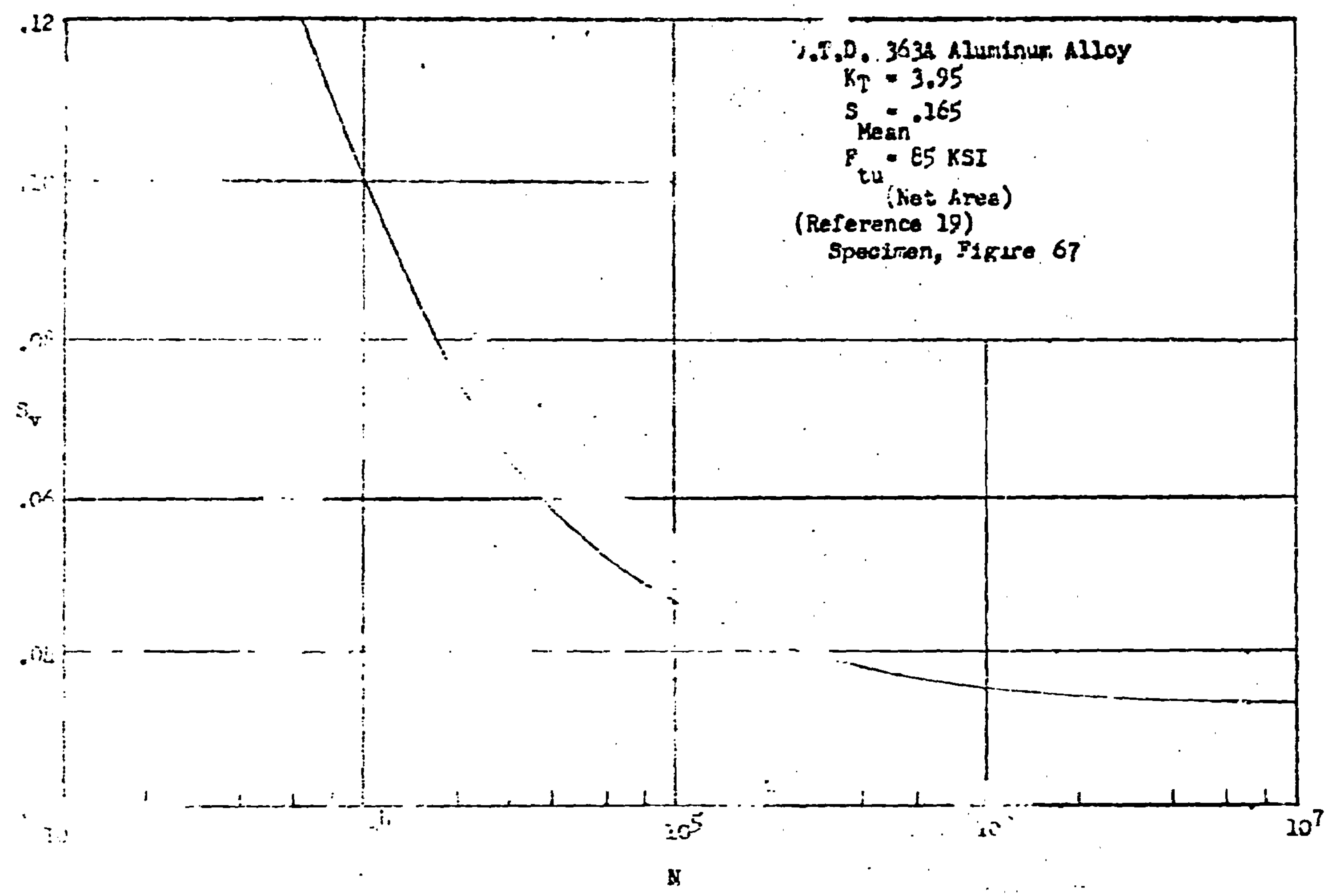

Figure S-N Curve for Notched Flate Specimens

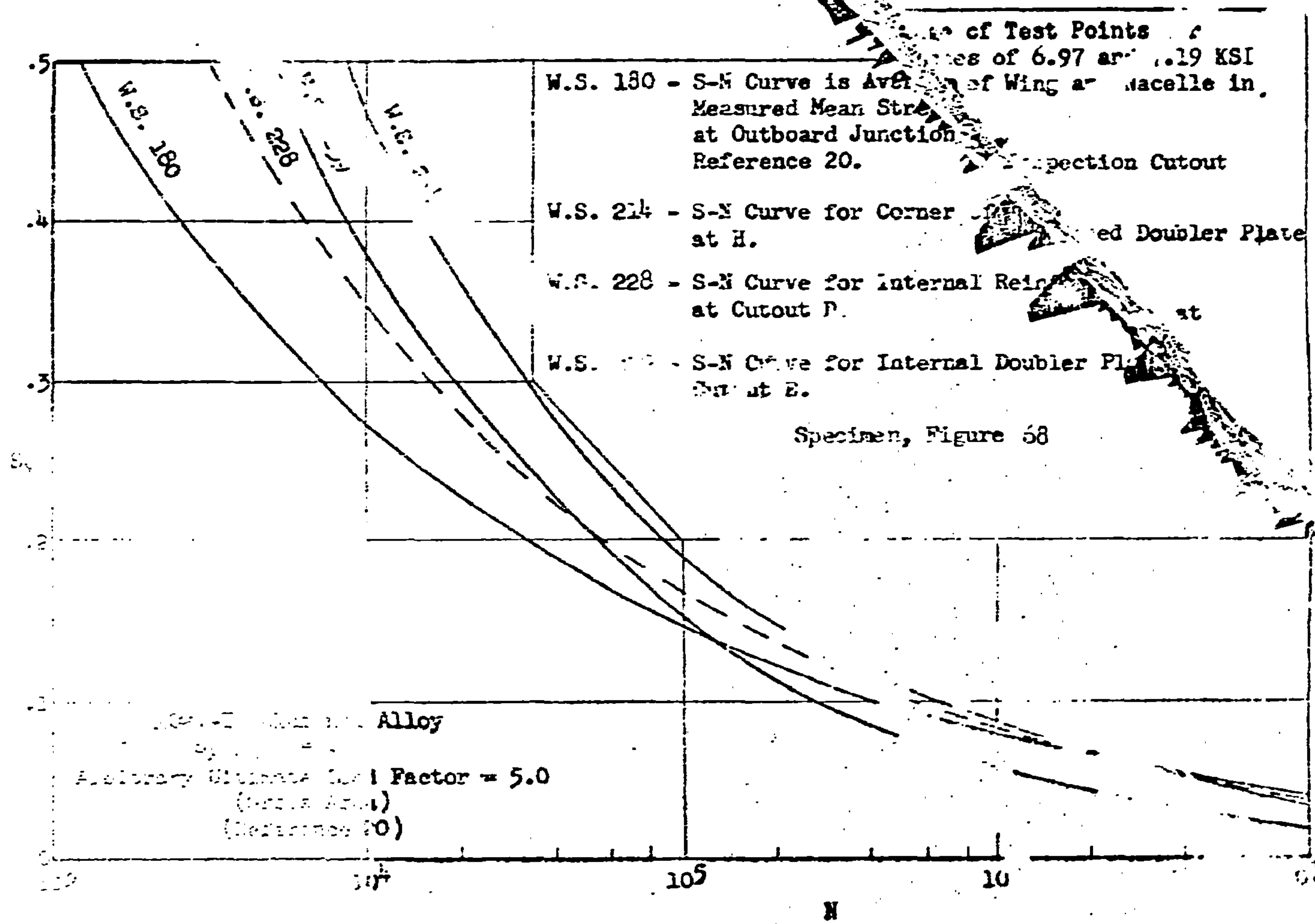

Figure S-N Curves for Wing Stations 180, 214, 228, and 239 of C.

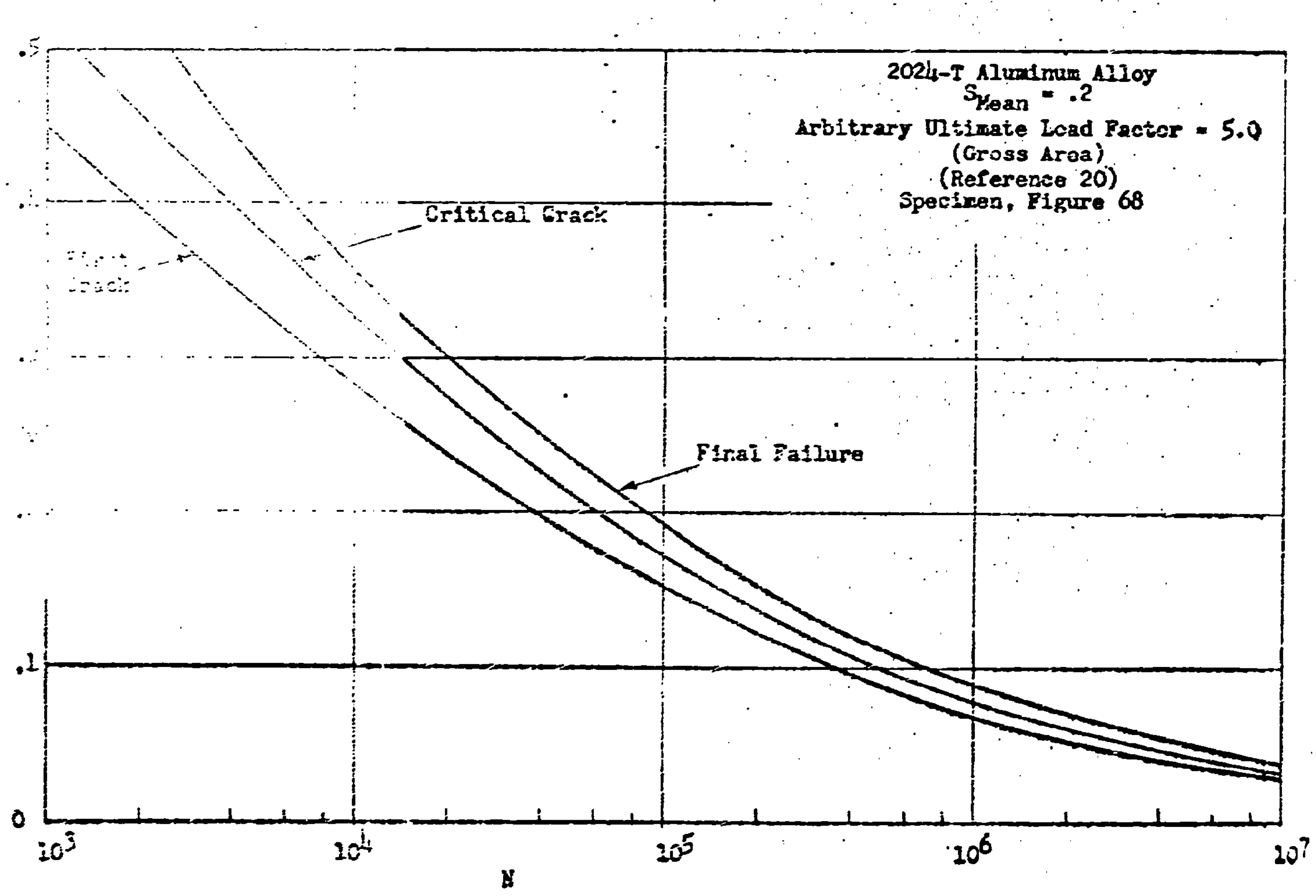

Figure 93 Average S-N Curves for Complete C-46 Wing

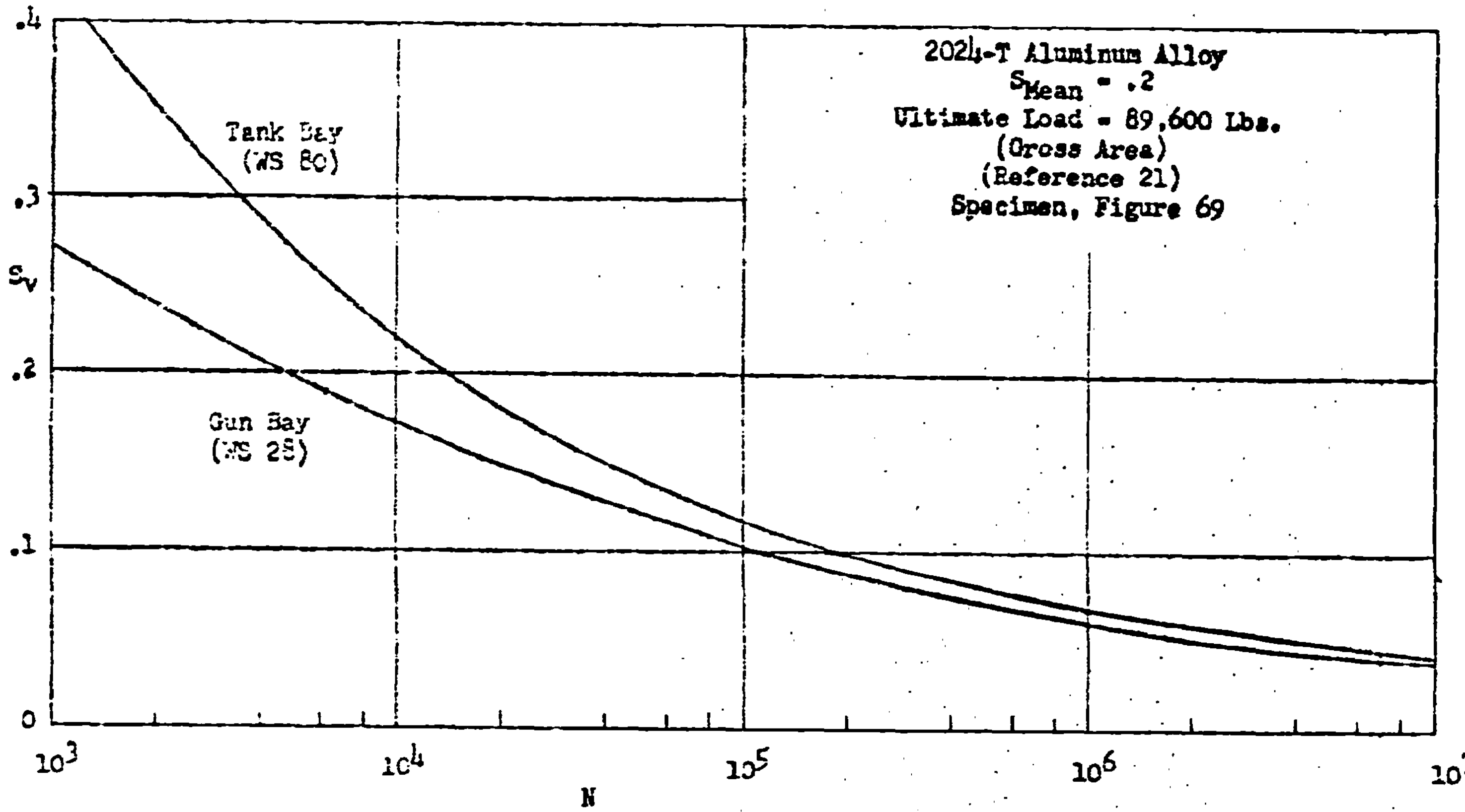

Figure 94 S-N Curves for Initial Failure of P51 Wing

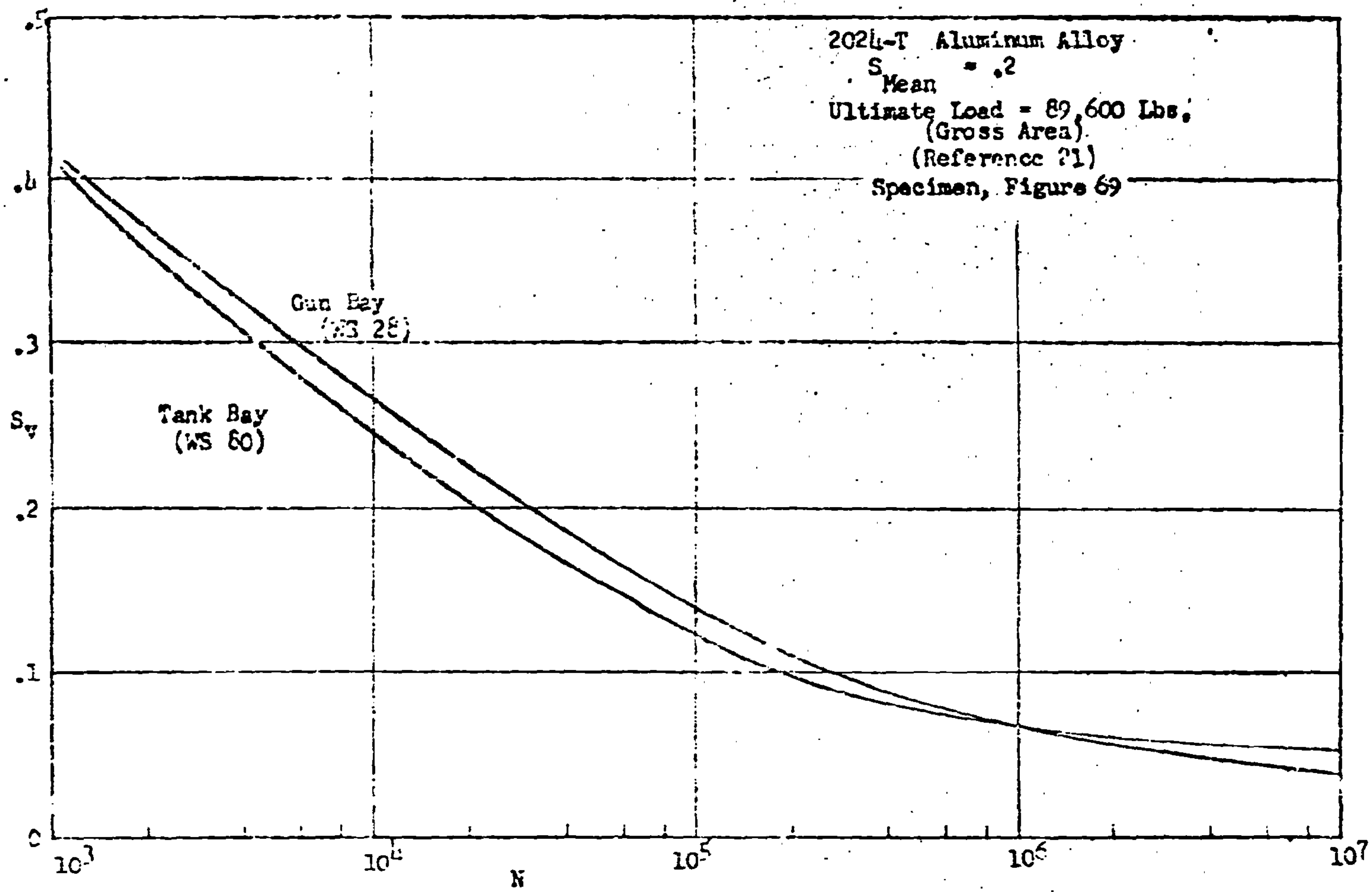

Figure 95 S-N Curves for Final Failure of P51 Wing

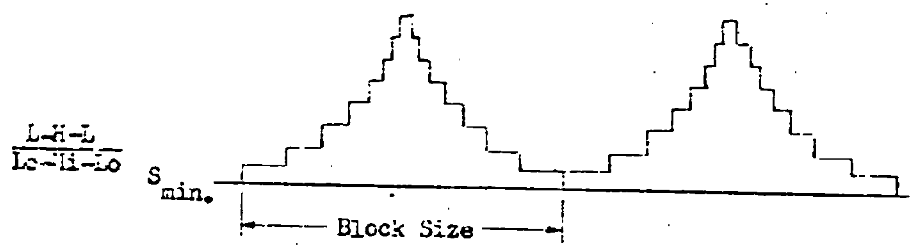

Figure 95 Schematic Diagram of Lo-Hi-Lo Maneuver Loading Sequence

TABLE 44

UNIT MANEUVER LOADING SPECTRA AND S-N DATA
FOR DOUBLE SHEAR RIVETED JOINTS
2024-T3 ALCLAD
(Reference 17)

F_{tu} = 61.1 KSI (Net Area)

Loading Step	S_{max}	S_v	n	N
		S_{min} = .0833		
1	.117	.0169	3200	-
2	.183	.0499	1800	540000
3	.250	.0833	1100	170000
4	.317	.1169	620	77000
5	.383	.1499	350	42000
6	.450	.1833	200	24000
7	.517	.2169	120	14000
8	.583	.2499	68	9300
9	.650	.2833	39	6000
		(M1*)	Σ 7497	
		S_{min} = .0625		
1	.088	.0128	3200	-
2	.138	.0378	1800	9000000
3	.188	.0628	1100	420000
4	.238	.0878	620	190000
5	.288	.1128	350	97000
6	.338	.1378	200	57000
7	.388	.1628	120	35000
8	.438	.1878	68	24000
9	.488	.2128	39	16000
		(M2)	Σ 7497	
		S_{min} = .050		
1	.070	.010	3200	-
2	.110	.030	1800	-
3	.150	.050	1100	1300000
4	.190	.070	620	400000
5	.230	.090	350	200000
6	.270	.110	200	120000
7	.310	.130	120	76000
8	.350	.150	68	50000
9	.390	.170	39	35000
		(M3)	Σ 7497	

* Test Group No.

TABLE 45

UNIT MANEUVER LOADING SPECTRA AND S-N DATA FOR UNNOTCHED SHEET
7075-T6 ALCLAD
(Reference 17)

F_{tu} = 76.8 KSI (Net Area)

Loading Step	S_{max}	S_v	n	N	S_{max}	S_v	n	N
	S_{min} = .125				S_{min} = .100			
1	.175	.025	3200	-	.140	.020	3200	-
2	.275	.075	1800	-	.220	.060	1800	-
3	.375	.125	1100	470000	.300	.100	1100	6000000
4	.475	.175	620	140000	.380	.140	620	300000
5	.575	.225	350	71000	.460	.180	350	140000
6	.675	.275	200	40000	.540	.220	200	80000
7	.775	.325	120	22000	.620	.260	120	52000
8	.875	.375	68	9000	.700	.300	68	34000
9	.975	.425	39	1300	.780	.340	39	20000
		(M4*)	Σ 7497			(M5)	Σ 7497	
	S_{min} = .0833				S_{min} = .0625			
1	.117	.0168	3200	-	.088	.0128	3200	-
2	.183	.0498	1800	-	.138	.0378	1800	-
3	.250	.0834	1100	-	.188	.0628	1100	-
4	.317	.1168	620	680000	.238	.0878	620	-
5	.383	.1498	350	230000	.288	.1128	350	850000
6	.450	.1334	200	135000	.338	.1378	200	340000
7	.517	.2168	120	86000	.388	.1628	120	200000
8	.583	.2498	68	58000	.438	.1878	68	130000
9	.650	.2834	39	41000	.488	.2128	39	92000
		(M6)	Σ 7497			(M7)	Σ 7497	

*Test Group No.

TABLE 46

UNIT MANEUVER LOADING SPECTRA AND S-N DATA FOR BUTT JOINTS
7075-T6 ALCLAD
(Reference 17)

F_{tu} = 53.0 KSI (Gross Area)

Loading Step	S_{max}	S_v	n	N
		S_{min} = .100		
1	.14	.02	3200	-
2	.22	.06	1800	2700000
3	.30	.10	1100	300000
4	.38	.14	620	71000
5	.46	.18	350	20000
6	.54	.22	200	8600
7	.62	.26	120	4200
8	.70	.30	68	2000
9	.78	.34	39	900
		(M8*)	Σ 7497	
		S_{min} = .0833		
1	.117	.0168	3200	-
2	.183	.0498	1800	-
3	.250	.0833	1100	700000
4	.317	.1168	620	190000
5	.383	.1498	350	62000
6	.450	.1833	200	21000
7	.517	.2168	120	10000
8	.583	.2498	68	5500
9	.650	.2833	39	3100
		(M9)	Σ 7497	
		S_{min} = .0625		
1	.088	.0127	3200	-
2	.138	.0377	1800	-
3	.188	.0627	1100	-
4	.238	.0877	620	750000
5	.288	.1127	350	270000
6	.338	.1377	200	120000
7	.388	.1627	120	50000
8	.438	.1877	68	23000
9	.488	.2127	39	12500
		(M10)	Σ 7497	

* Test Group No.

TABLE 47

UNIT MANEUVER LOADING SPECTRA AND S-N DATA
FOR STRIPS WITH CENTRALLY LOCATED HOLE
Cr-Mo STEEL
(Reference 17)

F_{tu} = 150.8 KSI (Net Area)

Loading Step	S_{max}	S_v	n	N
		S_{min} = .111		
1	.156	.0225	3200	-
2	.244	.0665	1800	-
3	.333	.1110	1100	-
4	.422	.1555	620	220000
5	.511	.2000	350	84000
6	.600	.2445	200	40000
7	.689	.2890	120	21000
8	.778	.3335	68	10000
9	.867	.3780	39	3800
		(M11*)	Σ 7497	
		S_{min} = .100		
1	.140	.020	3200	-
2	.220	.060	1800	-
3	.300	.100	1100	-
4	.380	.140	620	400000
5	.460	.180	350	130000
6	.540	.220	200	59000
7	.620	.260	120	32000
8	.700	.300	68	17500
9	.780	.340	39	9000
		(M12)	Σ 7497	
		S_{min} = .0833		
1	.117	.0168	3200	-
2	.183	.0498	1800	-
3	.250	.0834	1100	-
4	.317	.1168	620	-
5	.383	.1498	350	280000
6	.450	.1834	200	120000
7	.517	.2168	120	63000
8	.583	.2498	68	38000
9	.650	.2834	39	23000
		(M13)	Σ 7497	

* Test Group No.

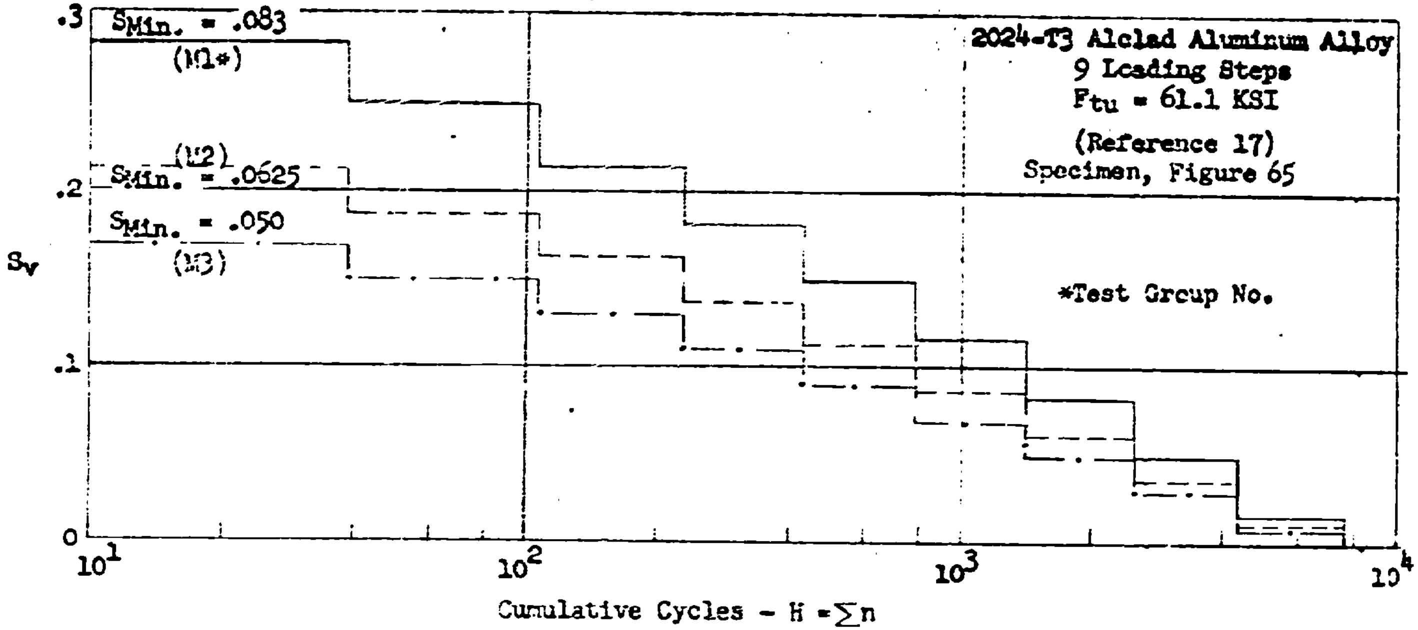

Figure 97 Unit Maneuver Loading Spectra for Double Shear Riveted Joint Specimens.

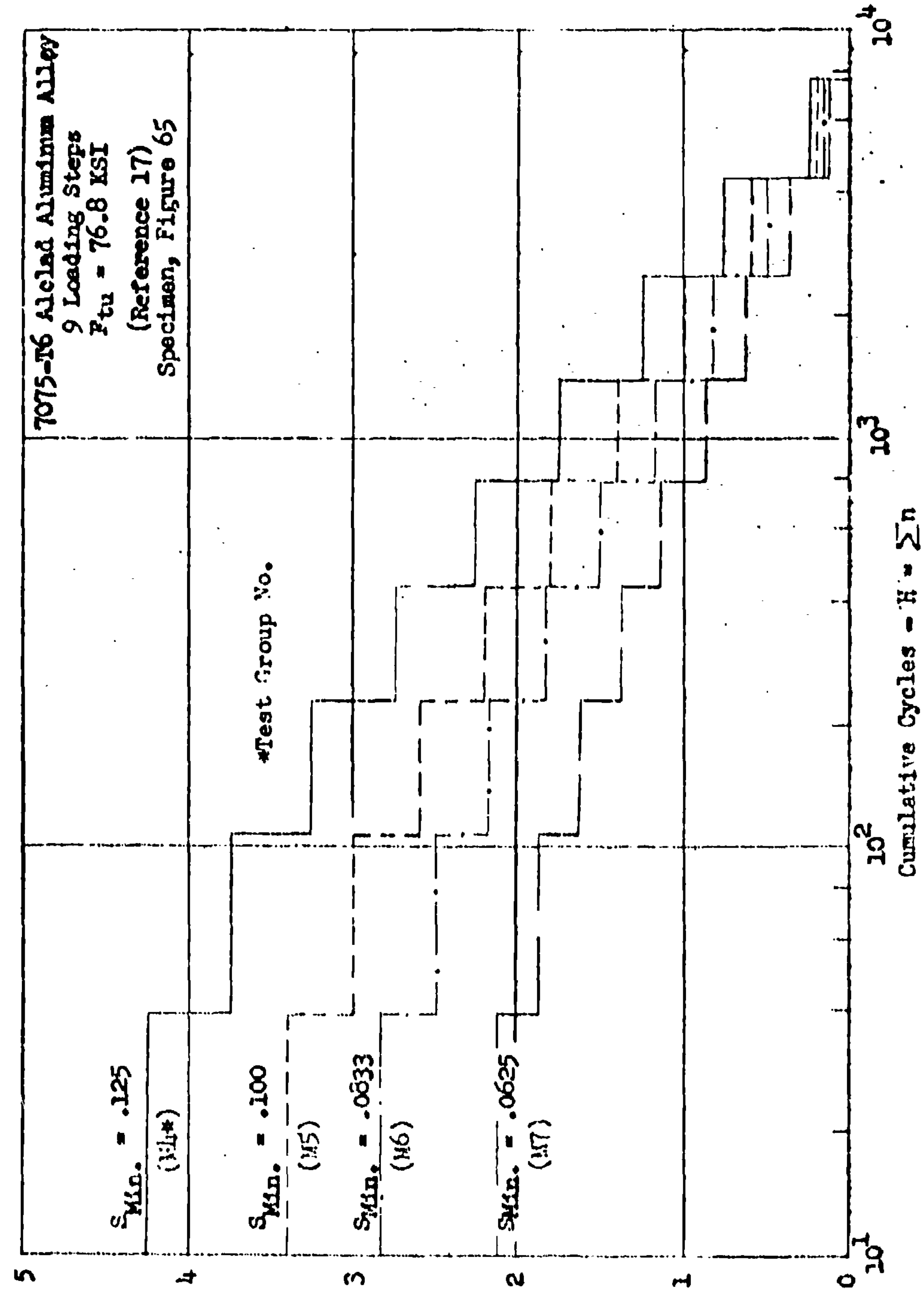

Figure 98 Unit Maneuver Loading Spectra for Unnotched Sheet Specimens.

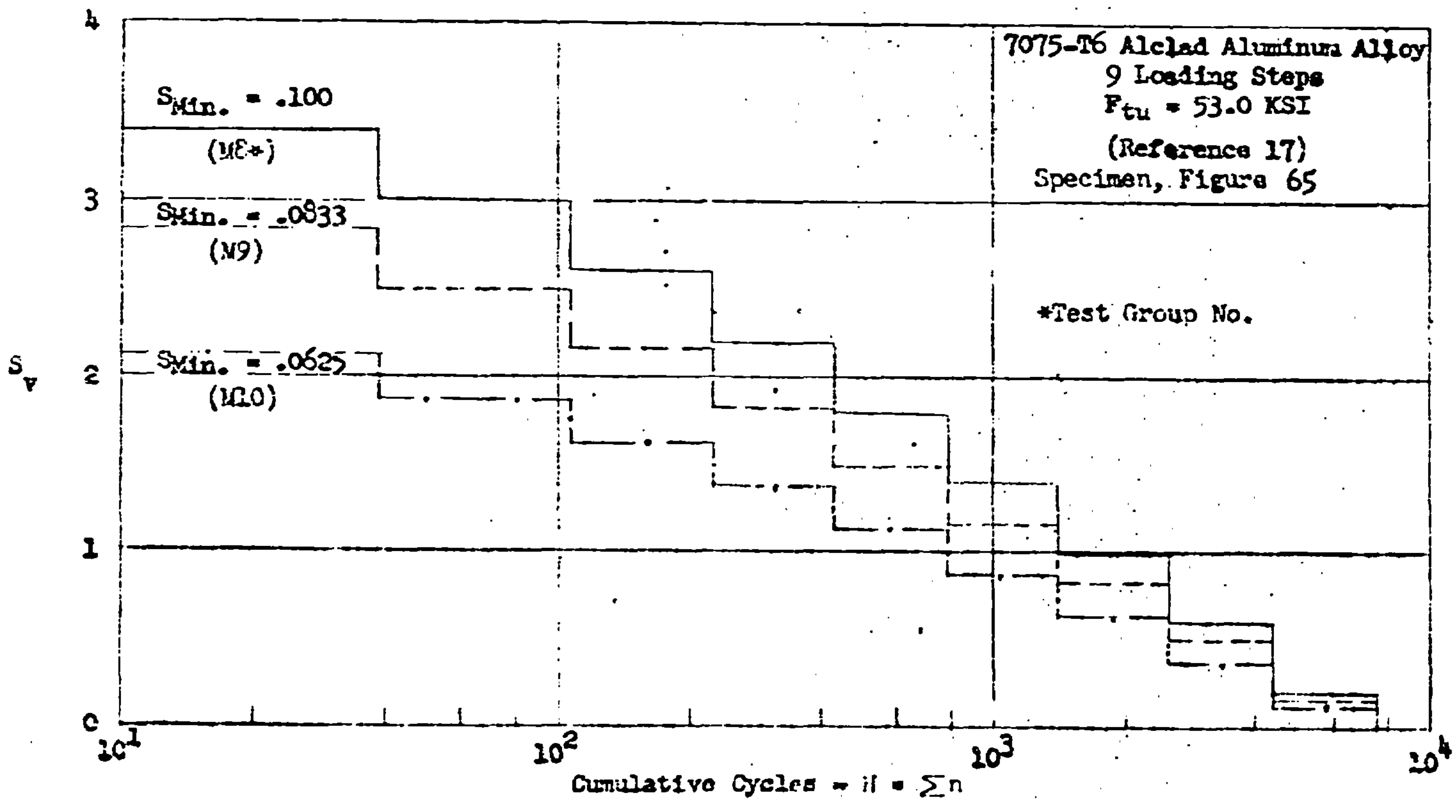

Figure 99 Unit Maneuver Loading Spectra for Butt Joint Specimens.

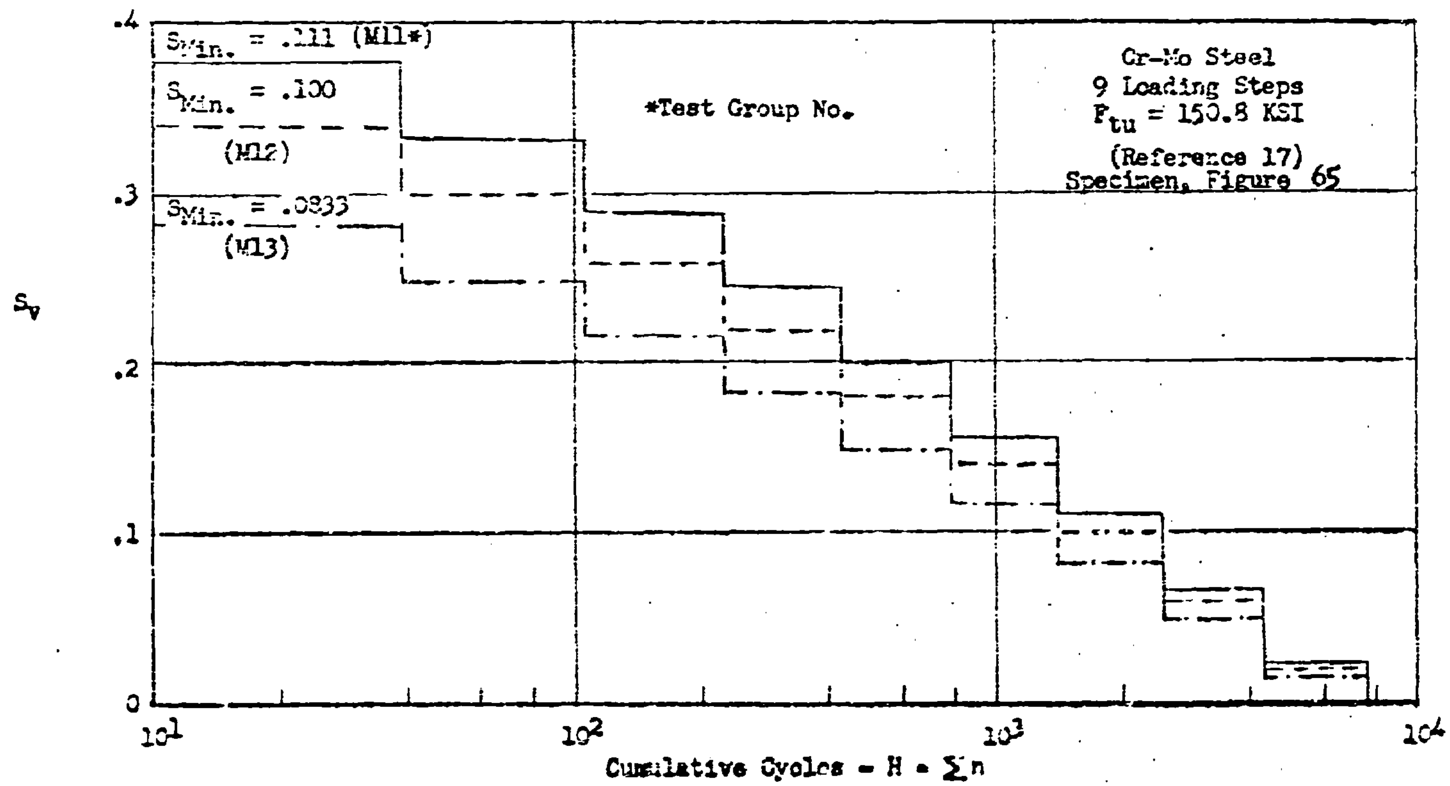

Figure 100 Unit Maneuver Loading Spectra for Strip Specimens with a Centrally Located Hole.

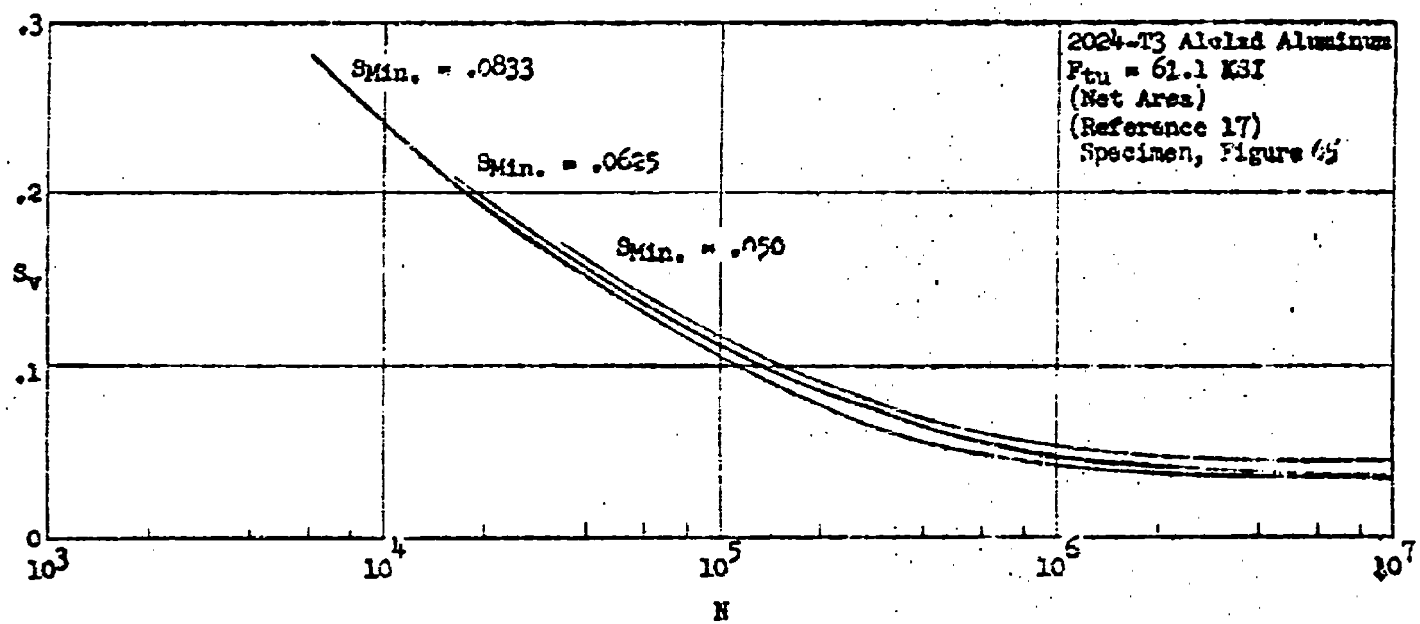

Figure 101. S-N Curves for Double Shear Riveted Joint Specimens. Constant Minimum Stress. (For Maneuver Type Loading)

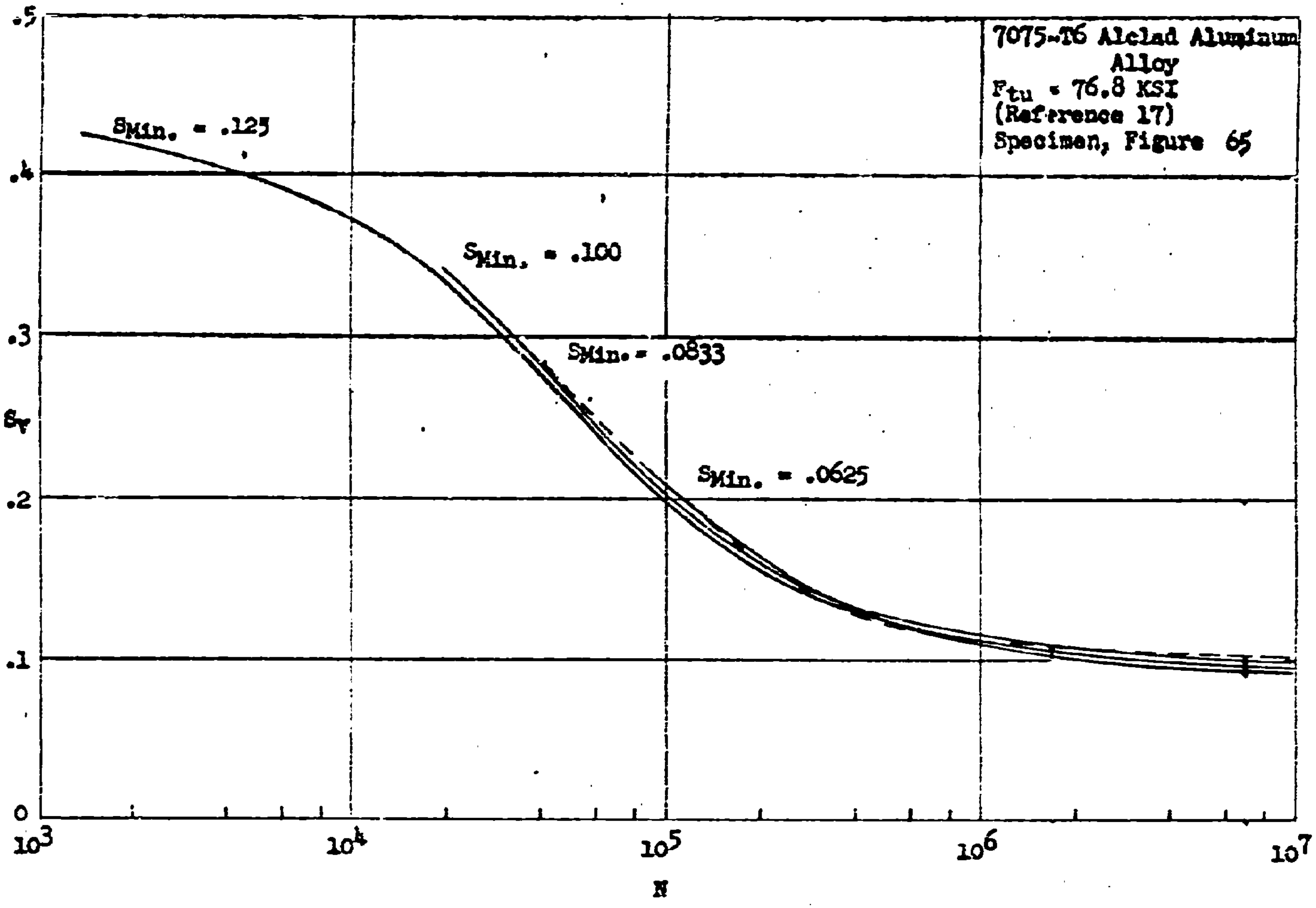

Figure 102 S-N Curves for Unnotched Sheet Specimens. Constant Minimum Stress. (For Maneuver Type Loading)

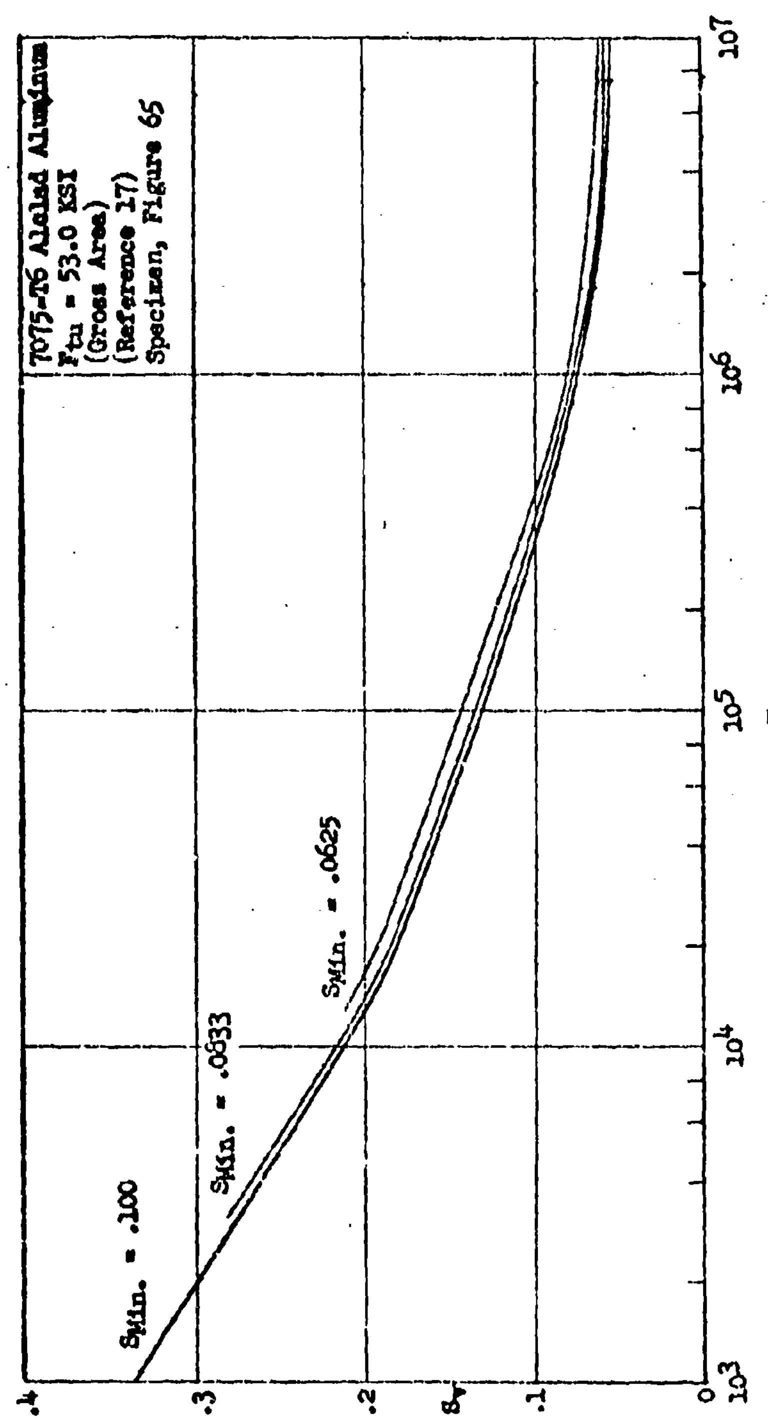

Figure 103 S-N Curves for Butt Joint Specimens. Constant Minimum Stress. (For Maneuver Type Loading)

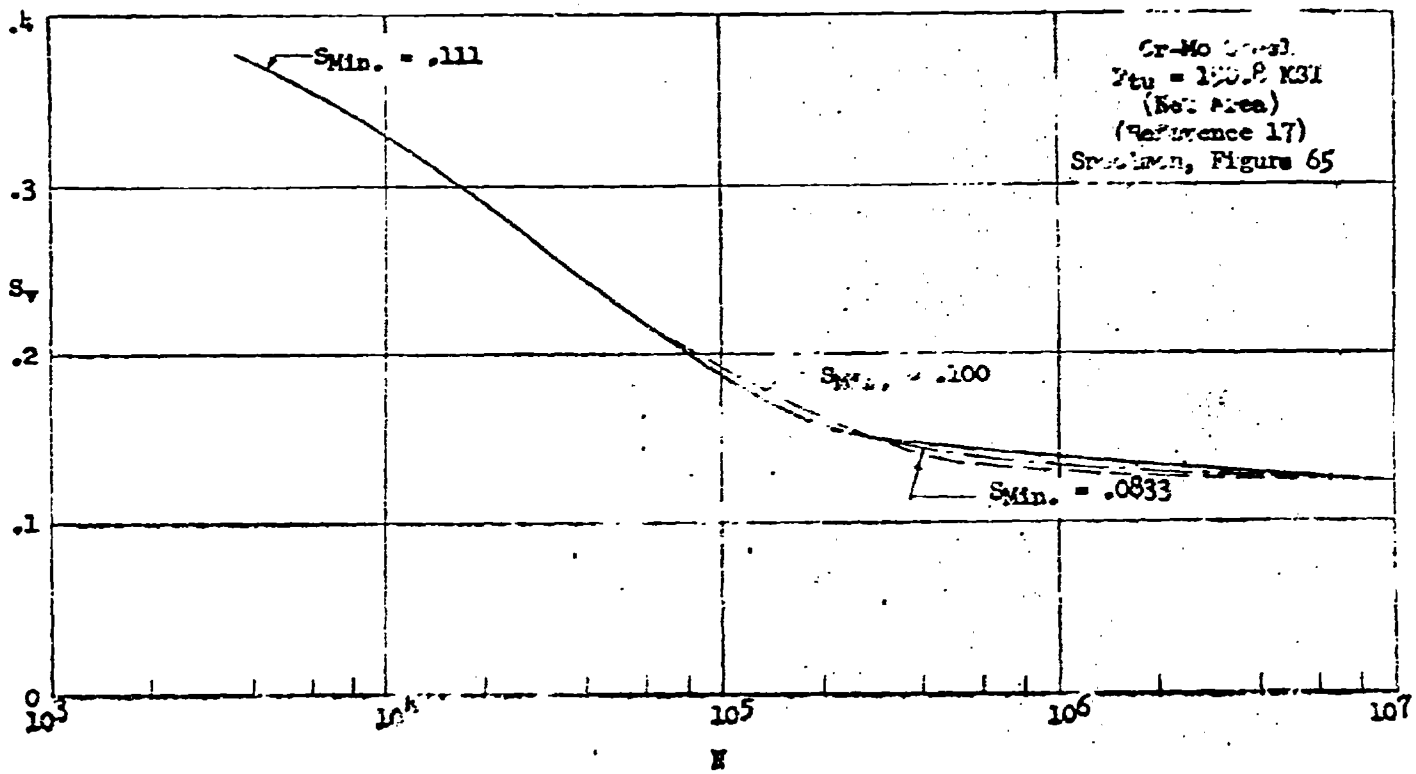

Figure 64 S-N Curves for Strip Specimens with Centrally Located Hole.
Constant Minimum Stress. (For Maneuver Type Loading)

TABLE 48

EXPERIMENTAL FATIGUE LIVES FOR GUST LOADING SPECTRA

(Table is Continued on Next Two Pages)

Test Group No.	Material	Specimen	S_{Mean}	Number of Loading Steps	Type of Spectrum Curve	Sequence	Block Size	Number of Specimens	Test Life (10^6 Cycles) Minimum	Maximum	Geometric Mean	Ref.
G1	2024-T3	Notched Sheet	.241	18	Gust 5	Lo-Hi	[illegible]	3	8.000	8.100	8.049	
G2						Lo-Hi	[illegible]	9	2.500	5.000	3.872	
G3						Hi-Lo	[illegible]	3	7.410	17.700	11.888	
G4						Hi-Lo	[illegible]	6	8.506	26.036	14.555	
G5					Gust B	CR	500000	8	3.654	10.143	6.938	
G6				18	Gust A	[illegible]	100000	4	1.403	2.501	1.824	
G7				8		Lo-Hi	100200	3	.501	.701	.595	
G8						Hi-Lo	100200	3	2.007	2.609	2.294	
G9						Lo-Hi-Lo		3	1.454	1.854	1.612	
G10						Hi-Lo-Hi	100200	3	1.376	1.756	1.519	
G11						CR	50100	3	1.704	2.253	2.020	
G12			.241				100200	4	.903	[illegible]	1.215	
G13			0				50000	6	.350	[illegible]	.479	
G14	2024-T3		0			CR	100000	3	.302	[illegible]	.364	16
G15	7075-T6		.241			Lo-Hi	10200	3	.377	[illegible]	.443	
G16						Lo-Hi	50900	4	.356	[illegible]	.452	
G17						Hi-Lo	50900	4	1.121	1.527	1.268	
G18						Lo-Hi-Lo	10200	4	.509	1.013	.762	
G19						Hi-Lo-Hi	50900	4	.866	1.069	.976	
G20						CR	10200	3	.590	.736	.661	
G21			.241			CR	50900	4	.458	.712	.600	
G22			.121			Lo-Hi-Lo	30200	3	.297	.468	.385	
G23			.121			CR	30200	6	.211	.400	.282	
G24			0			Lo-Hi	30000	6	.180	.510	.255	
G25						Hi-Lo		5	.390	.600	.496	
G26		Notched				Lo-Hi-Lo		3	.405	.615	.498	
G27	7075-T6	Sheet	0	8	Gust A	CR	30000	6	.210	.775	.394	

TABLE 48
(Table is completed on next page.)

Test Group No.	Material	Type of Specimen	S_{Mean}	Number of Loading Steps	Sequence	Block Size	Number of Specimens	Test Life (10^6 Cycles) Minimum	Maximum	Geometric Mean	Ref.
G28		Double	.253	9	Lo-Hi-Lo	360280	2	.324	.522	.411	
G29	2024-T3	Shear	.152				3	3.260	5.980	4.788	
G30	Alclad	Riveted	.101				3	13.690	27.400	21.732	
G31		Joints	.081				2	62.400	270.000	129.700	
G32		Unnotched	.201				2	24.100	27.400	25.710	
G33		Sheet	.161				2	58.700	98.000	75.875	
G34	7075-T6		.145				2	127.000	181.000	151.966	17
	Alclad										
G35		Butt	.250				4	2.050	4.030	2.994	
G36		Joints	.167				2	27.000	28.100	27.558	
G37			.125				2	72.700	140.000	100.956	
G38		Strips	.286				2	3.310	4.970	4.060	
G39	Cr-Mo	w/hole	.222				2	12.100	26.600	17.902	
	Steel										
G40			.182	9	Lo-Hi-Lo	360280	3	45.000	63.000	50.367	
G41		(a)	.212	6	Lo-Hi-(c)	1599000	1			1.599	
G42	2024-T3			6	Hi-Lo-(c)	2279000	1			2.279	
G43	Alclad			6		2848000	1			2.848	
G44				5		457700	1			.458	18
G45		(b)		5		164400	1			.164	
G46	7075-T6			5	Hi-Lo (c)	92900	1			.093	
G47	Alclad	(a)	.212	6	Lo-Hi (c)	1228000	1			1.228	
	D.T.D.										
G48	363A	Notched	.165	9	Lo-Hi-Lo	13290	6	.093	.279	.133	
G49	Aluminum	Plate	.165	9	Lo-Hi-Lo	6290	6	.088	.145	.122	19
G50	Alloy		.165	10	Lo-Hi-Lo	5410	5	.032	.282	.074	

(a) lap joint with one row of flush rivets
(b) lap joint with two rows of flush rivets
(c) sequence applied only once

TABLE 48

(Concluding Page of Table)

Test Group No.	Material		Type of Specimen	S_{Mean}	Number of Loading Steps	Sequence	Block Size	Number of Specimens	Test Life (10^6 Cycles) Minimum	Maximum	Geometric Mean	Ref.
G51	2024-T	C-46 Wing	WS 180	.20	16	QR	59670	4	.970	8.314	4.179	
G52		C-46 Wing	WS 214					6	3.487	8.712	4.453	
G53		C-46 Wing	WS 228					5	.354	7.459	2.307	
G54		C-46 Wing	WS 239					5	1.253	3.879	2.070	20
G55		C-46 Wing	(d)					6	.354	2.507	1.252	
G56		C-46 Wing	(e)					6	1.418	6.906	3.344	
G57		C-46 Wing	(f)		16	QR	59670	6	7.160	13.100	9.656	
G58		P51 Wing	Gun Bay		11	TR	500000	3	.276	.596	.417	
G59		P51 Wing	Initial Failure		3	Lo-Hi-Lo	32860	4	.240	1.120	.557	
G60		P51 Wing	Tank Bay		11	TR	500000	2	1.260	1.835	1.521	
G61		P51 Wing	Initial Failure		3	Lo-Hi-Lo	32860	7	.669	1.470	.953	21
G62		P51 Wing	Gun Bay		11	TR	500000	4	2.025	3.150	2.520	
G63		P51 Wing	Final Failure		3	Lo-Hi-Lo	32860	3	.990	2.300	1.495	
G64		P51 Wing	Tank Bay		11	TR	500000	2	1.782	2.280	2.017	
G65	2024-T	P51 Wing	Final Failure	.20	3	Lo-Hi-Lo	32860	5	.774	1.935	1.039	

(d) first crack initiated in complete wing
(e) Initiation of critical crack that propagated to failure when loading continued
(f) final failure of complete wing

TABLE 49

EXPERIMENTAL FATIGUE LIVES FOR MANEUVER LOADING SPECTRA

(Reference 17)

Test Group No.	Material	Type of Specimen	S_{min}	Number of Loading Steps	Sequence	Block Size	Number of Specimens	Test Life (10^6 Cycles) Min.	Max.	Geometric Mean
M1	2024-T3 Alclad	Double Shear Riveted Joint	.0833	9	Lo-Hi-Lo	7497	2	.252	.334	.308
M2			.0625				2	.465	.532	.499
M3			.050				2	.825	.990	.903
M4	7075-T6 Alclad	Unnotched Sheet	.125				2	.206	.206	.206
M5			.100				2	.645	.787	.716
M6			.0833				3	.630	1.120	.903
M7			.0625				2	1.454	3.359	2.219
M8		Butt Joint	.100				2	.066	.071	.069
M9			.0833				2	.190	.243	.214
M10			.0625				2	1.095	1.994	1.477
M11	Cr-Mo Steel	Strip w/hole	.111				2	.168	.208	.198
M12			.100				2	.352	.389	.370
M13			.0833	9	Lo-Hi-Lo	7497	2	1.042	1.042	1.042

APPENDIX D

ORIGINAL TEST RESULTS

This appendix presents a description of the test equipment, descriptions of the test specimens, and tabulation and graphical results of the experimental work completed in this program. Also included is the statistical analysis of the constant amplitude coupon S-N data. These data are presented in three part

Part 1. Constant amplitude axial load S-N data from simple coupons.

- Statistical analysis of constant amplitude S-N data.
- Experimental S-N data.
- Construction of S-N Curves by interpolation.

Part 2. Spectral Axial load data from simple coupons.

- Description of equipment and procedures for obtaining experimental data on coupon specimens.
- Unit Loading Spectra
- Experimental Lives
- Test Histories

Part 3. Fatigue Test Results of a Complex Specimen

- Specimen Description
- Test Set-up
- Test Results

APPENDIX D

PART 1 - CONSTANT AMPLITUDE AXIAL LOAD S-N DATA FROM SIMPLE COUPONS

Statistical Analysis of Constant Amplitude S-N Data

The multiple variables and the limited number of individual test specimens per test condition (five coupons each) led to the use of special statistical methods for small samples. The method of linear regression was chosen to analyze the results of the constant amplitude S-N test data. This method has been suggested by Weibull in reference 33, as well as by other investigators. It considers the frequency distribution of log $(S_T - S_E)$ when log N is held constant. While Figure 105 shows that this method can lead to an approximately normal distribution, the small sample size for each combination of stress concentration factor K_T and mean stress f_{mean} in Table 50 does not always make it possible to arrive at statistically significant conclusions with a high degree of confidence.

TABLE 50

TEST CONFIGURATIONS FOR S-N DATA

K_T	f_{mean}, gross area, KSI				
	-10	-5	0	10	15
3	X	X		X	X
4	X	X	X	X	X
7	X	X	X	X	X
10	X	X		X	X

The eighteen test configurations listed comprise the 450 specimens in Table 52. Twenty-five specimens were tested for each combination of K_T and f_{mean}, with five of these specimens being tested at each of five convenient varying stress levels, which did not exceed 25 KSI. Some additional test configurations are given in Table 53 which were not statistically analyzed.

In Weibull's use of the method of linear regression with small sample size, the ($n = 5 \times 5$) or twenty-five specimens are pooled and the following S-N function is assumed (reference 33).

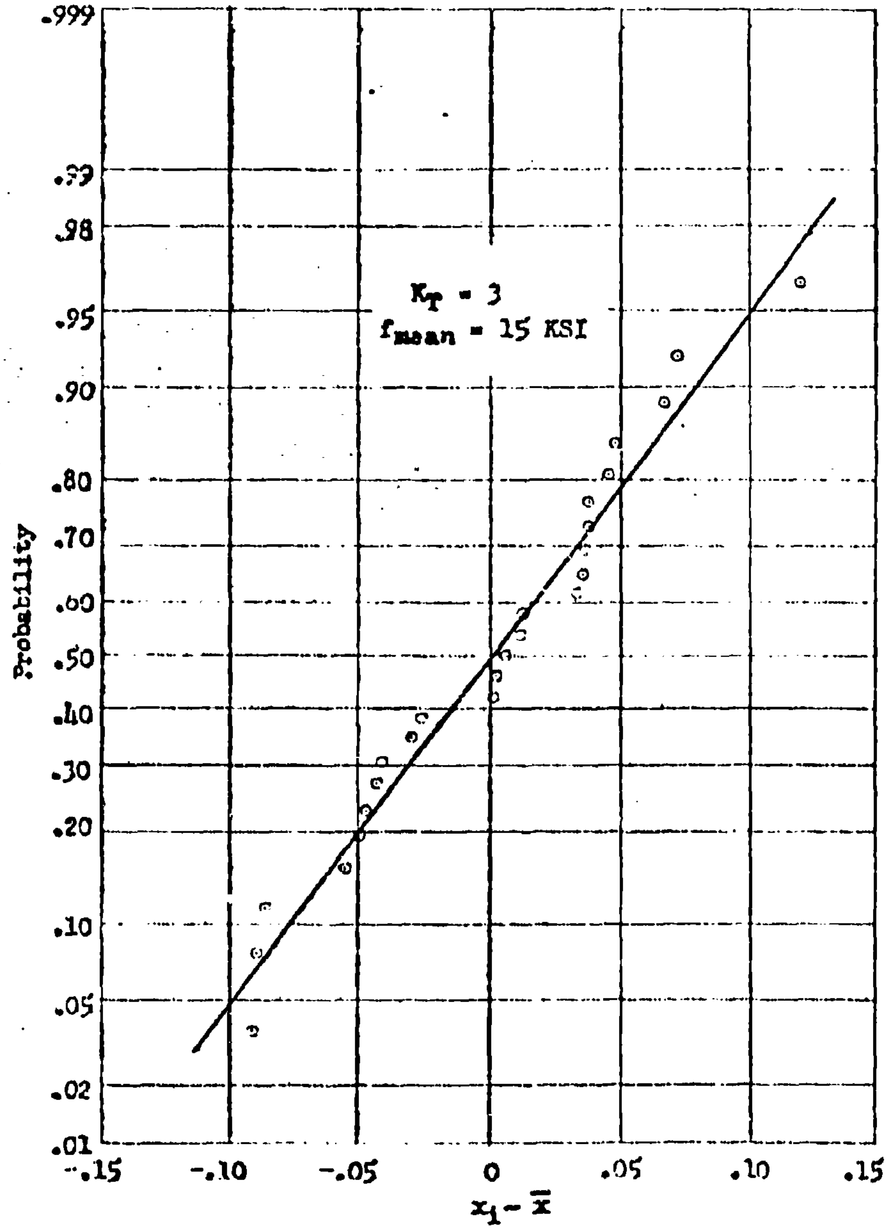

Figure 105 Deviation in Δ Log S_v from the Least Square Best Fit Straight Line on a Plot of Log S_v versus Log N

$$S_v = S_E + p\,N^u \qquad \text{(D1)}$$

This form corresponds to Equation (A6) of Appendix A when

$$p = \alpha^u$$

and

$$u = \frac{1}{\beta}$$

The endurance limit S_E is itself a statistical variate, and Equation (D1) must be solved for known or estimated values of S_E. For a given value of S_E, Equation (D1) can be written in the form

$$\log (S_v - S_E) = \log p + u \log N \qquad \text{(D2)}$$

Designating $y = \log (S_v - S_E)$ as the dependent and $x = \log N$ as the independent variable, the method of linear regression may be applied with

$$y = y_o + u\,x \qquad \text{(D3)}$$

and the coefficients u and y_o of the straight regression line are determined by

$$u = \frac{\sum (x_i - \bar{x})(y_i - \bar{y})}{\sum (x_i - \bar{x})^2} \qquad \text{(D4)}$$

and

$$y_o = \log p = \bar{y} - u\,\bar{x} \qquad \text{(D5)}$$

where

$$\bar{x} = \frac{\sum x_i}{n} \quad ; \quad \bar{y} = \frac{\sum y_i}{n} \qquad \text{(D6)}$$

The method is strictly correct only if the population variances of y are homogeneous; that means, the standard deviation in y is independent of x. The deviations from the regression line should be normally distributed. An unbiased estimate of the variance from regression of the population ($n = \infty$) is given by

$$\{\text{var}\} = \frac{\sum [y_i - (y_o + u\,x_i)]^2}{n-2} \qquad \text{(D7)}$$

For any given value x^*, confidence limits for the computed value $y^* = y_o + u x^*$ are easily set according to Cramer (reference 34).

Upper confidence limit

$$y_u = (y_o + u x^*) + (t_{\alpha/2;\nu}) \sqrt{\{\text{var}\} \left\{\frac{1}{n} + \frac{(x^* - \bar{x})^2}{\sum (x_i - \bar{x})^2}\right\}} \tag{D8}$$

Lower confidence limit

$$y_l = (y_o + u x^*) - (t_{\alpha/2;\nu}) \sqrt{\{\text{var}\} \left\{\frac{1}{n} + \frac{(x^* - \bar{x})^2}{\sum (x_i - \bar{x})^2}\right\}} \tag{D9}$$

Values of $t_{\alpha/2;\nu}$ corresponding to the required confidence coefficient $(1 - \alpha)$ and the given degree of freedom $\nu = n - 2$ can be found in reference 34; for instance, the values are given in Table 51 for $n = 25$ test specimens.

TABLE 51

Student's t - value for $\nu = 23$ Degree of Freedom

Confidence (%)	20	40	60	80	90	95	98	99	99.9
t - value	.256	.532	.858	1.319	1.714	2.069	2.500	2.807	3.767

Plausible values must be assumed for the endurance limit before this statistical procedure can be applied to S-N data. The actual value selected for the endurance limit, S_E, as pointed out in reference 33, will have only a small effect on the analytical matching of S-N data in the mid-stress range. A more accurate linear interpretation of S-N data over the entire stress range may sometimes be provided by a statistical fit of Equation (D10) to S-N data.

$$N = \frac{\gamma}{S_v^{\delta}} \tag{D10}$$

The improvement in matching S-N data in the high and low stress ranges occurs when S-N data follow the linear trend that is indicated in Figure 47 . When plotted in the form of log $(S_v - S_E)$ versus log N, the straight

line variation in Figure 47 degenerates into a curve as shown in Figure 57, where two portions of the resulting curve are approximated by straight lines. This curvilinear variation with log (S_w - S_E) led to the use of linear regression based on Equation (D10). Statistical parameters for this equation constitute a special case for Equation (D1), being the same as that secured by setting S_E equal to zero in Equation (D1) and in the subsequent statistical development.

The use of linear regression with Equation (D10) lead to more likely conditions for a straight line fit to the entire stress range of S-N data. It led to the S-N curves in Figures 106 to 123 that were faired within the ± 90 per cent confidence limits. This fairing was made to reduce as much as possible the merging and intersections in cross plots of the data. The faired S-N curves intersected in only one case at the upper end (f_y = 25 ksi) and were tangent in one place near the endurance limit. Agreement was generally good with the test data although the resulting S-N curves did not flatten out in the vicinity of the assumed endurance limit at $N = 10^7$ cycles.

TABLE 52
S–N DATA FOR NOTCHED SHEET COUPONS
(Table is continued on the next two pages)
All Stresses are Based on Gross Area

$K_T = 3$, $f_{mean} = -10$		$K_T = 3$, $f_{mean} = -5$		$K_T = 3$, $f_{mean} = 10$		$K_T = 3$, $f_{mean} = 15$		$K_T = 4$, $f_{mean} = -10$		$K_T = 4$, $f_{mean} = -5$	
f_v KSI	N	f_v KSI	N	f_v KSI	N	f_v KSI	N	f_v KSI	N	f_v KSI	N
25	601	25	901	25	765	25	660	25	1215	25	500
25	640	25	1031	25	1509	25	915	25	1519	25	610
25	1425	25	1384	25	1666	25	965	25	1597	25	806
25	2044	25	1642	25	2476	25	1072	25	2424	25	812
25	5055	25	2760	25	2621	25	1101	25	2843	25	873
20	2144	20	3300	20	2765	20	3272	20	1290	20	1245
20	6200	20	3954	20	3130	20	3904	20	2445	20	1650
20	7500	20	3960	20	4641	20	4269	20	3379	20	1686
20	7573	20	6315	20	6264	20	4998	20	3600	20	2274
20	11660	20	6377	20	8091	20	5200	20	5179	20	2460
15	10600	15	10800	15	9000	15	7995	15	12600	15	3600
15	37500	15	12600	15	10800	15	8722	15	12600	15	5400
15	39600	15	23400	15	10800	15	10655	15	14400	15	6650
15	43200	15	27000	15	16200	15	10707	15	13200	15	6800
15	108000	15	41400	15	19800	15	11295	15	16200	15	7050
10	100800	10	7200	10	27000	10	23400	12.5	13860	10	27600
10	135000	10	36000	10	27540	10	32400	12.5	11400	10	63000
10	203400	10	75600	10	49680	10	34200	12.5	16920	10	62800
10	302400	10	270000	10	52800	10	43600	12.5	54600	10	86400
10	385200	10	295560	10	55800	10	84600	12.5	79740	10	93600
7.5	484200	5	374400	5	196560	5	176400	10	37440	5.5	163000
7.5	525600	5	522000	5	198300	5	180000	10	91800	5.5	189000
7.5	698400	5	1644500	5	198540	5	232200	10	117000	5.5	1306800
7.5	1674000	5	*	5	201600	5	246600	10	124200	5.5	1998000
7.5	2719600	5	*	5	239400	5	460800	10	3700000	5.5	3601000

* 10^7 cycles (no failure)

TABLE 52
(Table is completed on next page)
All Stresses are Based on Gross Area

$K_T = 4$, $f_{mean} = 0$		$K_T = 4$, $f_{mean} = 10$		$K_T = 4$, $f_{mean} = 15$		$K_T = 7$, $f_{mean} = -10$		$K_T = 7$, $f_{mean} = -5$		$K_T = 7$, $f_{mean} = 0$	
f_v KSI	N	f_v KSI	N	f_v KSI	N	f_v KSI	N	f_v KSI	N	f_v KSI	N
25	331	25	150	25	171	20	343	25	36	20	142
25	342	25	250	25	175	20	450	25	119	20	215
25	393	25	260	25	180	20	516	25	140	20	224
25	445	25	324	25	212	20	590	25	172	20	277
25	537	25	350	25	315	20	664	25	183	20	360
20	670	20	521	20	491	15	474	20	195	15	386
20	744	20	531	20	540	15	743	20	226	15	413
20	914	20	640	20	690	15	1006	20	247	15	573
20	975	20	820	20	1030	15	1200	20	293	15	636
20	1016	20	1001	20	1203	15	1883	20	296	15	884
15	3600	15	1860	15	1471	10	9540	15	465	10	1200
15	4283	15	2500	15	2325	10	12600	15	672	10	1800
15	4468	15	2900	15	2600	10	14400	15	748	10	2310
15	6460	15	5946	15	3053	10	41400	15	753	10	3150
15	7200	15	6150	15	3170	10	52200	15	813	10	4633
10	26280	10	9000	10	6300	7.5	14580	10	6150	7.5	14400
10	25800	10	9600	10	6450	7.5	40140	10	6300	7.5	16740
10	29700	10	10500	10	7200	7.5	102780	10	7872	7.5	19800
10	36180	10	12600	10	7950	7.5	147600	10	8100	7.5	32400
10	37600	10	27000	10	15040	7.5	148500	10	8620	7.5	34200
5	2098500	4	61200	3	90000	5	185000	4	178200	5	51400
5	3979500	4	63000	3	174600	5	240000	4	847800	5	101500
5	3440000	4	64800	3	370800	5	390400	4	911700	5	102600
5	6378000	4	92800	3	406800	5	651600	4	1000000	5	111900
5	8109720	4	872000	3	2196000	5	691700	4	*	5	941600

* 10^7 cycles (no failure)

TABLE 52
(Concluding Page of Table)
All Stresses are Based on Gross Area

$K_T = 7$, $f_{mean} = 10$		$K_T = 7$, $f_{mean} = 15$		$K_T = 10$, $f_{mean} = -10$		$K_T = 10$, $f_{mean} = -5$		$K_T = 10$, $f_{mean} = 10$		$K_T = 10$, $f_{mean} = 15$	
f_Y KSI	N	f_Y KSI	N	f_Y KSI	N	f_Y KSI	N	f_Y KSI	N	f_Y KSI	N
20	100	20	90	20	147	15	450	15	156	15	125
20	130	20	160	20	263	15	450	15	168	15	184
20	240	20	180	20	336	15	562	15	177	15	199
20	250	20	190	20	415	15	753	15	179	15	202
20	350	20	230	20	501	15	1855	15	200	15	242
15	383	15	360	15	360	10	760	10	493	10	450
15	425	15	430	15	478	10	1031	10	728	10	605
15	440	15	460	15	575	10	1231	10	766	10	655
15	668	15	480	15	685	10	2331	10	794	10	761
15	706	15	1033	15	3387	10	3300	10	1021	10	861
10	1500	10	500	10	1660	7.5	916	7.5	772	5	4331
10	2450	10	900	10	2215	7.5	3600	7.5	1391	5	4500
10	3600	10	1510	10	3215	7.5	4438	7.5	1462	5	4924
10	4189	10	1880	10	4500	7.5	7200	7.5	1501	5	5400
10	4950	10	2040	10	9011	7.5	22544	7.5	1766	5	6300
5	12600	5	10800	7.5	28800	5.5	23300	5	2880	2.5	25200
5	12600	5	12600	7.5	45000	5.5	36000	5	6176	2.5	28800
5	14400	5	12960	7.5	66600	5.5	36000	5	6343	2.5	30600
5	17460	5	14250	7.5	72000	5.5	43200	5	6999	2.5	57600
5	25200	5	17280	7.5	73800	5.5	88200	5	7258	2.5	64800
2.5	88200	2	84600	5	185400	4	48600	2.5	25200	1.5	340200
2.5	88200	2	84600	5	352800	4	55800	2.5	36000	1.5	648000
2.5	129600	2	185400	5	658800	4	144000	2.5	73440	1.5	4104900
2.5	691000	2	342000	5	1420200	4	824760	2.5	82620	1.5	4696200
2.5	1296000	2	*	5	3216600	4	838480	2.5	576000	1.5	*

* 10^7 cycles (no failure)

TABLE 53

S-N DATA FOR NOTCHED SHEET COUPONS
All Stresses are Based on Gross Area

$K_T=4$; $f_{mean}=1.125$ KSI		$K_T=4$; $f_{mean}=4.5$ KSI		$K_T=4$; $f_{mean}=7$ KSI		$K_T=4$; $f_{mean}=2.4$ KSI	
f_v KSI	N	f_v KSI	N	f_v KSI	N	f_v KSI	N
4.225	$>10^7$	7.5	25200	15	3342	10.4	12015
4.225	$>10^7$	7.5	32400	15	3465	10.4	14856
4.225	$>1.5\,(10)^7$	7.5	41400	15	3537		
		7.5	43400	15	4075		
		7.5	43800	15	4330		
		7.5	45000				

$K_T=7$; $f_{mean}=1.125$ KSI		$K_T=7$; $f_{mean}=4.5$ KSI		$K_T=7$; $f_{mean}=7$ KSI		$K_T=7$; $f_{mean}=2.6$ KSI	
f_v KSI	N	f_v KSI	N	f_v KSI	N	f_v KSI	N
4.225	364000	7.5	9900	15	485	10.2	1356
4.225	144000	7.5	10600	15	502	10.2	1332
4.225	148000	7.5	11900	15	503		
4.225	$>10^7$	7.5	13700	15	529		
4.225	$>10^7$	7.5	14600	15	540		
4.225	$>10^7$	7.5	14700				

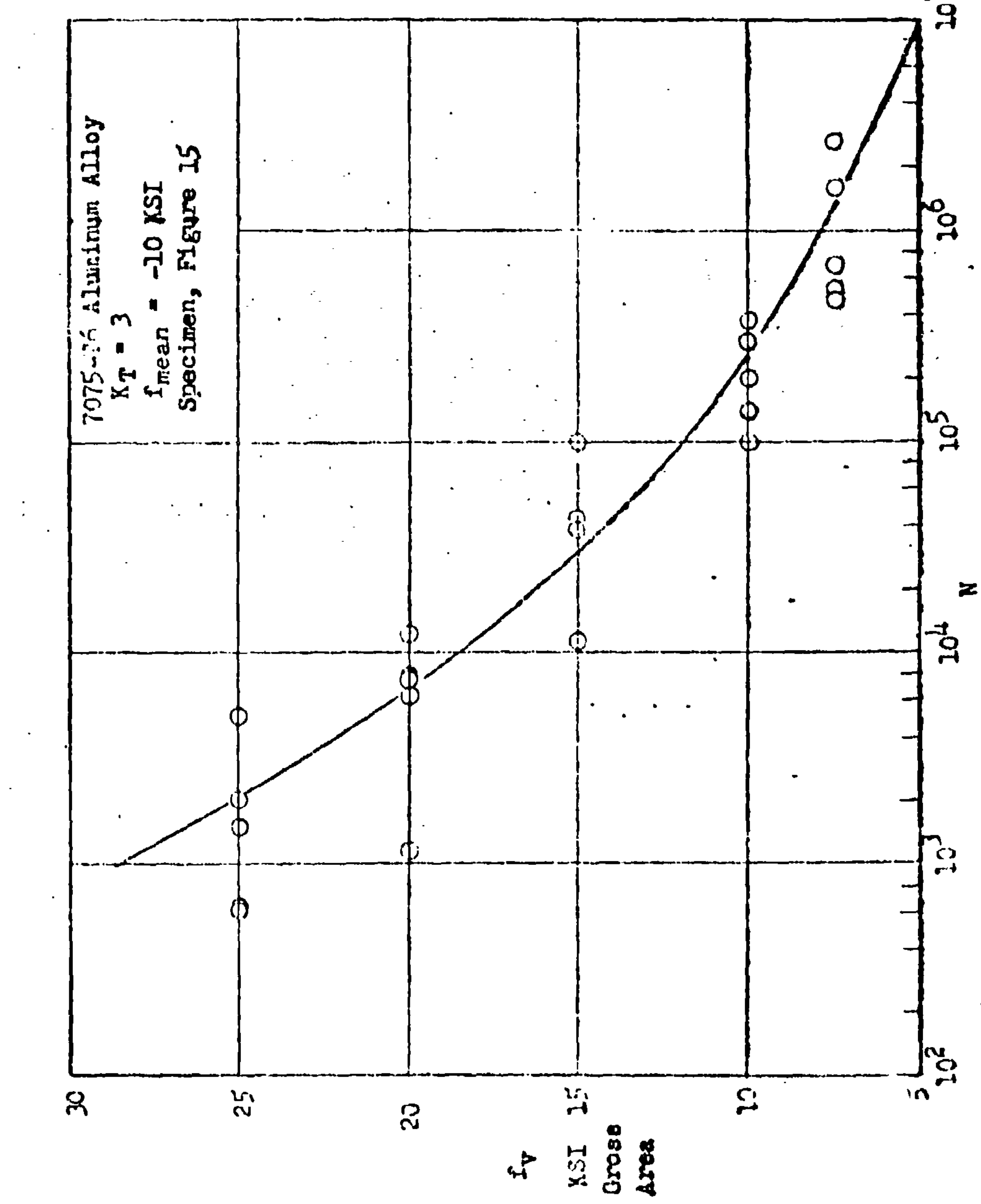

Figure 106 Experimental S-N Curve for Notched Sheet Coupons

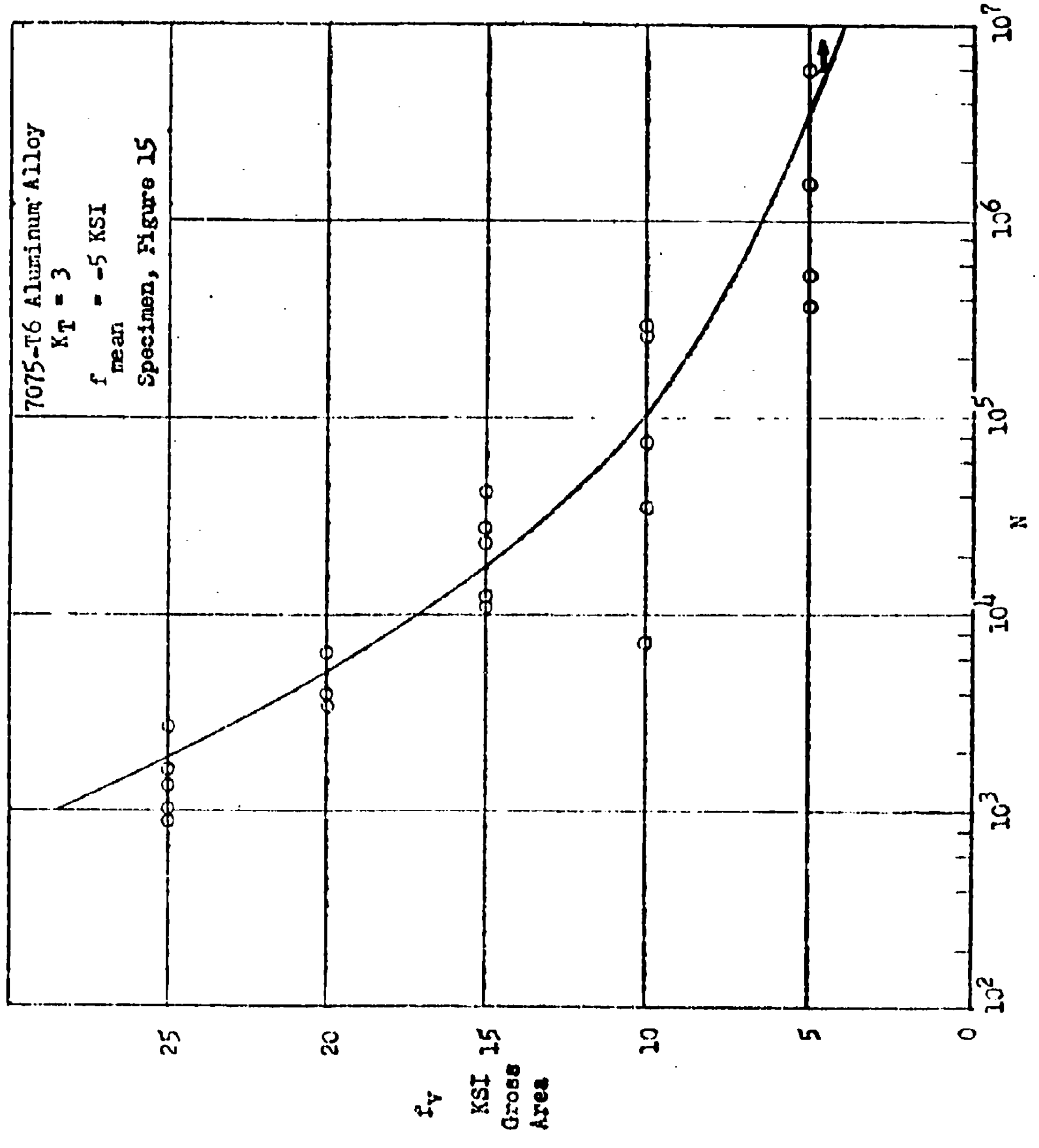

Figure 107 Experimental S-N Curve for Notched Sheet Coupons

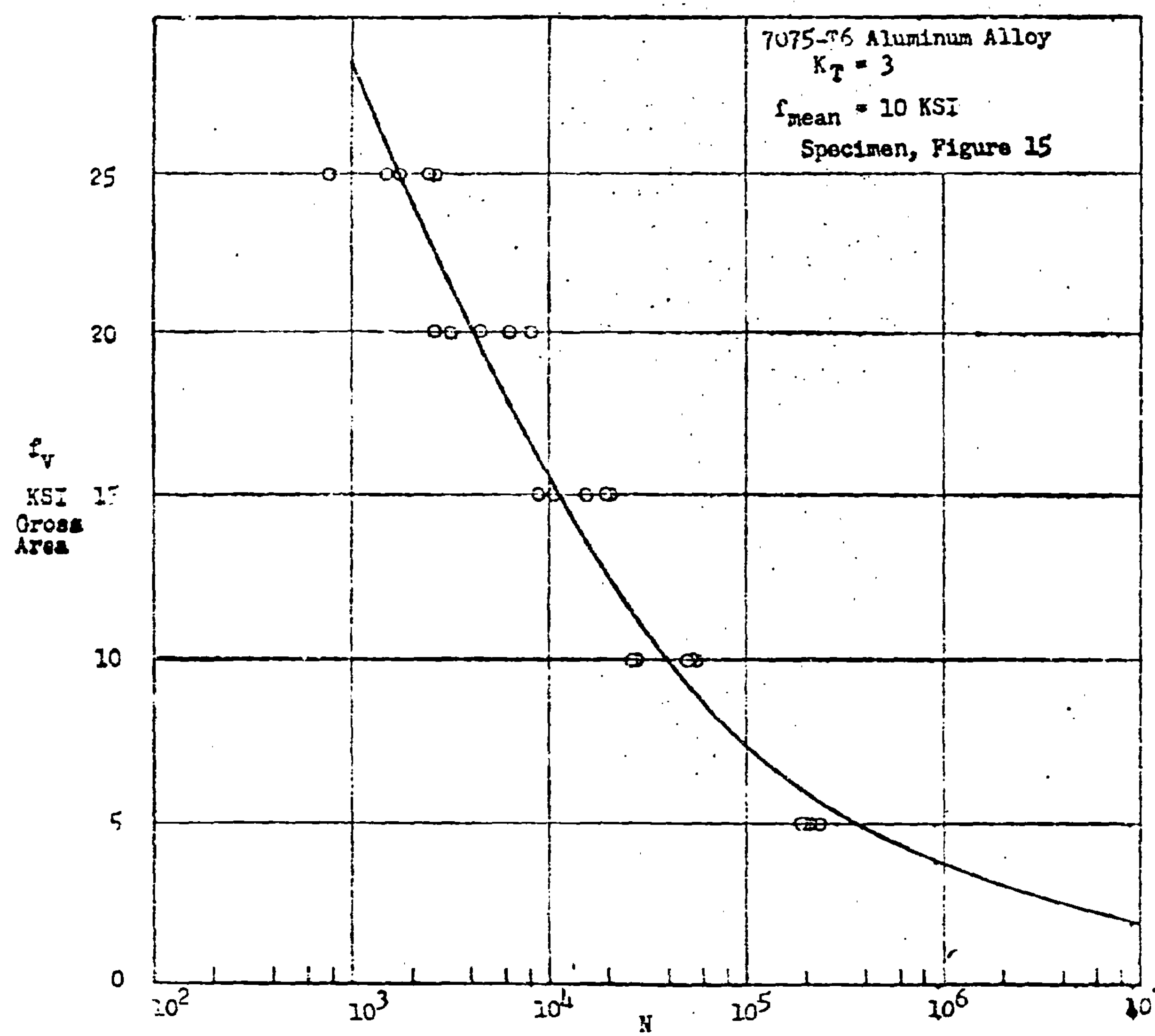

Figure 108 Experimental S-N Curve for Notched Sheet Coupons

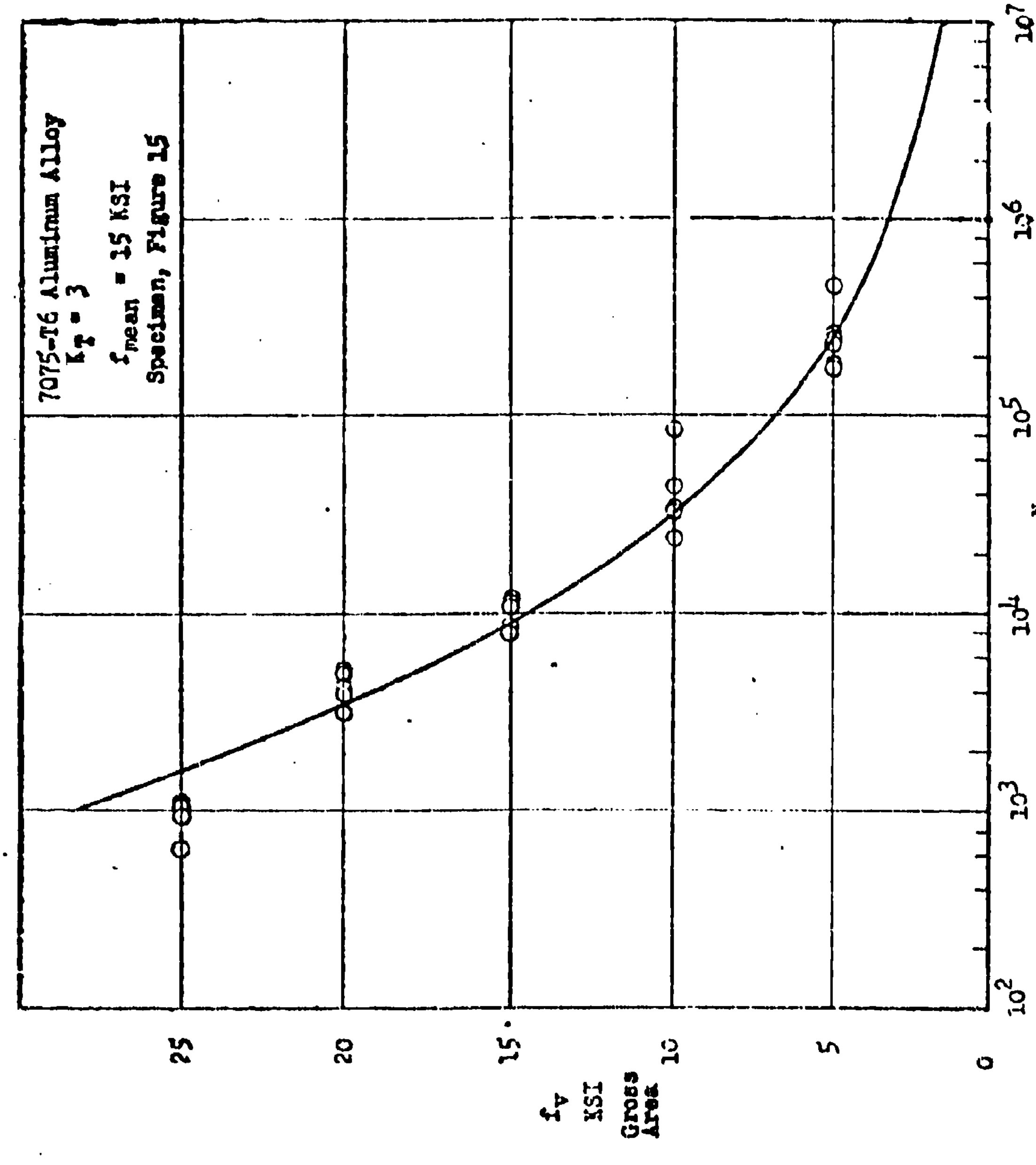

Figure 109 Experimental S-N Curve for Notched Sheet Coupons

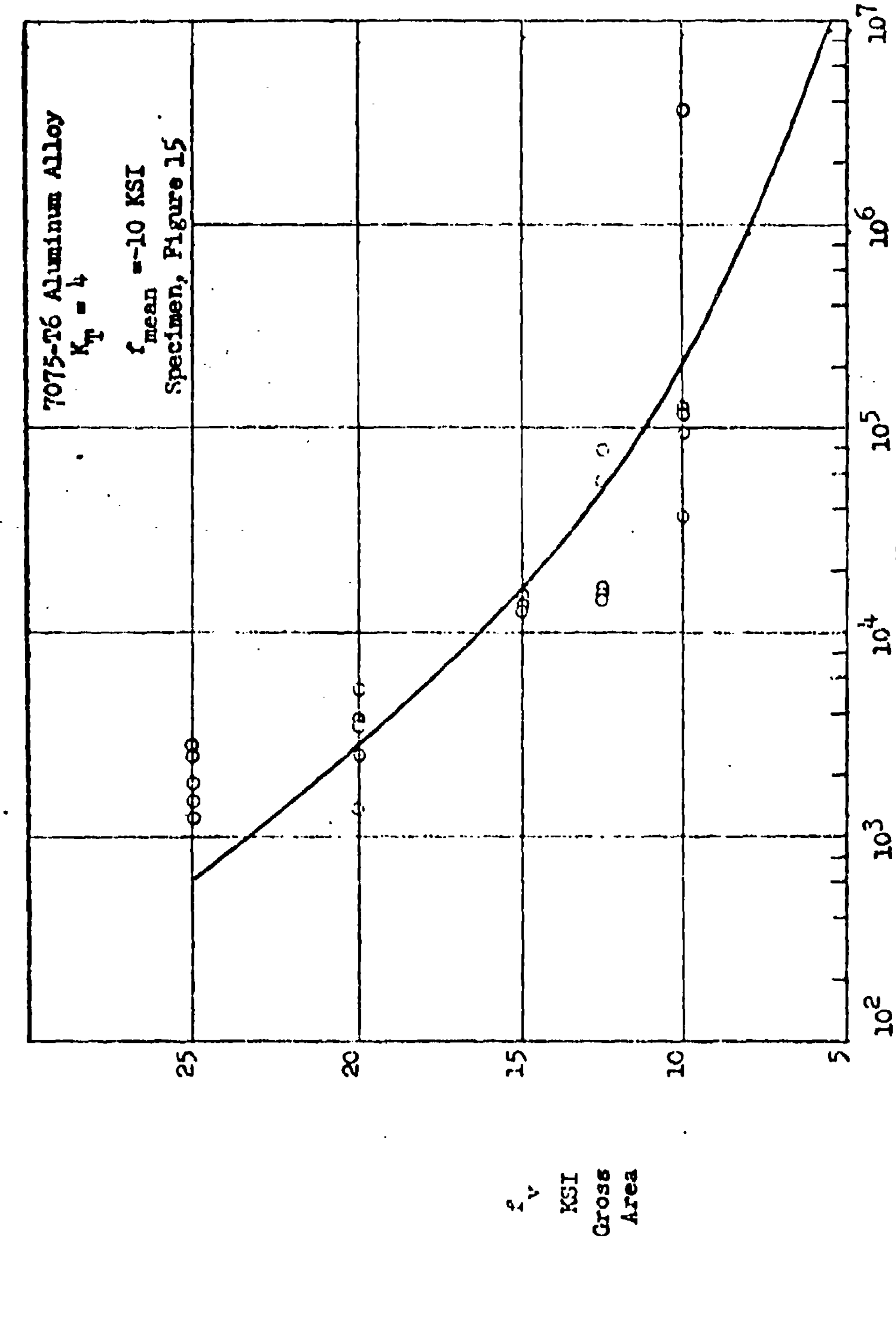

Figure 110 Experimental S-N Curve for Notched Sheet Coupons

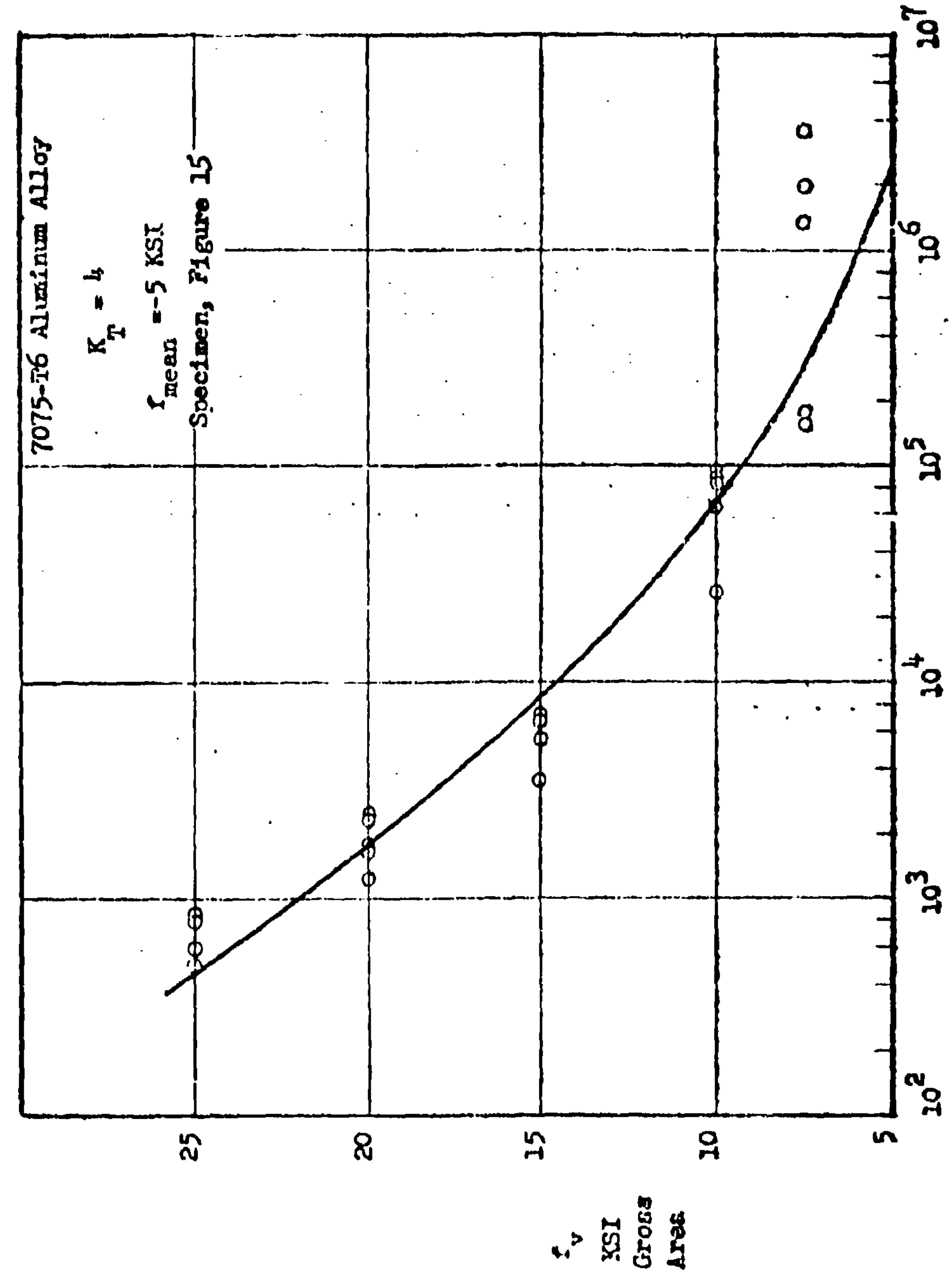

Figure 111 Experimental S-N Curve for Notched Sheet Coupons

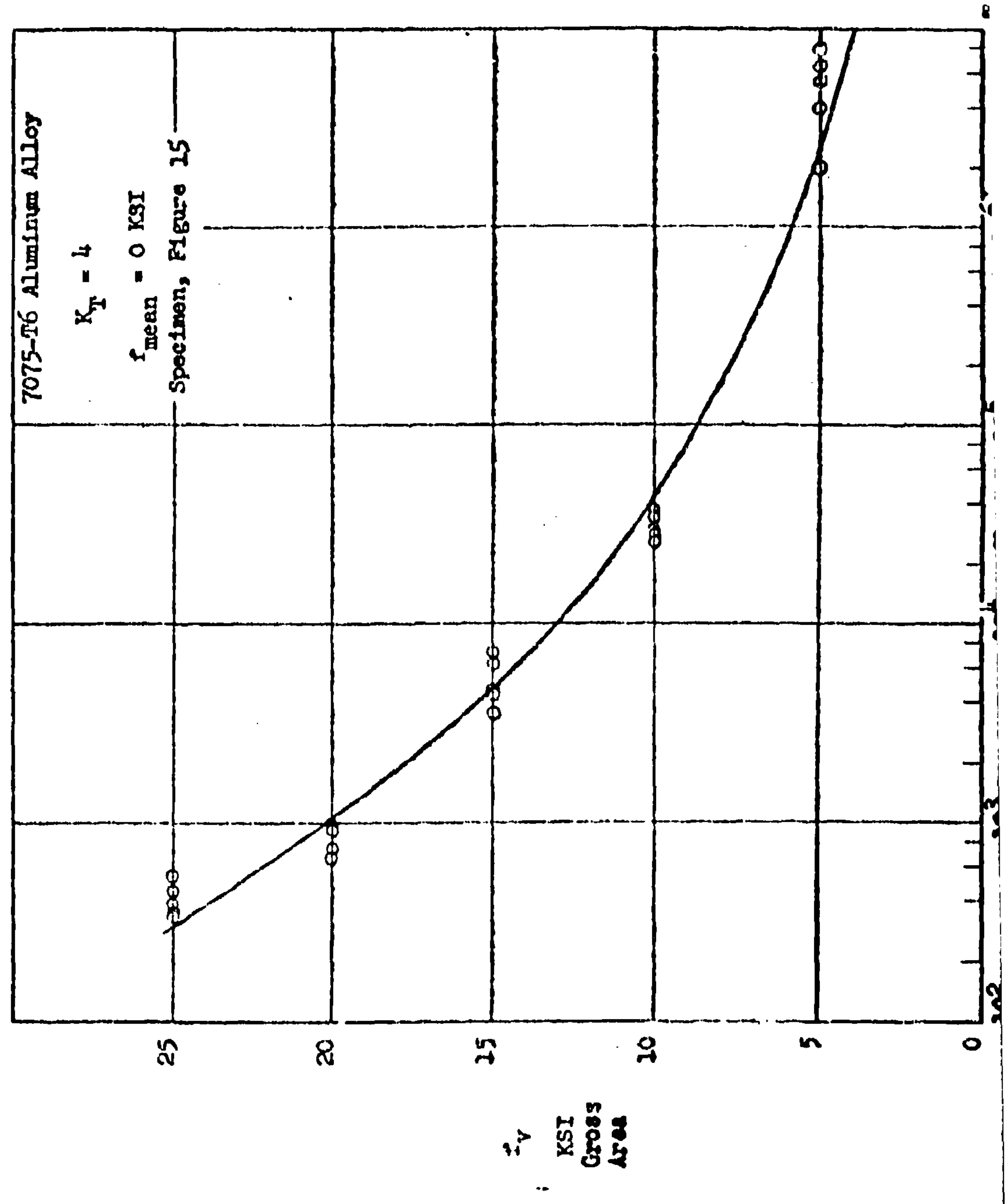
7075-T6 Aluminum Alloy
K_T = 4
f_mean = 0 KSI
Specimen, Figure 15
25
20
15
10
5
0
f_v
KSI
Gross
Area

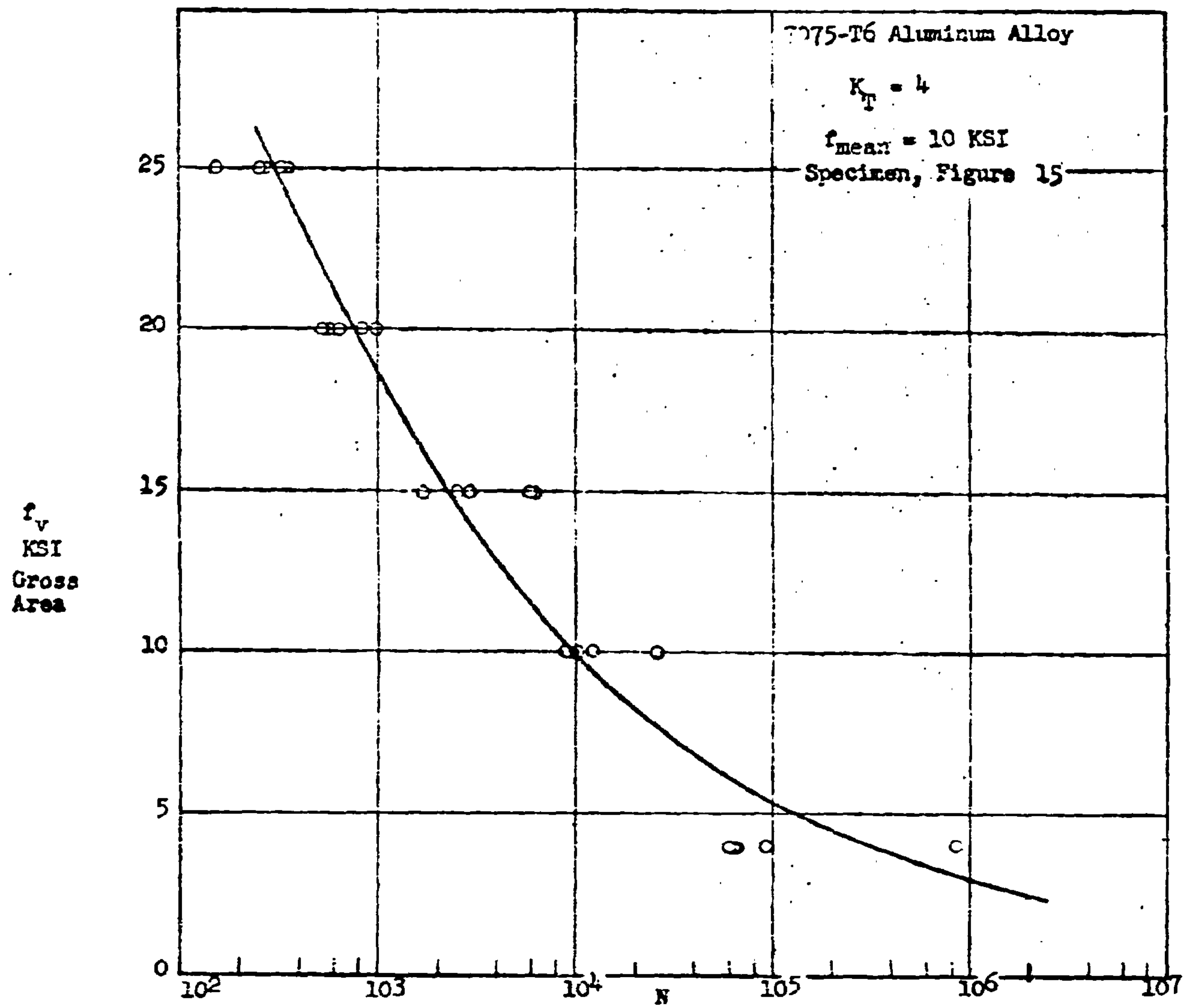

Figure 113 Experimental S-N Curve for Notched Sheet Coupons

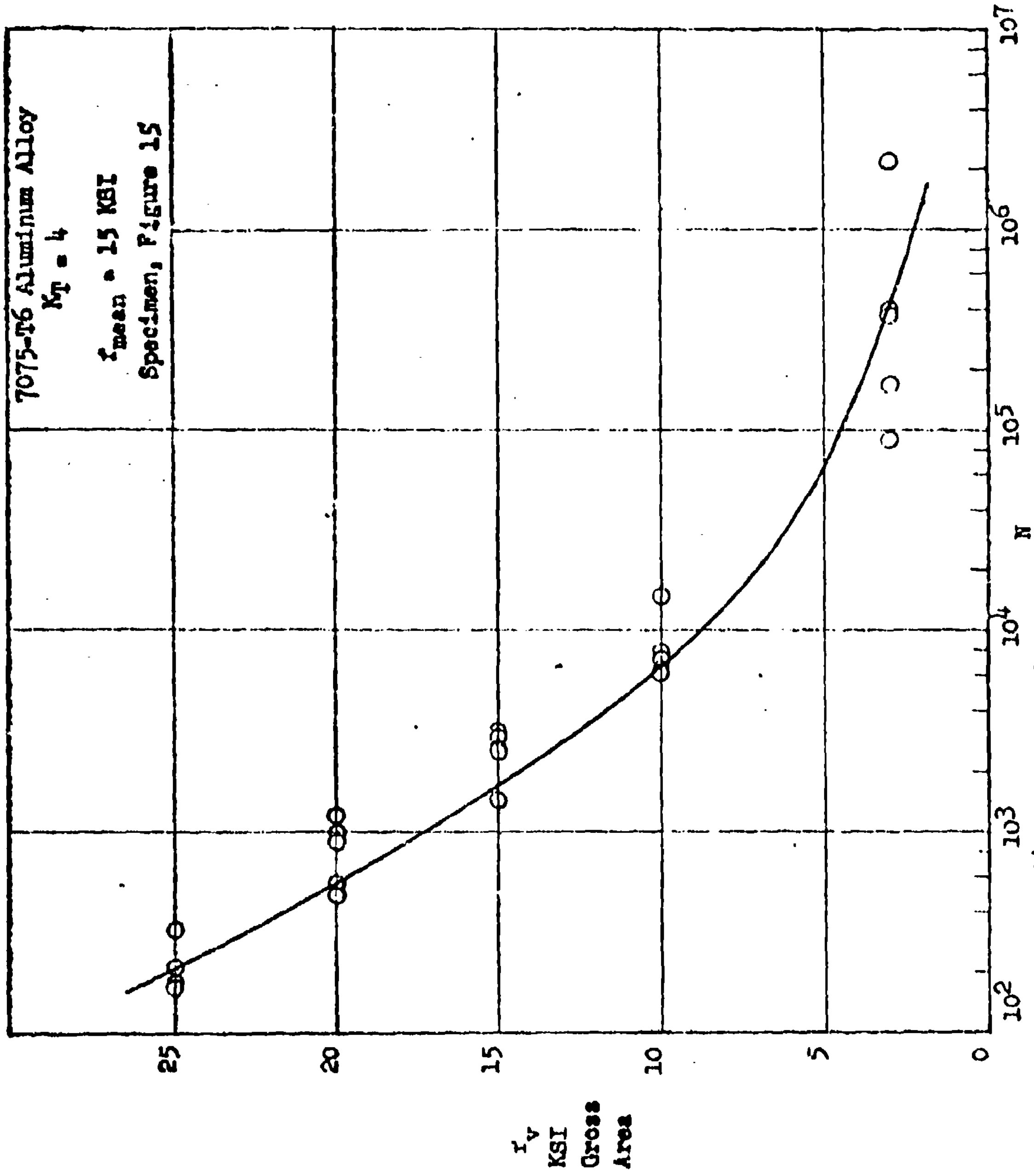

Figure 114 Experimental S-N Curve for Notched Sheet Coupons

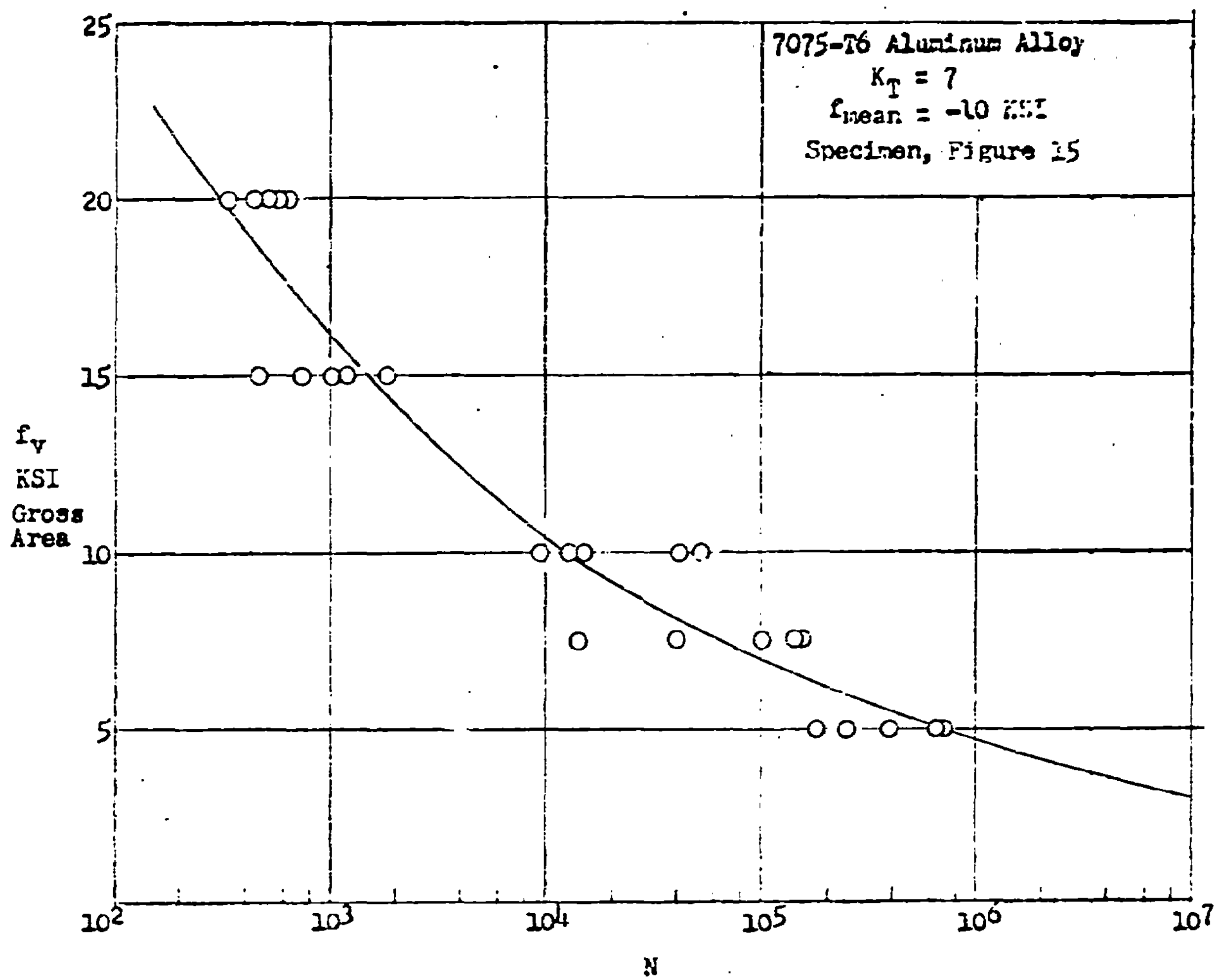

Figure 115 Experimental S-N Curve for Notched Sheet Coupons

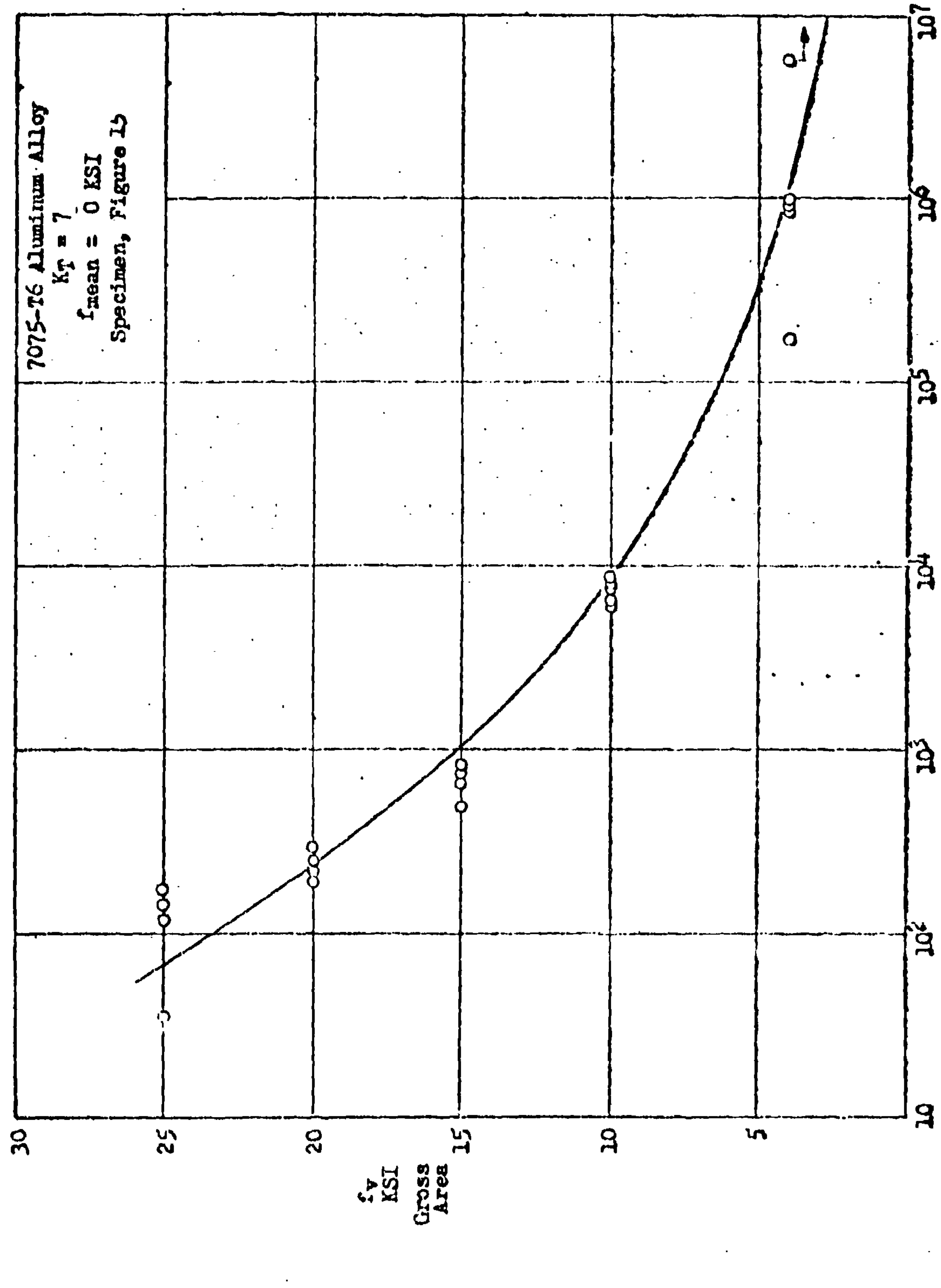

Figure 116 Experimental S-N Curve for Notched Sheet Coupons

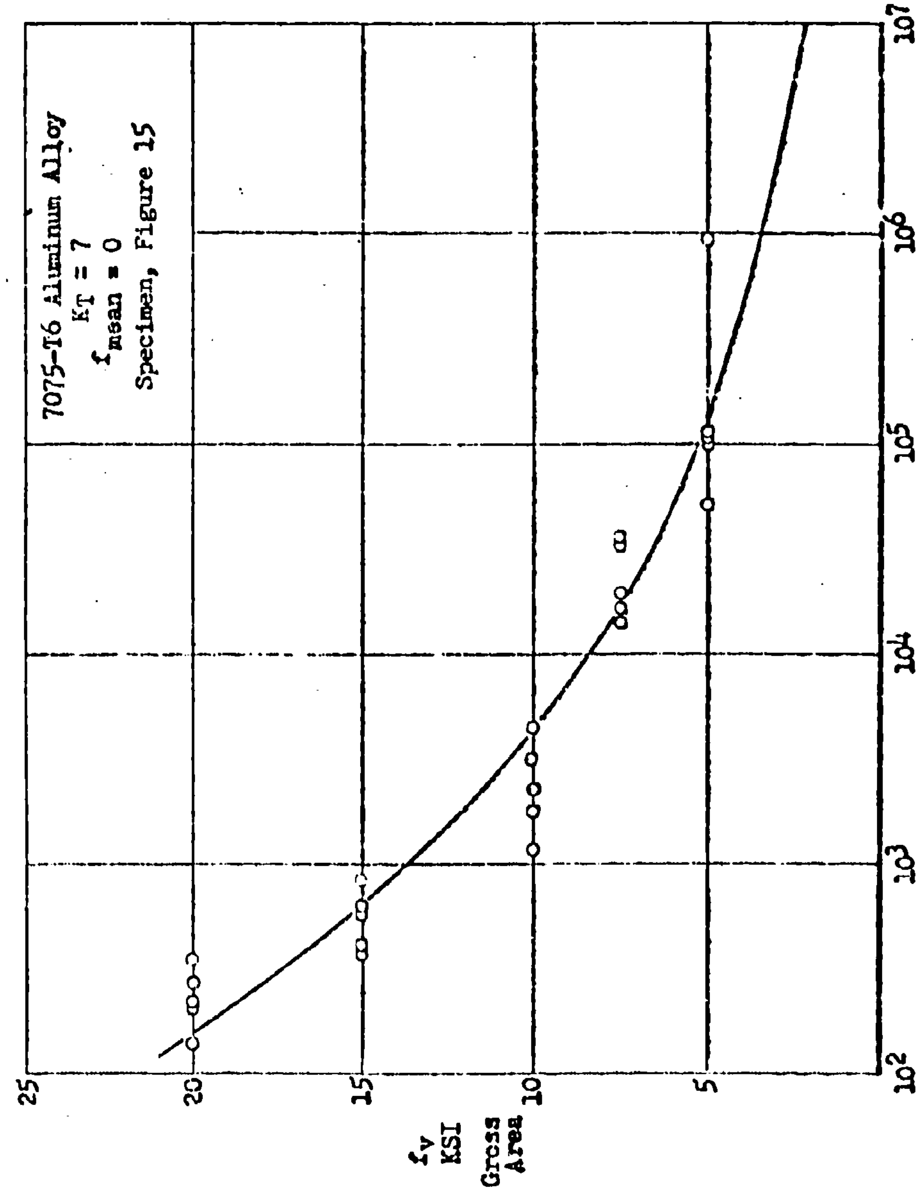

Figure 117 Experimental S-N Curve for Notched Sheet Coupons

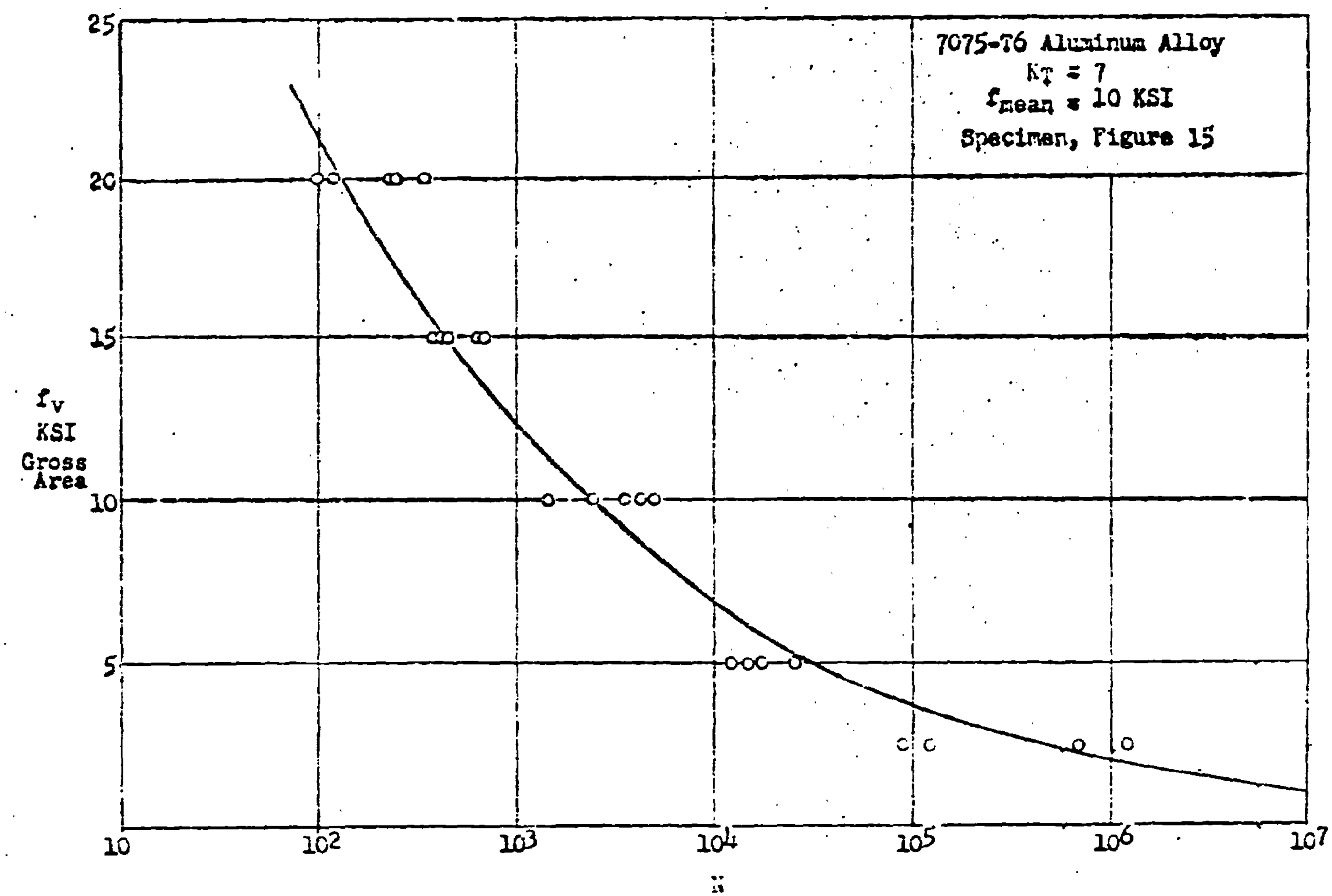

Figure 118 Experimental S-N Curve for Notched Sheet Coupons

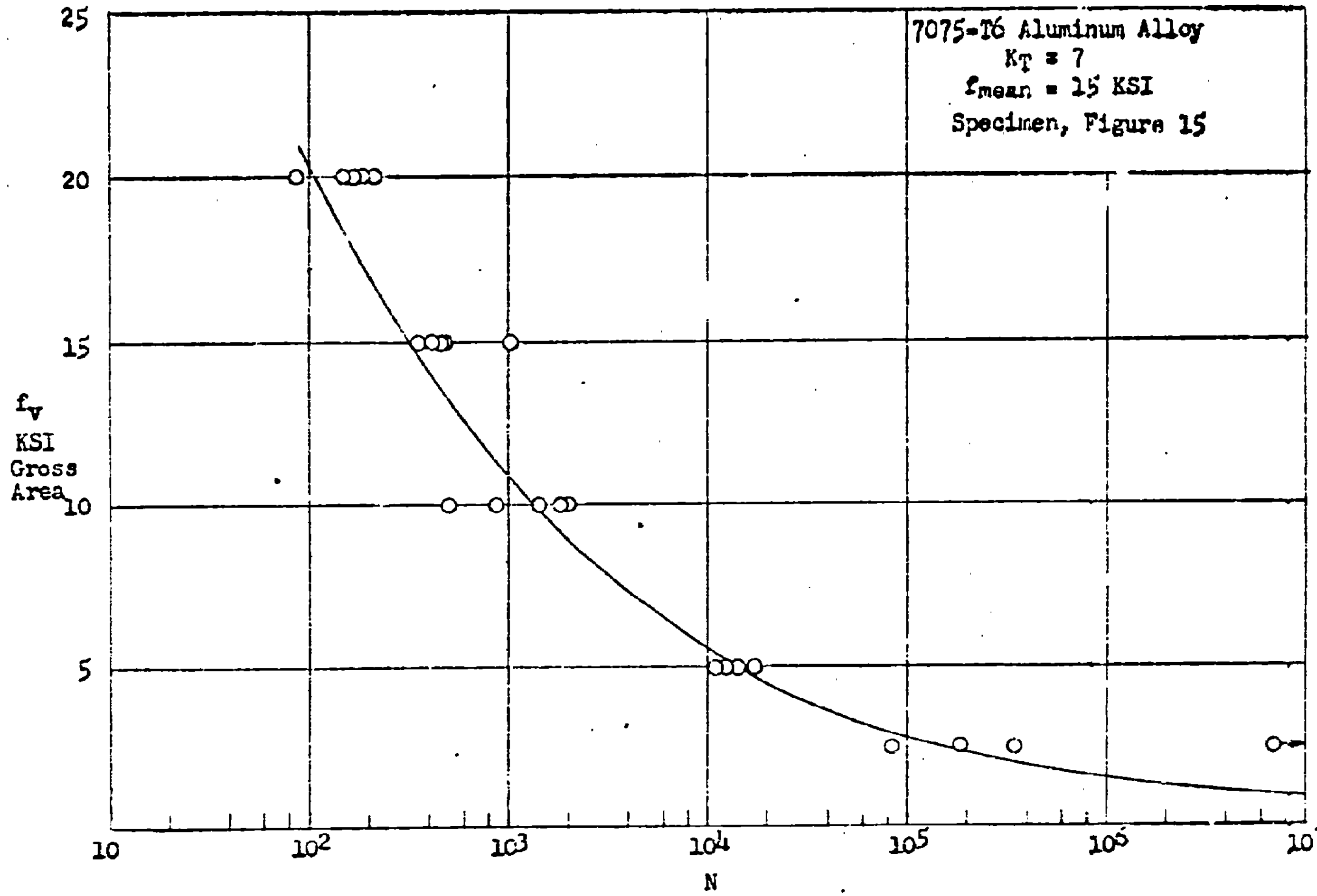

Figure 119 Experimental S-N Curve for Notched Sheet Coupons

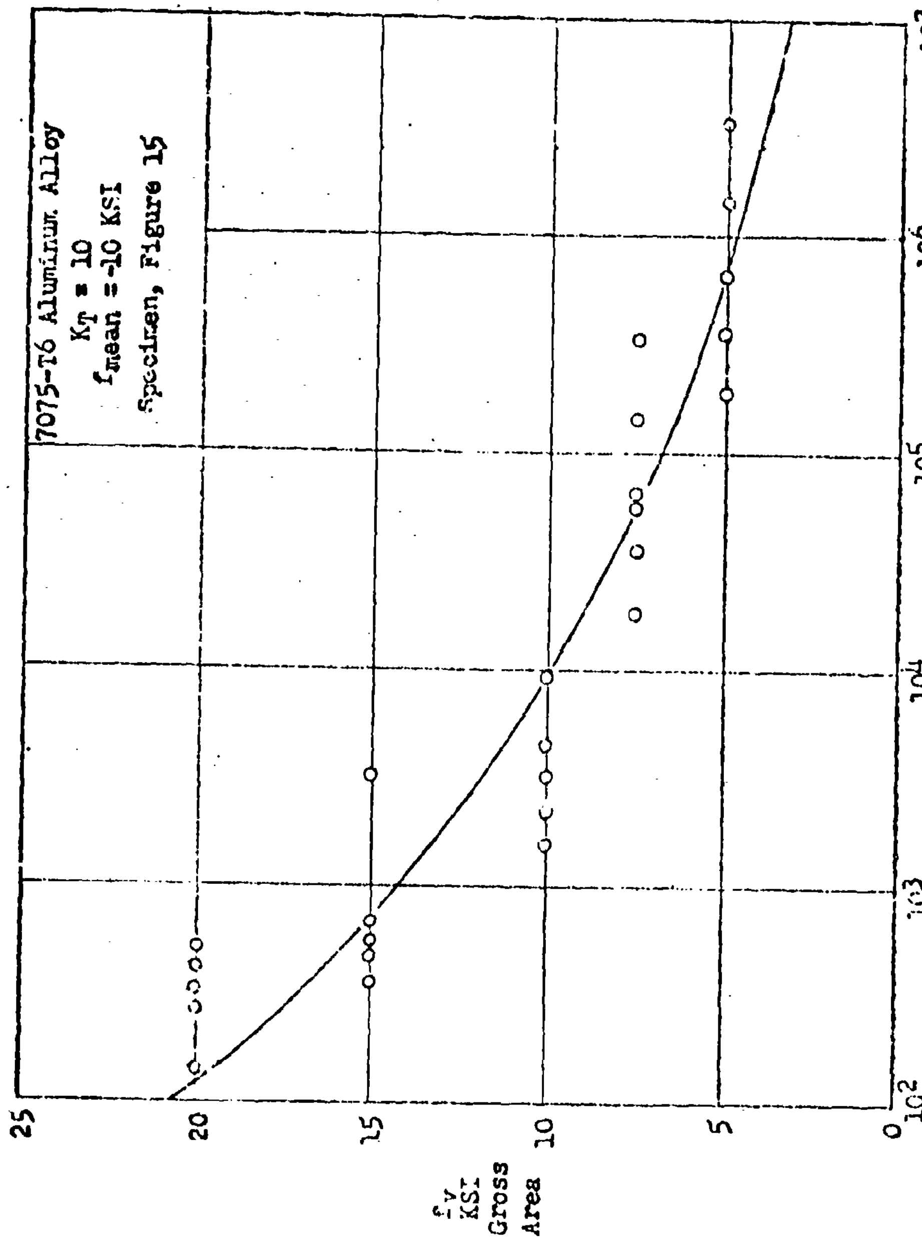

Figure 120 Experimental S-N Curve for Notched Sheet Coupons

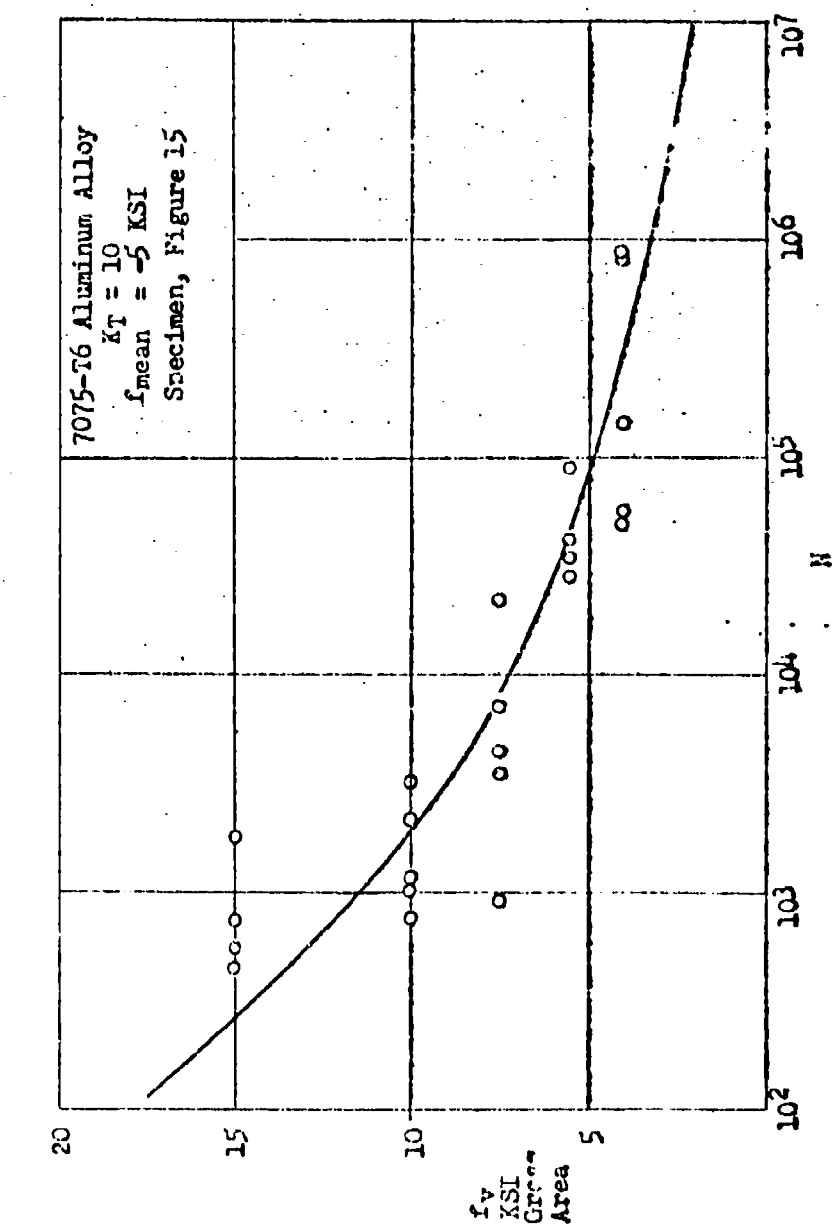

Figure 121 Experimental S-N Curve for Notched Sheet Coupons

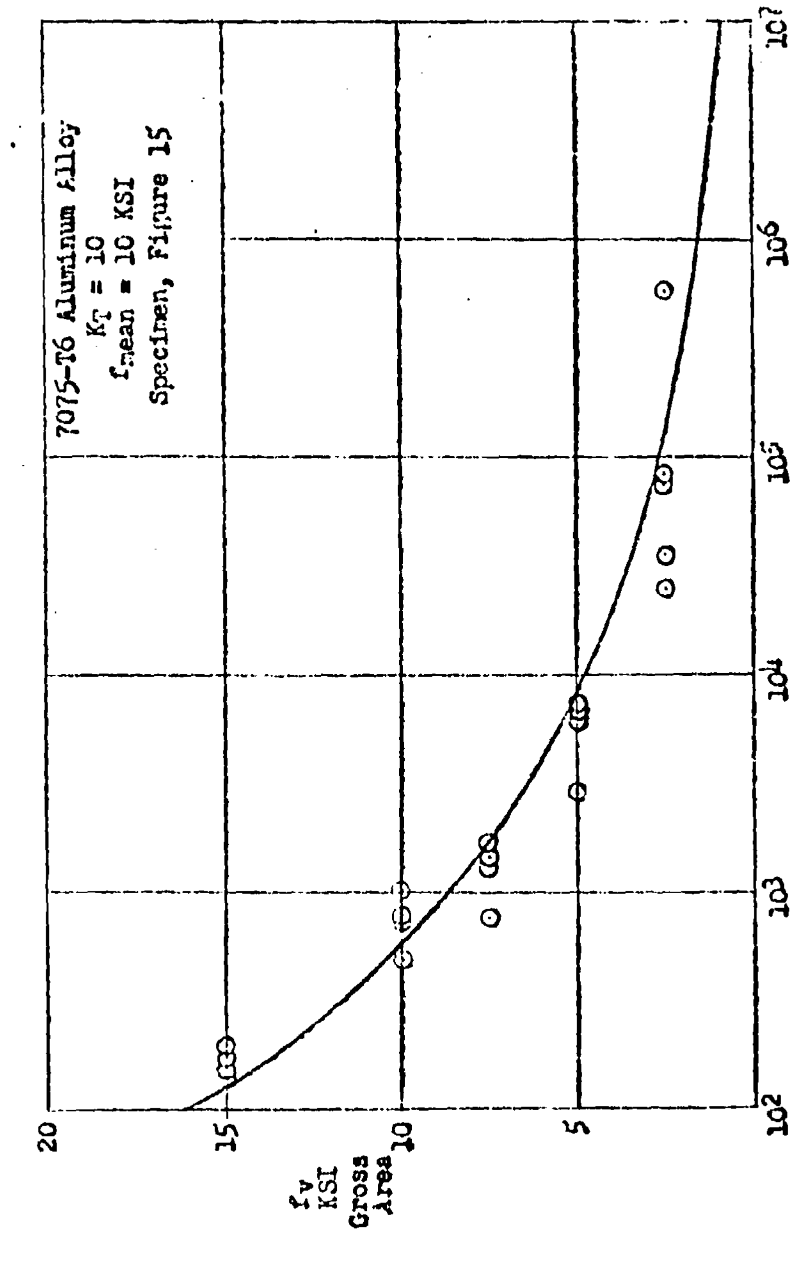

Figure 122 Experimental S-N Curve for Notched Sheet Coupons

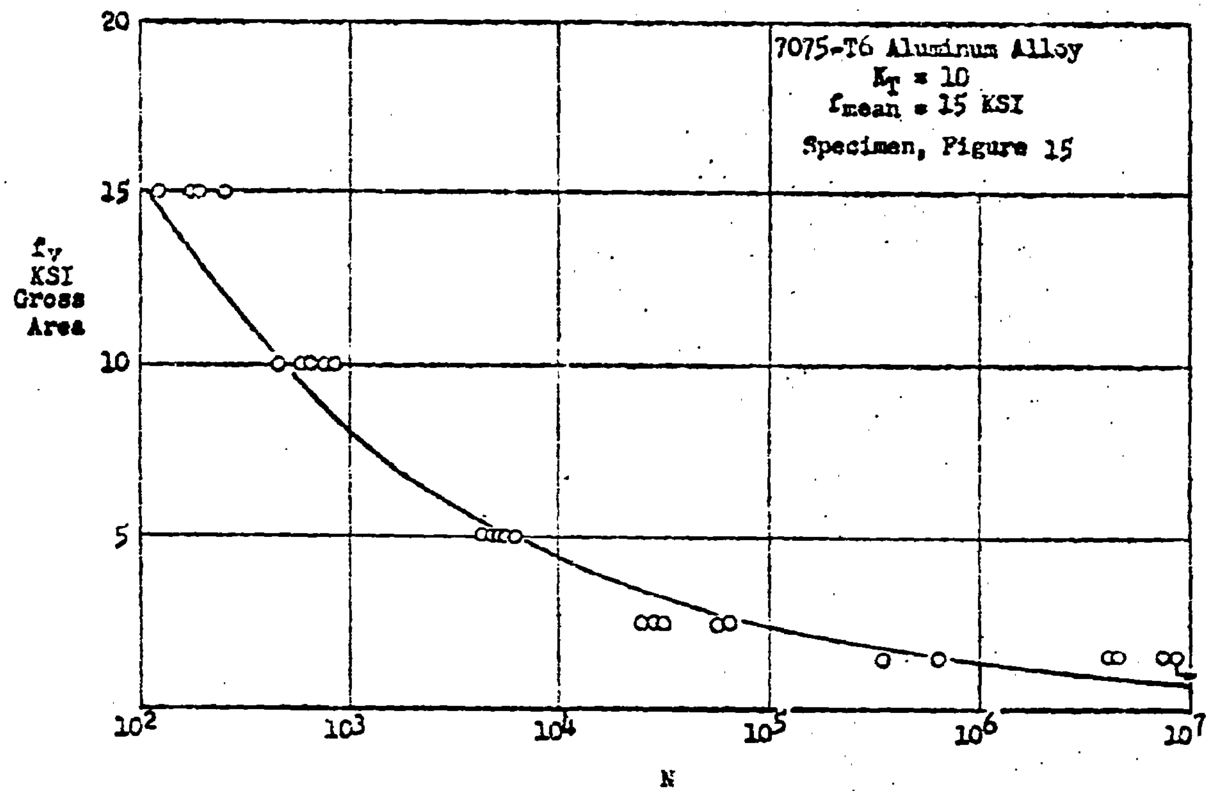

Figure 123 Experimental S-N Curve for Notched Sheet Coupons

CONSTRUCTION OF S-N CURVES BY INTERPOLATION

The complete fatigue loading history for an airframe structure contains several types of varying load spectra, each acting at different mean load levels. One spectrum in particular, the high-performance fighter-trainer maneuver load history, is characterized by an essentially constant minimum load with the varying load excursions to a maximum magnitude and returning to the original minimum. For fighter-maneuver spectra, the normally defined mean load thus varies with each cycle. Interpolation procedures are required to provide the S-N curves for each of these two basic types of loading.

A. S-N curves of allowable symmetrical varying stresses about a constant mean stress of any specified value are most readily obtained from interpolation of S-N data plotted on a Christensen diagram along lines of the specified constant mean stress. Figure 124 illustrates this operation. The S-N curves in Figure 126 were obtained in this manner from Figure 124, and those in Figure 127 were obtained in a similar manner from Figure 125.

B. S-N curves of allowable unsymmetrical varying stresses above a constant minimum stress of any specified value are readily obtained by interpolation of S-N data plotted on a Christensen diagram along lines of the specified constant minimum stress. Figure 124 illustrates how this procedure results in a 45° line originating at the constant minimum stress in the rectilinear plot that leads to the S-N curve plotted in Figure 128. This latter figure also contains an S-N curve that was derived in the same manner from Figure 125.

C. S-N curves of allowable stresses with any ratio of $R = \frac{F_{min}}{F_{max}}$ may be obtained by interpolation along a radial line of slope $\frac{1}{R}$ on the $F_{min} - F_{max}$ scale.

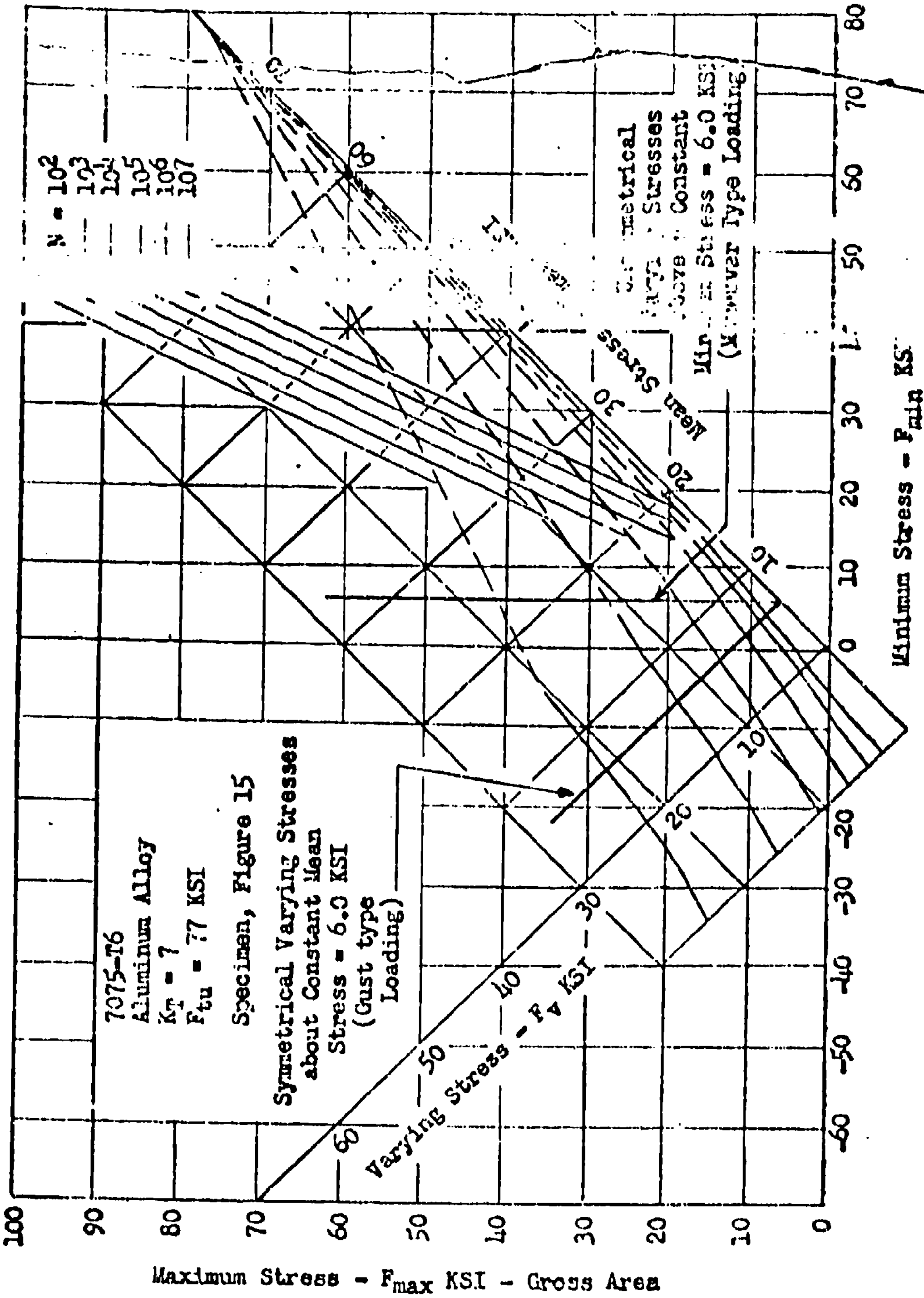

Figure 124 Christensen Diagram-Axial Loading, Coupon Test S-N Data - K_T = 7

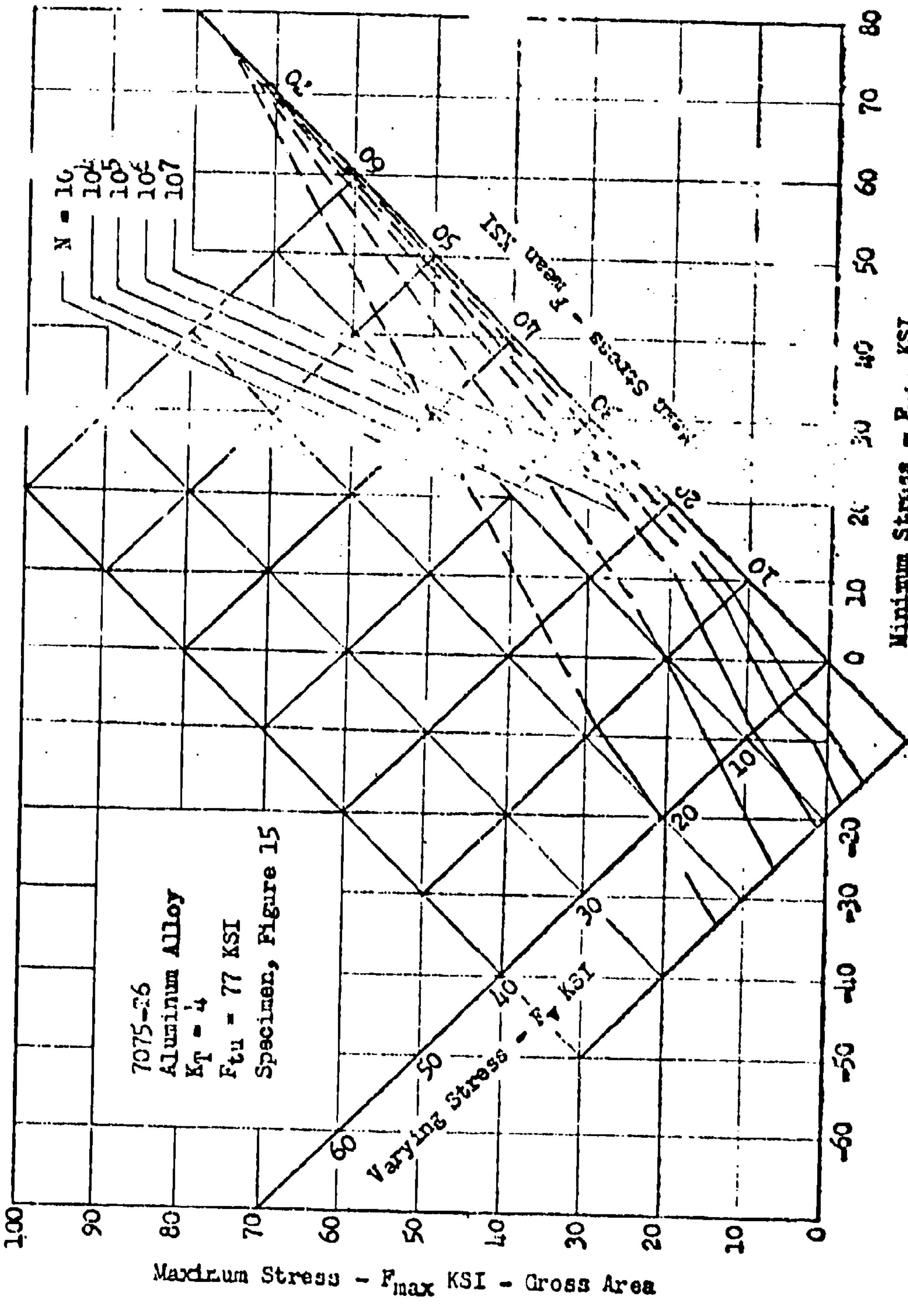

Figure 125 Christensen Diagram-Axial Loading, Coupon Test S-N Data - $K_T = 4$

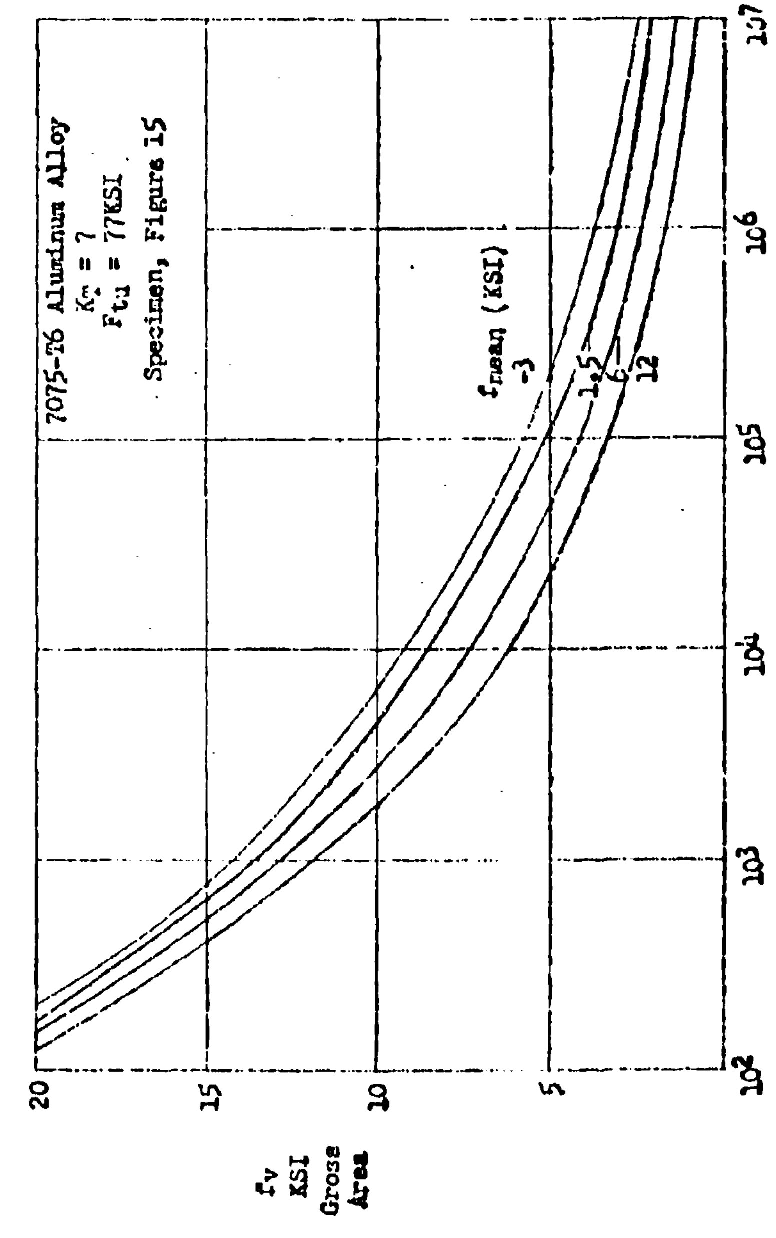

Figure 126 Interpolated S-N Curves for Notched Sheet Coupons - K_T = 7

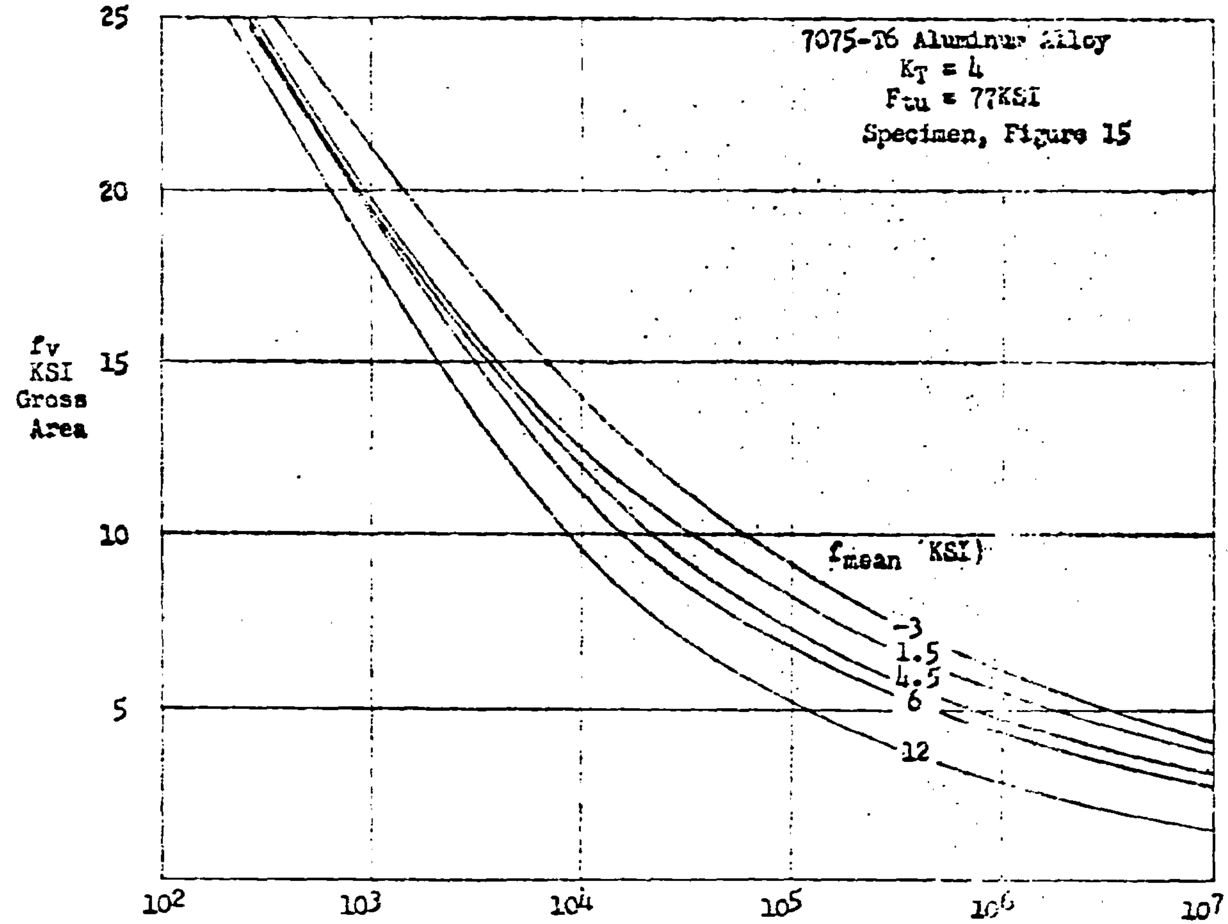

Figure 127 Interpolated S-N Curves for Notched Sheet Coupons - K_T - 4

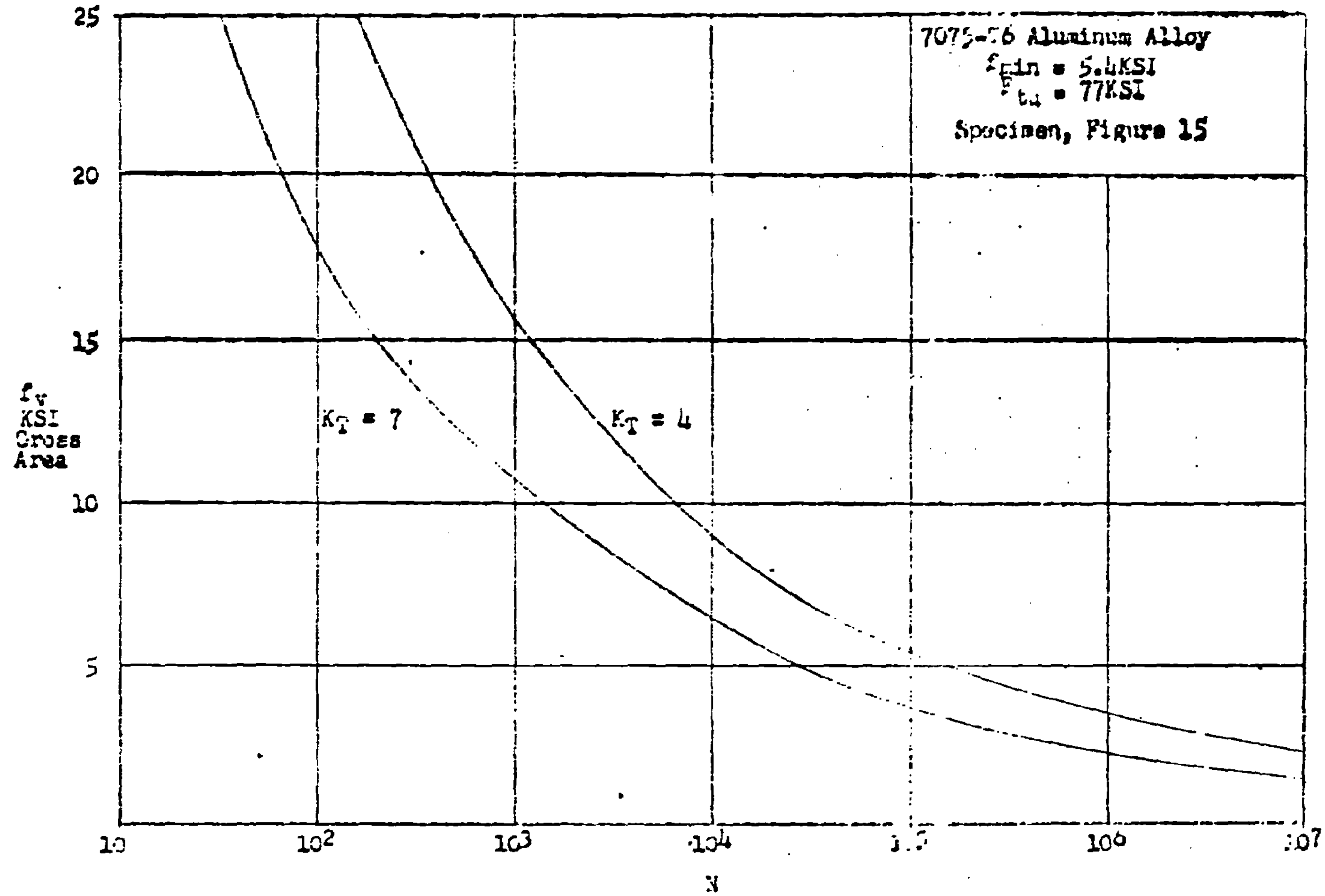

Figure 128 Interpolated S-N Curves for Notched Sheet Coupons Constant Minimum Stress
(For Maneuver Type Loading)

APPENDIX D

PART 2 - SPECTRAL AXIAL LOAD DATA FROM SIMPLE COUPONS

DESCRIPTION OF EQUIPMENT AND PROCEDURES FOR OBTAINING EXPERIMENTAL DATA ON COUPON SPECIMENS

This appendix describes the procedures and equipment employed in accomplishing the experimental and data processing phases of this investigation. An analysis is also presented of the degree of accuracy of the specimen loading histories as a reflection of the command signal emanating from the programming tape. In addition, discussion is presented relative to significant problems encountered in development of methods and equipment.

CONSTRUCTION OF LOADING TAPES

Random Gust Loading Tapes

A one-inch multi-channel magnetic tape recording of a complete flight of an instrumented B-47 airplane was obtained from the Boeing Airplane Company. A photograph of the equipment which was used for converting the flight data to test input tapes is shown as Figure 130. A full length oscillograph of this instrumentation tape was visually scanned in order to identify signals of high cyclic activity. The signals representing the bending moments occurring at the wing root during a 96-minute low altitude pass (800 feet at 280 knots) was selected for adaptation to specimen loading signals for this investigation.

The selected flight record was transcribed on dual-channel 1/4-inch magnetic tape, as shown schematically on Figure 131. The flight record was passed through an electronic scanning system which continuously determined and subtracted out variations of mean load from the initial mean value. The mean variations were recorded on Channel No. 2 and the resulting dynamic signal was recorded on Channel No. 1. In order to obtain the shortest testing time possible within the frequency limitations of the testing equipment, the 96-minute flight histories were compressed to about 6 minutes for the wing root trace. Ten copies of the transcribed wing root trace were recorded and spliced together into one-hour continuous programming tape.

In an effort to obtain a random trace with a markedly different spectrum shape, the dynamic signal (Channel No. 1) of the wing root programming tape was re-recorded through a non-linear amplification system. To illustrate the change in shape produced, spectral representations based on zero crossing peak counts of the wing root, modified wing root unit programming tapes are shown on Figure 132.

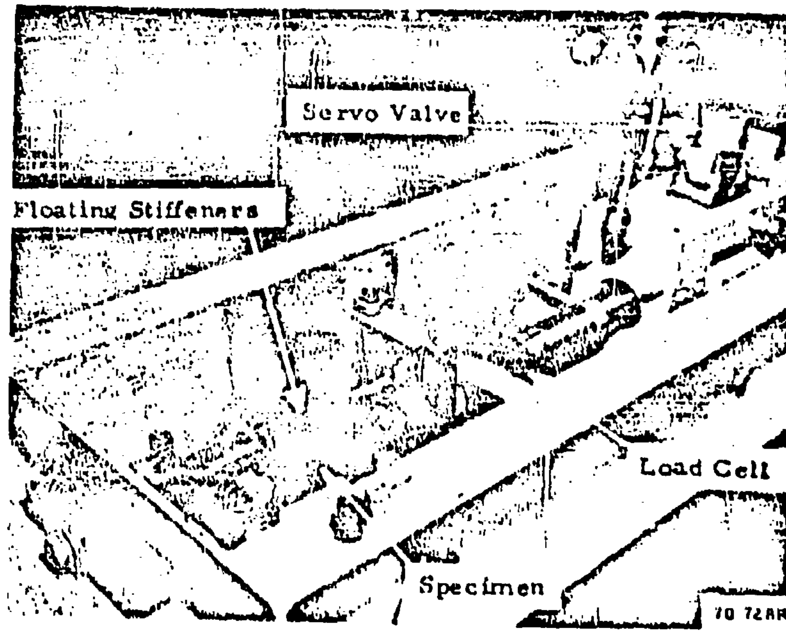

Figure 129 Close-up of Specimen Installation

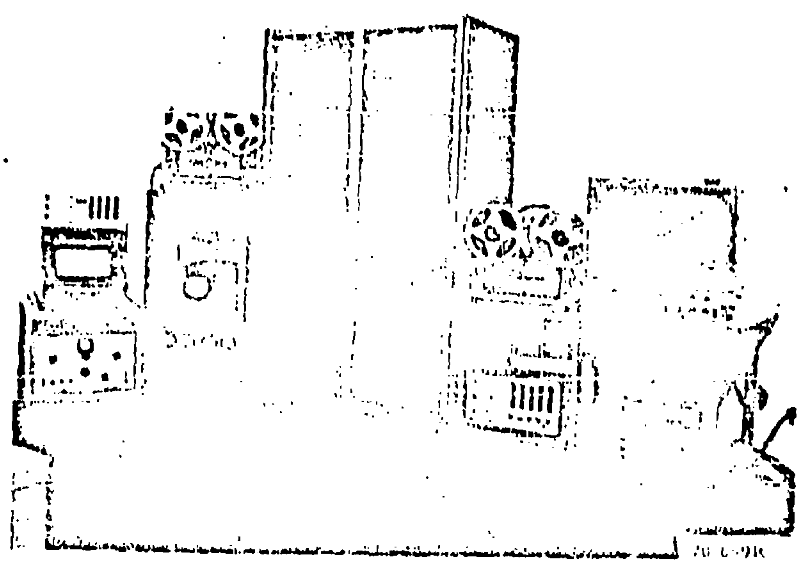
Figure 130 General View of Tape Construction and Data Reduction Equipment

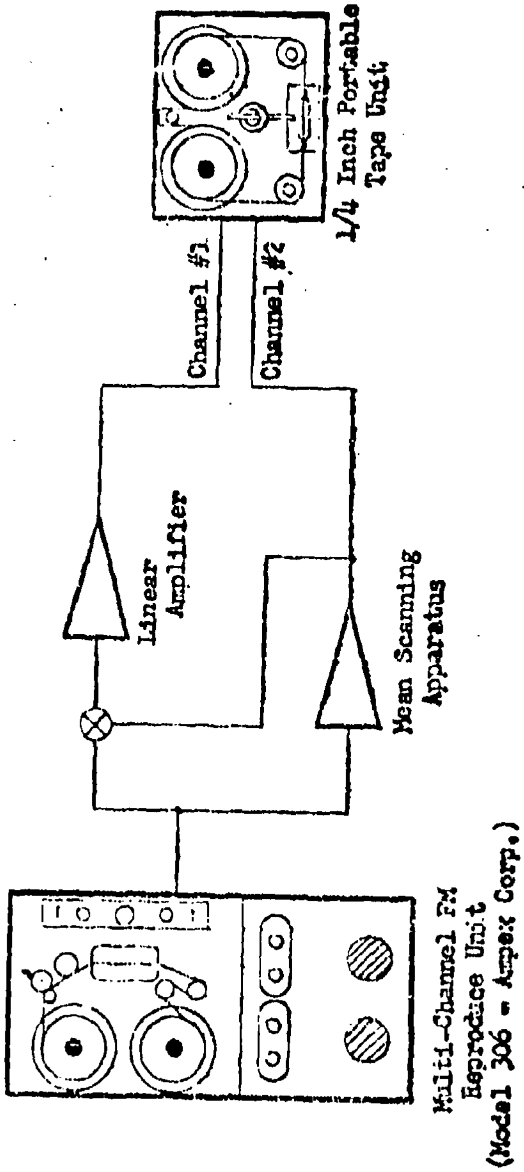

Figure 131 Schematic of Transcription of Flight Record

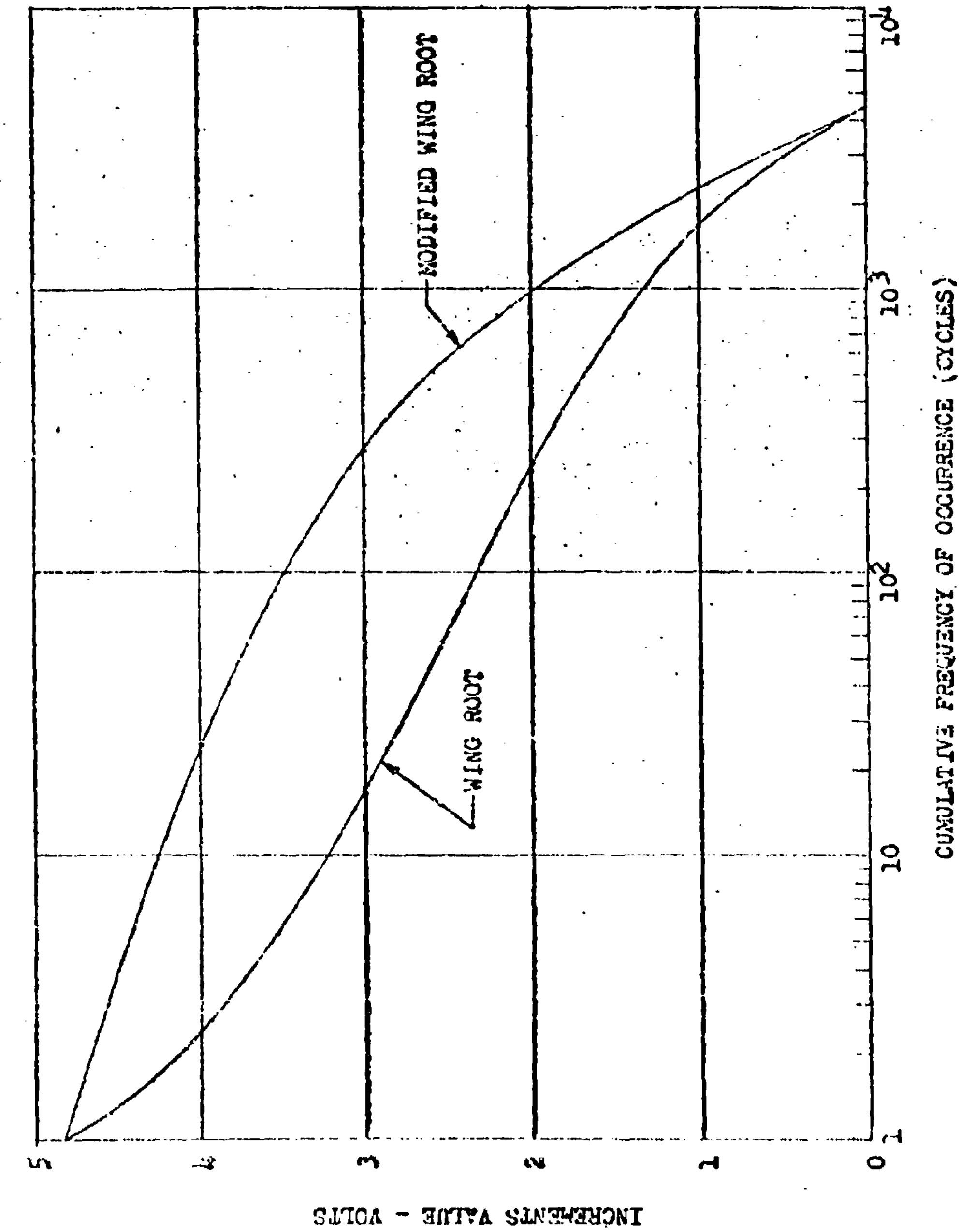

FIGURE 132 MEAN CROSSING PEAK COUNT-WING ROOT AND MODIFIED WING ROOT TRACES

The system used to electrically alter the spectrum shape of a random trace is shown schematically on Figure 133 A desired input-output voltage pattern was drawn on the oscilloscope display screen and the non-linear amplification system was calibrated to match this relationship. Spectrum modification was accomplished by rerecording the tape through this calibrated setup.

FATIGUE TESTING PROGRAM

The limited flight loading histories recorded by the 96-minute wing trace was insufficient to provide the desired characteristics of a representative extende random service loading history. To obtain the desired loading history, the random wing root programming signal was modified. The maximum positive and nega tive loads were made symmetrical and larger loads were inserted so as to repres a longer service loading spectrum.

Repetitions of 10 basic sections of the random signal (identified as A_1, A_2, B_1 B_2 ..... E_1, E_2) were spliced together to make four programming tapes, each approximately one hour long. The A_1 section was obtained by rerecording the the basic wing root signal through a non-linear amplifier such that the maximum negative excursion was limited to match the maximum positive excursion. This operation is similar to that used in making the unit modified wing trace and was shown schematically on Figure 133. The B_1 section was obtained by rerecording the A_1 section through the non-linear amplifier such that the maximum positive and negative excursions are increased about 15%, the next smaller excursions are amplified only slightly and the smallest excursions experience negligible change. The C_1, D_1 and E_1 sections are obtained in the same manner with the maximum positive and negative excursions increased by approximately 20%, 30%, and 40% respectively, over the maximum A_1 excursions. The A_2 through E_2 sections were obtained by rerecording the A_1 through E_1 sections through a 75% linear amplification system. These 10 basic sections are summarized below.

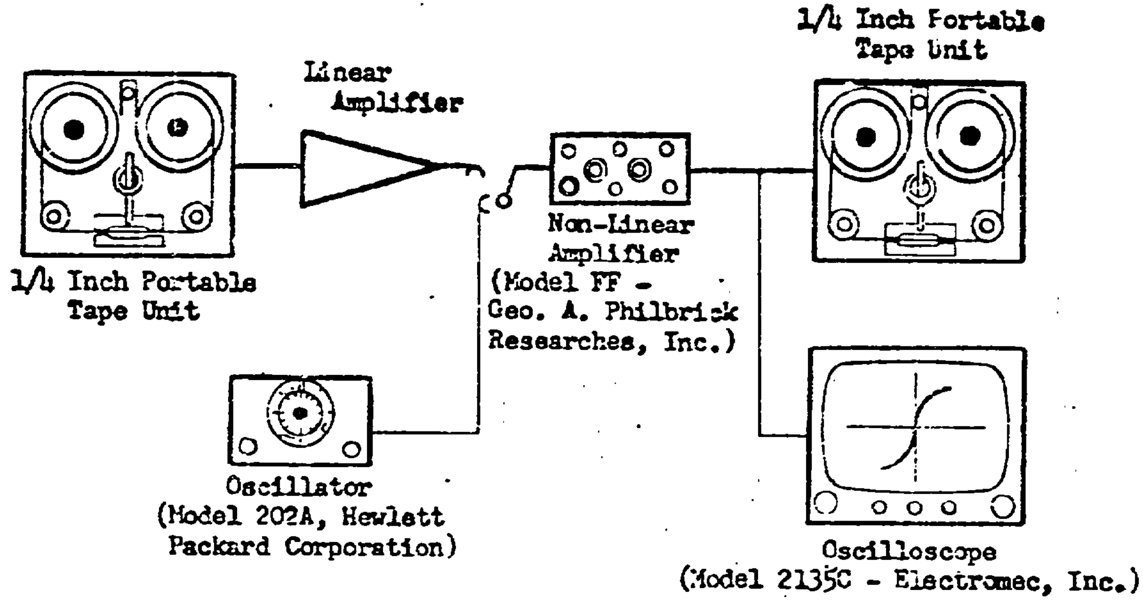

Figure 133 Schematic of System for Altering Spectrum Shapes

A_1	Unit wing root signal modified so that maximum positive and negative excursions are approximately equal.
A_2	Section A_1 x 75% (linear amplifications)
B_1	Section A_1 modified so that maximum positive and negative excursions amplified approximately 15%.
B_2	Section B_1 x 75% (linear amplification)
C_1	Section A_1 modified so that maximum positive and negative excursions amplified approximately 20%
C_2	Section C_1 x 75% (linear amplification)
D_1	Section A_1 modified so that maximum positive and negative excursions amplified approximately 30%
D_2	Section D_1 x 75% (linear amplification)
E_1	Section A_1 modified so that maximum positive and negative excursions amplified approximately 40%
E_2	Section E_1 x 75% (linear amplification)

Four programming tapes (identified as Tape Nos. 49, 50, 51 and 52) were then constructed by splicing the 10 basic sections together in the following sequence.

Tape No. 49

A_1	A_2	A_1	A_2	C_1	A_2	A_1	A_2	A_1	C_2

Tape No. 50

A_1	A_2	A_1	A_2	D_1	A_2	A_1	A_2	A_1	D_2

Tape No. 51

A_1	A_2	A_1	A_2	E_1	A_2	A_1	A_2	A_1	E_2

Tape No. 52

A_1	A_2	A_1	B_2	B_1	A_1	A_2	A_2	B_1	B_2

These four tapes were utilized for testing specimens in the following 14-hour sequence to obtain the desired extended random gust loading spectrum.

Test Sequence	Loading Tape No.
1	52
2	49
3	52
4	52
5	50
6	49
7	49
8	52
9	50
10	52
11	52
12	52
13	49
14	51

Random Military Manuever Tape

Because of the unavailability of an appropriate recording of representative military manuever loadings, a tape was constructed to be consistent with the loading spectrum for fighter aircraft which is described in specification MIL-A-8866.

The unit wing root programming trace was played through the non-linear amplification system so that the negative excursions were suppressed and the positive excursions were modulated to match the spectrum described above. This operation was similar to that described in making the modified wing root trace which was shown schematically in Figure 132.

Step Ordered Gust Loading Tapes

Cyclic step-ordered loading tapes were constructed to simulate the average test life of a given group of random loading histories. Three combinations of stress interval and block size were used:

(1) 1,000 psi stress interval and 1/10 block size
(2) 1,000 psi stress interval and 1/20 block size
(3) 4,000 psi stress interval and 1/20 block size

The system used to construct the step-ordered loading tapes is shown schematically on Figure 134.

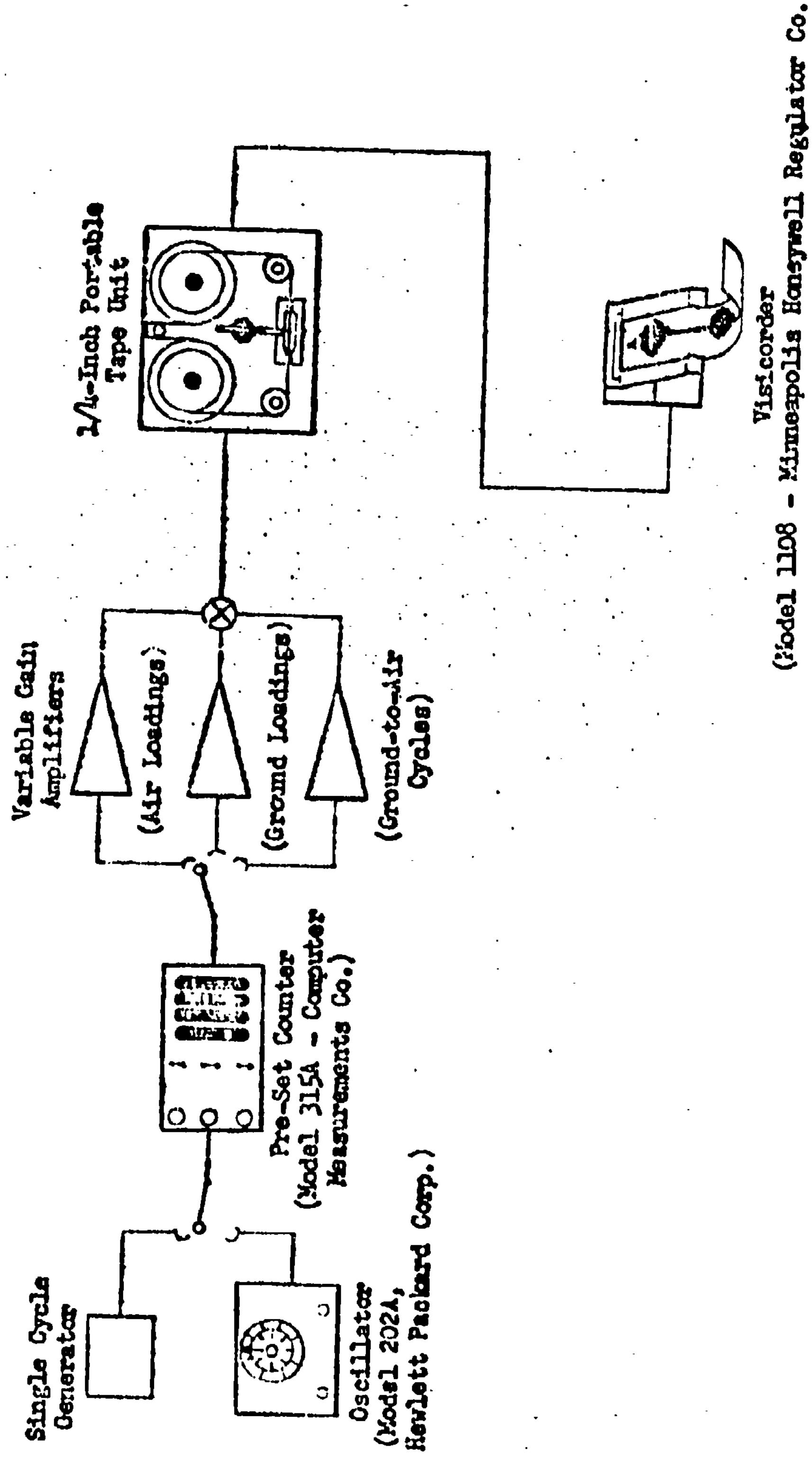

Figure 134 Schematic of Step Ordered Tape Generation

The procedure used in constructing an ordered loading tape is shown in the following examples

For a given average random test history, construct an ordered programming tape of 1,000 psi stress interval size, and 1/10 block size.

(1) Graph the random test history spectrum.
(2) Observe and record in columnar form the cumulative frequency count at the half range intervals (500 psi, 1500 psi, 2500 psi, etc.) on the random spectrum.

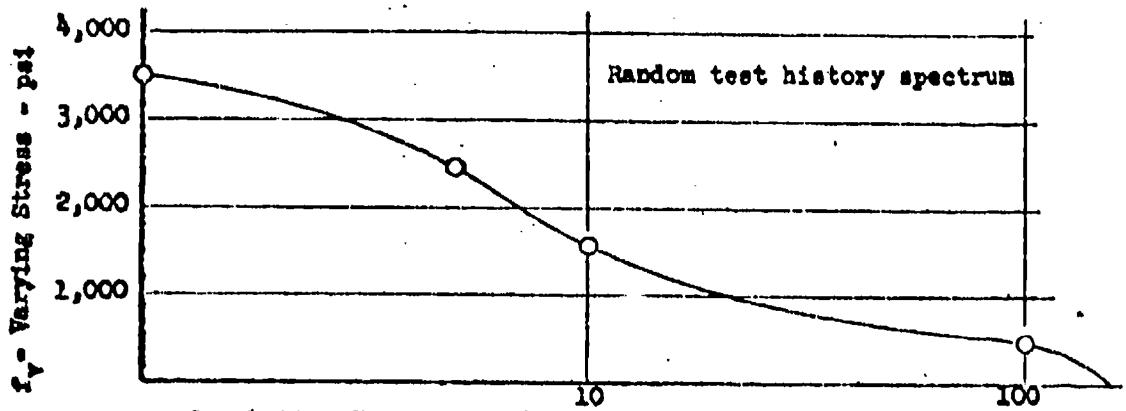

(3) Determine the total number of cycles to be applied at each stress level (1000 psi, 2000 psi, 3000 psi, etc.) by calculating differences between the cumulative counts observed in step (2).

(4) Divide the total number of cycles for each stress level calculated in step (3) by ten. This determines the number of cycles to be applied in each unit spectrum at each stress level. Distribute each fractional cycle to the corresponding half life.

(5) Construct a test programming schedule for the "stress level-cycle" combinations from step (4).

f_v	$\sum n$	n	Unit Spectrum Number									
			(1)	(2)	(3)	(4)	(5)	(6)	(7)	(8)	(9)	(10)
500	100											
1,000		90	9	9	9	9	9	9	9	9	9	9
1,500	10											
2,000		5	1		1		1		1		1	
2,500	5											
3,000		4	1			1		1			1	
3,500	1	1					1					

(6) Employing an "oscillator-preset counter-recorder" combination, (shown schematically in Figure 134) record the ordered loading tape as described in the programming schedule constructed in step (5).

Unit Spectrum No. 1 Unit Spectrum No. 2 Unit Spectrum No. 3

Step Ordered Military Maneuver Loadings

Step ordered loading tapes were constructed representing the average random military maneuver test histories. These ordered loading tapes were constructed utilizing the same procedure used in making the step ordered gust loading tapes except that the negative excursions were suppressed by passing the generated signal through a diode.

Step Ordered Composite Loading Tapes

Step ordered programming tapes were constructed representing random composite test histories. These ordered tapes were constructed for both gust and military maneuver type air loadings employing the same procedure described in the example above. Air loadings, ground loadings, and ground-to-air transitions were treated as three separate random spectra and separate programming schedules were made for each spectrum. The complete ordered composite tape was made as follows:

(1) The first unit spectrum of air loadings was recorded, as tabulated on its programming schedule, about the mean load for which the corresponding random air loadings were applied.

(2) The first unit spectrum of ground loadings was also recorded, as shown on its programming schedule, at the mean load at which the corresponding random ground loadings were applied.

(3) The first unit spectrum of ground-to-air cycles was recorded such that the peak-to-peak excursion extended from the air loading mean to the ground loading mean.

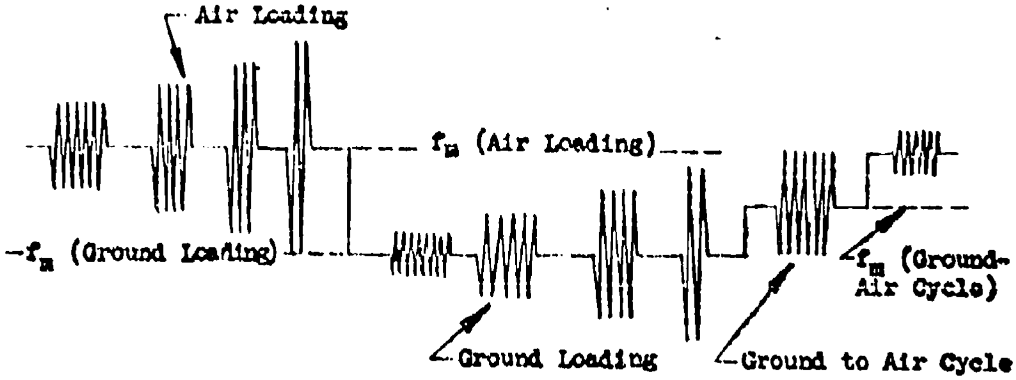

The procedure described above was used to generate the first unit composite loading spectrum. The succeeding spectrum units were constructed in the same manner.

The standard equipment items used in this tape construction work are indicated on the schematics on Figures 133 and 134. The portable tape unit is a two-channel frequency-modulated 1/4-inch record and playback unit. The tape deck is a series 30 recorder manufactured by American Electronics, Inc., and the electronics were designed and developed by Lockheed. Characteristic of this unit are:

Carrier frequency - 3,400 cps
Tape speed - 7 1/2 inches per second
Minimum signal to noise ratio - 40 db
Maximum record voltage - 9.0 volts
Playback filtering - 60 or 500 cps

SPECIMEN LOADING

The specimen loading system which was developed for this investigation was basically simple in mechanical detail, utilizing for the most part standard commercial equipment for signal input, hydraulic load control and loading readout. However, to appreciate the demands upon the system it must be realized that in this investigation the primary testing requirement involved application of specimen loadings which faithfully followed command signals of a very complex nature. The controlled application of such loadings dictated the selection and development of servo control circuitry and the development of special test monitoring techniques. A description of the loading system is presented below followed by a brief discussion of several problems encountered during testing.

DESCRIPTION OF SPECIMEN LOADING EQUIPMENT

Fatigue loading equipment was developed for the rapid application of the loadings defined by signals on the magnetic tapes described in preceding paragraphs. This equipment basically provides an electro-hydraulic servo system consisting of a test specimen in series with a servo valve-jack combination, with the loadings programmed by the signal from magnetic tape. This system is shown schematically on Figure 135.

As shown on this figure, the output signal from the programmer is fed into the servo loop through the summing junction. The amplified input signal programs the action of the servo valve in metering cyclic flow of oil to the fore and aft parts of the servo jack. The output signal of the load transducer strain gage is amplified and fed back into the summing junction closing the loop. The instantaneous summing of these two opposing signals at the input side of the servo valve ideally results in the specimen experiencing the loading history represented by the signal on the loading tape. In utilizing such a system due cognizance was given to inherent mechanical and electrical limitations of the entire system, especially with respect to frequency response and flow characteristics of the servo valve.

The 1/4 inch programming tape unit used for spectral loading input is the same basic unit as the 1/4 inch portable tape unit which was used for preparation of the program tapes except that it does not have recording capabilities. The servo loop command and feed-back electronics were basically Model K2-W operational amplifiers in series with Model K2-P chopper stabilizing amplifiers, manufactured by George A. Philbrick Researches, Inc. A diode clipper was mounted in the electrical circuit between the tape unit and the summing junction which limited the amplitude of the programming signal supplied to the summing junction in case of signal overload. This diode clipper was also basically a Model K2-W operational amplifier.

The servo jack was a Lockheed designed hydraulic actuator with a maximum static force rating of 17,000 pounds. The servo valve employed to program the action of the hydraulic actuator was a Model 26 Flow Control Valve, manufactured by Hydraulic Research and Manufacturing Company. This servo valve has a flow control range from 0.15 to 10 gpm for an operating pressure range of

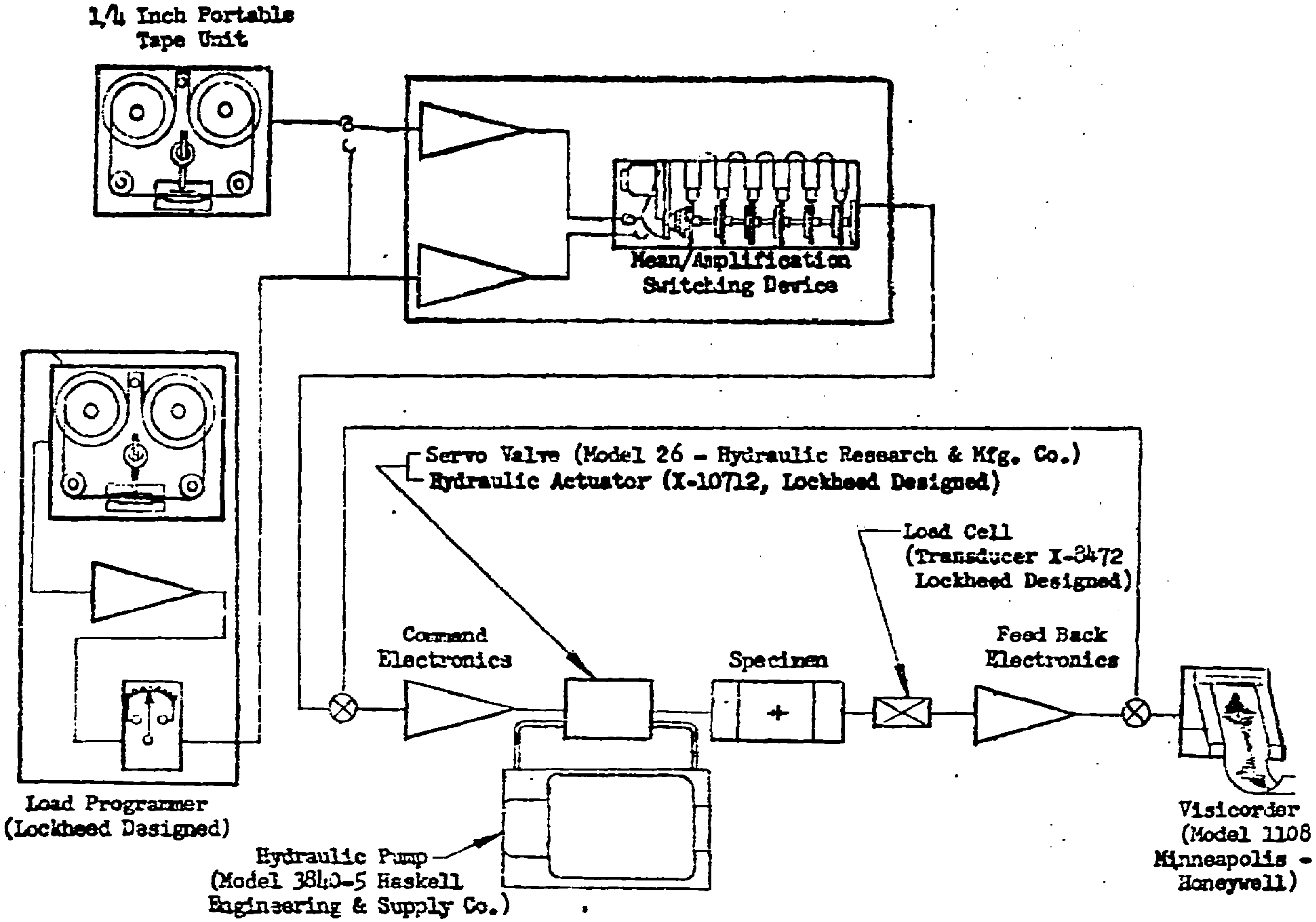

Figure 135 Schematic of Test Loading System

150 to 4,000 psi. The transducer used as the sensing unit in the system was a Lockheed designed strain gaged load cell. This transducer is cylindrical in constructional detail and is equipped with a full bridge gage installation, the electrical output being essentially insensitive to bending strain. Four complete loading systems were developed for this testing program and are shown in operation on Figure 136. The tape playback unit, the electronics and associated components for programming two separate servo loops were mounted in a self-contained unit as shown on Figure 137. A photograph of a valve-jack combination, load transducer and specimen, all rigidly mounted in one of the loading fixtures, is shown on Figure 129. The specimen was mounted in the test fixture by rigid friction grips, and floating stiffeners were used on the unsupported edges of the specimen to prevent buckling as shown in Figure 129. A failure wire was cemented to the specimen in the area of maximum stress concentration and connected to a relay. Upon initiation of a fatigue crack the failure wire circuit was interrupted, instantaneously blocking off hydraulic flow to the actuator.

PROCEDURE FOR SPECTRAL LOADING OF SPECIMENS

Prior to the application of loads to each specimen, the loading system was calibrated and adjusted to produce the applicable loading history represented on programming tape. Although several steps in the calibration and dynamic loading procedure were common to all spectral tests, certain steps were followed only for particular types of loading history. Outlines of the procedures follow.

Loading Histories Having Constant Mean Load Values

(1) From known transducer data, a calibration factor of load versus electrical output was determined which related the maximum signal voltage on the program tape to the highest load to be applied to the specimen. This maximum signal was recorded on an oscillograph for later reference.

(2) A dummy specimen, serving merely as a load link during calibration was installed in the test fixture and the static mean load was applied by dialing in the equivalent voltage to the servo valve circuit.

(3) The required dynamic signal amplification was set, based on the loading tape voltage calibration factor.

(4) The maximum dynamic load was applied to the dummy specimen and the load cell signal output was recorded on an oscillograph for comparison with the static signal previously recorded.

(5) Deviation of the maximum loading cycle from the desired load level was corrected by a compensating adjustment of the signal amplification, and step 4 was repeated.

(6) When the desired loading level for the maximum cycle was obtained the calibrating system was replaced by a test specimen.

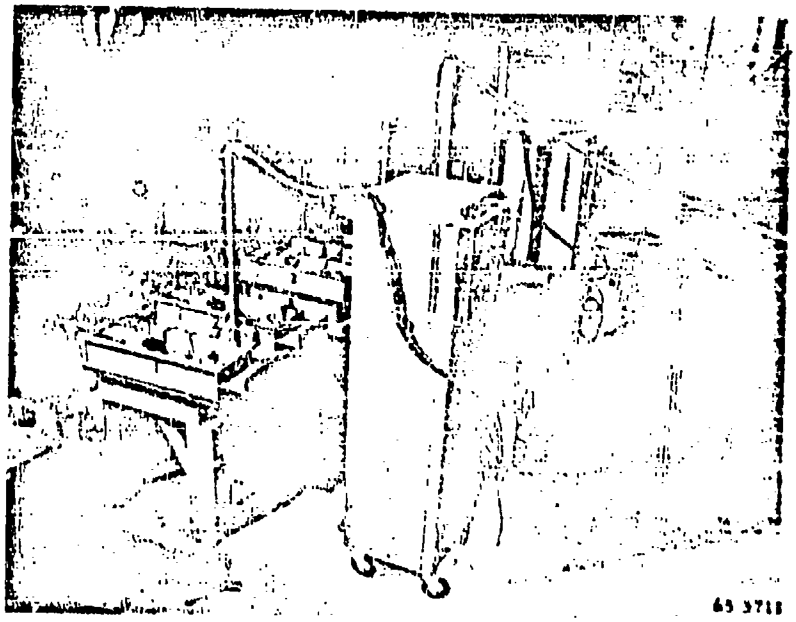

Figure 136 General View of Specimen Loading Apparatus

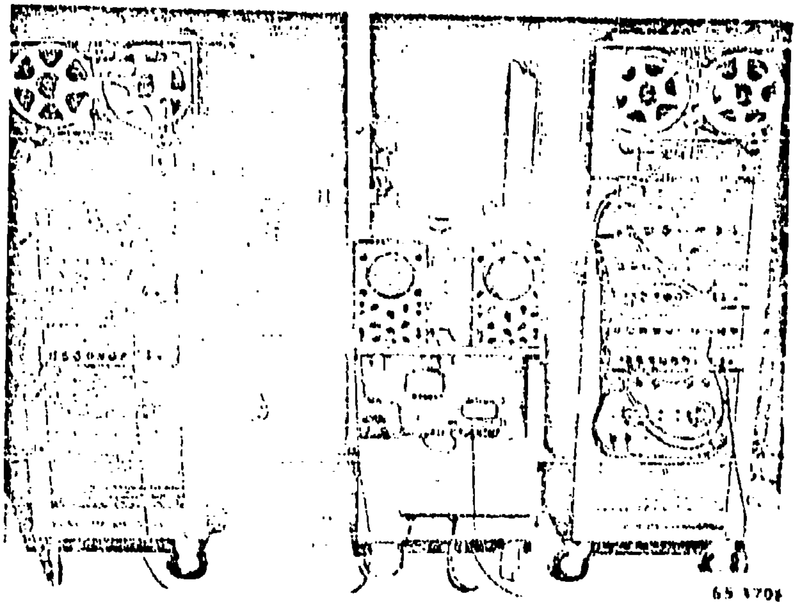

Figure 137 Magnetic Tape Loading Control Units

(7) The loading trace was then applied to the test specimen. The maximum loading cycle was periodically monitored on the oscillograph and required adjustments made to the amplification of the dynamic signal to maintain the desired loading level.

(8) Testing was continued until the initiation of a fatigue crack interrupted the failure wire circuit terminating the loadings. In addition, interruption of the failure wire circuit cut off the power source to the electrical timing device recording the duration of specimen life.

The full range of random loadings applied to the test specimen were periodically monitored to determine the spectrum content of the applied loads, and as an added check on the stability of the frequency response of the loading system. Monitoring of these random loadings was accomplished by recording on magnetic tape the output signal from the load transducer for each unit loading trace applied. These unit monitor tapes were then electrically counted as described later in the data reduction section.

Periodic monitoring checks were also made of the ordered loadings applied to the specimen. Monitoring of the ordered loadings applied in the preliminary investigation was accomplished in the manner described above for the random loadings. Monitoring of the step ordered loadings consisted of periodic recording on an oscillograph of the load transducer output signal for the complete ordered loading trace. The loads for each group of cycles were calculated from the oscillographic record and compared with the schedule from which the loading tape was constructed.

Loading Histories Having Variable Mean Load Values

Random composite loadings with gust type air loadings were produced by using the same loading tape signal for both air loadings and ground loadings. The ground loading trace was similar to the air loadings except that different static mean load and amplification of the dynamic signal were used. The loading tape signal was routed through an electro-mechanical device which periodically shifted both static mean load and amplification of the dynamic trace. The procedure for alternately applying these two loading traces from the same input signal was as follows:

(1) A calibration factor for the load programming system was determined relating specimen load to loading tape voltage and a calibration signal was recorded on an oscillograph. The input voltage relationships required to define the desired loading history were then calculated.

(2) With a dummy specimen installed in the loading fixture, the switching device was locked in one of the spectrum loading positions and the static mean load was applied with a bias voltage.

(3) The required dynamic signal amplification was set based on the loading tape voltage relationships calculated in Step 1 above.

(4) The maximum dynamic signal was applied to the calibrating specimen and recorded on an oscillograph for comparison with the previously recorded loading system calibration factor.

(5) Deviation of the maximum loading cycle from the desired load level was corrected by a compensating adjustment of the signal amplification and the repetition of Step 4.

(6) The switching device was then locked in the second loading condition and Steps 2 through 5 were repeated to obtain its desired dynamic trace amplification.

(7) After the desired loading levels for the maximum loading cycle were obtained, the calibrating specimen was replaced by a test specimen.

(8) The loading trace was then applied to the specimen and the switching device was started at the commencement of the dynamic signal.

(9) The maximum composite loading cycle was periodically monitored on the oscillograph and the required adjustments were made to the amplification of the dynamic signal to maintain the desired loading level.

(10) Testing was continued until a fatigue crack developed. The loading was terminated by failure of the previously described failure wire and the test duration was recorded.

Random composite military maneuver loadings were produced by employing the signals from two separate loading tapes. To apply these loadings the portable tape unit used in the tape construction work was operated in parallel with the programming tape unit as shown schematically on Figure 135. These two signals were fed into the same switching device used in applying the random composite gust loadings. The switching apparatus alternately switched static mean loads and the dynamic signal inputs. The setup, calibration, testing and monitoring were also accomplished in the manner described above for random composite gust loadings.

Ordered composite loading tapes were constructed so that the relationship between the static mean load and the dynamic loading level was recorded on the tape. Thus only one signal amplification was required for the composite tape to apply the desired composite loading spectra. The procedure for setting the loading levels, testing and monitoring, was the same as described for the single spectrum loadings.

Discussion of Loading System Development

In developing this loading system a number of problems were encountered. The resolution of the overall problem of applying the same loading history to the specimen for repeated applications of the same loading trace required considerable effort. Many factors contributing to this overall problem complicated the development of a completely reliable loading system throughout a major portion of the preliminary investigation. Some of the contributing problems are discussed in the following paragraphs.

In order to extend the operating frequency range of the servo valve and system, electrical lead networks were developed. A flat frequency response over the range of 0 to 45 cps with attenuation of 3 db at 60 cps within a

maximum allowable deviation of ±2% was set up as the performance standard. Values for the lead network components were determined from the frequency response of the basic system. In addition individual lead networks were tailored to compensate for the cumulative effect of the characteristics of each servo loop in order to meet these requirements.

In the continued effort to improve the overall loading system performance, the meter originally used in setting the level of the input loading trace was replaced by a direct reading oscillograph (Visicorder). The use of the oscillograph permitted utilization of a dynamic signal for calibrating the loading tapes. This more realistic method of setting the loading level with a dynamic signal in the frequency range of the applied loading cycles greatly improved the control of variations in frequency response.

Due to deterioration in servo valve performance and aging of electronic components, it was necessary to monitor continuously the frequency response of the servo system. A function generator was used in conjunction with an oscillograph to check the servo system response and by adjustment of the forward and feedback gains of the servo amplifier, the system response could be maintained within the limits of the ±2% deviation.

Variations were noted, during the early testing stage, between loading histories sampled at discrete intervals for the same input trace. This was concluded to be due mainly to large fluctuations of the hydraulic oil temperature occurring over a normal operating period since corresponding fluctuations were also observed in the frequency response of the loading system. Stabilization of the hydraulic oil temperature through the use of an immersion heater or regulation of cooling water through a heat exchanger greatly reduced these response variations.

Proper mechanical operation of the servo valve demands that the hydraulic fluid be filtered of all particles which are greater than approximately 25 microns in diameter. In order to assure reasonable filter life the entire hydraulic system was maintained as free as practicable of contaminants. The formation of varnish or generation of corrosion particles results in costly shutdown periods and is a constant threat to the attainment of reliable test data. Therefore MIL H 5606-A hydraulic fluid was selected because of its stable and non-corrosive characteristics. This particular problem proved to be a costly one during the early stages of the testing phase of this investigation.

Bearing in mind that the specimen loading system was, of necessity, highly responsive to tape signal command, it can readily be seen that it was imperative that loading input tapes remain as free as possible of extraneous signals which might affect testing validity. These false signals may be of such strength to cause serious overloading or destruction of the specimen. In an effort to produce and maintain loading input tapes essentially free of false signals, special tape handling procedures were adopted. Electrical means were also employed to repress false signals of any significant magnitude, during load application.

In passing a magnetic tape across a signal reproduce-head any irregularity of the tape surface causes a momentary loss of playback signal known as a drop-out, resulting in the appearance of a maximum voltage at the output terminals of the tape unit reproduce-electronics. The response characteristics of an electro hydraulic servo loop are such that the loading system instantaneously applies the maximum possible load to the test specimen. The major causes of tape drop-outs are improper tape splices, flaking of the magnetic surface, and minute dust particles collecting on the tape surface. A method of completely eliminating drop-outs was not achieved, but by a continual effort in guarding against conditions conducive to their origin, their occurrence was effectively minimized.

The principal efforts extended in minimizing the occurrence of drop-outs were as follows:

1. Dust protective shields were installed around the area of the loading tape and signal reproduce-equipment. A practice of periodic cleaning was rigorously followed.

2. Multi-pass loading tapes were constructed by splicing together recorded sections of the unit loading trace. These loading tapes were rerecorded onto splice-free tape for use on the load programming units. In the event of accidental damage or flaking of the magnetic coating of the test loading tape, resulting in a permanent drop-out, a duplicate splice-free copy was made of the originally spliced multi-pass tape.

3. Where single drop-outs or other strong extraneous signals existed which were not the result of splicing, electrical means involving the use of diode clippers were utilized to subdue the strength of the signal. To this end the clipper circuit was adjusted to cut off all signal strength which was in excess of that signal representing the highest spectral load.

CONSTANT LOAD AMPLITUDE TESTING EQUIPMENT

As noted in the main body of the report, sets of S-N curves were developed as reference data for the random loading and spectrum loading tests. The S-N tests were conducted in resonant beam fatigue test machines. In this type of fatigue machine, loads are developed by means of a motor-driven rotating eccentric weight fastened at the free end of a pivoted beam. This beam is tuned to a frequency slightly higher than the driving frequency produced by the motor (1800 rpm). The test specimen is mounted normal to the axis of the beam and so is loaded axially by the beam displacements. Static and dynamic loads are measured and monitored using the output of strain gages mounted on a load cell which is loaded in series with the test specimen.

DATA REDUCTION

DESCRIPTION OF COUNT METHODS

At [illegible] art of this program a large number of count methods were reviewed in te[illegible] their applicability. All of these methods were variations of three basic count methods: "Peak Count," "Range Count" and "Interval Crossing Count." One of these three basic types of count methods was then selected for further use as applied to the gust data records used in this study. This was the mean crossing peak count method. The manner in which the selected count method was applied is described below.

Mean Crossing Peak Count

Given load-time trace $y = f(t)$

(1) Establish load levels of interest $y_1, y_2, y_3 \ldots y_n$ above and below mean

$$\bar{y} = \frac{1}{T}\int_0^T f(t)dt$$

(2) Establish all points at which $y = \bar{y}$, that is , where load-time trace crosses mean.

(3) Between two successive crossings of the mean establish:

a) The maximum value of load-time trace for portions greater than mean (peak).

b) The minimum value of load-time trace for portions less than mean (valley).

(4) Count the number of peak maximum values above any paticular level of interest.

(5) Count the number of valley minimum values below any particular level of interest.

(6) Summarize counts.

This Procedure is Illustrated in Figure 138.

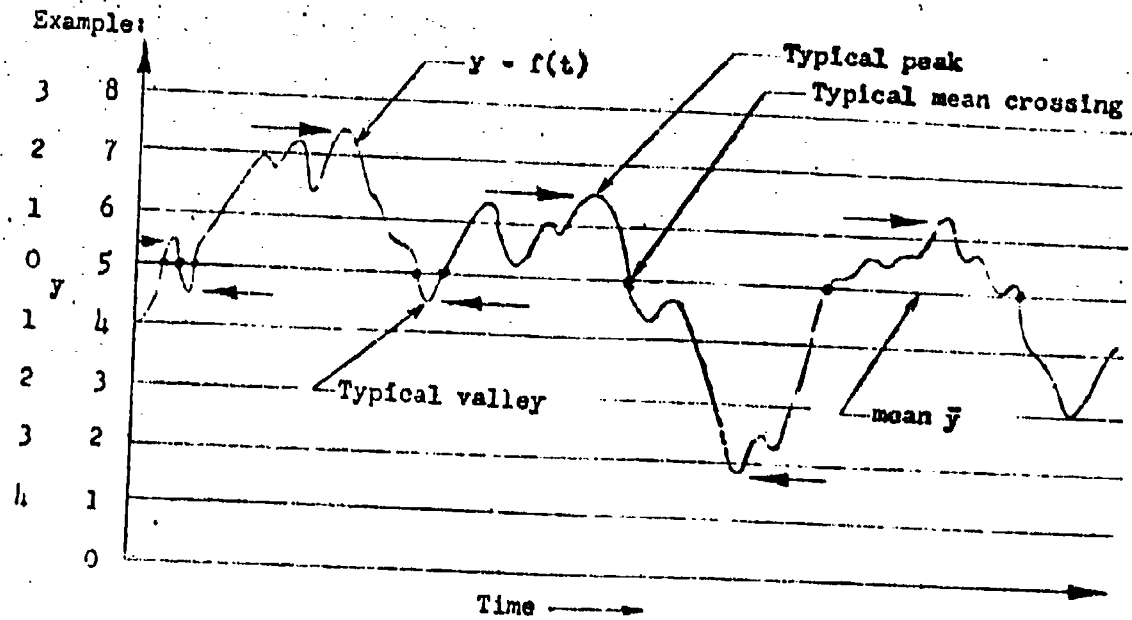

Level of Interest	0	1	2	3	4
Peak Count	4	3	1	0	0
Valley Count	3	1	1	1	0

Figure 138 Definition of the Mean Crossing Peak Count Method

ELECTRICAL COUNTING SYSTEMS

An integrated system was developed for high speed statistical analysis of random and ordered spectra employing analog methods. A counting system was developed for obtaining a mean crossing peak count at counting rates up to 500 cycles per second. This integrated system basically consists of a magnetic tape input unit, an analog computer and an electronic totalizing counter. Figure 130 shows this system programmed for counting.

The magnetic tape input unit was the 1/4 inch portable tape unit used in the construction of the loading tapes. A Model 521C electronic counter manufactured by the Hewlett Packard Corporation was employed to record the statistical data from the counting circuit.

The analog computer consists of eight standard K5-U computing amplifiers and twenty K2-W operational amplifiers manufactured and packaged in a self-contained unit by George Philbrick Researches, Inc. Four separate input signals can be scaled, the polarity inverted, and then summed in the K5-U computing amplifiers. In addition, a reference voltage of either polarity can be subtracted from its final output. The K2-W is a basic operational amplifier in that no input or feedback resistors are associated with it. By adding resistors, capacitors, and diodes externally the K2-W can be made to operate as an inverter, filter, mean integrator, buffer, peak follower, or voltage crossing detector. Schematical representations are shown on Figures 139 and 140 for the operational configurations in which these amplifiers were employed in the counting circuit. In addition, the counting circuit developed for the mean crossing peak count method is shown schematically in Figure 141.

The initial calibration of this circuit was based on use of a five-minute section of the original B-47 wing root loading trace. This trace was recorded on 1/4 inch magnetic tape suitable for electrical counting and an oscillograph was made. The visible trace was scanned and the mean crossing peak count was tabulated. This tabulation was then used as a guide in assessing the performance of the counting circuit.

In the development of this counting system certain problems were encountered which were largely due to the demand for unique applications of analog computer elements. A number of possible circuits were evaluated in the search for counting systems which were accurate and reliable. The selection and use of high quality components was a requisite to the reliable performance of all circuits. Precision carbon resistors and high quality mylar capacitors were used exclusively in all operational amplifier circuitry. Silicon crystal diodes were used in the initial phases of counting circuit development but later proved to possess insufficient reverse impedance to reset the peak follower in all instances. Vacuum tube diodes were substituted, providing reliable operation of the peak follower circuit.

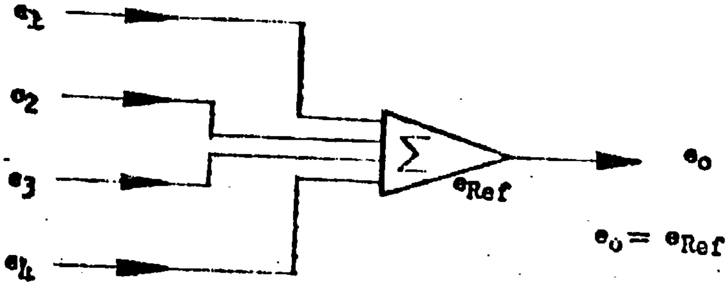

$$e_o = e_{Ref} + \sum (a_1e_1 + a_2e_2 + a_3e_3 + a_4e_4)$$

K5-U Computing Amplifier

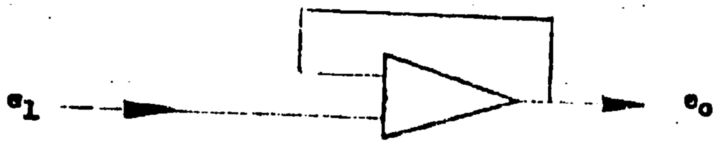

$$e_o \approx e_1$$

Buffer - K2-W Operational Amplifier

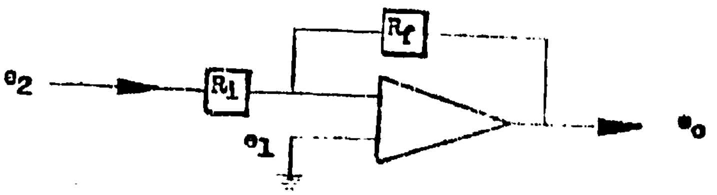

$$e_o \approx - \frac{R_f}{R_1} e_2$$

Inverter - K2-W Operational Amplifier

Figure 139 Applications of Basic Computer Elements

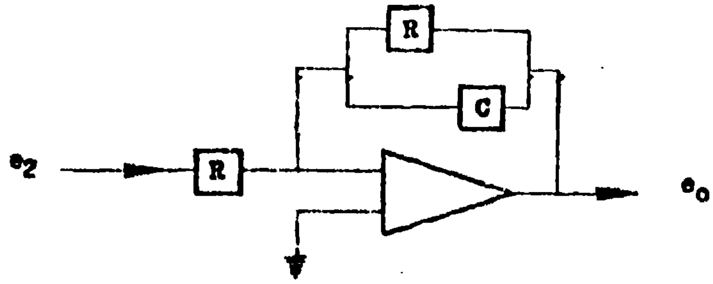

for filter $RC \ll 1$, $e_o \approx - e_2$

for mean integrator $RC \gg 1$,

$$e_o = \frac{1}{t}\int_o^t e_2 dt$$

Filter and Mean Integrator
K2-W Operational Amplifier

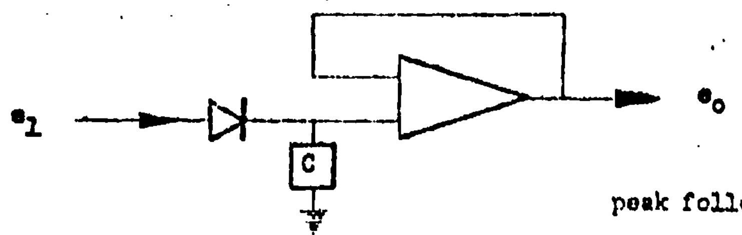

peak follower $e_o \approx + \left| + e_{1_{max}} \right|$

Peak Follower - K2-W Operational Amplifier

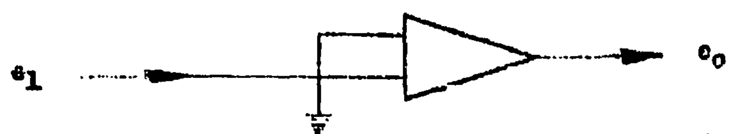

$e_o = +70 \Big|_{e_1 > 0}$; $e_o = -70 \Big|_{e_1 < 0}$

Voltage Crossing Detector
K2-W Operational Amplifier

Figure 140 Applications of Basic Computer Elements

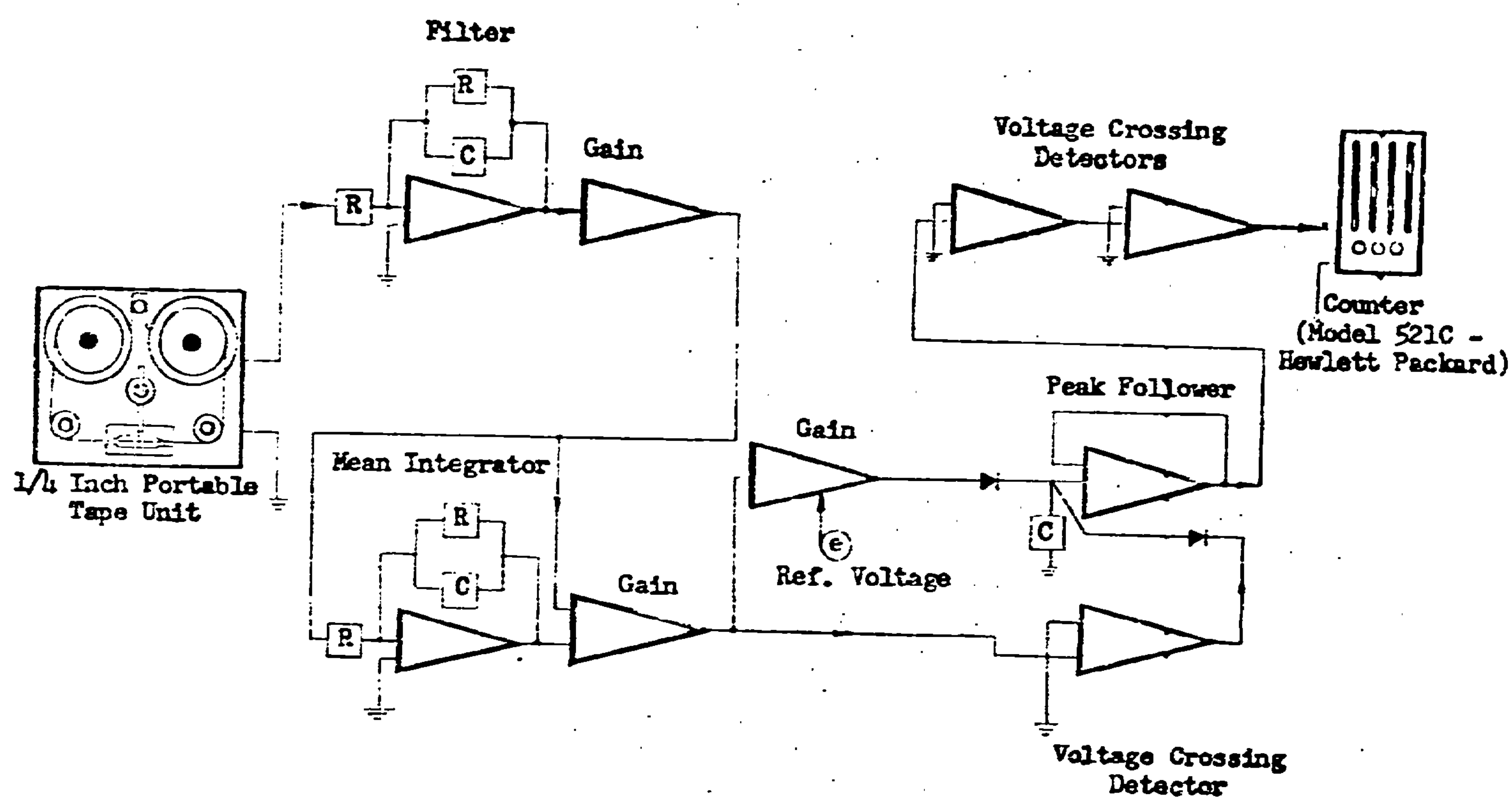

Figure 141 Schematic of Computing Circuit for the Mean Crossing Peak Count

Procedure for Counting Random Spectra

Monitor tapes for the load transducer output signal, representing the specimen loading history, were recorded for a unit section of each random programming tape. These unit loading signals were then programmed through the computing circuit and their count distributions were recorded in columnar form.

The counting of a particular monitor tape was accomplished in the following manner:

(1) The counting circuit was installed on the analog computer and a schedule was made of the load levels at which counts were desired.

(2) The load level was dialed into the computer and the monitor tape signal was programmed to the counting circuit.

(3) Cumulative counts were displayed on the electronic counter as the unit section of monitor signal was transmitted through the computing circuit.

(4) When all of the monitor tape signals had been played through the computing circuit, the total cumulative counts were recorded for permanent record and the sequence was repeated for each load level in the counting schedule.

Procedure for Counting Ordered Spectra

Monitor tapes were also recorded from the load transducer output signal for a unit section of each ordered loading tape constructed in the preliminary investigation. These monitor tapes were counted in the same manner as described above for counting the random spectra.

Counting of the monitor tape output signal for the step ordered loading tapes constructed in the principal part of this investigation was obtained in the following manner.

(1) An oscillographic record was made of the load transducer output signal for the full length of each step ordered programming tape.

(2) The amplitude at each load interval was scaled and the load level determined by comparison with a known calibration.

ANALYSIS OF ACCURACY

A step by step procedure of the testing, monitoring, and counting operation is summarized below. The values of maximum possible error at each step in this procedure are shown. The nature of such error sources is noted in the procedure outline and also keyed to the schematic diagram shown in Figure 142.

These individual errors were added directly to obtain the maximum error limits shown graphically on Figure 143. However, a more realistic evaluation of the accuracy of the presented data is obtained from the 95% probability error limits presented graphically on Figure 144.

TEST PROCEDURE USING MULTI-PASS LOADING SPECTRUM PROGRAMMING TAPE	% of Error
(1) Apply static calibration of load cell H to Visicorder (J)	
a) Load cell calibration	±1.0
(2) Start tape transport (A) and play output signal thru tape electronics (B) and servo loop (D-E-F-H) and record load cell (H) output on Visicorder J. Compare maximum dynamic range to static calibration on Visicorder (step 1) and adjust gain pot C to apply desired maximum specimen stress	
a) Stability of programmer electronics (B)	±0.5
b) Stability of servo command electronics (D)	±0.02
c) Frequency response deviation (E)	±2.0
d) Specimen cross sectional area variation (F)	±1.5
e) Stability of load cell monitor electronics (I)	±0.02
f) Visicorder frequency response (J)	±3.0
g) Reading accuracy - comparison Visicorder calibrations (J)	±2.0
(3) Continuous loading applied to specimen with calibration techniques (steps 1 and 2) applied periodically	
a) Variation of frequency response	±0.5

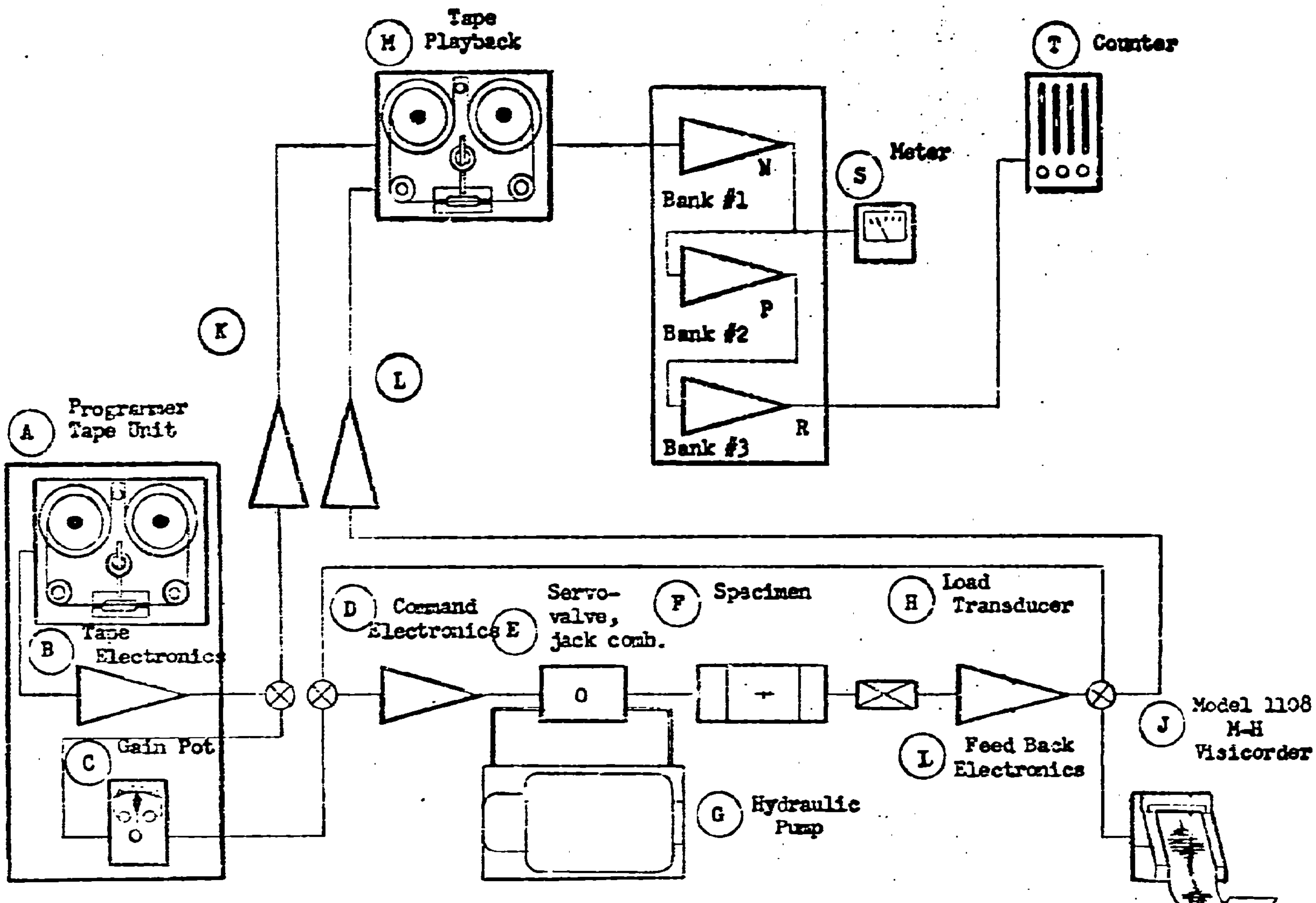

Figure 142 Schematic of Complete Testing, Monitoring and Counting Process

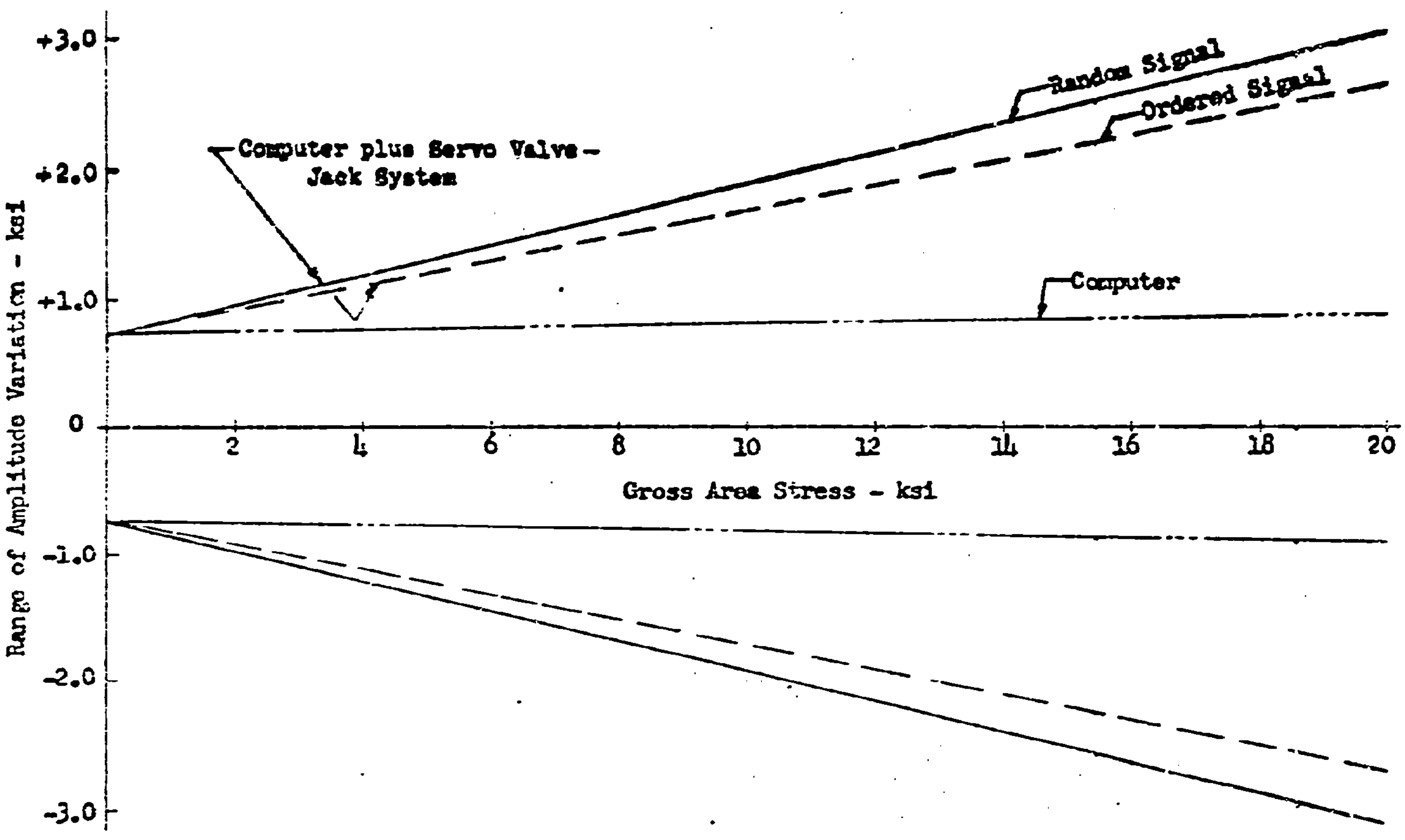

Figure 143 Maximum Error Limits

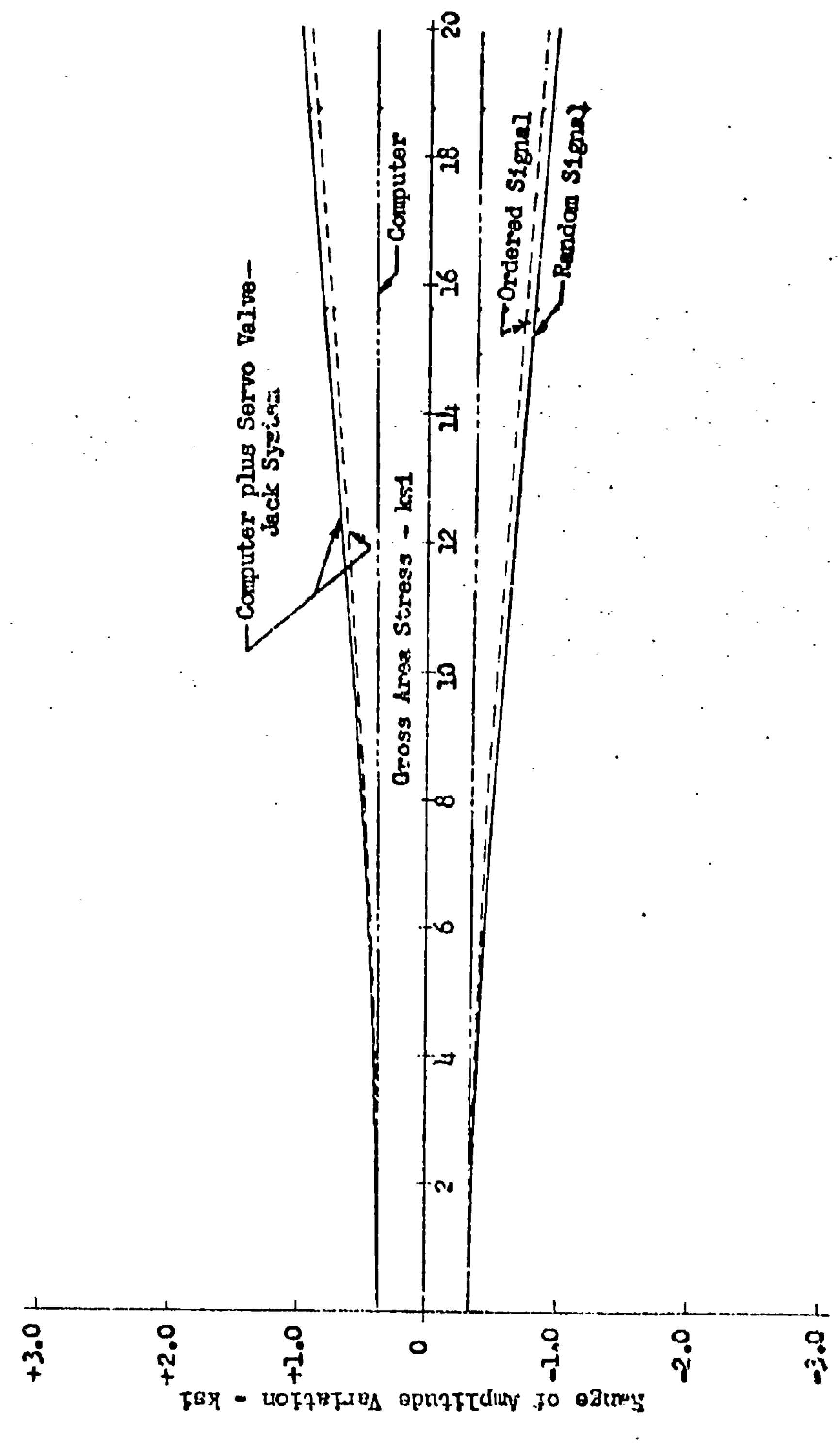

FIGURE 144 95% PROBABILITY ERROR LIMITS

PROCEDURE FOR RECORDING MONITOR TAPE
OF SPECIMEN LOADING HISTORY

		% of Error
(1)	Output signal of load cell (H) played through monitor electronics (L) and unit section of basic data recorded on recorder (M).	
	a) Stability of load cell monitor electronics (I).	---
	b) Stability of recorder electronics (L).	±0.5

PROCEDURE FOR COUNTING MONITOR TAPE

(1)	Program monitor signal into computer (N), (P) & (R) and observe occurrences of data characteristics on counter (R).	
	a) Balance computer bank No. 2 (P).	±0.09 *
	b) Balance computer bank No. 3 (R).	±0.09 *
	c) Zero output computer bank No. 1 (N) (read meter (S)) for "tape-zero" input.	±0.09 *
	d) Adjust output computer bank No. 1 (N) (read meter (S)) for tape calibration input to desired signal amplification level.	±0.225 *
	e) Dial desired signal count level in computer bank No. 3 (R) and observe number of counts on counter (T).	---
	f) Stability of computer bank No. 1 (N).	±0.5
	g) Stability of computer bank No. 2 (P).	±0.2475 *
	h) Stability of computer bank No. 3 (R).	±0.2

It should be noted that the error analysis described above applies to the complete testing-counting process. It therefore establishes the accuracy of the specimen test history curves presented in the report.

* KSI Constant

MATERIAL STRENGTH

The results of static tensile tests on the 7075-T6 bare aluminum material used in the investigation are presented in Table 54. The geometry of the rectangular 2 inch gage length conformed to ASTM Standard E8-57T. The longitudinal grained tensile test specimens were taken along the longitudinal axis of each sheet of material.

TABLE 54

STATIC TENSILE PROPERTIES OF
7075-T6 BARE ALUMINUM SHEET, .040 GAGE

Spec. No.	Sheet No. 1			Sheet No. 2			Sheet No. 3			Sheet No. 4			Sheet No. 5		
	F_{tu} (ksi)	F_{ty} (ksi)	% Elong.	F_{tu} (ksi)	F_{ty} (ksi)	% Elong.	F_{tu} (ksi)	F_{ty} (ksi)	% Elong.	F_{tu} (ksi)	F_{ty} (ksi)	% Elong.	F_{tu} (ksi)	F_{ty} (ksi)	% Elong.
1	85.4	78.2	11.0	85.4	78.5	11.5	85.8	78.6	11.0	84.9	77.2	11.0	85.7	78.6	11.0
2	86.1	79.0	12.0	85.2	78.3	10.5	84.8	77.7	11.0	85.4	78.3	11.0	85.5	78.4	10.5
3	85.4	77.8	11.0	84.5	77.1	11.0	85.1	78.3	11.0	85.4	78.5	10.5	86.0	78.1	11.0
4	85.7	78.7	10.5	84.3	76.2	11.0	85.9	78.8	11.0	84.8	76.5	11.0	84.5	76.7	9.0
5	85.0	77.4	11.0	85.1	77.9	11.5	85.9	78.7	12.0	85.6	78.3	12.0	84.5	76.4	10.0
6	85.2	77.2	12.0	84.7	77.9	11.0	85.4	77.0	10.5	85.8	78.7	11.0	86.1	79.2	12.0
7	85.2	78.3	11.0	84.7	77.4	11.5	85.5	78.5	11.5	86.1	78.8	11.0	85.9	78.7	11.0
8	85.6	78.1	12.0	85.3	78.3	10.0	85.1	78.2	11.5	85.4	78.5	11.0	86.0	78.8	12.5
9	84.8	76.8	13.0	84.0	76.3	11.0	85.1	77.5	10.5	85.6	78.7	11.5	85.9	76.6	11.0
10	85.3	78.1	11.0	85.6	78.5	11.0	85.8	79.1	11.0	85.4	78.5	11.0	85.3	78.0	11.0
11	84.8	77.2	11.5	85.2	77.9	11.5	85.1	78.1	10.5	85.0	77.9	11.0	85.7	78.2	11.0
12	85.7	78.3	12.0	85.3	78.1	12.0	84.1	76.5	11.5	85.4	78.5	11.0	85.6	78.5	11.0
13	85.1	78.1	12.0	84.9	77.2	12.0	85.0	78.0	10.5						
14	85.9	79.1	11.0	85.5	78.3	12.0	83.6	75.3	11.5						
15	83.7	76.3	12.0	84.5	77.8	11.0	84.4	77.6	12.0						
16	84.8	77.5	12.0	84.5	77.2	12.0	84.6	77.6	11.5						

Note: The static test specimens were selected along the longitudinal centerline of each 48 x 144 inch sheet. The longitudinal axis of each specimen was parallel to the direction of sheet rolling.

TABLE 55

UNIT LOW PEAK GUST LOADING SPECTRA AND S-N DATA FOR NOTCHED SHEET COUPONS
7075-T6 ALUMINUM ALLOY
$K_T = 4$
$f_{mean} = 6$ KSI $S_{mean} = .071$

$F_{tu} = 85$ KSI (Gross Area)

Loading Step	f_v KSI	S_v	n	N
18 LOADING STEPS				
1	.60	.0071	715900	--
2	1.78	.0209	511588	--
3	2.97	.0349	280342	6000000
4	4.16	.0489	112479	1200000
5	5.35	.0629	32231	320000
6	6.54	.0769	7519	120000
7	7.42	.0873	1184	68000
8	8.02	.0944	561	46000
9	8.60	.1012	379	32000
10	9.20	.1082	211	24000
11	9.75	.1147	119	18500
12	10.35	.1218	125	14000
13	11.15	.1312	81	10200
14	11.75	.1382	18	8400
15	11.98	.1409	4	7800
16	12.28	.1445	17	7200
17	12.80	.1506	15	6000
18	13.55	.1594	13	4800
		(066*)	Σ 1662800	
4 LOADING STEPS				
1	4.20	.0494	25408	1000000
2	8.15	.0959	582	43000
3	12.00	.1412	11	7800
4	14.00	.1647	.10	4200
			Σ 26000	

* Test Group No.

TABLE 56

UNIT LOW PEAK GUST LOADING SPECTRA AND S-N DATA FOR NOTCHED SHEET COUPONS
7075-T6 ALUMINUM ALLOY

$K_T = 4$

$f_{mean} = 6$ KSI $S_{mean} = .071$

$F_{tu} = 85$ KSI (Gross Area)

Loading Step	f_V KSI	S_V	n	N	f_V KSI	S_V	n	N
			14 LOADING STEPS					
1	1.10	.0129	25057		1.09	.0128	50098	∞
2	2.10	.0247	17005		2.14	.0236	34105	∞
3	3.10	.0365	9986	4500000	3.05	.0359	19970	5200000
4	4.15	.0468	5231	1100000	4.05	.0474	10422	1300000
5	5.00	.0588	1832	450000	5.05	.0594	3636	440000
6	6.05	.0712	627	180000	6.05	.0709	1248	180000
7	7.00	.0824	163	90000	7.05	.0827	324	86000
8	8.00	.0941	59	47000	8.05	.0947	118	45000
9	9.05	.1065	23	26000	9.07	.1067	45	25000
10	10.00	.1176	9.9	16500	10.25	.1206	20	15000
11	11.00	.1294	4.5	11000	10.60	.1247	8.8	13000
12	12.00	.1412	1.5	7800	11.40	.1341	3.9	9500
13	12.95	.1524	.74	5800	12.60	.1482	.98	6400
14	14.00	.1647	.25	4200	14.00	.1647	.50	4200
		(068*)	Σ 60000			(069)	Σ 120000	

* Test Group No.

TABLE 57

UNIT LOW PEAK GUST LOADING SPECTRA AND S-N DATA FOR NOTCHED SHEET COUPONS
7075-T6 ALUMINUM ALLOY
$K_T = 7$
$f_{mean} = 6$ KSI $\quad S_{mean} = .071$

$F_{tu} = 85$ KSI (Gross Area)

Loading Step	f_v KSI	S_v	n	N	f_v KSI	S_v	n	N
	17 LOADING STEPS				13 LOADING STEPS			
1	.60	.0071	100308		1.10	.0129	4497	∞
2	1.78	.0209	71917	3900000	1.95	.0229	2124	2400000
3	2.97	.0349	39417	980000	2.79	.0328	1291	520000
4	4.16	.0489	15803	110000	3.72	.0438	703	170000
5	5.35	.0629	4551	42000	4.66	.0548	256	70000
6	6.54	.0769	1068	17000	5.66	.0666	89	32000
7	7.42	.0873	166	9900	6.68	.0786	23	15000
8	8.02	.0944	100	6900	7.70	.0906	10	8000
9	8.60	.1012	35	5100	8.76	.1031	3.5	4800
10	9.20	.1082	29	3800	9.75	.1147	1.5	3000
11	9.75	.1147	18	3000	11.00	.1294	.70	1800
12	10.35	.1218	18	2300	11.91	.1401	.20	1300
13	11.15	.1312	10	1700	13.10	.1541	.10	890
14	11.75	.1382	4.0	1400				
15	11.98	.1409	1.0	1300				
16	12.28	.1445	2.4	1150				
17	12.80	.1506	2.0	950				
		(070*)	Σ 233400			(071)	Σ 9000	

* Test Group No.

TABLE 58

UNIT HIGH PEAK GUST LOADING SPECTRA AND S-N DATA FOR NOTCHED SHEET COUPONS
7075-T6 ALUMINUM ALLOY
$K_T = 4$
$f_{mean} = 12$ KSI $S_{mean} = .141$

$F_{tu} = 85$ KSI (Gross Area)

Loading Step	f_v KSI	S_v	n	N
		23 LOADING STEPS		
1	.5	.0059	107200	∞
2	1.5	.0176	83784	10000000
3	2.5	.0294	70408	1500000
4	3.5	.0412	49593	420000
5	4.5	.0529	32123	170000
6	5.5	.0647	19296	80000
7	6.5	.0765	9663	41000
8	7.5	.0882	4035	24000
9	8.5	.1000	1658	15000
10	9.5	.1118	691	10000
11	10.5	.1235	287	7400
12	11.5	.1353	151	5500
13	12.5	.1471	77	4100
14	13.5	.1588	42	3100
15	14.5	.1706	29	2400
16	15.5	.1824	16	1900
17	16.10	.1894	2.0	1600
18	16.51	.1942	6.0	1500
19	16.92	.1991	1.0	1300
20	17.50	.2059	5.0	1200
21	18.14	.2134	1.3	960
22	18.64	.2193	1.5	890
23	19.26	.2266	.70	760
		(072*)	Σ 379100	
		5 LOADING STEPS		
1	4.13	.0486	8389	230000
2	8.25	.0971	828	17000
3	12.35	.1453	30	4300
4	16.05	.1888	2.9	1590
5	18.30	.2153	.096	940
		(073)	Σ 9250	

* Test Group No.

TABLE 59

UNIT HIGH PEAK GUST LOADING SPECTRA AND S-N DATA FOR NOTCHED SHEET COUPONS
7075-T6 ALUMINUM ALLOY

$K_T = 4$

$f_{mean} = 12$ KSI $\quad S_{mean} = .141$

$F_{tu} = 85$ KSI (Gross Area)

Loading Step	f_v KSI	S_v	n	N	f_v KSI	S_v	n	N
				19 LOADING STEPS				
1	.96	.0113	5033	--	1.49	.0175	10043	10000000
2	1.79	.0211	3511	4500000	2.46	.0289	6993	1600000
3	2.65	.0312	3290	1100000	3.34	.0393	6594	500000
4	3.55	.0418	1842	380000	4.50	.0529	3697	170000
5	4.48	.0527	1139	175000	5.30	.0624	2298	88000
6	5.45	.0641	592	81000	6.36	.0748	1199	45000
7	6.35	.0747	355	45000	7.35	.0865	708	26000
8	7.35	.0865	133	26000	8.40	.0988	263	15000
9	8.38	.0986	59	16000	9.50	.1118	117	10000
10	9.35	.1100	23	10000	10.50	.1235	45	7400
11	10.85	.1276	9.9	5500	11.60	.1365	20	5200
12	11.90	.1400	4.9	4900	12.50	.1471	9.8	4100
13	12.80	.1506	3.0	3800	13.60	.1600	5.9	3000
14	13.80	.1624	2.0	2900	13.80	.1624	3.8	2900
15	14.90	.1753	.99	2200	15.10	.1776	2.0	2100
16	15.90	.1871	.50	1700	15.90	.1871	.98	1700
17	17.20	.2024	.30	1250	17.00	.2000	.56	1300
18	18.05	.2124	.10	1000	18.00	.2118	.21	1000
19	18.30	.2153	.10	960	18.30	.2153	.21	960
		(G74*)	Σ 16000			(G75)	Σ 32000	

* Test Group No.

TABLE 60

UNIT HIGH PEAK GUST LOADING SPECTRA AND S-N DATA FOR NOTCHED SHEET COUPONS
7075-T6 ALUMINUM ALLOY
$K_T = 7$
$f_{mean} = 12$ KSI $S_{mean} = .141$

$F_{tu} = 85$ KSI (Gross Area)

Loading Step	f_v KSI	S_v	n	N	f_v KSI	S_v	n	N
	14 LOADING STEPS				17 LOADING STEPS			
1	.84	.0099	25147	9000000	1.05	.0124	767	5400000
2	2.50	.0294	18066	280000	2.00	.0235	621	700000
3	4.16	.0489	9964	41000	3.00	.0353	444	140000
4	5.84	.0687	4005	13000	3.90	.0459	286	54000
5	7.50	.0882	1170	5100	4.90	.0576	194	24000
6	9.16	.1078	278	2400	5.80	.0682	102	13000
7	10.42	.1226	43	1500	6.80	.0800	48	7000
8	11.24	.1322	21	1150	8.00	.0941	20	3900
9	12.08	.1421	15	900	9.00	.1059	8.9	2600
10	12.92	.1520	7	710	9.80	.1152	3.6	1900
11	13.66	.1607	4.6	570	10.60	.1247	1.4	1400
12	14.48	.1704	4.4	480	11.70	.1376	.91	980
13	15.58	.1833	3.2	350	12.70	.1494	.40	740
14	16.40	.1929	.60	290	14.00	.1647	.31	530
15					14.90	.1753	.15	420
16					16.00	.1882	.10	320
17					16.20	.1906	.044	300
	(G76*)		Σ 58700		(G77)		Σ 2500	

* Test Group No.

TABLE 61

UNIT CONCAVE UPWARD AND CONCAVE DOWNWARD GUST LOADING SPECTRA AND S-N DATA FOR NOTCHED SHEET COUPONS
7075-T6 ALUMINUM ALLOY

$K_T = 4$

$f_{mean} = 12$ KSI $\quad S_{mean} = .141$

$F_{tu} = 85$KSI (Gross Area)

7 Loading Steps

Loading Step	f_v KSI	S_v	n	N	f_v KSI	S_v	n	N
				Concave Upward				
1	1	.0118	157310	20000000	1	.0118	456200	20000000
2	3	.0353	62150	750000	3	.0353	269000	750000
3	5	.0588	44890	110000	5	.0588	83450	110000
4	7	.0624	6900	31000	7	.0824	15070	31000
5	9	.1059	1140	12000	9	.1059	1450	12000
6	11	.1294	190	6300	11	.1294	350	6300
7	12.75	.1500	50	3800	12.75	.1500	80	3800
		(G78*)	Σ272600			(G79)	Σ825600	
				Concave Downward				
1	1	.0118	65590	20000000	1	.0118	38340	20000000
2	3	.0353	61210	750000	3	.0353	42920	750000
3	5	.0588	32800	110000	5	.0588	27000	110000
4	7	.0624	24920	31000	7	.0624	19970	31000
5	9	.1059	9960	12000	9	.1059	12020	12000
6	11	.1294	2030	6300	11	.1294	4490	6300
7	12.75	.1500	210	3800	12.75	.1500	400	3800
		(G80)	Σ196700			(G81)	Σ145100	

* Test Group No.

TABLE 62

UNIT FIGHTER MANEUVER LOADING SPECTRA AND S-N DATA FOR NOTCHED SHEET COUPONS
7075-T6 ALUMINUM ALLOY
$K_T = 4$
$f_{min} = 5.4$ KSI $S_{min} = .064$

$F_{tu} = 85$ KSI (Gross Area)

Loading Step	f_v KSI	S_v	n	N	f_v KSI	S_v	n	N
				11 LOADING STEPS				
1	.71	.0084	5971	∞	1.68	.0198	350	∞
2	2.13	.0251	4795	∞	3.50	.0412	235	1000000
3	4.27	.0502	7085	350000	5.75	.0676	175	78000
4	7.10	.0835	5029	26000	7.80	.0918	125	18000
5	9.92	.1167	2860	7000	10.00	.1176	85	6600
6	12.78	.1504	1351	2400	12.10	.1424	56	3100
7	14.90	.1753	264	1200	14.20	.1671	29	1500
8	16.30	.1918	164	820	16.50	.1941	12	780
9	18.45	.2171	113	500	18.30	.2153	5.4	520
10	20.25	.2382	12	360	20.15	.2371	1.6	360
11	20.81	.2448	6.3	320	21.00	.2471	.28	310
		(M14*)	Σ 27700			(M15)	Σ 1100	

* Test Group No.

TABLE 63

UNIT FIGHTER MANEUVER LOADING SPECTRA AND S-N DATA FOR NOTCHED SHEET COUPONS
7075-T6 ALUMINUM ALLOY
$K_T = 4$
$f_{min} = 5.4$ KSI $S_{min} = .064$

$F_{tu} = 85$ KSI (Gross Area)

Loading Step	f_v KSI	S_v	n	N	Loading Step	f_v KSI	S_v	n	N
40 LOADING STEPS									
1	.470	.0055	100	--	21	10.450	.1229	15	5700
2	.845	.0099	75	--	22	11.050	.1300	15	4400
3	1.175	.0138	75	--	23	11.750	.1382	12	3500
4	1.555	.0183	75	--	24	12.250	.1441	11	2900
5	1.930	.0227	75	--	25	12.850	.1512	7.8	2300
6	2.400	.0282	60	7200000	26	13.550	.1594	5.9	1800
7	2.920	.0344	55	2600000	27	14.150	.1665	5.9	1600
8	3.500	.0412	45	1000000	28	14.650	.1724	5.8	1300
9	3.955	.0465	45	510000	29	15.150	.1782	3.9	1100
10	4.475	.0526	45	300000	30	15.700	.1847	2.9	940
11	5.000	.0588	40	155000	31	16.300	.1918	2.0	820
12	5.555	.0654	35	88000	32	16.850	.1982	2.0	710
13	6.050	.0712	35	58000	33	17.350	.2041	1.5	640
14	6.650	.0782	32	37000	34	17.850	.2100	.98	570
15	7.150	.0841	30	26000	35	18.300	.2153	.96	520
16	7.750	.0912	25	18000	36	18.850	.2218	.70	470
17	8.300	.0976	23	14000	37	19.400	.2282	.58	420
18	8.550	.1006	20	12000	38	20.000	.2353	.50	370
19	9.400	.1106	20	8600	39	20.300	.2388	.40	350
20	10.000	.1176	19	6700	40	21.000	.2471	.30	310
							(M16*)	Σ 1000	

* Test Group No.

TABLE 64

UNIT GROUND LOADING SPECTRA AND S-N DATA FOR NOTCHED SHEET COUPONS

7075-T6 ALUMINUM ALLOY

$X_T = 7$

$f_{mean} = -3$ KSI $\qquad S_{mean} = -.035$

$F_{tu} = 85$ KSI (Gross Area)

Loading Step	f_v KSI	S_v	n	N	f_v KSI	S_v	n	N
	18 Loading Steps				11 Loading Steps			
1	.48	.0056	236392	-	1.10	.0129	10553	-
2	1.44	.0169	174558	-	2.07	.0244	7010	-
3	2.38	.0280	96152	-	3.10	.0365	2831	2900000
4	3.32	.0391	38265	1800000	4.07	.0479	980	580000
5	4.28	.0504	10869	470000	5.15	.0606	98	180000
6	5.23	.0615	2542	160000	6.25	.0735	38	70000
7	5.94	.0699	409	90000	7.32	.0861	15	33000
8	6.42	.0755	184	62000	8.50	.1000	4.3	15000
9	6.89	.0811	124	43000	9.05	.1065	1.5	10500
10	7.36	.0866	71	31000	9.90	.1165	.41	6800
11	7.80	.0918	44	23000	10.50	.1235	.19	5000
12	8.28	.0974	42	18000				
13	8.90	.1047	25	12000				
14	9.33	.1104	8	9000				
15	9.56	.1125	2	7800				
16	9.80	.1153	4.3	7000				
17	10.22	.1202	4.3	5400				
18	10.80	.1271	3.8	4200				
		(T1*)	Σ 559700			(T2)	Σ 21500	

* Test Group No.

TABLE 65

UNIT COMPOSITE LOW PEAK GUST, GROUND AND GROUND-AIR-GROUND LOADING SPECTRUM, AND S-N DATA FOR NOTCHED SHEET COUPONS

7075-T6 ALUMINUM ALLOY

$K_T = 4$

$F_{tu} = 85$ KSI (GROSS AREA)

LOADING STEP	f_v KSI	S_v	n	N
	26 LOADING STEPS			
	LOW PEAK GUST LOADING			
	$f_{mean} = 6$ KSI; $S_{mean} = .071$			
1	1.15	.0135	5549	∞
2	2.20	.0259	4036	∞
3	3.25	.0382	2018	8400000
4	4.35	.0512	940	900000
5	5.35	.0629	386	330000
6	6.40	.0753	114	135000
7	7.45	.0876	27	65000
8	8.25	.0971	9.9	40000
9	9.15	.1076	4.0	24000
10	10.15	.1194	2.4	15000
11	11.20	.1318	.99	10000
12	12.05	.1418	.41	8600
13	13.00	.1529	.19	5700
			Σ13100	
	GROUND LOADING			
	$f_{mean} = -3$ KSI; $S_{mean} = -.035$			
14	1.20	.0141	2969	∞
15	2.20	.0259	2078	∞
16	3.30	.0388	1088	∞
17	4.50	.0529	495	5200000
18	5.65	.0665	208	1500000
19	6.75	.0794	64	550000
20	7.60	.0894	15	270000
21	8.65	.1018	5.9	136000
22	9.40	.1106	2.0	90000
23	10.30	.1212	.99	52000
24	11.45	.1347	.60	29000
25	12.00	.1412	.41	22600
			Σ6930	
	GROUND-AIR-GROUND LOADING			
	$f_{mean} = 1.5$ KSI; $S_{mean} = .018$			
26	4.90	.0576	1170	2100000
Total		(CG1*)	Σ21200	

* Test Group No.

TABLE 66

UNIT COMPOSITE LOW PEAK GUST, GROUND AND GROUND-AIR-GROUND LOADING SPECTRUM, AND S-N DATA FOR NOTCHED SHEET COUPONS

7075-T6 ALUMINUM ALLOY

$K_T = 7$

F_{tu} = 85 KSI (GROSS AREA)

LOADING STEP	f_v KSI	S_v	n	N
	21 LOADING STEPS			
	LOW PEAK GUST LOADING			
	f_{mean} = 6 KSI; S_{mean} = .071			
1	1.30	.0153	511	∞
2	2.30	.0271	325	2900000
3	3.20	.0376	220	320000
4	4.20	.0494	90	110000
5	5.10	.0600	34	49000
6	6.00	.0706	12	25000
7	7.20	.0847	2.5	11000
8	8.70	.1024	.81	4900
9	9.10	.1071	.35	4000
10	10.00	.1176	.21	2700
11	11.00	.1294	.052	1800
			Σ1200	
	GROUND LOADING			
	f_{mean} = -3 KSI; S_{mean} = -.035			
12	1.30	.0153	290	∞
13	2.30	.0271	190	∞
14	3.30	.0388	84	1800000
15	4.30	.0506	29	450000
16	5.20	.0612	5.2	165000
17	6.25	.0735	1.1	69000
18	7.25	.0853	.35	34000
19	8.35	.0982	.16	17000
20	8.85	.1041	.052	12000
			Σ600	
	GROUND-AIR-GROUND LOADING			
	f_{mean} = 1.5 KSI; S_{mean} = .018			
21	4.65	.0547	102	140000
Total		(CG2*)	Σ1900	

* Test Group No.

TABLE 67

UNIT COMPOSITE HIGH PEAK GUST, GROUND AND GROUND-AIR-GROUND LOADING SPECTRA, AND S-N DATA FOR NOTCHED SHEET COUPONS
7075-T6 ALUMINUM ALLOY
$K_T = 4$
$F_{tu} = 85$ KSI (GROSS AREA)

LOADING STEP	f_v KSI	S_v	n	N	f_v KSI	S_v	n	N
	28 LOADING STEPS							
	High Peak Gust Loading; f_{mean} = 12 KSI; S_{mean} = .141							
1	1.15	.0135	606	∞	1.10	.0129	2560	∞
2	2.40	.0282	505	1800000	2.30	.0271	2560	2000000
3	3.40	.0400	429	470000	3.00	.0353	1598	770000
4	4.30	.0506	257	190000	3.90	.0459	1064	280000
5	5.40	.0635	158	86000	4.80	.0565	580	132000
6	6.35	.0747	84	46000	5.85	.0688	387	63000
7	7.65	.0900	40	22000	7.00	.0824	169	31000
8	8.55	.1006	17	14300	8.00	.0941	73	18500
9	9.55	.1124	5.9	9800	9.00	.1059	24	12000
10	10.60	.1247	3.0	7100	10.20	.1200	13	8100
11	11.50	.1353	1.4	5500	11.05	.1300	4.8	5500
12	12.60	.1482	.69	4000	12.10	.1424	3.4	4600
13	13.60	.1600	.39	3000	13.05	.1535	1.5	3500
14	14.80	.1741	.21	2250	14.00	.1647	.97	2760
15	15.40	.1812	.16	1960	14.90	.1753	.51	2200
16	15.80	.1859	.092	1760	16.0	.1882	.34	1670
17	16.30	.1918	.046	1560	16.85	.1982	.11	1360
18	—	—	—	—	18.30	.2153	.11	960
			Σ2110				Σ9040	
	Ground Loading; f_{mean} = -3 KSI; S_{mean} = -.035							
19	1.25	.0147	553	∞	1.10	.0129	435	∞
20	2.10	.0247	286	∞	2.05	.0241	348	∞
21	3.10	.0365	133	∞	3.05	.0359	126	∞
22	4.20	.0494	44	7800000	4.00	.0471	46	10000000
23	5.00	.0588	6.9	3000000	5.00	.0588	9.2	3000000
24	6.00	.0706	2.0	1070000	6.05	.0712	2.4	980000
25	6.90	.0812	.64	480000	7.00	.0824	.63	450000
26	7.95	.0935	.25	220000	8.05	.0947	.40	192000
27	8.65	.1018	.046	134000	9.30	.1094	.11	93000
28	8.95	.1053	.046	116000	—	—	—	—
			Σ1030				Σ970	
	Ground-Air-Ground Loading; f_{mean} = 4.5 KSI; S_{mean} = .053							
29	7.95	.0935	182	65000	7.85	.0924	89	67000
Total		(CG3 *)	Σ3320			(CG4)	Σ10100	

* Test Group No.

TABLE 68

UNIT COMPOSITE FIGHTER MANEUVER, GROUND AND GROUND-AIR-GROUND LOADING SPECTRUM, AND S-N DATA FOR NOTCHED SHEET COUPONS 7075-T6 Aluminum Alloy

$K_T = 4$

$f_{tu} = 85$ KSI (Gross Area)

Loading Steps	f_v KSI	S_v	n	N
		29 Loading Steps		
		FIGHTER MANEUVER LOADING $f_{min} = 5.45$ KSI; $S_{min} = .064$		
1	.71	.0084	1870	∞
2	2.13	.0251	1496	13000000
3	4.27	.0502	2224	340000
4	7.10	.0835	1574	27000
5	9.92	.1167	896	6500
6	12.78	.1504	423	2400
7	14.90	.1753	83	1200
8	16.30	.1918	51	820
9	18.42	.2167	35	510
10	20.25	.2382	3.9	340
11	20.80	.2447	2.0	310
			Σ8660	
		GROUND LOADING $f_{mean} = -3$ KSI; $S_{mean} = -.035$		
12	.42	.0049	849	∞
13	1.44	.0169	628	∞
14	2.38	.0280	345	∞
15	3.32	.0391	138	∞
16	4.28	.0504	39	7000000
17	5.22	.0614	9.1	2200000
18	5.94	.0699	1.5	1100000
19	6.42	.0755	.63	740000
20	6.89	.0811	.44	500000
21	7.36	.0866	.25	330000
22	7.80	.0918	.15	240000
23	8.28	.0974	.21	170000
24	8.90	.1047	.037	120000
25	9.38	.1104	.055	90000
26	9.56	.1125	.002	80000
27	9.80	.1153	.016	70000
28	10.22	.1202	.003	54000
			Σ2010	
		GROUND-AIR-GROUND LOADING $f_{mean} = 1.22$ KSI; $S_{mean} = .014$		
29	4.22	.0496	287	5000000
Total			(CM1*)Σ11000	

* Test Group No.

TABLE 69

EXPERIMENTAL FATIGUE LIVES FOR GUST LOADING SPECTRA
7075-T6 ALUMINUM ALLOY

(Table is completed on next three pages)

Test Group No.	Specimen No.	Type of Specimen	K_T	S_{mean}	No. of Loading Steps	Type of Spectrum Curve	Sequence	Block Size	Test Life (10^6 Cycles)
	318	Notched	4	.071		Low			1.936
G66	362	Sheet			18	Peak	True	1662800	1.470
	393	Coupon					Random	(Avg.)	1.792
	305								1.453
									1.650*
	364								1.394
	365								.458
G67	368				4		Lo-Hi	26000	2.103
	370								2.046
	377								1.030
									1.230 *
	372								4.918
	376								3.178
G68	381				14		Lo-Hi	60000	4.189
	385								3.777
	394								5.070
									4.165 *
	378								4.555
	387								5.386
G69	388				14		Lo-Hi	120000	5.390
	392								5.874
	391		4						10.056
									6.005 *
	299		7		17				.252
	300				15				.170
G70	301				17		True	233400	.239
	302	Notched			17		Random	(Avg.)	.200
	303	Sheet			17	Low			.326
	304	Coupon	7	.071	17	Peak			.213
									.228 *

* Geometric mean of test life

TABLE 69

EXPERIMENTAL FATIGUE LIVES FOR GUST LOADING SPECTRA
7075-T6 ALUMINUM ALLOY

(Table is continued on next page)

Test Group No.	Specimen No.	Type of Specimen	K_T	S_{mean}	No. of Loading Steps	Type of Spectrum Curve	Sequence	Block Size	Test Life (10^6 Cycles)
G71	348	Notched Sheet Coupon	7	.071	13	Low Peak	Low-Hi	9000	.211
	350								.289
	351								.305
	355								.254
	356		7	.071		Low Peak			.228
									.255*
G72	279		4	.141	23	High Peak	True Random	379100 (Avg.)	.652
	285				21				.396
	287				21				.457
	288				21				.335
	290				21				.259
	291				21				.326
	292				21				.248
									.359*
G73	326				5		Lo-Hi	9250	.304
	331								.145
	332								.153
	334								.188
	336								.306
	337								.207
	339								.498
	340								.353
									.248*
G74	313				13		Lo-Hi	16000	.415
	320								.470
	328								.814
	335								.441
	341	Notched Sheet Coupon	4	.141		High Peak			.928
									.579*

* Geometric mean of test life

TABLE 69

EXPERIMENTAL FATIGUE LIVES FOR GUST LOADING SPECTRA
7075-T6 ALUMINUM ALLOY

(Table is concluded on next page)

Test Group No.	Specimen No.	Type of Specimen	K_T	S_{mean}	No. of Loading Steps	Type of Spectrum Curve	Sequence	Block Size	Test Life (10^6 Cycles)
	307	Notched	4	.141		High			.319
	308	Sheet				Peak			.289
G75	309	Coupon			19		Lo-Hi	32000	.288
	310								.224
	312		4						.257
									.274 *
	274		7		13				.0566
	280				14				.0957
G76	281				13		True	58700	.0566
	282				13		Random	(Avg.)	.0392
	283				13				.0522
	284				13				.0522
									.0567*
	293								.0630
	294								.0582
G77	295				17		Lo-Hi	2500	.0630
	296	Notched							.0680
	297	Sheet				High			.0413
	298	Coupon	7	.141		Peak			.0555
									[illegible]*

* Geometric mean of test life

TABLE 69

EXPERIMENTAL FATIGUE LIVES FOR GUST LOADING SPECTRA
7075-T6 ALUMINUM ALLOY
(Concluding page of table)

Test Group No.	Specimen No.	Type of Specimen	K_T	S_{mean}	No. of Loading Steps	Type of Spectrum Curve	Sequence	Block Size	Test Life (10^6 Cycles)
G78	70	Notched Sheet Coupon	4	.141	7	Concave Upward	True Random	272600 (Avg.)	.300
	72								.309
	85								.260
	88								.254
	92								.277
	93								.240
	114								.262
	115								.228
	126								.359
	128								.239
									.270*
G79	251				7	Concave Upward	Lo-Hi	825600 (Avg.)	1.020
	252								.780
	255								.536
	256								.808
	258								.985
									.804*
G80	173				7	Concave Downward	True Random	196700 (Avg.)	.168
	175								.259
	176								.157
	177								.203
									.193*
G81	246				7	Concave Downward	Lo-Hi	145100 (Avg.)	.134
	247								.118
	248								.147
	249								.141
	250	Notched Sheet Coupon	4	.141					.187
									.144*

* Geometric Mean of Test Life

TABLE 70

EXPERIMENTAL FATIGUE LIVES FOR GROUND LOADING SPECTRA

7075-T6 ALUMINUM ALLOY

Test Group No.	Specimen No.	Type of Specimen	K_T	S_{mean}	No. of Loading Steps	Sequence	Block Size	Test Life (10^6 cycles)
T1	416 417 418 419 422 423	Notched Sheet Coupon	7	-.035	18	True Random	559700 (Avg.)	.783 .500 .552 .579 .496 .448 .550 *
T2	461 462 465 466 469 471	Notched Sheet Coupon	7	-.035	11	Lo-Hi	21500	.775 .748 1.010 1.268 .900 1.309 .978 *

* Geometric mean of test life

TABLE 71

EXPERIMENTAL FATIGUE LIVES FOR FIGHTER MANEUVER LOADING SPECTRA
7075-T6 ALUMINUM ALLOY

Test Group No.	Specimen No.	Type of Specimen	K_T	S_{min}	No. of Loading Steps	Sequence	Block Size	Test Life (10^6 Cycles)
	342	Notched Sheet Coupon	4					.0264
	343							.0220
	344							.0176
M14	345			.064	11	True Random	27700 (Avg.)	.0308
	346							.0440
	347							.0264
	349							.0264
								.0267*
	399							.0129
	400							.0129
M15	401			.064	11	Lo-Hi	1100	.0097
	404							.0193
	406							.0150
								.0136 *
	410							.0082
	411							.0174
M16	413	Notched Sheet Coupon	4	.064	40	Lo-Hi	1000	.0123
	414							.0123
	415							.0133
								.0123 *

* Geometric mean of test life

TABLE 72

EXPERIMENTAL FATIGUE LIVES FOR COMPOSITE MANEUVER LOADING SPECTRUM
7075-T6 ALUMINUM ALLOY

True Random Loading Sequence

Test Group No.	Specimen No.	Type of Specimen	K_T	S_{min}	S_{mean}	No. of Loading Steps	Block Size	Test Life (10^6 Cycles)
	488							.0091
	489	Notched		Fighter	Ground -.035		11000	.0103
CM1	490	Sheet	4	Maneuver	G-A-G	29	(Avg.)	.0121
	499	Coupon		.064	.014			.0098
	500							.0135
								.0108*

* Geometric Mean of Test Life

TABLE 73

EXPERIMENTAL FATIGUE LIVES FOR COMPOSITE GUST LOADING SPECTRA

7075-T6 ALUMINUM ALLOY

Lo-Hi Loading Sequence

Test Group No.	Specimen No.	Type of Specimen	K_T	S_{mean}	No. of Loading Steps	Block Size	Test Life (10^6 cycles)
CG1	475	Notched Sheet Coupon	4	Gust .071, Ground -.035, G-A-G .018	26	21200	1.092
	480						.571
	481						1.242
	485						.754
	487						1.694
							.998 *
CG2	478		7	Gust .071, Ground -.035, G-A-G .018	21	1900	.134
	479						.138
	482						.083
	484						.110
	486						.084
							.107 *
CG3	467		4	Gust .141, Ground -.035, G-A-G .053	28	3300	.145
	470						.191
	472						.117
	473						.118
	474						.151
							.142 *
CG4	509		4	Gust .141, Ground -.035, G-A-G .053	28	10100	.200
	510						.259
	511						.338
	512						.221
	513						.276
	514	Notched Sheet Coupon					.269
	517						.177
	518						.301
							.250 *

* Geometric mean of test data

TABLE 74

LOW PEAK RANDOM GUST LOADING HISTORIES
(MEAN CROSSING PEAK COUNTS)

f_{mean} = 6,000 psi
K_T = 4.0

Test Group No. G66

Varying Stress (psi)	Cumulative Frequency of Load Cycle Occurrences			
	Specimen No.305	Specimen No.318	Specimen No.362	Specimen No.393
0	1,452,900	1,935,750	1,470,300	1,792,200
1,190	827,300	1,102,600	837,050	1,020,600
2,380	380,300	507,050	384,750	469,100
3,560	135,380	180,500	136,990	166,960
4,750	37,113	49,490	37,539	45,774
5,950	8,952	11,939	9,057	11,043
7,120	2,382.7	3,181.5	2,411.3	2,938.6
7,720	1,326.0	1,811.2	1,371.7	1,672.6
8,310	859.5	1,148.4	869.1	1,060.0
8,900	527.7	705.3	534.3	650.8
9,500	344.1	460.3	348.7	424.3
10,000	239.9	321.5	243.3	295.6
10,700	91.1	122.4	93.1	112.3
11,600	60.2	80.7	61.7	74.0
11,900	22.6	30.5	23.7	27.6
12,050	21.0	28.6	22.0	25.6
12,500	10.2	13.2	10.2	11.5
13,100	7.7	10.0	7.7	8.7
14,000	2.0	3.0	2.0	2.0

TABLE 75

LOW PEAK ORDERED GUST LOADING HISTORIES

Stress Interval = 4,000 psi
Unit Spectrum = 1/20 avg. random test history
f_{mean} = 6,000 psi
K_T = 4.0

Test Group No. 067

Varying Stress (psi)	Cumulative Frequency of Load Cycle Occurrences				
	Specimen No. 364	Specimen No. 365	Specimen No. 368	Specimen No. 370	Specimen No. 377
2,100	1,393,865	457,862	2,103,148	2,045,683	1,029,604
6,180	31,805	10,202	48,008	46,808	23,404
10,080	588	189	888	866	433
14,000	5	2	8	8	4
No. of Blocks	53.61	17.61	80.89	78.68	39.60

TABLE 76

LOW PEAK ORDERED GUST LOADING HISTORIES

Stress Interval = 1,000 psi
Unit Spectrum = 1/20 avg. random test life
f_{mean} = 6,000 psi
K_T = 4.0

Test Group No. G68

Varying Stress (psi)	Cumulative Frequency of Load Cycle Occurrences				
	Specimen No. 372	Specimen No. 376	Specimen No. 381	Specimen No. 385	Specimen No. 394
550	4,918,201	3,177,840	4,189,201	3,777,001	5,070,000
1,600	2,868,201	1,852,840	2,439,201	2,202,001	2,945,000
2,600	1,474,201	951,840	1,249,201	1,131,001	1,512,000
3,620	654,201	421,840	552,001	501,001	672,000
4,580	223,701	143,590	189,751	170,501	231,000
5,520	72,901	46,800	62,101	55,801	75,600
6,520	21,466	13,780	18,285	16,431	22,260
7,500	8,101	5,200	6,901	6,201	8,400
8,520	3,241	2,080	2,761	2,481	3,360
9,520	1,378	884	1,174	1,055	1,428
10,500	568	364	484	435	588
11,500	203	130	173	156	210
12,480	81	52	69	63	84
14,000	20	13	17	16	21
No. of Blocks	81.97	52.96	69.82	62.95	84.50

TABLE 77

LOW PEAK ORDERED GUST LOADING HISTORIES

Stress Interval = 1,000 psi
Unit Spectrum = 1/10 avg. random test history
f_{mean} = 6,000 psi
K_T = 4.0

Test Group No. G69

Varying Stress (psi)	Cumulative Frequency of Load Cycle Occurrences				
	Specimen No.378	Specimen NO.387	Specimen No.388	Specimen No.391	Specimen No.392
540	4,552,819	5,385,622	5,390,422	10,056,042	5,874,024
1,620	2,652,819	3,135,622	3,140,422	5,856,042	3,424,024
2,590	1,360,819	1,605,622	1,610,422	3,000,042	1,758,024
3,540	600,819	705,622	710,422	1,328,042	778,024
4,540	203,519	242,022	242,022	456,542	264,024
5,540	66,619	79,222	79,222	149,442	86,424
6,530	19,629	23,342	23,342	44,032	25,464
7,540	7,419	8,822	8,822	16,642	9,624
8,600	2,979	3,542	3,542	6,682	3,864
9,660	1,277	1,518	1,518	2,864	1,656
10,420	537	638	638	1,204	696
11,000	204	242	242	457	264
12,000	56	66	66	125	72
14,000	19	22	22	42	24
No. of Blocks	37.94	44.88	44.92	83.80	48.95

TABLE 78

LOW PEAK RANDOM GUST LOADING HISTORIES
(MEAN CROSSING PEAK COUNTS)

f_{mean} = 6,000 psi
K_T = 7.0

Test Group No. 070

Varying Stress (psi)	Cumulative Frequency of Load Cycle Occurrences					
	Specimen No.299	Specimen No.300	Specimen No.301	Specimen No.302	Specimen No.303	Specimen No.304
0	252,300	169,650	239,250	200,100	326,250	213,150
1,190	143,700	97,050	136,500	114,100	185,900	121,600
2,380	65,900	44,800	62,700	52,450	85,500	56,000
3,560	23,480	15,980	22,360	18,630	30,460	19.940
4,750	6,437	4,440	6,157	5,142	8,349	5,507
5,950	1,552	1,079.5	1,488	1,246	2,018.5	1,338
7,120	411.8	286.0	397.3	328.3	538.6	354.3
7,720	234.4	163.6	227.2	187.6	306.2	202.0
8,310	148.5	103.5	144.1	118.9	193.7	127.7
8,900	90.9	62.7	88.3	72.3	119.2	77.6
9,500	60.0	40.8	58.4	47.5	77.4	50.6
10,000	41.8	28.4	40.8	33.3	53.7	35.3
10,700	16.1	11.3	16.1	13.6	19.7	13.6
11,600	10.6	7.3	10.6	9.0	12.9	9.0
11,900	3.9	1.1	3.9	2.6	5.0	2.6
12,050	3.6	1.0	3.6	2.5	4.6	2.5
12,500	1.4		1.4	1.3	1.4	1.3
13,100	1.0		1.0	1.0	1.0	1.0

TABLE 79

LOW PEAK ORDERED GUST LOADING HISTORIES

Stress Interval = 1,000 psi
Unit Spectrum = 1/20 avg. random test history
f_{mean} = 6,000 psi
K_T = 7.0

Test Group No. C71

Varying Stress (psi)	Cumulative Frequency of Load Cycle Occurrences Specimen No.348	Specimen No.350	Specimen No.351	Specimen No.355	Specimen No.356
550	211,141	289,080	305,371	253,531	228,242
1,520	104,421	145,280	153,731	127,121	113,502
2,370	55,201	76,800	80,971	67,201	60,002
3,260	25,301	35,200	36,771	30,801	27,502
4,190	8,971	12,480	12,871	10,921	9,752
5,160	2,991	4,160	4,291	3,641	3,252
6,170	921	1,280	1,321	1,121	1,002
7,190	300	416	430	365	327
8,230	139	192	199	169	152
9,260	58	80	83	71	64
10,380	23	32	33	29	26
11,460	7	9	10	9	8
13,100	2	3	3	3	3
No. of Blocks	23.46	32.12	33.93	28.17	25.36

TABLE 80

HIGH PEAK RANDOM GUST LOADING HISTORIES
(MEAN CROSSING PEAK COUNTS)

f_{mean} = 12,000 psi
K_T = 4.0

Test Group No. G72

Varying Stress (psi)	Cumulative Frequency of Load Cycle Occurrences						
	Specimen No.279	Specimen No.285	Specimen No.287	Specimen No.288	Specimen No.290	Specimen No.291	Specimen No.292
0	652,500	395,850	456,750	334,950	239,250	326,250	247,950
1,000	467,600	283,800	327,500	240,300	171,700	234,100	177,900
2,000	323,760	196,350	226,600	166,250	118,700	161,950	123,000
3,000	202,550	122,850	141,750	104,050	74,250	101,350	76,950
4,000	117,200	71,020	82,020	60,220	42,960	58,670	44,510
5,000	61,830	37,520	43,500	31,800	22,720	30,970	23,550
6,000	28,650	17,345	20,075	14,710	10,585	14,335	10,960
7,000	12,030	7,285	8,445	6,180	4,455	6,025	4,610
8,000	5,100	3,082	3,582	2,615	1,893	2,550	1,958
9,000	2,250	1,364	1,583	1,157.5	833.5	1,129	862
10,000	1,145	697	805	590.0	424.0	575	439
11,000	567.3	346.2	400	292.6	210.2	285.6	217.2
12,000	311.4	190.2	219.6	160.2	115.7	156.6	119.3
13,000	179.7	109.5	126.4	91.9	67.1	90.0	69.0
14,000	108.4	65.7	76.0	54.8	40.5	53.8	41.6

(Continued on next page)

TABLE 80 (Continued)

Varying Stress (psi)	Cumulative Frequency of Load Cycle Occurrences						
	Specimen No.279	Specimen No.285	Specimen No.287	Specimen No.288	Specimen No.290	Specimen No.291	Specimen No.292
15,000	39.7	22.9	27.3	18.7	15.1	18.7	15.1
16,000	28.8	16.6	19.8	13.6	11.0	13.6	11.0
16,190	27.3	15.7	18.7	12.8	10.4	12.8	10.4
16,830	9.2	6.2	6.2	4.6	3.6	4.6	3.6
17,000	4.9	3.0	3.0	1.5	1.5	1.5	1.5
18,000	3.7	2.2	2.2	1.1	1.1	1.1	1.1
18,290	3.4	2.0	2.0	1.0	1.0	1.0	1.0
19,000	1.2						
19,520	1.0						

(End of Table 80)

TABLE 81

HIGH PEAK ORDERED GUST LOADING HISTORIES

Stress Interval = 4,000 psi
Unit Spectrum = 1/20 avg. random test history
f_{mean} = 12,000 psi
K_T = 4.0

Test Group No. 073

Varying Stress (psi)	Cumulative Frequency of Load Cycle Occurrences			
	Specimen No.326	Specimen No.331	Specimen No.332	Specimen No.334
2,070	304,232	144,578	152,718	188,145
6,190	28,000	13,126	14,001	17,500
10,350	1,056	496	529	660
14,200	96	46	49	60
18,300	3	2	2	2
Spectrum Units	32.89	15.63	16.51	20.34
Varying Stress (psi)	Cumulative Frequency of Load Cycle Occurrences			
	Specimen No.336	Specimen No.337	Specimen No.339	Specimen No.340
2,070	305,713	207,478	497,650	353,350
6,190	28,875	19,250	46,375	33,250
10,350	1,089	726	1,749	1,254
14,200	99	66	159	114
18,300	3	2	5	4
No. of Blocks	33.05	22.43	53.80	38.20

TABLE 82

HIGH PEAK ORDERED GUST LOADING HISTORIES

Stress Interval = 1,000
Unit Spectrum = 1/20 avg. random test history
f_{mean} = 12,000 psi
K_T = 4.0

Test Group No. 674

Varying Stress (psi)	Cumulative Frequency of Load Cycle Occurrences				
	Specimen No.313	Specimen No.320	Specimen No.328	Specimen No.335	Specimen No.341
480	414,882	470,401	813,600	441,281	928,161
1,320	284,882	320,401	558,600	301,281	638,001
2,220	193,882	217,501	380,100	203,281	435,001
3,100	108,082	121,801	211,800	113,401	243,601
4,020	59,982	68,151	117,500	63,451	136,301
4,960	30,082	34,801	60,000	32,400	69,601
5,900	15,002	17,401	30,000	16,201	34,801
6,850	6,002	6,961	12,000	6,481	13,921
7,860	2,527	3,046	5,250	2,836	6,091
8,860	1,127	1,306	2,250	1,216	2,611
10,100	552	639	1,100	595	1,277
11,380	302	349	600	325	697
12,350	177	204	350	190	407
13,300	102	117	200	109	233
14,350	52	59	100	55	117
15,400	27	30	50	28	59
16,550	14	15	25	14	30
17,620	6	6	10	6	12
18,300	3	3	5	3	6
No. of Blocks	25.93	29.40	50.85	27.58	58.01

TABLE 83

HIGH PEAK ORDERED GUST LOADING HISTORIES

Stress Interval = 1,000
Unit Spectrum = 1/10 avg. random test history
f_{mean} = 12,000
K_T = 4.0

Test Group No. G75

Varying Stress (psi)	Cumulative Frequency of Load Cycle Occurrences				
	Specimen No.307	Specimen No.308	Specimen No.309	Specimen No.310	Specimen No.312
750	319,040	288,960	288,000	224,319	256,961
1,980	219,040	198,000	198,000	153,999	176,001
2,900	149,040	135,000	135,000	104,999	120,001
3,920	83,040	75,600	75,600	58,799	67,201
4,900	46,040	42,300	42,300	32,899	37,601
5,830	23,040	21,600	21,600	16,799	19,201
6,850	11,040	10,800	10,800	8,399	9,601
7,880	4,320	4,320	4,320	3,359	3,841
8,950	1,890	1,890	1,890	1,469	1,681
10,000	810	810	810	629	721
11,050	396	396	396	307	353
12,050	216	216	216	167	193
13,050	126	126	126	97	113
13,700	72	72	72	55	65
14,450	36	36	36	27	33
15,500	18	18	18	13	17
16,450	9	9	9	6	9
17,500	4	4	4	2	4
18,300	2	2	2	1	2
No. of Blocks	9.97	9.03	9.00	7.01	8.03

TABLE 84

HIGH PEAK RANDOM GUST LOADING HISTORIES
(MEAN CROSSING PEAK COUNTS)

f_{mean} = 12,000 psi

K_T = 7.0

Test Group No. 076

Varying Stress (psi)	Cumulative Frequency of Load Cycle Occurrences					
	Specimen No.274	Specimen No.280	Specimen No.281	Specimen No.282	Specimen No.283	Specimen No.284
0	56,550	95,700	56,550	39,150	52,200	52,200
1,670	32,400	54,500	32,400	22,600	29,800	29,800
3,330	15,000	25,100	15,000	10,600	13,700	13,700
5,000	5,360	9,000	5,360	3,880	4,860	4,860
6,670	1,504	2,479	1,504	1,092	1,354	1,354
8,330	369	606	369	267.5	329	329
10,000	99.1	159.1	99.1	70.8	86.6	86.6
10,830	56.8	88.9	56.8	40.5	49.6	49.6
11,660	35.6	55.5	35.6	25.8	31.2	31.2
12,500	21.1	33.5	21.1	15.8	18.4	18.4
13,330	13.5	21.5	13.5	10.3	11.9	11.9
14,000	9.2	14.7	9.2	7.2	8.2	8.2
14,960	3.1	5.0	3.1	3.1	3.1	3.1
16,190	2.0	3.3	2.0	2.0	2.0	2.0
16,620		1.0				

TABLE 85

HIGH PEAK ORDERED GUST LOADING HISTORIES

Stress Interval = 1,000 psi
Unit Spectrum = 1/20 avg. random test history
f_{mean} = 12,000 psi
K_T = 7.0

Test Group No. 077

Varying Stress (psi)	Cumulative Frequency of Load Cycle Occurrences					
	Specimen No.293	Specimen No.294	Specimen No.295	Specimen No.296	Specimen No.297	Specimen No.298
530	63,002	58,249	63,002	68,001	41,253	55,501
1,550	43,752	40,249	43,752	47,251	28,503	38,501
2,500	28,127	25,874	28,127	30,376	18,003	24,751
3,450	16,877	15,524	16,877	18,226	10,303	14,851
4,400	9,627	8,854	9,627	10,396	6,163	8,471
5,350	4,702	4,323	4,702	5,077	3,011	4,137
6,300	2,127	1,954	2,127	2,296	1,363	1,871
7,400	902	827	902	973	579	793
8,500	402	367	402	433	259	353
9,400	177	160	177	190	115	155
10,200	84	75	84	90	56	73
11,150	49	43	49	52	33	42
12,200	26	22	26	27	18	22
13,300	16	13	16	16	11	13
14,450	8	6	8	8	6	6
15,500	4	3	4	4	3	3
16,200	3	2	3	3	2	2
No. of Blocks	25.19	23.29	25.19	27.24	16.52	22.23

TABLE 86

TEST LOADING SPECTRA

	Cumulative Frequency of Occurrences (Cycles)				
Specimen No.	70	72	85	88	92
Trace	Wing Root	Wing Root	Wing Root	Wing Root	Wing Root
K_T	4	4	4	4	4
Record No.	17M-P4-4	17M-P4-4	17M-P4-4	17M-P4-4	17M-P3-3
Mean Stress (psi)	12,000	12,000	12,000	12,000	12,000
Trace Repetitions	69.7	71.8	60.5	59.1	79.2
Varying Stress (Gross Area) KSI	Random	Random	Random	Random	Random
	Test Group No. G78				
0	299,710	308,740	260,150	254,130	277,200
1.5					
2	153,340	157,960	133,100	130,020	67,320
4	66,215	68,210	57,475	56,145	39,600
6	9,061	9,334	7,865	7,683	8,712
8	1,533	1,580	1,331	1,300	1,584
10	293	302	254	248	396
11					
12	118	122	103	100	135
13.5	70	72	61	59	79

TABLE 66

TEST LOADING SPECTRA

(Continued)

	Cumulative Frequency of Occurrences (Cycles)				
Specimen No.	93	114	115	126	128
Trace	Wing Root	Wing Root	Wing Root	Wing Root	Wing Root
K_T	4	4	4	4	4
Record No.	17M-P4-4	17M-P3-3	17M-P4-4	17M-P3-3	17M-P4-4
Mean Stress (psi)	12,000	12,000	12,000	12,000	12,000
Trace Repetitions	55.7	74.8	53.0	102.5	55.6
Varying Stress (Gross Area) KSI	Random	Random	Random	Random	Random
	Test Group No. G78				
0	239,510	261,600	227,900	358,750	239,080
1.5					
2	122,540	63,580	116,600	87,125	122,320
4	52,915	37,400	50,350	51,250	52,820
6	7,241	8,228	6,890	11,275	7,228
8	1,225	1,496	1,166	2,050	1,223
10	234	374	223	512	234
12	95	127	90	174	94
12.25					
13.5	56	75	53	102	56

TABLE 86

TEST LOADING SPECTRA
(Continued)

	Cumulative Frequency of Occurrences (Cycles)				
Specimen No.	251	252	255	256	258
Trace	Wing Root	Wing Root	Wing Root	Wing Root	Wing Root
K_T	4	4	4	4	4
Record No.	46M-P4-4	46M-P2-1	46M-P4-4	46M-P4-4	46M-P2-1
Mean Stress (psi)	12,000	12,000	12,000	12,000	12,000
Trace Repetitions	217.0	156.0	114.0	172.0	197.0
Varying Stress (Gross Area) KSI	Ordered	Ordered	Ordered	Ordered	Ordered
	Test Group No. G79				
0	1,019,900	780,000	535,800	808,400	985,000
2	477,400	327,600	250,800	378,400	413,700
4	130,200	88,920	68,400	103,200	112,290
6	21,700	15,600	11,400	17,200	19,700
8	2,604	1,872	1,368	2,064	2,364
10	673	640	353	533	808
12	282	265	148	224	335
13.5	217	156	114	172	197

TABLE 86

TEST LOADING SPECTRA
(Continued)

	Cumulative Frequency of Occurrences (Cycles)			
Specimen No.	173	175	176	177
Trace	Mod. Wing Root	Mod. Wing Root	Mod. Wing Root	Mod. Wing Root
K_T	4	4	4	4
Record No.	30M-P4-4	30M-P4-4	30M-P4-4	30M-P4-4
Mean Stress (psi)	12,000	12,000	12,000	12,000
Trace Repetitions	37.3	57.6	34.9	45.1
Varying Stress (Gross Area) KSI	Random	Random	Random	Random
	Test Group No. G80			
0	167,850	259,200	157,050	202,950
2	111,900	172,800	104,700	135,300
4	59,680	92,160	55,840	72,160
6	31,705	46,360	29,665	38,335
8	10,444	16,128	9,772	12,628
8.6				
9.6				
10	1,940	2,995	1,815	2,345
10.35				
11.55				
12	213	328	199	257
13.5	37	58	35	45

TABLE 86

TEST LOADING SPECTRA
(Concluded)

	Cumulative Frequency of Occurrences (Cycles)				
Specimen No.	246	247	248	249	250
Trace	Mod. Wing Root	Mod. Wing Root	Mod. Wing Root	Mod. Wing Root	Mod. Wing Root
K_T	4	4	4	4	4
Record No.	44M-P2-1	44M-P4-4	44M-P2-1	44M-P4-4	44M-P2-1
Mean Stress (psi)	12,000	12,000	12,000	12,000	12,000
Trace Repetitions	31.1	27.4	34.1	32.7	43.5
Varying Stress (Gross Area) KSI	Ordered	Ordered	Ordered	Ordered	Ordered
	Test Group No. G81				
0	133,730	117,820	146,630	140,610	187,050
2	99,520	84,940	109,120	101,370	139,200
4	62,200	46,580	68,200	55,590	87,000
6	37,320	24,660	40,920	29,430	52,200
8	18,038	9,364	19,778	11,772	25,230
10	4,976	3,288	5,456	3,924	6,960
12	404	329	443	392	566
13.5	31	27	34	33	44

TABLE 87

RANDOM MILITARY MANEUVER LOADING HISTORIES
(PEAK COUNTS)
Minimum Stress = 5,450 psi
K_T = 4.0

Test Group No. M14

Incremental Stress (psi)	Cumulative Frequency of Load Cycle Occurrences					
	Specimen No.342	Specimen No.343	Specimen No.344	Specimen No.345	Specimen No.346	Specimen No. 347 & No. 349
0	26,400	22,000	17,600	30,800	44,000	26,400
2,840	20,700	17,250	13,800	24,150	34,500	20,700
5,680	16,100	13,450	10,760	18,830	26,900	16,100
11,400	9,360	7,800	6,240	10,920	15,600	9,360
17,000	4,560	3,800	3,040	5,320	7,600	4,560
22,700	1,830	1,525	1,220	2,135	3,050	1,830
28,400	540	450	360	630	900	540
31,200	288	240	192	336	480	288
34,000	132	110	88	154	220	132
39,800	24	20	16	28	40	24
41,200	12	10	8	14	20	12
42,050	6	5	4	7	10	6

TABLE 88

ORDERED MILITARY MANEUVER LOADING HISTORIES

Stress Interval = 4,000 psi
Unit Spectrum = 1/20 avg. random test history
Minimum Stress = 5,450 psi
K_T = 4.0

Test Group No. M15

Incremental Stress (psi)	Cumulative Frequency of Load Cycle Occurrences				
	Specimen No.399	Specimen No.400	Specimen No.401	Specimen No.404	Specimen No.406
1,680	12,900	12,898	9,676	19,345	15,001
5,180	8,700	8,698	6,526	13,045	10,101
9,250	5,880	5,878	4,411	8,815	6,811
13,550	3,780	3,778	2,836	5,665	4,361
17,800	2,280	2,278	1,711	3,415	2,611
22,100	1,260	1,258	946	1,885	1,421
26,300	588	586	442	877	637
30,700	240	238	181	355	260
34,800	84	82	64	121	91
38,450	24	22	19	34	26
42,000	3	3	3	5	4
No. of Blocks	12.00	11.99	9.00	17.99	13.95

TABLE 89

ORDERED MILITARY MANEUVER LOADING HISTORIES

Stress Interval = 1,000 psi
Unit Spectrum = 1/20 avg. random test history
Minimum Stress = 5,450 psi
K_T = 4.0

Test Group No. M16

Incremental Stress (psi)	Cumulative Frequency of Load Cycle Occurrences			
	Specimen No.410	Specimen No.411	Specimen Nos.413&414	Specimen No.415
470	8,201	17,425	12,298	13,271
1,320	7,401	15,725	11,098	11,971
2,020	6,801	14,450	10 198	10,996
2,730	6,201	13,175	9.298	10,021
3.480	5,601	11,900	8,398	9,046
4,330	5,001	10,625	7,498	8,071
5,320	4,521	9,605	6,778	7.291
6,420	4,081	8,670	6,118	6,576
7,460	3,721	7,905	5,578	5,991
8,430	3,361	7,140	5,038	5,406
9,480	3,001	6,375	4,498	4,821
10,560	2,721	5,780	4,078	4.366
11,600	2,401	5,100	3.598	3,846
12,700	2,121	4,505	3,178	3,391
13,800	1,881	3,995	2,818	3,001
14,900	1,681	3,570	2,518	2.676
16,050	1,425	3,026	2,134	2,260
16,850	1,241	2,635	1,858	1,961
17,950	1,081	2.295	1,618	1,701
19,400	921	1,955	1,378	1,441
20,450	769	1,632	1,150	1,194
21,500	649	1,377	970	999
22,800	529	1,122	790	804
24,000	441	935	658	661
25,100	345	731	514	517
26,400	281	595	418	421
27,700	233	493	346	349
28,800	185	391	274	277
29,800	137	289	202	205
30,850	105	221	154	157
32,000	81	170	118	121
33,150	65	136	94	97
34,200	49	102	70	73
35,200	37	77	52	55
36,150	29	60	40	43
37,150	21	43	29	31
38,250	15	31	21	22
39,400	10	21	14	15
40,300	7	16	11	11
42,000	4	9	6	6
No. of Blocks	8.00	17.00	11.99	12.95

TABLE 90

RANDOM GROUND LOADING HISTORIES
(MEAN CROSSING PEAK COUNTS)

f_{mean} = -3,000 psi
K_T = 7.0

Test Group No. T1

Varying Stress (psi)	Cumulative Frequency of Load Cycle Occurrences					
	Specimen No.416	Specimen No.417	Specimen No.418	Specimen No.419	Specimen No.422	Specimen No.423
0	783,000	500,250	552,450	578,550	495,900	448,050
950	452,400	289,000	319,300	334,200	286,250	258,700
1,920	208,250	133,000	146,850	153,800	131,550	119,050
2,850	73,600	47,040	51,950	54,400	46,450	42,150
3,800	20,050	12,846	14,168	14,818	12,656	11,460
4,750	4,843	3,107.5	3,424	3,583	3,057.5	2,770
5,700	1,287	827.9	911.2	953.7	813.9	738.5
6,180	715.9	461.0	507.3	530.4	453.4	410.9
6,650	458.9	295.6	325.1	339.4	290.1	262.9
7,130	286.2	184.3	202.6	211.6	180.3	164.3
7,600	187.4	120.4	133.2	138.0	117.6	107.2
8,000	129.4	83.0	91.8	94.8	80.9	73.7
8,550	48.8	31.1	34.6	34.6	29.8	26.6
9,250	32.8	20.8	23.1	23.1	19.8	17.8
9,500	11.0	6.7	7.8	7.8	6.7	6.7
9,620	10.2	6.2	7.2	7.2	6.2	6.2
9,980	4.4	2.7	2.7	2.7	2.7	2.7
10,450	3.4	2.0	2.0	2.0	2.0	2.0
11,150	1.0					

TABLE 91

ORDERED GROUND LOADING HISTORIES

Stress Interval = 1,000 psi
Unit Spectrum = 1/20 avg. random test history
f_{mean} = -3,000 psi
a_T = 7.0

Test Group No. 72

Varying Stress (psi)	Cumulative Frequency of Load Cycle Occurrences					
	Specimen No.461	Specimen No.462	Specimen No.465	Specimen No.466	Specimen No.469	Specimen No.471
550	775,438	747,757	1,010,085	1,268,351	900,009	1,309,422
1,580	396,008	380,257	516,585	648,851	459,009	668,922
2,580	144,008	136,007	187,585	235,851	165,009	241,192
3,580	41,408	39,107	53,635	67,701	47,159	69,012
4,610	5,768	5,447	7,370	9,291	6,569	9,612
5,700	2,168	2,047	2,770	3,491	2,469	3,612
6,780	692	653	884	1,113	788	1,152
7,910	296	279	378	475	337	492
8,780	87	82	111	139	99	144
9,480	22	20	28	34	25	36
10,500	7	6	9	11	8	12
No. of Blocks	36.07	34.78	46.98	58.99	41.86	60.90

TABLE 92

ORDERED COMPOSITE LOADING HISTORIES

(Spectra Based on Tests Having Approx. 11 Random Gust Loadings per Flight)

LOW PEAK GUST LOADINGS IN FLIGHT

Stress Interval = 1,000 psi
Unit Spectrum = 1/20 average random test history
K_T = 4.0

Test Group No. C01

Varying Stress (psi)	Cumulative Frequency of Load Cycles Occurrences				
	Specimen No. 475	Specimen No. 480	Specimen No. 481	Specimen No. 485	Specimen No. 487
	Gust Loadings f_{mean} = 6,000 psi				
580	674,501	351,000	766,987	467,505	1,040,000
1,680	388,501	202,500	442,487	269,505	600,000
2,720	180,501	94,500	206,487	125,505	280,000
3,8[illegible]	76,501	40,500	89,487	53,505	120,000
4,8[illegible]0	29,051	14,850	32,437	19,305	44,000
5,880	8,161	4,320	9,427	5,600	12,800
6,920	2,296	1,215	2,647	1,575	3,600
7,850	919	496	1,054	630	1,440
8,700	408	216	464	280	640
9,650	205	108	232	140	320
10,680	82	43	93	56	128
11,620	31	16	35	21	48
13,000	10	5	12	7	16
	Ground Loadings f_{mean} = -3,000 psi				
600	357,001	189,000	406,232	245,000	560,000
1,700	204,001	108,000	232,232	140,000	320,000
2,750	96,901	51,300	110,432	66,500	152,000
3,900	40,801	21,600	46,632	28,000	64,000
5,080	15,301	8,100	17,632	10,500	24,000
6,200	4,591	2,430	5,452	3,150	7,200
7,180	1,276	675	1,682	875	2,000
8,120	511	270	812	350	800
9,020	205	108	464	140	320
9,850	103	54	116	70	160
10,880	52	27	58	35	80
12,000	21	11	23	14	32
	Ground to Air Cycles f_{mean} = 1,500 psi				
4,000	60,486	31,249	68,788	41,510	94,287
No. of Blocks	51.54	26.96	58.62	35.59	79.97

TABLE 93

ORDERED COMPOSITE LOADING HISTORIES
(Spectra Based on Tests having approx. 12 Random Gust Loadings per Flight)

LOW PEAK GUST LOADINGS IN FLIGHT

Stress Interval = 1,000 psi
Unit Spectrum = 1/20 avg. random test history
K_T = 7.0

Test Group No. CG2

Varying Stress (psi)	Cumulative Frequency of Load Cycle Occurrences				
	Specimen No. 478	Specimen No. 479	Specimen No. 482	Specimen No. 484	Specimen No. 486
	Gust Loadings f_{mean} = 6,000 psi				
650	84,652	87,180	52,445	69,305	52,575
1,800	48,442	49,950	30,005	39,725	30,135
2,750	25,367	26,225	15,705	20,875	15,835
3,700	9,747	10,165	6,025	8,115	6,155
4,650	3,447	3,595	2,155	2,895	2,195
5,550	1,067	1,113	693	923	699
6,600	227	237	177	227	177
7,950	105	107	61	82	61
8,900	43	43	26	35	27
9,550	18	18	11	15	11
11,000	4	4	2	3	2
	Ground Loadings f_{mean} = -3,000 psi				
650	42,002	43,201	25,811	34,765	26,395
1,800	21,702	22,321	13,341	17,945	13,635
2,800	8,402	8,641	5,171	6,925	5,275
3,800	2,522	2,593	1,559	2,053	1,585
4,750	492	505	312	400	309
5,720	121	123	74	98	76
6,750	40	40	24	32	25
7,800	15	15	9	12	9
8,850	4	4	2	3	2
	Ground to Air Cycles f_{mean} = 1,500 psi				
4,650	7,280	7,488	4,472	5,928	4,545
No. of Blocks	70.54	72.61	43.57	57.93	43.98

TABLE 94

ORDERED COMPOSITE LOADING HISTORIES
(Spectra Based on Tests having approx. 13 Random Gust Loadings per Flight)

HIGH PEAK GUST LOADINGS IN FLIGHT

Test Group No. C03
Stress Interval = 1,000 psi
Unit Spectrum = 1/20 avg. random test history
K_T = 4.0

Varying Stress (psi)	Cumulative Frequency of Load Cycles Occurrences				
	Specimen No. 467	Specimen No. 470	Specimen No. 472	Specimen No. 473	Specimen No. 474
	Gust Loadings f_{mean} = 12,000 psi				
580	91,835	120,914	74,142	75,449	95,632
1,780	65,435	86,114	52,542	53,849	68,032
2,900	43,435	57,114	35,002	35,849	45,032
3,850	24,735	32,776	20,127	20,549	25,875
4,850	13,545	17,956	11,027	11,187	14,176
5,880	6,665	8,836	5,427	5,427	6,976
7,000	3,010	3,991	2,452	2,452	3,151
8,100	1,247	1,654	1,017	1,017	1,306
9,050	516	685	422	422	541
10,030	258	343	212	212	271
11,050	129	172	107	107	136
12,050	69	92	58	58	73
13,100	39	52	33	33	41
14,200	22	29	18	18	23
15,100	13	18	11	11	14
15,600	6	9	6	6	7
16,300	2	3	2	2	2
	Ground Loadings f_{mean} = -3,000 psi				
620	44,720	59,281	36,401	36,401	46,800
1,680	20,640	27,361	16,801	16,801	21,600
2,600	8,170	10,831	6,651	6,651	8,550
3,650	2,365	3,136	1,926	1,926	2,475
4,600	430	571	351	351	450
5,500	129	172	106	106	135
6,450	43	58	36	36	45
7,420	15	20	13	13	15
8,300	4	6	4	4	4
8,950	2	3	2	2	2
	Ground to Air Cycles f_{mean} = 4,500 psi				
7,950	7,955	10,545	6,475	6,475	8,325
No. of Blocks	43.56	57.04	35.28	35.67	45.44

TABLE 95

ORDERED COMPOSITE LOADING HISTORIES
(Spectra Based on Tests having approximately 110 Random Gust Loadings per Flight)

HIGH PEAK GUST LOADINGS IN FLIGHT
Test Group No. CG4
Stress interval = 1,000 psi
Unit Spectrum = 1/20 avg. random test history
K_T = 4.0

Varying Stress (psi)	Cumulative Frequency of Load Cycle Occurrences							
	Specimen No. 509	Specimen No. 510	Specimen No. 511	Specimen No. 512	Specimen No. 513	Specimen No. 514	Specimen No. 517	Specimen No. 518
	Gust Loadings f(mean) = 12,000 psi							
550	179,556	231,735	302,418	197,951	246,129	240,364	158,896	269,287
1,[illegible]20	129,556	166,735	217,418	142,951	176,129	172,864	113,896	194,287
2,450	79,556	101,735	132,418	87,951	108,002	107,864	68,896	119,287
3,[illegible]	47,556	60,135	79,201	52,751	64,302	64,664	40,303	71,287
4,350	25,556	32,503	42,901	28,551	35,102	34,964	22,103	38,287
5,320	13,556	17,503	23,101	15,351	18,902	18,764	11,903	20,302
6,420	5,702	7,503	9,901	6,551	8,102	7,964	5,103	8,702
7,500	2,377	3,128	4,126	2,701	3,377	3,251	2,128	3,627
8,500	952	1,253	1,651	1,051	1,352	1,301	853	1,452
9,600	477	623	826	526	667	651	428	727
10,620	230	303	397	253	326	313	207	350
11,580	135	178	232	148	191	183	122	205
12,580	68	93	116	74	96	92	62	103
13,520	39	52	66	42	55	53	36	59
14,450	20	27	33	21	28	27	19	30
15,450	10	14	16	10	14	14	10	15
16,420	4	6	6	4	6	6	4	6
18,300	2	3	3	2	3	3	2	3

(continued on next page)

TABLE 95 (Continued)

Varying Stress (psi)	Cumulative Frequency of Load Cycle Occurrences: Specimen No. 509	Specimen No. 510	Specimen No. 511	Specimen No. 512	Specimen No. 513	Specimen No. 514	Specimen No. 517	Specimen No. 518
			Ground Loadings f_{mean} = -3,000 psi					
550	19,002	25,013	33,004	21,004	27,004	26,004	17,004	29,005
1,520	10,452	13,763	19,154	11,554	14,854	14,304	9,354	15,955
2,550	3,612	4,763	6,274	3,994	5,134	4,944	3,234	5,615
3,520	1,142	1,513	1,984	1,264	1,624	1,564	1,024	1,745
4,500	230	313	400	256	328	316	208	353
5,520	68	88	119	77	98	95	63	106
6,520	22	28	36	24	30	30	20	33
7,520	10	13	16	11	14	14	9	15
9,300	2	3	3	2	3	3	2	3
			Ground to Air Cycles f_{mean} = 4,500 psi					
7,850	1,748	2,300	3,036	1,932	2,484	2,392	1,564	2,668
No. of Blocks	19.85	25.67	33.54	21.89	27.31	26.63	17.58	29.82

(End of Table)

TABLE 96

RANDOM COMPOSITE LOADING HISTORIES

MILITARY MANEUVER LOADINGS IN FLIGHT
$K_T = 4.0$
Test Group No. CML

Dynamic Stress (psi)	Cumulative Frequency of Load Cycle Occurrences Specimen No.488	Specimen No. 489	Specimen No. 490	Specimen No.499	Specimen No.500
(Incremental)	Military Maneuver Loadings Minimum Stress = 5,450 psi				
0	7,236	8,126	9,549	7,711	10,676
2,840	5,674	6,371	7,488	6,046	8,371
5,680	4,424	4,968	5,838	4,714	6,527
11,400	2,566	2,881	3,386	2,734	3,785
17,000	1,250	1,404	1,649	1,332	1,844
22,700	502	563	662	534	740
28,400	148	166	195	158	218
31,200	78	88	104	84.1	116
34,000	36.2	40.6	47.7	38.6	53.4
39,700	6.58	7.39	8.68	7.01	9.71
41,200	3.29	3.69	4.34	3.50	4.85
42,000	1.64	1.85	2.17	1.75	2.43
(Varying)	Ground Loadings $f_{mean} = -3,000$ psi				
0	1,682	1,888	2,216	1,793	2,478
950	971	1,090	1,280	1,036	1,431
1,920	446	501	588	476	658
2,850	158	177	208	168	233
3,800	43.0	48.2	56.6	45.8	63.3
4,750	10.4	11.6	13.7	11.1	15.3
5,700	2.75	3.09	3.63	2.94	4.06
6,180	1.53	1.72	2.02	1.63	2.26
6,650	0.982	1.10	1.29	1.05	1.45
7,130	0.61	0.69	0.81	0.65	0.90
7,600	0.41	0.45	0.53	0.43	0.59
8,000	0.28	0.31	0.36	0.29	0.41
8,550	0.10	0.12	0.14	0.11	0.15
9,250	0.070	0.078	0.092	0.074	0.10
9,500	0.024	0.026	0.031	0.025	0.035
9,620	0.022	0.024	0.029	0.023	0.032
9,980	0.008	0.009	0.011	0.009	0.012
10,450	0.006	0.007	0.008	0.006	0.009
	Ground-Air-Ground Loading $f_{mean} = 1,225$ psi				
4,225	240	270	317	256	354

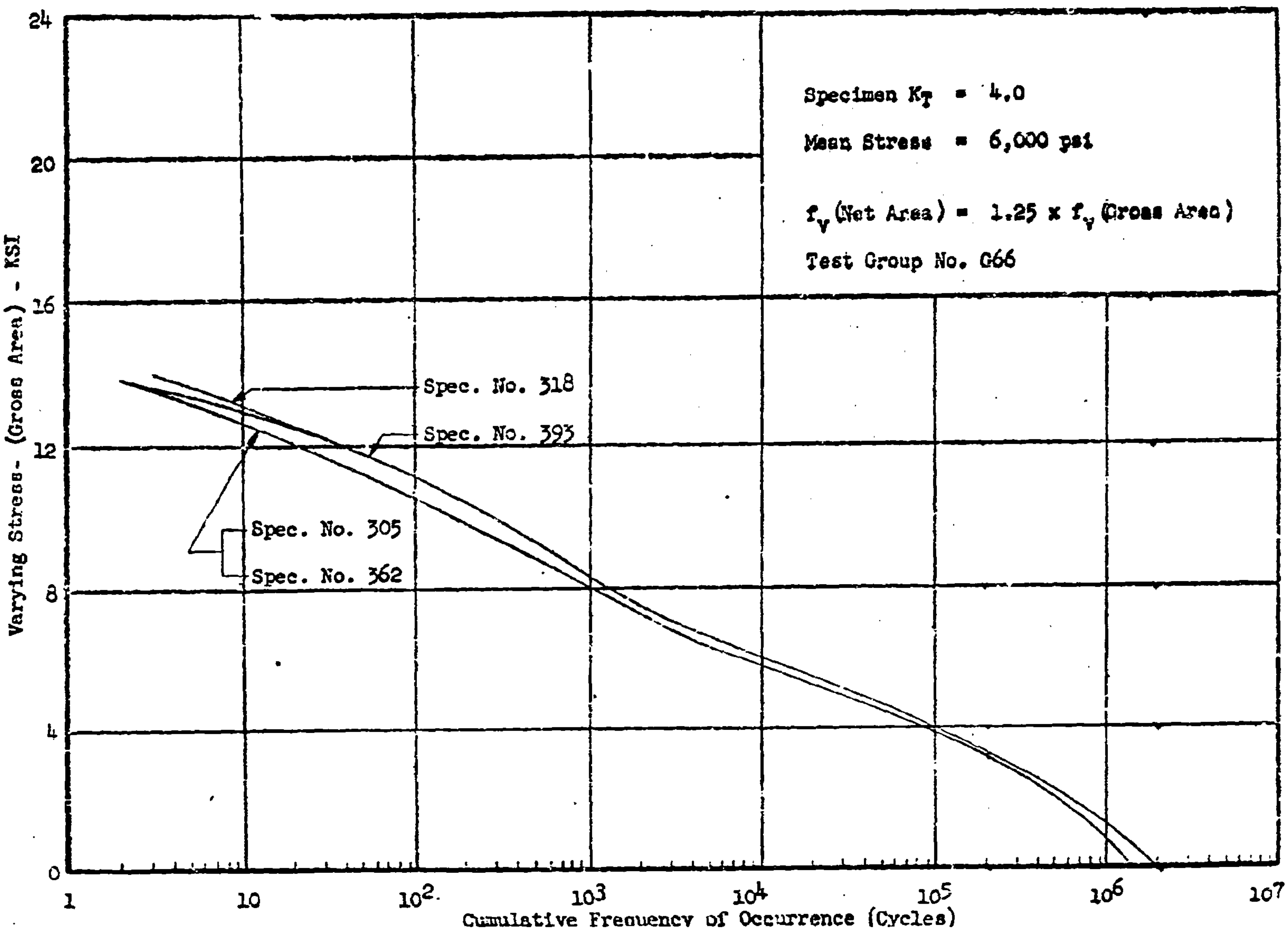

Figure 145 Random Low Peak Gust Loading Test Data

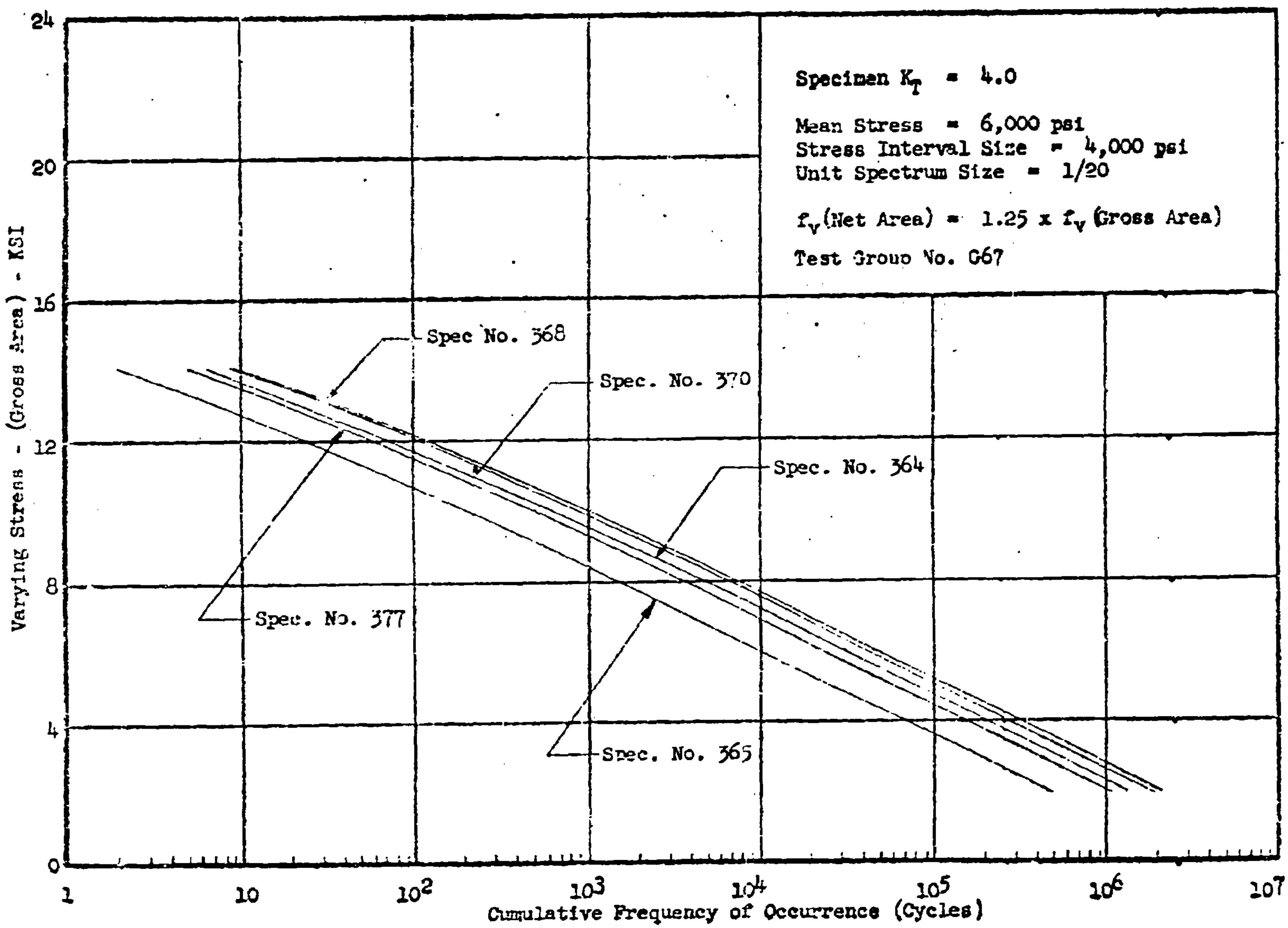

Figure 146 Ordered Low Peak Gust Loading Test Data

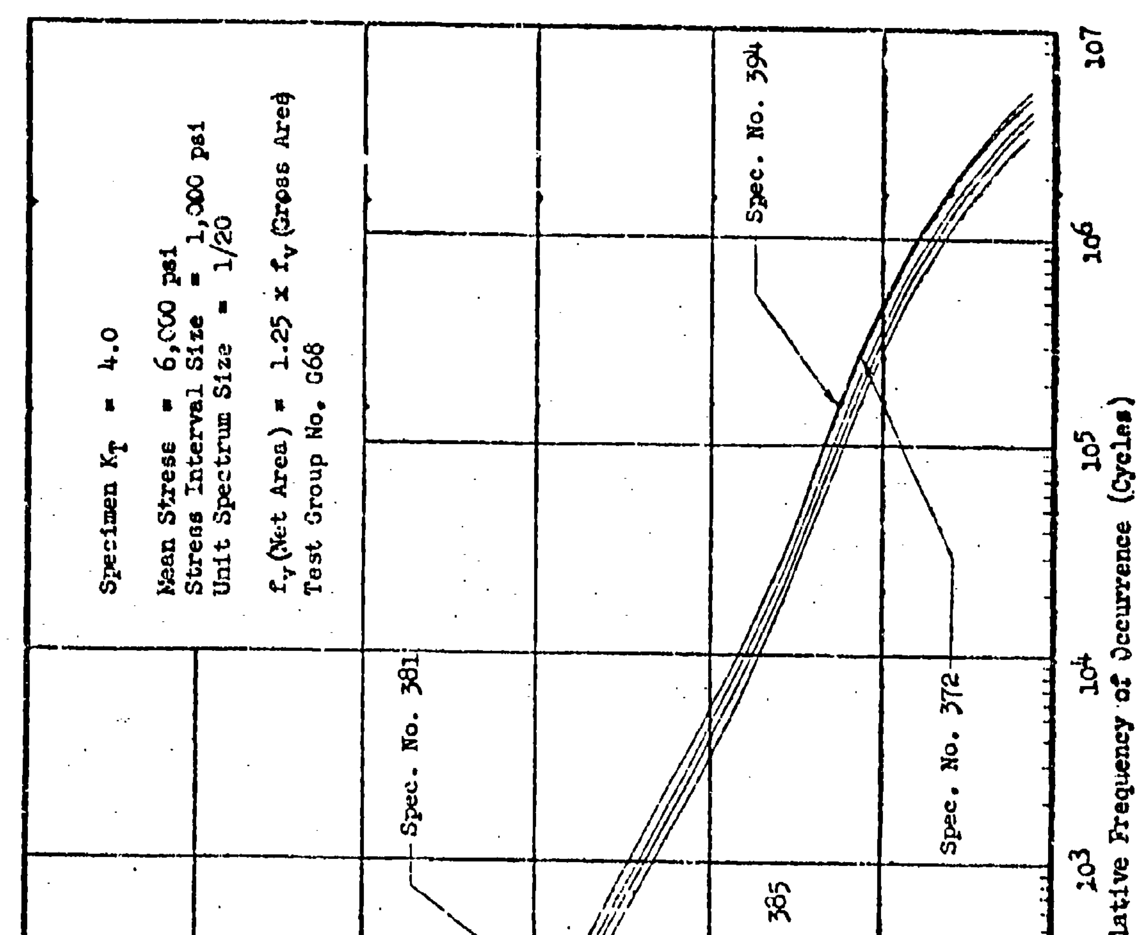

Figure 147 Ordered Low Peak Gust Loading Test Data

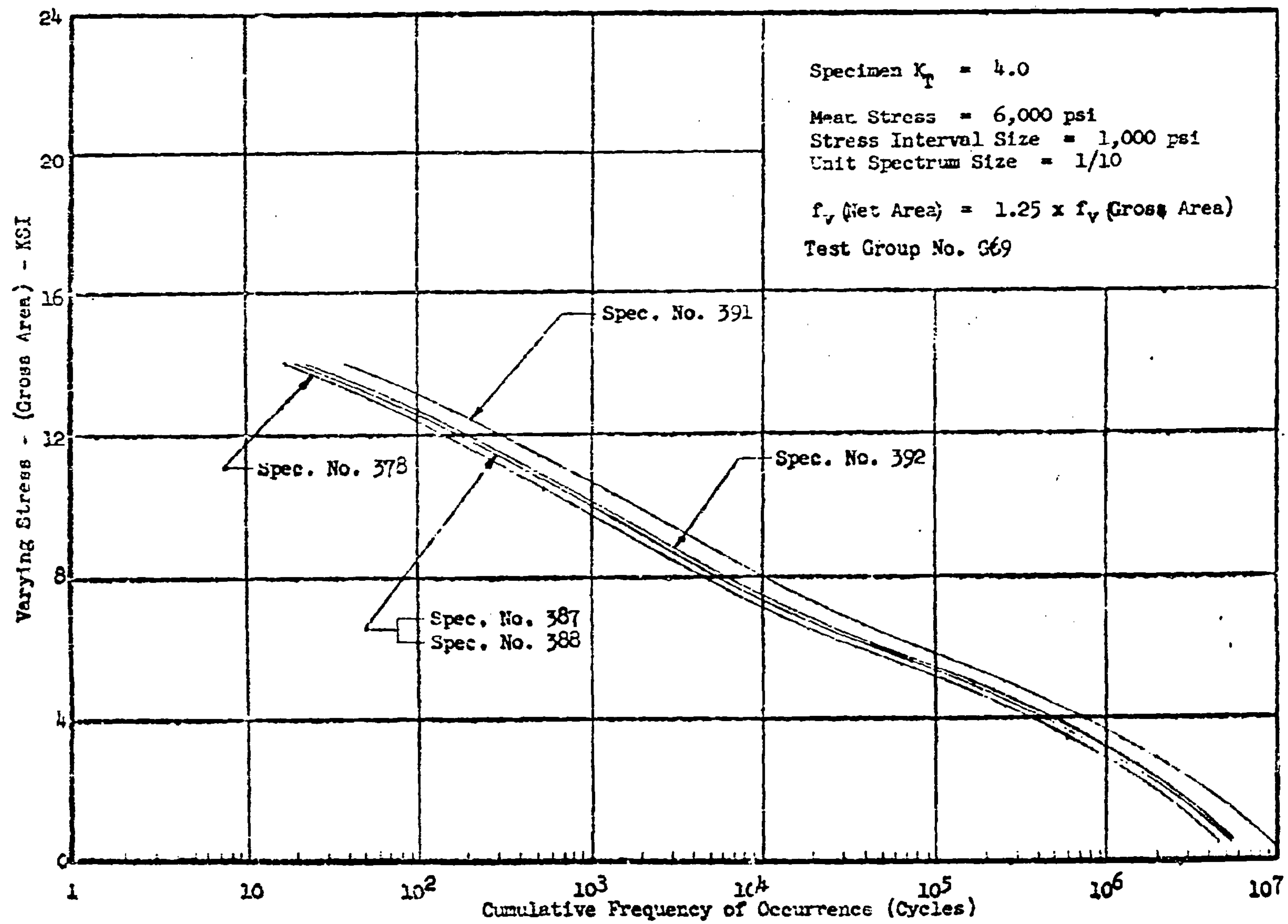

Figure 148 Ordered Low Peak Gust Loading Test Data

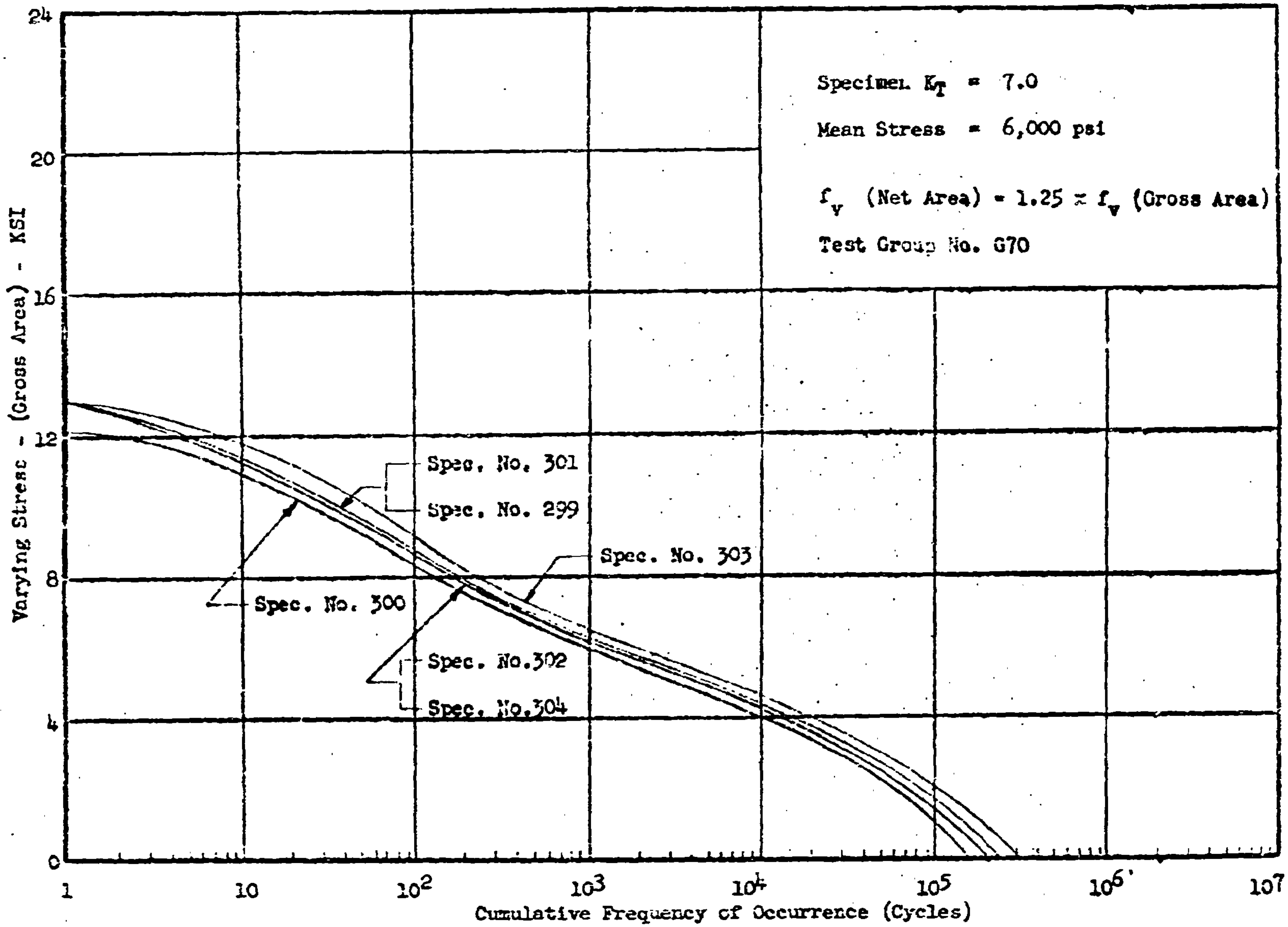

Figure 149 Random Low Peak Gust Loading Test Data

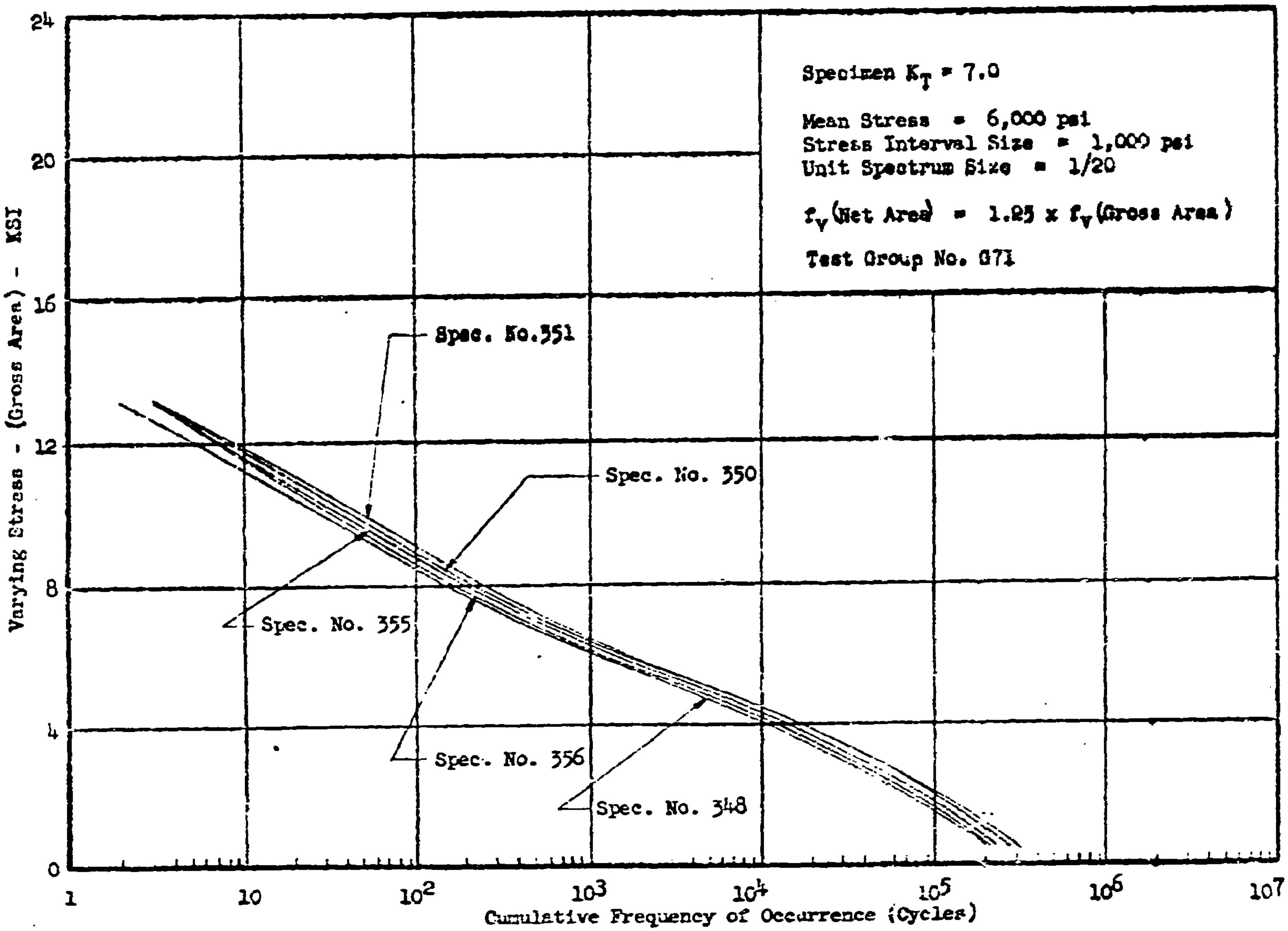

Figure 150 Ordered Low Peak Gust Loading Test Data

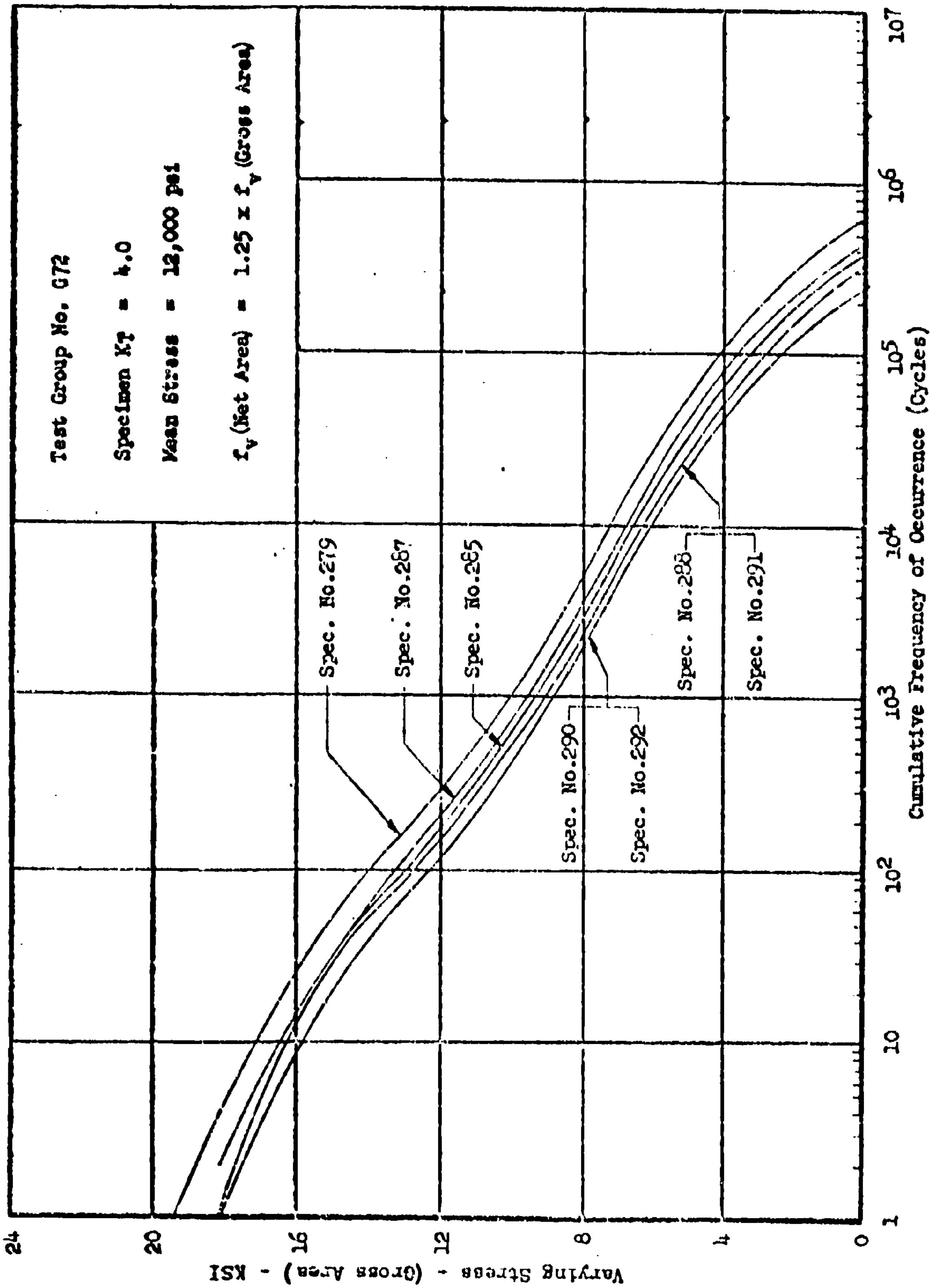

Figure 151 Random Peak Gust Loading Test Data

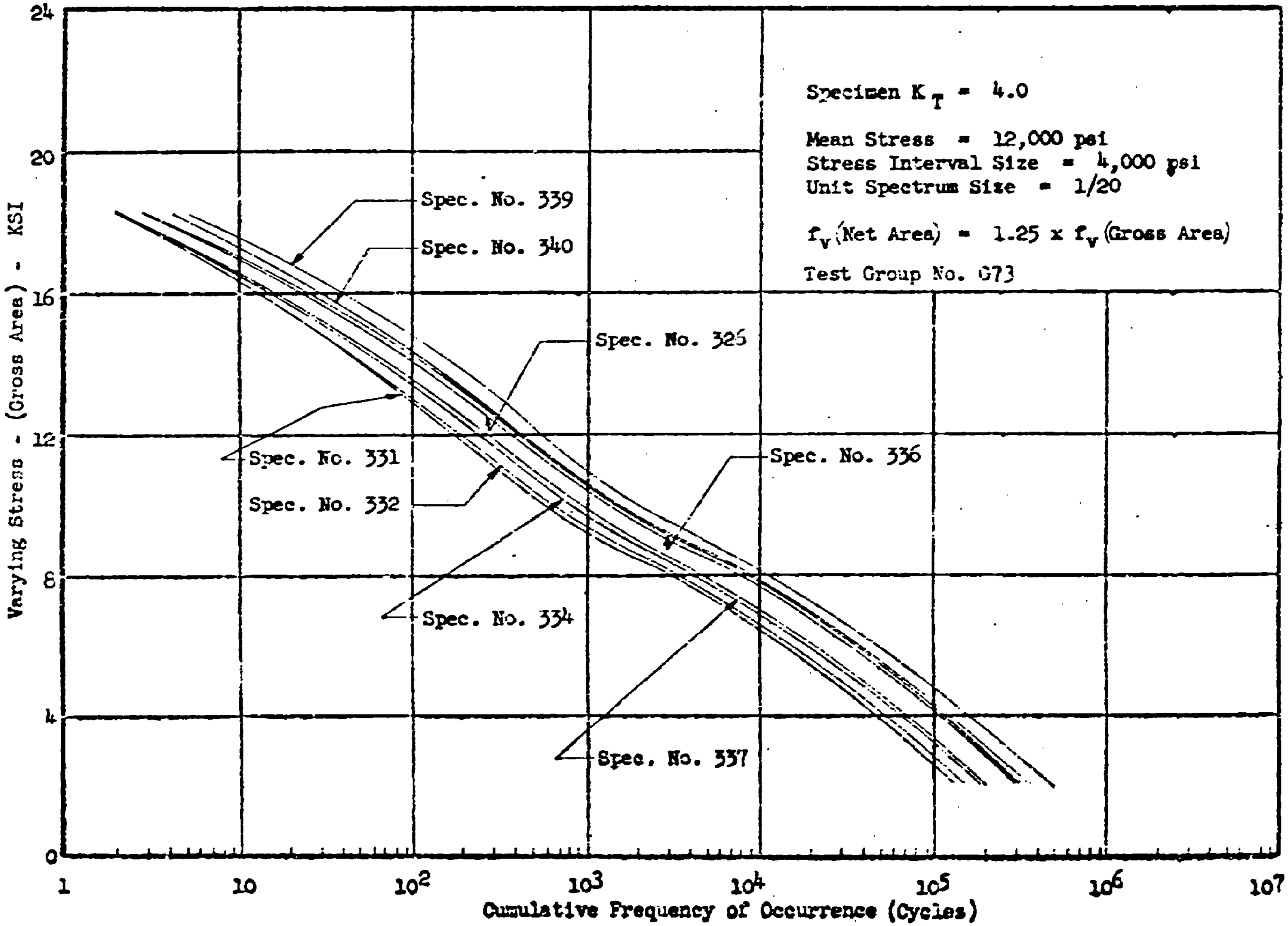

Figure 152 Ordered High Peak Gust Loading Test Data

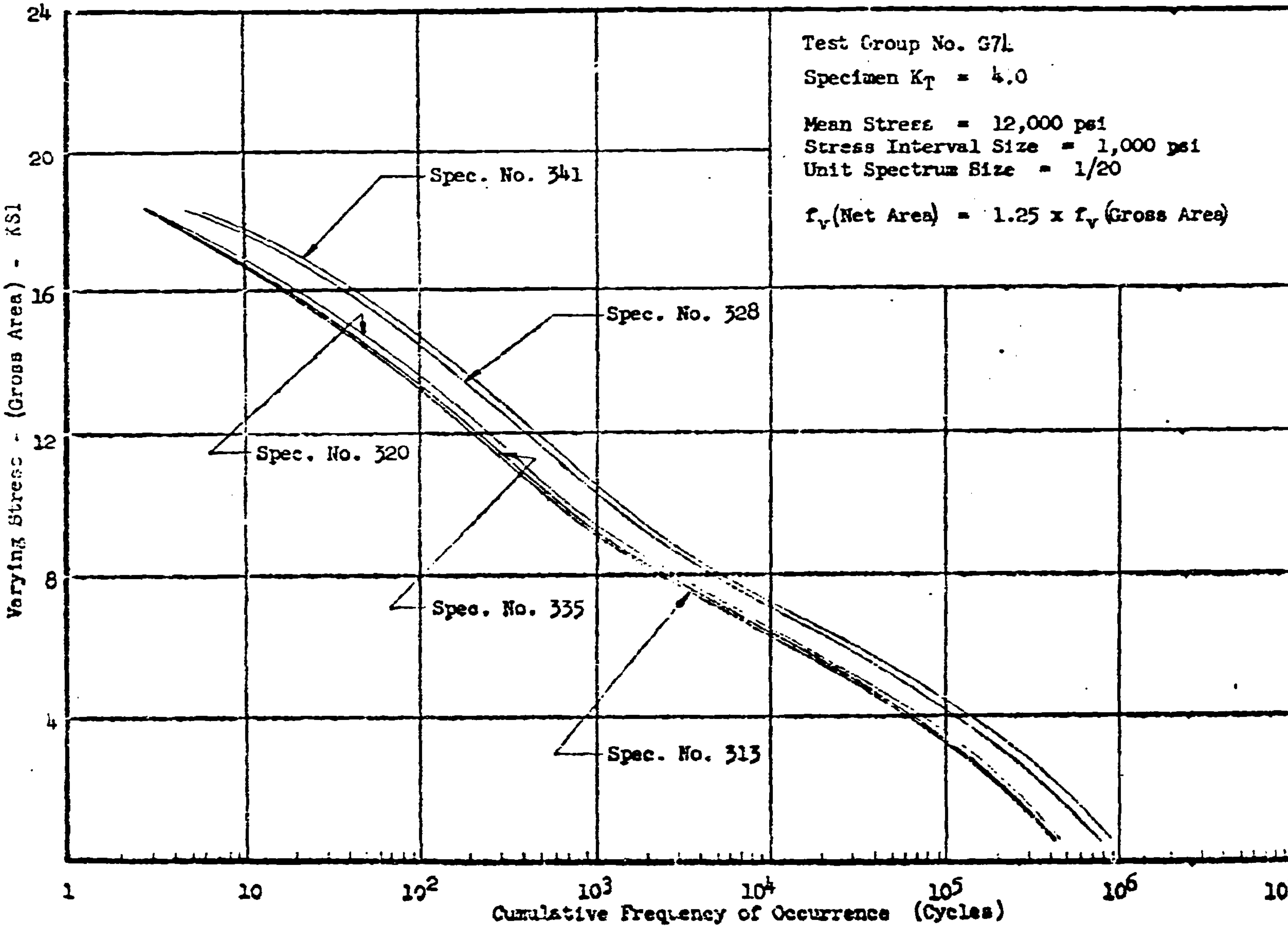

Figure 153 Ordered High Peak Gust Loading Test Data

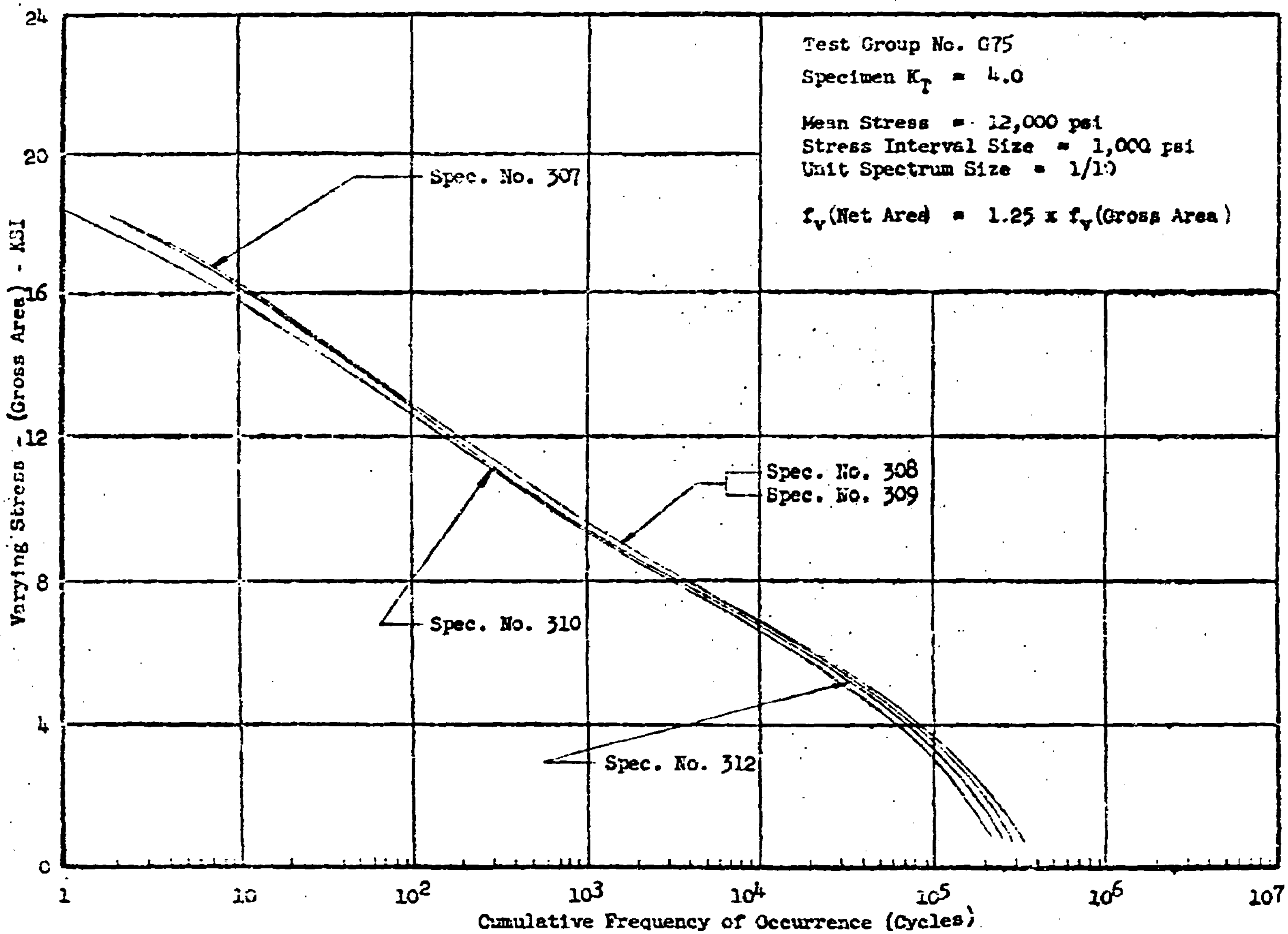

Figure 154 Ordered High Peak Gust Loading Test Data

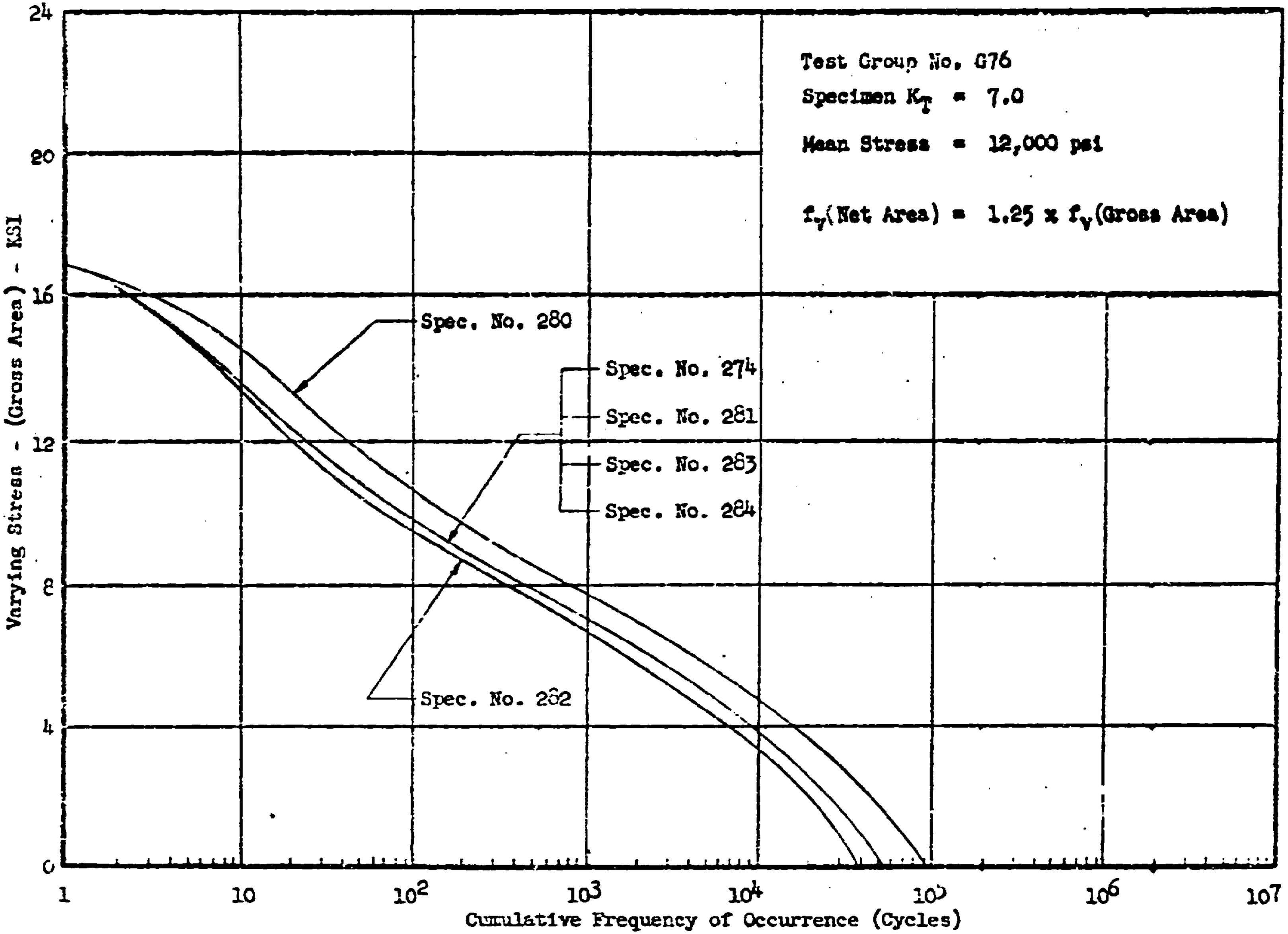

Figure 155 Random High Peak Gust Loading Test Data

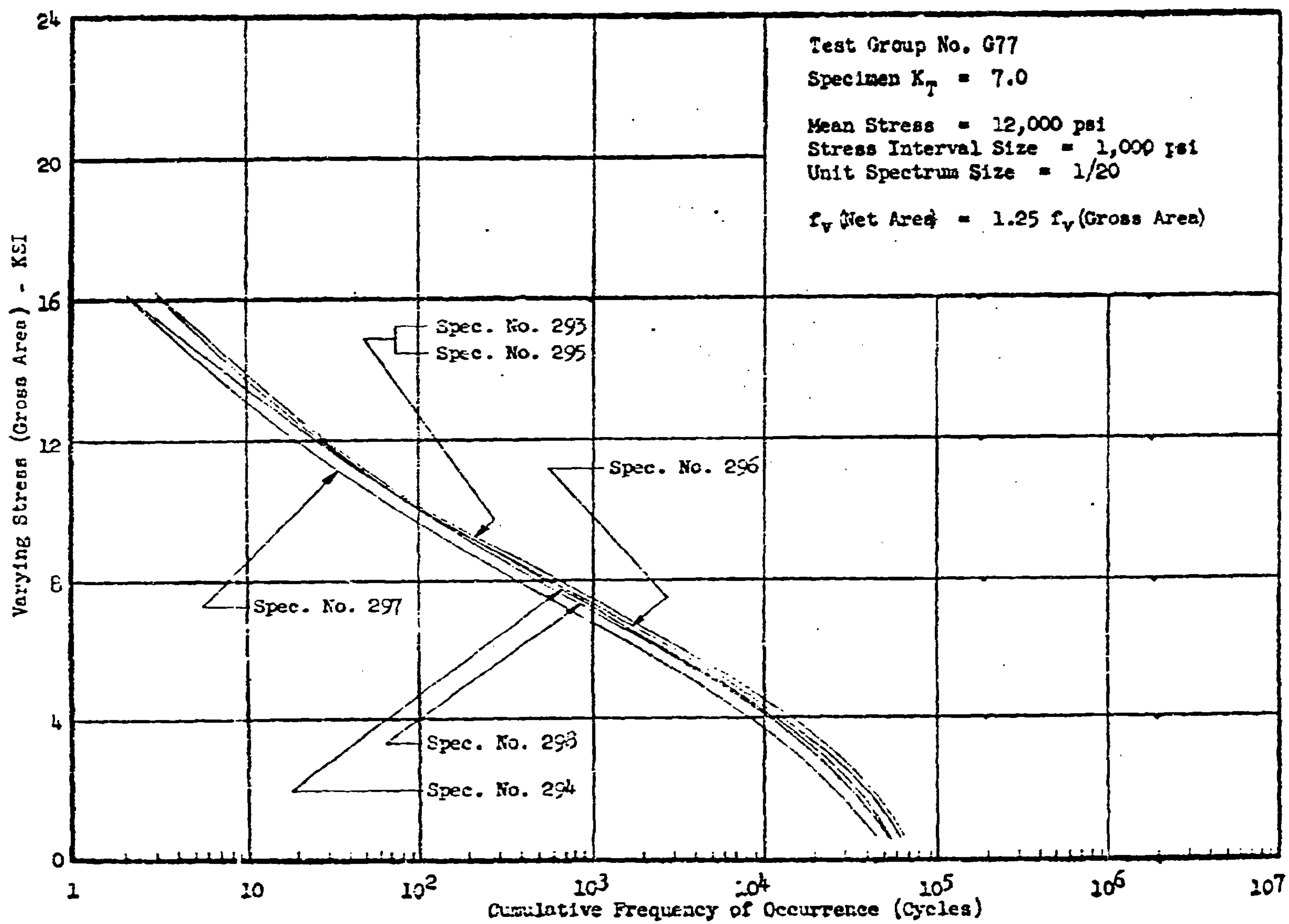

Figure 156 Ordered High Peak Gust Loading Test Data

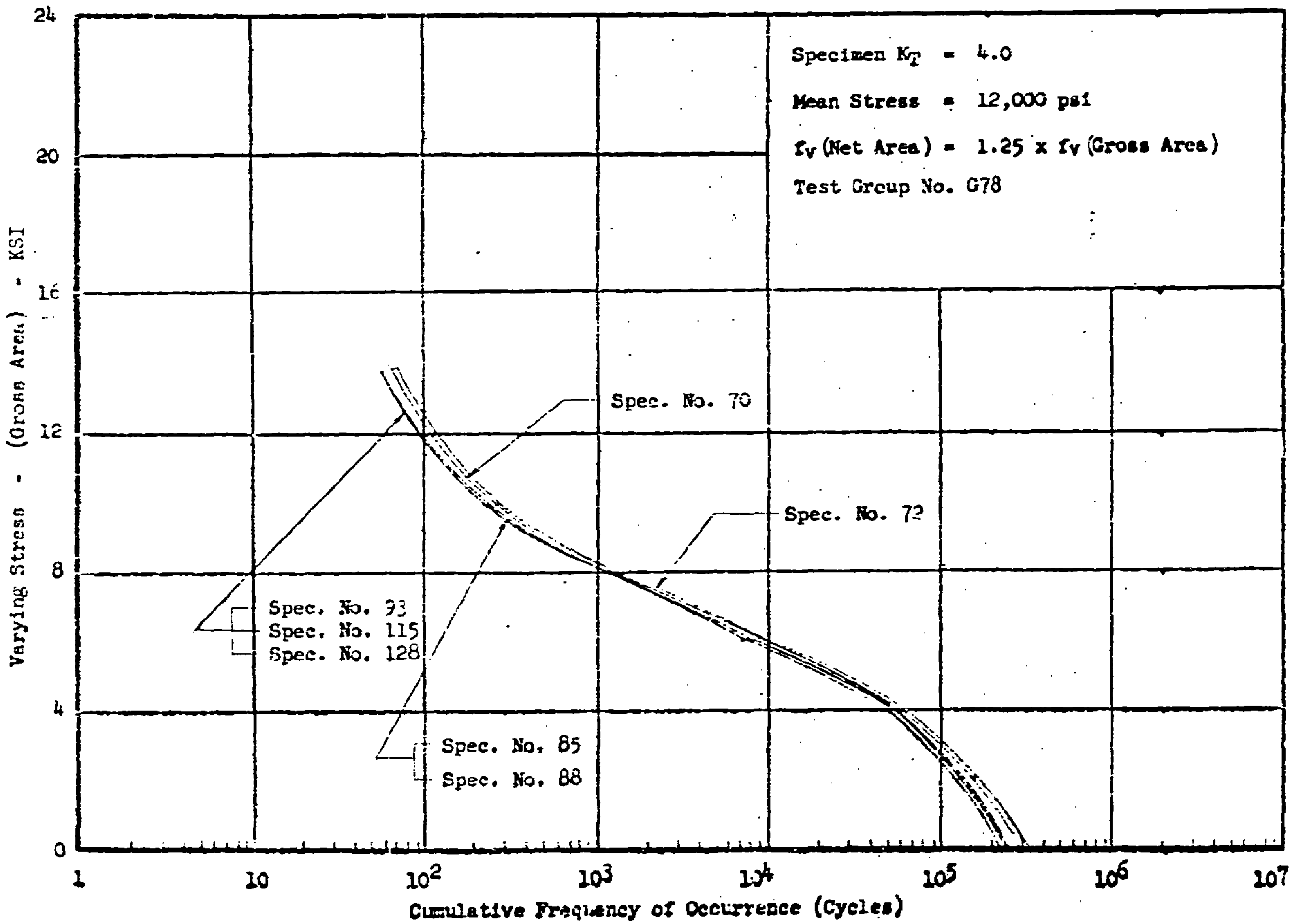

Figure 157 Wing Root Random Loading Test Data (Mean Crossing Peak Count)

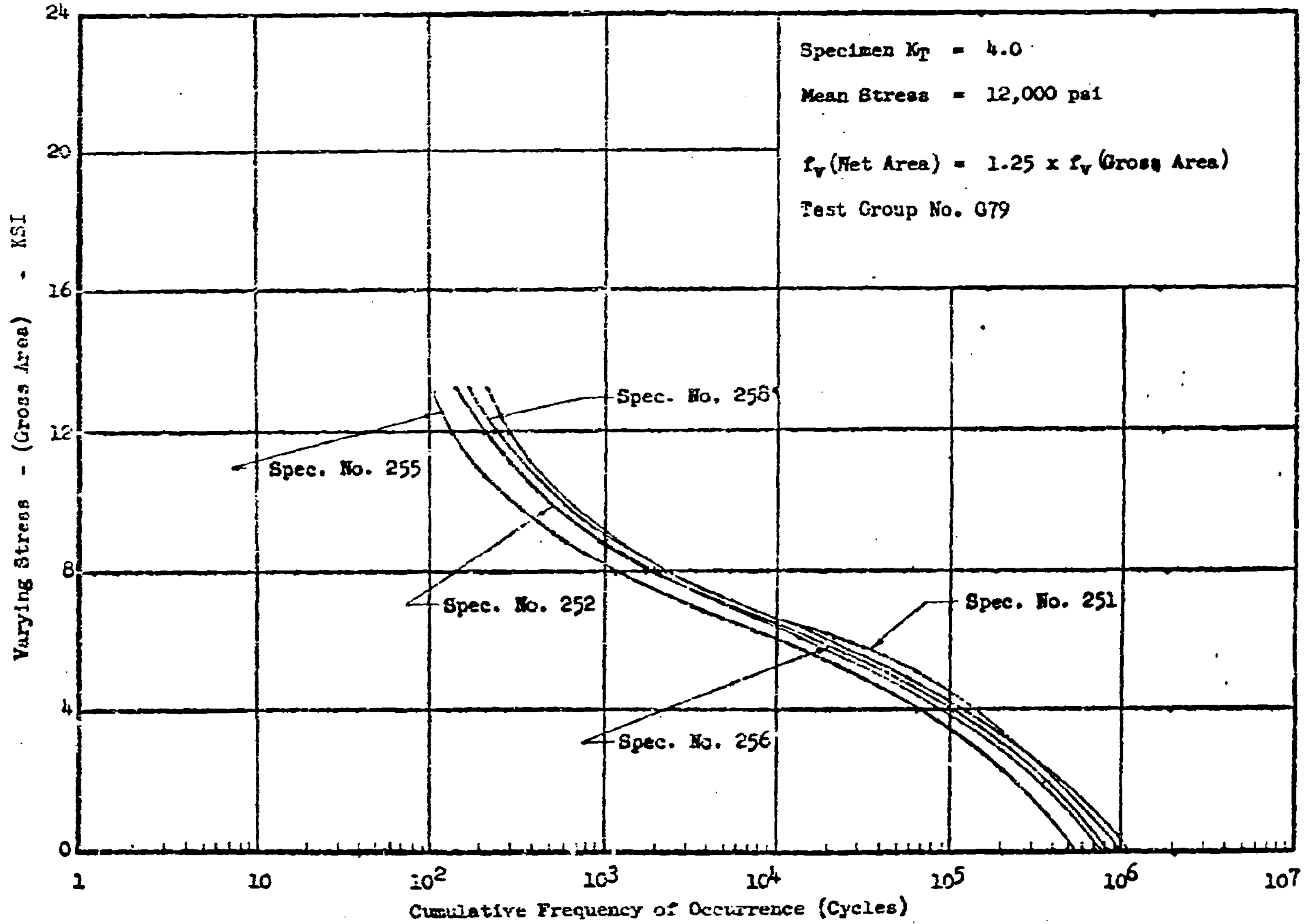

Figure 158 Wing Root Ordered Loading Test Data (Mean Crossing Peak Count)

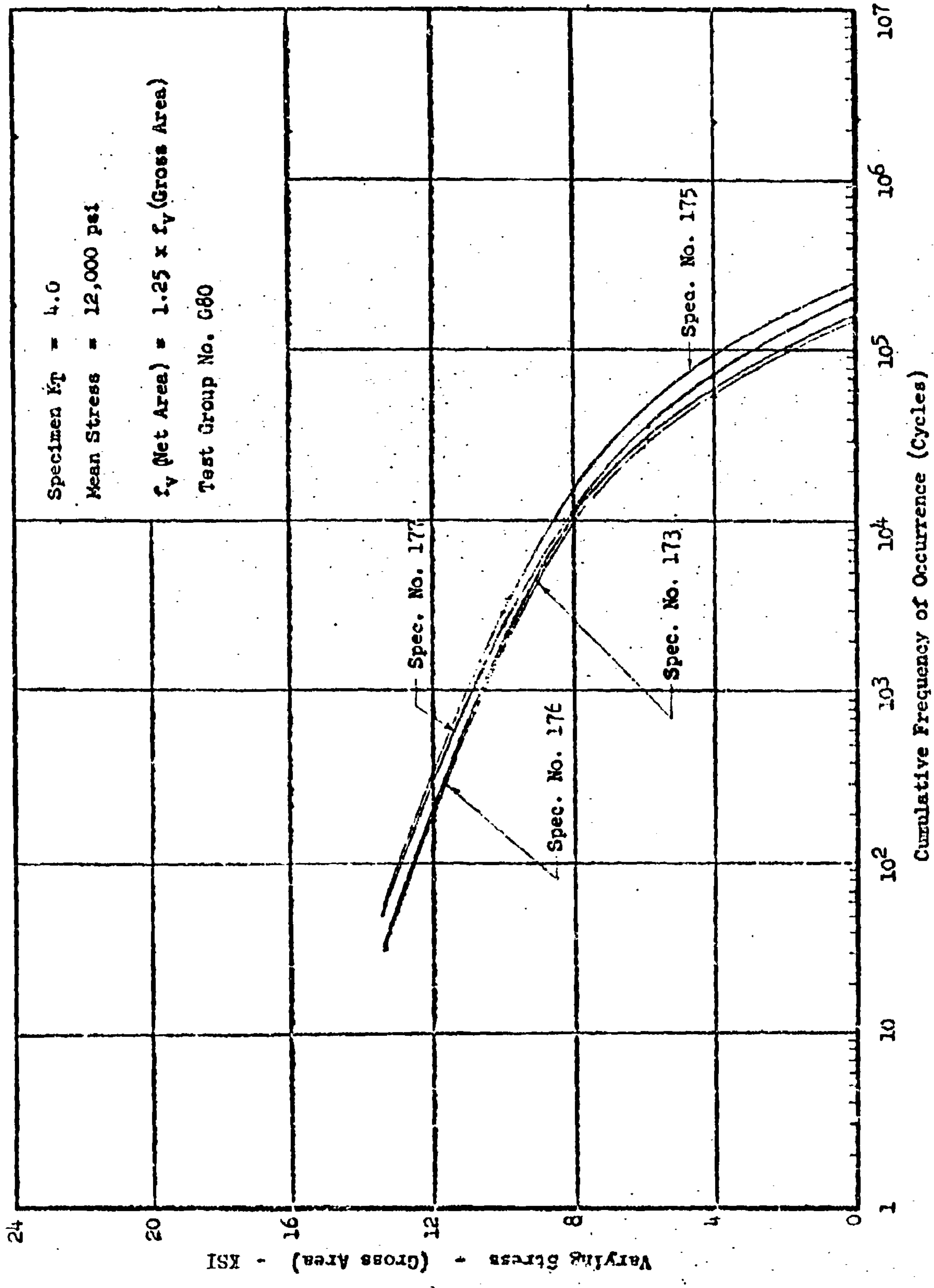

Figure 159 Modified Wing Root Random Loading Test Data (Mean Crossing Peak Count)

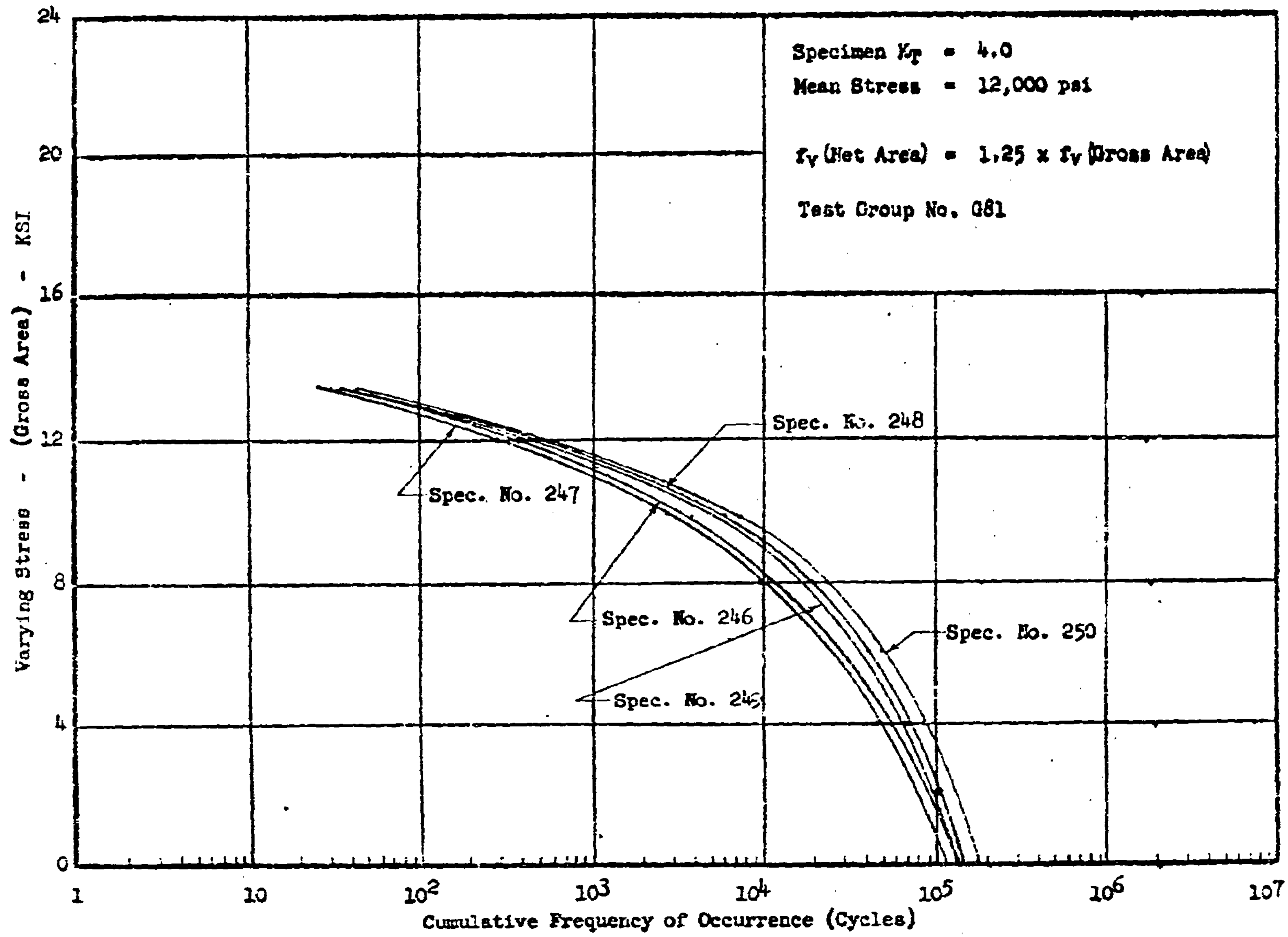

Figure 160 Modified Wing Root Ordered Loading

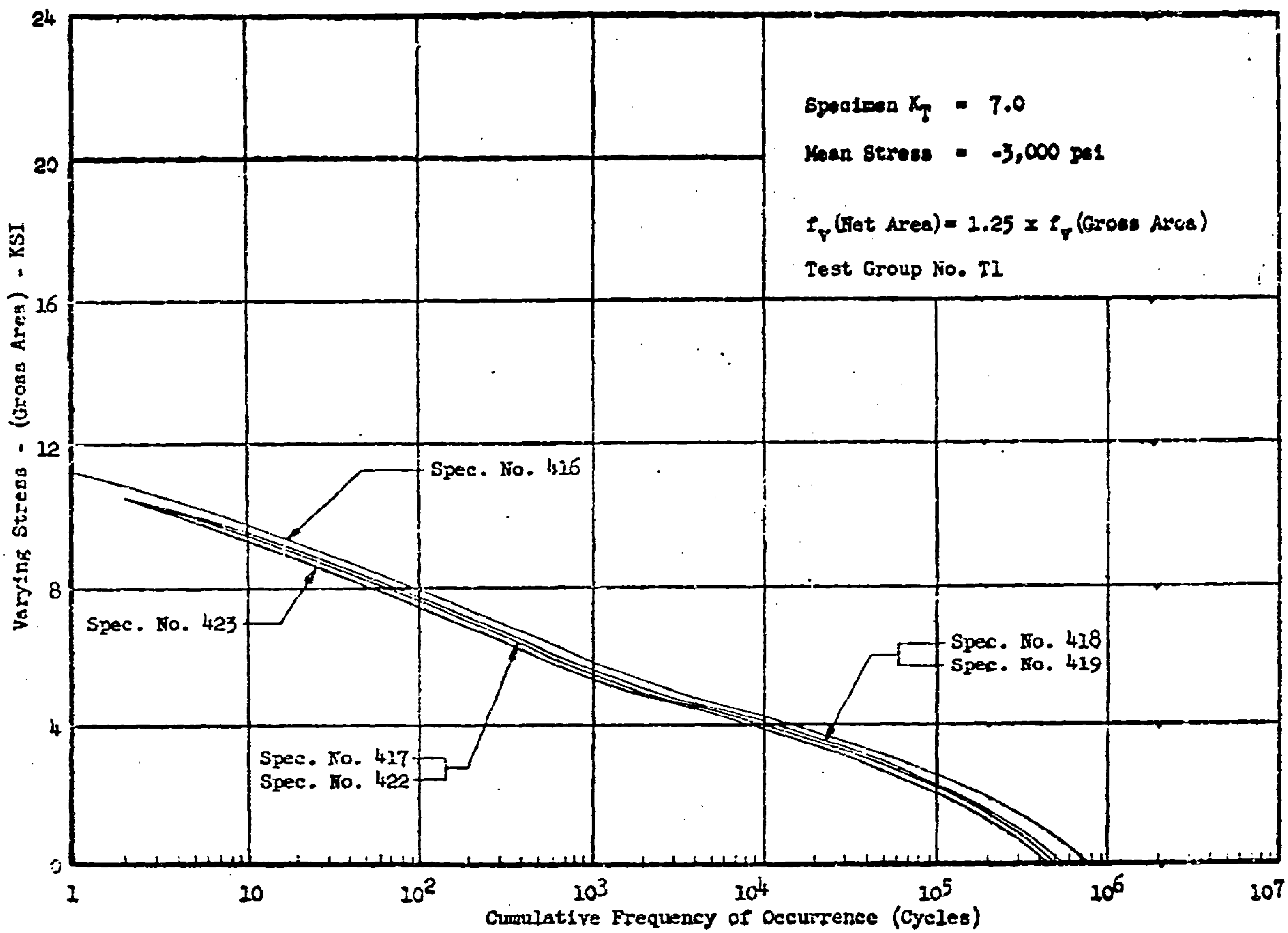

Figure 161 Random Ground Loading Test Data

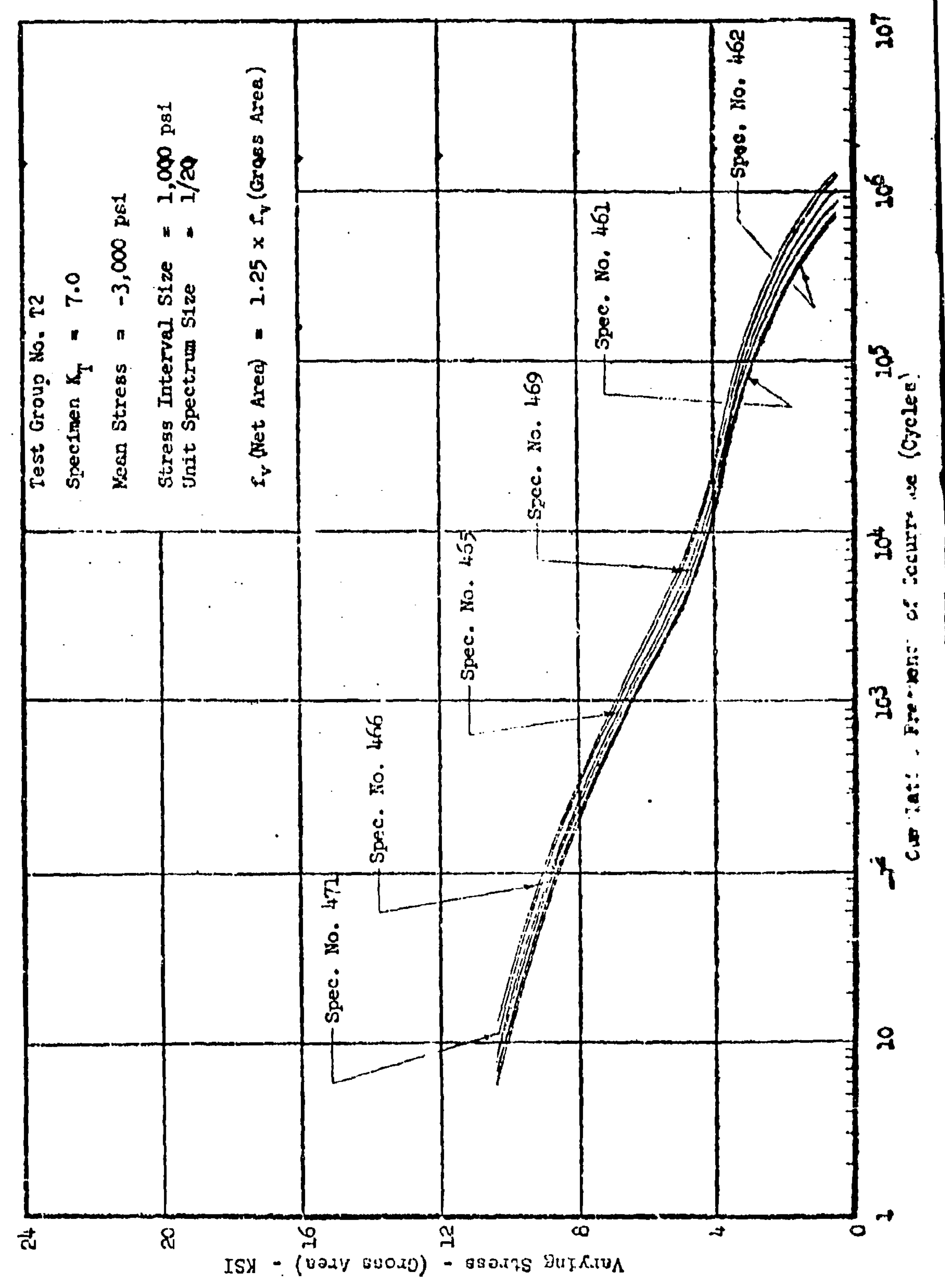
Test Group No. T2
Specimen K_T = 7.0
Mean Stress = -3,000 psi
Stress Interval Size = 1,000 psi
Unit Spectrum Size = 1/20
f_v (Net Area) = 1.25 x f_v (Gross Area)
Spec. No. 471
Spec. No. 466
Spec. No. 455
Spec. No. 469
Spec. No. 461
Spec. No. 462
Varying Stress - (Gross Area) - KSI
Cumulative Frequency of Occurrence (Cycles)

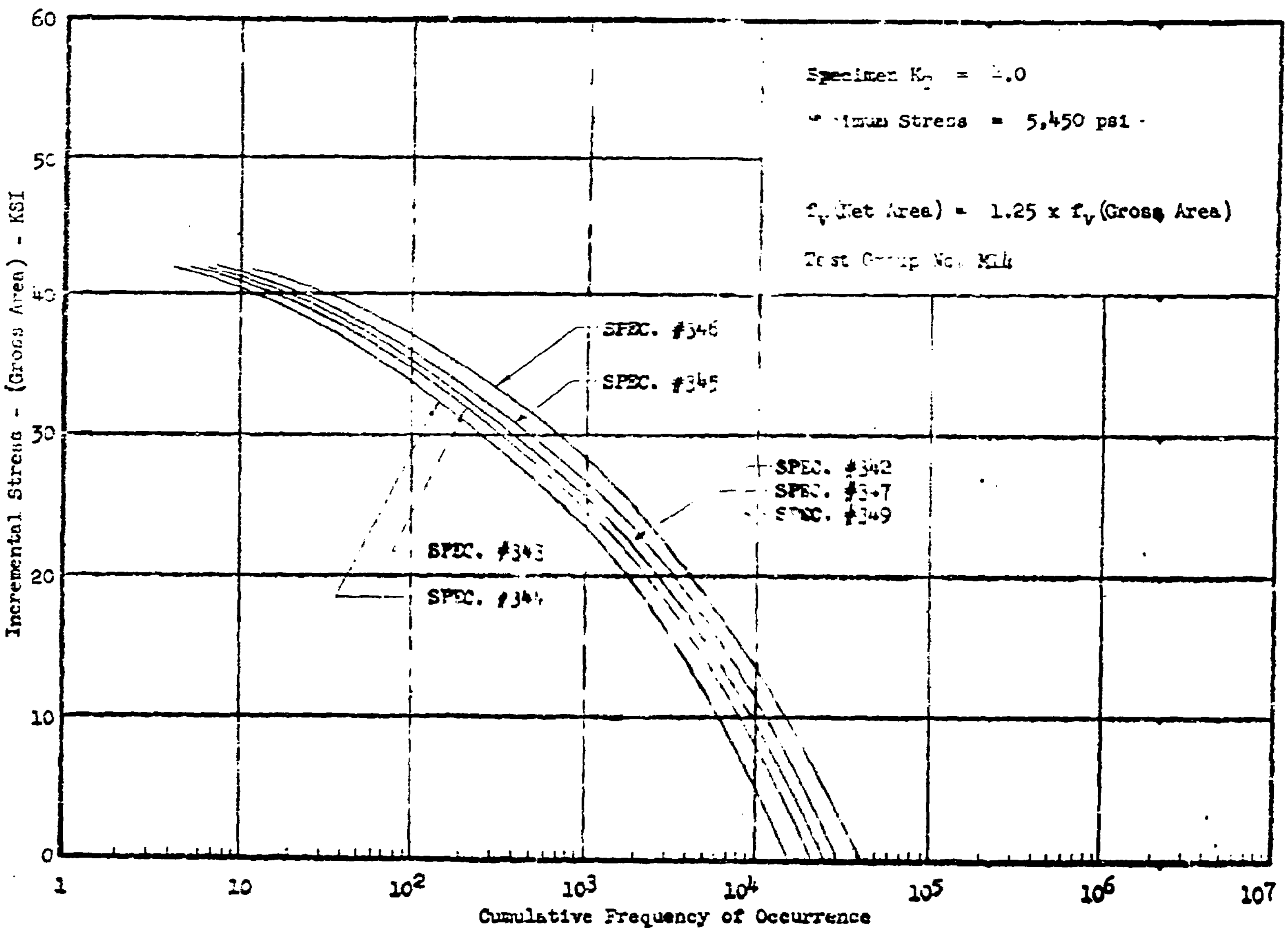

Figure 163 Random Military Maneuver Flight Loading Test D...

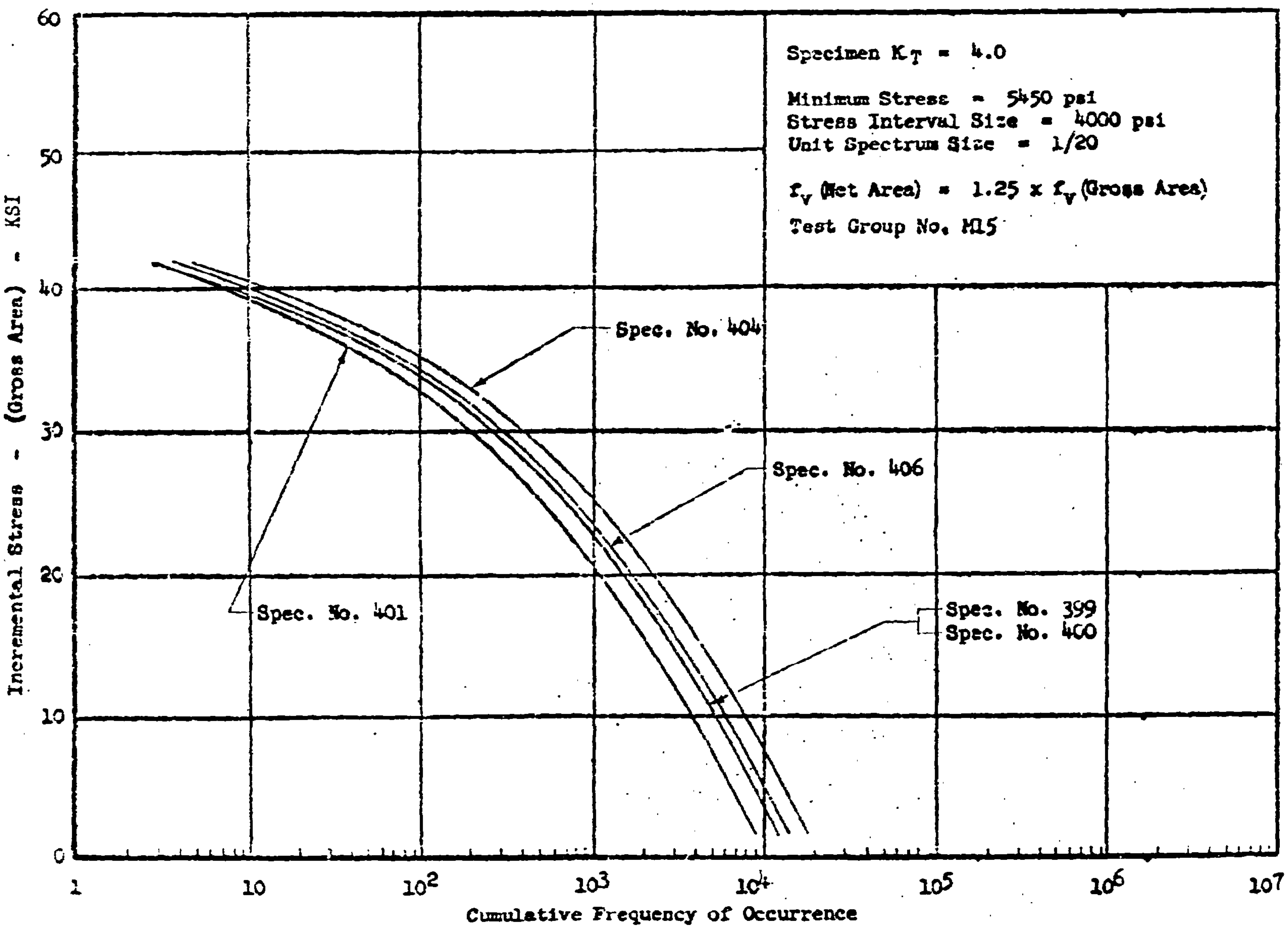

Figure 164 Ordered Military Maneuver Flight Loading Test Data

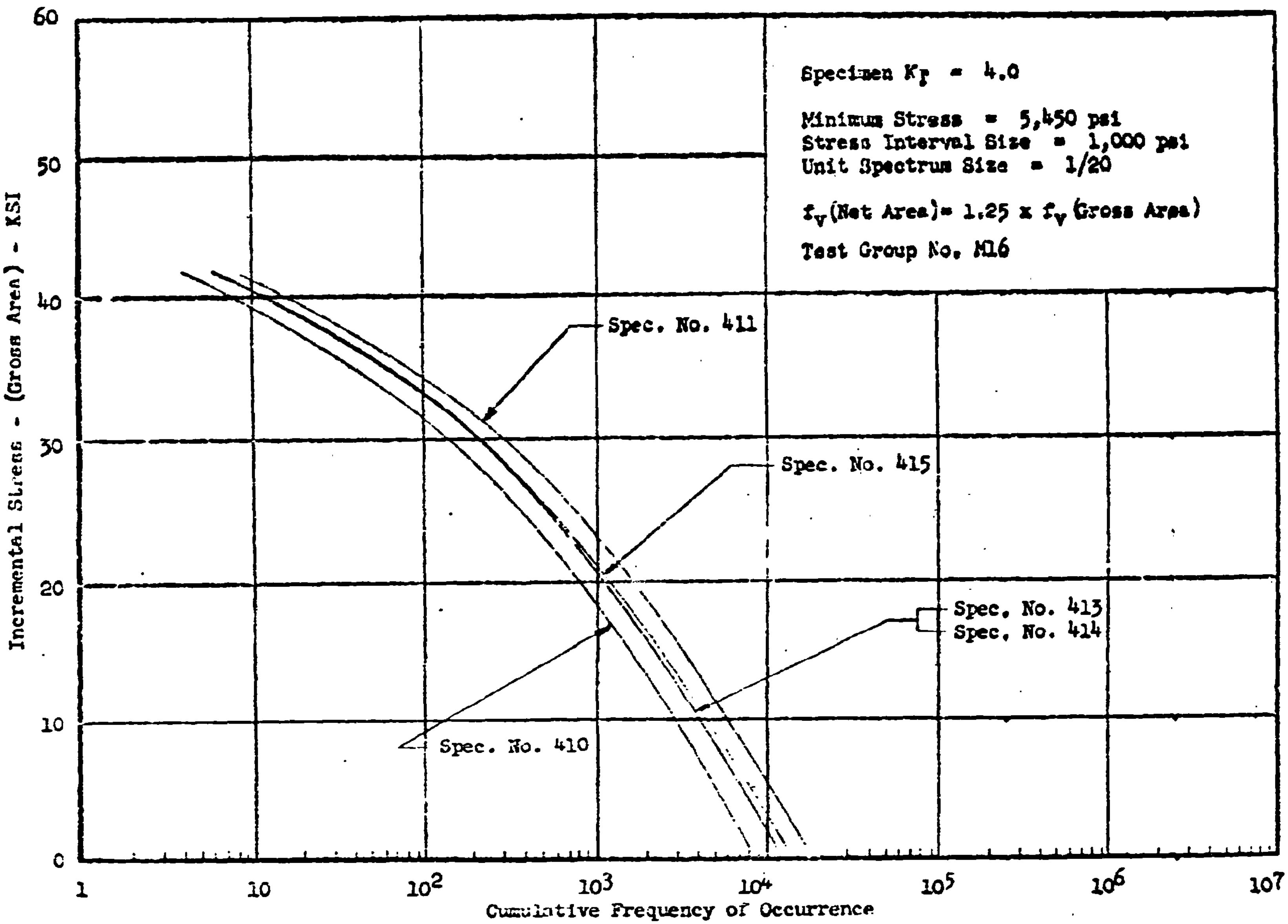

Figure 165 Ordered Military Maneuver Flight Loading Test Data

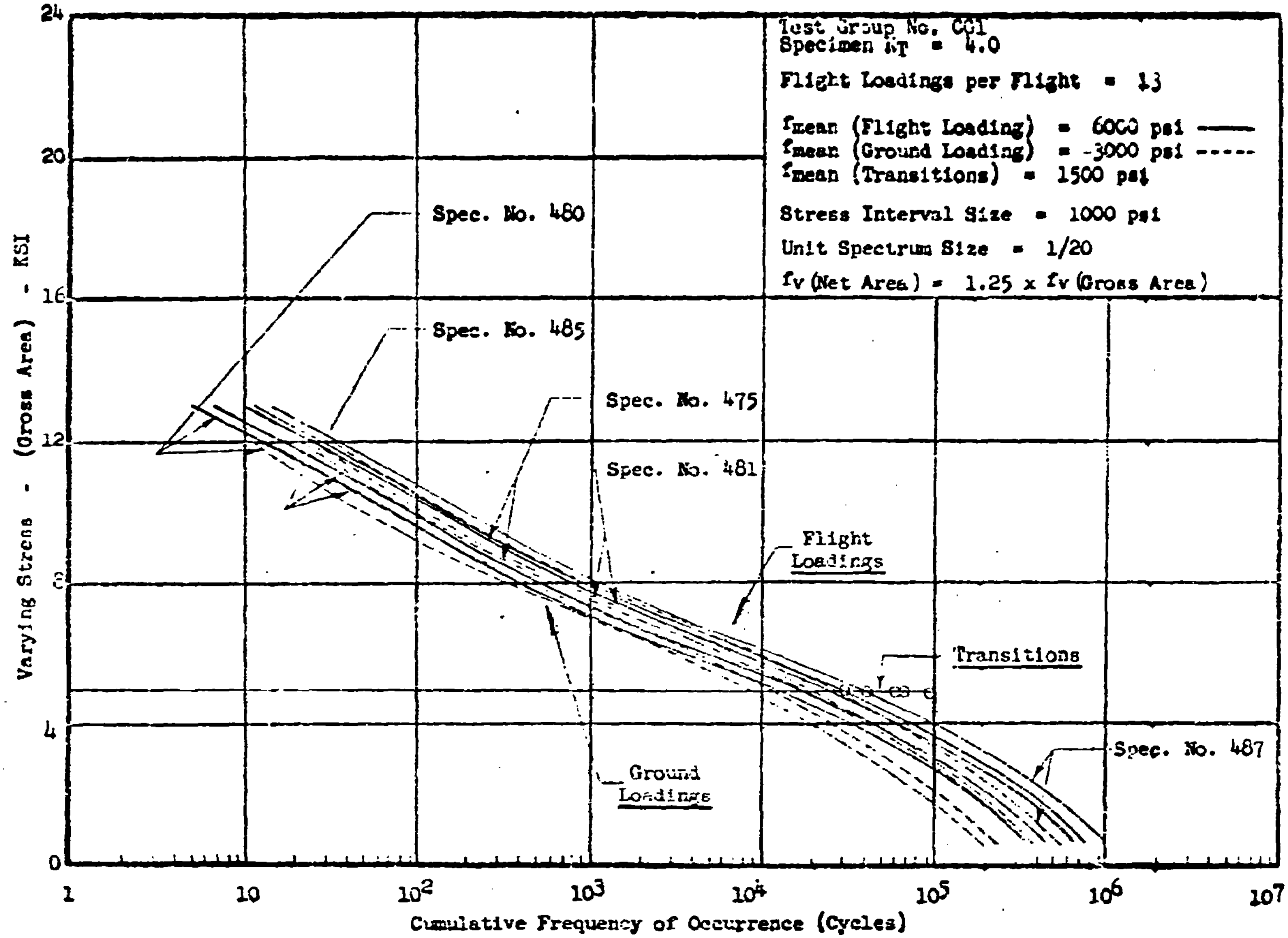

Figure 166 Ordered Composite Loading Test Data (Low Peak Gust Loadings in Flight)

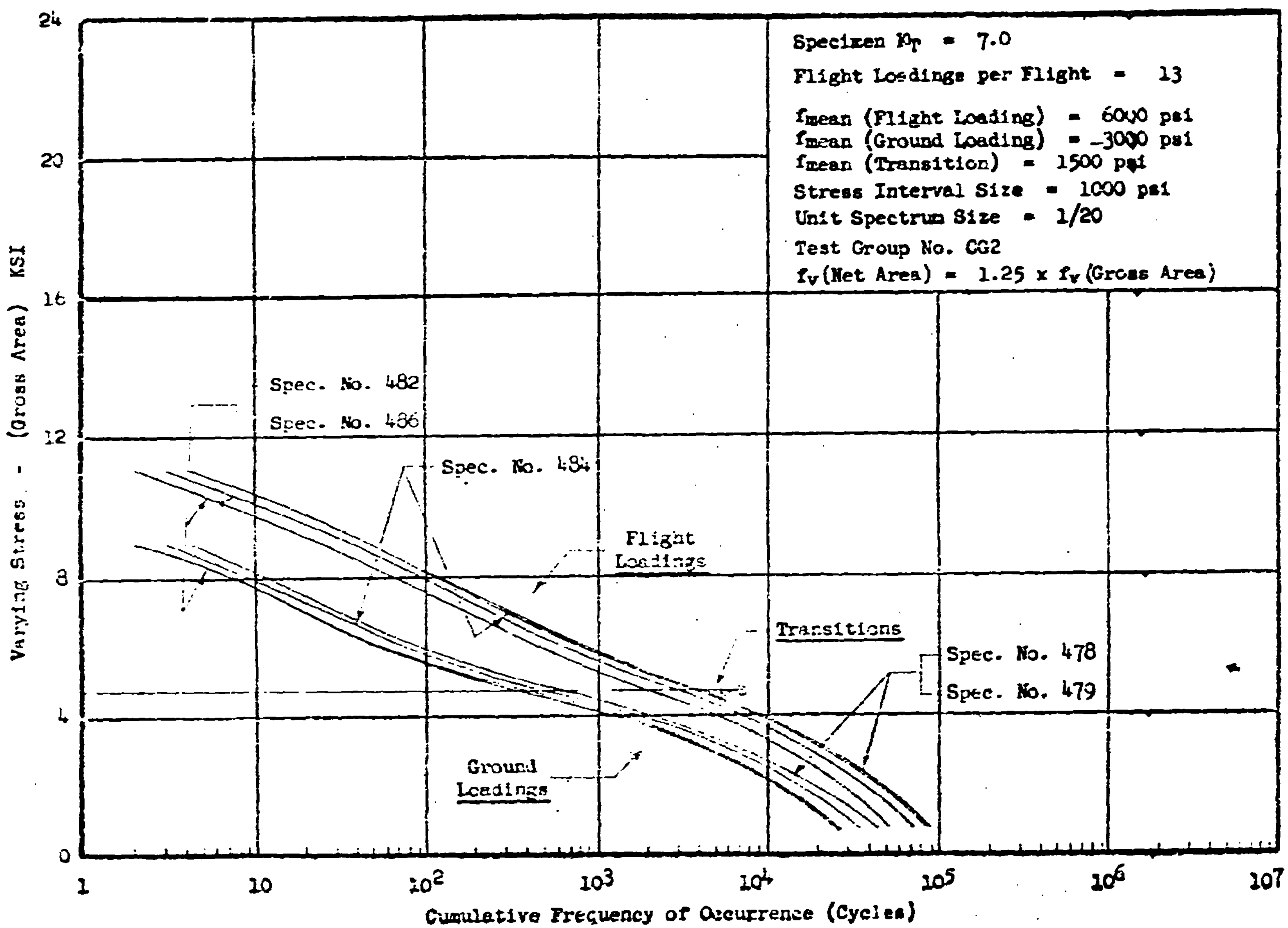

Figure 167 Ordered Composite Loading Test Data (Low Peak Gust Loadings in Flight)

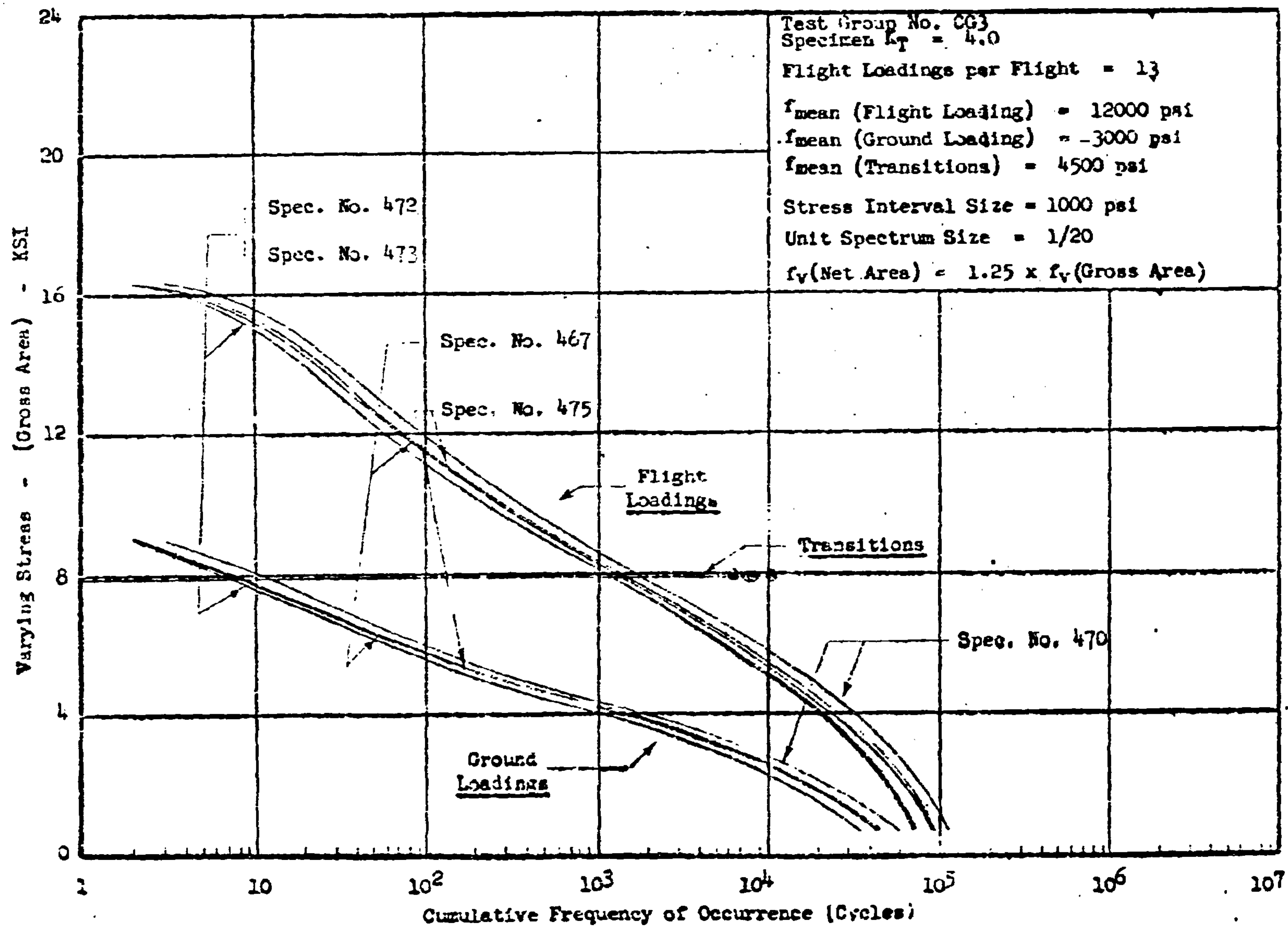

Figure 168 Ordered Composite Loading Data (High Peak Gust Loadings in Flight)

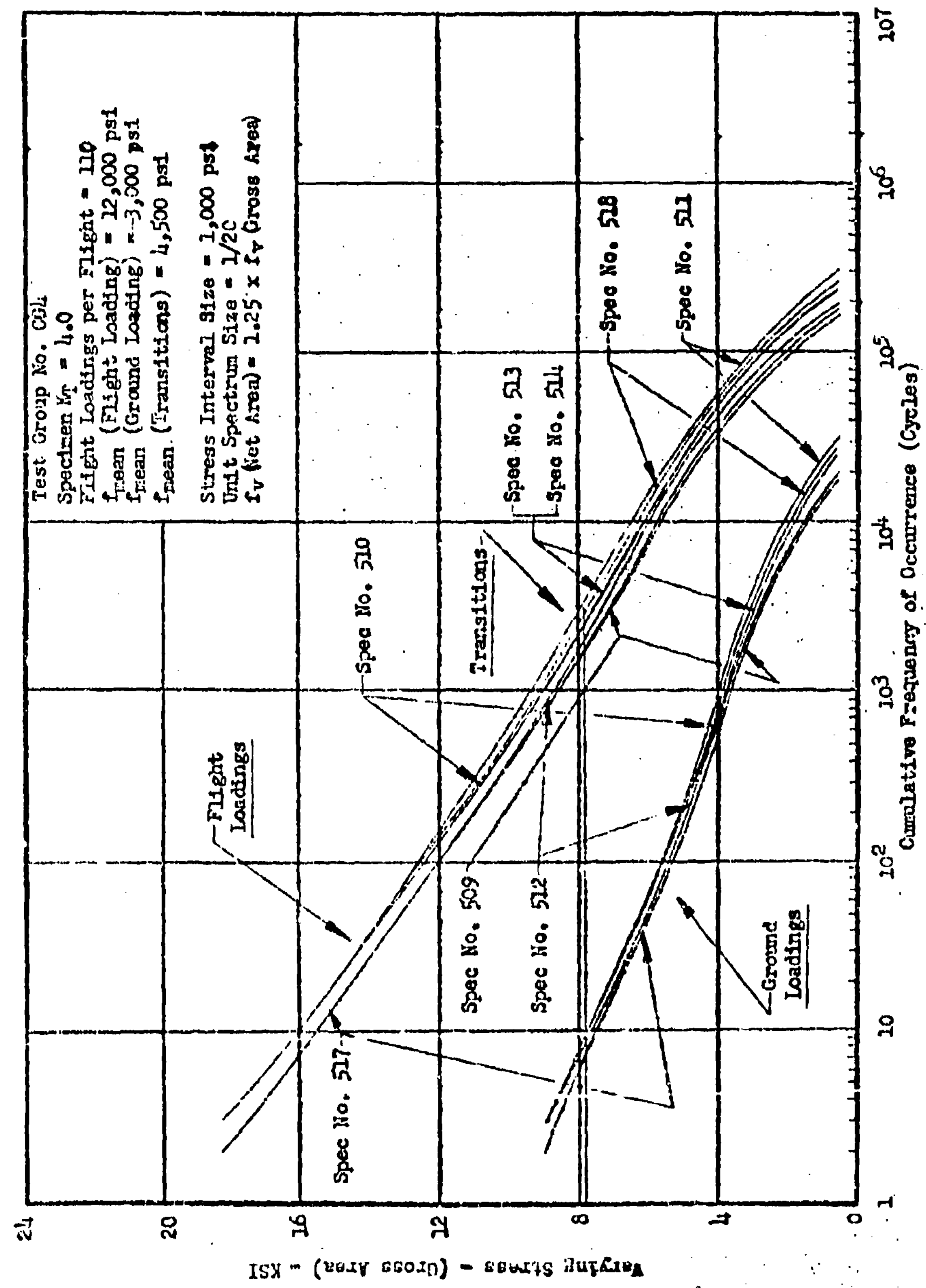

Figure 169 Ordered Composite Loading Test Data (High Peak Gust Loadings in Flight)

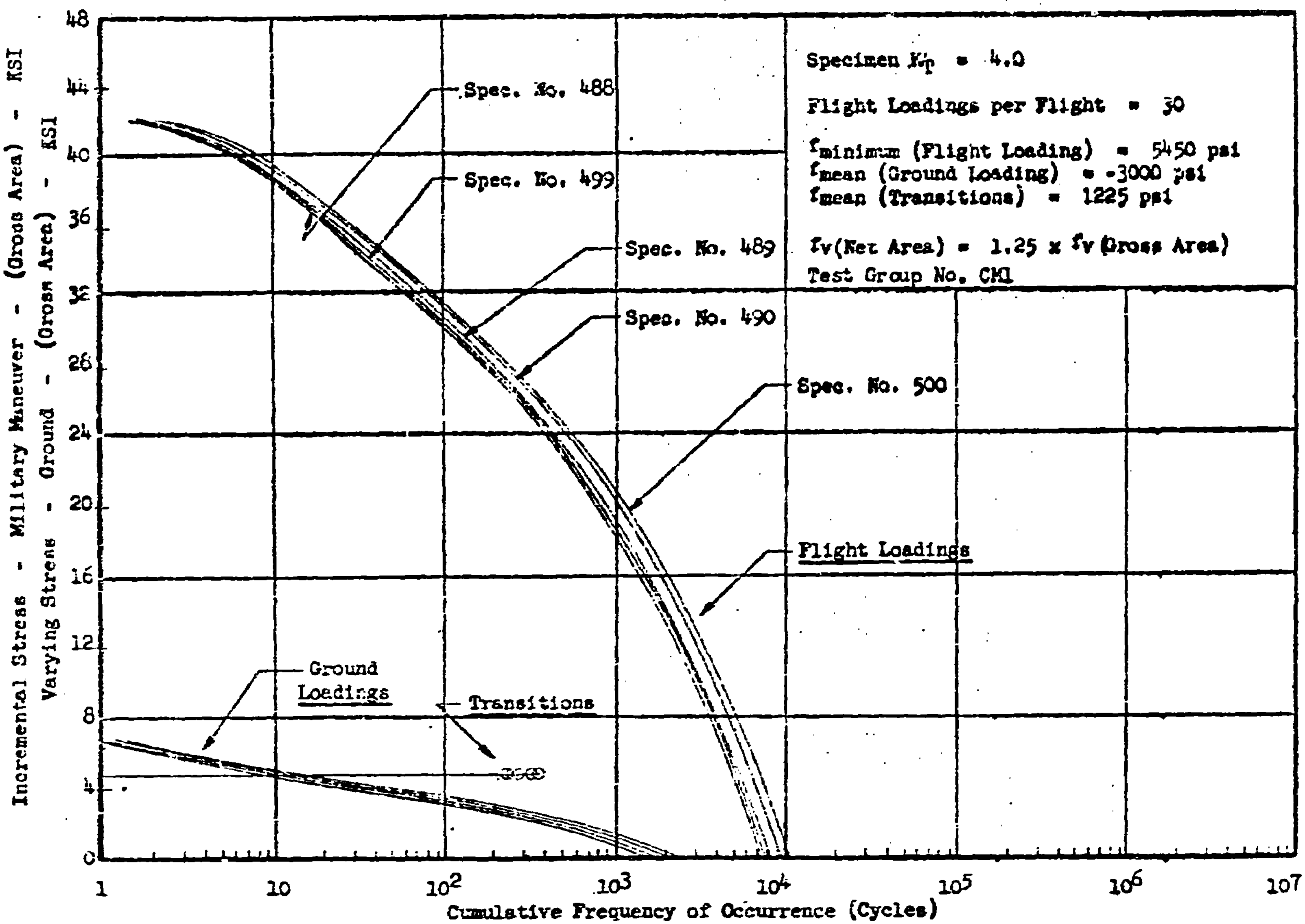

Figure 170 Random Composite Loading (Military Maneuver Flight Loadings)

APPENDIX D

PART 3 - FATIGUE TEST RESULTS OF A COMPLEX SPECIMEN

Introduction

In order to compare the fatigue life results derived from simple coupon data described in other sections of this report, it was planned to fatigue test fifteen typical complex joint specimens representative of contemporary aircraft construction. The joint selected is illustrated in Figure 41. The test spectra to be applied were representative of two types of loading, gust and maneuver, and a composite set in which ground taxi loads and ground-air-ground loading cycles defined by a static mean ground to a static mean flight range were combined with gust loads in flight on one group of specimens, and with maneuver loads in flight in another group of specimens. The test equipment and specimen description, along with the experimental results in tabular, graphical, and photographic form, are presented in this appendix.

The Specimen

The specimen is constructed of two basically identical panel sections of integrally stiffened skin typical of current wing tension surface design. The two panels are joined by a double shear butt splice arrangement, with one splice plate recessed for flush outer contour, and the other splice plate containing an integral flange for a rib support connection. The material is aluminum alloy extrusion 7075-T6 of Specification QQ-A-277. Mechanical properties determined from tensile coupons of the specimen material are listed in Table 9 , which indicates satisfactory agreement with the specification requirements. The panels are assembled with 12 Hi-Lok fasteners of one quarter inch diameter as indicated in Figure 41.

Test Set-up

Each of the panel assemblies was installed in a Lockheed-designed 500,000-pound fatigue testing machine as shown in Figure 43. To facilitate the fatigue testing, and since it was desired to have these panels tested in groups of three's, the tandem arrangement was adopted. In practice, the first of two such panels to fail was replaced by a third test panel; however, the second panel to fail was replaced simply by a dummy panel in order that the testing might be continued without disturbing the adjustment of the test machine.

Figure 44 presents a schematic diagram of the test machine which is partially shown in Figure 43. This machine, which was designed and built particularly for the ordered spectrum testing of wing surface structure, is a fairly conventional inertia-drive resonance machine utilizing inertia reaction and incorporating a spring-coupled hydraulic static loading system. It is normally operated subresonance with amplification factors of less than 50. Dynamic load control when running is provided by test frequency adjustment, and the driving eccentric weight is manually adjustable over a range of more than 20 to 1 to provide additional set-up control.

For the subject test program an auxiliary, more sensitive, load-measuring transducer was bolted to the face of the permanently installed 500,000-pound transducer in series with the two test panels (Figure 43). This load transducer consisted mainly of an I-section upon which were mounted 16 electrical strain gages arranged to measure axial loads up to plus or minus 100,000 pounds independent of moments in either transverse plane and independent of shear eccentricity.

Test Procedure

In the spectrum testing of the panels, relatively high amplitude, low-cycle loadings were applied by means of a hydraulic jack, part of the hydraulic static loading system previously mentioned, at frequencies ranging from 1 to 200 cycles per minute. Control of these hydraulic loadings was maintained through a Weston 4-way solenoid valve which in turn was actuated by a special cyclic control device incorporating a Schmitt Trigger. This load control device consisted principally of a two-level voltage sensor, each level of which could be adjusted independently of the other level to "trigger" the solenoid valve whenever a paticular voltage, generated by the previously calibrated load measuring transducer, was amplified and fed into it. And, since the principle function of any electrical strain gage type of transducer is to generate a voltage proportional to the load which is being applied to it, it was simply a case of manually selecting the upper and lower load levels and then allowing the hydraulic jack to cycle back and forth between these points.

Lower amplitude, hi-cycle loadings (dynamic) were applied at approximately 1,200 cycles per minute by means of the rotating eccentric weight shown in Figure 44. These loads were manually selected by means of a hand-operated vari-drive coupled to the eccentric shaft. Loads were visually controlled through a calibrated dynamic strain indicator which, as in the case of the cyclic load control device previously described, was used to determine indirectly the actual load being felt by the load transducer. Calibration of this strain indicator was made at the beginning of each work day using a calibration box which has previously been calibrated against known loads applied directly to the transducer in a Baldwin-Southwark universal test machine at the Lockheed Physical Test Laboratory.

For both types of loadings, hydraulic and dynamic, loads were selected that would give the required stress levels shown in Figures 179 through 184 at the minimum cross section of the panel assemblies. This minimum cross section was always near the center section of one of the two panel sections comprising the panel assembly.

As an additional check on the accuracy of the applied loadings, stresses at minimum cross section of the panels were measured independently (both statically and dynamically) through pairs of strain gages installed on the stringers and on the skin at these areas. These strain surveys showed the stresses at the minimum areas to be within plus or minus 2% of the required axial stresses as determined by measured loads at the transducer.

Test Results

Panel No. 1 was loaded statically in the aforementioned fatigue machine and after 350 applications of the basic air loading spectrum had failed to

produce any evidence of fatigue cracking (Table 98). Careful inspection of this panel, prior to the static test, was made after the panel had been disassembled. The panel was then reassembled, using new Hi-Lok fasteners after it was determined that the only visible fatigue "damage" consisted of minor fretting at the faying surfaces within the joint area (Figure 171).

The static tension load was applied at a steady rate of 500 pounds per second until failure. Failure occurred at 66,000 pounds (giving an ultimate tensile stress of 80,950 psi across the minimum cross section of the smaller of the two panel sections) and consisted of the fracture of both the tee and of one of the panel sections at the joint (Figure 171).

The remaining 14 panels were spectrum tested to failure - Panels 2 through 6 to a spectrum of air loads representing amplifications of the basic spectrum used in the spectrum test of Panel No. 1 (Figure 179 through 181); Panels 7 through 9 to a single maneuver loading spectrum (Figure 182); Panels 10 and 13 to a composite spectrum representing gust, ground-to-air, and ground loadings (Figure 183) and Panels 14 and 15 to a composite spectrum of ground, ground-to-air, and maneuver loadings (Figure 184).

With the exception of Panels 7 through 9, all spectrum loadings were applied one block at a time, with the smallest loads being applied first.

In the case of Panel No. 7, the first 230 blocks were applied one at a time; however, the last seventy were applied ten blocks at a time.

For Panels 8 and 9, the blocks were applied ten at a time from the beginning of the testing, and, in addition, the lowest load level was omitted from the spectrum.

For Panel No. 9, the next two lowest load levels were dropped at the end of 500 blocks.

Panels 11 and 12 are not reported since both panels failed in compression because of a failure in the hydraulic loading system of the fatigue testing machine.

The mechanical properties of the joint material are given in Table 97. Spectral test results for minimum gross area stresses are presented in Tables 99 to 104 and Figures 179 to 184. The stress conversion factors in Table 105 were used to convert the panel stresses for minimum gross area into stresses for gross area at point of fracture in Tables 106 to 109.

The results of these spectral fatigue tests are analysed on the basis of stresses for both minimum gross area and gross area at point of fracture, and compared in Section V of the main body of this report.

TABLE 97

MECHANICAL PROPERTIES OF JOINT MATERIAL

Coupon	Ultimate (KSI)	Yield (KSI)	% Elong.*	Red. Area %
A. Integrally Stiffened Panel Coupons Longitudinal Grain				
E-1	87.6	79.4	9	16
E-2	92.3	84.2	9	16
E-3	93.0	84.9	9	14
E-4	90.1	81.4	10	15
E-5	88.6	80.2	10	15
E-6	90.5	82.6	9	16
Aver.	90.4	82.1	9.3	
Spec. QQ-A-277	80	72	7	
B. Splice Plate Coupons Transverse Grain				
S-1	74.7	63.1	12	
S-2	71.5	59.6	12	
S-3	73.2	61.6	12	
S-4	74.5	62.9	10	
S-5	72.4	61.0	11	
S-6	73.8	62.0	12	
S-7	72.2	60.7	12	
S-8	75.6	64.3	11	
Aver.	73.5	61.9	11.5	
Spec. QQ-A-287	73	63		
C. Splice Tee-Section Coupons Transverse Grain			**	
T-1	74.1	73.3	F.O.G.L.	
T-2	74.6	73.8	F.O.G.L.	
T-3	83.2	73.4	14	
T-4	76.3	72.9	F.O.G.L.	
T-5	84.0	73.8	12	
T-6	83.7	75.6	14	
T-7	83.1	72.7	14	
T-8	83.7	73.7	F.O.G.L.	
Aver.	80.3	73.7	13.5	
Spec. QQ-A-277	75	65		

* 1" Gage Length
** 0.5" Gage Length
F.O.G.L. - Failed Outside Gage Length

TABLE 98

SUMMARY OF PANEL TEST RESULTS
(Continued on next page)

Panel No.	Min. Area (in^2)	Loading Geometry (1)		No. of Applied Loading Blocks	Description of Panel Failures		Test Results
		Spectrum Description	Spectrum Step Size		Mode & Location	Ref. Photos (2)	
1	.8153	Air Loading f_{mean} = 12,000 psi	f_{vary} = 1,000 psi	350	No fatigue failure. Panel pulled statically. Failure occurred both in the tee & in one of the panel sections at the joint.	Fig. 171	Fig. 179
2	.8137	Air Loading f_{mean} = 23,400 psi	f_{vary} = 1,960 psi	52	No failure.		
		Air Loading f_{mean} = 30,600 psi	f_{vary} = 2,560 psi	3 Total: 55	Multiple fatigue failures in the tee between fillet radius and line of hi-lok holes at edge of collars.	Figs. 173 & 174	Fig. 180
3	.8151	Air Loading f_{mean} = 23,400 psi	f_{vary} = 1,960 psi	52	No failure.		
		Air Loading f_{mean} = 30,600 psi	f_{vary} = 2,560 psi	9	1/4 inch fatigue crack at edge of single hi-lok hole in the tee.	Figs. 175 & 176	Fig. 180
				2 Total: 63	Catastrophic failure at intersection of stringer run-out and fillet.		

(1) All stresses are those experienced at the minimum cross section of the panel assembly (Fig.41, Sec. B-B).

(2) Photographs, shown in Figs.171 thru 176, were selected as representative of the various types of fatigue failures incurred.

TABLE 98

SUMMARY OF PANEL TEST RESULTS
(Continued on next page)

Panel No.	Min. Area (in^2)	Loading Geometry (1)		No. of Applied Loading Blocks	Description of Panel Failures		Test Results
		Spectrum Description	Spectrum Step Size		Mode & Location	Ref. Photos (2)	
4	.8168	Air Loading $f_{mean} = 27,000$ psi	$f_{vary} =$ 2,240 psi	56-1/2	Single failure at intersection of stringer run-out and fillet radius, catastrophic.	Figs. 175 & 176	Fig.181
5	.8204	Air Loading $f_{mean} = 27,000$ psi	$f_{vary} =$ 2,240 psi	48-1/2	Single fatigue failure (1/2 inch crack) in tee between fillet & line of hi-lok holes at edge of a collar.	Figs. 173 & 174	Fig.181
6	.8332	Air Loading $f_{mean} = 27,000$ psi	$f_{vary} =$ 2,240 psi	58	Same as Panel No. 9	Fig. 172	Fig.181
7	.8197	Maneuver Loading $f_{min} = 7,600$ psi	$\Delta f_{max} =$ 5,650 psi	300	Same as Panel No. 9	Fig. 172	Fig.182
8	.8462	Maneuver Loading $f_{min} = 7,600$ psi	$\Delta f_{max} =$ 5,650 psi	460	Multiple fatigue failures in tee at edge of hi-lok holes.	Figs. 177 & 178	Fig.182
9	.8373	Maneuver Loading $f_{min} = 7,600$ psi	$\Delta f_{max} =$ 5,650 psi	600	Multiple hidden fatigue failures in a panel section at the hi-lok holes, panel failed catastrophically.	Fig. 172	Fig.182

(1) All stresses are those experienced at the minimum cross section of the panel assembly (Fig. 11, Sec. B-B).

(2) Photographs, shown in Figs. 171 thru 178, were selected as representative of the various types of fatigue failures incurred.

TABLE 96

SUMMARY OF PANEL TEST RESULTS

Panel No. (3)	Min. Area (in^2)	Loading Geometry (1)		No. of Applied Loading Blocks	Description of Panel Failures		Test Results
		Spectrum Description	Spectrum Step Size		Mode & Location	Ref. Photos (2)	
10	.8369	Air Loading f_{mean} = 27,000 psi G.T.A. Loading f_{mean} = 10,000 psi Ground Loading f_{mean} = -6,700 psi	f_{vary} = 2,240 psi f_{vary} = 16,560 psi f_{vary} = 2,220 psi	9-1/2	Same as Panel No. 9	Fig.172	Fig. 183
13	.8326	Air Loading f_{mean} = 27,000 psi G.T.A. Loading f_{mean} = 10,000 psi Ground Loading f_{mean} = -6,700 psi	f_{vary} = 2,240 psi f_{vary} = 16,560 psi f_{vary} = 2,220 psi	10	Same as Panel No. 4	Figs.175 & 176	Fig. 183
14	.8340	Ground Loading f_{mean} = -6,700 psi G.T.A. Loading f_{mean} = 450 psi Maneuver Loading f_{min} = 7,600 psi	f_{vary} = 2,220 psi f_{vary} = 7,160 psi Δf_{max} = 5,650 psi	5	Catastrophic failure starting at an outside hi-lok hole in the tee.	Figs.177 & 178	Fig. 184
15	.8178	Ground Loading f_{mean} = -6,700 psi G.T.A. Loading f_{mean} = 450 psi Maneuver Loading f_{min} = 7,600 psi	f_{vary} = 2,220 psi f_{vary} = 7,160 psi Δf_{max} = 5,650 psi	9	Same as Panel No. 9 except that both panel sections failed.	Fig. 172	Fig. 184

(1) All stresses are those experienced at the minimum cross section of the panel (Figure 41, Section B-B)
(2) Photographs selected are representative of the various types of fatigue failures incurred.
(3) Panels 11 & 12 were accidentally overloaded and were failed in compression.

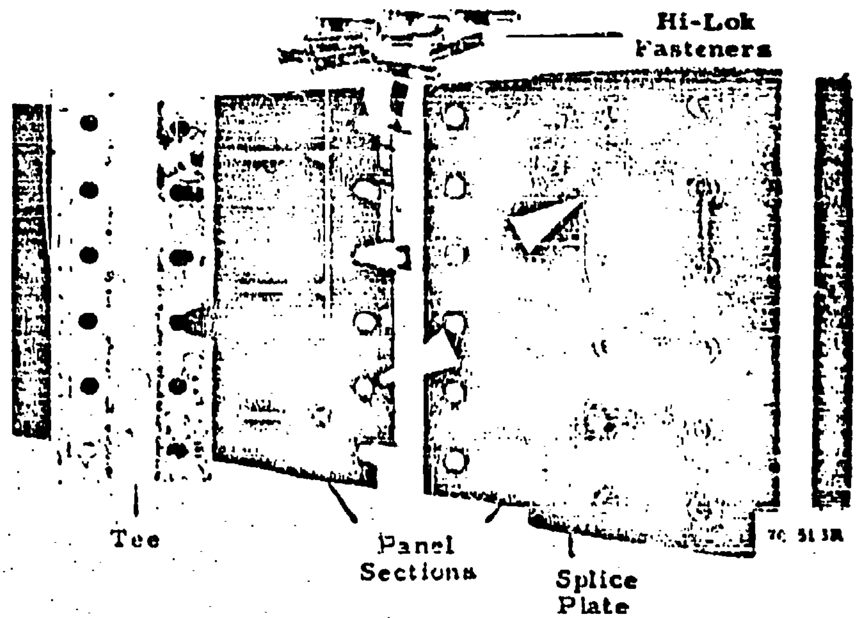

Figure 171 Panel Assembly No. 1, Pulled Statically. Fretting at the faying surfaces (arrows) was caused by previous, low-amplitude cycling.

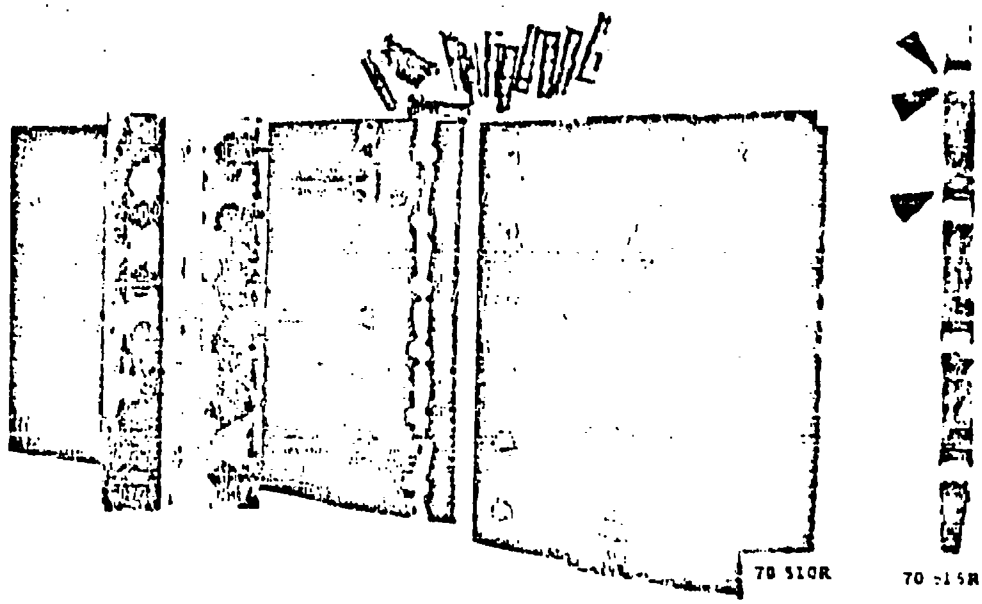

Figure 172 Panel Assembly No. 9. Fatigue failure of a panel section. Edges of all six holes showed evidence of fatigue cracking. Note beach marks (arrows) in the enlarged cross section.

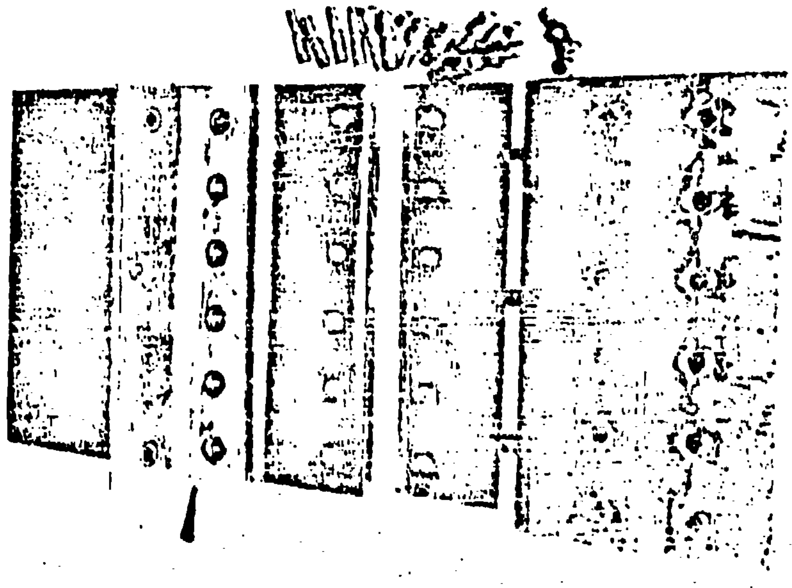

Figure 173 Panel Assembly No. 2. Fatigue failure of the tee (arrow) between lockbolt holes and the fillet radius.

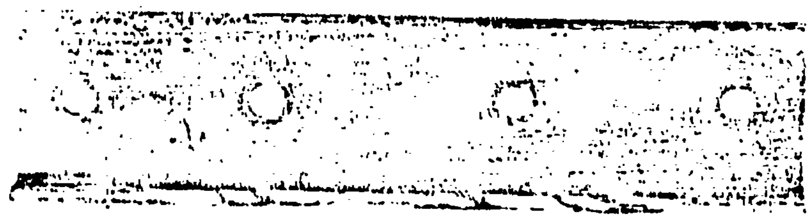

Figure 174 Cross section of the tee shown above. Multiple fatigue failures (bright semi-circular areas) coincide with scratches on the upper surface of the tee.

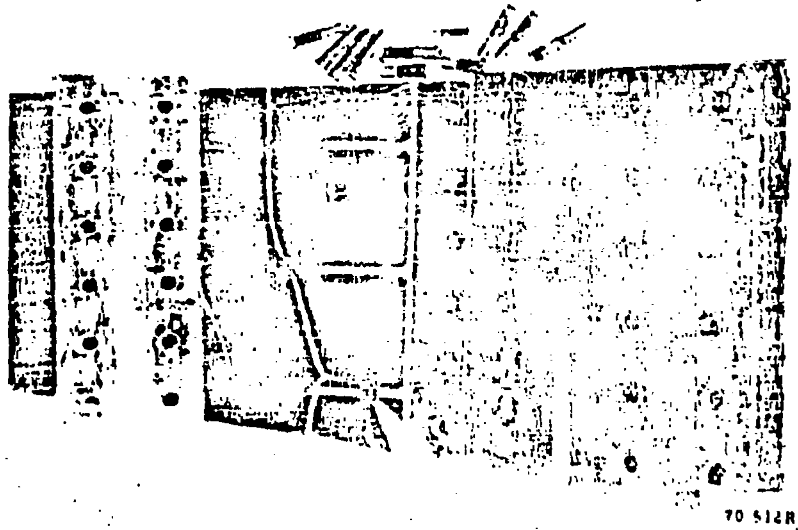

Figure 175 Panel Assembly No. 4. Fatigue failure in a panel section near the intersection of a stringer run-out and a fillet radius.

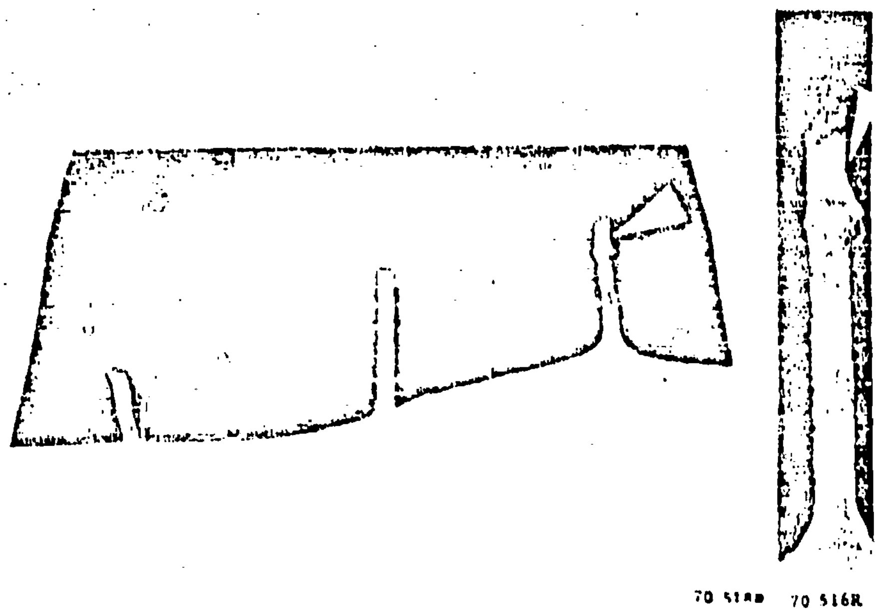

Figure 176 Two cross section views of the fatigue crack shown in the above photograph.

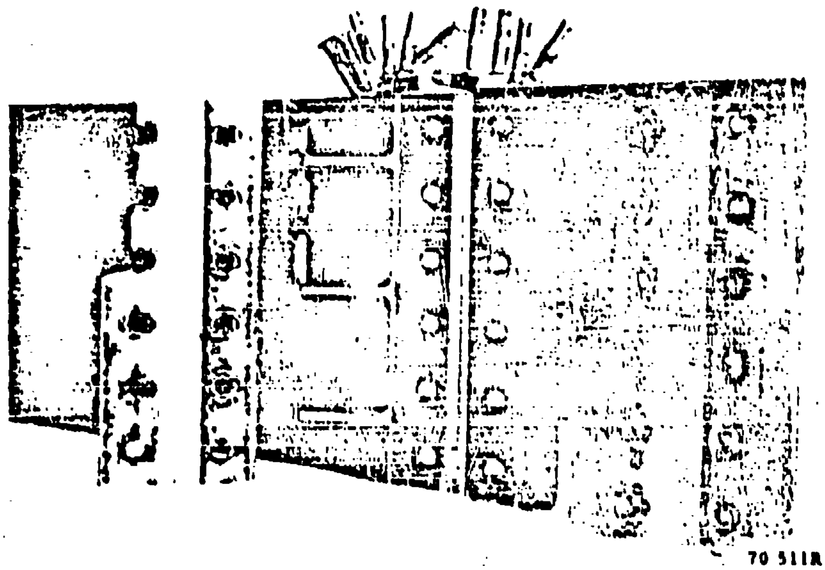

Figure 177 Panel Assembly No. 8. Fatigue failures in the tee section. Cracks originated at the edges of the two outside lockbolt holes.

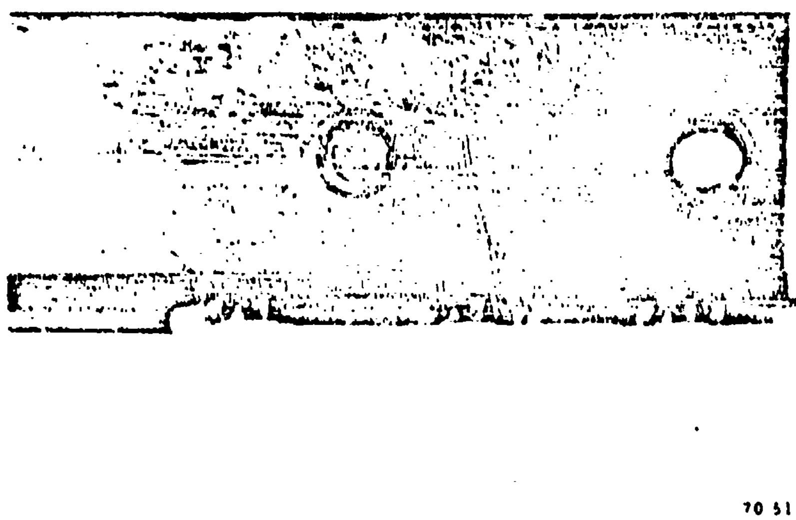

Figure 178 Cross section of the failed tee shown in the above photograph. Note beach marks (arrows).

TABLE 99

GUST LOADING HISTORY
LO-HI LOADING SEQUENCE
PANEL NO. 1
f_{mean} = 12,000 psi

Varying Stress (psi) *	Simple Frequency (cycles)
1	1,750,000
2	1,225,000
3	1,155,000
4	647,500
5	402,500
6	210,000
7	126,000
8	47,250
9	21,000
10	8,050
11	3,500
12	1,750
13	1,050
14	700
15	350
16	175
17	115
18	35
18.3	35

*Minimum cross sectional area.

TABLE 100

GUST LOADING HISTORY - LO-HI LOADING SEQUENCE

Test Group No. G82

PANEL NO. 2		PANEL NO. 3	
Varying Stress (psi) *	Simple Frequency Cycles	Varying Stress (psi) *	Simple Frequency Cycles
f_{mean} = 23,448 psi		f_{mean} = 23,408 psi	
1,954	260,000	1,951	260,000
3,908	182,000	3,901	182,000
5,862	171,600	5,852	171,600
7,816	96,200	7,803	96,200
9,770	59,800	9,753	59,800
11,724	31,200	11,704	31,200
13,678	18,720	13,654	18,720
15,632	7,020	15,605	7,020
17,586	3,120	17,556	3,120
19,540	1,196	19,506	1,196
21,494	520	21,458	520
23,448	260	23,409	260
25,402	156	25,358	156
27,357	104	27,309	104
29,311	52	29,260	52
31,265	27	31,211	27
33,219	17	33,162	17
35,173	6	35,112	6
35,759	6	35,697	6
No Failure - Loads Increased		No Failure - Loads Increased	
f_{mean} = 30,660 psi		f_{mean} = 30,610 psi	
2,555	15,000	2,550	45,000
5,110	10,500	5,101	31,500
7,666	9,900	7,653	29,700
10,221	5,550	10,204	16,650
12,776	3,450	12,755	10,350
15,331	1,800	15,305	5,400
17,887	1,080	17,857	3,240
20,442	405	20,407	1,215
22,997	147	22,957	540
25,552	46	25,508	207
28,109	20	28,061	90
30,662	10	30,609	45
33,219	6	33,162	27
35,774	4	35,713	18
38,329	2	38,264	9
40,885	2	40,814	5
43,440	1	43,365	3
45,995	0	45,915	1
46,762	0	46,681	1

*Minimum cross sectional area.

TABLE 101

GUST LOADING HISTORY
LO-HI LOADING SEQUENCE

Test Group No. 083

PANEL NO. 4		PANEL NO. 5		PANEL NO. 6	
Varying Stress (psi) *	Simple Frequency (Cycles)	Varying Stress (psi) *	Simple Frequency (Cycles)	Varying Stress (psi) *	Simple Frequency (Cycles)
f_{mean} = 27,152 psi		f_{mean} = 27,033 psi		f_{mean} = 26,618 psi	
2,262	285,000	2,252	245,000	2,218	290,000
4,525	199,500	4,505	171,500	4,436	203,000
6,788	188,100	6,758	161,700	6,655	191,400
9,051	105,450	9,011	90,650	8,873	107,300
11,313	65,550	11,263	56,350	11,091	66,700
13,576	34,200	13,516	29,400	13,310	34,800
15,839	20,520	15,770	17,280	15,582	20,880
18,102	7,695	18,022	6,480	17,746	7,830
20,365	3,420	20,275	2,880	19,964	3,480
22,627	1,311	22,527	1,104	22,182	1,334
24,890	570	24,780	480	24,400	580
27,152	282	27,032	240	26,618	290
29,415	168	29,285	144	28,836	174
31,677	112	31,537	96	31,054	116
33,941	56	33,791	48	33,273	58
36,203	29	36,044	24	35,491	29
38,466	18	38,296	15	37,710	18
40,728	6	40,549	5	39,927	6
41,408	6	41,225	5	40,593	6

*Minimum cross sectional area.

TABLE 102

FIGHTER MANEUVER LOADING HISTORIES
LO-HI LOADING SEQUENCE
Test Group No. M17

PANEL NO. 7		PANEL NO. 8		PANEL NO. 9	
Maximum Stress (psi) *	Simple Frequency (Cycles)	Maximum Stress (psi) *	Simple Frequency (Cycles)	Maximum Stress (psi) *	Simple Frequency (Cycles)
Minimum Stress = 7,865 psi		Minimum Stress = 7,601 psi		Minimum Stress = 7,680 psi	
13,606	80,500	13,181	80,500	13,320	80,500
19,363	70,500	18,759	110,450	18,957	117,500
25,123	52,500	24,338	82,250	24,595	87,500
30,882	37,500	29,917	58,750	30,234	75,000
36,641	25,500	35,497	39,950	35,872	51,000
42,399	16,800	41,075	26,320	41,509	33,600
48,158	8,700	46,654	13,630	47,147	17,400
53,917	3,900	52,233	6,110	52,786	7,800
59,675	1,450	57,811	2,350	58,423	2,972
65,434	508	63,391	810	64,061	1,033
68,314	90	66,181	144	66,881	184

*Minimum cross sectional area.

TABLE 103

COMPOSITE LOADING HISTORIES
GUST LOADINGS IN FLIGHT - LO-HI LOADING SEQUENCE

Test Group No. C05

PANEL NO. 10		PANEL NO. 13	
Varying Stress (psi) *	Simple Frequency (Cycles)	Varying Stress (psi) *	Simple Frequency (Cycles)
Gust Loadings			
f_{mean} = 26,500 psi		f_{mean} = 26,800 psi	
2,208	123,750	2,220	165,000
4,416	86,535	4,439	115,380
6,626	80,190	6,660	106,920
8,834	44,955	8,880	59,940
11,042	28,905	11,099	37,260
13,250	16,200	13,319	19,440
15,459	9,700	15,540	11,664
17,667	3,650	17,759	5,103
19,876	1,620	19,979	1,620
22,084	621	22,199	621
24,292	270	24,418	270
26,500	135	26,638	135
28,708	81	28,858	81
30,916	54	31,077	54
33,126	29	33,298	27
35,334	14	35,518	14
37,542	8	37,737	8
39,750	3	39,957	3
40,413	3	40,624	2
Ground Loadings			
f_{mean} = -6,630 psi		f_{mean} = -6,660 psi	
2,208	110,250	2,220	110,250
4,416	61,200	4,439	61,200
6,626	25,200	6,660	25,200
8,834	10,080	8,880	10,080
11,042	2,150	11,099	2,150
13,250	450	13,319	450
15,459	120	15,540	120
17,667	54	17,759	54
19,876	29	19,979	28
22,084	6	22,199	6
24,292	1	24,418	1
24,591	1	24,748	1
Ground to Air Cycles			
f_{mean} = 9,940 psi		f_{mean} = 10,000 psi	
16,561	32,500	16,647	32,500

*Minimum cross sectional area.

TABLE 104

COMPOSITE LOADING HISTORIES
FIGHTER MANEUVER LOADINGS IN FLIGHT
LO-HI LOADING SEQUENCE
Test Group No. CM2

PANEL NO. 14		PANEL NO. 15	
Dynamic Stress (psi) *	Simple Frequency (Cycles)	Dynamic Stress (psi) *	Simple Frequency (Cycles)
Maximum Stress			
Maneuver Loadings			
Minimum Stress = 7,725 psi		Minimum Stress = 7,875 psi	
13,372	24,500	13,629	44,100
19,032	20,750	19,397	37,350
24,692	18,500	25,166	33,300
30,353	15,250	30,935	27,450
36,013	9,250	36,704	16,650
41,672	5,750	42,471	10,350
47,333	2,500	48,241	4,500
52,993	2,000	54,010	3,600
58,653	661	59,778	1,485
64,313	112	65,547	228
67,144	28	68,432	56
Varying Stress			
Ground Loadings			
f_{mean} = -6,650 psi		f_{mean} = -6,780 psi	
2,216	61,250	2,258	110,250
4,432	34,000	4,517	61,200
6,648	14,000	6,776	25,200
8,864	5,600	9,034	10,080
11,080	1,075	11,293	1,935
13,296	225	13,551	405
15,513	60	15,810	108
17,728	27	18,068	49
19,944	14	20,327	26
22,160	3	22,585	5
24,376	1	24,843	1
24,750	0	25,179	1
Ground to Air Cycles			
f_{mean} = 442 psi		f_{mean} = 450 psi	
7,280	3,325	7,360	5,980

*Minimum cross sectional area.

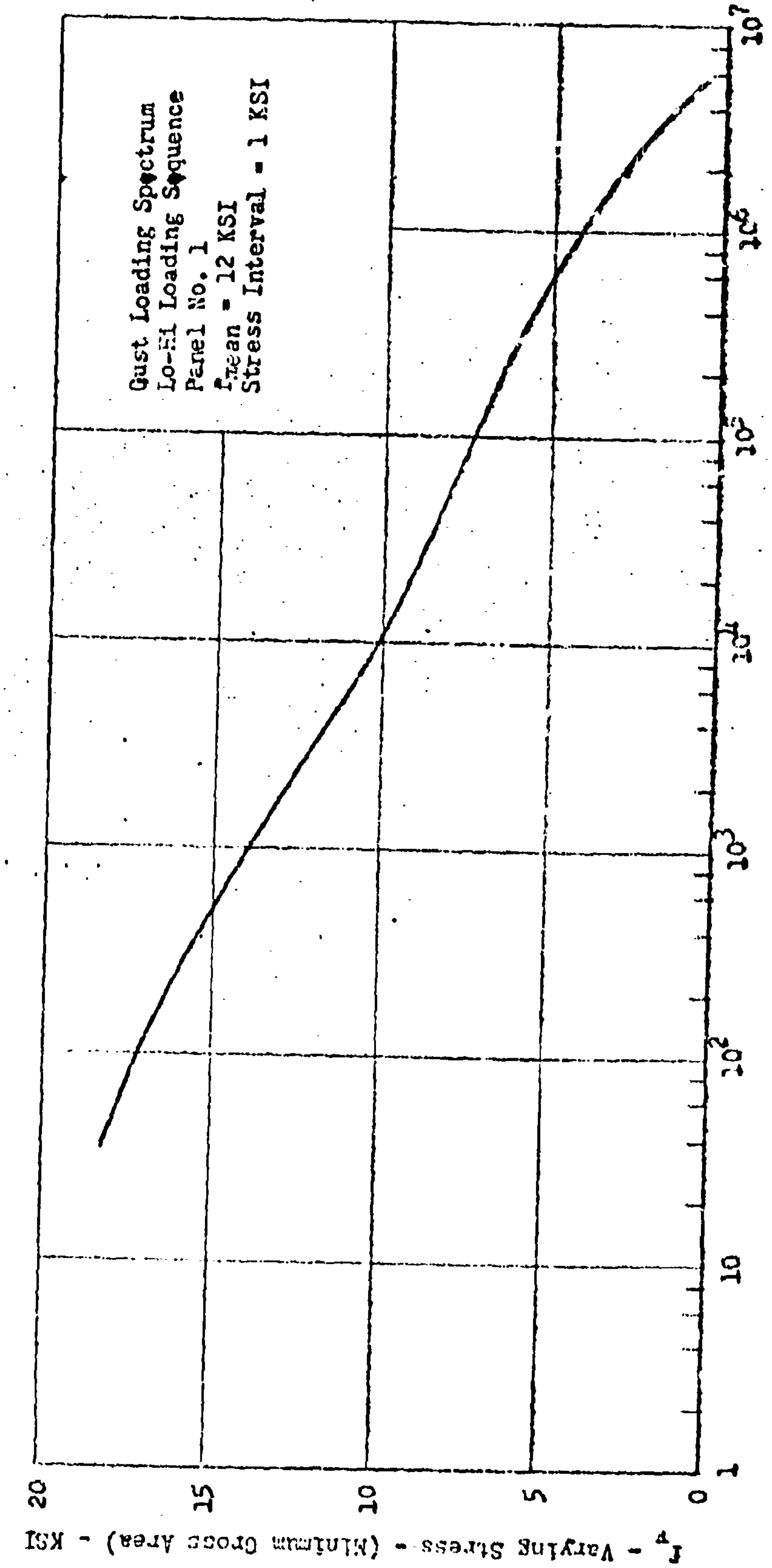

Cumulative Load Cycle Occurrences

Figure 179. Ordered Test Load History

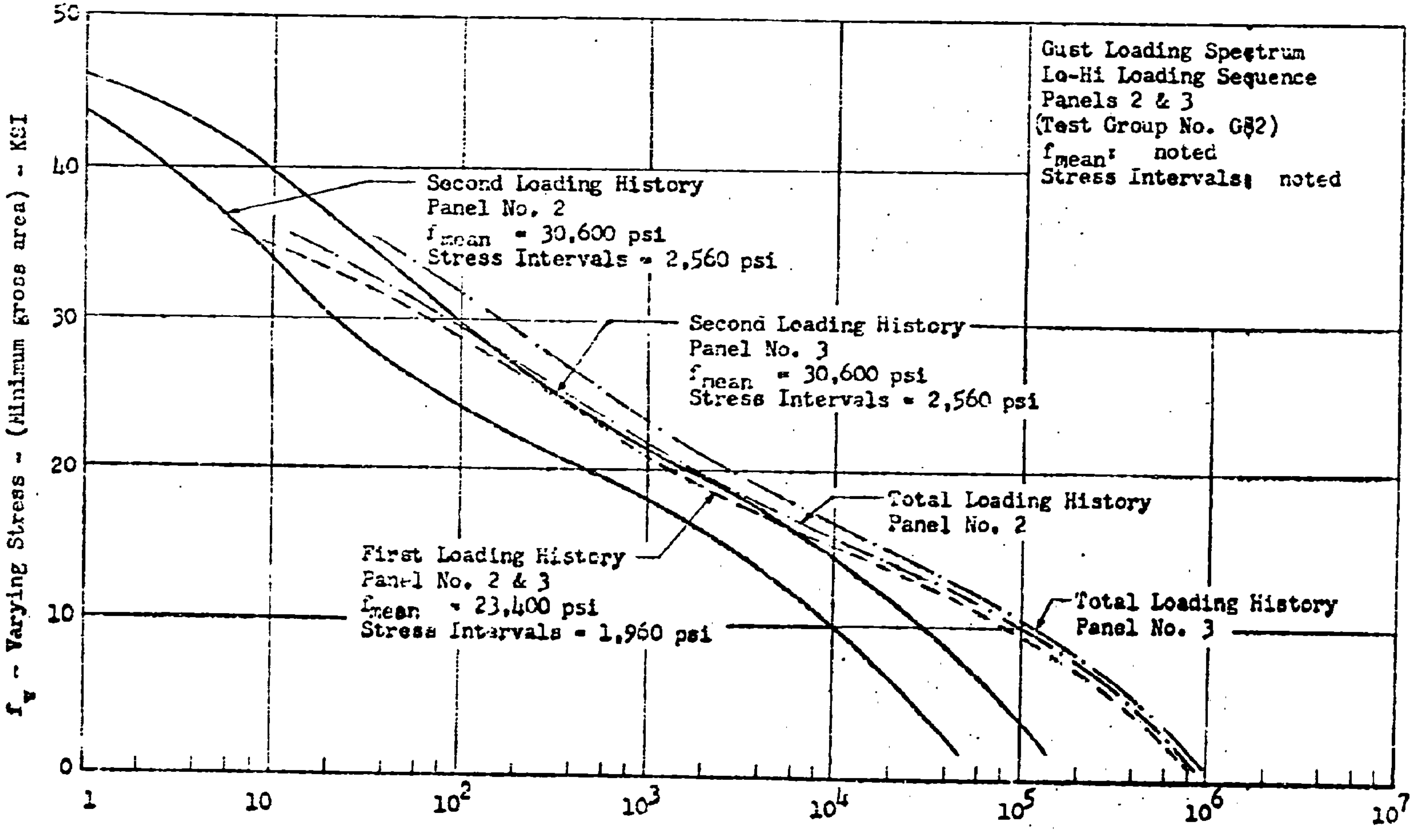

Cumulative Load Cycle Occurrences

Figure 180. Ordered Test Loading History

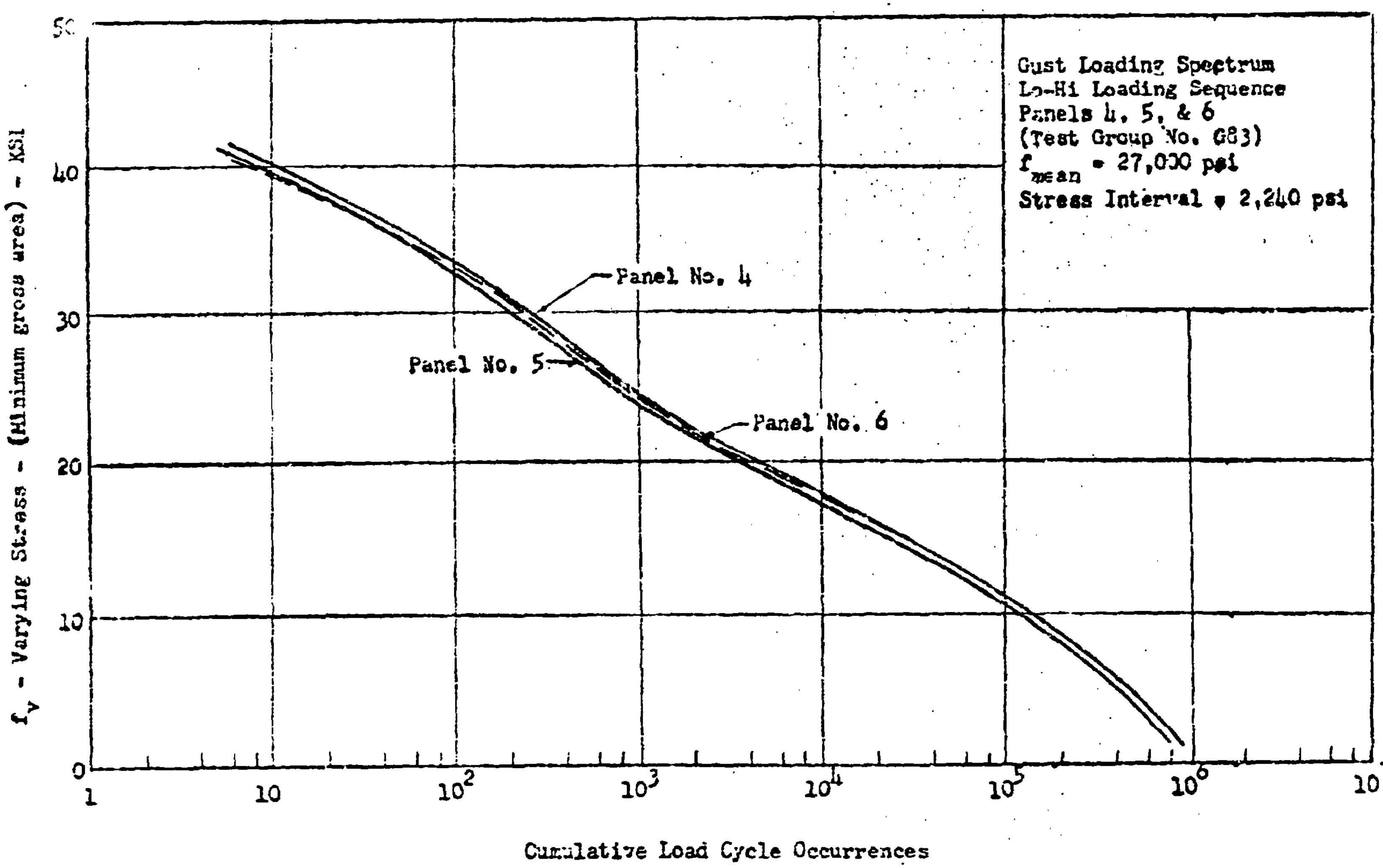

Figure 181. Ordered Test Loading History

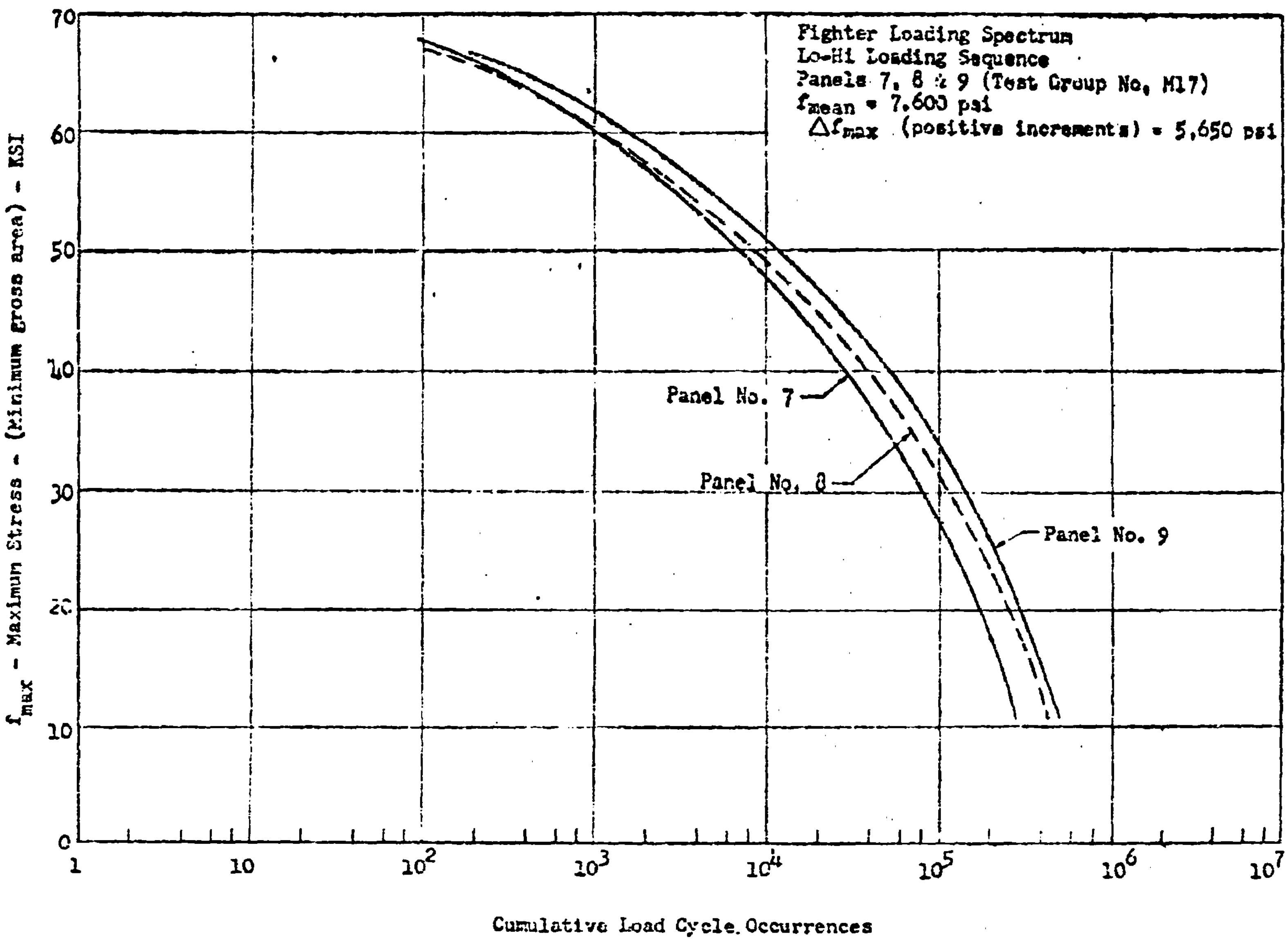

Figure 122. Ordered Test Loading History

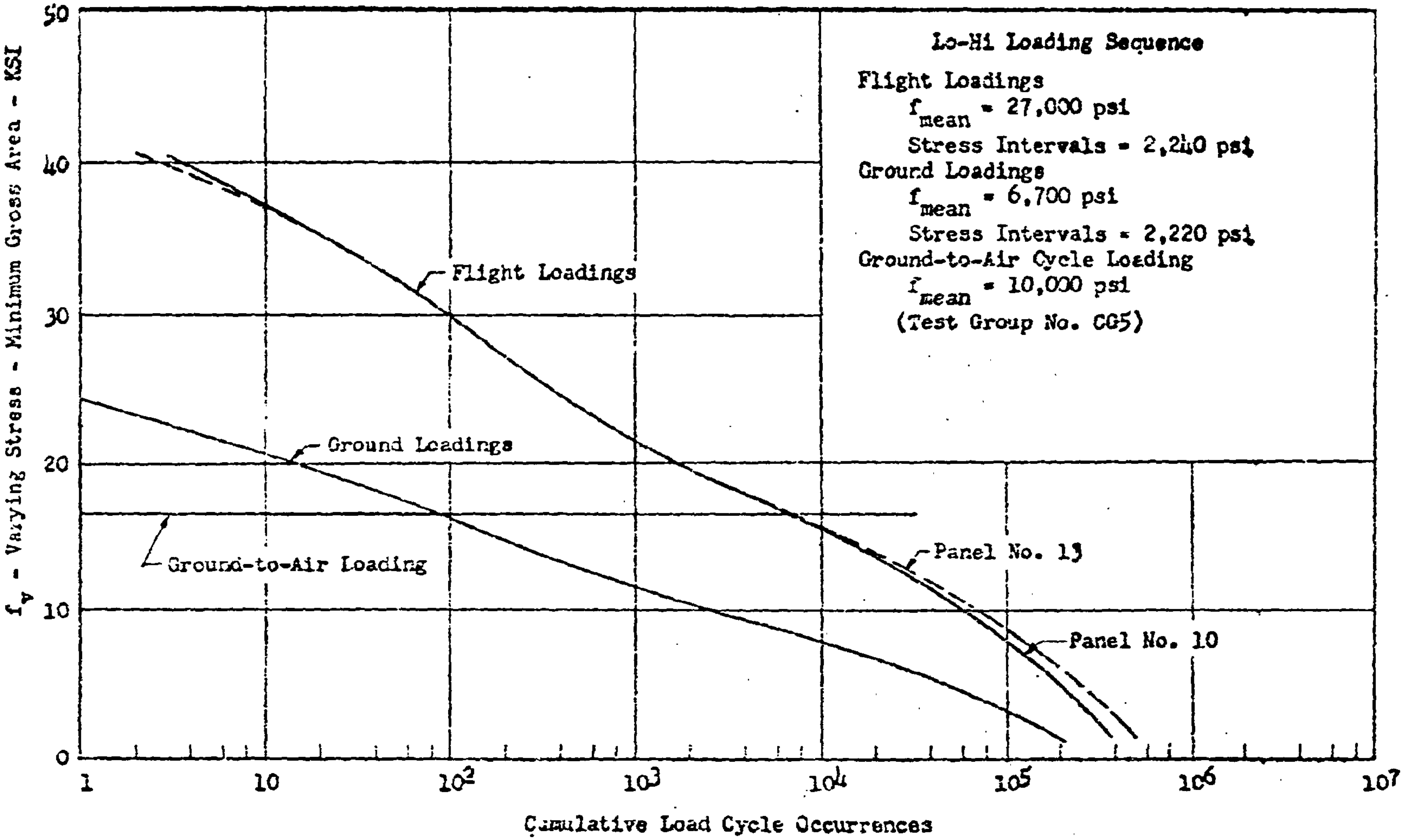

Figure 183. Ordered Composite Gust Loading Test Histories

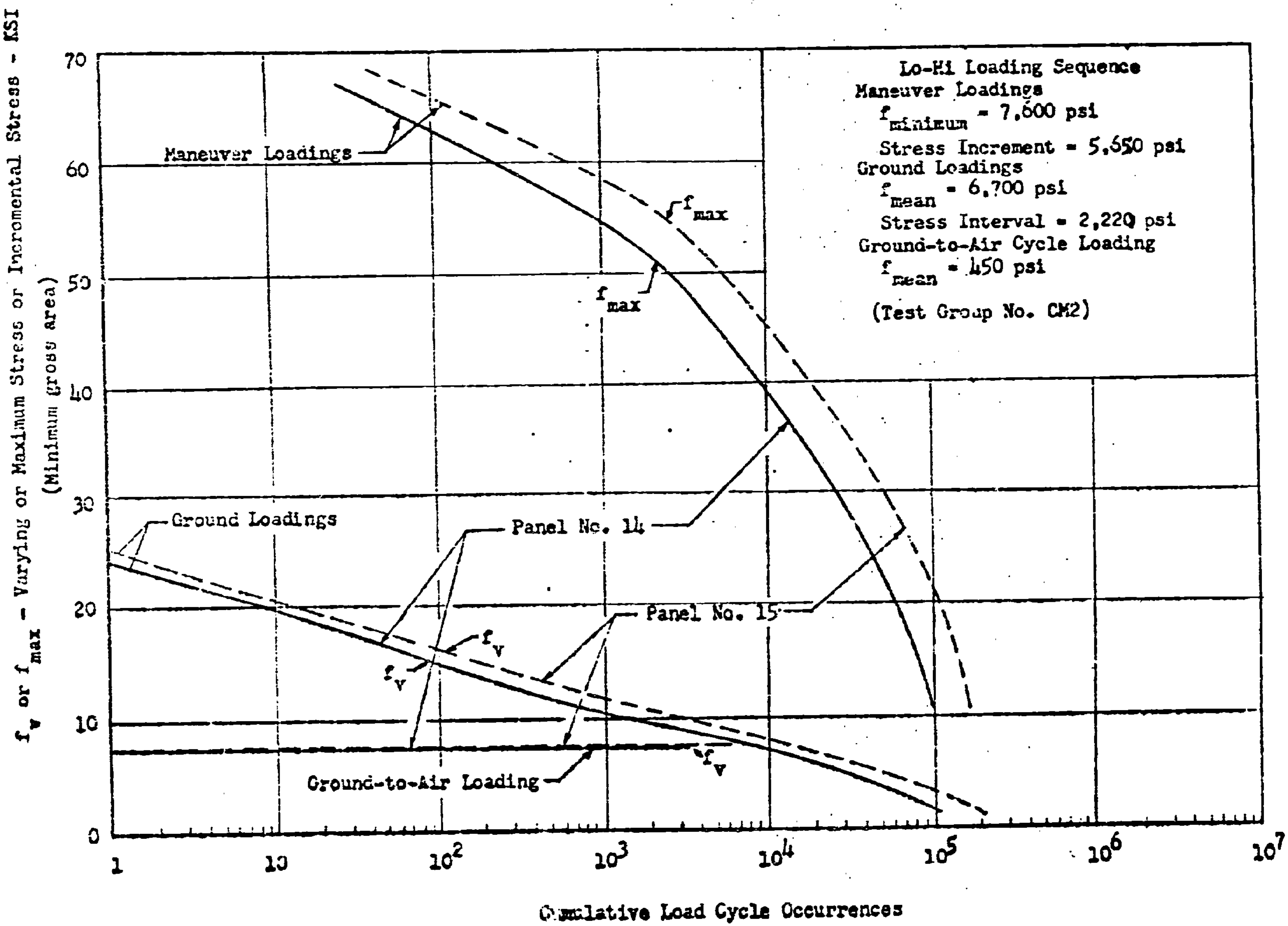

Figure 184. Ordered Composite Maneuver Loading Test Histories

TABLE 105

FACTORS USED TO CONVERT PANEL STRESSES FOR MINIMUM GROSS AREA INTO STRESSES FOR GROSS AREA AT POINT OF FRACTURE

Panel No.	Minimum Gross Area (in.^{2})	Point of Fracture	Area of Tee (in.^{2})	Area of Splice Plate (in.^{2})	Fractured Gross Area (in.^{2})	Stress Conversion Factors (1)
2	.8137	Tee	.7892	1.232	.2021[2]	.403
3	.8151	Tee	.7864	1.236	2.022[2]	.403
		Stringer Run-out			1.742[3]	.468
4	.8168	Stringer Run-out			1.543[3]	.529
5	.8204	Tee	.7869	1.226	2.013[2]	.406
6	.8332	Panel at Joint			1.649	.505
7	.8197	Panel at Joint			1.615	.508
8	.8462	Tee	.7892	1.228	2.017[2]	.420
9	.8373	Panel at Joint			1.580	.530
10	.8369	Panel at Joint			1.648	.508
13	.8326	Stringer Run-out			1.794[3]	.468
14	.8340	Tee	.7866	1.235	2.022[2]	.412
15	.8178	Panel at Joint			1.640	.499

1. Stress conversion factor is the ratio of minimum gross area to fractured gross area.
2. Total area for tee and splice plate.
3. Effective area of panel and stringer in vicinity of stringer run-out at joint.

TABLE 106

GROSS AREA STRESS SPECTRA IN VICINITY OF FRACTURE
IN PANEL 2 AT TEE AND IN PANEL 3* AT STRINGER RUN-OUT

Test Group No. G82

Loading Step	Panel 2 f_v KSI	Panel 2 n	Panel 3* f_v KSI	Panel 3* n
	f_{mean} = 9.45 KSI		f_{mean} = 11.00 KSI	
1	.79	260000	.91	260000
2	1.57	182000	1.83	182000
3	2.36	171600	2.74	171600
4	3.15	96200	3.65	96200
5	3.94	59800	4.56	59800
6	4.72	31200	5.48	31200
7	5.51	18720	6.39	18720
8	6.30	7020	7.30	7020
9	7.09	3120	8.22	3120
10	7.87	1196	9.13	1196
11	8.66	520	10.00	520
12	9.45	260	11.00	260
13	10.20	156	11.90	156
14	11.00	104	12.80	104
15	11.80	52	13.70	52
16	12.60	27	14.60	27
17	13.40	17	15.50	17
18	14.20	6	16.40	6
19	14.40	6	16.70	6
		≥ 832004		≥ 832004
	No Failure - Loads Increased			
	f_{mean} = 12.4 KSI		f_{mean} = 14.3 KSI	
20	1.03	15000	1.19	45000
21	2.06	10500	2.39	31500
22	3.09	9900	3.58	29700
23	4.12	5550	4.78	16650
24	5.15	3450	5.97	10350
25	6.18	1800	7.16	5400
26	7.21	1080	8.36	3240
27	8.24	405	9.55	1215
28	9.27	147	10.70	540
29	10.30	46	11.90	207
30	11.30	20	13.10	90
31	12.40	10	14.30	45
32	13.40	6	15.50	27
33	14.40	4	16.70	18
34	15.40	2	17.90	9
35	16.50	2	19.10	5
36	17.50	1	20.30	3
37	-	-	21.50	1
38	-	-	21.80	1
		≥ 47931		≥ 144001
TOTAL		≥ 879935		≥ 976005

* Stresses at point of fracture in Panel 3 are based on stress conversion factor (Table 105) for catastrophic failure at stringer run-out rather than stress conversion factor for initial failure at tee.

TABLE 107

GROSS AREA STRESS SPECTRA IN VICINITY OF FRACTURE IN PANEL 4 AT STRINGER RUN-OUT, IN PANEL 5 AT TEE AND IN PANEL 6 AT JOINT

Test Group No. G83

Loading Step	Panel 4 f_v KSI	Panel 4 n	Panel 5 f_v KSI	Panel 5 n	Panel 6 f_v KSI	Panel 6 n
1	1.20	255000	.92	245000	1.12	290000
2	2.39	199500	1.84	171500	2.24	203000
3	3.59	188100	2.76	161700	3.36	151400
4	4.79	105450	3.68	90650	4.48	107300
5	5.98	65550	4.60	56350	5.60	66700
6	7.18	34200	5.51	29400	6.72	34800
7	8.38	20520	6.43	17280	7.87	20880
8	9.58	7695	7.35	6400	8.96	7830
9	10.80	3420	8.27	2880	10.10	3480
10	12.00	1311	9.19	1104	11.20	1334
11	13.20	570	10.10	480	12.30	580
12	14.40	282	11.00	240	13.40	290
13	15.60	168	11.90	144	14.60	174
14	16.80	112	12.90	96	15.70	116
15	18.00	56	13.80	48	16.80	58
16	19.20	29	14.70	24	17.90	29
17	20.30	18	15.60	15	19.00	18
18	21.50	6	16.50	5	20.20	6
19	21.90	6	16.80	5	20.50	6
		Σ 911993		Σ 783401		Σ 928001

TABLE 108

GROSS AREA STRESS SPECTRA IN VICINITY OF FRACTURE IN PANELS 7 AND 9
AT JOINT AND IN PANEL 8 AT TEE

Test Group No. M17

Loading Step	Panel 7		Panel 8		Panel 9	
	f_v KSI	n	f_v KSI	n	f_v KSI	n
	f_{min} = 4.00 KSI		f_{min} = 3.19 KSI		f_{min} = 4.07 KSI	
1	1.46	80500	1.17	80500	1.49	80500
2	2.92	70500	2.34	110450	2.99	117500
3	4.38	52500	3.51	82250	4.48	67500
4	5.85	37500	4.69	56750	5.98	75000
5	7.31	25500	5.86	39950	7.47	51000
6	8.77	16800	7.0[illegible]	26320	8.96	33600
7	10.20	8700	8.2[illegible]	13630	10.60	17400
8	11.70	3900	9.37	6110	12.00	7500
9	13.20	1450	10.50	2350	13.40	2972
10	14.60	508	11.70	810	14.90	1033
11	15.40	90	12.[illegible]0	144	15.70	184
		Σ 2979[illegible]		Σ 421264		Σ 473989

TABLE 109

GROSS AREA STRESS SPECTRA IN VICINITY OF FRACTURE IN PANEL 10 AT JOINT AND PANEL 13 AT STRINGER RUN-OUT

Test Group No. CG5

Loading Step	Panel 10 f_v KSI	Panel 10 n	Panel 13 f_v KSI	Panel 13 n
	Gust Loading			
	f_{mean} = 13.50 KSI		f_{mean} = 12.40 KSI	
1	1.12	123750	1.03	165000
2	2.24	86535	2.06	115380
3	3.37	80190	3.09	106920
4	4.49	44955	4.12	59940
5	5.61	28905	5.15	37260
6	6.73	16200	6.18	19440
7	7.85	9700	7.12	11664
8	8.97	3650	8.24	5103
9	10.10	1620	9.27	1620
10	11.20	612	10.30	612
11	12.30	270	11.30	270
12	13.50	135	12.40	135
13	14.60	81	13.40	81
14	15.70	54	14.40	54
15	16.80	29	15.50	27
16	17.90	14	16.50	14
17	19.10	8	17.50	8
18	20.20	3	18.50	3
19	20.50	3	18.80	2
		Σ396723		Σ515542
	Ground Loading			
	f_{mean} = 3.37 KSI		f_{mean} = 3.09 KSI	
20	1.12	110250	1.03	110250
21	2.24	61200	2.06	61200
22	3.37	25200	3.09	25200
23	4.49	10080	4.12	10080
24	5.16	2150	5.15	2150
25	6.73	450	6.18	450
26	7.85	120	7.21	120
27	8.97	54	8.24	54
28	10.10	29	9.27	28
29	11.20	6	10.30	6
30	12.30	1	11.30	1
31	12.50	1	11.50	1
		Σ209541		Σ209540
	Ground-Air-Ground Loading			
	f_{mean} = 5.05 KSI		f_{mean} = 4.64 KSI	
32	8.41	32500	7.72	32500
TOTAL		Σ638764		Σ757582

TABLE 110

GROSS AREA STRESS SPECTRA IN VICINITY OF FRACTURE IN PANEL 14 AT TEE AND IN PANEL 15 AT JOINT

Test Group No. CM2

Loading Step	Panel 14 f_v KSI	Panel 14 n	Panel 15 f_v KSI	Panel 15 n
	Fighter Maneuver Loading			
	f_{min} = 3.18 KSI		f_{min} = 3.93 KSI	
1	1.16	24500	1.44	44100
2	2.33	20750	2.87	37350
3	3.50	18500	4.31	33300
4	4.66	15250	5.75	27450
5	5.83	9250	7.19	16650
6	6.99	5750	8.63	10350
7	8.16	2500	10.10	4500
8	9.33	2000	11.50	3600
9	10.50	661	12.90	1485
10	11.70	112	14.40	228
11	12.20	28	15.10	56
		Σ 99301		Σ 179069
	Ground Loading			
	f_{mean} = -2.74 KSI		f_{mean} = -3.38 KSI	
12	.91	61250	1.13	110250
13	1.83	34000	2.25	61200
14	2.74	14000	3.38	25200
15	3.65	5600	4.51	10080
16	4.56	1075	5.64	1935
17	5.48	225	6.76	405
18	6.39	60	7.89	108
19	7.30	27	9.02	49
20	8.22	14	10.10	25
21	9.13	3	11.30	5
22	10.00	1	12.40	1
23	-	-	12.60	1
		Σ 116255		[illegible]
	Ground-Air-Ground Loading			
	f_{mean} = .18 KSI		f_{mean} = .22 KSI	
24	3.00	3325	3.67	5980
TOTAL		[illegible]		Σ 394309

Aeronautical Systems Division, W-PAFB, Ohio.
Rpt No. ASD-TR-61-434, AN ENGINEERING EVALUATION OF METHODS FOR THE PREDICTION OF FATIGUE LIFE IN AIRFRAME STRUCTURES. Mar 62, 4[illegible]p. incl illus., tables, 35 refs.

Unclassified Report

Results of study are presented for comparison and verification of fatigue-life prediction methods suitable for handling complex problems encountered in design and operation of modern aircraft. Problems of airframe fatigue are analyzed from overall viewpoint of a system of design, development testing, and interpretation of fleet service history. From study of 20 proposed fatigue-life prediction methods, 10 were evaluated numerically with 78 complex spectral test results representing about 266 specimens.

(over)

1. Airframes
2. Fatigue

I. AFSC Project 1367, Task 136710
II. Contract AF33(616)-6974
III. Lockheed-California Co., A Div. of Lockheed Aircraft Corp., Burbank, California
IV. W. J. Crichlow, A. J. McCulloch, L. Young, et al
V. In ASTIA collection

Experimental program generated constant-amplitude, axial-load, S-N type data on simple notched coupons of 7075-T6 aluminum alloy sheet. New magnetic tape-controlled fatigue test machines were used to apply simple spectra of gust, maneuver, ground, composite spectra of flight gust, ground taxi, and ground-air-ground transitions and composite spectra of flight maneuver, ground taxi, and ground-air-ground transition. Specimens of complex joint were also fatigue-tested to same simple ordered gust and maneuver spectra, to the composite spectra of flight gust, ground taxi, and ground-air-ground transition cycles, and to composite flight maneuver, ground taxi, and ground-air-ground transition cycles. Data were analyzed to confirm or provide means of improving selected fatigue-life prediction methods.

Aeronautical Systems Division, W-PAFB, Ohio.
Rpt No. ASD-TR-61-434, AN ENGINEERING EVALUATION OF METHODS FOR THE PREDICTION OF FATIGUE LIFE IN AIRFRAME STRUCTURES. Mar 62, 4[illegible]p. incl illus., tables, 35 refs.

Unclassified Report

Results of study are presented for comparison and verification of fatigue-life prediction methods suitable for handling complex problems encountered in design and operation of modern aircraft. Problems of airframe fatigue are analyzed from overall viewpoint of a system of design, development testing, and interpretation of fleet service history. From study of 20 proposed fatigue-life prediction methods, 10 were evaluated numerically with 78 complex spectral test results representing about 266 specimens.

(over)

1. Airframes
2. Fatigue

I. AFSC Project 1367, Task 136710
II. Contract AF33(616)-6974
III. Lockheed-California Co., A Div. of Lockheed Aircraft Corp., Burbank, California
IV. W. J. Crichlow, A. J. McCulloch, L. Young, et al
V. In ASTIA collection

Experimental program generated constant-amplitude, axial-load, S-N type data on simple notched coupons of 7075-T6 aluminum alloy sheet. New magnetic tape-controlled fatigue test machines were used to apply simple spectra of gust, maneuver, ground, composite spectra of flight gust, ground taxi, and ground-air-ground transitions and composite spectra of flight maneuver, ground taxi, and ground-air-ground transition. Specimens of complex joint were also fatigue-tested to same simple ordered gust and maneuver spectra, to the composite spectra of flight gust, ground taxi, and ground-air-ground transition cycles, and to composite flight maneuver, ground taxi, and ground-air-ground transition cycles. Data were analyzed to confirm or provide means of improving selected fatigue-life prediction methods.

REPORT HAS BEEN DELIMITED

AND CLEARED FOR PUBLIC RELEASE

PER DOD DIRECTIVE 5200.20 AND

RESTRICTIONS ARE IMPOSED UPON

USE AND DISCLOSURE.

TRIBUTION STATEMENT A

PROVED FOR PUBLIC RELEASE;

TRIBUTION UNLIMITED.